frontiers | Research Topics

Parasites at the one health interface

Edited by
Mughees Aizaz Alvi, Hussam Askar, Hongbin Yan
and Sirikachorn Tangkawattana

Published in
Frontiers in Veterinary Science

FRONTIERS EBOOK COPYRIGHT STATEMENT

The copyright in the text of individual articles in this ebook is the property of their respective authors or their respective institutions or funders. The copyright in graphics and images within each article may be subject to copyright of other parties. In both cases this is subject to a license granted to Frontiers.

The compilation of articles constituting this ebook is the property of Frontiers.

Each article within this ebook, and the ebook itself, are published under the most recent version of the Creative Commons CC-BY licence. The version current at the date of publication of this ebook is CC-BY 4.0. If the CC-BY licence is updated, the licence granted by Frontiers is automatically updated to the new version.

When exercising any right under the CC-BY licence, Frontiers must be attributed as the original publisher of the article or ebook, as applicable.

Authors have the responsibility of ensuring that any graphics or other materials which are the property of others may be included in the CC-BY licence, but this should be checked before relying on the CC-BY licence to reproduce those materials. Any copyright notices relating to those materials must be complied with.

Copyright and source acknowledgement notices may not be removed and must be displayed in any copy, derivative work or partial copy which includes the elements in question.

All copyright, and all rights therein, are protected by national and international copyright laws. The above represents a summary only. For further information please read Frontiers' Conditions for Website Use and Copyright Statement, and the applicable CC-BY licence.

ISSN 1664-8714
ISBN 978-2-8325-7119-4
DOI 10.3389/978-2-8325-7119-4

Generative AI statement
Any alternative text (Alt text) provided alongside figures in the articles in this ebook has been generated by Frontiers with the support of artificial intelligence and reasonable efforts have been made to ensure accuracy, including review by the authors wherever possible. If you identify any issues, please contact us.

About Frontiers

Frontiers is more than just an open access publisher of scholarly articles: it is a pioneering approach to the world of academia, radically improving the way scholarly research is managed. The grand vision of Frontiers is a world where all people have an equal opportunity to seek, share and generate knowledge. Frontiers provides immediate and permanent online open access to all its publications, but this alone is not enough to realize our grand goals.

Frontiers journal series

The Frontiers journal series is a multi-tier and interdisciplinary set of open-access, online journals, promising a paradigm shift from the current review, selection and dissemination processes in academic publishing. All Frontiers journals are driven by researchers for researchers; therefore, they constitute a service to the scholarly community. At the same time, the *Frontiers journal series* operates on a revolutionary invention, the tiered publishing system, initially addressing specific communities of scholars, and gradually climbing up to broader public understanding, thus serving the interests of the lay society, too.

Dedication to quality

Each Frontiers article is a landmark of the highest quality, thanks to genuinely collaborative interactions between authors and review editors, who include some of the world's best academicians. Research must be certified by peers before entering a stream of knowledge that may eventually reach the public - and shape society; therefore, Frontiers only applies the most rigorous and unbiased reviews. Frontiers revolutionizes research publishing by freely delivering the most outstanding research, evaluated with no bias from both the academic and social point of view. By applying the most advanced information technologies, Frontiers is catapulting scholarly publishing into a new generation.

What are Frontiers Research Topics?

Frontiers Research Topics are very popular trademarks of the *Frontiers journals series*: they are collections of at least ten articles, all centered on a particular subject. With their unique mix of varied contributions from Original Research to Review Articles, Frontiers Research Topics unify the most influential researchers, the latest key findings and historical advances in a hot research area.

Find out more on how to host your own Frontiers Research Topic or contribute to one as an author by contacting the Frontiers editorial office: frontiersin.org/about/contact

Parasites at the one health interface

Topic editors

Mughees Aizaz Alvi — University of Agriculture, Faisalabad, Pakistan

Hussam Askar — Al Azhar University, Egypt

Hongbin Yan — Lanzhou Veterinary Research Institute, Chinese Academy of Agricultural Sciences, China

Sirikachorn Tangkawattana — Khon Kaen University, Thailand

Citation

Alvi, M. A., Askar, H., Yan, H., Tangkawattana, S., eds. (2025). *Parasites at the one health interface*. Lausanne: Frontiers Media SA. doi: 10.3389/978-2-8325-7119-4

Table of contents

05 Editorial: Parasites at the one health interface
Mughees Aizaz Alvi, Hong-Bin Yan, Hussam Askar and Sirikachorn Tangkawattana

08 Mechanism of Qingchang compound against coccidiosis based on network pharmacology-molecular docking
Zhiqiang Yan, Chunlin Chen, Shaoqin Zhai, Hongmei Tang, Maixun Zhu, Yuandi Yu and Hua Zheng

19 *In silico* and *in vivo* evaluation of the anti-cryptosporidial activity of eugenol
Hattan S. Gattan, Majed H. Wakid, Rowaid M. Qahwaji, Sarah Altwaim, Haifaa A. Mahjoub, Mashael S. Alfaifi, Hayam Elshazly, Wafa Abdullah I. Al-Megrin, Eman Abdullah Alshehri, Hatem A. Elshabrawy and Asmaa M. El-kady

33 Unveiling zoonotic threats: molecular identification of *Brugia* sp. infection in a lion
Witchuta Junsiri, Patchana Kamkong, Aunchisa Phojun and Piyanan Taweethavonsawat

40 Modulation of the rat intestinal microbiota in the course of *Anisakis pegreffii* infection
Min-hao Zeng, Shan Li, Qing-bo Lv, Xiao-xu Wang, Abdul Qadeer and Mohamed H. Mahmoud

51 Unrevealing the therapeutic potential of artesunate against emerging zoonotic *Babesia microti* infection in the murine model
Saqib Ali Fazilani, Wei An, Sihong Li, Mohammad Farooque Hassan, Muhammad Ishfaq, Shakeel Ahmed Lakho, Muhammad Farooque, Muhammad Shoaib and Xiuying Zhang

64 Burden and factors influencing intestinal parasitic infections among food handlers in Gondar City, Northwest Ethiopia
Michael Getie, Gizeaddis Belay, Azanaw Amare, Wondwossen Abebe and Teshiwal Deress

75 Case report: *Echinococcus multilocularis* infection in a dog showing gastrointestinal signs in Hokkaido, Japan
Izumi Kida, Naoki Hayashi, Nozomu Yokoyama, Noriyuki Nagata, Kazuyoshi Sasaoka, Noboru Sasaki, Keitaro Morishita, Kensuke Nakamura, Hirokazu Kouguchi, Kinpei Yagi, Ryo Nakao, Mitsuyoshi Takiguchi and Nariaki Nonaka

79 Wild rodents in three provinces of China exhibit a wide range of *Enterocytozoon bieneusi* diversity
Zhen-Qiu Gao, Hai-Tao Wang, Qing-Yu Hou, Ya Qin, Si-Yuan Qin, Quan Zhao and He Ma

88 Prior *Trichinella spiralis* infection protects against *Schistosoma mansoni* induced hepatic fibrosis
Asmaa M. El-kady, Sarah A. Altwaim, Majed H. Wakid, Alaa S. Banjar, Khalil Mohammed, Mashael S. Alfaifi, Hayam Elshazly, Wafa Abdullah I. Al-Megrin, Eman Abdullah Alshehri, Eman Sayed and Hatem A. Elshabrawy

105 Ecological factors associated with fox feces density in an *Echinococcus multilocularis* endemic zone in Japan
Megumi Fukui, Kohji Uraguchi, Himika Numa, Toru Suzuki, Michiko Karasawa, Kaoruko Maita, Terumi Yokozawa, Yoko Hayama and Kohei Makita

117 Evaluating prevalence, risk factors, and diagnostic techniques for *Cryptosporidium* infection in goats and surrounding water sources
Manahil Rafiq, Naimat Ullah Khan, Imad Khan, Mansoor Ahmad, Aiman Bibi, Mourad Ben Said, Hanène Belkahia, Muhammad Tariq, Silwat Saeed, Mostafa A. Abdel-Maksoud, Mohamed A. El-Tayeb, Sabiha Fatima, Bushra Hafeez Kiani, Akram A. Alfuraydi and Farhad Badshah

128 Investigation of *Hyalomma turanicum* and *Hyalomma asiaticum* in Pakistan, with notes on the detection of tickborne Rickettsiales
Zafar Ullah, Iram Liaqat, Mehran Khan, Abdulaziz Alouffi, Mashal M. Almutairi, Dmitry A. Apanaskevich, Tetsuya Tanaka and Abid Ali

139 Murine-related helminthiasis: a public health concern at solid waste sites around forest- adjacent communities in Thailand
Nattapon Maneepairoj, Paisin Lekcharoen, Kittipong Chaisiri and Supaphen Sripiboon

150 Impact of trypanosomiasis on male camel infertility
Sara Salah Abdel-Hakeem, Gaber Megahed, Ahmed M. Al-Hakami, Mohammed E. M. Tolba and Yasser F. M. Karar

164 Prediction of potential drug targets and key inhibitors (ZINC67974679, ZINC67982856, and ZINC05668040) against *Rickettsia felis* using integrated computational approaches
Sudais Rahman, Hsien Liu, Mohibuallah Shah, Mashal M. Almutairi, Iram Liaqat, Tetsuya Tanaka, Chien-Chin Chen, Abdulaziz Alouffi and Abid Ali

179 Existence of *Pentatrichomonas hominis* in Tibetan Antelope (*Pantholops hodgsonii*)
Shuo Liu, Jing-Hao Li, Si-Yuan Qin, Jing Jiang, Zhen-Jun Wang, Tao Ma, Jun-Hui Zhu, Hong-Li Geng, Wei-Lan Yan, Nian-Yu Xue, Yan Tang and He-Ting Sun

185 Prevalence and assemblage distribution of *Giardia intestinalis* in farmed mink, foxes, and raccoon dogs in northern China
Shuo Liu, Miao Zhang, Nian-Yu Xue, Hai-Tao Wang, Zhong-Yuan Li, Ya Qin, Xue-Min Li, Qing-Yu Hou, Jing Jiang, Xing Yang, Hong-Bo Ni and Jian-Xin Wen

194 One Health alert: zoonotic scabies from dromedary camels—A case report and call for vigilance
Hebel Christiana, Schuster Rolf Karl, Kinne Joerg and Wernery Ulrich

200 Ixodid ticks of Western Palearctic bats: ecology, host-parasite relationships, geographic distribution and zoonotic importance
Attila D. Sándor, Cristian Domșa, Áron Péter and Sándor Hornok

frontiers | Frontiers in Veterinary Science

TYPE Editorial
PUBLISHED 27 October 2025
DOI 10.3389/fvets.2025.1685326

Check for updates

OPEN ACCESS

EDITED AND REVIEWED BY
Antoinette Marsh,
The Ohio State University, United States

*CORRESPONDENCE
Mughees Aizaz Alvi
✉ mugheesaizazalvi@gmail.com
Hong-Bin Yan
✉ yanhongbin@caas.cn

RECEIVED 13 August 2025
ACCEPTED 09 October 2025
PUBLISHED 27 October 2025

CITATION
Alvi MA, Yan H-B, Askar H and Tangkawattana S (2025) Editorial: Parasites at the one health interface.
Front. Vet. Sci. 12:1685326.
doi: 10.3389/fvets.2025.1685326

COPYRIGHT
© 2025 Alvi, Yan, Askar and Tangkawattana. This is an open-access article distributed under the terms of the Creative Commons Attribution License (CC BY). The use, distribution or reproduction in other forums is permitted, provided the original author(s) and the copyright owner(s) are credited and that the original publication in this journal is cited, in accordance with accepted academic practice. No use, distribution or reproduction is permitted which does not comply with these terms.

Editorial: Parasites at the one health interface

Mughees Aizaz Alvi[1]*, Hong-Bin Yan[2]*, Hussam Askar[3,4] and Sirikachorn Tangkawattana[5]

[1]Department of Clinical Medicine and Surgery, University of Agriculture, Faisalabad, Pakistan, [2]State Key Laboratory for Animal Disease Control and Prevention, College of Veterinary Medicine, Lanzhou University, Gansu Province Research Center for Basic Disciplines of Pathogen Biology, Key Laboratory of Veterinary Parasitology of Gansu Province, Key Laboratory of Veterinary Etiological Biology and Key Laboratory of Ruminant Disease Prevention and Control (West), Ministry of Agricultural and Rural Affairs, National Para-reference Laboratory for Animal Echinococcosis, Lanzhou Veterinary Research Institute, Chinese Academy of Agricultural Sciences, Lanzhou, China, [3]Faculty of Science, Al-Azhar University, Assiut, Egypt, [4]State Key Laboratory for Animal Disease Control and Prevention, Lanzhou Veterinary Research Institute, Chinese Academy of Agricultural Sciences, Lanzhou, China, [5]Faculty of Veterinary Medicine, Khon Kaen University, Khon Kaen, Thailand

KEYWORDS

One Health, zoonotic parasites, parasitic diseases, surveillance and control, neglected tropical diseases

Editorial on the Research Topic
Parasites at the one health interface

Relationships among human health, animal health, environmental health, both interrelationships in general and the connection specifically between human and animals, have become particularly important given the emergence of new infectious diseases, changing environmental conditions, and escalating animal-human interactions. Parasitic diseases are examples of the multidimensional nature of the issues encountered on this interface, which often occurs because of complicated ecological, socioeconomic and behavioral factors. The aspects of parasitic and parasitic-vector borne diseases as threats to global health, as well at the interface of One Health are presented with a rich set of contributions varying from field based, surveillance based and specific parasites.

Framing the One Health agenda through parasite research

In essence, the One Health framework fosters the use of transdisciplinary approaches in order to learn and reduce the threat of zoonoses. The existence of parasites is featured as a direct and indirect disease mediator, and they have been affected by ecological fluctuations, global business, human utilization of the land, wildlife encounters, and climate change. The articles that are a part of this Research Topic highlight the role of parasites as important ecosystem health sentinels and as under-recognized risks to human and animal health.

Echinococcosis is an exemplary reflection of such nuance, through infections of *Echinococcus multilocularis* (a zoonotic highly pathogenic cestode in humans). Japanese investigators offer two articles that examine this parasite in two different perspectives. Kida et al. report a unique example of *E. multilocularis* infection in domestic dog with evidence of gastrointestinal manifestations in Hokkaido, highlighting its hazard and the need to monitor this parasite in companion animal veterinary practices.

Simultaneously, Fukui et al. evaluate the ecologic drivers, including vegetation and proximity to urban centers, affecting the density of fox feces (through which the prevalence of parasites can be inferred) in endemic regions thereby connecting wildlife ecology to the monitoring of population health.

Likewise, zoonotic scabies has re-emerged. According to Christiana et al., there is an alarming incident of *Sarcoptes scabiei* infection passed from dromedary camels to humans is posing a risk to the occupational health of pastoral societies and highlights the need to focus on awareness of diagnostics. Such examples indicate the changing boundaries of zoonotic parasitism and the need to have early warning systems that have to be integrated within both the veterinary and human health care systems.

Expanding the host spectrum: wildlife and domestic interfaces

Parasitological surveillance of the wildlife species is often neglected, yet the species are important in a disease ecology context. Liu, Li, et al. document the existence of *Pentatrichomonas hominis* in the Tibetan antelope- a species that is not only ecologically sensitive but also one that is indicative of the high-altitude ecosystem. This is indicative of the possibility of translocation, adaptation of parasites in other species living on distant habitats enhanced by the overlap of livestock and wildlife and the resultant climatic changes. On a similar note, Gao et al. cite a huge variation in *Enterocytozoon bieneusi* genotypes in wild rodents in three Chinese provinces, establishing the role of reservoir species in maintaining and transmitting parasites in the wild.

There are also other zoonotic nematodes in the form of the zoonotic filarial nematode genera, *Brugia* which crosses surprising boundaries. Infection with *Brugia* sp. has been identified in a captive lion, which is an extension of the known host ranges and pose a risk to zoo personnel and those who handle wild animals (Junsiri et al.). Likewise, Liu, Zhang, et al. revealed the presence of *Giardia intestinalis* in commercial farm raised fur animals in the north of China, including mink, foxes, and raccoon dogs, which indicates that industrialized animal culture forms a facilitator of protozoan spread amongst the animal units. These case studies indicate the immediacy of embeddedness of wildlife, exotic and farm-raised animals disease and health status in the expanded One Health approaches.

Human-associated parasitism: neglect, burden, and risk factors

Marginalized populations are frequently overrepresented in parasitic diseases. Getie et al. examined the burden of intestinal parasitic infection in food handlers in Gondar City, Ethiopia, and it was found that the outcomes demonstrated high incidence rates and the cause was due to poor hygiene habits and low education levels. In their study, the researchers emphasize the necessity of specific public health education and the regular screening of the employees within the food industry, particularly in low-resource countries. Parallel to these findings, we have Thailand where Maneepairoj et al. addressed helminth infection around forest-proximal waste stations, and examined rodents and murine-related parasites. They determined that ecological degradation, substandard sanitation, and close proximity to humans are common factors which creates conditions promoting cross-species parasites and increase the risk of parasite exposure to humans.

Ullah et al. investigated the prevalence of the *Hyalomma* tick species on livestock in Pakistan. The investigators found the presence of Rickettsiales DNA, pointing to a dual parasitic-vector status, illuminating the possible underestimation of threats to livestock productivity and even human health in arid regions.

Environmental spillover and water-linked transmission

Water is one of the major channels in the spread of parasitic infections, particularly in pastoral and peri-urban areas. Rafiq et al. investigated *Cryptosporidium* prevalence of goats and local water, linking the infectivity of the pathogen to pollute the environment and sustain infection rates. Their work contributes to the need to introduce combined livestock-water monitoring and protozoa diagnosis enhancement in order to reduce the contamination of the environment.

Investigation of novel treatments for cryptosporidiosis is another important area. Gattan et al. describe their investigation of the anti-cryptosporidial effect of eugenol, a natural compound, through both initial *in vitro* and subsequent *in vivo* evaluations. The positive results support the utility of plant-based and inexpensive therapeutic solutions, particularly, amid antimicrobial resistance growth and the lack of effective treatments of cryptosporidiosis in general.

Novel therapeutics and predictive computational approaches

Translational dimensions of parasite research can be well illustrated in contributions that discuss the field of drug research, and disease modulation. Rahman et al. used computational biology tools to identify effective inhibitors (ZINC67974679, ZINC67982856, and ZINC05668040) against *Rickettsia felis*, a pathogen causative in the flea-borne spotted fever disease. The combined power of their multiple methods (virtual screening, pharmacokinetic modeling, and docking analysis), illustrate the future direction of parasitic disease research through rapid, non-expensive, and precision based methods.

Fazilani et al. discussed the possible use of artesunate in the therapy of *Babesia microti* infection in mice, as the drug demonstrates strong antiprotozoal activity. This makes it possible to repurpose drugs on neglected parasitic diseases where there are few investments in the pharmaceutical industry.

Within these series of One Health and zoonotic parasites papers, a study evaluating cross-protection, underscores the importance of parasite immunomodulation, El-kady et al. showed that predisposed *Trichinella spiralis* infection may prevent the development of hepatic fibrosis caused by *Schistosoma mansoni*, indicating that immunomodulatory strategies stimulated by the interaction of two organisms may be a promising solution.

Microbiota and immunological frontiers

Zeng et al., explored an innovative aspect of gastrointestinal parasites and host microbiome. This study evaluated rats infected with *Anisakis pegreffii* and showed that parasitic infection can bias the host's microbial community. The authors discussed the impact of parasitic infection on disease outcomes and the immune system. The potential therapeutics or diagnostics that may emerge can take advantage of these microbiome-parasite interactions and may be based not on eliminating the parasite, but on altering the host's microbial landscape.

Moving forward: integration, surveillance, and equity

The various studies and their findings included within this Research Topic demonstrate the diversity of biologic complexity of parasite infections related to One Health. Under the One Health movement, there are several main priorities for the future which include the followings:

1. Fortifying surveillance: surveillance should be enhanced, not only between dogs living in our cities and rodents living in our forests, but also on a species and ecosystem level to identify any emerging threats in a timely manner.
2. Cross-sectoral collaboration: parasitology research need to utilize the molecular biology, computational science, social sciences and veterinary epidemiology toolboxes to be able to deliver a complete and multidisciplinary solution.
3. Building capacity in low-resource environments: a large proportion of the biggest disease burdens of parasite are in the locations with the poorest diagnostic capacity. Local laboratories and field-based training, as well as community education, are also of utmost importance for resource investment.
4. Drug innovation and repurposing: although natural compounds continue to achieve pharmaceutical success, nature already has given us a successful drug, eugenol, and repurposing it and similar compounds can develop new drug candidates, as seen with artesunate.
5. Climate and ecological awareness: research needs to be adjusted to the changing parasite ranges due to global environmental changes with the concurrent ecological models and the long-term surveillance have to become important components of the needed analysis.

The contributions to this Research Topic enhance our knowledge about the topic of parasitism at the interface between human, animals, and the environment and help to emphasize the relevancy of the parasitic diseases on the world health. To deal with these aspects, one will need innovation, equity, and collaboration which are the features of the One Health philosophy.

Author contributions

MA: Writing – original draft. H-BY: Writing – original draft. HA: Writing – original draft. ST: Writing – original draft.

Funding

The author(s) declare that no financial support was received for the research and/or publication of this article.

Conflict of interest

The authors declare that the research was conducted in the absence of any commercial or financial relationships that could be construed as a potential conflict of interest.

Generative AI statement

The author(s) declare that no Gen AI was used in the creation of this manuscript.

Any alternative text (alt text) provided alongside figures in this article has been generated by Frontiers with the support of artificial intelligence and reasonable efforts have been made to ensure accuracy, including review by the authors wherever possible. If you identify any issues, please contact us.

Publisher's note

All claims expressed in this article are solely those of the authors and do not necessarily represent those of their affiliated organizations, or those of the publisher, the editors and the reviewers. Any product that may be evaluated in this article, or claim that may be made by its manufacturer, is not guaranteed or endorsed by the publisher.

frontiers | Frontiers in Veterinary Science

TYPE Original Research
PUBLISHED 01 March 2024
DOI 10.3389/fvets.2024.1361552

Check for updates

OPEN ACCESS

EDITED BY
Hongbin Yan,
Chinese Academy of Agricultural Sciences, China

REVIEWED BY
Muhammad Tahir Aleem,
Nanjing Agricultural University, China
Warda Qamar,
University of Agriculture, Pakistan
Mian Hafeez,
University of Veterinary and Animal Sciences, Pakistan

*CORRESPONDENCE
Zhiqiang Yan
✉ yanzhiqiang202012@163.com
Yuandi Yu
✉ yuyd@cqaa.cn
Hua Zheng
✉ zheng_121_16@163.com

†These authors have contributed equally to this work

RECEIVED 26 December 2023
ACCEPTED 22 February 2024
PUBLISHED 01 March 2024

CITATION
Yan Z, Chen C, Zhai S, Tang H, Zhu M, Yu Y and Zheng H (2024) Mechanism of Qingchang compound against coccidiosis based on network pharmacology-molecular docking.
Front. Vet. Sci. 11:1361552.
doi: 10.3389/fvets.2024.1361552

COPYRIGHT
© 2024 Yan, Chen, Zhai, Tang, Zhu, Yu and Zheng. This is an open-access article distributed under the terms of the Creative Commons Attribution License (CC BY). The use, distribution or reproduction in other forums is permitted, provided the original author(s) and the copyright owner(s) are credited and that the original publication in this journal is cited, in accordance with accepted academic practice. No use, distribution or reproduction is permitted which does not comply with these terms.

Mechanism of Qingchang compound against coccidiosis based on network pharmacology-molecular docking

Zhiqiang Yan[1*†], Chunlin Chen[1,2†], Shaoqin Zhai[1], Hongmei Tang[1], Maixun Zhu[1], Yuandi Yu[1*] and Hua Zheng[2*]

[1]Chongqing Academy of Animal Sciences, Rongchang, China, [2]Chongqing Research Center of Veterinary Biological Products Engineering Technology, Chongqing, China

The aim of this study was to investigate the anti-*Eimeria tenella* mechanism of Qingchang Compound (QCC) and provide a basis for its clinical application. The active ingredients, active ingredient-disease intersection targets, and possible pathways of QCC for the treatment of chicken coccidiosis were analyzed, the binding ability of pharmacodynamic components and target proteins was determined by network pharmacology and the molecular docking, and a model of infection with coccidiosis was constructed to verify and analyze the mechanism of action of QCC against coccidiosis. Among the 57 components that met the screening conditions, the main bioactive components were quercetin, dichroine, and artemisinin, with IL-1β, IL-6, IL-10, IFN-γ, and IL-8 as the core targets. Simultaneously, the KEGG signaling pathway of QCC anti-coccidiosis in chickens was enriched, including cytokine-cytokine receptor interactions. The results showed that the main pharmacodynamic components of QCC and the core targets could bind well; artemisinin and alpine possessed the largest negative binding energies and presented the most stable binding states. In addition, *in vivo* studies showed that QCC reduced blood stool in chickens with coccidiosis, restored cecal injury, and significantly reduced the mRNA and protein expression levels of IL-1β, IL-10, and IFN-γ in ceca ($p < 0.01$). Our results suggest that the main active ingredients of QCC are artemisinin and alpine and its mechanism of action against coccidiosis may be related to the reduction of the inflammatory response by acting on specific cytokines.

KEYWORDS

Qingchang compound, network pharmacology, molecular docking, experimental verification, main components, core target

1 Introduction

Chicken coccidiosis is a protozoan disease caused by coccidian parasites belonging to the phylum Apicomplexa, class Sporozoa, order Eucoccidiorida, family *Eimeriidae*, and genus *Eimeria*. The main causative agents of chicken coccidiosis are seven species of *Eimeria*, namely *Eimeria tenella*, *E. necatrix*, *E. brunetti*, *E. maxima*, *E. acervulina*, *E. mitis*, and *E. praecox*, among which *E. tenella* is the most pathogenic. This disease primarily affects young and juvenile chickens (1–4). It has been reported that the annual economic loss to China's chicken

industry due to coccidiosis is up to 5 billion yuan, and drug expenditure alone is approximately 1.56–1.95 billion yuan (5).

Although, the chemotherapeutic drugs (Diclazuril and Sulfonamides) were mainly agents, it had a severe resistance in coccidia isolated from chicken farms, manifesting as broad, crossover, or multidrug resistance (6). Therefore, researchers have conducted in multiple directions, including live vaccines, recombinant vaccines, and medicinal plants (7–9). However, live vaccines have problems of poor stability, easy virulence regression, and uneven immunity, thus the application of live vaccines for coccidia needs further improvement. At present, the development and clinical application of recombinant proteins targeting coccidia require a long time. Traditional Chinese medicine is widely used in veterinary clinics because it is difficult for microorganisms to develop drug resistance to these widely sourced herbal prescriptions. Hence, the research and development of veterinary traditional Chinese medicine anti-coccidial drugs aligns with the market demand and national policy.

The main characteristic of veterinary Chinese medicinal compounds is the combination of multiple components and targets; however, traditional research of compound therapeutics has mainly involved a single target and pathway. Research on the mechanisms of traditional Chinese medicines against parasite has mainly focused on the direct effects of drugs on the activation of the host's immune function. The direct drug effects include recognition, movement, adhesion, invasion, and intracellular development, whereas the activation of the host's immune function includes both specific and non-specific immunity, making it difficult to fully explain the pharmacological effects and molecular mechanisms of Chinese veterinary drug compounds. In recent years, network pharmacology has been widely used to reveal the pharmacodynamic components, action of signaling channels, and compatibility connotations of Chinese veterinary drugs with the overall research mode of "multi-component-multi-target disease" (10–12). Currently, research on the anti-coccidiosis effect of QCC in chickens is mostly limited to pharmacodynamic studies, and there are few reports on the anti-coccidiosis mechanism(s) of action of this herb. The traditional methods for studying the possible mechanism of action of veterinary Chinese medicine against coccidiosis are tedious, time consuming, and expensive. In contrast, the use of network pharmacology and molecular docking in this regard presents significant advantages (efficient, accurate, and comprehensive) (13). In this study, the main pharmacodynamic components, core targets, and enriched signaling pathways of QCC were analyzed using modern Chinese medicine network pharmacology and molecular docking, the core targets of the drug were verified through animal studies, and the anti-coccidiosis mechanism of action of QCC was determined.

2 Materials and methods

2.1 Network pharmacology analysis of the anti-coccidiosis effect of QCC in chickens

2.1.1 Construction of a drug-active ingredient-target network for QCC

The filtering conditions for the TCMSP database were Oral Bioavailability (OB) ≥ 30% and Drug-likeness (DL) ≥ 0.18. Through literature review, we identified the active components of four Chinese herbs—Artemisiae annuae herba, Dichroae radix, Agrimonia pilosa, and Sanguisorbae radix—and supplemented or cross-verified the data retrieved. Target information for these active components was downloaded from the TCMSP database. Component target proteins and gene names were matched using UniProt.[1] The drugs, active components, and potential targets were imported into Cytoscape 3.8.2 software (Bloomage BioTechnology Corporation Limited, China) to construct a drug-active component-target network to identify important candidate components.

2.1.2 Screening of targets for the prevention and treatment of chicken coccidiosis with QCC and construction of a protein–protein interaction network

In the GeneCards,[2] OMIM,[3] and NCBI[4] databases, we conducted keyword searches using the terms "Avian Coccidiosis," "Coccidiosis in Chicken," and "Chicken coccidia" to obtain targets related to coccidiosis in chickens. Species filtering was then performed using UniProt, and a Venn diagram was generated online.[5] The targets of Artemisiae annuae herba, Dichroae radix, Agrimonia pilosa, Sanguisorbae radix, and chicken coccidiosis were imported separately. The intersection of these sets was used to identify common targets, which serve as targets for treating chicken coccidiosis with QCC. The intersecting targets obtained from the Venn diagram were imported into the String database.[6] The species "Gallus" was selected, and a minimum interaction score of "medium confidence (0.400)" was chosen. After the protein–protein interaction (PPI) network was obtained, a TSV-format file was downloaded. This file was imported into Cytoscape 3.8.2 to construct a PPI network. The "Analyze Network" function was used to perform network analysis, calculating the degree values for all nodes in the network. Targets that ranked the highest based on their degree values were selected and used for subsequent molecular docking verification.

2.1.3 Gene ontology enrichment analysis and KEGG pathway enrichment analysis for targets of QCC in chicken coccidiosis

Gene Ontology (GO) and Kyoto Encyclopedia of Genes and Genomes (KEGG) pathway enrichment analyses were performed on the potential target genes through the DAVID website.[7] The input for potential targets was restricted to chicken species. The resulting GO analysis was filtered based on a p-value of less than 0.05, and the KEGG analysis was filtered based on a p-value of less than 0.01. The results were sorted according to the number of enriched genes, and the top 20 entries were selected for both. Bubble charts and bar graphs were created to identify the main biological processes (BP), primary cellular components (CC), and principal molecular functions (MF) involved, as well as key signaling pathways implicated.

1 https://www.uniprot.org/
2 https://www.genecards.org/
3 https://omim.org/
4 https://www.ncbi.nlm.nih.gov/
5 http://www.bioinformatics.com.cn/
6 https://string-db.org/
7 https://david.Ncifcrf.gov/

2.1.4 Molecular docking verification of core active components and targets of QCC

The 3D structures of the components of Artemisiae annuae herba, Dichroae radix, Agrimonia pilosa, and Sanguisorbae radix were obtained from the PubChem database and converted to the moL2 format using OpenBabel. They were then imported into PyMOL for addition of hydrogen, charging, and other treatments. The protein conformations were screened using the RCSB PDB database.[8] The selection criteria included having a well-defined protein structure obtained through X-ray crystallography with a crystal resolution smaller than 3A. These proteins were then processed to remove water and small molecules and treated with hydrogen addition, charge addition, and non-polar hydrogen merging in Autodock Tools 1.5.6. Docking calculations between large and small molecules were performed using AutoDock Tools. Receptor–ligand pairs were sorted and screened based on binding free energy (affinity in kcal/mol). A compound is considered to spontaneously bind and interact with a protein if its binding energy is <0 kcal/mol, with lower-energy conformations being more stable. Generally, a binding energy of <-1.2 kcal/mol indicates good binding efficiency (14). Visualization was performed using PyMOL 2.3.2 software.

2.2 Experimental validation of QCC against chicken coccidiosis

2.2.1 Preparation of QCC and tender *Eimeria* oocysts

A precise amount of QCC (Artemisiae annuae herba, Dichroae radix, Agrimonia pilosa, and Radix Sanguisorbae = 5:2:2:1) was weighed and soaked in distilled water for 0.5 h, followed by extraction in 75% ethanol for 1 h, and subsequent water extraction for 1 h. The extracts from both processes were combined and concentrated to yield a solution with a concentration of 1.0 g/mL of raw medicine, which was then set aside for later use.

Tender *E.* oocysts were obtained from the Chongqing Academy of Animal Science. Gavage feeding of sporulated oocysts was performed in chickens to revitalize the oocysts. Fecal samples from the chickens were collected upon the appearance of bloody feces to isolate the oocysts. Harvested *E.* oocysts were cultured in 2.5% potassium dichromate solution at 28°C for 3 days (10). During this period, oocyst status was monitored. Culturing was halted when sporulation and hatching rates exceeded 90%, and the sporulated oocysts were collected and set aside.

2.2.2 Experimental grouping and treatment

One-day-old Ross broiler chicks purchased from a poultry farm in Chongqing were allowed *ad libitum* access to food and water. The feed did not contain any additives. After reaching 16 days of age, the chicks were transferred to flame-sterilized cages.

Thirty 16 days-old Ross broiler chicks were randomly divided into three groups: Control, Model, and QCC. Except for the Control group, the other two groups were orally gavaged with 1×10^4 sporulated oocysts per chicken. Five days post inoculation, the QCC group was orally administered QCC extract at a dose of 2.4 g/kg. An equivalent volume of physiological saline was administered to the Control and Model groups. The treatment was administered once daily for a continuous period of 7 days. All chickens had *ad libitum* access to food and water, and the feed provided did not contain any additives.

2.2.3 Effect of QCC on clinical manifestations and cecal tissue of chickens with coccidiosis

During this study, the clinical manifestations of the chickens were observed and recorded, including their mental state, feeding, fur, movement, and fecal state. At the end of the study, all chickens were dissected, and the ceca was collected, fixed with 4% paraformaldehyde, embedded in paraffin, sliced, and stained with hematoxylin and eosin. Pathological changes in the tissues were observed under a microscope, and a microscopic imaging system was used to capture images.

2.2.4 Quantification of target gene mRNA levels using qPCR

At the end of the experiment, eight chickens from each group were randomly euthanized. The cecal tissue samples were collected aseptically and immediately stored in liquid nitrogen until further use. Total RNA was extracted from the cecal tissue following the protocol provided in the TRIzol reagent kit. Subsequently, cDNA was synthesized by reverse transcription and used as a template for real-time quantitative PCR (qPCR) analysis. The qPCR products were visualized and photographed using a gel imaging system. The density of the target bands was quantified using image analysis software, and the relative mRNA expression levels of the target genes were calculated using the $2^{-\Delta\Delta Ct}$ method. The primers were designed and synthesized according to gallus IL-1β (NM_204524.1), IL-6 (NM_204628.1), IL-10 (NM_001004414), IL-8 (DQ393272), and IFN-γ (NM_205149.1) gene sequences published in GenBank, all of which were synthesized by Bioengineering (Shanghai) Co., Ltd. The details of the primers used for real-time qPCR amplification are presented in Table 1.

2.2.5 Statistical analysis

All data were analyzed with SPSS 25.0 statistical software and are presented as means ± SD. One-way analysis of variance (ANOVA) was used to analyze data between groups, and the LSD method was used for pairwise comparisons. Statistical significance was set at $p < 0.05$ and 0.01. The letters a, b, and c indicate $p < 0.05$, and A, B, and C indicate $p < 0.01$.

3 Results

3.1 Screening results of active components and target sites of QCC

After screening through the TCMSP database, 57 compounds were identified that met the criteria of OB ≥30% and DL ≥0.18. Among them, 22 were from Artemisiae annuae herba, 17 were from Dichroae radix, and an additional compound, dichroine, was included because of its importance, resulting in 18 compounds from Dichroae radix. Additionally, five compounds were identified from Agrimonia pilosa and 13 from Sanguisorbae radix. After deduplication, a total of 51 unique compounds were identified. *Artemisia annua*'s active components corresponded to 210 target sites; Dichroae radix's active

8 https://www.rcsb.org/

TABLE 1 Primer sequence of qPCR.

Gene	Primer name	Primer sequence	Length of amplification product (bp)
IL-1β	F	GGCCTGAGTCATGCATCGTT	125
	R	ATAAATACCTCCACCCCGACAA	
IL-6	F	GAGGGCCGTTCGCTATTTG	93
	R	GCCATGTGGCAGATTGGTAA	
IL-10	F	ACCTTTGGCTGCCAGTCTGT	167
	R	CAGGTGAAGAAGCGGTGACA	
IL-8	F	CCTGGTTTCAGCTGCTCTGT	129
	R	GGCGTCAGCTTCACATCTTG	
IFN-γ	F	AACCTTCCTGATGGCGTGAA	137
	R	AAACTCGGAGGATCCACCAG	
β-Actin	F	ATGGCTCCGGTATGTGCAA	142
	R	TGGGCTTCATCACCAACGTA	

components corresponded to 52 target sites; Agrimonia pilosa's active components corresponded to 178 target sites; and Sanguisorbae radix's active components corresponded to 182 target sites. After eliminating the duplicates, 228 unique target sites were identified.

3.2 Screening of QCC bioactive ingredients and therapeutic targets for chicken coccidiosis

Following searches in the GeneCards, OMIM, and NCBI databases, 101 disease-target sites were identified. After species-specific filtering, 89 unique disease target sites were identified. Using Venn diagram analyses, 14 intersecting target sites were identified among the active constituents of Artemisiae annuae herba, Dichroae radix, Agrimonia pilosa, and Sanguisorbae radix and disease-specific targets for chicken coccidiosis (Figure 1A). A pharmacological network of drug-active component targets was constructed for Artemisiae annuae herba, Dichroae radix, Agrimonia pilosa, and Sanguisorbae radix. In this network, blue nodes represent potential target sites, pink nodes represent effective compounds, and yellow nodes represent drugs. The graph incorporates 51 compound nodes and 228 potential target nodes. Based on their prominence in the network, the top five compounds were quercetin, kaempferol, luteolin, artemisinin, and berberine. From the perspective of individual compound-target networks and based on the theory of network pharmacology, these five compounds could potentially account for the majority of the therapeutic effects of QCC and may represent the primary active substances in Artemisiae annuae herba, Dichroae radix, Agrimonia pilosa, and Sanguisorbae radix (Figure 1B). An analysis was conducted on the intersecting target sites obtained from both the constituent and disease-specific targets using Venn diagrams on the STRING website, resulting in a PPI network (Figure 1C). The network comprises 12 nodes and 46 edges. The size of each node symbolizes its degree value, whereas the color gradient from light to dark represents betweenness centrality. The thickness and color of the edges indicate the edge betweenness and combined score, respectively. Topological analysis of the PPI network identified hub proteins within this network. Based on their degree values, the top five proteins were IL-1β, IL-6, IL-10, IFN-γ, and IL-8. GO enrichment analysis was performed on potential target genes using DAVID. A total of 31 GO terms were identified, including 27 related to BP, one related to CC, and three related to MF (Figure 1D). The top 10 terms in each category are shown in Figure 1E. KEGG pathway analysis yielded a total of 11 enriched pathways.

3.3 Molecular docking validation of core active components and target interactions of QCC

Significant compounds such as quercetin, kaempferol, luteolin, artemisinin, and berberine were docked with the core target proteins IL-1β, IL-6, IL-10, IFN-γ, and IL-8. The docking results are listed in Table 2. All docking binding energies were less than −1.2 kcal/mol, indicating that the active components artemisinin, berberine, quercetin, kaempferol, and luteolin from Artemisiae annuae herba, Dichroae radix, Agrimonia pilosa, and Sanguisorbae radix could spontaneously bind with core targets (Table 3). Docking results were visualized using PyMOL software, and detailed docking interactions were observed under magnification (Figure 2). These findings suggested that QCC could exert its anti-coccidial effects through components like artemisinin, berberine, quercetin, kaempferol, and luteolin targeting IL-1β, IL-6, IL-10, IFN-γ, and IL-8.

3.4 Effects of QCC on the clinical manifestations of chickens with coccidiosis

Apart from the control group, chickens in both the model and drug treatment groups began to display symptoms of coccidiosis on the 4th day post-inoculation with sporulated oocysts. Symptoms included bloody feces, poor mental state, dull feather coat, decreased food intake, and blood in the cecal cavity. After administering QCC, clinical symptoms improved. The feces became more formed, and only trace amounts of blood were present (Figure 3). The mental state of

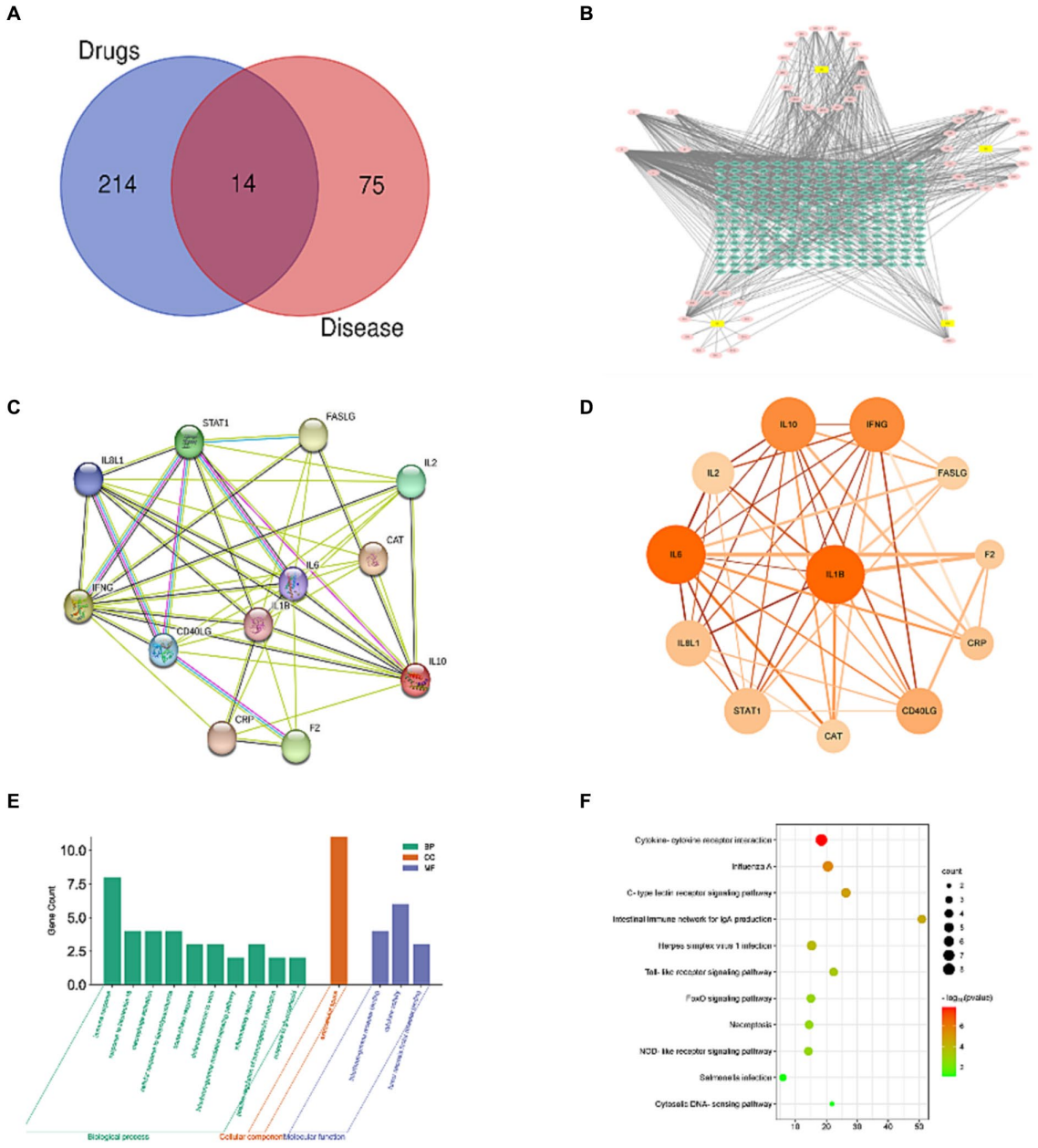

FIGURE 1
Network pharmacology analysis. **(A)** Venn diagram of intersection of QCC and anti-coccidiosis targets; **(B)** active ingredients-target network of QCC; **(C)** protein–protein interaction (PPI) network within the common targets; **(D)** enrichment analysis of GO biological processes; **(E)** enrichment analysis of pathway signaling.

the chickens improved, food intake returned to normal, and blood in the cecal cavity was not evident.

3.5 Effects of QCC on cecal tissue in chickens with coccidiosis

The cecal tissue structure of chickens in the control group was normal, the cells were neatly arranged and there was no obvious histopathological damage. Cecal tissue from the model group showed a large range of inflammatory cell infiltration, and coccidia bodies were observed in epithelial cells. Further, the mucosal layer was severely damaged. In the QCC group, no coccidiosis was found in the cecum epithelial cells; however, a small area of inflammatory cell infiltration and epithelial cell shedding was observed (Figure 4).

3.6 Effect of QCC on the mRNA expression levels of cecal IL-1β, IL-6, IL-8, IL-10, and IFN-γ in chickens with coccidiosis

At the end of the study, there was no significant difference in the mRNA expression of IL-6 and IL-8 ($p > 0.05$) in cecum tissues. The mRNA expression levels of IL-1β, IL-10, and IFN-γ in the model

TABLE 2 Detailed information of ingredients among four herbal medicines in QCC.

ID number	Molecule name	Source
MOL000098	Quercetin	Artemisiae annuae herba, Agrimonia pilosa, Radix Sanguisorbae
MOL000422	Kaempferol	Artemisiae annuae herba, Agrimonia pilosa, Radix Sanguisorbae
MOL000006	Luteolin	Artemisiae annuae herba, Agrimonia Pilosa, Radix Sanguisorbae
MOL000358	beta-sitosterol	Radix Sanguisorbae
MOL000354	Isorhamnetin	Artemisiae annuae herba
MOL000449	Stigmasterol	Dichroae radix, Artemisiae annuae herba
MOL008199	α-Dichroine	Dichroae Radix
MOL008182	Alpha-berbine	Dichroae radix
MOL008193	4,8-dimethoxy-1-methyl-3-(3-methyl-2-oxobutyl)quinolin-2-one	Dichroae radix
MOL005229	Artemetin	Artemisiae annuae herba
MOL001002	Ellagic acid	Agrimonia pilosa
MOL008177	7-4,8-dimethoxy-1-methyl-3-(3-methyl-2-oxobut-3-enyl) quinolin-2-one	Dichroae radix
MOL004609	Areapillin	Artemisiae annuae herba
MOL008178	3-(2-keto-3-methyl-but-3-enyl)-4,8-dimethoxy-carbostyril	Dichroae radix
MOL002235	EUPATIN	Artemisiae annuae herba
MOL007423	6,8-di-c-glucosylapigenin	Artemisiae annuae herba
MOL004083	Tamarixetin	Artemisiae annuae herba

TABLE 3 Binding energy of core-active ingredients in QCC with core anti-coccidiosis targets.

Molecule name	Binding protein	Binding energy (kcal/mol)
Quercetin	IL-1β	−7.22
Quercetin	IFN-γ	−4.7
Quercetin	IL-6	−5.5
Quercetin	IL-8	−3.79
Quercetin	IL-10	−3.78
Kaempferol	IL-1β	−6.79
Kaempferol	IFN-γ	−4.99
Kaempferol	IL-6	−5.58
Kaempferol	IL-8	−4.32
Kaempferol	IL-10	−4.02
Luteolin	IL-1β	−7.11
Luteolin	IFN-γ	−4.94
Luteolin	IL-6	−5.93
Luteolin	IL-8	−4.44
Luteolin	IL-10	−4.68
Artemetin	IL-1β	−8.19
Artemetin	IFN-γ	−6.88
Artemetin	IL-6	−6.85
Artemetin	IL-8	−6.26
Artemetin	IL-10	−6.23
Dichroine	IL-1β	−8.74
Dichroine	IFN-γ	−6.8
Dichroine	IL-6	−8.76
Dichroine	IL-8	−6.01
Dichroine	IL-10	−6.98

group were high, and the difference was significant compared with that in the control group ($p < 0.01$). The mRNA expression levels of IL-1β, IL-10, and IFN-γ in the QCC group were reduced, and the difference was significant compared with that in the model group ($p < 0.01$) (Figure 5).

3.7 Effect of QCC on protein expression levels of cecal IL-1β, IL-6, IL-8, IL-10, and IFN-γ in chickens with coccidiosis

At the end of the study, there was no significant difference in the protein expression of IL-6 and IL-8 in the cecum tissues from all the groups ($p > 0.05$). Protein expression of IL-1β and IFN-γ in the QCC group was significantly lower than in the model group ($p < 0.01$). Compared to the control group, the protein expression of IL-10 in the cecum of the model and drug groups increased significantly ($p < 0.01$), but there was no significant difference between the model and QCC groups ($p > 0.05$) (Figure 6).

4 Analysis and discussion

Chicken coccidiosis is an acute inflammatory intestinal protozoal disease with high incidence rate and mortality, which is globally prevalent and non-seasonal (15, 16). The use of anticoccidial chemicals, coccidiocides, coccidiostats, and ionophores has been a common practice in modern poultry production for controlling avian coccidiosis. However, the emergence of drug resistance and increasing consumer demand for meat free of residues has prompted the development of alternative control methods (17). In recent years, research has found that some traditional Chinese veterinary medicine, plant extracts, essential oils and probiotics, have significant anti coccidiosis activity with minimal side effects, and low susceptibility to drug resistance, such as Artemisia brevifolia Extract could enhancing the immunomodulatory potential against coccidiosis (18), herbal formula extract highly reduced the coccidian multiplication rate and reduced the severity of intestinal lesions (19). *Citrus sinensis* Essential Oil and Star Anise (*Illicium verum*) Essential Oil supplementation lowered oocysts shedding in faeces and faecal score (20, 21). Among these alternative insecticides, veterinary traditional Chinese medicine has a relatively complete medication theory and history. According to historical experience, some TCMs with "cold taste and bitter" properties, such as Artemisiae annuae herba and Dichroae radix, have antiparasitic effects. Qingchang Compound (QCC) is a traditional Chinese medicine for veterinary use with efficacy against chicken coccidiosis, which has undergone early stage clinical trials alongside Artemisiae annuae herba, Dichroae radix, Agrimonia pilosa, and Sanguisorbae radix (22). Our study preliminarily predicted and validated the activity of the top five active ingredients (quercetin, kaempferol, luteolin, artemisinin, and dichroine) in QCC and their affinity with five core targets (IL-1β, IL-6, IL-10, IFN-γ, and IL-8).

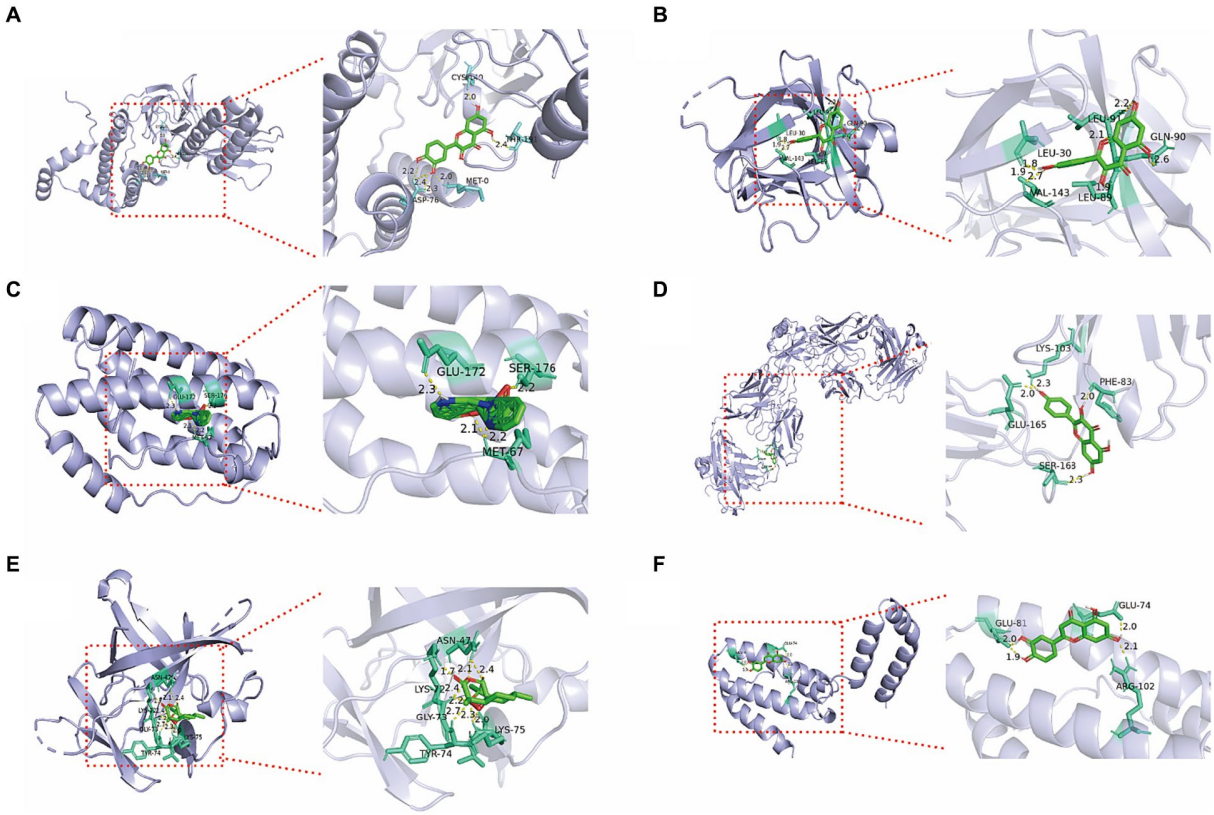

FIGURE 2
Molecular docking 3D diagram of core active ingredients in QCC with core anti-coccidiosis targets. **(A)** Quercetin-IFN-γ; **(B)** Quercetin-IL-1β; **(C)** Dichroine-IL-6; **(D)** Kaempferol IL-8; **(E)** Artemetin-IL1β; **(F)** Luteolin-IL-10.

Further study revealed that QCC could improve the clinical symptoms of cecal coccidiosis in chickens, reduce cecal tissue injuries, and downregulate the expression of IL-1β, IL-10, and INF-γ.

In this study, the main components of QCC with anti-coccidiosis efficacy in chickens were analyzed by network pharmacology, and the main bioactive components (artemisinin, dichroine, quercetin, kaempferol, and luteolin) exhibit strong anti-parasitic activity. Previous studies have confirmed that the *Artemisia annua* and Atractylodes lancea has significant anti-coccidial effects (23). Artemisinin, the main active component of the traditional Chinese medicine *Artemisia annua*, can induce apoptosis of second-generation merozoites by reducing mitochondrial membrane potential, leading to a remarkable suppression of the upregulated mRNA levels of NF-κB and interleukin-17A in the ceca during *Eimeria* tenella infection (23, 24). In addition, artemisinin can bind to membrane proteins (ATP transporters) in the asexual reproductive stage of plasmodium falciparum to reduce the infectivity of plasmodium malaria parasites (25, 26), and then promote the functional recovery by regulating the body's inflammatory response. The natural product dichroine and its synthetic derivatives has been proved that can disrupt the activity of synthetase by regulating the gene encoding gluprolyl-tRNA synthetase in plasmodium falciparum (27). The anti-parasitic effects of quercetin, kaempferol, and luteolin are primarily manifested in their ability to inhibit the inflammatory response induced by parasites (28–30). Therefore, we speculate that the anti-coccidiosis effect of QCC is mainly related to artemisinin, dichroine, quercetin, kaempferol, and luteolin, which may be related to their direct inhibition of parasite reproduction and reduction of excessive inflammatory responses.

Molecular docking is an important method for studying the interactions between ligands and receptors, predicting their binding modes and affinities, and searching for candidate compounds based on the docking results (31). We determined that the core targets (IL-1β, IL-6, IL-10, IFN-γ, and IL-8) of QCC can effectively bind with the core pharmacological components, among which artemisinin and alpine showed the largest negative binding energies and most stable binding abilities. And those of IL-1β and IFN-γ to each major component were low, indicating that it could bind spontaneously with the main component. When infected with coccidia, T lymphocytes can secrete various cytokines (the main is IFN-γ, IL-1β), which in turn play a role in anti-infection and immune protection (32). IFN-γ plays a crucial role in resisting intracellular parasitic protozoa, and directly kills parasites or inhibit their growth in the host (33). IL-1β is an important pro-inflammatory factor in the body, which can enhance the host's resistance to coccidian infection, but can also exacerbate intestinal damage and dysfunction (34). Therefore, it is speculated that the therapeutic substances of QCC can regulate the synthesis and secretion of IL-1β, IFN-γ, and IL-8 through the aforementioned interactions, thereby modulating intestinal inflammation and achieving therapeutic effects against nematode infections. In addition, KEGG analysis showed that these targets are mainly focused on the cytokine receptor interaction and influenza a pathway, indicating that future research should focus on these pathways.

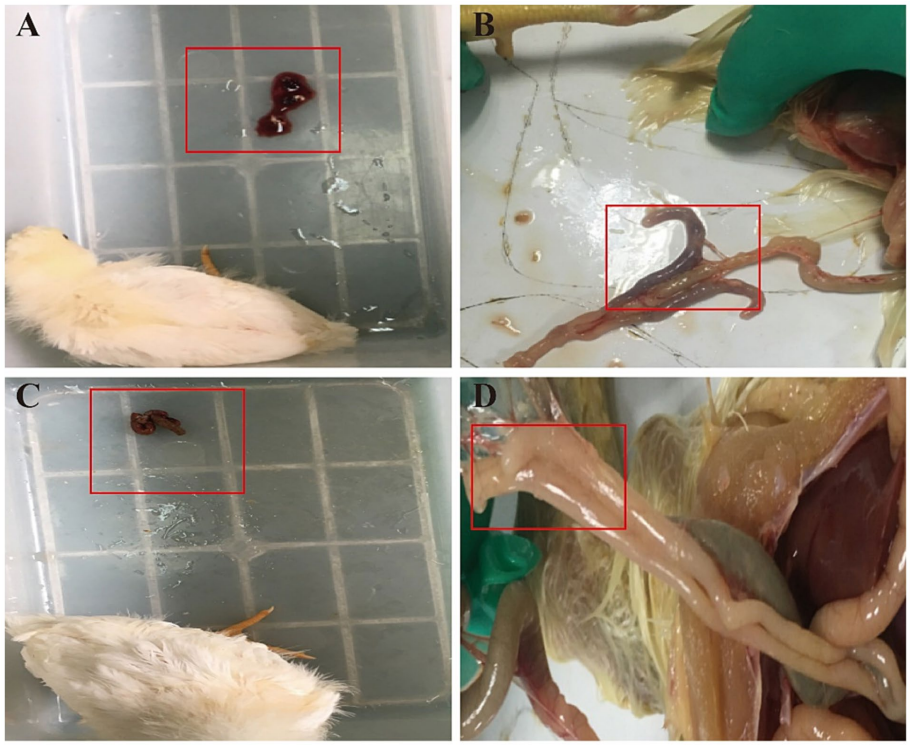

FIGURE 3
Effect of QCC on clinical manifestations of chickens with coccidiosis. **(A)** The red box indicates that there is a large amount of blood in the feces. **(B)** The red box indicates that the cecum is dark red with clots. **(C)** The red box indicates that a small amount of blood could be found in feces. **(D)** The red box indicates that the cecum is smooth, no swelling, with a smooth outer wall and no obvious blood was found.

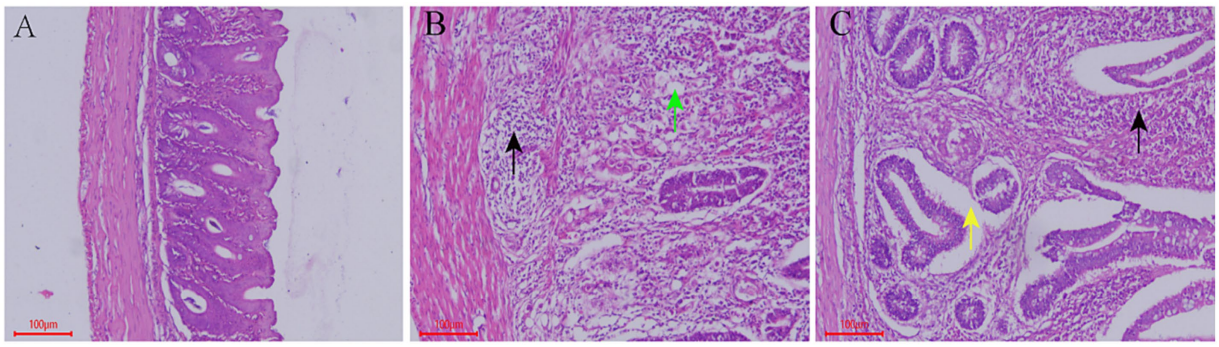

FIGURE 4
Effect of QCC on Cecal Tissue of Coccidiosis Chickens. **(A)** Control group, HE, Bar = 100 μm, 100×; **(B)** model group, HE, Bar = 100 μm, 100×. A large number of inflammatory cells infiltrate (black arrow), and numerous parasite bodies are seen in glandular epithelial cells (green arrow); **(C)** QCC group, HE, Bar = 100 μm, 100×. Inflammatory cell infiltration (black arrow), glandular epithelial cells detached from the basal portion (yellow arrow).

In vivo study, IL-1β, INF-γ, and IL-10 mRNA were significantly increased in chicken ceca after infection with coccidiosis, the results were consistent with those of previous studies (35, 36). This paper found that QCC can reduce the expression levels of IL-1β, INF-γ, and IL-10. IL-1β is one of the important pro-inflammatory factors involved in intestinal inflammation, which promotes the production of inflammatory transmitters, the multiplication and differentiation of B cells, and stimulates the expression of immune molecules in body cells, thereby improving the level of humoral and cellular immunity (37). INF-γ is an important active substance that regulates the balance of the Th1/Th2 immune responses and plays an important role in immune regulation (38), which has been reported to be the most important cytokine in the fight against coccidiosis infection (39). IL-10 reduces the degree of intestinal inflammation by inhibiting the release of IL-1, IL-6, and IL-8 (40). Combine with our results, we believe that after treatment with QCC, the body is in a state of low inflammatory response and a low degree of infection, which may be related to the decrease in bloody stool and alleviation of intestinal tissue damage. In the next study, we will verify the effects of the effective ingredients of QCC on the body and investigate whether there is synergy among artemisinin, dichroine, quercetin, kaempferol, and luteolin.

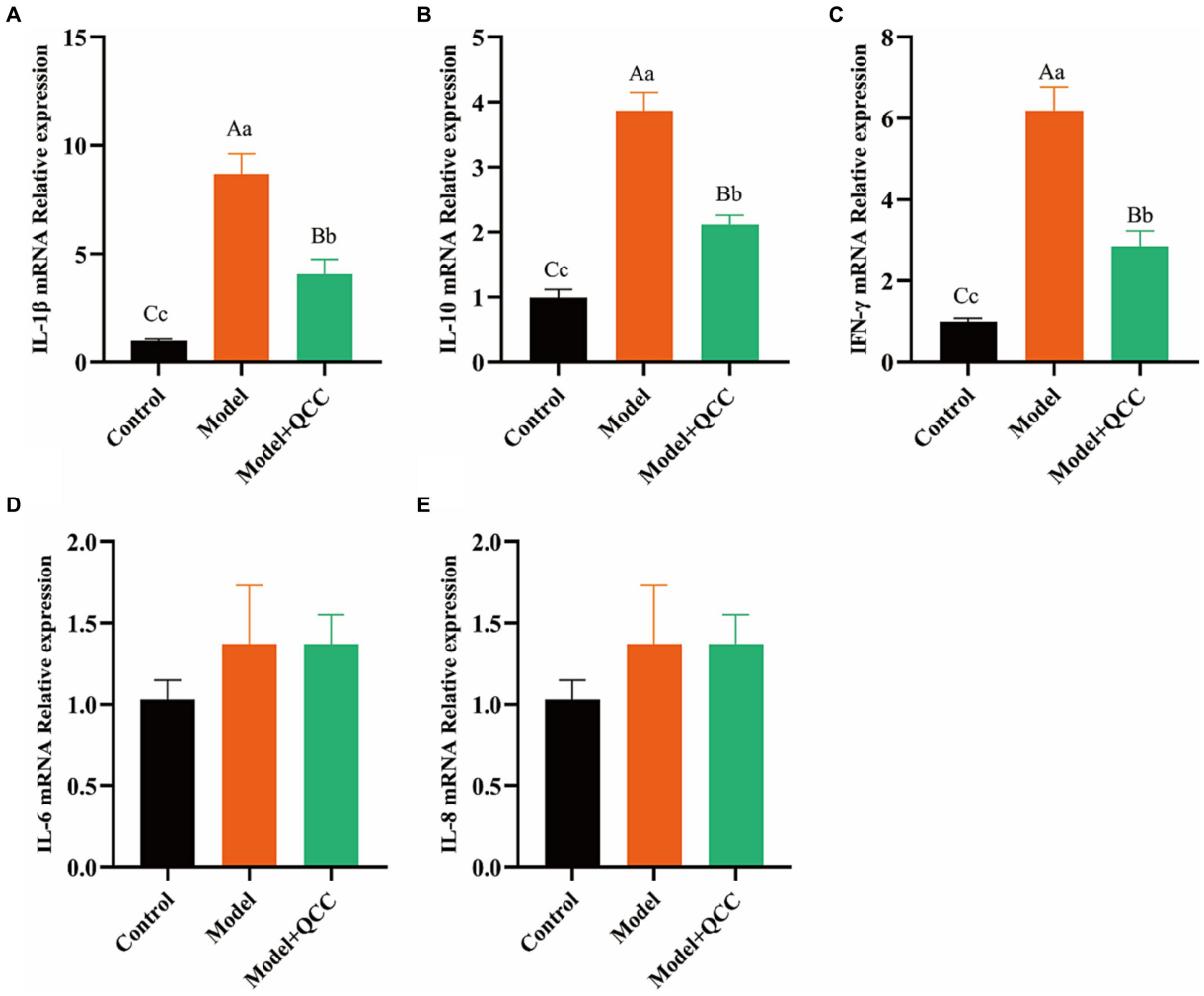

FIGURE 5
The mRNA expression of coccidiosis after QCC treated in caecum. The mRNA expresses of IL-1β **(A)**, IL-10 **(B)**, IFN-γ **(C)**, IL-6 **(D)**, IL-8 **(E)**. Different lower-case letters on the column mark indicate significant difference ($p < 0.05$), and different capital letters on the superscript indicate extremely significant difference ($p < 0.01$).

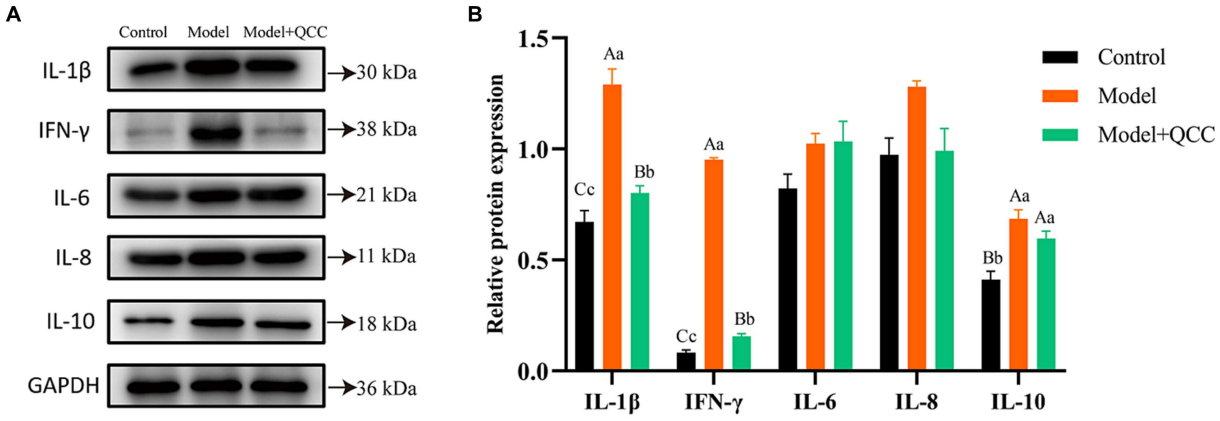

FIGURE 6
The protein expression of coccidiosis after QCC treated in caecum. The western bolt bar **(A)** and protein expression **(B)** of IL-1β, IL-10, IFN-γ, IL-6, and IL-8. Different lower-case letters on the column mark indicate significant difference ($p < 0.05$), and different capital letters on the superscript indicate extremely significant difference ($p < 0.01$).

5 Conclusion

QCC can reduce blood content in feces and intestinal damage in coccidiosis infected chickens by regulating inflammation-related cytokines, reducing the intestinal inflammatory response, and preventing the development of parasites in intestinal epithelial cells, thereby possessing anti-coccidiosis activity.

Data availability statement

The datasets presented in this study can be found in online repositories. The names of the repository/repositories and accession number(s) can be found in the article/supplementary material.

Ethics statement

The animal studies were approved by the ethics approval reference number for the use of animals was XKY-20230420, which approved by the Chongqing Academy of Animal Science Animal Ethics Committee. The studies were conducted in accordance with the local legislation and institutional requirements. Written informed consent was obtained from the owners for the participation of their animals in this study.

Author contributions

ZY: Writing – original draft. CC: Data curation, Writing – review & editing. SZ: Formal analysis, Investigation, Writing – original draft. HT: Resources, Writing – review & editing. MZ: Methodology, Writing – original draft. YY: Writing – original draft. HZ: Writing – original draft.

Funding

The author(s) declare financial support was received for the research, authorship, and/or publication of this article. The experimental materials and reagents of this project are all funded by Chongqing Natural Science Foundation Chongqing Natural Science Foundation Project (cstc2019jcyj-msxmX 0061).

Conflict of interest

The authors declare that the research was conducted in the absence of any commercial or financial relationships that could be construed as a potential conflict of interest.

Publisher's note

All claims expressed in this article are solely those of the authors and do not necessarily represent those of their affiliated organizations, or those of the publisher, the editors and the reviewers. Any product that may be evaluated in this article, or claim that may be made by its manufacturer, is not guaranteed or endorsed by the publisher.

References

1. Blake DP, Knox J, Dehaeck B, Huntington B, Rathinam T, Ravipati V, et al. Re-calculating the cost of coccidiosis in chickens. *Vet Res*. (2020) 51:115. doi: 10.1186/s13567-020-00837-2

2. Bortoluzzi C, Perez-Calvo E, Olsen PB, van der Vaart S, van Eerden E, Schmeisser J, et al. Effect of microbial muramidase supplementation in diets formulated with different fiber profiles for broiler chickens raised under various coccidiosis management programs. *Poult Sci*. (2023) 102:102955. doi: 10.1016/j.psj.2023.102955

3. Gulzar N, Andleeb S, Raza A, Ali S, Liaqat I, Raja SA, et al. Acute toxicity, anti-diabetic, and anti-cancerous potential of Trillium govanianum-conjugated silver nanoparticles in Balb/c mice. *Curr Pharm Biotechnol*. (2023) 24:124025. doi: 10.2174/1389201024666230818124025

4. Bremner A, Kim S, Morris KM, Nolan MJ, Borowska D, Wu Z, et al. Kinetics of the cellular and transcriptomic response to Eimeria maxima in relatively resistant and susceptible chicken lines. *Front Immunol*. (2021) 12:653085. doi: 10.3389/fimmu.2021.653085

5. Mao X, Dou Y, Fan X, Yu B, He J, Zheng P, et al. The effect of dietary Yucca schidigera extract supplementation on productive performance, egg quality, and gut health in laying hens with Clostridium perfringens and coccidia challenge. *Poult Sci*. (2023) 102:102822. doi: 10.1016/j.psj.2023.102822

6. Chapman HD, Rathinam T. Focused review: the role of drug combinations for the control of coccidiosis in commercially reared chickens. *Int J Parasitol Drugs Drug Resist*. (2022) 18:32–42. doi: 10.1016/j.ijpddr.2022.01.001

7. Lakho S, Haseeb M, Huang J, Hasan M, Khand F, Leghari A, et al. Eimeria tenella 14-kDa phosphohistidine phosphatase stimulates maturation of chicken dendritic cells and mediates DC-induced T cell priming in a Th1 cytokine interface. *Res Vet Sci*. (2022) 152:61–71. doi: 10.1016/j.rvsc.2022.07.022

8. Haseeb M, Huang J, Lakho S, Yang Z, Hasan M, Ehsan M, et al. Em14-3-3 delivered by PLGA and chitosan nanoparticles conferred improved protection in chicken against Eimeria maxima. *Parasitol Res*. (2022) 121:675–89. doi: 10.1007/s00436-021-07420-4

9. Jamil M, Aleem M, Shaukat A, Khan A, Mohsin M, Rehman T, et al. Medicinal plants as an alternative to control poultry parasitic diseases. *Life*. (2022) 12:449. doi: 10.3390/life12030449

10. Yan Z, Chen Q, Fu L, Fu W, Zheng H, Tang H, et al. Effect of Qing Chang oral liquid on the treatment of artificially infected chicken coccidiosis and the cellular immunity. *Vet Med Sci*. (2022) 8:2504–10. doi: 10.1002/vms3.922

11. Luo Y, Yang S, Wen M, Wang B, Liu J, Li S, et al. Insights into the mechanisms of triptolide nephrotoxicity through network pharmacology-based analysis and RNA-seq. *Front Plant Sci*. (2023) 14:1144583. doi: 10.3389/fpls.2023.1144583

12. Yang W, Zhang Y, Gao J, Hu P, Yang Y, Xu X. A meta-analysis of the Zilongjin tablets for non-small cell lung cancer and its network pharmacology of action against NSCLC and COVID-19. *Front Med*. (2023) 10:1080121. doi: 10.3389/fmed.2023.1080121

13. Zhang P, Zhang D, Zhou W, Wang L, Wang B, Zhang T, et al. Network pharmacology: towards the artificial intelligence-based precision traditional Chinese medicine. *Brief Bioinform*. (2023) 25:518. doi: 10.1093/bib/bbad518

14. Liang X, Xie H, Yu L, Ouyang J, Peng Q, Chen K, et al. Study on the effects and mechanisms of Wenzhong Bushen formula in improving ovarian reserve decline in mice based on network pharmacology. *J Ethnopharmacol*. (2024) 324:117756. doi: 10.1016/j.jep.2024.117756

15. Mesa-Pineda C, Navarro-Ruíz JL, López-Osorio S, Chaparro-Gutiérrez JJ, Gómez-Osorio LM. Chicken coccidiosis: from the parasite lifecycle to control of the disease. *Front Vet Sci*. (2021) 8:787653. doi: 10.3389/fvets.2021.787653

16. Fatoba AJ, Adeleke MA. Diagnosis and control of chicken coccidiosis. A recent update. *J Parasit Dis*. (2018) 42:483–93. doi: 10.1007/s12639-018-1048-1

17. Muthamilselvan T, Kuo T, Wu Y, Yang W. Herbal remedies for coccidiosis control. A review of plants, compounds, and anticoccidial actions. *Evid Based Complement Alternat Med*. (2016) 2016:2657981. doi: 10.1155/2016/2657981

18. Kashif H, Asghar A, Hamdan A, Abdulrahman M, Ahmad A, Atif R, et al. Immunomodulatory effects of Artemisia brevifolia extract against experimentally induced coccidiosis in broiler chicken. *Pak Vet J*. (2023) 43:333–8. doi: 10.29261/pakvetj/2023.026

19. Pop L, Varga E, Coroian M, Nedian M, Mircean V, Dumitrache M, et al. Efficacy of a commercial herbal formula in chicken experimental coccidiosis. *Parasites Vect*. (2019) 12:343. doi: 10.1186/s13071-019-3595-4

20. Aqsa I, Abdullah A. Anticoccidial efficacy of Citrus sinensis essential oil in broiler chicken. *Pak Vet J*. (2022) 42:461–6. doi: 10.29261/pakvetj/2022.082

21. Nawal A, Khalid M, Zohaib S, Kostadin K, Junaid A, Muhammad A, et al. Anticoccidial activity of star Anise (Illicium verum) essential oil in broiler chicks. *Pak Vet J*. (2023) 43:553–8. doi: 10.29261/pakvetj/2023.050

22. Yan Z, Xu D, Fu W, Chen C, Tang H, Zhu M, et al. Screening of traditional Chinese medicine prescription against chicken coccidiosis and its pathological effects on cecal tissue of sick chicken. *J Southern Agric*. (2019) 2019:2322–8. doi: 10.3969/j.issn

23. Jiao J, Yang Y, Liu M, Li J, Cui Y, Yin S, et al. Artemisinin and Artemisia annua leaves alleviate Eimeria tenella infection by facilitating apoptosis of host cells and suppressing inflammatory response. *Vet Parasitol*. (2018) 254:172–7. doi: 10.1016/j.vetpar.2018.03.017

24. Mo P, Ma Q, Zhao X, Cheng N, Tao J, Li J. Apoptotic effects of antimalarial artemisinin on the second generation merozoites of Eimeria tenella and parasitized host cells. *Vet Parasitol*. (2014) 206:297–303. doi: 10.1016/j.vetpar.2014.09.025

25. Ismail HM, Barton V, Phanchana M, Charoensutthivarakul S, Wong MHL, Hemingway J, et al. Artemisinin activity-based probes identify multiple molecular targets within the asexual stage of the malaria parasites plasmodium falciparum 3D7. *Proc Natl Acad Sci USA*. (2016) 113:2080–5. doi: 10.1073/pnas.1600459113

26. Sun L, Chen Z, Ni Y, He Z. Network pharmacology-based approach to explore the underlying mechanism of sinomenine on sepsis-induced myocardial injury in rats. *Front Pharmacol*. (2023) 14:1138858. doi: 10.3389/fphar.2023.1138858

27. Herman JD, Pepper LR, Cortese JF, Estiu G, Galinsky K, Zuzarte-Luis V, et al. The cytoplasmic prolyl-tRNA synthetase of the malaria parasite is a dual-stage target of febrifugine and its analogs. *Sci Transl Med*. (2015) 7:288ra77. doi: 10.1126/scitranslmed.aaa3575

28. Sabya S, Amit K, Priya R, Shubhankar K, Sandeep K. Therapeutic potential of quercetin-loaded Nanoemulsion against experimental visceral Leishmaniasis: in vitro/ex vivo studies and mechanistic insights. *Mol Pharm*. (2022) 19:3367–84. doi: 10.1021/acs.molpharmaceut.2c00492

29. Hanif H, Abdollahi V, Javani Jouni F, Nikoukar M, Rahimi Esboei B, Shams E, et al. Quercetin nano phytosome: as a novel anti-leishmania and anti-malarial natural product. *J Parasit Dis*. (2023) 47:257–64. doi: 10.1007/s12639-022-01561-8

30. Abo M, Metwally K, El-Menyawy H, Hegab F, El-Wakil E. Assessment of the potential prophylactic and therapeutic effects of kaempferol on experimental Trichinella spiralis infection. *J Helminthol*. (2023) 97:e36. doi: 10.1017/S0022149X23000184

31. Siham O, Nuha A, Yassir A. Immunoinformatics, molecular docking and dynamics simulation approaches unveil a multi epitope-based potent peptide vaccine candidate against avian leukosis virus. *Sci Rep*. (2024) 14:2870. doi: 10.1038/s41598-024-53048-6

32. Li J, Yang X, Jia Z, Ma C, Pan X, Ma D. Activation of ChTLR15/ChNF-κB-ChNLRP3/ChIL-1β signaling transduction pathway mediated inflammatory responses to E. tenella infection. *Vet Res*. (2021) 52:15. doi: 10.1186/s13567-020-00885-8

33. Pu X, Pan Y, Xiang Q, Lu M, Xu L, Yan R, et al. Inhibitory effect of Eimeria maxima IFN-γ inhibitory molecules on the immune function of T cell subsets in chickens. *Poult Sci*. (2023) 102:103098. doi: 10.1016/j.psj.2023.103098

34. Bai B, Liu Q, Kong R, Jia Z, Chen H, Zhi W, et al. Role of Nrf2/HO-1 pathway on inhibiting activation of ChTLR15/ChNLRP3 inflammatory pathway stimulated by E. Tenella sporozoites. *Poult Sci*. (2024) 103:103445. doi: 10.1016/j.psj.2024.103445

35. Min W, Lillehoj H, Burnside J, Weining K, Staeheli P, Zhu J. Adjuvant effects of IL-1beta, IL-2, IL-8, IL-15, IFN-alpha, IFN-gamma TGF-beta4 and lymphotactin on DNA vaccination against Eimeria acervulina. *Vaccine*. (2001) 20:267–74. doi: 10.1016/s0264-410x(01)00270-5

36. Hong Y, Lillehoj H, Lee S, Dalloul R, Lillehoj E. Analysis of chicken cytokine and chemokine gene expression following Eimeria acervulina and Eimeria tenella infections. *Vet Immunol Immunopathol*. (2006) 114:209–23. doi: 10.1016/j.vetimm.2006.07.007

37. Casillas-Ramírez A, Micó-Carnero M, Sánchez-González A, Maroto-Serrat C, Trostchansky A, Peralta C. NO-IL-6/10-IL-1β axis: a new pathway in steatotic and non-steatotic liver grafts from brain-dead donor rats. *Front Immunol*. (2023) 14:1178909. doi: 10.3389/fimmu.2023.1178909

38. Jiang S, Sun B, Zhang Y, Han J, Zhou Y, Pan C, et al. The immediate adverse drug reactions induced by ShenMai injection are mediated by thymus-derived T cells and associated with RhoA/ROCK signaling pathway. *Front Immunol*. (2023) 14:1135701. doi: 10.3389/fimmu.2023.1135701

39. Liu J, Liu L, Li L, Tian D, Li W, Xu L, et al. Protective immunity induced by Eimeria common antigen 14-3-3 against Eimeria tenella, Eimeria acervulina and Eimeria maxima. *BMC Vet Res*. (2018) 14:337. doi: 10.1186/s12917-018-1665-z

40. Yang Y, Liu Q, Deng S, Shao Q, Peng L, Ling Y, et al. Human umbilical cord derived mesenchymal stem cells overexpressing HO-1 attenuate neural injury and enhance functional recovery by inhibiting inflammation in stroke mice. *CNS Neurosci Ther*. (2023) 30:14412. doi: 10.1111/cns.14412

frontiers | Frontiers in Veterinary Science

TYPE Original Research
PUBLISHED 07 March 2024
DOI 10.3389/fvets.2024.1374116

Check for updates

OPEN ACCESS

EDITED BY
Hussam Askar,
Al Azhar University, Egypt

REVIEWED BY
Mona Mahmoud,
King Abdullah Medical City, Saudi Arabia
Ukpe Ajima,
University of Jos, Nigeria

*CORRESPONDENCE
Hatem A. Elshabrawy
✉ hatem.elshabrawy@shsu.edu
Asmaa M. El-kady
✉ asmaa.elkady@med.svu.edu.eg

RECEIVED 21 January 2024
ACCEPTED 14 February 2024
PUBLISHED 07 March 2024

CITATION
Gattan HS, Wakid MH, Qahwaji RM, Altwaim S, Mahjoub HA, Alfaifi MS, Elshazly H, Al-Megrin WAI, Alshehri EA, Elshabrawy HA and El-kady AM (2024) *In silico* and *in vivo* evaluation of the anti-cryptosporidial activity of eugenol. *Front. Vet. Sci.* 11:1374116. doi: 10.3389/fvets.2024.1374116

COPYRIGHT
© 2024 Gattan, Wakid, Qahwaji, Altwaim, Mahjoub, Alfaifi, Elshazly, Al-Megrin, Alshehri, Elshabrawy and El-kady. This is an open-access article distributed under the terms of the Creative Commons Attribution License (CC BY). The use, distribution or reproduction in other forums is permitted, provided the original author(s) and the copyright owner(s) are credited and that the original publication in this journal is cited, in accordance with accepted academic practice. No use, distribution or reproduction is permitted which does not comply with these terms.

In silico and *in vivo* evaluation of the anti-cryptosporidial activity of eugenol

Hattan S. Gattan[1,2], Majed H. Wakid[1,2], Rowaid M. Qahwaji[1], Sarah Altwaim[2,3], Haifaa A. Mahjoub[4], Mashael S. Alfaifi[5], Hayam Elshazly[6,7], Wafa Abdullah I. Al-Megrin[8], Eman Abdullah Alshehri[9], Hatem A. Elshabrawy[10]* and Asmaa M. El-kady[11]*

[1]Department of Medical Laboratory Sciences, Faculty of Applied Medical Sciences, King Abdulaziz University, Jeddah, Saudi Arabia, [2]Special Infectious Agents Unit, King Fahd Medical Research Center, Jeddah, Saudi Arabia, [3]Department of Clinical Microbiology and Immunology, Faculty of Medicine, King Abdulaziz University, Jeddah, Saudi Arabia, [4]Biological Sciences Department, College of Sciences and Arts, King Abdulaziz University, Rabigh, Saudi Arabia, [5]Department of Epidemiology, Faculty of Public Health and Health Informatics, Umm Al-Qura University, Mecca, Saudi Arabia, [6]Department of Biology, Faculty of Sciences-Scientific Departments, Qassim University, Buraidah, Saudi Arabia, [7]Department of Zoology, Faculty of Science, Beni-Suef University, Beni Suef, Egypt, [8]Department of Biology, College of Science, Princess Nourah Bint Abdulrahman University, Riyadh, Saudi Arabia, [9]Department of Zoology, College of Science, King Saud University, Riyadh, Saudi Arabia, [10]Department of Molecular and Cellular Biology, College of Osteopathic Medicine, Sam Houston State University, Conroe, TX, United States, [11]Department of Medical Parasitology, Faculty of Medicine, South Valley University, Qena, Egypt

Background: Cryptosporidiosis is an opportunistic parasitic disease widely distributed worldwide. Although *Cryptosporidium* sp. causes asymptomatic infection in healthy people, it may lead to severe illness in immunocompromised individuals. Limited effective therapeutic alternatives are available against cryptosporidiosis in this category of patients. So, there is an urgent need for therapeutic alternatives for cryptosporidiosis. Recently, the potential uses of Eugenol (EUG) have been considered a promising novel treatment for bacterial and parasitic infections. Consequently, it is suggested to investigate the effect of EUG as an option for the treatment of cryptosporidiosis.

Materials and methods: The *in silico* bioinformatics analysis was used to predict and determine the binding affinities and intermolecular interactions of EUG and Nitazoxanide (NTZ) toward several *Cryptosporidium parvum* (*C. parvum*) Iowa II target proteins. For animal study, five groups of immunosuppressed Swiss albino mice (10 mice each) were used. Group I was left uninfected (control), and four groups were infected with 1,000 oocysts of *Cryptosporidium* sp. The first infected group was left untreated. The remaining three infected groups received NTZ, EUG, and EUG + NTZ, respectively, on the 6th day post-infection (dpi). All mice were sacrificed 30 dpi. The efficacy of the used formulas was assessed by counting the number of *C. parvum* oocysts excreted in stool of infected mice, histopathological examination of the ileum and liver tissues and determination of the expression of iNOS in the ileum of mice in different animal groups.

Results: treatment with EUG resulted in a significant reduction in the number of oocysts secreted in stool when compared to infected untreated mice. In addition, oocyst excretion was significantly reduced in mice received a combination therapy of EUG and NTZ when compared with those received NTZ alone. EUG succeeded in reverting the histopathological alterations induced by *Cryptosporidium* infection either alone or in combination with NTZ. Moreover,

mice received EUG showed marked reduction of the expression of iNOS in ileal tissues.

Conclusion: Based on the results, the present study signified a basis for utilizing EUG as an affordable, safe, and alternative therapy combined with NTZ in the management of cryptosporidiosis.

KEYWORDS

Cryptosporidium, immunocompromised, eugenol, nitazoxanide, iNOS

Introduction

Cryptosporidiosis is a global opportunistic parasitic disease caused by the protozoan *Cryptosporidium* species (1). These parasites can infect mainly the epithelial cells of the jejunum and ileum of vertebrates after direct contact with the excreted oocysts in fecal materials or in the contaminated food, water, or drinks. Although, parasite development is relatively confined to the terminal jejunum and ileum, in immunosuppressed hosts the entire gastrointestinal tract as well as the biliary and pancreatic ducts may be infected and less frequently the respiratory tract (2).

Cryptosporidiosis may be self-limiting, or severe life-threatening condition depending on the immune status of the host (3–5). in immunocompetent individuals, *Cryptosporidium* infection may be a symptomatic or typically results in an episode of watery diarrhea (6). On the contrary, those with impaired immune systems such as infants, elderly and immunocompromised patients due to organ transplantation, AIDS and cancer therapy are more prone to infection with chronic, prolonged illness that is challenging to cure and may even be fatal (5, 7). In immunocompromised patients, cryptosporidiosis may cause severe life-threatening diarrhea and extra-intestinal disseminations resulting in bile duct obstruction, pancreatitis, papillary stenosis, and sclerosing cholangitis (5, 7, 8). Therefore, cryptosporidiosis is among the most serious opportunistic infections in immunocompromised patients (7).

Treatment options for cryptosporidiosis are extremely limited; there is no available vaccine is for this parasite, and nitazoxanide (NTZ) is the only FDA-approved drug for cryptosporidiosis. It promotes recovery in immunocompetent individuals but unfortunately has a very poor efficacy in children and in patients with acquired immunodeficiency syndrome (AIDS) (9). Treatment of the cause of immunosuppression has been found to reduce the severity of cryptosporidiosis in patients with Human immunodeficiency virus (HIV) and is not an option in immunocompromised patients without HIV infection (10, 11). Moreover, HIV patients in developing countries cannot afford anti-retrovirals, which results in the re-emergence of cryptosporidiosis (12).

Eugenol (EUG) (derived from the clove name, *Eugenia caryophyllata*) is the major phenolic constituent in several essential oils in clove, nutmeg, cinnamon, and basil (13). Due to its medicinal significance, EUG attracted the attention of researchers and created a vast field of study for its potential use as a medicine to treat a variety of disorders. Several pharmacological properties have been reported for EUG such as anesthetic, antioxidant, antibacterial, anti-helminthic, anti-inflammatory, anti-carcinogenic, schistosomicidal, anti-leishmanial, and anti-giardial properties (14–21).

Molecular docking is considered an important method that analyzes orientation of ligands into the binding sites of their targets. Searching algorithms generate poses that are ranked according to their scoring functions (22). For *Cryptosporidium*, the parasite depends mainly on glycolysis as a source of energy using LDH as a key for this process. So, this enzyme was used in many studies for assessment as a target protein for new therapeutics. In the present study we aim to assess the therapeutic potential of EUG in the treatment of cryptosporidiosis in immunocompromised mice and to use the *in-silico* bioinformatics analysis to predict and determine the binding affinities and many non-covalent intermolecular interactions of EUG and NTZ toward several *C. parvum* lowa II target proteins, including LDH, SerRS, TryptoRS, and MAPK1.

Materials and methods

In silico bioinformatics analysis

For ligands preparation, the PubChem database[1] was used to obtain the canonical smiles of EUG (EUG, 2-methoxy-4-prop-2-enylphenol, MF:$C_{10}H_{12}O_2$, MW:164.201 g/mol, CID: 3314) and NTZ [2-[(5-nitro-1,3-thiazol-2-yl)carbamoyl]phenyl] acetate, MF: $C_{12}H_9N_3O_5S$, MW: 307.28 g/mol, CID: 41684. Furthermore, ACD/ChemSketch program was used to generate, clean, and optimize the chemical structures of EUG and NTZ that were saved as MDL MOL-file formats. Moreover, OpenBabel GUI v2.3.2 software was used to minimize energy of the selected ligand compounds that converted from MDL MOL to PDB-file formats. For target proteins preparation, the crystal x-ray structures of *C. parvum* lowa II lactate dehydrogenase (LDH, PDB ID: 4ND1, 2.15 Å) (23, 24), cytoplasmic seryl-tRNA synthetase (SerRS, PDB ID: 6OTE, 2.95 Å), tryptophanyl-tRNA synthetase (TrpRS, PDB ID: 3HV0, 2.42 Å) (25), and mitogen-activated protein kinase1 (MAPK1, PDB ID: 3OZ6, 2.37 Å) were retrieved from the RCSB-PDB database[2] as PDB-file formats. For energy minimization, the target proteins were processed using Swiss-PdbViewer v4.1.0 program.

1 https://pubchem.ncbi.nlm.nih.gov/

2 http://www.rcsb.org/

Molecular docking was performed using Autodock v4.2.6 software that utilizes the estimated free energy of binding (kcal/mol) and inhibition constant (Ki) of EUG and NTZ toward their target proteins. For optimization, the structures of ligands were detected and chosen roots, which were saved as PDBQT-file formats. For protein optimization, water molecules, hetero atoms, and complex moieties were removed as well as polar hydrogen and Kollman and Gasteiger charges were added as PDBQT-file formats. For definition of the binding sites, the grid boxes were centered on macromolecules with 0.375 Å spacing, 18.017 X-, 2.772 Y-, and 28.774 Z-center, and 175 as several points in X-, Y-, and Z-dimensions. For the best docking conformation, Lamarckian Genetic Algorithm (GA) was applied in the drug-ligand interactions and 10 GA runs were performed with the following factors: 150 as population size, 250,000 as number of energy evaluations, and 27,000 as number of generations. The 10 conformations were clustered using a root-mean square deviation (RMSD) of 2.0 A. The least energy conformation was saved as a PDB-file format. If the binding energy is <−5 kJ/mol, it represents that the target protein has certain binding affinity toward the ligand (26–29). For the docked ligands, the elevated negative values of the estimated free energy of binding are positively correlated with their binding affinities and docking properties. For a better binding affinity, the binding energy should be lower (30). The pose with the best binding affinity was visualized using BIOVIA Discovery Studio Visualizer software.

Animals and infection

The present study was carried out in the Parasitology department, Faculty of Medicine, South Valley University, Qena, Egypt. Fifty laboratory bred male Swiss albino mice weighing approximately 20 g were used. The mice had a 10-day acclimatization period before being infected with *Cryptosporidium* oocyst. All mice were kept in cages with proper ventilation, free supplies of water, and standard pellet food at a maintained temperature of 25°C with 12 h of light and 12 h of darkness. To exclude parasitic infections, stools were examined daily for 3 days.

All the experimental animals were subjected to immune suppression using dexamethasone orally at a dose of 0.25 mg/g/day for 14 successive days prior to inoculation with *Cryptosporidium* oocysts (31). The mice continued to receive dexamethasone at the same dose throughout the experiment (32–34).

Animals were divided into five groups, each with ten mice, as following: GI: immunocompromised non-infected mice; GII: immunocompromised *Cryptosporidium*-infected untreated; GIII: immunocompromised, *Cryptosporidium* infected and treated with NTZ; GIV: immunocompromised, *Cryptosporidium* infected and treated with EUG; GV: immunocompromised, *Cryptosporidium* infected and treated with NTZ + EUG. *Cryptosporidium* oocysts were kindly supplied by Theodor Belharz Institute, Cairo, EGYPT and were genetically identified by Dr. Eman El-Wakil as *C. parvum* (35). Mice in groups GII to GV were orally infected with 1,000 oocysts of *C. parvum* resuspended in 200 µL PBS for each mouse (36–38).

NTZ (Sigma Pharma, Egypt), was administered in a daily dose of 200 mg/kg (39, 40), while EUG, (Geno Technology Inco India, CAT #P8776-54), was administered at a dose of 500 µg/kg/day (20). All drugs were administered orally to the mice starting from the 6th dpi for five consecutive days. To confirm the establishment of infection, fresh fecal pellets were collected from each mouse on the 2nd dpi and examined using the modified Ziehl-Neelsen (mZN) staining method. All mice were euthanized on the 30th dpi and tissues (ileum and livers) were collected for evaluation of the efficacy of drugs.

Assessment of infection and the drug efficacy

Stool examination

For evaluation of the efficacy of treatment, fresh fecal pellets were examined for each mouse on the 30th dpi and examined using the mZN staining to determine the amount of *C. parvum* oocysts excreted on the last day of the experiment. Each sample was emulsified in 10% formal saline and 1 mg was smeared, fixed and stained with mZN, *C. parvum* oocysts were counted microscopically in 10 fields under 100x objective lens. The following formula was used to determine the percent reduction (PR), which represented the decline in the number of oocysts in the treated group compared to the infected untreated group.

$$\text{Efficacy}\% = \frac{\text{mean oocysts count in control group} - \text{mean oocysts count in treated group}}{\text{mean oocyst count in control group}} \times 100$$

Histopathological examination

The last 2 cm of the ileum in addition to the liver were extracted from each euthanized animal, fixed in 10% formal saline, and processed into paraffin blocks. From each paraffin block, 3-mm thick portions were removed and stained with Hematoxylin & Eosin (H&E) by an independent pathologist (41). Intestinal tissue sections were examined for pathological findings and scored for the following: inflammation with villous atrophy (none = 0, slight = 1, moderate = 2, severe = 3); inflamed area/extent (mucosa = 1, mucosa and submucosa = 2, transmural = 3); surface ulceration (none = 0, focal = 1, diffuse = 2, complete loss of surface epithelium = 3, entire surface epithelium and crypt epithelium are lost = 4); percent involvement (1–25% = 1, 26–50% = 2, 51–75% = 3, 76–100% = 4) (42). Liver lesions were staged and graded according to the degree of periportal, periseptal interface hepatitis (piecemeal necrosis) (absent = 0, mild = 1, moderate = 2, severe = 3); confluent necrosis (absent = 0, focal = 1, zone 3 in some areas = 2, zone 3 in most areas = 3, zone 3 + occasional portal-central (P-C) bridging = 4, zone 3 + multiple P-C bridging = 5, panacinar or multiacinar = 6); focal (spotty) lytic necrosis, apoptosis and lobulitis per 10x objective (absent = 0, 1 focus = 1, 2–4 foci = 2, 5–10 foci = 3, > 10 foci = 4); portal lymphocytic inflammation (absent = 0, mild = 1, moderate = 2, marked = 3, strongly marked = 4).

Immunohistochemical staining

The terminal 2 cm of the ileum were sectioned into 4-micron sections, incubated overnight, then deparaffinized, rehydrated in alcohol, and rinsed with dH_2O. Endogenous peroxidase activity was blocked using 0.6% hydrogen peroxide (H_2O_2), then rinsed twice in PBS and boiled twice in Tris/EDTA buffer (pH 9.0). The rabbit

recombinant monoclonal inducible nitric oxide synthase (iNOS) antibody was then applied to tissue sections and incubated for an additional overnight period at room temperature (Clone No., Abcam, Cambridge, MA, United States). After washing excess reagent in PBS containing 0.05% Tween-20 (PBS-T), tissue sections were incubated with HRP-conjugated goat anti-rabbit secondary antibody (1:5,000) (Vivantis Technologies, Selangor Darul Ehsan, Malaysia) at 4°C. After 1 h, slides were washed with PBS-T, and then incubated with 0.05% diaminobenzidine (DAB) and 0.01% H_2O_2 for 3 min to enhance the peroxidase reaction color. The smears were counterstained with hematoxylin for 1 min, then dehydrated, mounted, and then examined microscopically at different magnifications.

Data analysis

The obtained data were analyzed using the Statistical Package for Social Sciences (SPSS) version 20 for Windows. All values were presented as mean ± standard deviation (SD). Analysis of Variance (ANOVA) followed by LSD *post hoc* analysis test was used for statistical comparison of different groups. p-value of < 0.05 was considered statistically significant.

Results

Evaluation of *in silico* bioinformatics findings

As reported in Table 1, the estimated free energy of binding of EUG toward *C. parvum* Iowa II LDH, SerRS, TrpRS, and MAPK1 targets were −6.95, −6.51, −5.93, and −6.02 kcal/mol, respectively. While the estimated free energy of binding of NTZ toward *C. parvum* Iowa II LDH, SerRS, TrpRS, and MAPK1 targets were −9.56, −7.41, −9.54, and −8.75 kcal/mol, respectively. Furthermore, the estimated inhibition constant values (Ki) of EUG toward LDH, SerRS, TrpRS, and MAPK1 targets were 8.08, 17.32, 44.64, and 39.51 μM, respectively. While the estimated Ki of NTZ toward LDH, SerRS, TrpRS, and MAPK1 targets were 97.69 nM, 3.71 μM, 102.43 nM, and 386.87 nM, respectively. Based on scoring functions, the strength of ligand-interacted forms is greatly associated to intermolecular binding and the interactions of the ligands and their target proteins such as classical/non-classical H-bond interaction, electrostatic interaction, and hydrophobic interaction (24), which confirmed our findings. As shown in Figures 1–4 and Table 1, the EUG and NTZ docked forms clearly demonstrated the different types, strength, and bond lengths of the intermolecular binding and interactions of EUG and NTZ toward their key amino acid residues of LDH, SerRS, TrpRS, and MAPK1 targets. Moreover, the NTZ-TrpRS docked form included an unfavorable acceptor-acceptor (Gly280B) interaction that could be reduced its stability compared to the EUG-TrpRS docked form (Figure 3; Table 1).

Cryptosporidium oocysts count in different animal groups

The mean number of oocysts excreted in stool in all treated animals decreased significantly after treatment with EUG, NTZ, or EUG + NTZ when compared to the infected non-treated group shown in Table 2 and Figure 5 ($p < 0.05$). Additionally, when compared to NTZ alone, treatment with EUG and NTZ significantly reduced the amount of fecal oocyst ($p = 0.02$). animal groups treated with the combination of EUG and NTZ showed the highest percent reduction in the number of fecal oocyst (93.44%), followed by NTZ (82.56%) and EUG alone (62.5%; Table 2).

Histopathology of the small intestine

In contrast to uninfected mice, sections of ileum of infected untreated group (GI) showed villous blunting with moderate transmural inflammatory cellular infiltration (mainly lymphocytes) involving more than 75% of the intestinal wall with marked reduction of goblet cells. Treatment of mice caused significant restoration of normal epithelial structure, restoration of goblet cells and lowered the inflammatory infiltration of the intestinal wall. EUG alone resulted in marked reduction of cellular infiltration, which was restricted to the mucosa only in less than 30% of the intestinal wall. Similar results were recognized in mice treated with NTZ where there was almost restoration of intestinal tissue, with mild chronic inflammatory cells infiltrate in the lamina propria with some dilated blood vessels. The best degree of improvement was recognized in the mice group treated with NTZ and EUG combination (Figure 6).

Histopathology of the liver

H&E-stained liver sections were used to examine the therapeutic effect of EUG in the alleviation of pathological changes in the liver of immunocompromised mice with cryptosporidiosis. Liver tissues of uninfected mice showed normal uniform plates of hepatocytes (Black arrows) with no evidence of injury. Liver tissues of infected untreated mice showed significant hydropic degeneration of hepatocytes (Black arrows), lytic necrosis (Black arrowheads) and confluent necrosis (Red arrow). Treated groups showed marked improvement in comparison to uninfected ones. In EUG treated mice, hepatocytes showed mild lobulitis (Red arrow) with no evidence of hydropic degeneration (Black arrows). On the other hand, mice treated with NTZ showed restoration of hepatocytes integrity with no evidence of injury. Combination of NTZ and EUG showed restoration of hepatocytes integrity with no evidence of injury (Figure 7).

Immunohistochemistry

Strong cytoplasmic expression of iNOS were detected in the intestinal epithelium of the infected untreated mice, while the treated groups revealed weaker expression with significant reduction of the mean percent of positive expression ($p = 0.002$). Mice that received combined treatment (NTZ + EUG) showed the lowest mean percentage of iNOS positive cells (Table 3 and Figure 8).

Discussion

Bioinformatics is a potent biological area that uses computational-based methods to evaluate the biological systems and provide some accurate predictions for several *in vitro* and *in vivo* studies and clinical

TABLE 1 The ligand-target protein binding properties.

Ligand-interacted properties			LDH (4ND1)	SerRS (6OTE)	TrpRS (3HV0)	MAPK1 (3OZ6)
EUG	Estimated free energy of binding (kcal/mol)		−6.95	−6.51	−5.93	−6.02
	Estimated inhibition constant (Ki)		8.08 µM	17.32 µM	44.64 µM	39.51 µM
	H-bonds	Amino Acids (Donor. Acceptor)	4 Conventional H-bonds (2 Asp143A (N…O), Val144A (N…O), Pro141A (O…O)); 2 carbon H-bonds (Asn140A (C…OD1), His195A (C…O))	2 Conventional H-bonds (Val114A (N…O), Asn113A (O…OD1)); carbon H-bonds (Asp377A (C…OD1))	2 Conventional H-bonds (Thr279B (OG1…O), Tyr278B (O…O)); 2 carbon H-bonds (Thr279B (*CA*…O), Gly280B (C…O)); Pi-Donor H-bond (Tyr278B (O-Pi))	Carbon H-bond (Asp4A (C…OD2)); Pi-Donor H-bond (Trp26A (O-Pi))
		Bond lengths (Å)	3.27, 3.21, 2.81, 2.81, 3.68, 2.67 Å	2.97, 3.22, 3.29 Å	2.65, 3.07, 2.97, 3.46, 4.18 Å	3.04, 3.83 Å
	Hydrophobic, miscellaneous, and electrostatic interactions		Alkyl hydrophobic Ile325A, Val322A	Pi-sigma, Pi-Pi stacked, and Pi-alkyl hydrophobic (Tyr378A, Trp108A)	Pi-Pi T-shaped hydrophobic (Tyr278B)	Pi-Pi Stacked, alkyl, and Pi-alkyl hydrophobic (Val7A, Val39A, Leu8A, Leu13A, Trp26A); electrostatic Pi-anion (Asp4A)
	Van der Waal's reactions		Arg109A, Leu142A, Gly194A, Gly196A, Gly198A, Met199A, Ser318A, Glu321A	Thr376A, Arg381A, Gly112A, Ile111A	Pro425B, Val424B, His426B, Gln430B, Arg281B, Gly282B, Thr315B, Gln318B, Gln401B, Phe434B	Tyr87A, Tyr11A, Lys41A, Ser28A
NTZ	Estimated free energy of binding (kcal/mol)		−9.56	−7.41	−9.54	−8.75
	Estimated inhibition constant (Ki)		97.69 nM	3.71 µM	102.43 nM	386.87 nM
	H-bonds	Amino Acids (Donor. Acceptor)	6 Conventional H-bonds (Arg109A (NH2…O), 2 Asn140A (ND2…O), 2 Arg171A (NH1/NH2…O), Thr245A (OG1…O)); Pi-Donor H-bond (Asn140A (N…Pi orbitals))	2 Conventional H-bonds (Asp290A (N…O), Trp292A (N…O)); carbon H-bonds (Asp290A (*CA*…O)); 2 Pi-Donor H-bonds (Lys289A (NZ…Pi), Thr291A (N…Pi))	2 conventional H-bonds (Gly282B (N…O), Ala427B (N…O)); Pi-Donor H-bond (Gln430B (NE2…Pi))	3 Conventional H-bonds (Arg163A (NH1…O), Tyr208A (N…O), Arg163A (N…O)); carbon H-bond (Arg157A (CD…O))
		Bond lengths (Å)	3.08, 2.73, 2.87, 3.18, 2.85, 3.24, 3.65 Å	2.95, 2.64, 3.07, 3.53, 3.93 Å	2.92, 3.19, 3.88 Å	2.87, 2.83, 2.84, 2.97 Å
	Hydrophobic, miscellaneous, and electrostatic interactions		Miscellaneous Pi-sulfur (His195A); amide-Pi-stacked hydrophobic (Ile136A); Pi-alkyl hydrophobic (Pro250A, Ala246A)	Pi-Pi T-shaped and Pi-alkyl hydrophobic (Trp292A); electrostatic Pi-cation (Lys289A)	Unfavorable acceptor-acceptor (Gly280B)	Pi-Pi T-shaped and Pi-alkyl hydrophobic (Val165A, Tyr208A, Arg163A, Arg157A)
	Van der Waal's reactions		Pro105A, Leu112A, Ser99A, Thr139A, Thr97A, Leu167A, Ile32A, Trp236A	Gly288A, Arg367A, Tyr363A	Pro295B, His426B, Pro425B, Thr279B, Val424b, Phe434B, Tyr278B, Gln401B, Arg281B, His292B, Glu318B, Lys319B	Arg164A, Arg57A, Ser158A, Asn161A, Phe159A, Thr206A, Gln259A, Lys207A

trials (24, 43). The molecular docking method determines ligand conformation and orientation within a targeted binding site. Searching through algorithms generates conformations that are ranked according to their scoring functions (22, 24). Plant essential oils potentially have ecotoxicological activities against several parasites and insects (44). EUG (4-allyl-2-methoxyphenol) is considered as a phenylpropanoid compound that represents a major component of plant essential oils and has an allyl chain-substituted guaiacol. Naturally, EUG is present in many plant families and several aromatic plants (45, 46). Previous studies reported that EUG has potent medicinal therapeutic applications including antimicrobial, antiviral, antiparasitic, anti-inflammatory, neuroprotective, antioxidant, anti-diabetic, anti-obesity, hypolipidemic, and anticancer potentials (47–49). In the present study, we targeted molecular docking simulation analysis to visualize, determine, and evaluate the binding affinities and inhibition potentials of EUG and NTZ against some *C. parvum* lowa II target proteins including LDH, SerRS, TrpRS, and MAPK1. In this study, the lower docking scores of the EUG- and NTZ-interacted

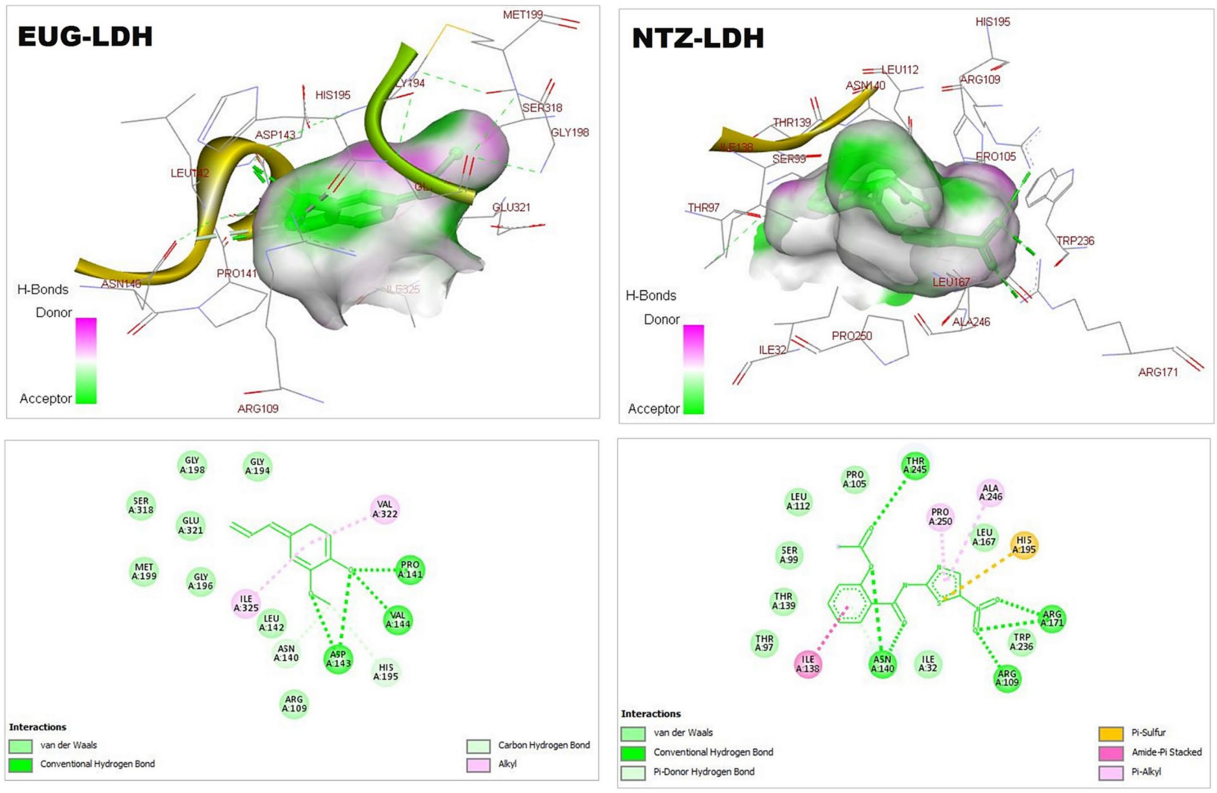

FIGURE 1
3D (upper panel) and 2D (lower panel) ligand-interacted forms show key amino acid residues of LDH using BIOVIA drug discovery studio visualizer. EUG, eugenol; NTZ, nitazoxanide; LDH, lactate dehydrogenase.

forms represented strength of the ligand-target protein binding activities, stability of the binding conformation, and variety of the intermolecular binding and interactions (Figures 1–4; Table 1), which confirmed recent findings (50).

Cryptosporidium is a protozoan parasite that potentially causes waterborne diseases. The parasite depends on glycolysis for energy production and cellular metabolism. *C. parvum* LDH is an essential regulator of glycolysis. The anti-cryptosporidial drugs aim to target and inhibit the biochemical and metabolic pathways of *C. parvum* (23). As critical substrate-binding sites, Arg171, Asn140, His195, Arg109, and Trp236 represent the catalytic amino acid residues of *C. parvum* LDH (23), which clearly presented in the EUG-LDH and NTZ-LDH docked forms (Figure 1).

C. parvum lowa II SerRS and TrpRS are considered as important protozoan enzymes that widely regulate protein biosynthesis (25). As shown in Figures 2, 3 and Table 1, the EUG and NTZ docked forms potentially demonstrated the binding affinities, inhibition potentials, and the intermolecular interactions of EUG and NTZ toward amino acid residues of *C. parvum* lowa II SerRS and TrpRS targets, which greatly predicted inhibition of differentiation, growth, and survival of *C. parvum* cells. Merritt et al. study reported that Glu318, Gln401, Gly280, Thr279, and Tyr278 as key amino acid residues represented the active site of *C. parvum* TrpRS (25), which clearly demonstrated in the EUG- and NTZ-interacted forms (Figure 3; Table 1). Moreover, the NTZ-TrpRS docked form had an unfavorable acceptor-acceptor (Gly280B) interaction that have reduced its stability compared to the EUG-TrpRS docked form.

MAPK is a serine/threonine protein kinase that regulates cellular growth, development, differentiation, survival, and interaction interactions between host and various pathogens, including parasites (51–53). In lung injury, inhibition of the MAPK3/MAPK1 signaling process highly reduces cellular inflammation, oxidative stress response, pro-inflammatory cytokines, and apoptotic signaling (50, 54, 55). This study reported that EUG and NTZ were introduced as *C. parvum* MAPK1 inhibitors that greatly confirmed findings of previous studies.

Immunosuppression may arise as a side effect of cancer treatment, in HIV-positive people, or following organ donation. Consequently, this category of patients are more prone to opportunistic infection including *Cryptosporidium* species with high probability of severe life-threatening illnesses especially with limited treatment options (56, 57). Some efforts have been focused on evaluating natural compounds, particularly essential oils against *C. parvum* (58). Therefore, the purpose of the present study was to assess the effectiveness of EUG in treating immunosuppressed mice infected with *C. parvum*. For the induction of a mouse model of immunosuppression, dexamethasone was used. Dexamethasone was used in the present study for induction of immune suppression following previous studies (31, 33, 34, 59, 60). Convincing evidence shows that EUG possesses potent antimicrobial, antifungal, antibacterial, and anti-parasitic properties (14–21), however, information about its anti-cryptosporidial properties is limited. So, we aimed to evaluate the efficacy of EUG against *C. parvum in vivo*. Our research revealed that EUG effectively combats *C. parvum* in immunocompromised mice. To the best of our knowledge, this is the first study that evaluates Euogenol anti-cryptosporidial activity *in vivo* in an immunocompromised mice model. Our findings show that EUG

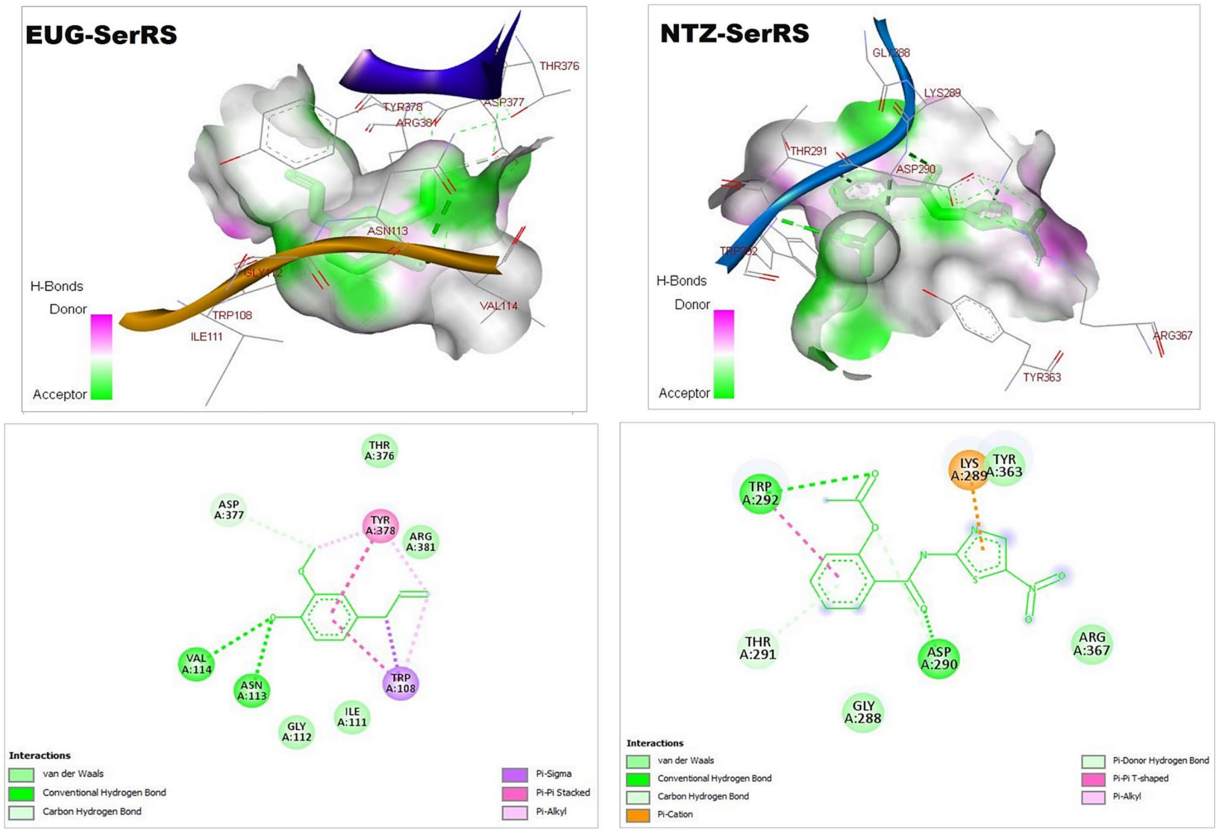

FIGURE 2
3D (upper panel) and 2D (lower panel) ligand-interacted forms show key amino acid residues of SerRS using BIOVIA drug discovery studio visualizer. EUG, eugenol; NTZ, nitazoxanide; SerRS, cytoplasmic seryl-tRNA synthetase.

has considerable anti-cryptosporidial action and a significant synergistic effect when combined with NTZ. Comparing treated and untreated mice, the current study found that EUG considerably reduced the degree of oocyst shedding. Additionally, when combined with NTZ, EUG significantly reduced the number of oocysts that were shed, as opposed to NTZ alone, which, according to earlier studies, was unable to entirely remove the oocysts (34).

Tasdemir et al. conducted an *in vitro* analysis of EUG's effectiveness against *Cryptosporidium* oocysts (61). According to their findings, thyme, oregano, and clove essential oils can significantly reduce the quantity of *Cryptosporidium* oocysts.

To further evaluate the effect of EUG on *C. parvum* induced pathological changes in the intestine and liver tissues, H & E-stained sections of both tissues were examined. Small intestine sections of animals infected with the *C. parvum* and subsequently treated with EUG either alone or in combination with NTZ showed a normal villous pattern with a mild lymphocytic inflammatory response noted in the villi and lamina propria. In the same line, EUG treatment-either alone or in combination with NTZ-restored normal liver histological structures and alleviated *Cryptosporidium* induced alterations.

Furthermore, immunohistochemical screening of iNOS antibody revealed strong cytoplasmic expression in the intestinal epithelium of infected untreated mice. In contrast, weak expression was observed in mice treated with EUG alone or in combination with NTZ. This confirmed the strong oxidative stress strived by the parasite and confirmed the effect of drugs in reducing oxidative stress in tissue. This result agrees with previous studies which demonstrated that mice and piglets infected with *Cryptosporidium*, were able to recover after treatment with iNOS inhibitor or peroxynitrite scavenger, suggesting that reactive nitrogen intermediates may serve as an early and innate defense against intestinal epithelial infection (62). It was documented that the synthesis of NO is increased in cryptosporidiosis, while the inhibition or absence of iNOS decreased epithelial infection and oocyst shedding (63).

The mechanisms behind the antiprotozoal effect of essential oils need further investigations to be fully understood. The high lipophilic nature of the essential oils allows easy absorption by the cell membrane and inhibition of the lipid metabolism of parasites. Another mode of action involves penetrating the membrane first, followed by modulation of cytoplasmic metabolic pathways or organelle function, rather than compromising the integrity of the parasite's membrane (64).

Conclusion

Cryptosporidium is an opportunistic causing with life threatening illness in immunocompromised individuals with limited treatment options. In the present study EUG was able to combat cryptosporidiosis alone and had a synergistic effect when added to NTZ. Mice received EUG alone or in combination with NTZ showed reduced fecal oocyst count and restored the normal histological structures of the liver and spleen when compared with non-treated mice. Based on the results, the present study signified a basis for utilizing EUG as an affordable,

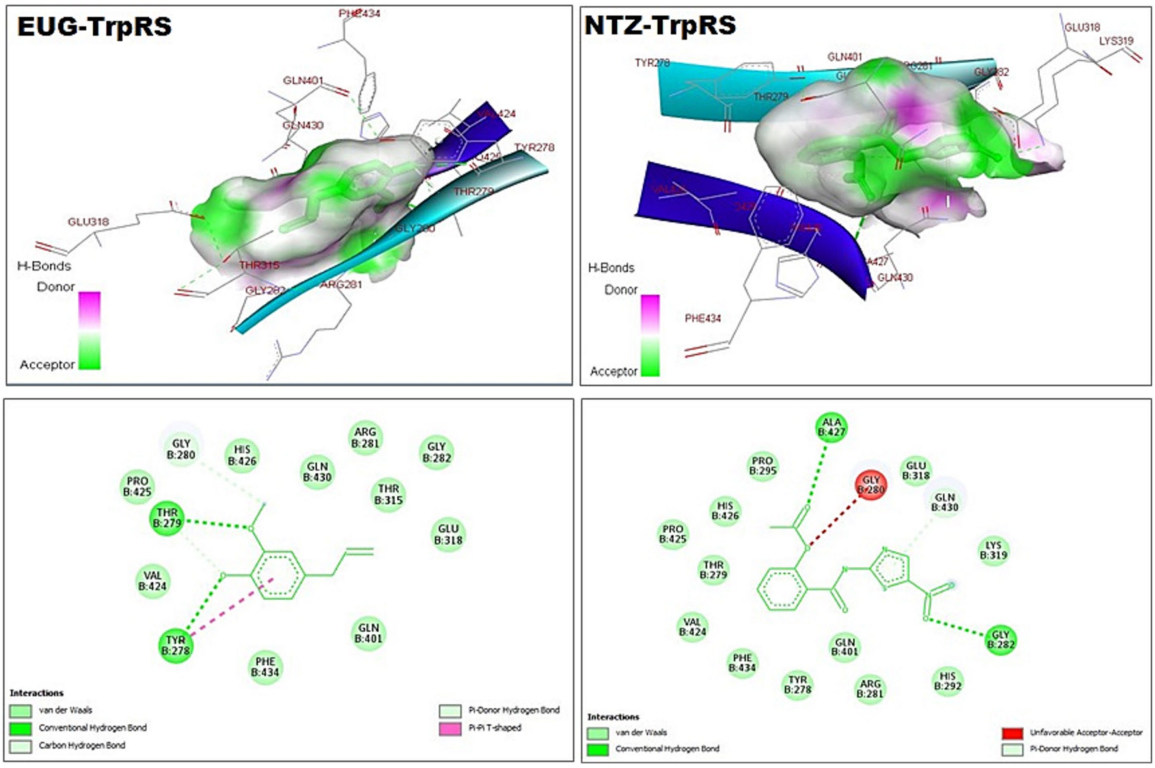

FIGURE 3
3D (upper panel) and 2D (lower panel) ligand-interacted forms show key amino acid residues of TrpRS using BIOVIA drug discovery studio visualizer. EUG, eugenol; NTZ, nitazoxanide; TrpRS, tryptophanyl-tRNA synthetase.

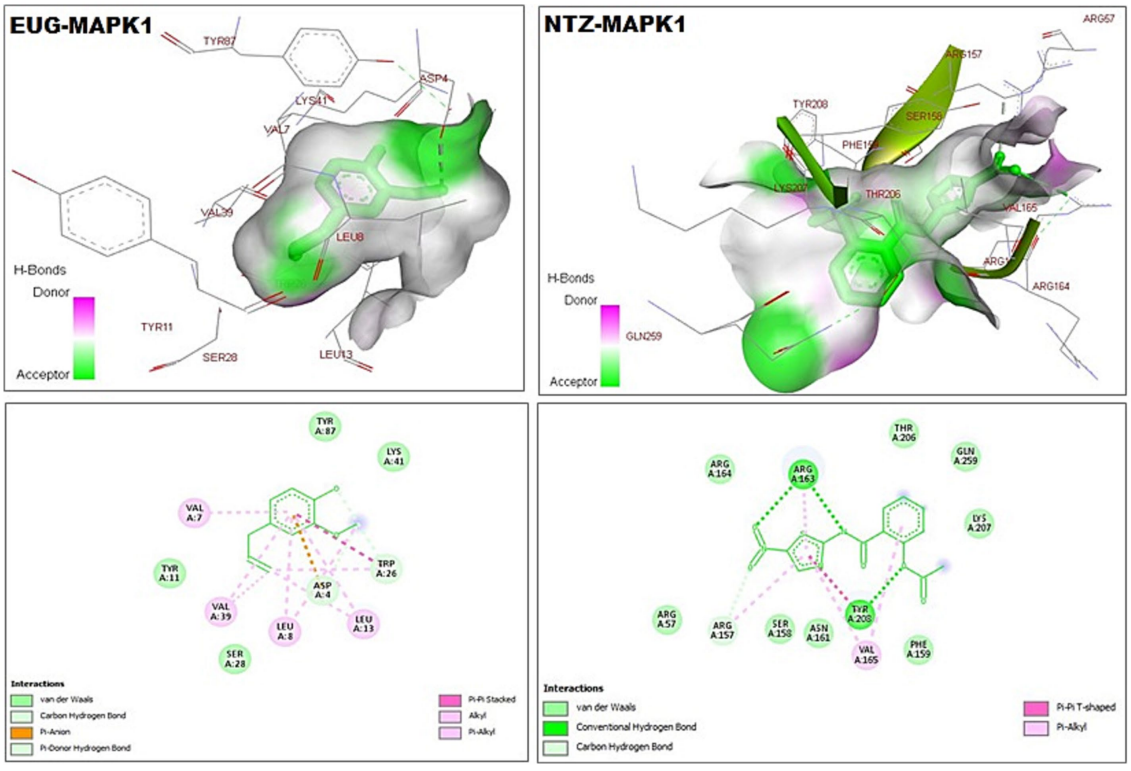

FIGURE 4
3D (upper panel) and 2D (lower panel) ligand-interacted forms show key amino acid residues of MAPK1 using BIOVIA drug discovery studio visualizer. EUG, eugenol; NTZ, nitazoxanide; MAPK1, mitogen-activated protein kinase1/serine–threonine protein kinase.

TABLE 2 Showing treatment with eugenol reduced oocysts counts in the stool of infected mice.

Animal group	Oocyst count/HPF Mean ± SD	%R	*p* value (among groups)	post hock test
Infected untreated	30.4 + 3.33		0.001*	
Infected + Eugenol	11.4 + 1.33	62.5%		a, b
Infected + NTZ	5.2 + 0.6	82.56%		a
Infected + Eugenol + NTZ	1.9 + 0.2	93.44%		a, c

Oocysts were counted in infected untreated mice and compared to counts in animals treated with NTZ or euogenol or both. Data are expressed as mean ± SD and were analyzed using ANOVA for pairwise comparison.
%R: percentage of reduction. SD: Standard deviation. * indicates statistical significance. Letter "a" indicates significant reductions in oocysts counts after treatments compared to infected untreated group. Letter "b" indicates a significant difference in oocysts versus NTZ treated group. Letter "c" indicates a significant difference in oocysts versus eugenol treated group.

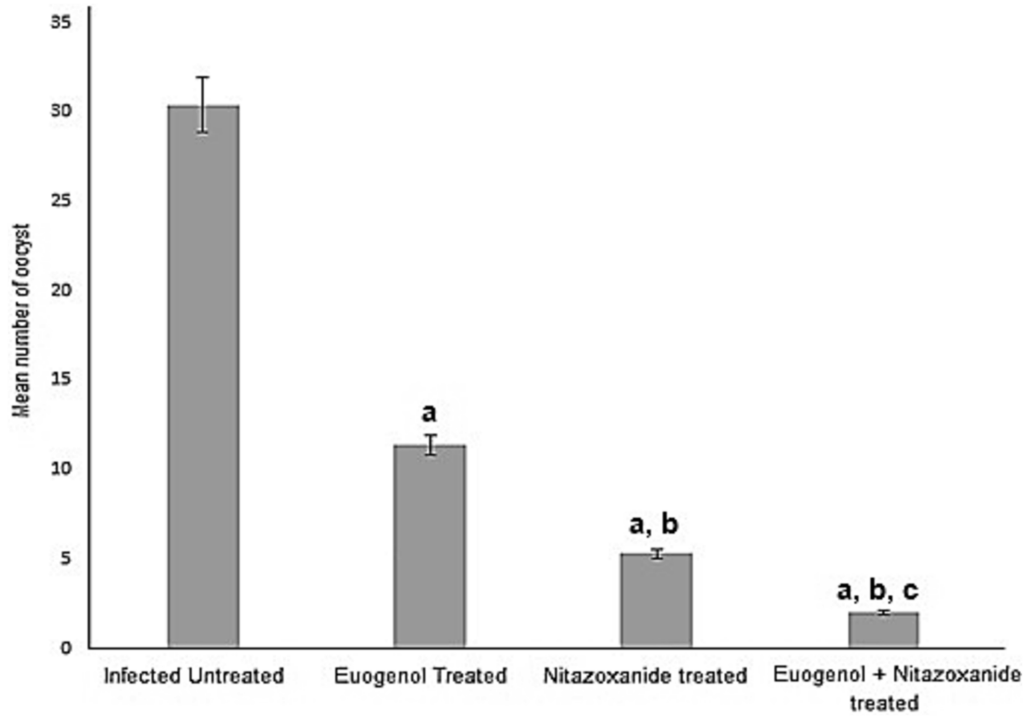

FIGURE 5
Treatment with eugenol reduced oocysts counts in the stool of infected mice. Oocysts were counted in infected untreated mice and compared to counts in animals treated with NTZ or EUG. Data are expressed as mean ± SD and were analyzed using ANOVA for pairwise comparison. Letter "a" indicates statistical difference compared to infected untreated group ($p < 0.001$). Letter "b" indicates statistical difference versus eugenol treated group ($p < 0.001$). Letter "c" indicates statistical difference versus NTZ treated group ($p < 0.001$).

safe, and alternative therapy combined with NTZ in the management of cryptosporidiosis.

Data availability statement

The original contributions presented in the study are included in the article/supplementary material, further inquiries can be directed to the corresponding authors.

Ethics statement

The animal study was approved by the Faculty of Medicine's Institutional Review Board and Ethics Committee at South Valley University, Qena, Egypt (SVU-MED-PAR008-4-22-9-436). The study was conducted in accordance with the local legislation and institutional requirements.

Author contributions

HG: Writing – review & editing. MW: Writing – review & editing. RQ: Writing – review & editing. SA: Writing – review & editing. HM: Writing – review & editing. MA: Writing – review & editing. HayE: Writing – original draft. WA-M: Funding acquisition, Writing – review & editing. EA: Writing – review & editing. HatE: Writing – original draft, Writing – review & editing. AE-k: Conceptualization, Data curation, Formal analysis, Funding acquisition, Investigation, Methodology, Project

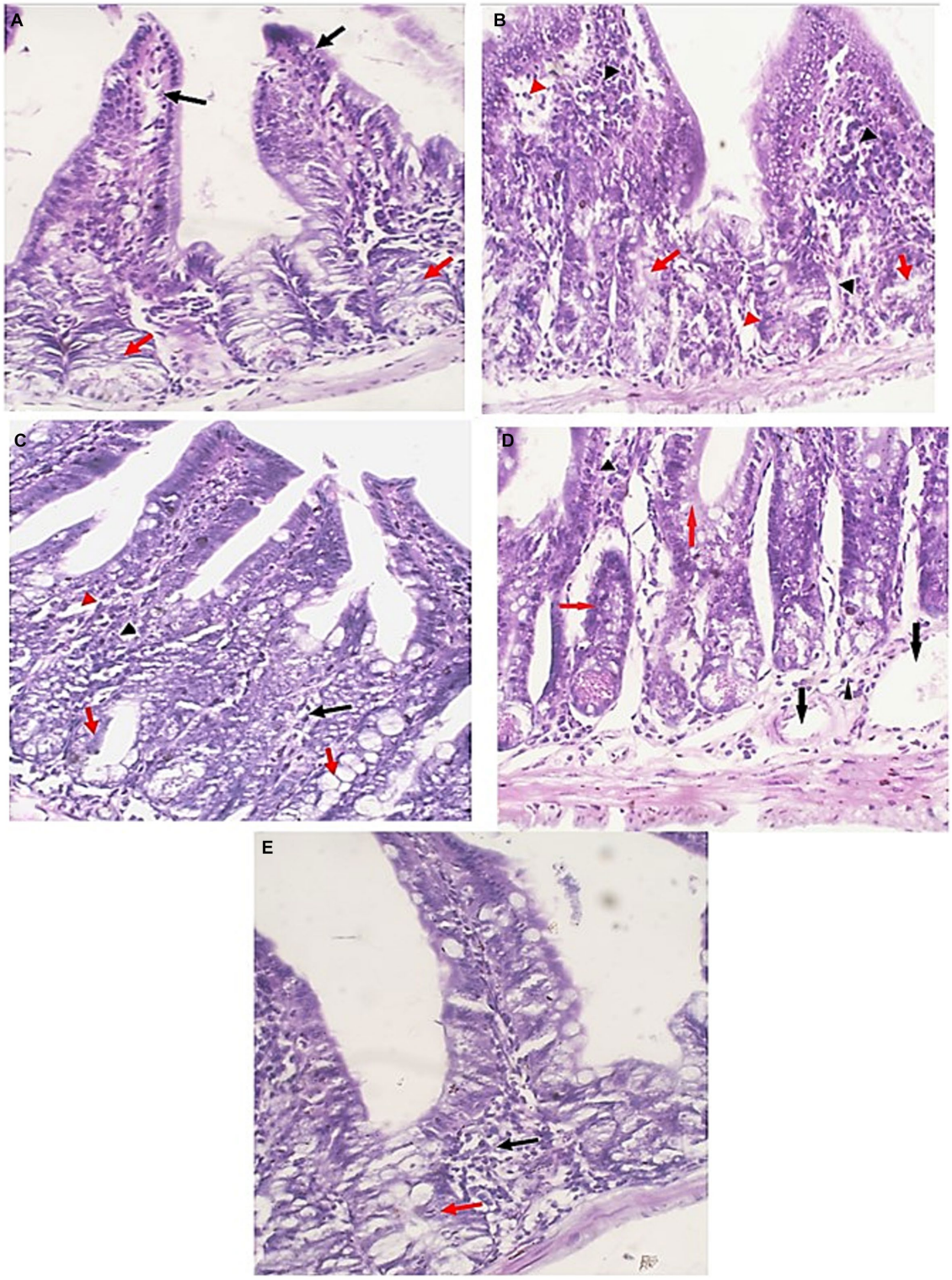

FIGURE 6
Small intestine sections of all studied groups. **(A)** Sections of uninfected untreated mice showing uniform intestinal tissue showing regular villi (Black arrows) with uniform crypts and glands in the lamina propria (Red arrows) (H&E, 400×). **(B)** Sections of infected untreated mice showing expansion of the lamina propria with chronic inflammatory cells (Black arrowheads). Glands (Red arrows) are distorted and attacked by chronic inflammatory cells. There are areas of edema (Red arrowheads) (H&E, 400×). **(C)** Sections of infected EUG treated mice showing significant reduction in the severity and the extent of inflammation (Black arrowheads) and edema (Red arrowheads) in the mucosa. Glands appear more uniform with no inflammatory cells attacking the glands (Red arrows) (H&E, 400×). **(D)** Sections of infected NTZ treated mice showing restoration of intestinal tissue, with mild chronic inflammatory cells infiltrate in the lamina propria (Black arrowheads). Glands retained their uniform regular outlines (Red arrows) with dilated blood vessels (Blue arrows) (H&E, 400×). **(E)** Sections of infected NTZ+ EUG treated mice showing restoration of intestinal tissue, with mild chronic inflammatory cells infiltrate in the lamina propria (Black arrowheads). Glands show uniform regular outlines (Red arrows) (H&E, 400×).

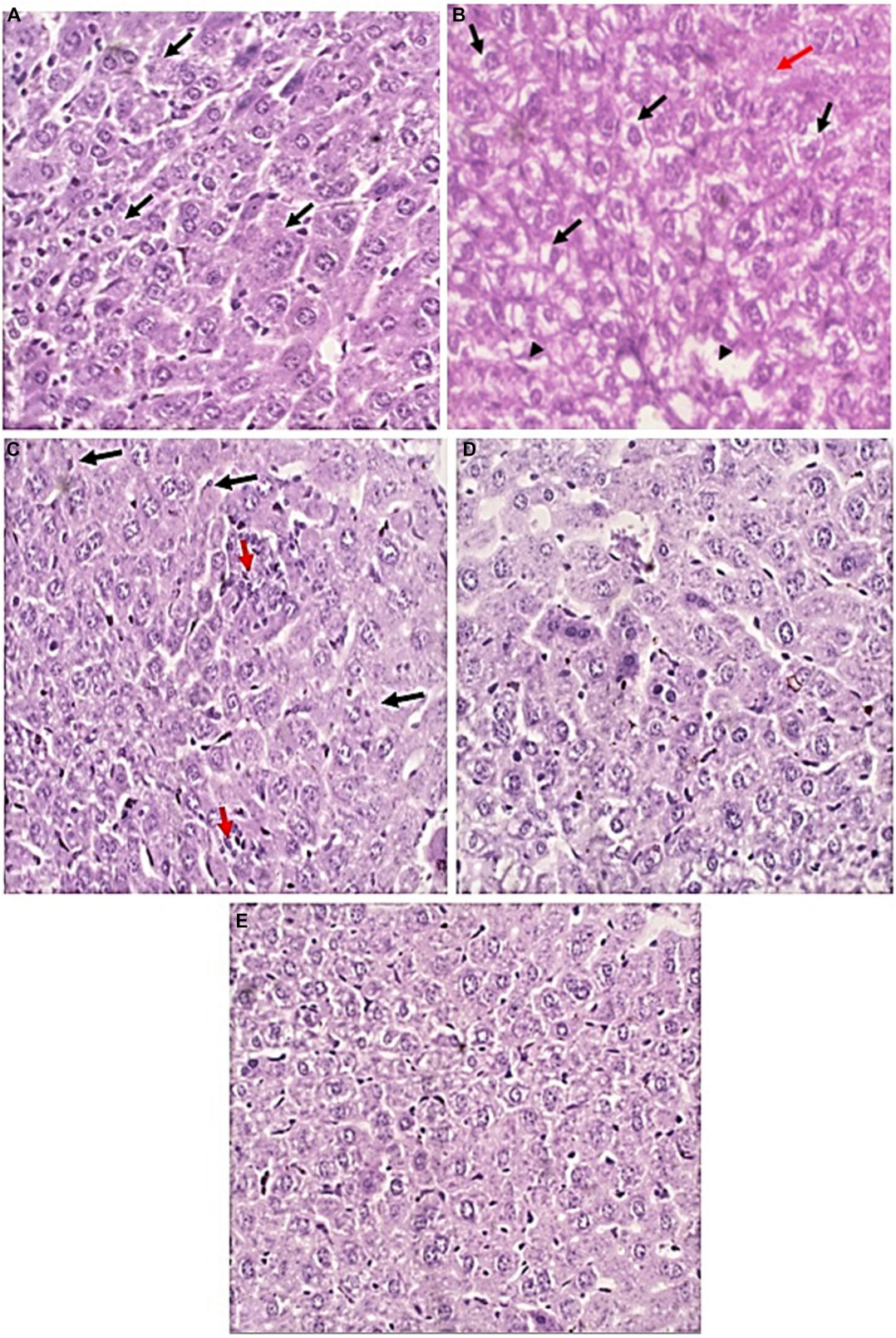

FIGURE 7
Liver sections of all studied groups. **(A)** Sections of uninfected untreated mice showing Uniform plates of hepatocytes (Black arrows) with no evidence of injury (H&E, 400×). **(B)** sections of infected untreated mice showing significant hydropic degeneration of hepatocytes (Black arrows). There are areas of lytic necrosis (Black arrowheads) with confluent necrosis (Red arrow) (H&E, 400×). **(C)** Sections of infected EUG treated mice showing Hepatocytes show no evidence of hydropic degeneration (Black arrows). There are two foci of lobulitis (Red arrow) (H&E, 400×) **(D)** Sections of infected NTZ treated mice showing restoration of hepatocytes integrity with no evidence of injury (H&E, 400×). **(E)** sections of infected NTZ+ EUG treated mice showing restoration of hepatocytes integrity with No evidence of injury.

TABLE 3 Showing the percentage of iNOS positive cells in ileal tissues of different animal groups.

Animal group	% of positive cells Mean ± SD	*p* value (among groups)	post hock test
Uninfected untreated	2.67 ± 1.2		
Infected untreated	40.01 ± 1.9	0.002*	a*
Infected + NTZ	23.2 ± 2.2		a*, b*
Infected + Eugenol	28.6 ± 2.1		a*, b*
Infected + Eugenol + NTZ	16.04 ± 2.5		a*, b*, c*

Data are expressed as mean ± SD and were analyzed using ANOVA for pairwise comparison. Letter "a" indicates statistical difference compared to infected untreated group ($p < 0.001$). Letter "b" indicates statistical difference versus eugenol treated group ($p < 0.001$). Letter "c" indicates statistical difference versus NTZ treated group ($p < 0.001$).

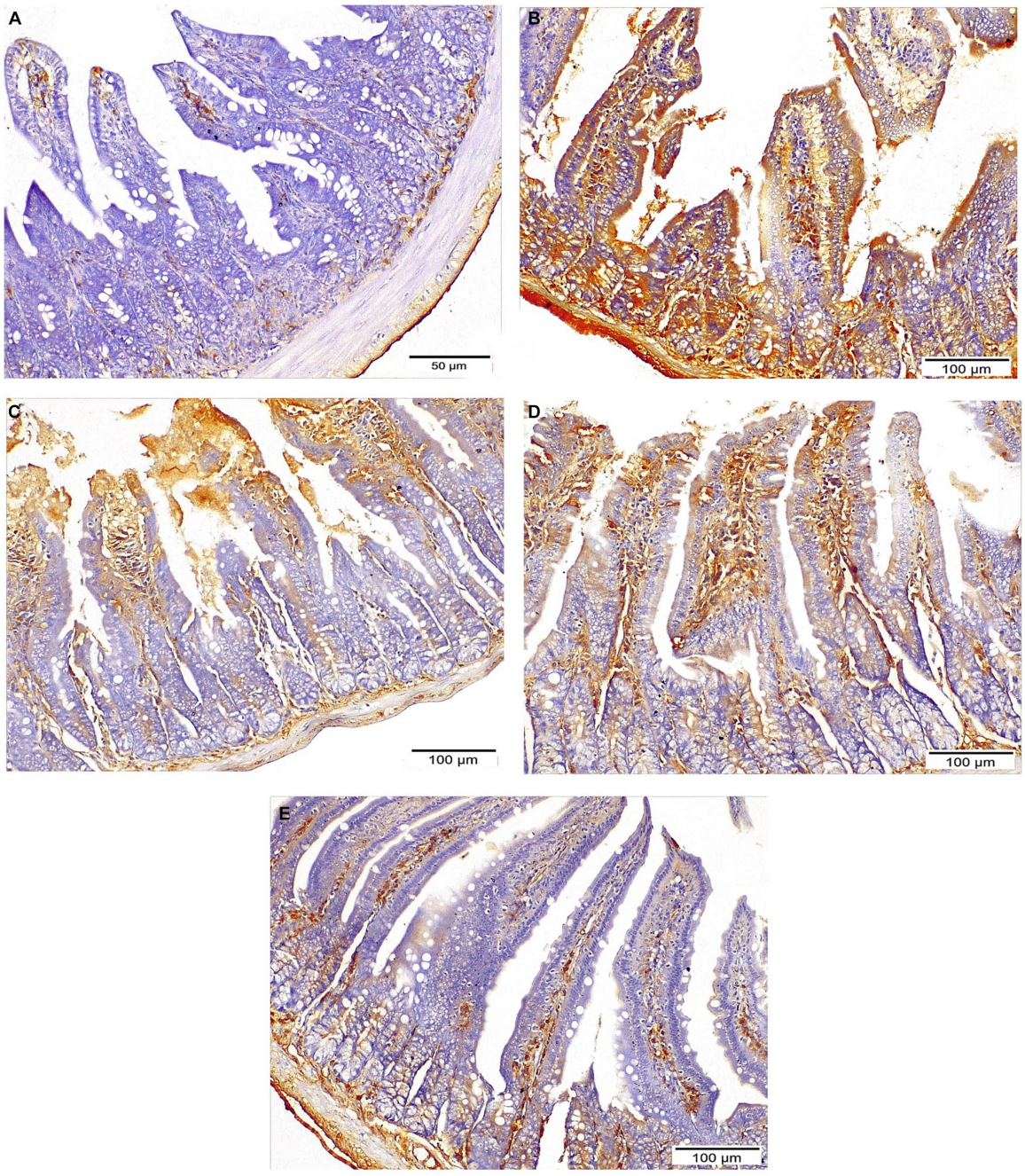

FIGURE 8
Sections of ileum showing INOS expression: **(A)** Negative expression in normal control mice. **(B)** Strong expression in infected untreated group (IHC ×200). **(C,D)** Moderate expression in both NTZ and EUG treated groups, respectively, (IHC ×200). **(E)** Mild diffuse expression in NTZ + EUG treated GROUP (IHC ×200).

administration, Resources, Software, Supervision, Validation, Visualization, Writing – original draft, Writing – review & editing.

Funding

The author(s) declare that financial support was received for the research, authorship, and/or publication of this article. The authors extend their acknowledgement to Princess Nourah bint Abdulrahman University Researchers Supporting Project number (PNURSP2024R39), Princess Nourah bint Abdulrahman University, Riyadh, Saudi Arabia and Researchers Supporting Project number (RSPD2024R859), King Saud University, Riyadh, Saudi Arabia.

Conflict of interest

The authors declare that the research was conducted in the absence of any commercial or financial relationships that could be construed as a potential conflict of interest.

Publisher's note

All claims expressed in this article are solely those of the authors and do not necessarily represent those of their affiliated organizations, or those of the publisher, the editors and the reviewers. Any product that may be evaluated in this article, or claim that may be made by its manufacturer, is not guaranteed or endorsed by the publisher.

References

1. Hafez EN, Hamed WFAE. The efficacy of *Citrus maxima* peels aqueous extract against cryptosporidiosis in immunecompromised mice. *Acta Parasitol*. (2021) 66:638–53. doi: 10.1007/s11686-020-00315-x

2. McCole DF, Eckmann L, Laurent F, Kagnoff MF. Intestinal epithelial cell apoptosis following *Cryptosporidium parvum* infection. *Infect Immun*. (2000) 68:1710–3. doi: 10.1128/IAI.68.3.1710-1713.2000

3. Cacciò SM, Chalmers RM. Human cryptosporidiosis in Europe. *Clin Microbiol Infect*. (2016) 22:471–80. doi: 10.1016/j.cmi.2016.04.021

4. Wang Z-D, Liu Q, Liu H-H, Li S, Zhang L, Zhao Y-K, et al. Prevalence of *Cryptosporidium*, *Microsporidia* and *Isospora* infection in HIV-infected people: a global systematic review and meta-analysis. *Parasit Vectors*. (2018) 11:28. doi: 10.1186/s13071-017-2558-x

5. Khalil IA, Troeger C, Rao PC, Blacker BF, Brown A, Brewer TG, et al. Morbidity, mortality, and long-term consequences associated with diarrhoea from *Cryptosporidium* infection in children younger than 5 years: a meta-analyses study. *Lancet Glob Health*. (2018) 6:e758–68. doi: 10.1016/s2214-109x(18)30283-3

6. Savioli L, Smith H, Thompson A. *Giardia* and *Cryptosporidium* join the 'neglected diseases initiative'. *Trends Parasitol*. (2006) 22:203–8. doi: 10.1016/j.pt.2006.02.015

7. Wang R-J, Li J-Q, Chen Y-C, Zhang L-X, Xiao L-H. Widespread occurrence of *Cryptosporidium* infections in patients with HIV/AIDS: epidemiology, clinical feature, diagnosis, and therapy. *Acta Trop*. (2018) 187:257–63. doi: 10.1016/j.actatropica.2018.08.018

8. Shoultz D, Hostos E, Choy R. Addressing *Cryptosporidium* infection among young children in low-income settings: the crucial role of new and existing drugs for reducing morbidity and mortality. *PLoS Negl Trop Dis*. (2016) 10:e0004242. doi: 10.1371/journal.pntd.0004242

9. Sparks H, Nair G, Castellanos-Gonzalez A, White AC. Treatment of *Cryptosporidium*: what we know, gaps, and the way forward. *Curr Trop Med Rep*. (2015) 2:181–7. doi: 10.1007/s40475-015-0056-9

10. Huston CD. The clofazimine for treatment of cryptosporidiosis in HIV-infected adults (CRYPTOFAZ) and lessons learned for anticryptosporidial drug development. *Clin Infect Dis*. (2021) 73:192–4. doi: 10.1093/cid/ciaa425

11. Maggi P, Larocca AMV, Quarto M, Serio G, Brandonisio O, Angarano G, et al. Effect of antiretroviral therapy on cryptosporidiosis and microsporidiosis in patients infected with human immunodeficiency virus type 1. *Eur J Clin Microbiol Infect Dis*. (2000) 19:213–7. doi: 10.1007/s100960050461

12. Nannini EC, Okhuysen PC. HIV 1 and the gut in the era of highly active antiretroviral therapy. *Curr Gastroenterol Rep*. (2002) 4:392–8. doi: 10.1007/s11894-002-0009-z

13. Raja M. Versatile and synergistic potential of eugenol: a review. *Pharm Anal Acta*. (2015) 6:06. doi: 10.4172/2153-2435.1000367

14. Ogata M, Hoshi M, Urano S, Endo T. Antioxidant activity of eugenol and related monomeric and dimeric compounds. *Chem Pharm Bull*. (2000) 48:1467–9. doi: 10.1248/cpb.48.1467

15. Miyazawa M, Hisama M. Suppression of chemical mutagen-induced SOS response by Alkylphenols from clove (*Syzygium aromaticum*) in the *Salmonella typhimurium* TA1535/pSK1002 Umu test. *J Agric Food Chem*. (2001) 49:4019–25. doi: 10.1021/jf0103469

16. Zhang Y, Lee B, Thompson M, Glass R, Lee RC, Figueroa D, et al. Lactulose–mannitol intestinal permeability test in children with diarrhea caused by rotavirus and *Cryptosporidium*. *J Pediatr Gastroenterol Nutr*. (2000) 31:16–21. doi: 10.1097/00005176-200007000-00006

17. Ündeğer Ü, Başaran A, Degen G, Başaran N. Antioxidant activities of major thyme ingredients and lack of (oxidative) DNA damage in V79 Chinese hamster lung fibroblast cells at low levels of carvacrol and thymol. *Food Chem Toxicol*. (2009) 47:2037–43. doi: 10.1016/j.fct.2009.05.020

18. Riella K, Marinho R, Santos J, Pereira-Filho R, Cardoso J, Albuquerque-Junior R, et al. anti-inflammatory and cicatrizing activities of thymol, a monoterpene of the essential oil from *Lippia gracilis*, in Rodents. *J Ethnopharmacol*. (2012) 143:656–63. doi: 10.1016/j.jep.2012.07.028

19. Catherine AA, Deepika H, Negi PS. Antibacterial activity of eugenol and peppermint oil in model food systems. *J Essent Oil Res*. (2012) 24:481–6. doi: 10.1080/10412905.2012.703513

20. El-Kady AM, Ahmad AA, Hassan TM, El-Deek HEM, Fouad SS, Althagfan SS. Eugenol, a potential schistosomicidal agent with anti-inflammatory and antifibrotic effects against *Schistosoma mansoni*, induced liver pathology. *Infect Drug Resist*. (2019) 12:709–19. doi: 10.2147/idr.S196544

21. Machado M, Dinis AM, Salgueiro L, Custódio JB, Cavaleiro C, Sousa MC. Anti-*Giardia* activity of *Syzygium aromaticum* essential oil and eugenol: effects on growth, viability, adherence and ultrastructure. *Exp Parasitol*. (2011) 127:732–9. doi: 10.1016/j.exppara.2011.01.011

22. Torres PHM, Sodero ACR, Jofily P, Silva-Jr FP. Key topics in molecular docking for drug design. *Int J Mol Sci*. (2019) 20:4574. doi: 10.3390/ijms20184574

23. Cook WJ, Senkovich O, Hernandez A, Speed H, Chattopadhyay D. Biochemical and structural characterization of *Cryptosporidium parvum* lactate dehydrogenase. *Int J Biol Macromol*. (2015) 74:608–19. doi: 10.1016/j.ijbiomac.2014.12.019

24. Pantsar T, Poso A. Binding affinity via docking: fact and fiction. *Molecules*. (2018) 23:1899. doi: 10.3390/molecules23081899

25. Merritt EA, Arakaki TL, Gillespie R, Napuli AJ, Kim JE, Buckner FS, et al. Crystal structures of three protozoan homologs of tryptophanyl-tRNA synthetase. *Mol Biochem Parasitol*. (2011) 177:20–8. doi: 10.1016/j.molbiopara.2011.01.003

26. Gaillard T. Evaluation of autodock and autodock Vina on the CASF-2013 benchmark. *J Chem Inf Model*. (2018) 58:1697–706. doi: 10.1021/acs.jcim.8b00312

27. Gurung AB, Bhattacharjee A, Ali MA. Exploring the physicochemical profile and the binding patterns of selected novel anticancer Himalayan plant derived active compounds with macromolecular targets. *Int J Med Inform*. (2016) 5:1–14. doi: 10.1016/j.imu.2016.09.004

28. Li H, Komori A, Li M, Chen X, Yang AWH, Sun X, et al. Multi-ligand molecular docking, simulation, free energy calculations and wavelet analysis of the synergistic effects between natural compounds baicalein and cubebin for the inhibition of the main protease of Sars-Cov-2. *J Mol Liq*. (2023) 374:121253. doi: 10.1016/j.molliq.2023.121253

29. Li H, Hung A, Yang AWH. Herb-target virtual screening and network pharmacology for prediction of molecular mechanism of Danggui Beimu Kushen Wan for prostate cancer. *Sci Rep*. (2021) 11:6656. doi: 10.1038/s41598-021-86141-1

30. Kumar DT, Iyer S, Christy JP, Siva R, Tayubi IA, Doss CGP, et al. A comparative computational approach toward pharmacological chaperones (Nn-Dnj and Ambroxol) on N370s and L444p mutations causing Gaucher's disease. *Adv Protein Chem Struct Biol*. (2019) 114:315–39. doi: 10.1016/bs.apcsb.2018.10.002

31. Esmat M, Abdel-Aal AA, Shalaby MA, Badawi M, Elaskary H, Yousif AB, et al. Efficacy of clofazimine and nitazoxanide combination in treating intestinal cryptosporidiosis and enhancing intestinal cellular regeneration in immunocompromised mice. *Food Waterborne Parasitol*. (2022) 27:e00161. doi: 10.1016/j.fawpar.2022.e00161

32. El-Wakil ES, Salem AE, Al-Ghandour AMF. Evaluation of possible prophylactic and therapeutic effect of mefloquine on experimental cryptosporidiosis in immunocompromised mice. *J Parasit Dis*. (2021) 45:380–93. doi: 10.1007/s12639-020-01315-4

33. Abdou AG, Harba NM, Afifi AF, Elnaidany NF. Assessment of *Cryptosporidium parvum* infection in immunocompetent and immunocompromised mice and its role in triggering intestinal dysplasia. *Int J Infect Dis*. (2013) 17:e593–600. doi: 10.1016/j.ijid.2012.11.023

34. Farid A, Tawfik A, Elsioufy B, Safwat G. *In vitro* and *in vivo* anti-*Cryptosporidium* and anti-inflammatory effects of *Aloe vera* gel in dexamethasone immunosuppressed mice. *Int J Parasitol Drugs Drug Resist*. (2021) 17:156–67. doi: 10.1016/j.ijpddr.2021.09.002

35. El-Wakil ES, El-Shazly MAM, El-Ashkar AM, Aboushousha T, Ghareeb MA. Chemical profiling of *Verbena officinalis* and assessment of its anti-cryptosporidial activity in experimentally infected immunocompromised mice. *Arab J Chem*. (2022) 15:103945. doi: 10.1016/j.arabjc.2022.103945

36. Metawea A, Bayoumy A, Ali I, Hammam O, Temsah K. Efficacy of nitazoxanide alone or loaded with silica nanoparticle for treatment of cryptosporidiosis in immunocompetent hosts. *Int J Med Arts*. (2021) 3:1229–39. doi: 10.21608/ijma.2021.55788.1237

37. Fahmy A, Alshenawy A, El-Wakil E, Hegab A. Efficacy of *Cyperus rotundus* extract against cryptosporidiosis and toxoplasmosis in murine infections. *Egypt Pharm J*. (2021) 20:242. doi: 10.4103/epj.epj_27_21

38. Ghareeb M, Sobeh M, Aboushousha T, Esmat M, Mohammed H, El-wakil E. Polyphenolic profile of *Herniaria hemistemon* aerial parts extract and assessment of its anti-cryptosporidiosis in a murine model: in silico supported *in vivo* study. *Pharmaceutics*. (2023) 15:415. doi: 10.3390/pharmaceutics15020415

39. Shahiduzzaman M, Daugschies A. Therapy and prevention of cryptosporidiosis in animals. *Vet Parasitol*. (2012) 188:203–14. doi: 10.1016/j.vetpar.2012.03.052

40. Li X, Brasseur P, Agnamey P, Leméteil D, Favennec L, Ballet J-J, et al. Long-lasting anticryptosporidial activity of nitazoxanide in an immunosuppressed rat model. *Folia Parasitol*. (2003) 50:19–22. doi: 10.14411/fp.2003.003

41. Feldman AT, Wolfe D. Tissue processing and hematoxylin and eosin staining. *Methods Mol Biol*. (2014) 1180:31–43. doi: 10.1007/978-1-4939-1050-2

42. Zhang Y, Zhao X, Zhu Y, Ma J, Ma H, Zhang H. Probiotic mixture protects dextran sulfate sodium-induced colitis by altering tight junction protein expressions and increasing Tregs. *Mediat Inflamm*. (2018) 2018:9416391–11. doi: 10.1155/2018/9416391

43. Moradi M, Golmohammadi R, Najafi A, Moosazadeh Moghaddam M, Fasihi-Ramandi M, Mirnejad R. A contemporary review on the important role of in silico approaches for managing different aspects of Covid-19 crisis. *Inform Med Unlocked*. (2022) 28:100862. doi: 10.1016/j.imu.2022.100862

44. Shang X-F, Dai L-X, Yang C-J, Guo X, Liu Y-Q, Miao X-L, et al. A value-added application of eugenol as acaricidal agent: the mechanism of action and the safety evaluation. *J Adv Res*. (2021) 34:149–58. doi: 10.1016/j.jare.2020.12.010

45. Barboza JN, Filho CSMB, Silva O, Medeiros JVR, de Sousa DP. An overview on the anti-inflammatory potential and antioxidant profile of eugenol. *Oxidative Med Cell Longev*. (2018) 2018:1–9. doi: 10.1155/2018/3957262

46. Genç Bilgiçli H, Kestane A, Taslimi P, Karabay O, Bytyqi-Damoni A, Zengin M, et al. Novel eugenol bearing oxypropanolamines: synthesis, characterization, antibacterial, antidiabetic, and anticholinergic potentials. *Bioorg Chem*. (2019) 88:102931. doi: 10.1016/j.bioorg.2019.102931

47. Nisar MF, Khadim M, Rafiq M, Chen J, Yang Y, Wan CC. Pharmacological properties and health benefits of eugenol: a comprehensive review. *Oxidative Med Cell Longev*. (2021) 2021:2497354. doi: 10.1155/2021/2497354

48. Bendre R, Rajput J, Bagul S, Karandikar P. Outlooks on medicinal properties of eugenol and its synthetic derivatives. *Nat Prod Chem Res*. (2016) 4:1–6. doi: 10.4172/2329-6836.1000212

49. Nam H, Kim MM. Eugenol with antioxidant activity inhibits Mmp-9 related to metastasis in human fibrosarcoma cells. *Food Chem Toxicol*. (2013) 55:106–12. doi: 10.1016/j.fct.2012.12.050

50. Hossain MA, Rahman MH, Sultana H, Ahsan A, Rayhan SI, Hasan MI, et al. An integrated in-silico pharmaco-bioinformatics approaches to identify synergistic effects of Covid-19 to HIV patients. *Comput Biol Med*. (2023) 155:1–21. doi: 10.1016/j.compbiomed.2023.106656

51. Kohno M, Tanimura S, Ozaki K. Targeting the extracellular signal-regulated kinase pathway in cancer therapy. *Biol Pharm Bull*. (2011) 34:1781–4. doi: 10.1248/bpb.34.1781

52. Li R, Wu K, Li Y, Liang X, Lai KP, Chen J. Integrative pharmacological mechanism of vitamin C combined with glycyrrhizic acid against Covid-19: findings of bioinformatics analyses. *Brief Bioinform*. (2021) 22:1161–74. doi: 10.1093/bib/bbaa141

53. Dai J, Gu L, Su Y, Wang Q, Zhao Y, Chen X, et al. Inhibition of curcumin on influenza A virus infection and influenzal pneumonia via oxidative stress, TLR2/4, P 38/JNK MAPK and Nf-κB pathways. *Int Immunopharmacol*. (2018) 54:177–87. doi: 10.1016/j.intimp.2017.11.009

54. Di Paola R, Crisafulli C, Mazzon E, Genovese T, Paterniti I, Bramanti P, et al. Effect of Pd98059, a selective Mapk3/Mapk1 inhibitor, on acute lung injury in mice. *Int J Immunopathol Pharmacol*. (2009) 22:937–50. doi: 10.1177/039463200902200409

55. Zhao L, Wang JL, Wang YR, Fa XZ. Apigenin attenuates copper-mediated B-amyloid neurotoxicity through antioxidation, mitochondrion protection and Mapk signal inactivation in an ad cell model. *Brain Res*. (2013) 1492:33–45. doi: 10.1016/j.brainres.2012.11.019

56. Abubakar I, Aliyu SH, Arumugam C, Usman NK, Hunter PR. Treatment of cryptosporidiosis in immunocompromised individuals: systematic review and Meta-analysis. *Br J Clin Pharmacol*. (2007) 63:387–93. doi: 10.1111/j.1365-2125.2007.02873.x

57. Miyamoto Y, Eckmann L. Drug development against the major diarrhea-causing parasites of the small intestine, *Cryptosporidium* and *Giardia*. *Front Microbiol*. (2015) 6:1208. doi: 10.3389/fmicb.2015.01208

58. Jin Z, Ma J, Zhu G, Zhang H. Discovery of novel anti-cryptosporidial activities from natural products by *in vitro* high-throughput phenotypic screening. *Front Microbiol*. (2019) 10:1999. doi: 10.3389/fmicb.2019.01999

59. Baishanbo A, Gargala G, Duclos C, François A, Rossignol J-F, Ballet J, et al. Efficacy of nitazoxanide and paromomycin in biliary tract cryptosporidiosis in an immunosuppressed gerbil model. *J Antimicrob Chemother*. (2006) 57:353–5. doi: 10.1093/jac/dki456

60. Gargala G, François A, Favennec L, Rossignol J-F. Activity of halogeno-thiazolides against *Cryptosporidium parvum* in experimentally infected immunosuppressed gerbils (*Meriones unguiculatus*). *Antimicrob Agents Chemother*. (2013) 57:2821–3. doi: 10.1128/AAC.01538-12

61. Tasdemir D, Kaiser M, Demirci B, Demirci F, Baser KHC. Antiprotozoal activity of Turkish *Origanum onites* essential oil and its components. *Molecules (Basel, Switzerland)*. (2019) 24:4421. doi: 10.3390/molecules24234421

62. Abdelhamed EF, Fawzy EM, Ahmed SM, Zalat RS, Rashed HE. Effect of nitazoxanide, artesunate loaded polymeric nano fiber and their combination on experimental cryptosporidiosis. *Iran J Parasitol*. (2019) 14:240–9. doi: 10.18502/ijpa.v14i2.1136

63. Gookin JL, Duckett LL, Armstrong MU, Stauffer SH, Finnegan CP, Murtaugh MP, et al. Nitric oxide synthase stimulates prostaglandin synthesis and barrier function in *C. parvum*-infected porcine ileum. *Am J Physiol Gastrointest Liver Physiol*. (2004) 287:G571–81. doi: 10.1152/ajpgi.00413.2003

64. Elshafie HS, Armentano MF, Carmosino M, Bufo SA, De Feo V, Camele I, et al. Cytotoxic activity of *Origanum vulgare* L. on hepatocellular carcinoma cell line HepG2 and evaluation of its biological activity. *Molecules*. (2017) 22:1435. doi: 10.3390/molecules22091435

65. Cabada MM, White AC Jr. Treatment of cryptosporidiosis: do we know what we think we know? *Curr Opin Infect Dis*. (2010) 23:494–9. doi: 10.1097/QCO.0b013e32833de052

66. Amadi B, Mwiya M, Sianongo S, Payne L, Watuka A, Katubulushi M, et al. High dose prolonged treatment with nitazoxanide is not effective for cryptosporidiosis in HIV positive Zambian children: a randomised controlled trial. *BMC Infect Dis*. (2009) 9:1–7. doi: 10.1186/1471-2334-9-195

frontiers | Frontiers in Veterinary Science

TYPE Brief Research Report
PUBLISHED 12 April 2024
DOI 10.3389/fvets.2024.1376208

Check for updates

OPEN ACCESS

EDITED BY
Sirikachorn Tangkawattana,
Khon Kaen University, Thailand

REVIEWED BY
Georgiana Deak,
University of Agricultural Sciences and Veterinary Medicine of Cluj-Napoca, Romania
Zorica D. Dakić,
University of Belgrade, Serbia

*CORRESPONDENCE
Piyanan Taweethavonsawat
✉ Piyanan.T@chula.ac.th

RECEIVED 25 January 2024
ACCEPTED 08 March 2024
PUBLISHED 12 April 2024

CITATION
Junsiri W, Kamkong P, Phojun A and Taweethavonsawat P (2024) Unveiling zoonotic threats: molecular identification of *Brugia* sp. infection in a lion.
Front. Vet. Sci. 11:1376208.
doi: 10.3389/fvets.2024.1376208

COPYRIGHT
© 2024 Junsiri, Kamkong, Phojun and Taweethavonsawat. This is an open-access article distributed under the terms of the Creative Commons Attribution License (CC BY). The use, distribution or reproduction in other forums is permitted, provided the original author(s) and the copyright owner(s) are credited and that the original publication in this journal is cited, in accordance with accepted academic practice. No use, distribution or reproduction is permitted which does not comply with these terms.

Unveiling zoonotic threats: molecular identification of *Brugia* sp. infection in a lion

Witchuta Junsiri[1], Patchana Kamkong[1], Aunchisa Phojun[2] and Piyanan Taweethavonsawat[1,3]*

[1]Parasitology Unit, Department of Veterinary Pathology, Faculty of Veterinary Science, Chulalongkorn University, Bangkok, Thailand, [2]Nakhon Ratchasima Zoo, The Zoological Park Organization, Nakhon Ratchasima, Thailand, [3]Biomarkers in Animals Parasitology Research Unit, Chulalongkorn University, Bangkok, Thailand

Brugia malayi and *B. pahangi*, potential zoonotic pathogens transmitted by mosquitoes, are believed to primarily infect dogs and cats as reservoir hosts. Although previous studies have indicated nematode infections in lions, particularly in zoo environments where human contact with these reservoirs is possible, limited documentation exists regarding *Brugia* sp. infections in lions in Thailand. This study aims to investigate a case of *Brugia* infection in a lion from a zoo in Thailand. The blood sample was collected and examined from a female lion, using staining methods to morphologically identify microfilaria at the genus level. Subsequently, the PCR was employed targeting specific genes, including mitochondrial 12S rDNA, 18S rDNA, cytochrome oxidase I (COI) and *Wolbachia* surface protein (*wsp*), to confirm the species of the filarial nematode parasite. The genetic sequencing results revealed a high similarity (99–100%) to *B. malayi* for the 12S rDNA, 18S rDNA, COI and *wsp* genes. Phylogenetic analysis based on nucleotide sequences from the 12S rDNA, 18S rDNA, COI and *wsp* genes showed that the sequences from this study belong to different clusters. This marks the inaugural documentation of molecular identification of *Brugia* infection in a lion, signifying that lions could function as reservoirs for this parasite and present a potential public health risk in the region. Our research underscores the effectiveness of molecular techniques and phylogenetic analysis in discerning and comprehending the evolution of filarial parasites. Additionally, it emphasizes the significance of these methods in enhancing the diagnosis, control, and prevention of zoonotic filarial nematode infections.

KEYWORDS

***Brugia malayi*, lion, molecular analysis, PCR, Thailand**

1 Introduction

Brugia spp., nematodes of the Onchocercidae family, have a global presence in infecting the lymphatic system of mammals. Lymphatic disease, commonly referred to as elephantiasis, is regarded as the primary manifestation of filariasis (1). Among *Brugia* species of medical importance are *Brugia malayi* and *Brugia timori*, causative agents of lymphatic filariasis in south and southeast Asia (2, 3). *Brugia malayi* can also naturally infect mammals such as monkeys and cats (4–6). Other filarial species, such as *B. pahangi*, have been reported to have associations with domestic animals (7, 8). *Brugia pahangi*, a closely related species of *B. malayi*, is a lymphatic filarial worm of mammals, particularly of cats, dogs and wild carnivores (9, 10).

Although there have been reports of the presence of this parasite's microfilaria in human blood samples, it is not currently identified as a cause of human disease in its natural environment (11, 12).

Filarial nematodes have previously been reported in different species of wild or captive felids, such as *Dirofilaria immitis* has been found in Bengal tiger (*Panthera tigris*) (13, 14), snow leopard (*Uncia uncia*) (15), clouded leopard (*Neofelis nebulosa*) (16), African lion (*Panthera leo*) (17), leopard (*Panthera pardus pardus*) (18). *Dirofilaria striata* has been reported in Florida panthers (*Felis concolor coryi*) and the bobcat (*Lynx rufus*) (19). Genet cats (*Genetta tigrina*) were infected with *D. repens* in East Africa (20). To date, there have been no documented cases of lymphatic filariasis resulting from *Brugia* sp. infection in lions globally, including Thailand. Nevertheless, the result showed an instance of *Brugia* sp. infection in a captive lion from a private zoo in Thailand. Molecular characterization of the infection was achieved through the analysis of the 12S rDNA, 18S rDNA, COI, and *wsp* genes.

2 Materials and methods

2.1 Sample collection

On October 27, 2022, a routine health examination was conducted on two lions (*Panthera leo*) at a private zoo. Both lions, a 2-year-old male and a 2-year-old female, weighing 90 kg each, were anesthetized for the examination. The lions had a body condition score of 3. Anesthesia was induced using a combination of 1 mg/kg xylazine (X-LAZINE, Thailand) and 4 mg/kg ketamine (Hameln Pharma, United Kingdom). Subsequently, blood samples were drawn from the femoral vein using EDTA tubes. These samples were then sent to a private standard laboratory center (Nakhon Ratchasima Province) to determine the presence of microfilariae through Giemsa staining (21) and Acid phosphatase staining (22). A blood sample was subjected to testing using an FIV/FeLV test kit (IDEXX, United States) and a CPV/CCV test kit (IDEXX, United States). The results revealed that a female lion tested positive for Brugian filariasis. The remaining EDTA blood from the Brugian filariasis-positive lion was preserved at −20°C for subsequent DNA extraction.

2.2 DNA extraction and molecular assay

For molecular identification, NucleoSpin® Blood (MACHEREY-NAGEL, Germany) was used to extract filarial nematode DNA according to the manufacturer's specifications. The DNA was used as a template for the PCRs with the GoTaq® Green Master Mix (Promega Corporation, United States), amplifying a section of the 12S rDNA, 18S rDNA, COI, and *wsp* genes. The cycling conditions for PCR and specific details of primer sequences were employed as outlined in Table 1. All PCR amplifications included *D. immitis* adult worm DNA as an amplification control, and nuclease-free water served as a no-template control. The amplified PCR products were stained with RedSafe™ Nucleic Acid Staining Solution (INtRON Biotechnology, Korea) and checked in 1.5% agarose gel. Further amplified DNA product was excised from the gel and purified using a PCR clean-up gel extraction kit (NucleoSpin® Gel and PCR Clean-up, MACHEREY-NAGEL, Germany) as per the manufacturer's instructions. Purified PCR products were carried out in both directions and confirmed by barcode taq (BT) sequencing. DNA sequences obtained in the study were identified using BLAST with sequences available in the GenBank database. The 12S rDNA, 18S rDNA, COI and *wsp* sequences obtained from this study were aligned along with the reference sequences retrieved from NCBI using CLUSTALW. Finally, the phylogenetic analysis was performed using MEGA X software (27). The maximum likelihood algorithm was used as the best fit model with 1,000 bootstrap replicates (28) and the nucleotide distance was calculated using the p-distance method (29).

3 Results

3.1 Parasite identification

A 2-year-old female lion blood sample was brought to Vet Central Lab for screening of microfilariae. The Giemsa blood smear taken from the positive case showed the presence of sheathed microfilariae. These sheathed microfilariae had a pink sheath, with a head-space at the front and two clear tail nuclei at the back (Figure 1A). Histochemical staining was performed to confirm species identification by acid phosphatase activity in microfilariae. When the sheathed microfilariae were stained with acid phosphatase, a pattern of four points staining emerged, indicating acid phosphatase activity at the amphid (AM), excretory pore (EP), anal pore (AP), and phasmid (PM) (Figure 1B). When it comes to *B. malayi* microfilaria, bright red points were seen, which were easily visible even under low magnification.

3.2 Similarity analysis

The primers used for PCR amplification successfully detected filarial nematode DNA in the blood samples. The *Brugia* sp. was specifically identified through PCR products of various sizes, including 484 bp (12S rDNA gene), 753 bp (18S rDNA gene), 672 bp (COI gene) and 723 bp (*wsp* gene). These PCR products were then sequenced and analyzed using BLAST. The BLAST results demonstrated that the 12S rDNA, 18S rDNA, COI and *wsp* sequences shared a high level of identity (99–100%) with *B. malayi*. The nucleotide sequence data mentioned in the paper have been deposited in GenBank, as indicated in Supplementary Table S1. Comparative analysis of the sequences revealed a high sequence similarity percentage (99.7–100%, 95.2–100%, 99.5–100% and 99.4–100%) for the 12S rDNA, 18S rDNA, COI and *wsp* sequences, respectively (Supplementary Tables S2–S5).

3.3 Phylogenetic analysis

The genetic relationships among *B. malayi* isolates can be more accurately determined by representing them in a phylogenetic tree. In our study, the Maximum Likelihood (ML) was used to construct these trees. By aligning the sequences of the *B. malayi* 12S rDNA gene obtained in our study with other sequences from GenBank, divided the resulting phylogenetic tree into 14 clusters. Notably, a *B. malayi* sequence identified in our study was placed in cluster 1 along with

TABLE 1 Primer list for the optimized *Brugia* sp. detection protocol.

Target gene	Primers	Sequence (5′–3′)	Annealing temperature (° C)	Product size (bp)	References
12S rDNA	12sF	GTTCCAGAATAATCGGCTA	52	484	(23)
	12sRdeg	ATTGACGGATGRTTTGTACC			
18S rDNA	18SF	TCGTCATTGCTGCGGTTAAA	54	753	(24)
	18SR	GGTTCAAGCCACTGCGATTAA			
COI	cox1intF	TGATTGGTGGTTT TGGTAA	54	672	(25)
	cox1intR	ATAAGTACGAGTATCAATATC			
wsp	WSPF	AACTGCTTTAGTGGCGTTGC	60	723	(26)
	WSPR	TTAAACATTAACCCAGCTTCTGTGC			

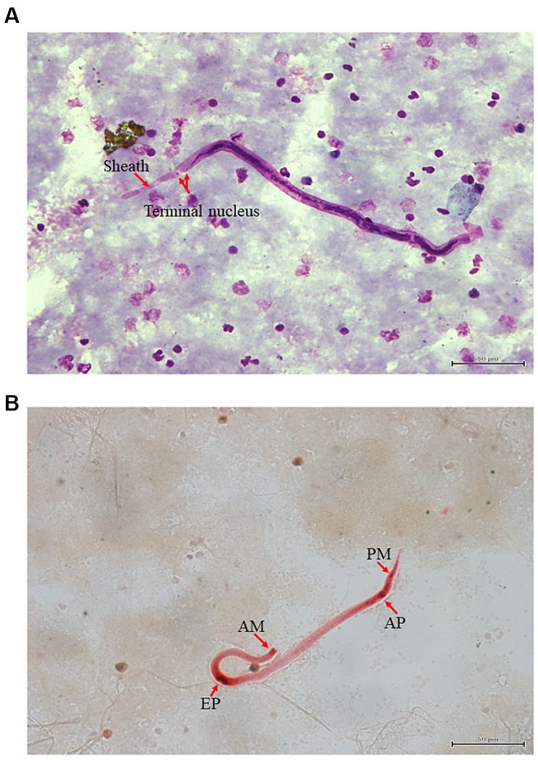

FIGURE 1
Microscopic examination using Giemsa and Acid phosphatase straining **(A,B)**: Giemsa staining of microfilaria infection from lion (*Panthera leo*) in Thailand. Red arrow indicates the presence of sheathed microfilaria **(A)**. *Brugia* microfilaria showing acid phosphatase activity at the amphid (AM), excretory pore (EP), anal pore (AP) and phasmid (PM) **(B)**.

sequences from the UK, USA, and Thailand (Figure 2). In the phylogenetic tree of the 18S rDNA gene, the sequences were classified into 20 clusters within the phylogram. Interestingly, a *B. malayi* sequence from a lion in Thailand was assigned to cluster 9 and showed genetic similarities with sequences from the UK and USA, indicating the genetic variability of the *B. malayi* 18S rDNA sequence in Thailand (Figure 3). The COI gene sequences were also analyzed, which were grouped into 8 clusters. A *B. malayi* COI gene sequence from a lion in Thailand was classified into cluster 1, alongside other *B. malayi* COI sequences from Thailand, Vietnam, and the USA (Supplementary Figure S1). Furthermore, the phylogenetic analysis of the *wsp* gene in *Wolbachia* endosymbionts revealed clear separation into 18 clusters. Within the cluster associated with *Brugia* sp., a more detailed subdivision into 9 subclusters was observed (Supplementary Figure S2). The *B. malayi* sequence identified in our investigation was classified within the 1st cluster, exhibiting genetic affinities with sequences originating from the USA.

4 Discussion

Presently, there is a lack of literature on *Brugia* infection in zoos and wildlife animals in Thailand. However, to the best of our knowledge, this study is the inaugural one to present both morphological and molecular characterization of *Brugia* sp. infection in captive zoo lions in Thailand. Morphological assessment is employed to identify potential causes, and subsequent molecular characterization aids in pinpointing the most likely parasitic source. Knowledge of lion parasites mainly from zoo lions and mostly focused on intestinal parasites (30, 31). Limited information exists regarding the prevalence of parasites in free-ranging lions (32). Parasites in lions have been documented in various regions, including Tanzania, Ethiopia, South Africa, the USA, Italy, India, and Malaysia (16, 18, 19, 31–34) with a few notable exceptions where a particular group of parasites has been studied, such as blood parasites (35–39), intestinal parasites (32, 40) or where the results of veterinary examinations in a National Park (33) have been reported. A previous study reported that *Dirofilaria* sp. is a common parasite of lions in the Kruger Park (33), while our study found microfilaria of *Brugia* sp. infected in lion. The result of this study similar to result reported by Zahedi et al. (16) who found microfilaria of *Brugia* in a clouded leopard (*Neofelis nebulosa*). However, the study found a mixed infection of *B. pahangi* and *D. immitis*, which differs from our study that reported the infection of *B. malayi*.

The criteria for morphological identification of microfilariae include their size, sheath, and nuclear column (41). Filarial infection with multiple species and morphological alterations of microfilariae are not easily differentiated morphologically even by trained persons (42). Histochemical staining to detect acid phosphatase activity can overcome most of these problems (43). Our result showed the lion microfilariae are sheathed with four points staining pattern with acid phosphatase activity at the amphid (AM), excretory pore (EP), anal pore (AP) and phasmid (PM). Moreover, *B. malayi* microfilaria had

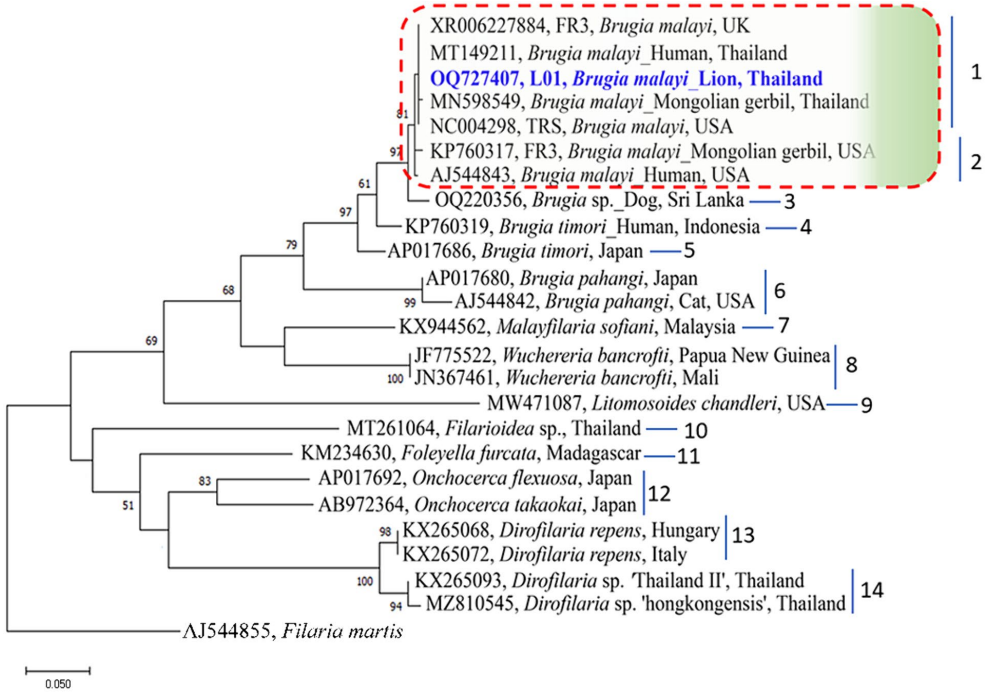

FIGURE 2
Phylogenetic tree based on an alignment of 12S rDNA gene sequences. Bootstrap confidence values (1,000 replicates) are shown as percentages. Values less than 50% are omitted. The units for the scale bar are substitutions per site. NCBI accession numbers are included. The 12S rDNA sequence of *B. malayi* from lion in Thailand, with taxon name shown in blue color and bold font, was generated as part of this study. Letters to the right of the bracketed branches denote the clusters. *Filaria martis* was used as out group.

bright red points that were distinctly visible even under low power. Species identification based on morphology also requires analysis of the adult-stage filaria. Unfortunately, our study did not find adult-stage filaria in lions. Nevertheless, the prevalence of microfilaria in lions should be noted and sampled for further analysis.

Routinely, diagnosis is carried out through microscopic examination of the morphology in microfilariae isolated from blood. It is known that *B. malayi* and *B. pahangi* are very similar morphologically. However, species identification by Giemsa staining is not sufficient (43). Although acid phosphatase staining is effective it is not reproducible and the procedure is complicated (44). Molecular methods based on species-specific PCRs are simple and easy to perform and have been introduced for discrimination of *Brugia* sp. (6, 44). Molecular diagnostic methods, based on the amplification of parasite DNA by PCR methods have the advantage of being more sensitive in detecting parasites than the usual microscopy methods, especially in case of low mf densities, as well as increased certainty in the identification of the species or even strain level. This study applied molecular phylogenetic analysis of 12S rDNA, 18S rDNA, COI, and *wsp* nucleotide sequences for confirmation of *Brugia* sp. in a single lion reservoir. In the tree analysis, the phylogenetic tree based on 12S rDNA, 18S rDNA and COI gene sequences were grouped with *B. malayi* sequences from other animals and other countries such as Thailand, Vietnam and USA. Notably, a *B. malayi* isolate obtained from a lion in a Thai zoo exhibited close genetic proximity to isolates from humans and dogs, suggesting a potential reservoir host. While suspicions of *B. malayi* presence in dogs have persisted concerning lymphatic filariasis, reports of *B. malayi* infection in lions were previously nonexistent. Our findings provide evidence for the potential role of lions as reservoir hosts for *B. malayi*. Moreover, there have been reports of *B. malayi* infection in humans in southern Thailand, particularly in regions near the Thai-Malaysian border. Studies have identified *Mansonia* sp. as a significant carrier of infective *Brugia* larvae in these areas, suggesting its role as one of the primary vectors for *B. malayi* in southern Thailand (45, 46). However, conclusive determination of the lion's reservoir capacity in endemic areas necessitates further on-site investigations involving animals in the vicinity of the zoo.

The primer set COXI-int-F and COXI-int-R employed in our study functioned as universal primers, capable of amplifying the COI region from 11 diverse species of blood and tissue filariae, including *B. malayi*, *B. pahangi*, *D. immitis*, *D. repens*, *Wuchereria bancrofti*, and *Onchocerca* spp. (25). In a 2019 study by Satjawongvanit et al., the detection of filarial nematode DNA in blood samples from domestic dogs in the Bangkok Metropolitan Region, Thailand, was accomplished using COI and internal transcribed spacer 1 (ITS1) gene-based PCR. Based on partial nucleotide sequences of the COI gene (~690 bp), they identified three species in domestic dogs: *D. immitis* (57.89%), *B. pahangi* (22.81%), and *B. malayi* (7.02%). The study emphasized the utility of the COI gene as a valuable marker for distinguishing between *D. immitis*, *B. pahangi*, and *B. malayi*, making COI-based PCR a suitable tool for detecting filarial nematode infections in dogs (47). Additionally, mitochondrial 12S rDNA primers were employed to construct the phylogeny. Although both the 12S rDNA and COI gene were deemed useful markers for detecting filarial nematodes in our study, Gaillard et al. (48) reported that the

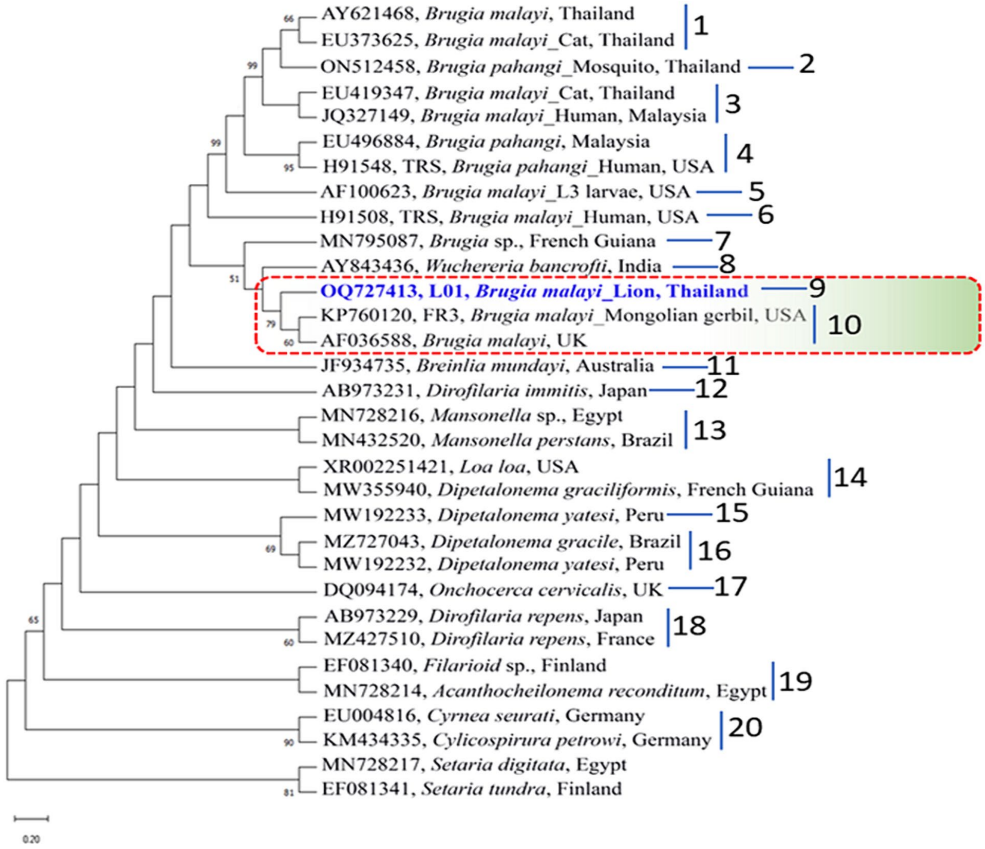

FIGURE 3
Phylogenetic tree based on an alignment of 18S rDNA gene sequences. Bootstrap confidence values (1,000 replicates) are shown as percentages. Values less than 50% are omitted. The units for the scale bar are substitutions per site. NCBI accession numbers are included. The 18S rDNA sequence of *B. malayi* from lion in Thailand, with taxon name shown in blue color and bold font, was generated as part of this study. Letters to the right of the bracketed branches denote the clusters. *Setaria digitata* and *S. tundra* were used as out group.

phylogenetic analyses and amplification of the 12S rDNA gene demonstrated less discriminating power compared to the COI fragment.

The phylogenetic trees of *wsp* gene for *Wolbachia* endosymbiont were distinctly separated into 2 groups *B. malayi* and *B. pahangi*. However, the results of *wsp* showed little differences in nucleotide sequences between the two *Brugia* species with is differs from previous reports by Bazzocchi et al. (49) who showed that the sequences of *B. malayi* and *B. pahangi* were grouped in *wsp* phylogeny. However, all the phylogenetic relationships which are unquestioned for the host nematodes are matched by the *Wolbachia* phylogeny based on *wsp* this indicated that the *Wolbachia*-filaria association is stable and species-specific.

5 Conclusion

To the authors' knowledge, this case represents the initial occurrence of *Brugia* infection in a captive lion from Thailand. The nematode was identified through both morphological and molecular methods, revealing a *B. malayi* infection, which has been documented in domestic animals within Thailand. Nonetheless, our findings bring attention to the insufficient understanding concerning the diversity of *Brugia* species and the interactions between hosts and parasites in wildlife animals from Thailand. This knowledge gap has potential implications in the fields of veterinary medicine and public health.

Data availability statement

The datasets presented in this study can be found in online repositories. The names of the repository/repositories and accession number(s) can be found in the article/Supplementary material.

Ethics statement

The requirement of ethical approval was waived by Biosafety Committee of Chulalongkorn University, Faculty of Veterinary Science (IBC 2231033) for the studies involving animals because this study was a part of the routine health check at a private farm, for which ethical approval was not obligatory. All procedures conducted during the study adhered to the relevant guidelines and regulations. The studies were conducted in accordance with the local legislation and institutional requirements. Written informed consent was not obtained from the owners for the participation of their animals in this study because this was a part

of the routine health check at Nakhon Ratchasima Zoo, Zoological Park Organization of Thailand, for which ethical approval was not obligatory.

Author contributions

WJ: Conceptualization, Investigation, Methodology, Validation, Writing – original draft. PK: Investigation, Methodology, Visualization, Writing – original draft. AP: Investigation, Resources, Visualization, Writing – original draft. PT: Writing – original draft, Writing – review & editing.

Funding

The author(s) declare that financial support was received for the research, authorship, and/or publication of this article. This research was supported the Thailand Science Research and Innovation Fund, Chulalongkorn University (FOODF67310022), Thailand and the Second Century Fund (C2F), Chulalongkorn University.

Conflict of interest

The authors declare that the research was conducted in the absence of any commercial or financial relationships that could be construed as a potential conflict of interest.

Publisher's note

All claims expressed in this article are solely those of the authors and do not necessarily represent those of their affiliated organizations, or those of the publisher, the editors and the reviewers. Any product that may be evaluated in this article, or claim that may be made by its manufacturer, is not guaranteed or endorsed by the publisher.

Supplementary material

The Supplementary material for this article can be found online at: https://www.frontiersin.org/articles/10.3389/fvets.2024.1376208/full#supplementary-material

SUPPLEMENTARY FIGURE 1.
Phylogenetic tree based on an alignment of COI gene sequences. Bootstrap confidence values (1,000 replicates) are shown as percentages. Values less than 50% are omitted. The units for the scale bar are substitutions per site. NCBI accession numbers are included. The COI sequence of B. malayi from lion in Thailand, with taxon name shown in blue color and bold font, was generated as part of this study. Letters to the right of the bracketed branches denote the clusters. Setaria tundra and S. labiatopapilosa were used as out group.

SUPPLEMENTARY FIGURE 2.
Phylogenetic tree based on an alignment of wsp sequences. Bootstrap confidence values (1,000 replicates) are shown as percentages. Values less than 50% are omitted. The units for the scale bar are substitutions per site. NCBI accession numbers are included. The wsp sequence of B. malayi from lions in Thailand, with taxon name shown in blue color and bold font, was generated as part of this study. Letters to the right of the bracketed branches denote the clusters. Wolbachia endosymbiont of Aedes albopictus was used as out group.

References

1. Eberhard ML. Zoonotic filariasis. *Trop Med Infect Dis*. (2006) 2:1189–203. doi: 10.1016/B978-0-443-06668-9.50106-X

2. Bizhani N, Hafshejani SH, Mohammadi N, Rezaei M, Rokni MB. Lymphatic filariasis in Asia: a systematic review and meta-analysis. *Parasitol Res*. (2021) 120:411–22. doi: 10.1007/s00436-020-06991-y

3. Dickson BFR, Graves PM, McBride WJ. Lymphatic filariasis in mainland Southeast Asia: a systematic review and meta-analysis of prevalence and disease burden. *Trop Med Infect Dis*. (2017) 2:32. doi: 10.3390/tropicalmed2030032

4. Edeson JFB, Wilson T. The epidemiology of filariasis due to Wuchereria bancrofti and Brugia malayi. *Annu Rev Entomol*. (1964) 9:245–68. doi: 10.1146/annurev.en.09.010164.001333

5. Kanjanopas K, Choochote W, Jitpakdi A, Suvannadabba S, Loymak S, Chungpivat S, et al. Brugia malayi in a naturally infected cat from Narathiwat province, southern Thailand. *Southeast Asian J Trop Med Public Health*. (2001) 32:585–7.

6. Chansiri K, Tejangkura T, Kwaosak P, Sarataphan N, Phantana S, Sukhumsirichart W. PCR based method for identification of zoonostic Brugia malayi microfilariae in domestic cats. *Mol Cell Probes*. (2002) 16:129–35. doi: 10.1006/mcpr.2001.0402

7. Nuchprayoon S, Sangprakarn S, Junpee A, Nithiuthai S, Chungpivat S, Poovorawan Y. Differentiation of Brugia malayi and Brugia pahangi by PCR-RFLP of ITS1 and ITS2. *Southeast Asian J Trop Med Public Health*. (2003) 34:67–73.

8. Rawangchue T, Sripirom N, Sungpradit S. Surveillance of zoonotic Brugia pahangi in monastery cats, Samphran district, Nakhon Pathom, Thailand. *Thai J Vet Med*. (2022) 52:117–25. doi: 10.56808/2985-1130.3196

9. Denham DA, Mcgreevy PB. Brugian filariasis: epidemiological and experimental studies. *Adv Parasitol*. (1977) 15:243–309. doi: 10.1016/S0065-308X(08)60530-8

10. Lau Y, Lee W, Xia J, Zhang G, Razali R, Anwar A, et al. Draft genome of Brugia pahangi: high similarity between B. Pahangi and B. Malayi. *Parasit Vectors*. (2015) 8:451. doi: 10.1186/s13071-015-1064-2

11. Palmieri JR, Ratiwayanto S, Masbar S, Tirtokusumo S, Rusch J, Marwoto HA. Evidence of possible natural infections of man with Brugia pahangi in South Kalimantan (Borneo), Indonesia. *Trop Geogr Med*. (1985) 37:239–44.

12. Tan LH, Fong MY, Mahmud R, Muslim A, Lau YL, Kamarulzaman A. Zoonotic Brugia pahangi filariasis in a suburbia of Kuala Lumpur City, Malaysia. *Parasitol Int*. (2011) 60:111–3. doi: 10.1016/j.parint.2010.09.010

13. Kennedy S, Patton S. Heartworms in a Bengal Tiger (*Panthera tigris*). *J Zoo Anim Med*. (1981) 12:20–2. doi: 10.2307/20094502

14. Atkins C, Moresco A, Litster A. Prevalence of naturally occurring Dirofilaria immitis infection among nondomestic cats housed in an area in which heartworms are endemic. *J Am Vet Med Assoc*. (2005) 227:139–43. doi: 10.2460/javma.2005.227.139

15. Murata K, Yanai T, Agatsuma T, Uni S. Dirofilaria immitis infection of a snow leopard (*Uncia uncia*) in a Japanese zoo with mitochondrial DNA analysis. *J Vet Med Sci*. (2003) 65:945–7. doi: 10.1292/jvms.65.945

16. Zahedi M, Vellayan S, Jeffery J, Krishnasamy M. A case of double infection with Brugia pahangi Buckley and Edeson, 1956 and Dirofilaria immitis Leidy 1856, in a Malaysian clouded leopard, *Neofelis nebulosa*. *Vet Parasitol*. (1986) 21:135–7. doi: 10.1016/0304-4017(86)90154-8

17. Ruiz de Ybáñez MR, Martínez-Carrasco C, Martínez JJ, Ortiz JM, Attout T, Bain O. Dirofilaria immitis in an African lion (*Panthera leo*). *Vet Rec*. (2006) 158:240–2. doi: 10.1136/vr.158.7.240

18. Mazzariol S, Cassini R, Voltan L, Aresu L, Regalbono AF. Heartworm (Dirofilaria immitis) infection in a leopard (*Panthera pardus pardus*) housed in a zoological park in North-Eastern Italy. *Parasit Vectors*. (2010) 3:25. doi: 10.1186/1756-3305-3-25

19. Lamm MG, Roelke ME, Greiner EC, Steible CK. Microfilariae in the free-ranging Florida panther (*Felis concolor coryi*). *J Helminthol Soc Wash*. (1997) 64:137–41.

20. Nelson GS, Heisch RB, Furlong M. Studies in filariasis in East Africa. II. Filarial infections in man, animals, and mosquitoes on the Kenya coast. *Trans R Soc Trop Med Hyg*. (1962) 56:202–17. doi: 10.1016/0035-9203(62)90155-4

21. Rosenblatt JE. Laboratory diagnosis of infections due to blood and tissue parasites. *Clin Infect Dis*. (2009) 49:1103–8. doi: 10.1086/605574

22. Chalifoux L, Hunt RD. Histochemical differentiation of Dirofilaria immitis and Dipetalonema reconditum. *J Am Vet Med Assoc*. (1971) 158:601–5.

23. Casiraghi M, Bain O, Guerrero R, Martin C, Pocacqua V, Gardner SL, et al. Mapping the presence of *Wolbachia pipientis* on the phylogeny of filarial nematodes: evidence for symbiont loss during evolution. *Int J Parasitol*. (2004) 34:191–203. doi: 10.1016/j.ijpara.2003.10.004

24. Laidoudi Y, Ringot D, Watier-Grillot S, Davoust B, Mediannikov O. A cardiac and subcutaneous canine dirofilariosis outbreak in a kennel in Central France. *Parasite*. (2019) 26:72. doi: 10.1051/parasite/2019073

25. Casiraghi M, Anderson T, Bandi C, Bazzocchi C, Genchi C. A phylogenetic analysis of filarial nematodes: comparison with the phylogeny of Wolbachia endosymbionts. *Parasitology*. (2001) 122:93–103. doi: 10.1017/S0031182000007149

26. Junsiri W, Kamkong P, Chinkangsadarn T, Ouisuwan S, Taweethavonsawat P. Molecular identification and genetic diversity of equine ocular setariasis in Thailand based on the COI, 12S rDNA, and ITS1 regions. *Infect Genet Evol*. (2023) 110:105425. doi: 10.1016/j.meegid.2023.105425

27. Kumar S, Stecher G, Li M, Knyaz C, Tamura C. MEGA X: molecular evolutionary genetics analysis across computing platforms. *Mol Biol Evol*. (2018) 35:1547–9. doi: 10.1093/molbev/msy096

28. Felsenstein J. Confidence limits on phylogenies: an approach using the bootstrap. *Evolution*. (1985) 39:783–91. doi: 10.2307/2408678

29. Nei M, Kumar S. *Molecular evolution and phylogenetics*. New York: Oxford University Press (2000).

30. Müller-Graf CDM. A Coprological survey of intestinal parasites of wild lions (*Panthera leo*) in the Serengeti and the Ngorongoro crater, Tanzania, East Africa. *J Parasitol*. (1995) 81:812–4. doi: 10.2307/3283987

31. Dashe D, Berhanu A. Study on gastrointestinal parasitism of wild animals in captivity at the zoological garden of Haramaya University, Ethiopia. *Open J Vet Med*. (2020) 10:173–84. doi: 10.4236/ojvm.2020.109015

32. Bjork KE, Averbeck GA, Stromberg BE. Parasites and parasite stages of free-ranging wild lions (*Panthera leo*) of northern Tanzania. *J Zoo Wildl Med*. (2000) 31:56–61. doi: 10.1638/1042-7260(2000)031[0056:PAPSOF]2.0.CO;2

33. Young E. Some important parasitic and other diseases of lion, *Panthera leo*. In the Kruger1national park. *J S Afr Vet Assoc*. (1975) 46:181–3.

34. Pawar RM, Lakshmikantan U, Hasan S, Poornachandar A, Shivaji S. Detection and molecular characterization of ascarid nematode infection (Toxascaris leonina and Toxocara cati) in captive Asiatic lions (*Panthera leo persica*). *Acta Parasitol*. (2012) 57:67–73. doi: 10.2478/s11686-012-0012-y

35. Dennig HK, Brocklesby DW. Babesia pantherae sp. nov., a piroplasm of the leopard (*Panthera pardus*). *Parasitology*. (1972) 64:525–32. doi: 10.1017/S0031182000045595

36. Averbeck GA, Bjork KE, Packer C, Herbst L. Prevalence of hematozoans in lions (*Panthera leo*) and cheetah (*Acinonyx jubatus*) in Serengeti National Park and Ngorongoro crater, Tanzania. *J Wildl Dis*. (1990) 26:392–4. doi: 10.7589/0090-3558-26.3.392

37. Lopez-Rebollar LM, Penzhorn BL, de Waal DT, Lewis BD. A possible new piroplasm in lions from the republic of South Africa. *J Wildl Dis*. (1999) 35:82–5. doi: 10.7589/0090-3558-35.1.82

38. Bosman AM, Venter EH, Penzhorn BL. Occurrence of Babesia felis and Babesia leo in various wild felid species and domestic cats in southern Africa, based on reverse line blot analysis. *Vet Parasitol*. (2007) 144:33–8. doi: 10.1016/j.vetpar.2006.09.025

39. Squarre D, Nakamura Y, Hayashida K, Kawai N, Chambaro H, Namangala B, et al. Investigation of the piroplasm diversity circulating in wildlife and cattle of the greater Kafue ecosystem, Zambia. *Parasit Vectors*. (2020) 13:599. doi: 10.1186/s13071-020-04475-7

40. Mukarati NL, Vassilev GD, Tagwireyi WM, Tavengwa M. Occurrence, prevalence and intensity of internal parasite infections of African lions (*Panthera leo*) in enclosures at a recreation park in Zimbabwe. *J Zoo Wildl Med*. (2013) 44:686–93. doi: 10.1638/2012-0273R.1

41. Mathison BA, Couturier MR, Pritt BS. Diagnostic identification and differentiation of microfilariae. *J Clin Microbiol*. (2019) 57:e00706–19. doi: 10.1128/JCM.00706-19

42. Ravindran R, Varghese S, Nair SN, Balan VM, Lakshmanan B, Ashruf RM, et al. Canine filarial infections in a human Brugia malayi endemic area of India. *Biomed Res Int*. (2014) 2014:630160:1–9. doi: 10.1155/2014/630160

43. Yen PK, Mak JW. Histochemical differentiation of Brugia, Wuchereria, Dirofilaria and Breinlia microfilariae. *Ann Trop Med Parasitol*. (1978) 72:157–62. doi: 10.1080/00034983.1978.11719298

44. Nuchprayoon S, Junpee A, Poovorawan Y, Scott AL. Detection and differentiation of filarial parasites by universal primers and polymerase chain reaction-restriction fragment length polymorphism analysis. *Am J Trop Med Hyg*. (2005) 73:895–900. doi: 10.4269/ajtmh.2005.73.895

45. Meetham P, Kumlert R, Gopinath D, Yongchaitrakul S, Tootong T, Rojanapanus S, et al. Five years of post-validation surveillance of lymphatic filariasis in Thailand. *Infect Dis Poverty*. (2023) 12:113. doi: 10.1186/s40249-023-01158-0

46. Zielke E, Hinz E, Sucharit S. Lymphatic filariasis in Thailand: a review on distribution and transmission. *Tropenmed Parasitol*. (1993) 15:141–8.

47. Satjawongvanit H, Phumee A, Tiawsirisup S, Sungpradit S, Brownell N, Siriyasatien P, et al. Molecular analysis of canine filaria and its Wolbachia endosymbionts in domestic dogs collected from two animal university hospitals in Bangkok metropolitan region, Thailand. *Pathogens*. (2019) 8:114. doi: 10.3390/pathogens8030114

48. Gaillard CM, Pion SD, Hamou H, Sirima C, Bizet C, Lemarcis T, et al. Detection of DNA of filariae closely related to Mansonella perstans in faecal samples from wild non-human primates from Cameroon and Gabon. *Parasit Vectors*. (2020) 13:313. doi: 10.1186/s13071-020-04184-1

49. Bazzocchi C, Jamnongluk W, O'Neill SL, Tim JC, Anderson TJC, Genchi C, et al. Wsp gene sequences from the Wolbachia of filarial nematodes. *Curr Microbiol*. (2000) 41:96–100. doi: 10.1007/s002840010100

frontiers | Frontiers in Veterinary Science

TYPE Original Research
PUBLISHED 09 May 2024
DOI 10.3389/fvets.2024.1403920

Check for updates

OPEN ACCESS

EDITED BY
Hussam Askar,
Al Azhar University, Egypt

REVIEWED BY
Bernardo Pereira Moreira,
University of Giessen, Germany
Mahmoud Abdelhamid,
Aswan University, Egypt

*CORRESPONDENCE
Min-hao Zeng
✉ zengminhao@stu.just.edu.cn
Shan Li
✉ slove0408@163.com

†These authors have contributed equally to this work

RECEIVED 20 March 2024
ACCEPTED 29 April 2024
PUBLISHED 09 May 2024

CITATION
Zeng M-h, Li S, Lv Q-b, Wang X-x, Qadeer A and Mahmoud MH (2024) Modulation of the rat intestinal microbiota in the course of *Anisakis pegreffii* infection. *Front. Vet. Sci.* 11:1403920. doi: 10.3389/fvets.2024.1403920

COPYRIGHT
© 2024 Zeng, Li, Lv, Wang, Qadeer and Mahmoud. This is an open-access article distributed under the terms of the Creative Commons Attribution License (CC BY). The use, distribution or reproduction in other forums is permitted, provided the original author(s) and the copyright owner(s) are credited and that the original publication in this journal is cited, in accordance with accepted academic practice. No use, distribution or reproduction is permitted which does not comply with these terms.

Modulation of the rat intestinal microbiota in the course of *Anisakis pegreffii* infection

Min-hao Zeng[1*†], Shan Li[2*†], Qing-bo Lv[3], Xiao-xu Wang[1], Abdul Qadeer[4] and Mohamed H. Mahmoud[5]

[1]School of Biotechnology, Jiangsu University of Science and Technology, Zhenjiang, China, [2]Jiangxi Provincial Key Laboratory of Cell Precision Therapy, School of Basic Medical Sciences, Jiujiang University, Jiujiang, China, [3]Key Laboratory of Zoonosis Research, Institute of Zoonosis, College of Veterinary Medicine, Ministry of Education, Jilin University, Changchun, China, [4]Department of Cell Biology, School of Life Sciences, Central South University, Changsha, China, [5]Department of Biochemistry, College of Science, King Saud University, Riyadh, Saudi Arabia

Background: *Anisakis* are globally distributed, marine parasitic nematodes that can cause human health problems, including symptoms such as vomiting, acute diarrhea, and allergic reactions. As parasitic nematodes that primarily affect the patient's digestive tract, intestinal helminths can interact directly with the host microbiota through physical contact, chemicals, or nutrient competition. It is widely accepted that the host microbiota plays a crucial role in the regulation of immunity.

Materials and methods: Nematodes collected from the abdominal cavity of marine fish were identified by molecular biology and live worms were artificially infected in rats. Infection was determined by indirect ELISA based on rat serum and worm extraction. Feces were collected for 16S rDNA-based analysis of microbiota diversity.

Results: Molecular biology identification based on ITS sequences identified the collected nematodes as *A. pegreffii*. The success of the artificial infection was determined by indirect ELISA based on serum and worm extraction from artificially infected rats. Microbiota diversity analysis showed that a total of 773 ASVs were generated, and PCoA showed that the infected group was differentiated from the control group. The control group contained five characterized genera (*Prevotellaceae* NK3B31 group, *Turicibacter*, *Clostridium sensu stricto* 1, *Candidatus Stoquefichus*, *Lachnospira*) and the infected group contained nine characterized genera (*Rodentibacter*, *Christensenella*, *Dubosiella*, *Streptococcus*, *Anaeroplasma*, *Lactococcus*, *Papillibacter*, *Desulfovibrio*, *Roseburia*). Based on the Wilcoxon test, four processes were found to be significant: bacterial secretion system, bacterial invasion of epithelial cells, bacterial chemotaxis, and ABC transporters.

Conclusion: This study is the first to analyze the diversity of the intestinal microbiota of rats infected with *A. pegreffii* and to determine the damage and regulation of metabolism and immunity caused by the infection in the rat gut. The findings provide a basis for further research on host-helminth-microbe correlationships.

KEYWORDS

***Anisakis pegreffii*, rat, microbiota, diversity analysis, host effects**

1 Introduction

Anisakiasis is a parasitic disease caused by the ingestion of larvae of the Anisakis nematode. These larvae are commonly found in marine fish worldwide. Consumption of raw or undercooked fish poses a risk of infection due to the presence of Anisakis larvae within the fish tissue (1). Symptoms of Anisakiasis typically include gastrointestinal disturbances such as vomiting, nausea and diarrhea (2). Additionally, allergic reactions and ectopic parasitism may occur due to the migration of the nematode larvae, presenting a potential health threat (3–6). The infection is prevalent globally and is particularly associated with regions where raw or lightly processed seafood is commonly consumed, such as Japan, Korea, China, Taiwan, Portugal, and Chile (7). In 2010, the European Food Safety Authority (EFSA) estimated that there were around 20,000 reported cases of Anisakiasis worldwide. In Japan alone, the average annual incidence of Anisakiasis in 2018–2019 was 19,737, based on insurance claims records (8, 9). Anisakiasis is widely prevalent in seas around the globe, have been identified by the FAO (Food and Agriculture Organization of the United Nations) as one of the 10 most important parasites affecting humans and fish (10).

As parasitic nematodes that primarily affect the patient's digestive tract, intestinal helminths can interact directly with the host microbiota through physical contact, chemical compounds, or nutritional competition. It is widely recognized that the host microflora plays a crucial role in regulating immunity (11–13). Parasites can also indirectly impact immunity and other physiological processes by regulating the host gut microbiota (14). Changes in gut microbes can also protect the host from parasites (15). Research has demonstrated that *Haemonchus contortus* has a significant impact on the gastrointestinal microbiota in lambs. It also reduces the α-diversity of the gastrointestinal microbial community in the rumen, abomasum, and duodenum, and disrupts the partitioning of amino acids for protein digestion and absorption (16). *Ascaris lumbricoides*, belonging to the superfamily Ascaridoidea along with Anisakis, is also capable of reducing the microbiota diversity of the porcine gut and altering the metabolic potential of the host (17).

It is of great interest to investigate whether Anisakiasis induces changes in the host gut microbiota. Using 16S rRNA sequence-based NGS sequencing and bioinformatics analysis, we researched the response of rat fecal microbiota communities to Anisakiasis to gain insight into how *A. pegreffii* affects host gut microbiota and metabolism. This statement provides a basis for further studies on the interactions between *Anisakis*-hosts-microbiota.

2 Materials and methods

2.1 Parasites collection

We obtained fresh, unfrozen marine fish such as Little Yellow Croaker (*Larimichthys polyactis*) and Largehead hairtail (*Trichiurus lepturus*) from markets in Shanghai City, China. The fish were dissected using scissors to expose the organs and digestive tract. Nematodes were isolated from tissues including the abdominal cavity, stomach, intestines, gonads, and muscles using forceps or needles. The worms were then washed three times with saline solution to remove any attached fish tissue.

2.2 Identification of parasites

The nematodes were categorized by microscopic observation and genomic DNA was extracted from randomly selected worms for molecular identification. In brief, the nematodes were homogenized in 200 μL of lysis buffer (Tris–HCl 100 mM, EDTA 25 mM, NaCl 500 mM, Protease K 10 μL), then incubated at 56°C for 6 h. After centrifugation at 12,000 rpm for 5 min to remove the precipitate, 200uL of Tris-saturated phenol: chloroform: isoamyl alcohol mixture (25, 24, 1, pH 8.0) were added, and then centrifuged at 12,000 rpm for another 5 min. The supernatant aqueous phase was transferred to a new tube. To extract genomic DNA, 200 μL of pre-cooled anhydrous ethanol was added to the sample, followed by thorough mixing. The mixture was then centrifuged at 12,000 rpm for 10 min, and the supernatant was carefully removed, leaving the precipitate behind. Wash the precipitate twice with 200 μL of 75% ethanol. Finally, dissolve the precipitate with ddH_2O. Genomic DNA was used as the template for PCR. The molecular identification by PCR was based on the ITS (Internal Transcribed Spacer) rDNA regions, the sequences were amplified using NC5 (5′- GTA GGT GAA CCT GCG GAA GGA TCA TT −3′) and NC2 (5′- TTA GTT TCT TTT CCT CCG CT −3′) primers (18, 19). PCR reaction (20 μL) contained 10 μL 2 × Hieff PCR Master Mix (Yeasen, Shanghai, China), 0.2 μL of each 10 μM NC5 and NC2 primers, ddH_2O up to 20 min were performed on the following conditions: 95°C for 3 min (initial denaturation), then 35 cycles of 95°C for 15 s (denaturation), 55°C for 15 s (annealing), and 72°C for 1 min (extension), and a final extension at 72°C for 5 min. The PCR products were analyzed by PCR-RFLP using *Hinf* I endonuclease (NEB, Beijing, China) and the PCR products were sequenced (20). For the elongation factor (EF1 α-1 nDNA) nuclear gene, the sequences were amplified using EF-F (5′- TCC TCA AGC GTT GTT ATC TGT T − 3′) and EF-R (5′- AGT TTT GCC ACT AGC GGT TCC -3′). The PCR reaction was essentially the same as above, but with an annealing temperature of 58°C (21). After sequencing, the obtained sequences and peak maps were aligned with the reference of EF1 α-1 nDNA sequences using SnapGene software 4.2.4[1].

2.3 Artificial infection of rats

With reference to the methodology of previous studies, a total of 6 5-6-week-old Sprague–Dawley (SD) rats were artificially infected with 10 live *A. pegreffii* using the infant rectal drug delivery tubes (22). Briefly, active worms are inserted into the tube stretching from the mouth of the tubes, the tubes were inserted into the rats' stomach, and a syringe was used to push the worms into the stomach. Six additional rats were used as negative controls. Serum samples were collected at the 1, 2, 3, and 5 weeks after infection, and feces were collected at 5 weeks after infection. The collected samples were either stored at −80°C or directly used in additional experiments. Five *A. pegreffii* were homogenized in pre-cold PBS (Phosphate Buffered Saline). The precipitate was removed by centrifugation, and the supernatant protein solution was filtered using a 0.22 μm filter. The concentration was determined using a BCA kit (Beyotime, Shanghai, China). An

1 www.snapgene.com

indirect ELISA was performed using worm extraction proteins and rat serum to diagnose the success of the artificial infection. Briefly, 96-well microtiter plates were coated with 1 μg of worm extraction protein in 100 μL of carbonate buffer (150 mM Na2CO3, 349 mM NaHCO3, pH 9.6) and incubated at 4°C overnight. After washing three times, the plates were blocked with 5% bovine serum albumin (BSA) for 2 h at 37°C. Sbsequently, rat sera diluted in PBST at 1:400 were added for 2 h at 37°C. HRP-conjugated goat anti-rat IgG antibody (Servicebio, Wuhan, China) was used as a secondary antibody at a 1:5000 dilution, and the reaction were revealed by TMB (Beyotime, Shanghai, China) for 15 min at 37°C and stopped by 2 M H2SO4. The reaction was measured at 450 nm with an ELISA reader. Data are represented as the mean ± standard deviation (SD), and the *t*-test was used for comparisons between the two groups. GraphPad Prism 8.3.1 (GraphPad Software, Inc., San Diego, CA, United States) was utilized for statistical analysis and generating graphs. *p*-values <0.05 were considered statistically significant.

2.4 Analysis of 16S rRNA gene sequences

The extraction of fecal genomic DNA and the 16S amplification were both provided by Wuhan Wanmo Technology Co., Ltd. The 16S rDNA V3-V4 region of the sample DNA was amplified using common primers 341-F (5′- CCT AYG GGR BGC ASC AG −3′) and 806-R (5′- GGA CTA CNN GGG TAT CTA AT −3′), and the resulting products were used to construct the libraries (21), which were then sequenced using the BGISEQ-500 platform. Poor quality bases of the paired-end sequence data were trimmed using Trimmomatic v0.36 (23) and were merged using FLASH v1.20 (24). The sequences were then imported into QIIME2 (25). Species annotation was performed on the obtained Amplicon Sequence Variants (ASVs) based on the 16S bacterial ribosomal databases SILVA (Release 128) (26), RDP (v1.6) (27), and Greengene (Release 13.5) (28), and the number of annotations and scores were counted at the phylum, family, and genus levels, and beta diversity was analyzed by PCoA based on Bray-Curtis and Jaccard distance. Species differing between groups were screened using Linear discriminant analysis Effect Size (LEfSe), (LDA > 2 as the threshold). The results of the analysis were visualized through the online tool TUTOOL[2].

3 Results

3.1 Diagnosis for *Anisakis pegreffii* infection in rats

The ITS fragment (approximately 1,000 bp) from each sample was amplified (Figure 1A). The PCR-RFLP showed three sharp fragments of 370, 300 and 250 bp consistent with *A. pegreffii* (Figure 1B). After sequencing, the target sequence showed 99.5% identity with *A. simplex* and up to 100% identity with *A. pegreffii* (GenBank Accession: AY821739.1 and MF820020.1, in Supplementary Figure S1). Based on the EF1 α-1 sequence of *A. simplex* (s. s.) and *A. pereffii* (GenBank Accession: KP326558.1 and MH443145.1), the sequences of the larvae obtained in this study were consistent with *A. pegreffii* and did not exist overlapping peaks (Figures 1C,D). Therefore, based on the detection method we used, the larvae used in this study were preliminarily identified as *A. pegreffii*. Based on the diagnostic results of the indirect ELISA assay, the results of all rat sera in the infection group were significantly higher than those of the control group at 2 weeks post-infection (wpi). As the duration of infection increased, the optical density 450 nm and P/N (Positive group/Negative group) values of the ELISA results for the infection group also increased significantly. At 5 wpi, the mean P/N values for both the infection and control groups were as high as 11.6 (Figure 1E). Therefore, the rats in the infected group were diagnosed with *A. pegreffii* infection, while those in the negative group were not infected.

3.2 *Anisakis pegreffii* restructure microbiota community in rats

A total of 773 ASVs were generated. The number of ASVs increased gradually with the sequencing depth, which met the analysis requirements (Supplementary Figure S2A). The relative abundance curves of the top 200 ASVs were smooth, indicating an even distribution of ASVs (Supplementary Figure S2B). At more than 3 biological replicates in each of the infection and control groups, the cumulative species curve tended to flatten, and the number of species did not significantly change with additional replicates. The number of replicates met the analysis requirements (Supplementary Figure S2C). Alpha diversity was assessed using Shannon's index at various levels. The results indicated no significant differences in diversity (Figure 2A). However, beta-diversity analyses revealed a significant separation of clustering profiles of the PCoA indices based on Bray-Curtis and Jaccard (Figures 2B,C). This suggests that *A. pegreffii* infections have a significant impact on the composition of the gut microbiota.

A total of 11 Phylum were obtained from the annotation of the two groups, with roughly the same composition in both groups (Figure 2D). Among them, Firmicutes and Bacteroidota were the dominant Phylum in both groups. In the control group, 61.93% of the species belonged to Firmicutes, with an abundance of 59.75, and 29.66% of the species belonged to Bacteroidota, with an abundance of 33.89%. In the infected group, 58.82% of the species belonged to the Firmicutes Phylum with an abundance of 40.15 and 32.86% of the species belonged to the Anamorph Phylum with an abundance of 35.76%. The abundance of the Proteobacteria Phylum was higher in the infected group compared to the control group. The top 50 Families and Genera in terms of abundance were selected and analyzed at the Family and Genus level, respectively, and it was evident that there were significant changes between the infected group and the control group at the Family and Genus level (Figures 2E,F).

The relative abundance of the top 30 families and genera in each group was statistically analyzed (Figures 3A,B). The families with more than 10% abundance in the control group were Lactobacillaceae, Lachnospiraceae and Prevotellaceae, and the families with more than 10% abundance in the infected group were Enterobacteriaceae, Bacteroidaceae, Lachnospiraceae, Lactobacillaceae and Muribaculaceae; compared to the control group, the relative abundance of Enterobacteriaceae in the infected group increased by 18.4%, Bacteroidaceae by 7.42%,

2 http://cloudtutu.com.cn/

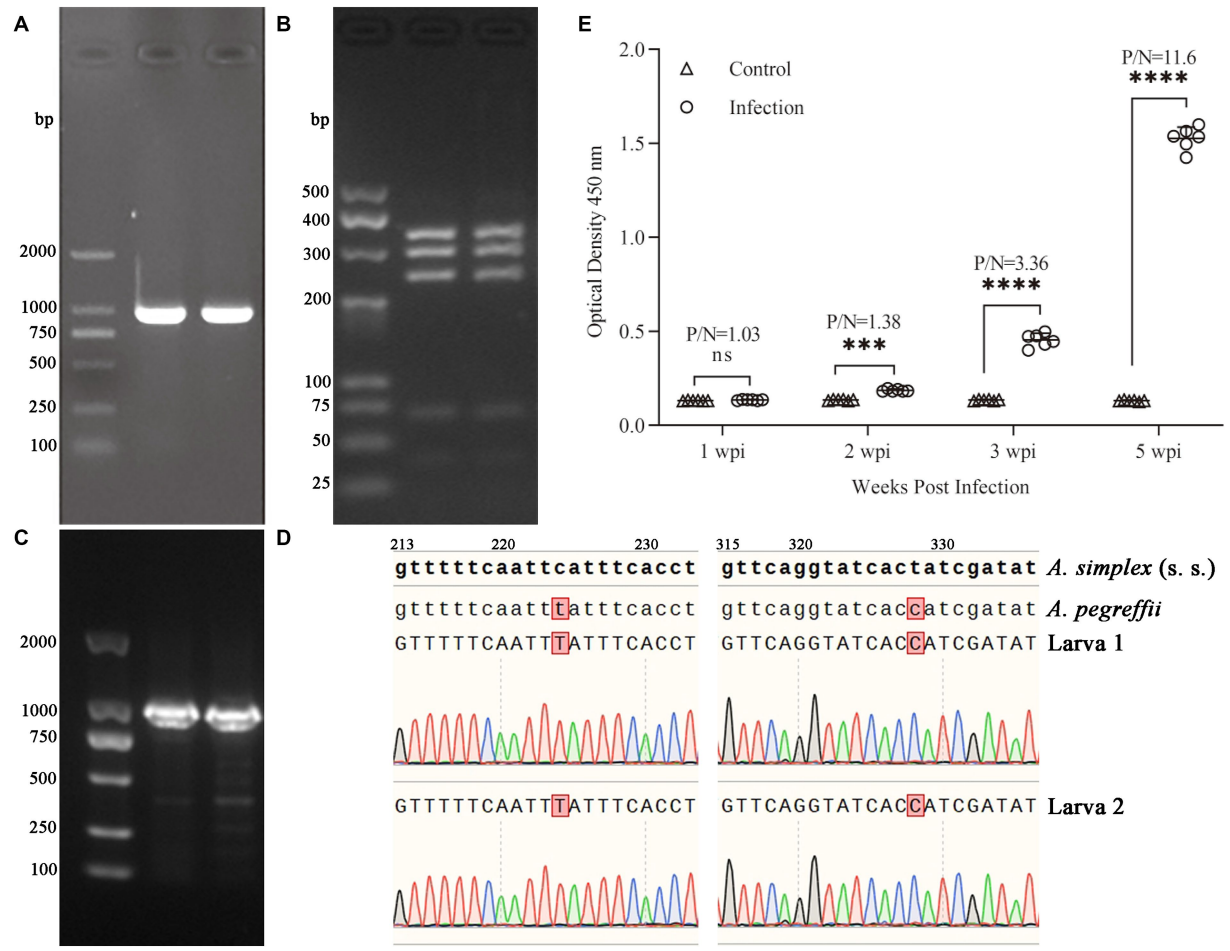

FIGURE 1
Electrophoresis of PCR products for ITS sequences in 1.0% agarose gel **(A)** and PCR-RFLP in 3.5% agarose gel **(B)** of *A. pegreffii*. The fragment sizes were all as expected. Results of electropherogram in 1.0% agarose gel **(C)** and alignment **(D)** of EF1 α-1 sequences. Indirect ELISA results **(E)** showed that OD450 of the infected group was significantly higher than that of the control group, and the P/N (Positive/Negative) values had reached 3.36 at 3 wpi, indicating that the rats were successfully infected with *A. pegreffii*.

Lactobacillaceae by 14.05%, Prevotellaceae by 8.46% and Peptostreptococcaceae by 4.28%. The genera with an abundance greater than 10% in the control group were *Lactobacillus* and Muribaculaceae, and the genera with an abundance greater than 10% in the infected group were *Bacteroides*, *Lactobacillus*, and Muribaculaceae; the relative abundance of *Escherichia-Shigella* genera increased by 19.71%, *Bacteroides* by 8.07%, and Lachnospiraceae_NK4A136_group by 3.00% compared to the control group increased by 19.71%, *Bacteroides* by 8.07% and Lachnospiraceae_NK4A136_group by 3.00% compared to the control group (Figures 3C,D).

For discovering significant biomarkers between different groups, the LEfSe analysis was performed. The characteristic homogeneous genera in each group were screened and the results are shown in Figure 4A, and the intergroup differences present at each genus level are shown in Figure 4B. The control group contained five characterized genera (Prevotellaceae NK3B31 group, *Turicibacter*, *Clostridium sensu stricto* 1, *Candidatus Stoquefichus*, *Lachnospira*) and the infected group contained nine characterized genera (*Rodentibacter*, *Christensenella*, *Dubosiella*, *Streptococcus*, *Anaeroplasma*, *Lactococcus*, *Papillibacter*, *Desulfovibrio*, *Roseburia*).

3.3 Reorganization for intestinal microbiota correlation

To represent the effect of *A. pegreffii* infection on rat intestinal microbiota, intragroup abundance correlation network diagrams were constructed at the Genus level, respectively. The correlation coefficients were analyzed based on the Spearman method for the 60 most abundant Genera, with the parameters of $R > 0.6$ and $p < 0.01$ (Figure 5). In the control group, the network' formed two large clusters, while the remaining genera formed smaller connections. The core genera were identified as *Butyricimonas*, *Alloprevotella*, Lachnospiraceae_UCG-006, A2, g_Erysipelotrichaceae, and g_Desulfovibrionaceae based on their weighted degree of centrality. The infection group exhibited two significantly large clusters in the network, which were connected to smaller clusters. The core genera identified were *Lachnoclostridium*, *Eubacterium_coprostanoligenes_* group, Lachnospiraceae_UCG-006, and *Alistipes*. Significant changes in abundance and connectivity of differential marker genera in the interactions network are shown in Table 1. Out of all the differential genera, 9 were absent in the network between the control and infection groups, 6 were present only in the interactions network with the

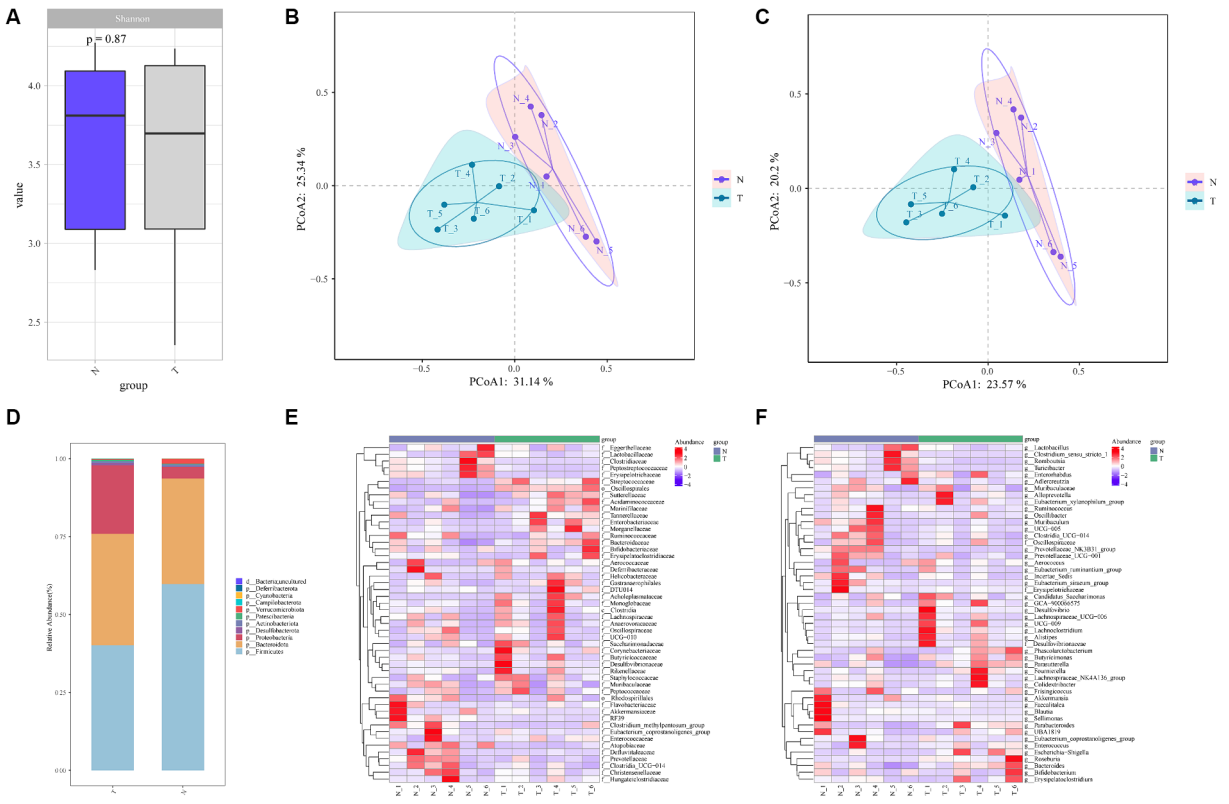

FIGURE 2
Alpha and beta diversity analyses between feces microbiota of *A. pegreffii* infection rats and control rats. N-negative control samples, T-infection samples. **(A)** Shannon Index Box Chart indicated no significant differences in alpha diversity. Beta-diversity analyses of clustering profiles based on Bray-Curtis **(B)** and Jaccard **(C)** showed the existence of significantly differences in beta diversity. **(D)** Bar plot of species composition at Phylum level. **(E)** Family level heatmap maps. **(F)** Genus-level heatmap maps.

control group, and 8 were present only in the interactions network with the infected group. Three genera were present in the interaction network for both the control and infected groups. The *Prevotellaceae_* NK3B31_group had greater weighted centrality in both groups, while *Romboutsia* and *Lachnoclostridium* had greater weighted centrality in the infected group compared to the control group.

3.4 Functional gene composition of intestinal microbiota in response to *Anisakis pegreffi*

To further research on metabolic differences in microbiota, based on the ASVs and abundances identified by 16S rDNA, the PICRUSt2 tool was used to predict metagenomic functional information (29). Based on the relative abundance of the top 30 functions, the Bray distance was calculated between samples and hierarchical clustering was performed (Figure 6A). The infection group and control group were not clustered together and did not form two independent clusters. The results of the PCoA analysis showed partial overlap between the infected and control groups (Figure 6B). The analysis of the differences between the within and between groups indicated that the between-group difference was larger than the within-group difference ($R > 0$) for the infected and control groups, but it was not significant ($p > 0.01$) (Figure 6C). Based on the Wilcoxon test, four processes were found to be significant: bacterial secretion system, bacterial invasion of epithelial cells, bacterial chemotaxis, and ABC transporters (Figure 6D). All these processes were more abundant in the infection group than in the control group.

4 Discussion

Animal models of infection are widely employed to investigate the cause-effect relationships between helminth colonization, shifts in gut microbial composition, and modifications in the immune or metabolic functions of the host (30). However, interactions between helminths and the gut microbiota vary significantly depending on the specific host–parasite combination being studied (31). Consequently, comparing data across different host–parasite systems, even if they involve the same helminth species, could potentially lead to misunderstandings. Conversely, research on naturally infected humans may offer insights into the relationships between gut microbial composition and infection with one or more parasites (32). Moreover, such studies often lack evidence of a causal link between specific gut microbial signatures and susceptibility to or the pathophysiology of infection (33). Therefore, it is important to conduct complementary studies that involve naturally infected human populations in endemic regions alongside experimental animal models to advance our understanding of the

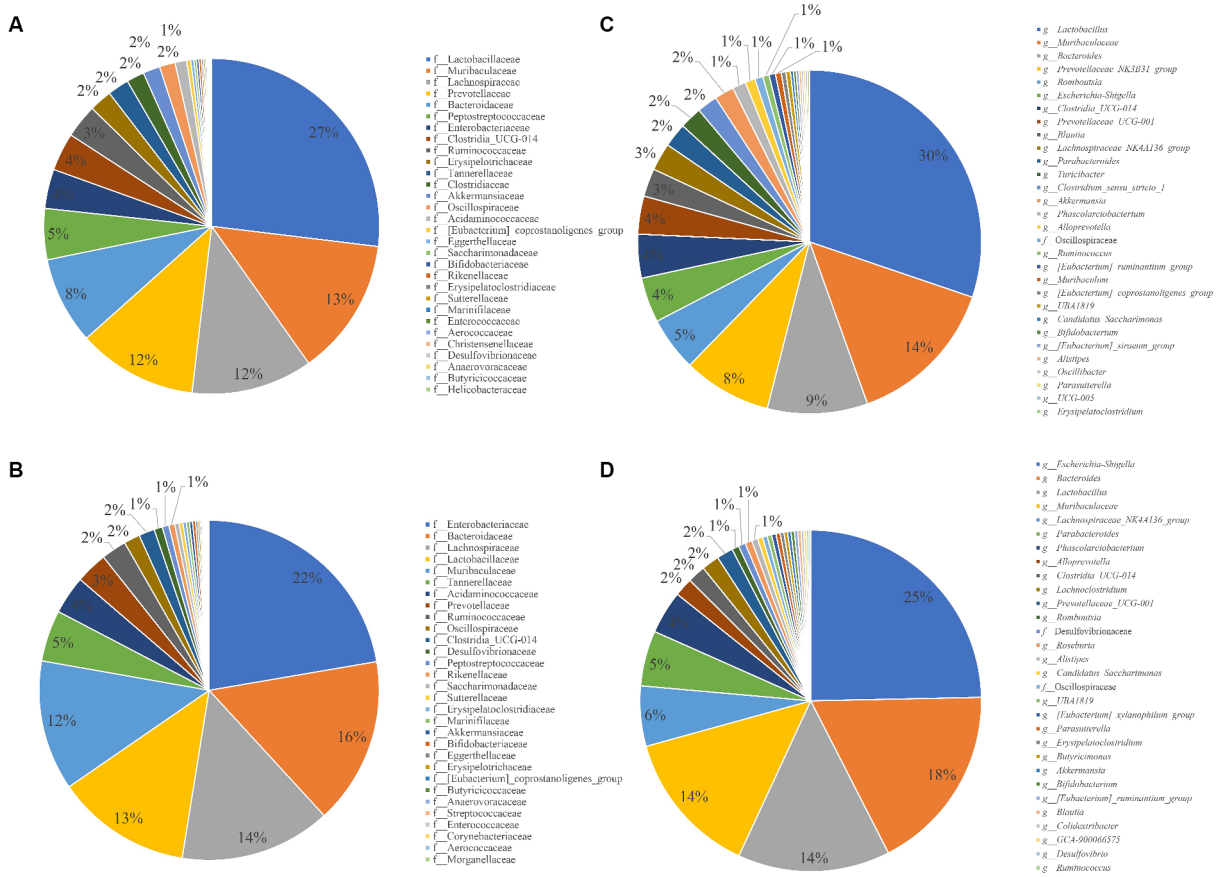

FIGURE 3
Pie chart for the proportion of species in different groups and taxonomic levels. **(A)** Composition of gut microbiota at family level in control group. **(B)** Composition of gut microbiota at family level in Infection group. **(C)** Control group at the Genus level. **(D)** Infection group at the Genus level.

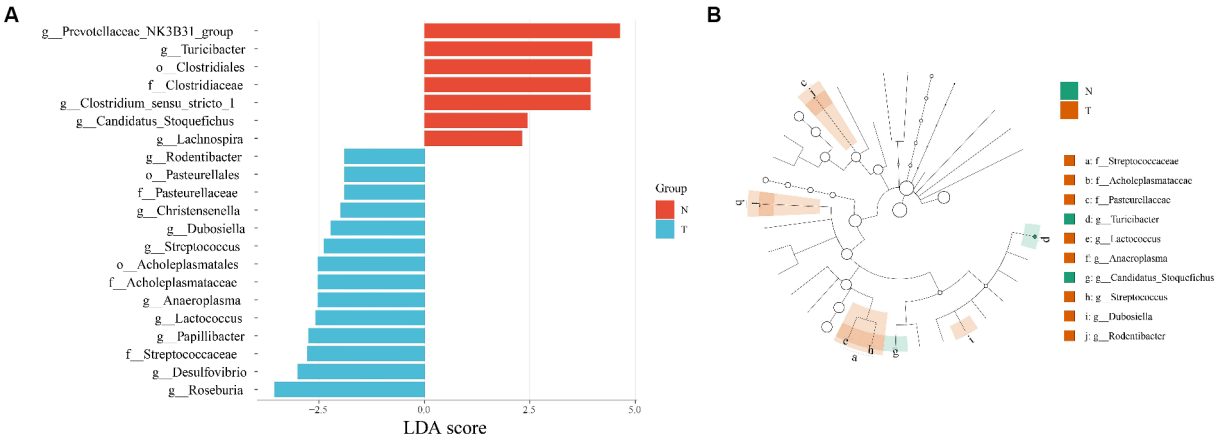

FIGURE 4
Distribution of LDA values **(A)** and evolutionary branching maps **(B)** of divergent species.

role of the gut microbiota in human parasitic diseases (34). The gut microbiota is a crucial element of the immune system and overall health (35). In this study, rats were used to examine the links between *A. pegreffii* infections and the composition of the host gut microbiota. As far as we know, this is the first-ever study investigating the associations between Anisakiasis and the gut microbiota of the host (rats).

Given the recognized risk posed by *Anisakis* nematodes, further investigation into their impact on the host is warranted (36). Our current study found that *A. pegreffii* infection did not lead to

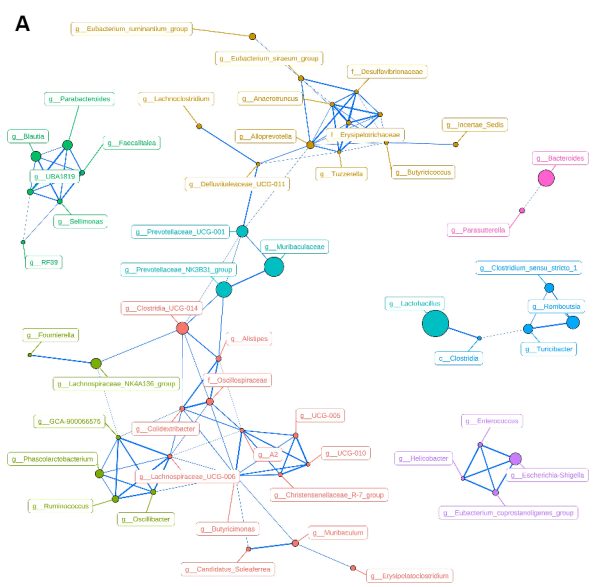

FIGURE 5
Network analysis chart in control group **(A)** and Infection group **(B)**.

significant alterations in the alpha diversity of rat gut microbiota. However, differences in beta diversity were observed, which is in line with previous research (32, 37, 38). Interestingly, we observed a significant reduction in the abundance of the Genus *Turicibacter* and the Order Clostridiales in the infected group, suggesting potential intestinal inflammation (39). This finding is consistent with the results of research that showed a decrease in Clostridiales due to *Toxocara canis* infection. Despite the known ability of Firmicutes bacteria to metabolize free fatty acids and bile acids, resulting in the production of butyrate, the reduced abundance of Firmicutes phylum in our study did not reflect anti-inflammatory properties (40, 41).

The Prevotellaceae_NK3B31_group is a key group of intestinal microorganisms, typically considered for their roles as probiotic bacteria producing short-chain fatty acid (SCFA). They are capable of producing various essential salts and fatty acids from dietary fiber, thereby playing a significant role in animal growth and development. Moreover, an increase in the abundance of the population of this group has been associated with the mitigation of gastric ulcer pathology (42–45). The high weighted degree of centrality of this bacterial group in both the control and infected groups indicates its importance in the intestinal tract of both groups of test animals. However, a significant decrease in the abundance (8% in control groups, 0.1% in infection groups) of this genus in the infection group resulted in a substantial alteration in gut microbiota diversity. Bacteria of the genus *Turicibacter* are also important members of the mammalian gut microbiota with evidence suggesting their involvement in modifying host bile acids and lipids, thereby regulating host lipid metabolism (46, 47). In the infection group, there was a significant decrease in the relative abundance of this genus (2% in control groups, 0.038% in infection groups), leading to a diminished capacity to regulate the overall gut microbiota. Intestinal helminth infections often increase the microbial origin of SCFAs, which can help regulate allergic diseases (48). However, this phenomenon was not observed in the present study. The Genus *Clostridium*_sensu_stricto_1 is known for its production of butyrate, which plays an important role in the development of intestinal epithelial cells and hosts energy supply (49, 50). In the present study, the relative abundance of this genus was significantly reduced (1.9% in control groups, 0.031% in infection groups), along with its ability to regulate the gut microbiota. The decreased level of *Romboutsia* (4.9% in control groups, 0.65% in infection groups) can lead to an increase in intestinal pH, subsequently promoting the proliferation of harmful bacteria like *Streptococcus* (0.007% in control groups, 0.052% in infection groups) (51). In heavily infected individuals with roundworms, *Streptococcus* was found to be the most prevalent bacteria in the intestines, significantly decreasing the pro-inflammatory activity of the host colonic mucosa (52, 53). The metabolism of butyric acid in the host's intestines has been significantly altered. Indigestible complex carbohydrates, such as dietary fiber, serve as an energy source for specific bacteria, resulting in the production of various short-chain fatty acid molecules, including butyrate. These microbial compounds play a role in regulating various metabolic pathways in the gut and other parts of the body, such as the liver, adipose tissue, muscle, and brain. It's now well-established that these metabolites have a significant impact on several physiological processes, including energy balance, glucose, and lipid metabolism, inflammation, as well as immunity, and cancer (54–56). Interestingly, the infection group showed enrichment of *Roseburia* (0.015% in control groups, 0.64% in infection groups), typically considered a probiotic that produces butyric acid and contributes to asthma prevention in children (57).

Moreover, the presence of *Lactococcus* was augmented in the infected cohort, aimed at curbing the onset of hypersensitivity reactions (58). The increase in both *Desulfovibrio* (0.043% in control groups, 0.198% in infection groups) and *Streptococcus* may indicate issues with bile acid metabolism, which aligns with the previously mentioned decrease in fatty acid synthesis. The Genus *Desulfovibrio* is commonly regarded as a harmful group of bacteria that produces reduced sulfate, generating

TABLE 1 Weighted degree of divergent species with significant changes in the relative abundance.

Species	Weighted degree		Wilcoxon *p*-values
	Control	Infection	
Romboutsia	1.943984	5.653698	0.015152
Lachnoclostridium	0.967048	12.45731	0.025974
Prevotellaceae_NK3B31_group	4.726978	4.724962	0.002165
RF39	1.848676	-	0.012907
Butyricicoccus	6.533377	-	0.02472
Eubacterium_siraeum_group	4.706891	-	0.016711
Escherichia-Shigella	2.963387	-	0.041126
Turicibacter	2.844556	-	0.002165
*Clostridium*_sensu_stricto_1	1.897321	-	0.002165
Desulfovibrio	-	7.60785	0.009622
Papillibacter	-	4.859768	0.002778
Streptococcus	-	1.947273	0.007796
f__Peptococcaceae	-	1.883714	0.008658
Roseburia	-	1.881372	0.007796
Eubacterium_ventriosum_group	-	1.877816	0.041126
Anaeroplasma	-	0.98638	0.002778
Lactococcus	-	0.96375	0.004337
Christensenella	-	-	0.002671
Candidatus_Stoquefichus	-	-	0.002778
Dubosiella	-	-	0.009622
Anaerostignum	-	-	0.028441
Christensenellaceae	-	-	0.036379
Faecalibaculum	-	-	0.019373
Lachnospira	-	-	0.009622
Rodentibacter	-	-	0.009622
Erysipelotrichaceae	-	-	0.012592

endogenous H_2S that can be detrimental to the organism (59, 60). The relative abundance of *Desulfovibrio* spp. is elevated in the intestinal tract of individuals with colitis, inflammatory bowel disease, and irritable bowel syndrome (61–63). The genus of *Escherichia-Shigella* was more abundant in the infection group (4.104% in control groups, 23.82% in infection groups), which is typically associated with dysentery (64). Additionally, it is positively associated with sulfate toxin metabolism (65). The genus *Bacteroides* was more abundant in the infection group (9.11% in control groups, 17.19% in infection groups) and can produce toxins that cause secretory diarrhea and colonic epithelial damage, leading to chronic colitis and colorectal cancer (66, 67). Bacteria have the potential to harm the host's health by invading tissue sites and evading the immune system. One of the ways they achieve this is through the secretion of virulent proteins, which can be released into the host cell or surrounding environment (68). Nevertheless, a more in-depth comprehension of the alterations in the intestinal microbiota in infected states can facilitate the treatment by improving the microbiological environment. For instance, the regulation of the composition of gut microbes may be employed to alleviate systemic inflammation and cardiovascular disease caused by chronic nephritis (69). Such research is also frequently employed in the investigation of neurological disorders (70–72).

In this study, based on the analysis of microbiota diversity and functional prediction, the infected group exhibited notable increases in the Bacterial secretion system, invasion of epithelial cells, and ABC transporter functions, implying significant microbiota-induced impact to the host gut.

5 Conclusion

In this study, rats infected with *A. pegreffii* were obtained by artificial infection and infection was determined by indirect ELISA diagnosis based on worm extraction. For the first time, the microbiota diversity analysis of host feces was performed using 16S sequencing. The results indicate that rats infected with *A. pegreffii* exhibited significant changes in microbiota diversity. The rats' SCFAs metabolism was affected, which in turn affected their nutrient metabolism and immune function. The increase in the abundance of pathogenic enteric bacteria indicated that the gut flora had been invaded by pathogens. It provides a basis for future research on host-helminth-microbiota correlations and microbiota metabolism.

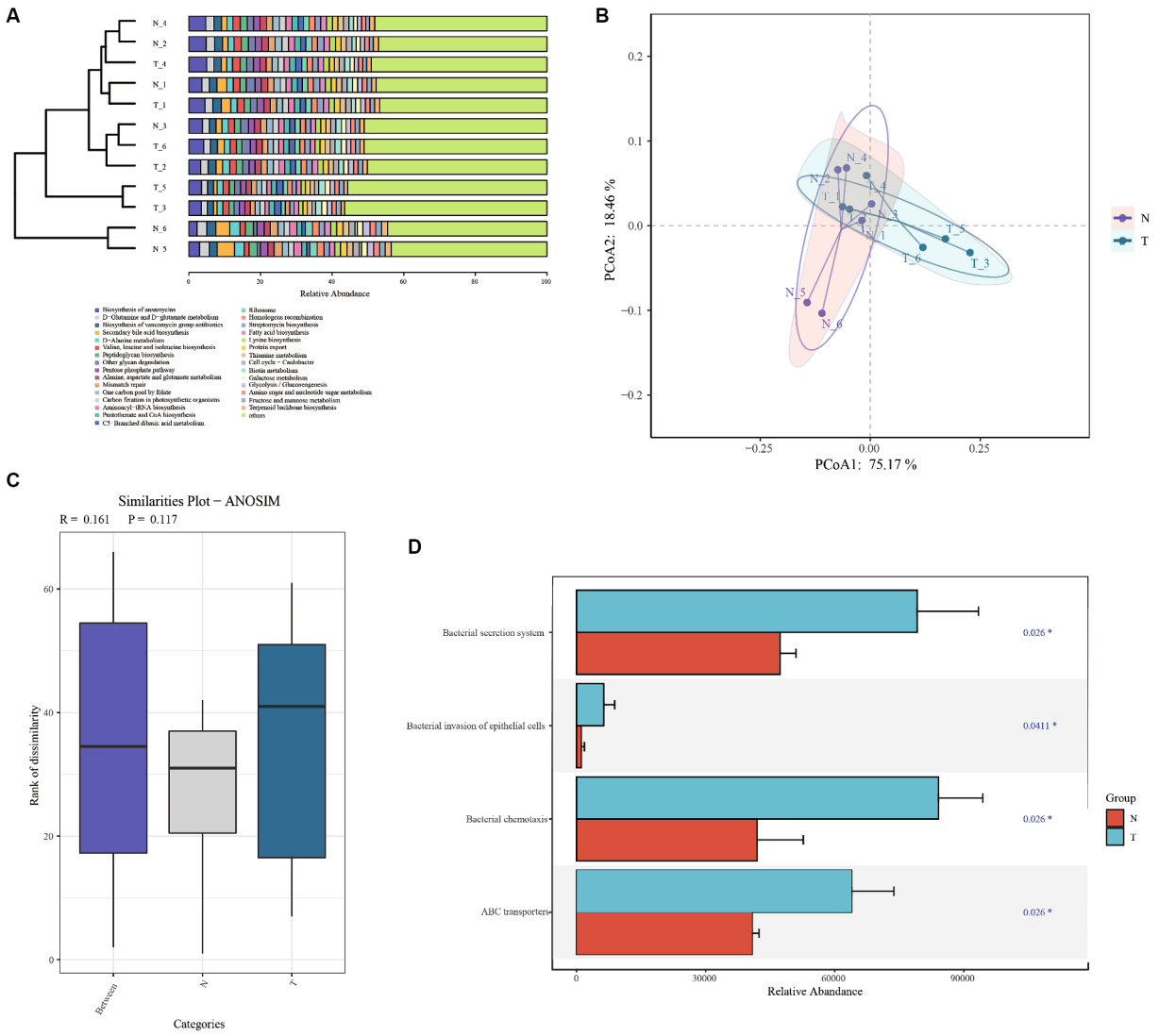

FIGURE 6
Functional analysis based on PICRUSt predictions. **(A)** Bray Cluster analysis and functional composition stacking map. **(B)** Bray Curtis PCoA analysis plots. **(C)** Anosim analysis based on functional gene abundance. **(D)** Significantly differential functional genes bar chart.

Data availability statement

The datasets presented in this study can be found in online repositories. The names of the repository/repositories and accession number(s) can be found at: https://www.ncbi.nlm.nih.gov/, PRJNA1088275.

Ethics statement

The animal study was approved by Medical Science and Technology Ethics Committee of Jiujiang University. The study was conducted in accordance with the local legislation and institutional requirements.

Author contributions

M-hZ: Conceptualization, Data curation, Formal analysis, Investigation, Methodology, Software, Validation, Visualization, Writing – original draft, Writing – review & editing. SL: Methodology, Supervision, Validation, Writing – review & editing. Q-bL: Data curation, Software, Writing – review & editing. X-xW: Conceptualization, Data curation, Investigation, Writing – review & editing. AQ: Investigation, Methodology, Writing – review & editing. MM: Funding acquisition, Resources, Writing – review & editing.

Funding

The author(s) declare that financial support was received for the research, authorship, and/or publication of this article. The authors would like to extend their gratitude to King Saud University (Riyadh, Saudi Arabia) for funding this research through Researchers supporting Project number (RSP-2024-R406).

Conflict of interest

The authors declare that the research was conducted in the absence of any commercial or financial relationships that could be construed as a potential conflict of interest.

Publisher's note

All claims expressed in this article are solely those of the authors and do not necessarily represent those of their affiliated organizations, or those of the publisher, the editors and the reviewers. Any product that may be evaluated in this article, or claim that may be made by its manufacturer, is not guaranteed or endorsed by the publisher.

Supplementary material

The Supplementary material for this article can be found online at: https://www.frontiersin.org/articles/10.3389/fvets.2024.1403920/full#supplementary-material

References

1. Buchmann K, Mehrdana F. Effects of Anisakid nematodes Anisakis Simplex (S.L.), Pseudoterranova Decipiens (S.L.) and *Contracaecum Osculatum* (S.L.) on Fish and consumer health. *Food Waterborne Parasitol.* (2016) 4:13–22. doi: 10.1016/j.fawpar.2016.07.003

2. Marcelino L, Garfias C, Zaheer T, Maqsood A, Bamarni S, Abdullah B, et al. Potential of Anisakiasis in foodborne zoonosis. *Pak Vet J.* (2022) 42:433–44. doi: 10.29261/pakvetj/2022.080

3. Villazanakretzer DL, Napolitano PG, Cummings KF, Magann EF. Fish parasites: a growing concern during pregnancy. *Obstet Gynecol Surv.* (2016) 71:253–9. doi: 10.1097/ogx.0000000000000303

4. Takano K, Okuni T, Murayama K, Himi T. A case study of Anisakiasis in the palatine tonsils. *Adv Otorhinolaryngol.* (2016) 77:125–7. doi: 10.1159/000441903

5. Groudan K, Martins T, Schmelkin IJ. Gastric Anisakiasis masquerading as gastroesophageal reflux disease. *Case Rep Gastrointest Med.* (2023) 2023:8635340–4. doi: 10.1155/2023/8635340

6. Ramanan P, Blumberg AK, Mathison B, Pritt BS. Parametrial Anisakidosis. *J Clin Microbiol.* (2013) 51:3430–4. doi: 10.1128/jcm.01398-13

7. Mattiucci S. Molecular epidemiology of Anisakis and Anisakiasis: an ecological and evolutionary road map. *Adv Parasitol.* (2018) 99:93–263. doi: 10.1016/bs.apar.2017.12.001

8. Ahuir-Baraja AE, Llobat L, Garijo MM. Effectiveness of gutting blue whiting (*Micromesistius Poutassou*, Risso, 1827), in Spanish supermarkets as an Anisakidosis safety measure. *Food Secur.* (2021) 10:862. doi: 10.3390/foods10040862

9. Sugiyama H, Shiroyama M, Yamamoto I, Ishikawa T, Morishima Y. Anisakiasis annual incidence and causative species, Japan, 2018-2019. *Emerg Infect Dis.* (2022) 28:2105–8. doi: 10.3201/eid2810.220627

10. Huss HH, Ababouch L, Gram L. *Assessment and management of seafood safety and quality*. Rome: FAO (2003).

11. Ruff WE, Greiling TM, Kriegel MA. Host-microbiota interactions in immune-mediated diseases. *Nat Rev Microbiol.* (2020) 18:521–38. doi: 10.1038/s41579-020-0367-2

12. El-Sayed A, Aleya L, Kamel M. Microbiota's role in health and diseases. *Environ Sci Pollut Res Int.* (2021) 28:36967–83. doi: 10.1007/s11356-021-14593-z

13. Martel J, Chang SH, Ko YF, Hwang TL, Young JD, Ojcius DM. Gut barrier disruption and chronic disease. *Trends Endocrinol Metab.* (2022) 33:247–65. doi: 10.1016/j.tem.2022.01.002

14. Hooper LV, Littman DR, Macpherson AJ. Interactions between the microbiota and the immune system. *Science.* (2012) 336:1268–73. doi: 10.1126/science.1223490

15. Jaenike J, Unckless R, Cockburn SN, Boelio LM, Perlman SJ. Adaptation via Symbiosis: recent spread of a Drosophila defensive symbiont. *Science.* (2010) 329:212–5. doi: 10.1126/science.1188235

16. Xiang H, Fang Y, Tan ZL, Zhong RZ. Haemonchus Contortus infection alters gastrointestinal microbial community composition, protein digestion and amino acid allocations in lambs. *Front Microbiol.* (2022) 12:15. doi: 10.3389/fmicb.2021.797746

17. Wang Y, Liu F, Urban JF Jr, Paerewijck O, Geldhof P, Li RW. Ascaris Suum infection was associated with a worm-independent reduction in microbial diversity and altered metabolic potential in the porcine gut microbiome. *Int J Parasitol.* (2019) 49:247–56. doi: 10.1016/j.ijpara.2018.10.007

18. Gasser RB, Bott NJ, Chilton NB, Hunt P, Beveridge I. Toward practical, DNA-based diagnostic methods for parasitic nematodes of livestock — bionomic and biotechnological implications. *Biotechnol Adv.* (2008) 26:325–34. doi: 10.1016/j.biotechadv.2008.03.003

19. Gasser RB, Rossi L, Zhu X. Identification of Nematodirus species (Nematoda: Molineidae) from wild ruminants in Italy using ribosomal DNA markers. *Int J Parasitol.* (1999) 29:1809–17. doi: 10.1016/s0020-7519(99)00123-x

20. D'Amelio S, Mathiopoulos KD, Santos CP, Pugachev ON, Webb SC, Picanço M, et al. Genetic markers in ribosomal DNA for the identification of members of the genus Anisakis (Nematoda: Ascaridoidea) defined by polymerase-chain-reaction-based restriction fragment length polymorphism. *Int J Parasitol.* (2000) 30:223–6. doi: 10.1016/s0020-7519(99)00178-2

21. Mattiucci S, Acerra V, Paoletti M, Cipriani P, Levsen A, Webb SC, et al. No more time to stay 'Single' in the detection of Anisakis Pegreffii, *A. simplex* (S. S.) and hybridization events between them: a multi-marker nuclear genotyping approach. *Parasitology.* (2016) 143:998–1011. doi: 10.1017/s0031182016000330

22. Figueiredo I, Cardoso L, Teixeira G, Lopes L, São Clemente SC, Vericimo MA. A technique for the intra-gastric Administration of Live Larvae of Anisakis Simplex in mice. *Exp Parasitol.* (2012) 130:285–7. doi: 10.1016/j.exppara.2012.01.004

23. Bolger AM, Lohse M, Usadel B. Trimmomatic: a flexible trimmer for Illumina sequence data. *Bioinformatics.* (2014) 30:2114–20. doi: 10.1093/bioinformatics/btu170

24. Magoč T, Salzberg SL. Flash: fast length adjustment of short reads to improve genome assemblies. *Bioinformatics.* (2011) 27:2957–63. doi: 10.1093/bioinformatics/btr507

25. Bolyen E, Rideout JR, Dillon MR, Bokulich NA, Abnet CC, Al-Ghalith GA, et al. Reproducible, interactive, scalable and extensible microbiome data science using Qiime 2. *Nat Biotechnol.* (2019) 37:852–7. doi: 10.1038/s41587-019-0209-9

26. Yilmaz P, Parfrey LW, Yarza P, Gerken J, Pruesse E, Quast C, et al. The Silva and "all-species living tree project (Ltp)" taxonomic frameworks. *Nucleic Acids Res.* (2013) 42:D643–8. doi: 10.1093/nar/gkt1209

27. Cole JR, Wang Q, Fish JA, Chai B, McGarrell DM, Sun Y, et al. Ribosomal database project: data and tools for high throughput Rrna analysis. *Nucleic Acids Res.* (2014) 42:D633–42. doi: 10.1093/nar/gkt1244

28. DeSantis TZ, Hugenholtz P, Larsen N, Rojas M, Brodie EL, Keller K, et al. Greengenes, a chimera-checked 16s Rrna gene database and workbench compatible with arb. *Appl Environ Microbiol.* (2006) 72:5069–72. doi: 10.1128/aem.03006-05

29. Douglas GM, Maffei VJ, Zaneveld JR, Yurgel SN, Brown JR, Taylor CM, et al. Picrust 2 for prediction of metagenome functions. *Nat Biotechnol.* (2020) 38:685–8. doi: 10.1038/s41587-020-0548-6

30. Cortés A, Toledo R, Cantacessi C. Classic models for new perspectives: delving into helminth-microbiota-immune system interactions. *Trends Parasitol.* (2018) 34:640–54. doi: 10.1016/j.pt.2018.05.009

31. Cortés A, Peachey L, Scotti R, Jenkins TP, Cantacessi C. Helminth-microbiota cross-talk - a journey through the vertebrate digestive system. *Mol Biochem Parasitol.* (2019) 233:111222. doi: 10.1016/j.molbiopara.2019.111222

32. Cortés A, Peachey LE, Jenkins TP, Scotti R, Cantacessi C. Helminths and microbes within the vertebrate gut-not all studies are created equal. *Parasitology.* (2019) 146:1371–8. doi: 10.1017/s003118201900088x

33. Arrieta MC, Walter J, Finlay BB. Human microbiota-associated mice: a model with challenges. *Cell Host Microbe.* (2016) 19:575–8. doi: 10.1016/j.chom.2016.04.014

34. Cortés A, Clare S, Costain A, Almeida A, McCarthy C, Harcourt K, et al. Baseline gut microbiota composition is associated with *Schistosoma Mansoni* infection burden in rodent models. *Front Immunol.* (2020) 11:593838. doi: 10.3389/fimmu.2020.593838

35. Lloyd-Price J, Mahurkar A, Rahnavard G, Crabtree J, Orvis J, Hall AB, et al. Strains, functions and dynamics in the expanded human microbiome project. *Nature.* (2017) 550:61–6. doi: 10.1038/nature23889

36. Bao M, Pierce GJ, Pascual S, González-Muñoz M, Mattiucci S, Mladineo I, et al. Assessing the risk of an emerging zoonosis of worldwide concern: Anisakiasis. *Sci Rep.* (2017) 7:43699. doi: 10.1038/srep43699

37. Scotti R, Southern S, Boinett C, Jenkins TP, Cortés A, Cantacessi C. Michelindb: a web-based tool for Mining of Helminth-Microbiota Interaction Datasets, and a Meta-analysis of current research. *Microbiome.* (2020) 8:10. doi: 10.1186/s40168-019-0782-7

38. Stracke K, Adisakwattana P, Phuanukoonnon S, Yoonuan T, Poodeepiyasawat A, Dekumyoy P, et al. Field evaluation of the gut microbiome composition of pre-school and school-aged children in Tha Song Yang, Thailand, following Oral Mda for Sth infections. *PLoS Negl Trop Dis.* (2021) 15:e0009597. doi: 10.1371/journal.pntd.0009597

39. Sun XM, Hao CY, Wu AQ, Luo ZN, El-Ashram S, Alouffi A, et al. Trichinella spiralis-induced immunomodulation signatures on gut microbiota and metabolic pathways in mice. *PLoS Pathog*. (2024) 20:e1011893. doi: 10.1371/journal.ppat.1011893

40. Zhong H, Penders J, Shi Z, Ren H, Cai K, Fang C, et al. Impact of early events and lifestyle on the gut microbiota and metabolic phenotypes in Young school-age children. *Microbiome*. (2019) 7:2. doi: 10.1186/s40168-018-0608-z

41. Kupritz J, Angelova A, Nutman TB, Gazzinelli-Guimaraes PH. Helminth-induced human gastrointestinal Dysbiosis: a systematic review and Meta-analysis reveals insights into altered taxon diversity and microbial gradient collapse. *MBio*. (2021) 12:e0289021. doi: 10.1128/mBio.02890-21

42. Wang J, Ji H, Wang S, Liu H, Zhang W, Zhang D, et al. Probiotic *Lactobacillus Plantarum* promotes intestinal barrier function by strengthening the epithelium and modulating gut microbiota. *Front Microbiol*. (2018) 9:1953. doi: 10.3389/fmicb.2018.01953

43. Feng L, Bao T, Bai L, Mu X, Ta N, Bao M, et al. Mongolian medicine formulae Ruda-6 alleviates indomethacin-induced gastric ulcer by regulating gut microbiome and serum metabolomics in rats. *J Ethnopharmacol*. (2023) 314:116545. doi: 10.1016/j.jep.2023.116545

44. Wang D, Tang G, Zhao L, Wang M, Chen L, Zhao C, et al. Potential roles of the rectum keystone microbiota in modulating the microbial community and growth performance in goat model. *J Anim Sci Biotechnol*. (2023) 14:55. doi: 10.1186/s40104-023-00850-3

45. Hu W, Huang L, Zhou Z, Yin L, Tang J. Diallyl disulfide (dads) ameliorates intestinal *Candida Albicans* infection by modulating the gut microbiota and metabolites and providing intestinal protection in mice. *Front Cell Infect Microbiol*. (2021) 11:743454. doi: 10.3389/fcimb.2021.743454

46. Lynch JB, Gonzalez EL, Choy K, Faull KF, Jewell T, Arellano A, et al. Gut microbiota Turicibacter strains differentially modify bile acids and host lipids. *Nat Commun*. (2023) 14:3669. doi: 10.1038/s41467-023-39403-7

47. Li H, Liu C, Huang S, Wang X, Cao M, Gu T, et al. Multi-omics analyses demonstrate the modulating role of gut microbiota on the associations of unbalanced dietary intake with gastrointestinal symptoms in children with autism Spectrum disorder. *Gut Microbes*. (2023) 15:2281350. doi: 10.1080/19490976.2023.2281350

48. Zaiss MM, Rapin A, Lebon L, Dubey LK, Mosconi I, Sarter K, et al. The intestinal microbiota contributes to the ability of helminths to modulate allergic inflammation. *Immunity*. (2015) 43:998–1010. doi: 10.1016/j.immuni.2015.09.012

49. Pryde SE, Duncan SH, Hold GL, Stewart CS, Flint HJ. The microbiology of butyrate formation in the human Colon. *FEMS Microbiol Lett*. (2002) 217:133–9. doi: 10.1111/j.1574-6968.2002.tb11467.x

50. Pei Y, Chen C, Mu Y, Yang Y, Feng Z, Li B, et al. Integrated microbiome and metabolome analysis reveals a positive change in the intestinal environment of Myostatin edited large White pigs. *Front Microbiol*. (2021) 12:12. doi: 10.3389/fmicb.2021.628685

51. Sieng S, Chen P, Wang N, Xu JY, Han Q. Toxocara Canis-induced changes in host intestinal microbial communities. *Parasit Vectors*. (2023) 16:462. doi: 10.1186/s13071-023-06072-w

52. Klomkliew P, Sawaswong V, Chanchaem P, Nimsamer P, Adisakwattana P, Phuphisut O, et al. Gut Bacteriome and metabolome of Ascaris Lumbricoides in patients. *Sci Rep*. (2022) 12:19524. doi: 10.1038/s41598-022-23608-9

53. Vitetta L, Llewellyn H, Oldfield D. Gut Dysbiosis and the intestinal microbiome: *Streptococcus Thermophilus* a key probiotic for reducing uremia. *Microorganisms*. (2019) 7:228. doi: 10.3390/microorganisms7080228

54. de Vos WM, Tilg H, Van Hul M, Cani PD. Gut microbiome and health: mechanistic insights. *Gut*. (2022) 71:1020–32. doi: 10.1136/gutjnl-2021-326789

55. Frost G, Sleeth ML, Sahuri-Arisoylu M, Lizarbe B, Cerdan S, Brody L, et al. The short-chain fatty acid acetate reduces appetite via a central homeostatic mechanism. *Nat Commun*. (2014) 5:3611. doi: 10.1038/ncomms4611

56. Cani PD, Jordan BF. Gut microbiota-mediated inflammation in obesity: a link with gastrointestinal Cancer. *Nat Rev Gastroenterol Hepatol*. (2018) 15:671–82. doi: 10.1038/s41575-018-0025-6

57. Depner M, Taft DH, Kirjavainen PV, Kalanetra KM, Karvonen AM, Peschel S, et al. Maturation of the gut microbiome during the first year of life contributes to the protective farm effect on childhood asthma. *Nat Med*. (2020) 26:1766–75. doi: 10.1038/s41591-020-1095-x

58. Zhang JD, Liu J, Zhu SW, Fang Y, Wang B, Jia Q, et al. Berberine alleviates visceral hypersensitivity in rats by altering gut microbiome and suppressing spinal microglial activation. *Acta Pharmacol Sin*. (2021) 42:1821–33. doi: 10.1038/s41401-020-00601-4

59. Verstreken I, Laleman W, Wauters G, Verhaegen J. *Desulfovibrio Desulfuricans* bacteremia in an immunocompromised host with a liver graft and ulcerative colitis. *J Clin Microbiol*. (2012) 50:199–201. doi: 10.1128/jcm.00987-11

60. Murros KE, Huynh VA, Takala TM, Saris PEJ. Desulfovibrio Bacteria are associated with Parkinson's disease. *Front Cell Infect Microbiol*. (2021) 11:652617. doi: 10.3389/fcimb.2021.652617

61. Gobert AP, Sagrestani G, Delmas E, Wilson KT, Verriere TG, Dapoigny M, et al. The human intestinal microbiota of constipated-predominant irritable bowel syndrome patients exhibits anti-inflammatory properties. *Sci Rep*. (2016) 6:39399. doi: 10.1038/srep39399

62. He P, Zhang Y, Chen R, Tong Z, Zhang M, Wu H. The Maca protein ameliorates Dss-induced colitis in mice by modulating the gut microbiota and production of Scfas. *Food Funct*. (2023) 14:10329–46. doi: 10.1039/d3fo03654e

63. Singh SB, Coffman CN, Varga MG, Carroll-Portillo A, Braun CA, Lin HC. Intestinal alkaline phosphatase prevents sulfate reducing Bacteria-induced increased tight junction permeability by inhibiting snail pathway. *Front Cell Infect Microbiol*. (2022) 12:882498. doi: 10.3389/fcimb.2022.882498

64. Fung CC, Octavia S, Mooney AM, Lan R. Virulence variations in Shigella and Enteroinvasive *Escherichia Coli* using the *Caenorhabditis Elegans* model. *FEMS Microbiol Lett*. (2015) 362:1–5. doi: 10.1093/femsle/fnu045

65. Hayashi T, Yamashita T, Watanabe H, Kami K, Yoshida N, Tabata T, et al. Gut microbiome and plasma microbiome-related metabolites in patients with decompensated and compensated heart failure. *Circ J*. (2018) 83:182–92. doi: 10.1253/circj.CJ-18-0468

66. Chung L, Thiele Orberg E, Geis AL, Chan JL, Fu K, DeStefano Shields CE, et al. *Bacteroides Fragilis* toxin coordinates a pro-carcinogenic inflammatory Cascade via targeting of colonic epithelial cells. *Cell Host Microbe*. (2018) 23:203–14.e5. doi: 10.1016/j.chom.2018.01.007

67. Valguarnera E, Wardenburg JB. Good gone bad: one toxin away from disease for *Bacteroides Fragilis*. *J Mol Biol*. (2020) 432:765–85. doi: 10.1016/j.jmb.2019.12.003

68. Green ER, Mecsas J. Bacterial secretion systems: an overview. *Microbiol Spectr*. (2016) 4:2015. doi: 10.1128/microbiolspec.VMBF-0012-2015

69. Mafra D, Lobo JC, Barros AF, Koppe L, Vaziri ND, Fouque D. Role of altered intestinal microbiota in systemic inflammation and cardiovascular disease in chronic kidney disease. *Future Microbiol*. (2014) 9:399–410. doi: 10.2217/fmb.13.165

70. Berer K, Mues M, Koutrolos M, Rasbi ZA, Boziki M, Johner C, et al. Commensal microbiota and myelin autoantigen cooperate to trigger autoimmune demyelination. *Nature*. (2011) 479:538–41. doi: 10.1038/nature10554

71. Bravo JA, Forsythe P, Chew MV, Escaravage E, Savignac HM, Dinan TG, et al. Ingestion of Lactobacillus strain regulates emotional behavior and central Gaba receptor expression in a mouse via the Vagus nerve. *Proc Natl Acad Sci USA*. (2011) 108:16050–5. doi: 10.1073/pnas.1102999108

72. Jabeen Z, Bukhari SA, Malik SA, Hussain G, Kamal S. Improved gut microbiota escalates muscle function rehabilitation and ameliorates oxidative stress following mechanically induced peripheral nerve injury in mice. *Pak Vet J*. (2023) 43:707–13. doi: 10.29261/pakvetj/2023.098

frontiers | Frontiers in Veterinary Science

TYPE Original Research
PUBLISHED 09 May 2024
DOI 10.3389/fvets.2024.1383291

Check for updates

OPEN ACCESS

EDITED BY
Mughees Aizaz Alvi,
University of Agriculture, Faisalabad, Pakistan

REVIEWED BY
Abu Hazafa,
University of Salerno, Italy
İbrahim Hakkı Ciğerci,
Afyon Kocatepe University, Türkiye

*CORRESPONDENCE
Xiuying Zhang
✉ zhangxiuying@neau.edu.cn

RECEIVED 07 February 2024
ACCEPTED 01 April 2024
PUBLISHED 09 May 2024

CITATION
Fazilani SA, An W, Li S, Hassan MF, Ishfaq M, Lakho SA, Farooque M, Shoaib M and Zhang X (2024) Unrevealing the therapeutic potential of artesunate against emerging zoonotic *Babesia microti* infection in the murine model. *Front. Vet. Sci.* 11:1383291. doi: 10.3389/fvets.2024.1383291

COPYRIGHT
© 2024 Fazilani, An, Li, Hassan, Ishfaq, Lakho, Farooque, Shoaib and Zhang. This is an open-access article distributed under the terms of the Creative Commons Attribution License (CC BY). The use, distribution or reproduction in other forums is permitted, provided the original author(s) and the copyright owner(s) are credited and that the original publication in this journal is cited, in accordance with accepted academic practice. No use, distribution or reproduction is permitted which does not comply with these terms.

Unrevealing the therapeutic potential of artesunate against emerging zoonotic *Babesia microti* infection in the murine model

Saqib Ali Fazilani[1,2], Wei An[3], Sihong Li[4], Mohammad Farooque Hassan[5], Muhammad Ishfaq[6], Shakeel Ahmed Lakho[7], Muhammad Farooque[8], Muhammad Shoaib[9] and Xiuying Zhang[1]*

[1]Heilongjiang Key Laboratory for Animal Disease Control and Pharmaceutical Development. Faculty of Basic Veterinary Science, College of Veterinary Medicine, Northeast Agricultural University, Harbin, China, [2]Department of Veterinary Pharmacology and Toxicology, Faculty of Biosciences, Shaheed Benazir Bhutto University of Veterinary and Animal Sciences, Sakrand, Pakistan, [3]Technical Centre of Chengdu Customs, Chengdu, China, [4]College of Animal Science and Technology and College of Veterinary Medicine of Zhejiang A&F University, Hangzhou, China, [5]Department of Veterinary Pathology, Faculty of Veterinary Sciences, Shaheed Benazir Bhutto University of Veterinary and Animal Sciences, Sakrand, Pakistan, [6]Huanggang Normal University, Huanggang, China, [7]Department of Veterinary Parasitology, Faculty of Veterinary Sciences, Shaheed Benazir Bhutto University of Veterinary and Animal Sciences, Sakrand, Pakistan, [8]Faculty of Veterinary and Animal Sciences, Ziauddin University Karachi, Karachi, Pakistan, [9]Key Laboratory of New Animal Drug Project, Gansu Province/Key Laboratory of Veterinary Pharmaceutical Development, Ministry of Agriculture and Rural Affairs, Lanzhou Institute of Husbandry and Pharmaceutical Sciences of Chinese Academy of Agriculture Sciences, Lanzhou, China

Babesiosis, a zoonotic blood protozoal disease, threatens humans and animals and is difficult to treat due to growing antimicrobial resistance. The study aimed to investigate the therapeutic efficacy of artesunate (AS), a well-known derivative of artemisinin, against *Babesia microti* (*B. microti*) using a murine infection model. Male BALB/c mice (6 weeks old; 15 per group) were chosen and randomly divided into 1) the control group, 2) *the B. microti* group, and 3) the *B. microti* + artesunate treatment groups. AS treatment at 2 mg/kg, 4 mg/kg, and 8 mg/kg of body weight significantly ($p < 0.05$) reduced the *B. microti* load in blood smears in a dose-dependent manner. Additionally, AS treatment mitigated the decrease in body weight and restored the normal state of the liver and spleen viscera index compared to the *B. microti*-infected group after 28 days. Hematological analysis revealed significant increases in RBC, WBC, and PLT counts post-AS treatment compared to the *B. microti*-infected group. Furthermore, AS administration resulted in significant reductions in total protein, bilirubin, ALT, AST, and ALP levels, along with reduced liver and spleen inflammation and lesions as observed through histopathological analysis. AS also elicited dose-dependent changes in mRNA and protein expression levels of apoptotic, proinflammatory, and anti-inflammatory cytokines in the liver compared to the control and *B. microti*-infected groups. Immunolabeling revealed decreased expression of apoptotic and inflammation-related proteins in AS-treated hepatic cytoplasm compared to the *B. microti*-infected group. AS also in dose-dependent manner decreased apoptotic protein and increased Bcl-2. Overall, these findings underscore the potential of AS as an anti-parasitic candidate in combating *B. microti* pathogenesis in an *in vivo* infection model, suggesting its promise for clinical trials as a treatment for babesiosis.

KEYWORDS

artesunate, babesiosis, histopathology, blood-borne pathogen, apoptosis, immune response, inflammation

1 Introduction

Babesiosis, a protozoal infection, manifests as a parasitic condition capable of infecting diverse vertebrate hosts, including penguins, pigs, and humans. Recently, there has been a notable rise in zoonotic *Babesia* infections, and the number of species capable of infecting humans consistently rising (1). It is becoming more common, and this raises concerns in the veterinary and medical fields. *B. microti* primarily disseminates through rodents and small mammals in North America and Asia. Over the past two decades, over a hundred cases of *B. microti* infection have been identified in different provinces across China, which establishes that this protozoal pathogen is the main source of babesiosis in the Chinese population (2).

The replication of the parasite within the red blood cells (RBCs) leads to the manifestation of clinical indicators, such as fever, hemolytic anemia, loss of appetite, hemoglobinuria, and considerable weight loss. In more severe instances of infection, the affected individual may culminate in a fatality, thus causing significant global losses (3, 4). The incubation period starts after a tick bite primarily, and it ranges from 1 to 6 weeks (5). However, in conditions when this *B. microti* has been transmitted through a blood transfusion, the highest severity of parasitemia can appear within a short period and leads to a wide range of clinical manifestations, including acute respiratory distress syndrome, disseminated intravascular coagulation, congestive heart failure, and renal failure (6). The currently available therapeutic options for *B. microti* are limited, and the development of drug resistance warrants immediate consideration (4). Considering the growing increase in antimicrobial resistance, it is difficult to treat, and there is an urgent need for alternative treatments that can specifically target this diverse parasite (7).

Artesunate (AS) is alternatively referred to as dihydroartemisinin-12-α-succinate and belongs to the category of semisynthetic compounds characterized by a peroxide-bridged sesquiterpene lactone structure (8). This compound is the biologically active constituent in the traditional Chinese medicinal plant, *Artemisia annua*. Earlier, AS was an antimalarial drug and primarily used to treat malaria, but its effectiveness against other protozoan parasites, like *Babesia*, was also observed (9, 10). AS gained much attention from researchers due to its unique pharmacological properties against several diseases. In addition to its antimalarial activity, this drug showed efficacy against several diseases caused by viruses, bacteria, and protozoa. Studies showed the potential effect of AS on SARS-Covid-1, Covid-2, and Covid-19 (11), schistosomiasis (12), leishmaniasis (13), babesiosis (9), tuberculosis, and many livestock diseases (14). Studies showed that AS also has immunomodulatory effects on tumor necrosis factor-alpha (TNF-α) and interleukin-6 (IL-6) in rats (15). A previously conducted study showed that AS treatment in sepsis-induced lung injury showed attenuated caspase levels and decreased apoptotic protein expression (16).

To date, the effects of AS on experimental babesiosis in mice infection models have not been studied in detail at the histopathologic and apoptotic molecular levels. This study provides substantial evidence for this purpose and uncovers the potential effects of the drug on the pathogenicity of *Babesia* parasites. In this study, the therapeutic potential of AS in inhibiting the pathogenesis of babesiosis was evaluated by hematology, microscopy, and biochemistry analysis along with histopathological observation, immunohistochemistry analysis, real-time quantitative PCR (qPCR), and Western blot analysis to explore the molecular mechanisms of disease progression and treatment response. Additionally, the molecular and physiological aspects of *Babesia* pathogenesis and the potential ameliorative effect of artesunate therapy were studied.

2 Materials and methods

2.1 Experimental animals and parasites

The mice testing was approved by the Animal Care and Use Committee of Northeast Agricultural University; 6-week-old male mice BALB/c (weight: 0.032 ± 0.001 g/kg) were selected and purchased from Liaoning Changsheng Biotech (Benxi, Liaoning, China) for this study, and a confirmed *B. microti* strain was obtained via performing a PCR test (reference strain, ATCC 30221). Artesunate was purchased from MedChem Express, China, for intramuscular administration in mice. Before the treatment, all mice were acclimatized and housed in a 12-h/12-h light/dark cycle at 23°C with fresh water and *ad-libitum* feeding. After a 1-week adaptation period, the experimental mice were randomly divided into five groups (15 per group) as follows: (1) the control group (CG), (2) the *B. microti* group (BM), (3) the *B. microti* + artesunate (2 mg/kg) low-dose group (LG), (4) the *B. microti* + artesunate (4 mg/kg) medium-dose group (MG), and (5) the *B. microti* + artesunate (8 mg/kg) high-dose group (HG). The different concentrations of drugs were prepared by following the method of Carvalho et al. (17). The *B. microti* was intraperitoneally administered to mice with 1×10^7 parasites following the method (9). After induction of *B. microti* infection reached 30 to 40%, mice were treated with AS daily for 4 weeks, and blood smear microscopy was used to analyze the parasites every second day. Blood samples were collected for routine blood biochemistry analysis on weekly basis. The body weight was measured every 3 day and final measured at 28th day of study. After 4 weeks, all groups were euthanized, and organs (liver and spleen) were collected and processed for further experiments following the standard protocols.

2.2 Blood smear examination

The detection of *B. microti* in blood samples was carried out by following the methodology outlined in prior research (18). According to the Centers for Disease Control (CDC) and the World Health Organization (WHO), the blood smear is still the preferred and fastest method for the detection of *B. microti* parasite in blood (19). Blood smear films were allowed to air dry. Subsequently, they were fixed

through immersion in absolute methanol for 1 to 2 s. Following fixation, the films were left to dry at room temperature. A staining protocol was adopted, involving a 30% Giemsa solution (Abcam, China) application to the blood films for 15 min, maintaining a temperature of approximately 20°C. Upon completing the staining process, the slides were meticulously washed and dried before examination under a compound microscope (Nikon Instrument, Inc., Japan). This microscopic analysis employed a "100 X" lens and an immersion oil drop (20).

2.3 Hematology and blood profiling

The blood profile of red blood cells (RBCs), white blood cells (WBCs), and platelets (PLTs) were determined through Mindray BC-5000 Vet Auto Hematology Analyzer, Shenzhen Mindray Animal Medical Technology Co., Ltd., China, following the guidelines of the manufacturer.

2.4 Blood biochemical parameters of the liver

The determination of liver biochemical parameters includes total protein concentration, bilirubin concentration, as well as the activities of critical enzymes such as serum alanine transaminase (ALT), aspartate transaminase (AST), and alkaline phosphatase (ALP). Blood samples were collected from the tail vein of mice using a 25-gauge needle and centrifuged at 3,000 rpm for 10 min to separate serum. The serum was transferred to a clean tube for enzymatic analysis according to the manufacturer's kits method (Jiangsu Aidisheng Biological Technology Co., Ltd).

2.5 Histopathological observation

Hematoxylin–eosin (HE) staining was performed using the previous method (21). Specifically, the liver and spleen tissues were fixed with 4% paraformaldehyde, dried with gradient alcohol, cleared with dimethylbenzene, and then embedded in paraffin. A rotary microtome (Leica, Germany) was then used to slice the tissues into 5 µm thin slices. The tissue sections were inspected under a microscope using a Leica Aperio CS2 slide scanner (Wetzlar, Germany).

2.6 Quantitative real-time PCR (qRT-PCR)

Liver samples were used to extract total RNA, and the concentration and quantity of the extracted RNA were measured using a NanoDrop 2000 spectrophotometer (Thermo Fisher Scientific, United States) at 260 nm and 280 nm, respectively. RNA with absorbances between 1.8 and 2.1 at A260/A280 were utilized for the study. Then, first-strand cDNA was synthesized utilizing a method previously established by our research team (21). With the help of Primer 5.0 software, specific gene primers were made for targets like interleukin-2 (IL2), interferon-gamma (IFN-γ), Beclin 1, tumor necrosis factor-alpha (TNF-α), CD44, caspase-9, and Bax. As a reference for normalization, GAPDH was employed as a housekeeping gene. Specific gene primers and housekeeping gene primers for qPCR is given in Table 1. The qPCR process was executed utilizing the FastStart Universal SYBR Green Master (ROX) Kit from Roche, Shanghai, China. A pre-denaturation step at 95°C for 10 min was the first step in the amplification process. This was followed by 40 cycles of denaturation at 95°C for 15 s, annealing at 58°C for 30 s, extension at 95°C for 15 s, and final extension at 37°C for 30 s. The $2^{-\Delta\Delta CT}$ method was used for mRNA expression levels (22, 23).

2.7 Immunohistochemistry analysis

For immunohistochemistry staining, the liver tissues were first fixed in a solution with 4% paraformaldehyde; they were then embedded in paraffin. Sections of 4 µm thickness were then cut from these paraffin-embedded tissues. The antigen repair solution with citric acid (pH 6.0, Service Bio, China) was employed to enhance antigen retrieval. After this step, the slides were treated with a 10% rabbit serum (Service Bio) to block non-specific binding. The slides were placed in primary antibody (Table 2) and stored at 4°C overnight. Following this, the slices were subjected to DAB (3,3′-diaminobenzidine) treatment. Subsequently, the slides were dehydrated using alcohol and subjected to hematoxylin (Service Bio, China) staining. The stained slides were examined under a microscope (Nikon E-100 Tokyo, Japan). Images were captured using the Case Viewer program (3DHISTECH, Hungary Ltd.).

2.8 Western blotting analysis

Total proteins were extracted following our previous study (24). Then, protein samples were subjected to a series of steps following a previous technique in our laboratory (25). These include protein processing, electrophoresis, membrane transfer, containment, and antibody incubation. The protein bands were determined through a Hypersensitive ECL luminous solution kit (MA0186, Meilun Bio,

TABLE 1 Genes and their primer information used for qRT-PCR analysis.

Sr. No.	Genes	Primers (5′-3′)
1	IL-2	Forward: GGATCCATGATGTGCAAAGTACTG Reverse: CGGTCGACTTATTTTTGCAGATATCT
2	IFN- γ	Forward: GGATCCATGATGTGCAAAGTACTG Reverse: CGGTCGACTTATTTTTGCAGATATCT
3	Beclin 1	Forward: CGACTGGAGCAGGAAGAAG Reverse: TCTGAGCATAACGCATCT
4	TNF- α	Forward: CCG AGG CAG TCA GAT CAT CTT Reverse: AGC TGC CCC TCA GCT TGA
5	CD44	Forward: CCAGAAGGAACAGTGGTTTGGC Reverse: ACTGTCCTCTGGGCTTGGTGTT
6	Caspase 9	Forward: GTTTGAGGACCTTCGACCAGCT Reverse: CAACGTACCAGGAGCCACTCTT
7	Bax	Forward: TCAGGATGCGTCCACCAAGAAG Reverse: TGTGTCCACGGCGGCAATCATC
8	GAPDH	Forward: GCACGCCATCACTATCTT Reverse: GGACTCCACAACATACTCAG

TABLE 2 Primary antibodies, their manufacturers, and the dilution ratio used for Immunohistochmeistry analysis.

Primary antibody	First anti-item number	Primary antibody manufacturer	The dilution ratio of one antibody
TNF-α	bs-10802R	Bioss	1:400
Caspase 9	A2636	ABclonal	1:200
Bax	AY0553	Always	1:200
CD44	ab189524	Abcam	1:200

TABLE 3 Antibodies used in Western Blotting analysis, their product, and sourcing details.

No.	Antibodies	Product & source information
1	Bcl-2	Bcl-2; 1:500; Catalogue# HY-p80030, Med Chem Express, China
2	BAX	BAX; 1:500; Catalogue# HY-122760, Med Chem Express, China
3	ICAM-1	ICAM-1; 1:2000; Catalogue# HY-P80502; Med Chem Express, China
4	SICAM-1	Anti-ICAM-1; 1:250; Catalogue# AB171123; Abcam, China
5	CRP	Anti-CRP; 1:1000; Catalogue# FNab01995; FN-test, China
6	GAPDH	Anti-GAPDH; 1:5000; Catalogue# HY-P80137; Med Chem Express, China

Dalian, China), and the images were acquired by Tanon (Tanon Life Sciences Ltd. Shanghai, China). The optical density of the protein band was measured by using ImageJ software from the National Institutes of Health, United States. To ensure consistency, the relative protein expression levels were normalized to GAPDH, a housekeeping protein. The antibodies employed in this process are listed in Table 3.

2.9 Statistical analysis

To ensure accuracy and reproducibility, all the above tests were repeated triplicate for validation. Statistical analysis was performed using GraphPad Prism (Ver. 9.0) with one-way variance. Data are presented as mean ± SEM, with p-values <0.05 were considered statistically significant using the Tukey's method for post-hoc testing. Images were created with GraphPad Prism 9 (San Diego, CA).

3 Results

3.1 Effect of AS treatment on blood smear analysis of the *B. microti*-infected and treatment groups

Blood smears were prepared and examined for each of the experimental groups, which included the control group (CG), the *B. microti*-infected group (BM), and the *B. microti*-infected groups treated with varying dosages of artesunate 2 mg/kg (LG), 4 mg/kg (MG), and 8 mg/kg (HG). Notably, blood smear results showed Figure 1 that AS in a dose-dependent manner reduced the *B. microti* load in the treatment groups, LG, MG, and HG, as compared to the BM group. This observation underscores the potential influence of AS at the specified dosage on the staining characteristics of blood smears, thereby warranting further investigation and analysis within the context of this study.

3.2 Influence of *B. microti* infection and AS treatment on body weight, liver, and spleen viscera

In Figure 2, notable alterations in body weight, as well as in the liver and spleen viscera, were observed compared to the BM-infected group in mice on the 28th day of the study. Specifically, Figure 2A illustrates that a significant reduction of body weight in mice infected with BM compared with mice in the control group (CG) ($p < 0.05$) was evident. However, it is noteworthy that with the AS treatment 2 mg/kg (LG), 4 mg/kg (MG), and 8 mg/kg (HG) for 28 days, the body weight loss could be reversed and exhibited a recovery trend ($p < 0.05$).

Similarly, as depicted in Figures 2B,C, the weight of the liver and spleen viscera demonstrated a significant increase in mice infected with *B. microti* (BM) when compared to the control group (CG) ($p < 0.05$), whereas the liver and spleen viscera dimensions remained unchanged. Furthermore, a minor weight recovery was observed in mice treated with a dosage of 2 mg/kg (LG), while a substantial recovery was noted in mice treated with dosages of 4 mg/kg (MG) and 8 mg/kg (HG). These data underscore the potential therapeutic impact of AS on mitigating the observed reductions in body weight and organ viscera sizes induced by *B. microti* infection.

3.3 Effect of AS treatment on hematological parameters (WBC, RBC, and platelets)

A comprehensive analysis of hematologic parameters was conducted between the groups, encompassing the CG, BM, and AS-treated LG, MG, and HG. The findings showed that comparative evaluation of red blood cell count (RBCs, Figure 3A), white blood cell count (WBCs, Figure 3B), and platelet count (PLTs, Figure 3C) exhibited distinct patterns. Within the *B. microti*-infected group (BM), a significant reduction was observed in the counts of RBCs, WBCs, and PLTs when contrasted with the control group (CG) ($p < 0.05$). This reduction signifies the hematologic impact of *B. microti* infection on these critical blood cell populations.

Conversely, a dose-dependent trend was observed following AS administration. Specifically, the groups LG, MG, and HG exhibited a notable and significant increase ($p < 0.05$) in the counts of RBCs, WBCs, and PLTs. This increment in blood cell counts underscores the potential of AS treatment to positively influence altered hematologic parameters of *B. microti* infection.

3.4 Influence of AS on liver biochemistry

As shown in Figure 4, In contrast, the mice in the *B. microti*-infected (BM) group exhibited a significant ($p < 0.05$) increase in the

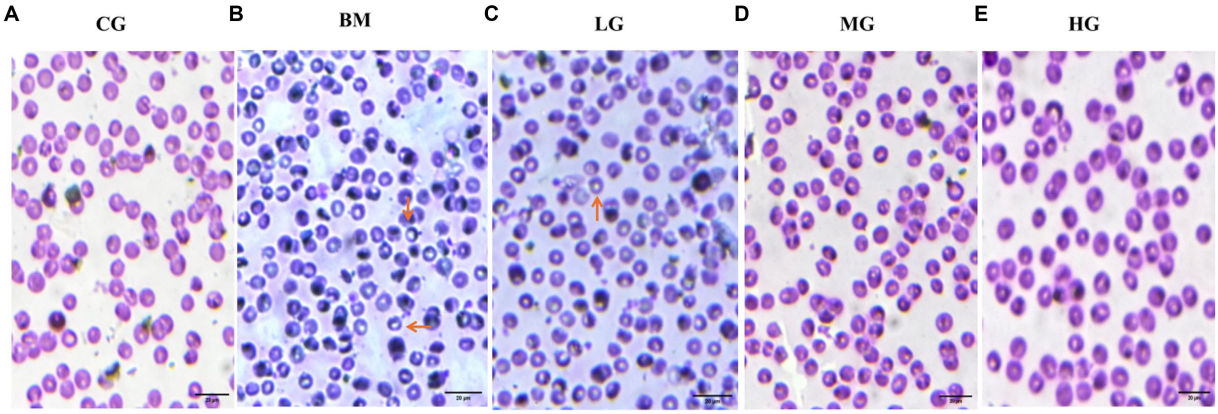

FIGURE 1
Results of Giemsa-stained thin blood smears (observed at 100X magnification). **(A)** The control group (CG), **(B)** the *B. microti* group (BM), **(C)** the *B. microti* + artesunate @2 mg/kg, low-dose group (LG), **(D)** the *B. microti* + artesunate @4mg/kg, medium-dose group (MG), **(E)** the *B. microti* + artesunate @8 mg/kg, high-dose group (HG). Arrows indicate the presence of *B. microti*, and scale bars represent 20 μm.

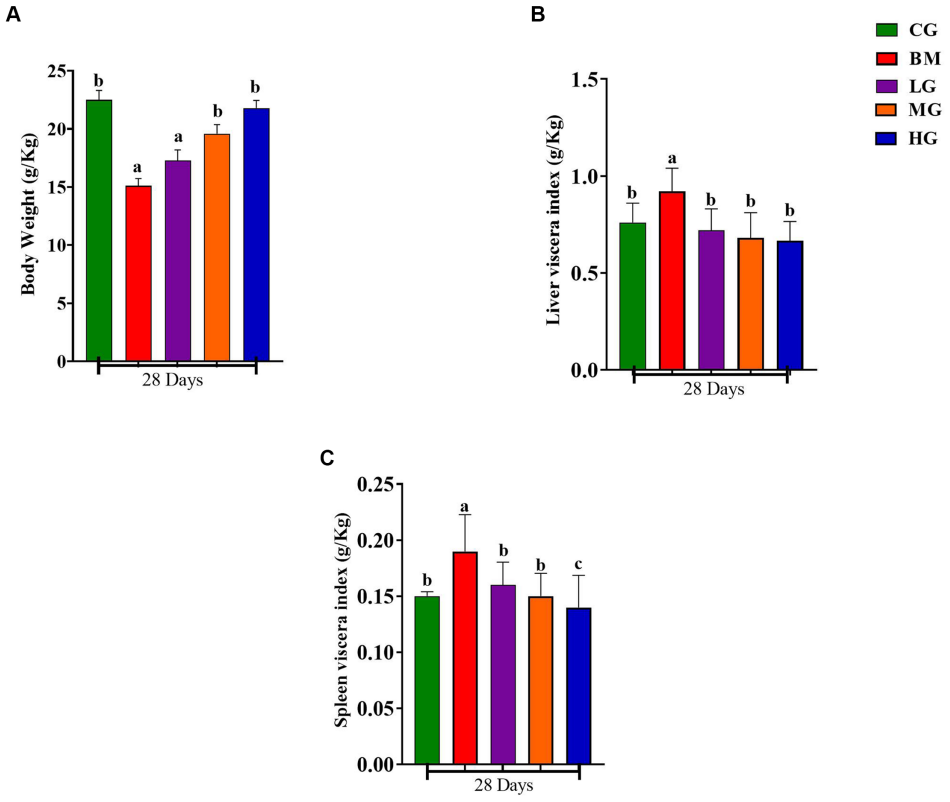

FIGURE 2
Results of body weight, liver, and spleen index. Experimental groups represented as the control group (CG), the *B. microti* group (BM), the *B. microti* + artesunate 2 mg/kg low-dose group (LG), the *B. microti* + artesunate 4 mg/kg medium-dose group (MG), and the *B. microti* + artesunate 8 mg/kg high-dose group (HG). **(A)** Results of body weight index. **(B)** Results of liver viscera index. **(C)** Results of spleen viscera index. Different lowercase letters represent significant differences between groups ($p < 0.05$).

concentration of aspartate transaminase (AST), Additionally, minor increases were observed in the levels of ALT, ALP, bilirubin, and total protein, compared to the control group (CG), throughout the 1st, 2nd, 3rd, and 4th weeks ($p < 0.05$). An increase in these blood biochemical parameters indicated liver injury.

Furthermore, it is noteworthy that mice treated with artesunate at dosages of 2 mg/kg (LG), 4 mg/kg (MG), and 8 mg/kg (HG) displayed minor decreases and recovered the elevated levels within the normal range as compared to the *B microti*-infected (BM) group ($p < 0.05$). These findings suggest that AS may play a role in mitigating the

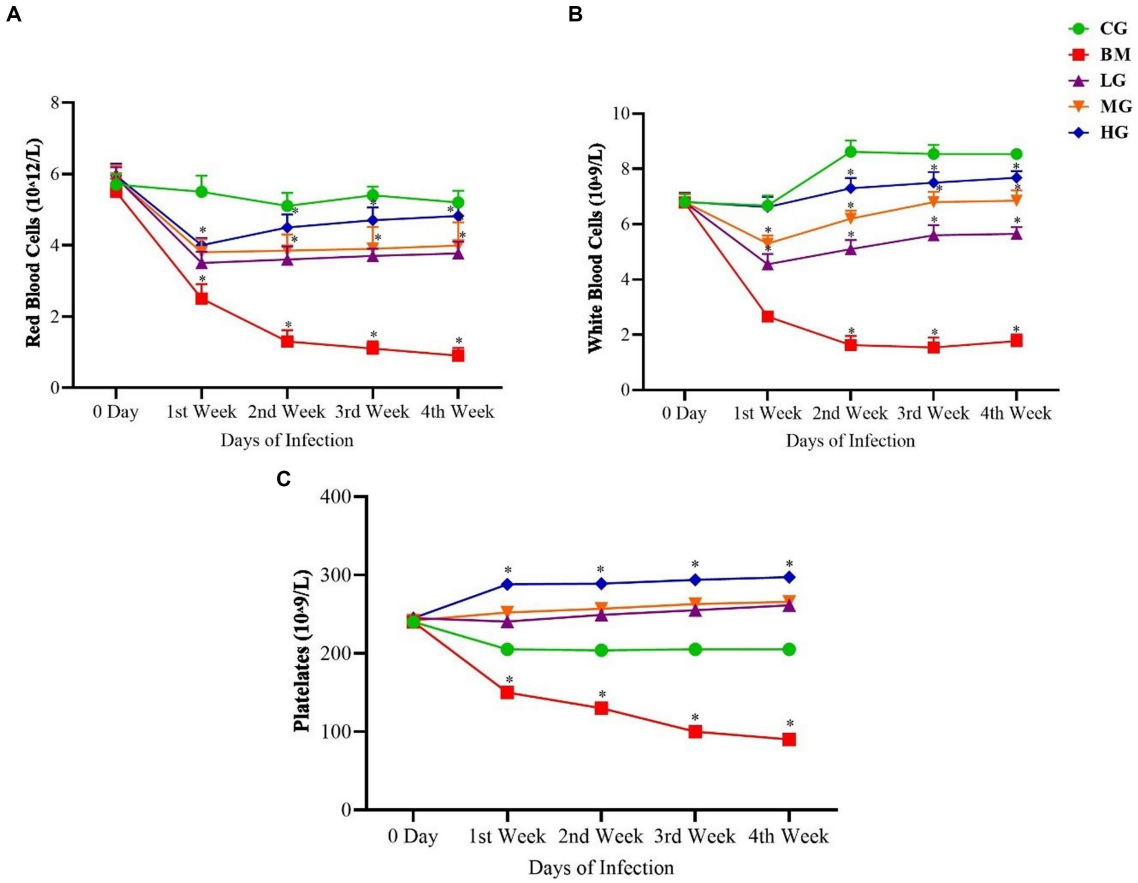

FIGURE 3
Results of **(A)** red blood cells (RBCs), **(B)** white blood cells (WBCs), and **(C)** platelets (PLTs). Experimental groups represented as the control group (CG), the *B. microti* group (BM), the *B. microti* + artesunate 2 mg/kg low-dose group (LG), the *B. microti* + artesunate 4 mg/kg medium-dose group (MG), and the *B. microti* + artesunate 8 mg/kg high-dose group (HG). The results are presented as means ± standard error of the mean (SEM). The data were analyzed, considering the significant differences with * ($p < 0.05$).

alterations in these biochemical parameters induced by *B. microti* infection.

3.5 Protective effect of AS treatment on histopathological changes in liver and spleen tissue

Our results showed that the liver histopathology of mice infected with *B. microti* (BM) (Figure 5A) exhibited moderate-to-severe inflammatory infiltrate and inflammatory lesions compared with the treatment group, this liver cellular inflammatory damage in the AS-treated groups significantly improved or recovered in a dose-dependent manner. The results here clearly indicate that hepatic lobules and central vein are unformed in appearance seen uniformly and well organized in the CG and HG groups to show that AS with a high dose of 8 mg/kg (HG) alleviated the liver damage and possess potent effect against *B. microti* infection.

Further, histopathology results of the spleen displayed a clear distinction between the red and white pulp structures, and marginal zones in the control group (CG) (Figure 5B). While the *B. microti* (BM) infection group showed serious congestion and enlarged red pulp. In a dose-dependent manner, we observed a recovered state of spleen cellular structure with weak red pulp cellularity and white pulp with clear marginal zones around follicles in the infected groups treated with artesunate (AS). This highlights AS efficacy against *B. microti* infection in liver and spleen tissues.

3.6 Effect of AS treatment and *B. microti* infection on expression levels of key markers of apoptosis and inflammation

To gain deeper insights into the potential effects of artesunate treatment in the context of *Babesia microti* infection, we investigated the mRNA expression levels of several key markers involved in apoptotic processes, and proinflammatory and anti-inflammatory pathways, such as Bax, Beclin 1, Caspase 9, CD44, IFN-γ, IL2, and TNF-α.

Our findings showed significant changes in mRNA expression levels of key regulatory genes of the apoptotic pathway (Bax, Beclin 1, and Caspase 9) in mice following the administration of AS in a dose-dependent manner. Notably, mice administered with AS at a high dosage of 8 mg/kg (HG) showed a significant reduction in the mRNA expression levels of Bax (Figure 6A), Beclin 1 (Figure 6B), and Caspase 9 (Figure 6C) in comparison with mice that were challenged

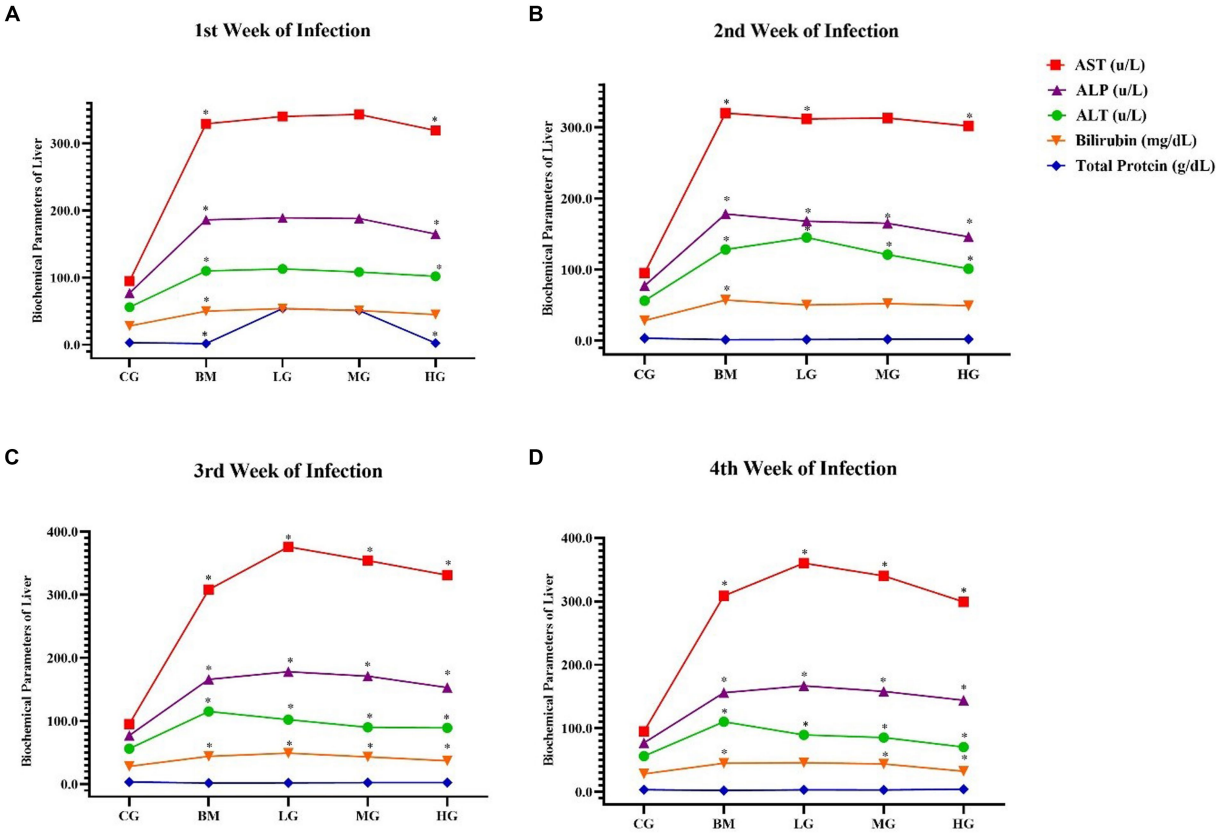

FIGURE 4
The results of blood biochemical parameters of the liver. Experimental groups, the control group (CG), the *B. microti* group (BM), the *B. microti* + artesunate 2 mg/kg low-dose group (LG), the *B. microti* + artesunate 4 mg/kg medium-dose group (MG), the *B. microti* + artesunate 8 mg/kg high-dose group (HG). **(A)** 1st week infection; **(B)** 2nd week infection; **(C)** 3rd week infection; and **(D)** 4th week of infection. The results are presented as means ± standard error of the mean (SEM). The collected data were analyzed, considering the significant differences with * ($p < 0.05$).

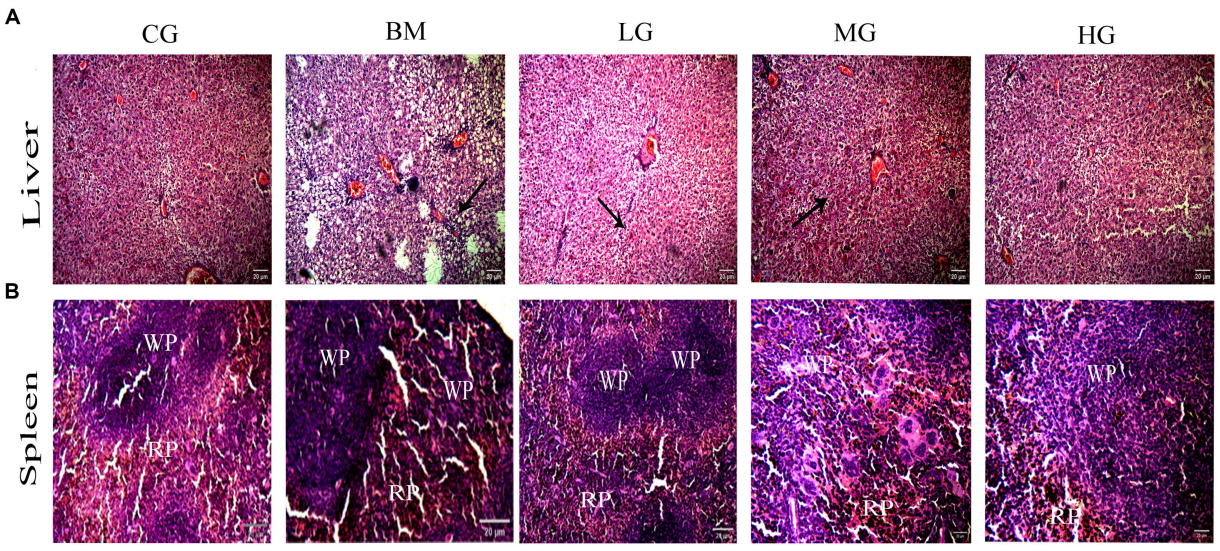

FIGURE 5
(A) Protective effect of AS treatment in liver on photomicrograph at 100 X magnification and scale bars 20 µm. Arrows show severe inflammatory lesions in the liver. **(B)** Effect of A S treatment on spleen photomicrograph at 100 X, Scale bar 20 µm. White pulp (WP) and red pulp (RP) structures in the *B. microti* group (BM). Recovery trend in the *B. microti* + artesunate 2 mg/kg low-dose group (LG), the *B. microti* + artesunate 4 mg/kg medium-dose group (MG), and the *B. microti* + artesunate 8 mg/kg high-dose group (HG) groups.

with *B. microti* (BM) alone ($p < 0.05$). These observations were particularly prominent during the 3rd and 4th weeks post-treatment. However, when AS was administered at lower doses of 2 mg/kg (LG), the expression patterns of these markers closely resembled those of the control group (CG). These findings further emphasize the potential of AS treatment to impact key apoptotic factors, indicating its role in reducing apoptosis induction.

We also investigated what role AS played in mice that were exposed to *B. microti* (BM) to see how it affected the levels of CD44, IFN-γ, IL2, and TNF-α cytokines. When compared to mice that were in (the BM) group and those that were given AS dosages had lower levels of these cytokines. Mice treated with AS at the medium dose of 4 mg/kg (MG) and high dose of 8 mg/kg (HG) exhibited a significant reduction in the expression of CD44 (Figure 6D), IFN-γ (Figure 6E), IL2 (Figure 6F), and TNF-α (Figure 6G) compared to those challenged with *B. microti* alone (BM) ($p < 0.05$). This marked reduction in cytokine expression was evident after the third and fourth weeks of treatment. Conversely, the treatment of mice with AS at a dose of 2 mg/kg resulted in significant changes, although it was not as effective as the treatment at doses 4 and 8 mg/kg (MG and HG) in the expression of these cytokines when compared to the control group (CG).

3.7 Effect of AS treatment and *B. microti* infection on immunohistochemistry of apoptosis and inflammation key marker proteins

The levels of important proteins like Bax, Caspase 9, CD44, and TNF-α in both the *B. microti* (BM) and AS treatment groups were detected with immunohistochemistry. In Figure 7, the hepatic cytoplasm of the mice infected with *B. microti* showcased a pronounced dark brown staining, suggesting the presence of considerable positive expression within the cytoplasmic compartment. Conversely, the hepatic cytoplasm exhibited a distinct blue coloration in the mice treated with AS at a dose of 8 mg/kg (HG). This blue hue indicates the absence of detectable protein expression. These results imply that AS effectively counteracts the infection induced by *B. microti* in mice.

3.8 Effect of AS on protein expression of apoptosis and inflammation markers

We investigated the expression profiles of two key factors, Bax and Bcl-2, that play important roles in apoptotic pathways, to learn more about how artesunate might help stop apoptosis in *B. microti* infections. Moreover, we also explored the impact of AS on inflammation markers, including SICAM-1, ICAM-1, and C-reactive protein. As shown in Figure 8A. Western blot analysis showed the protein expression of the proapoptotic factor Bax significantly increased, and the anti-apoptotic factor Bcl-2 decreased significantly ($p < 0.05$) in *the B. microti*-infected (BM) group. AS treatment normalizes Bax and Bcl-2 protein expression levels. Intriguingly, the expression pattern in the bar graph, Figures 8B,d,e show a significant ($p < 0.05$) decrease found at 2 (LG) and 8 mg/kg (HG) treatment groups in Bax. However, dose-dependent upregulation of Bcl-2 protein expression was found in AS treatment groups (LG, MG, and HG). This observation highlights the potential of AS treatment to modulate apoptotic processes in *B. microti* infection.

Furthermore, our investigation extended to the realm of inflammation markers. We examined protein expression ICAM-1, SICAM-1, and C-reactive protein levels, and results showed significant ($p < 0.05$) upregulation was found in the BM group as compared to the control (CG) and treatment groups. AS treatment at a low dose of 2 mg/kg (LG), medium dose of 4 mg/kg (MG), and 8 mg/kg (HG) significantly ($p < 0.05$) downregulated the alleviated level in a dose-dependent manner. However, a significant decrease was found at 4 mg/kg in SICAM-1 and ICAM-1 and 8 mg/kg in CRP protein expression.

4 Discussion

Animal health is suffering tremendously all over the world due to the spread of parasite infections, and babesiosis is one of the most prevalent diseases that is adversely affecting humans as well as animal populations on a very large scale (26–28). Currently, no drug of choice is available for the cure and treatment of human babesiosis. In animals, only diminazene aceturate is the first line of therapy in cases of severe babesiosis. Nowadays, severe drug resistance has developed against this drug (29). So far, many drugs are under research to find a new novel drug against the Babesia parasite. Artesunate is well known for its antimalarial properties; besides these, it has been extensively studied for antimicrobial, anti-inflammatory, antitumor, immunomodulatory, and antiparasitic properties. This drug is regarded as a potent antimalarial drug throughout the world (9, 30). The causative agents of malaria and babesia shared the same pathobiology and were also misdiagnosed in babesia as malaria (31, 32). So, this study was carried out in different aspects to know the potential effects of artesunate on physiological, serum biochemical, pathological, and immunomodulator response as well as the ameliorative and protective effects of AS against experimentally induced *B. microti* infection in mice.

We found that after a successful infection, it has been noted that *B. microti* has a high impact on body weight, liver, and spleen viscera index, causing weight loss, liver enlargement (hepatomegaly), and spleen enlargement (splenomegaly). This is due to decreased appetite, increased metabolism, red blood cell destruction, inflammation, immune cell infiltration, and heightened macrophage activity (33). A similar finding was observed in the *B. microti*-infected group and those treated with a lower dosage of AS of 2 mg/kg. The inability of the solely *B. microti*-infected group to recover by the 28-day mark underscores the severity of the infection. In contrast, the ameliorative effects observed in the AS-treated groups point toward its potential to mitigate the impact of the infection on growth and development. This trend becomes particularly evident with increasing AS dosages (4 mg/kg and 8 mg/kg), whereas dose-dependent improvement in body weight and organ indices is evident. The same finding was observed in experimentally induced leishmania parasites in mice at 37 days post-treatment significant increase in body weight and recovered state of liver and spleen viscera index with combined therapy of diminazene and chloroquine therapy (34).

B. microti is an intra-erythrocytic parasite that mainly infects red blood cells causing fever and severe forms of anemia, it gets

10.3389/fvets.2024.1383291

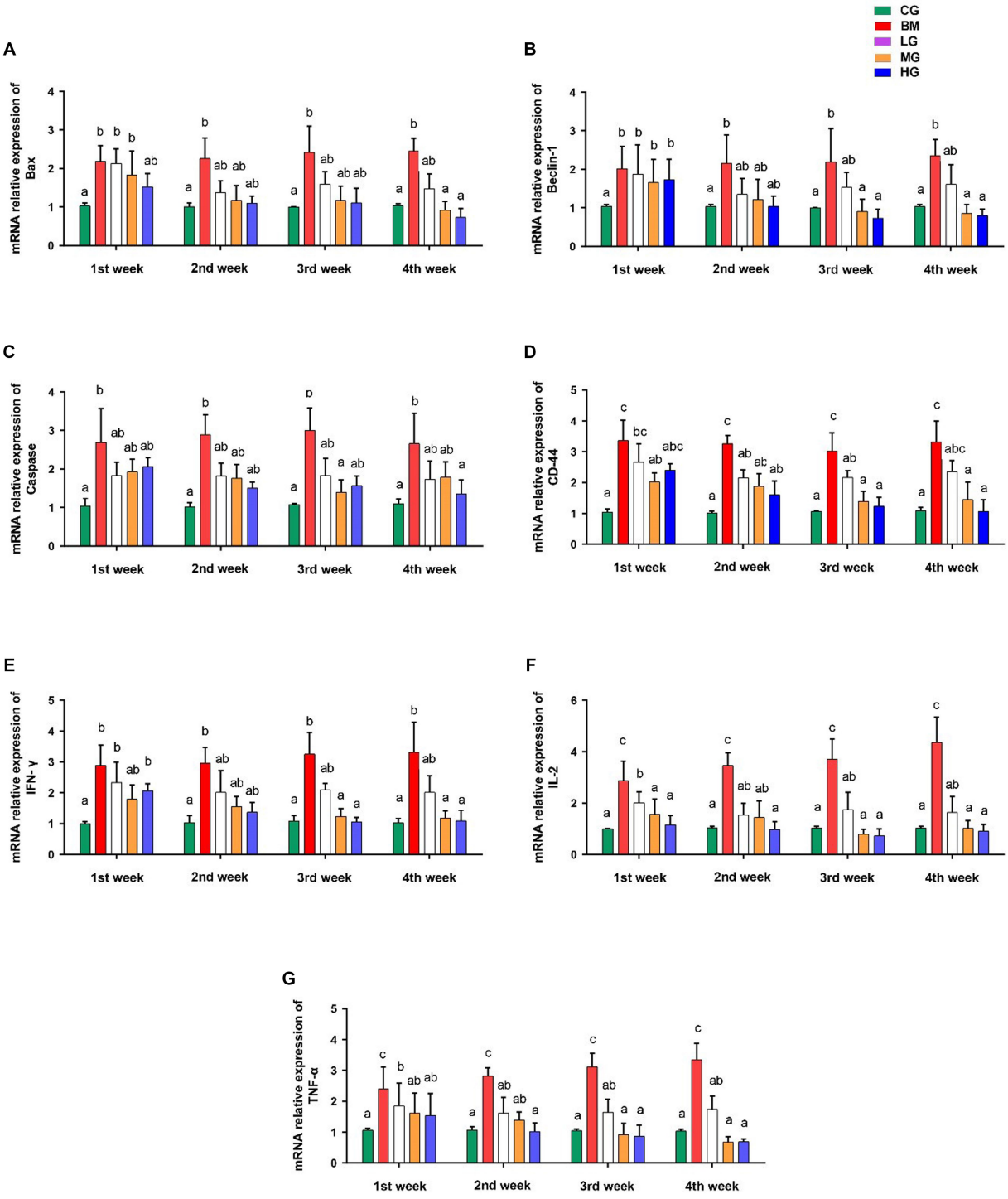

FIGURE 6
Results of mRNA expression profiles of key markers involved in apoptotic processes and proinflammatory and anti-inflammatory pathways. **(A)** Bax, **(B)** Beclin 1, **(C)** Caspase 9, **(D)** CD44, **(E)** IFN-γ, **(F)** IL2, and **(G)** TNF-α. However, experimental groups including the control group (CG), the *B. microti* group (BM), the *B. microti* + artesunate 2 mg/kg low-dose group (LG), the *B. microti* + artesunate 4 mg/kg medium-dose group (MG), and the *B. microti* + artesunate 8 mg/kg high-dose group (HG). The data were representative of three independent experiments, and the values are presented as the means ± SEM. $p \leq 0.05$ and $p \leq 0.01$ were considered significant. The same letters mean non-significant, and the different letters mean significant.

more attention from researchers due to its zoonotic importance. It can readily transmitted from infected rodents and small pet animals to humans (2, 35). We found treatment with AS at a higher dosage of 8 mg/kg yielded notable findings regarding the modulation of hematological parameters. The hematologic implications of AS administration are pronounced. The dose-dependent elevation in red blood cell (RBC), white blood cell (WBC), and platelet (PLT) counts consequent to AS treatment

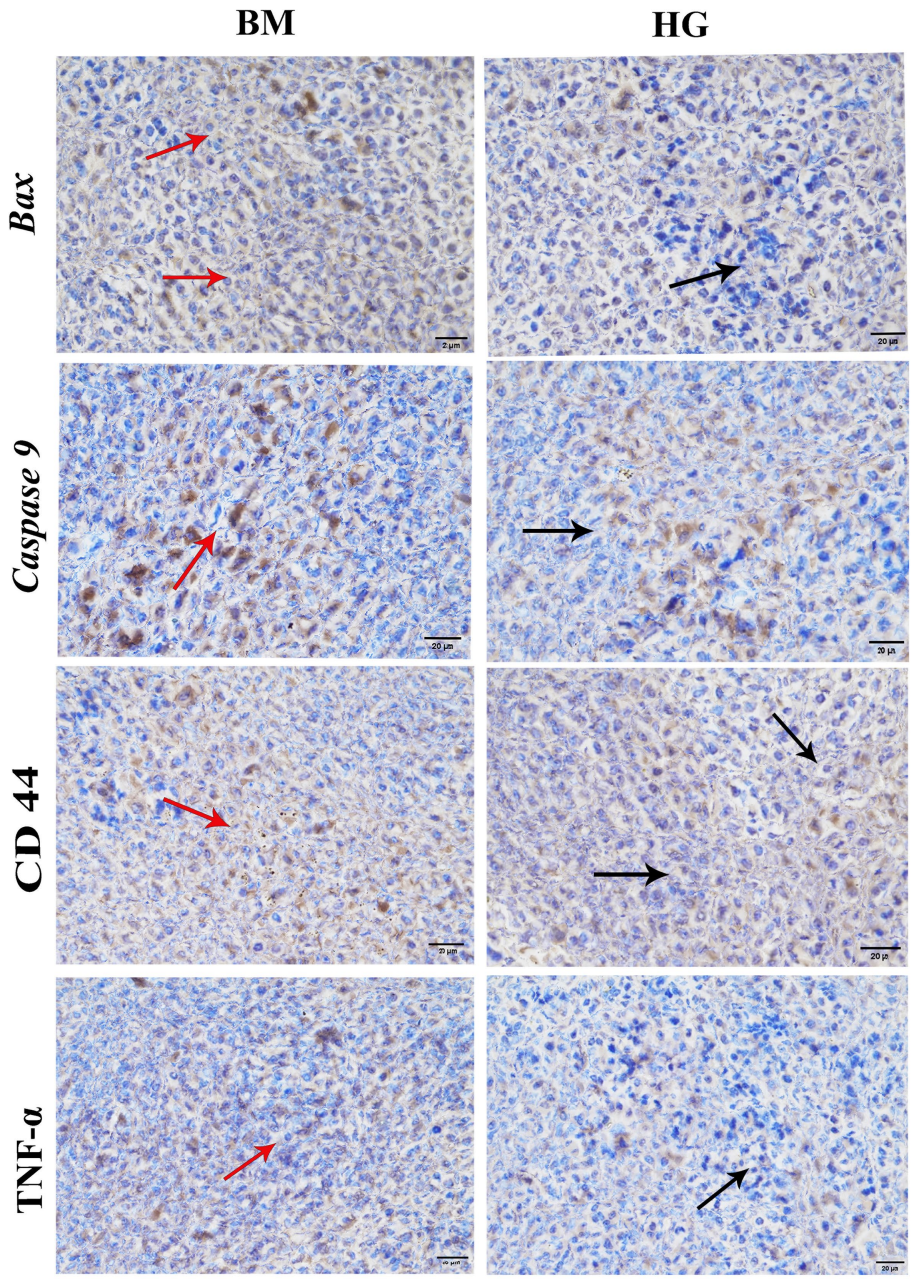

FIGURE 7
The result of immunohistochemistry analysis comparison between *the B. microti* (BM)-infected group and the *B. microti* + artesunate 8 mg/kg (HG) group. Red arrows indicated positive expression, whereas black arrows showed the absence of detectable proteins. Photomicrograph taken at 400X and scale bar 20 μm.

illuminate its role in positively impacting hematopoietic processes. This finding holds substantial clinical relevance, suggesting that AS treatment could potentially contribute to restoring hematologic homeostasis disrupted by *B. microti* infection. These findings are consistent with previous research in which patients infected with *Plasmodium falciparum*, following treatment with AS, exhibited a rapid recovery of vital hematological parameters. On the 42nd day post-treatment, a substantial restoration was observed in red blood cell (RBC) counts, white blood cell (WBC) counts, hemoglobin levels, and platelet counts. This resurgence in hematological indices underscores the efficacy of AS in promoting recovery and re-establishing normalcy in individuals afflicted by *Plasmodium falciparum* infection (36).

B.microti infection leads to abnormal liver function due to hepatocellular injury hemolysis and bile duct blockage leading to increased production of liver enzyme alanine transferase (ALT), alkaline phosphatase (ALP), bilirubin, and total protein count (37). In this context, we investigated AS treatment at varying dosages (2 mg/kg, 4 mg/kg, and 8 mg/kg) on mice with a focus on key biochemical parameters. Notably, the findings revealed significant reductions in the levels of alanine transaminase (ALT), alkaline phosphatase (ALP), and total protein in mice subjected to AS treatment when compared

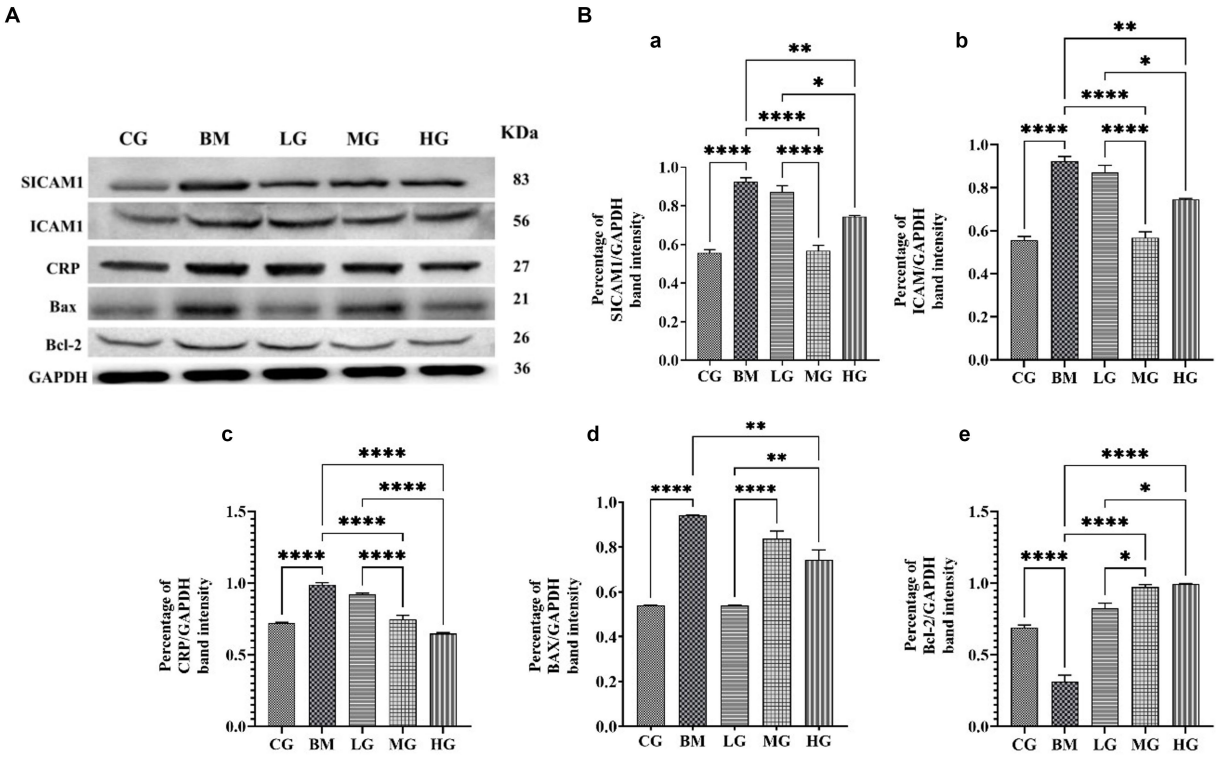

FIGURE 8
Regulating effect of artesunate (AS) after 4 weeks of treatment. **(A)** Shows protein levels of inflammation markers including SICAM-1, ICAM-1, and C-reactive protein and proapoptotic factor Bax and anti-apoptotic factor Bcl-2. **(B)** Shows a bar graph of the percentage of band intensity relative protein expression compared within the control group (CG), the *B. microti* (BM) group, and the experimental groups *B. microti* + artesunate 2 mg/kg low-dose group (LG), *B. microti* + artesunate 4 mg/kg medium-dose group, and 8 mg/kg high-dose group. **(a)** SICAM-1, **(b)** ICAM-1, **(c)** CRP, **(d)** BAX, **(e)** Bcl-2 bar graph, with asterisks representing a higher level of significance, "*" ($p < 0.05$) "**"($p < 0.01$) ***"($p < 0.001$)"****"($p < 0.0001$).

to the *B. microti*-infected group. Mice within the infection group displayed a significant increase in the concentration of aspartate transaminase (AST) throughout the study. Additionally, minor increases were observed in the levels of ALT, ALP, bilirubin, and total protein in this group when compared to the control group at various time points (1st, 2nd, 3rd, and 4th weeks). These observations underscore the biochemical alterations induced by *B. microti* infection, emphasizing the impact of the disease on liver function and protein metabolism. Furthermore, the animals treated with artesunate dosages of 2 mg/kg, 4 mg/kg, and 8 mg/kg exhibited a minor decrease in the levels of ALT, ALP, AST, bilirubin, and total protein when compared to the *B. microti*-infected group. This suggests that artesunate treatment may have a potential ameliorative effect on these biochemical parameters, attenuating the adverse consequences of *Babesia microti* infection. This study was in agreement with Abiodun (38).

The *B. microti* parasite inoculates the liver through the central hepatic vein and the spleen through the splenic artery. After entry, serous congestion of red pulp and proliferation of megakaryocytes lead to an acute phase of infection (33). In a previously conducted comparative study, the effect of artesunate and chloroquine treatment on histopathological damages caused by *Plasmodium berghei* in albino mice showed severe damage to the liver and spleen that was significantly reduced by artesunate treatment as compared to chloroquine (39). Similarly, we observed a dose-dependent manner recovery of spleen cellular structure with weak red pulp cellularity and white pulp with clear marginal zones around follicles. Hepatic lobules and central vein are unformed in appearance in the control and at high dosage (8 mg/kg) groups to show AS possesses potent effects of antiparasitic against *B. microti* infection.

Beyond its direct antiparasitic properties, AS may have additional therapeutic benefits due to its capacity to regulate the expression of apoptotic proteins Bax, Beclin, and Caspase activity through the destruction of contaminated cells, stop the infection from spreading, and encourage tissue regeneration (40). Recently, documented studies on 56 phytochemicals including AS showed significant reduction in TNF-α, IL2, CD44, and IFN-γ via NF-kB pathways *in vitro* and *in vivo* models (41). In our study, mice administered with AS at a dosage of 8 mg/kg showed a significant reduction in the mRNA expression levels of Bax, Beclin 1, and Caspase 9 in comparison to mice that were challenged with *B. microti* alone (Figure 6). Mice treated with AS at the medium dose of 4 mg/kg and high dose of 8 mg/kg exhibited a significant reduction in the expression of CD44, IFN-γ, IL2, and TNF-α compared to those challenged with *B. microti* alone. This modulation suggests a complex interplay between AS and cellular responses, potentially influencing the balance between cell survival and apoptosis.

The distinctive staining patterns observed in immunohistochemistry analysis showed hepatic cytoplasm between the *B. microti*-infected and AS at a higher dosage of 8 mg/kg showed the hepatic cytoplasm of the mice infected with *B. microti* showcased a pronounced strong tissue immune expression of Bax, Caspase 9,

CD44 and TNF-α staining, underscoring the presence of considerable positive expression within the cytoplasmic compartment. Conversely, the hepatic cytoplasm exhibited a distinct blue coloration in the mice treated with AS at a dose of 8 mg/kg. This blue hue indicates the absence of these detectable proteins Bax, Caspase 9, CD44, and TNF-α expression, this underscores the potential of AS treatment to influence protein expression dynamics within a cellular context. These findings are consistent with previous research that AS suppresses the oxidative and inflammatory processes by activating nuclear factor erythroid 2-related factor that inhibits caspase activity and reduces the apoptosis regulator Bax and Bcl-2 expression ratio by activating Nrf2 and downregulating ROS-dependent p38 mitogen-activated protein kinase in mice (42).

Babesiosis disrupts the delicate balance between apoptosis and inflammation, ICAM-1, a cell adhesion molecule, facilitates the interaction between leukocytes, immune cells, and endothelial cells, which line the blood vessels (43). CRP, a non-specific inflammatory marker produced by the liver, is used to assess the presence and severity of inflammation. SICAM-1, soluble form of ICAM-1, shed from the cell surface into the bloodstream provides a more sensitive and non-invasive measure of inflammation compared to ICAM-1 inflammatory mediators that are upregulated in response to this disturbance, as well as pro- and anti-apoptotic proteins such as Bax, a proapoptotic protein, which plays a critical role in initiating apoptosis by inducing mitochondrial damage and releasing cytochrome c (44). Our Western blot analysis showed a marked significant increase in expression levels of key apoptotic proteins Bax, and Bcl-2 expression decreased significantly ($p < 0.05$) in *the B. microti*-infected group, AS normalized Bax and Bcl-2 expression ratio. However, expression of inflammatory proteins (ICAM-1, SICAM-1, and C-reactive protein) was upregulated in the *B. microti*-infected group and AS treatment significantly ($p < 0.05$) downregulated this alleviation in a dose-dependent manner. This is a correlation with the results of De Mast et al. (43) and Park et al. (45) who noted elevated vWf, VCAM-1, SICAM-1, and C-reactive protein levels in children who have a microscopic asymptomatic malarial illness. This suggests that endothelial cells could be among the early host responses to the presence of parasites in the case of parasitemia. Our study results are also in agreement with the findings of Baric et al. (46) who checked ICAM-1, SICAM-1, and CRP levels through ELISA kit in dog blood samples suffering from canine babesiosis. These parameters were noted elevated before treatment but returned to normal after treatment which indicates the promising effects of AS for babesiosis treatment. The AS administration underscores the intricate role in regulating apoptotic pathways and alleviating inflammatory response during *B. microti* infection.

5 Conclusion

In conclusion, the present study provides potential evidence that AS may have a promising effect on *B. microti* infection by increasing body weight, recovering liver and spleen index state in mice, improving red blood cell (RBC), white blood cell (WBC), and platelet (PLT) counts, and restoring blood homeostasis, downregulating levels of alanine aminotransferase (ALT), aminotransferase glutamate (AST), alkaline phosphatase (ALP), and total protein; restoring cytoarchitectural damage in the liver and spleen; modulating the pathway of cellular apoptosis and attenuating in inflammatory response, and in a dose-dependent manner. Furthermore, these insights contribute significantly to understanding AS therapeutic mechanisms and their potential utility as an adjunctive treatment for Babesia infections.

Data availability statement

The raw data supporting the conclusions of this article will be made available by the authors, without undue reservation.

Ethics statement

The animal study was approved by the Institutional Research Ethics Committee, Northeast Agricultural University. The study was conducted in accordance with the local legislation and institutional requirements.

Author contributions

SF: Writing – original draft, Software, Methodology, Investigation, Formal analysis. WA: Writing – review & editing, Resources, Investigation, Formal analysis. SiL: Writing – review & editing, Validation, Project administration, Resources, Investigation. MH: Writing – review & editing, Validation. MI: Software, Data curation, Writing – review & editing. ShL: Validation, Formal analysis, Writing – review & editing, Software. MF: Methodology, Writing – review & editing, Software, Formal analysis. MS: Data curation, Writing – review & editing, Software, Formal analysis. XZ: Validation, Supervision, Project administration, Funding acquisition, Conceptualization, Writing – review & editing.

Funding

The author(s) declare that financial support was received for the research, authorship, and/or publication of this article. This study was supported by the National Natural Science Foundation of China (Grant no: 32072918).

Conflict of interest

The authors declare that the research was conducted in the absence of any commercial or financial relationships that could be construed as a potential conflict of interest.

Publisher's note

All claims expressed in this article are solely those of the authors and do not necessarily represent those of their affiliated organizations, or those of the publisher, the editors and the reviewers. Any product that may be evaluated in this article, or claim that may be made by its manufacturer, is not guaranteed or endorsed by the publisher.

References

1. Keroack CD, Elsworth B, Duraisingh MT. To kill a Piroplasm: genetic technologies to advance drug discovery and target identification in Babesia. *Int J Parasitol*. (2019) 49:153–63. doi: 10.1016/j.ijpara.2018.09.005

2. Hussain S, Hussain A, Aziz MU, Song B, Zeb J, George D, et al. A review of zoonotic Babesiosis as an emerging public health threat in Asia. *Pathogens*. (2021) 11:23. doi: 10.3390/pathogens11010023

3. Kavanaugh MJ, Decker CF. Babesiosis. *Dis Mon*. (2012) 58:355–60. doi: 10.1016/j.disamonth.2012.03.007

4. Alvi MA, Li L, Bahadur K, Ullah S, Saqib M, Ohiolei JA, et al. First comparative biochemical profile analysis of cystic fluids of Taenia Hydatigena and Echinococcus Granulosus obtained from slaughtered sheep and goats. *Pak Vet J*. (2022) 42:215–21. doi: 10.29261/pakvetj/2022.001

5. Tołkacz K, Rodo A, Wdowiarska A, Bajer A, Bednarska MJP. Impact of *Babesia microti* infection on the initiation and course of pregnancy in Balb/C mice. *Parasit Vectors*. (2021) 14:1–17. doi: 10.1186/s13071-021-04638-0

6. Jasik KP, Kleczka A, Franielczyk AJVS. Histopathological aspects of the influence of Babesia microti on the placentas of infected female rats. *Vet Sci*. (2024) 11:18. doi: 10.3390/vetsci11010018

7. Kandeel M, Rehman TU, Akhtar T, Zaheer T, Ahmad S, Ashraf U, et al. Anti-parasitic applications of nanoparticles: a review. *Pak Vet J*. (2022) 42:135–40. doi: 10.29261/pakvetj/2022.040

8. Aprioku J, Obianime A. Structure-activity-relationship (Sar) of Artemisinins on some biological Systems in Male Guinea Pigs. *Insight Pharm Sci*. (2011) 1:1–10. doi: 10.5567/IPHARMA-IK.2011.1.10

9. Goo Y-K, Terkawi MA, Jia H, Aboge GO, Ooka H, Nelson B, et al. Artesunate, a potential drug for treatment of Babesia infection. *Parasitol Int*. (2010) 59:481–6. doi: 10.1016/j.parint.2010.06.004

10. Swetanshu PS, Yadav S, Nde AL, Kumar VJ. Drugs for the control of parasitic diseases: current status and case studies In: AP Mishra and M Nigam, editors. *Parasitic Infections: Immune Responses and Therapeutics*. Hoboken, NJ: Wiley (2023)

11. Bae J-Y, Lee GE, Park H, Cho J, Kim Y-E, Lee J-Y, et al. Pyronaridine and Artesunate are potential antiviral drugs against Covid-19 and influenza. *bioRxiv*. (2020). doi: 10.1101/2020.07.28.225102

12. Utzinger J, Shuhua X, N'Goran EK, Bergquist R, Tanner M. The potential of Artemether for the control of schistosomiasis. *Int J Parasitol*. (2001) 31:1549–62. doi: 10.1016/S0020-7519(01)00297-1

13. Sen R, Bandyopadhyay S, Dutta A, Mandal G, Ganguly S, Saha P, et al. Artemisinin triggers induction of cell-cycle arrest and apoptosis in Leishmania Donovani promastigotes. *J Med Microbiol*. (2007) 56:1213–8. doi: 10.1099/jmm.0.47364-0

14. Martini MC, Zhang T, Williams JT, Abramovitch RB, Weathers PJ, Shell SS. Artemisia Annua and Artemisia Afra extracts exhibit strong bactericidal activity against *Mycobacterium Tuberculosis*. *J Ethnopharmacol*. (2020) 262:113191. doi: 10.1016/j.jep.2020.113191

15. Desrosiers MR, Mittleman A, Weathers PJ. Dried leaf *Artemisia Annua* improves bioavailability of artemisinin via cytochrome P450 inhibition and enhances artemisinin efficacy downstream. *Biomol Ther*. (2020) 10:254. doi: 10.3390/biom10020254

16. Zhang E, Wang J, Chen Q, Wang Z, Li D, Jiang N, et al. Artesunate ameliorates Sepsis-induced acute lung injury by activating the Mtor/Akt/Pi3k Axis. *Gene*. (2020) 759:144969. doi: 10.1016/j.gene.2020.144969

17. Carvalho LJ, Tuvshintulga B, Nugraha AB, Sivakumar T, Yokoyama N. Activities of Artesunate-based combinations and Tafenoquine against Babesia Bovis in vitro and Babesia Microti in vivo. *Parasit Vectors*. (2020) 13:1–9. doi: 10.1186/s13071-020-04235-7

18. Bukauskaitė D, Chagas CRF, Bernotienė R, Žiegytė R, Ilgūnas M, Iezhova T, et al. A new methodology for Sporogony research of avian Haemoproteids in laboratory-reared Culicoides Spp., with a description of the complete Sporogonic development of Haemoproteus pastoris. *Parasit Vectors*. (2019) 12:1–13. doi: 10.1186/s13071-019-3832-x

19. Akoolo L, Schlachter S, Khan R, Alter L, Rojtman AD, Gedroic K, et al. A novel quantitative PCR detects Babesia infection in patients not identified by currently available non-nucleic acid amplification tests. *BMC Microbiol*. (2017) 17:1–9. doi: 10.1186/s12866-017-0929-2

20. Shino Y, Itoh Y, Kubota T, Yano T, Sendo T, Oishi R. Role of poly (Adp-ribose) polymerase in cisplatin-induced injury in Llc-Pk1 cells. *Free Radic Biol Med*. (2003) 35:966–77. doi: 10.1016/S0891-5849(03)00470-2

21. Li S, Liu R, Wei G, Guo G, Yu H, Zhang Y, et al. Curcumin protects against aflatoxin B1-induced liver injury in broilers via the modulation of long non-coding RNA expression. *Ecotoxicol Environ Saf*. (2021) 208:111725. doi: 10.1016/j.ecoenv.2020.111725

22. Livak KJ, Schmittgen TD. Analysis of relative gene expression data using real-time quantitative Pcr and the 2− Δδct method. *Methods*. (2001) 25:402–8. doi: 10.1006/meth.2001.1262

23. Schmittgen TD, Livak KJ. Analyzing real-time Pcr data by the comparative Ct method. *Nat Protoc*. (2008) 3:1101–8. doi: 10.1038/nprot.2008.73

24. Zhang Y, Wang Y, Yang Y, Zhao D, Liu R, Li S, et al. Proteomic analysis of Itpr2 as a new therapeutic target for curcumin protection against Afb1-induced Pyroptosis. *Ecotoxicol Environ Saf*. (2023) 260:115073. doi: 10.1016/j.ecoenv.2023.115073

25. Wang H, Muhammad I, Li W, Sun X, Cheng P, Zhang X. Sensitivity of arbor acres broilers and chemoprevention of aflatoxin B1-induced liver injury by curcumin, a natural potent inducer of phase-ii enzymes and Nrf2. *Environ Toxicol Pharmacol*. (2018) 59:94–104. doi: 10.1016/j.etap.2018.03.003

26. Villanueva-Saz S, Borobia M, Fernández A, Jiménez C, Yzuel A, Verde MT, et al. Anaemia in sheep caused by *Babesia* and *Theileria* Haemoparasites. *Animals (Basel)*. (2022) 12:3341. doi: 10.3390/ani12233341

27. Rafique A, Nasir S, Ashraf A, Nawaz Z, Zahid FM, Abbas A, et al. Sero-surveillance and risk factors analysis of caprine toxoplasmosis in Faisalabad Punjab, Pakistan. *Pak Vet J*. (2022) 42:102–6. doi: 10.29261/pakvetj/2021.020

28. Aslam F, Saleem G, Ashraf K, Hafeez MA, Saqib MJPVJ. Identification and molecular characterization of Theileria Annulata with associated risk factors in naturally infected camels from selected districts in Punjab, Pakistan. *Pak Vet J*. (2023) 43:79–84. doi: 10.29261/pakvetj/2022.084

29. Tuvshintulga B, Sivakumar T, Yokoyama N, Igarashi I. Development of unstable resistance to Diminazene Aceturate in Babesia Bovis. *Int J Parasitol Drugs Drug Resist*. (2019) 9:87–92. doi: 10.1016/j.ijpddr.2019.02.001

30. Adebayo JO, Tijjani H, Adegunloye AP, Ishola AA, Balogun EA, Malomo SO. Enhancing the antimalarial activity of Artesunate. *Parasitol Res*. (2020) 119:2749–64. Epub 2020/07/09. doi: 10.1007/s00436-020-06786-1

31. Arsuaga M, González LM, Padial ES, Dinkessa AW, Sevilla E, Trigo E, et al. Misdiagnosis of Babesiosis as malaria, Equatorial Guinea, 2014. *Emerg Infec Dis*. (2018) 24:1588–9. doi: 10.3201/eid2408.180180

32. Marley SE, Eberhard ML, Steurer FJ, Ellis WL, McGreevy PB, Ruebush TK 2nd. Evaluation of selected antiprotozoal drugs in the Babesia Microti-Hamster model. *Antimicrob Agents Chemother*. (1997) 41:91–4. doi: 10.1128/aac.41.1.91

33. Djokic V, Akoolo L, Parveen N. Babesia Microti infection changes host spleen architecture and is cleared by a Th1 immune response. *Front Microbiol*. (2018) 9:85. doi: 10.3389/fmicb.2018.00085

34. Mwololo SW, Mutiso JM, Macharia JC, Bourdichon AJ, Gicheru MM. In vitro activity and in vivo efficacy of a combination therapy of Diminazene and chloroquine against murine visceral Leishmaniasis. *J Biomed Res*. (2015) 29:214–23. doi: 10.7555/JBR.29.20140072

35. Aguilar-Marcelino L, Bautista-Garfias CR, Zaheer T, Maqsood A, Bamarni SSI, Abdullah BH, et al. Potential of Anisakiasis in foodborne zoonosis. *Pak Vet J*. (2022) 42:433–44. doi: 10.29261/pakvetj/2022.080

36. Quang Bui P, Hong Huynh Q, Thanh Tran D, Thanh Le D, Quang Nguyen T, Van Truong H, et al. Pyronaridine-Artesunate efficacy and safety in uncomplicated *Plasmodium falciparum* malaria in areas of artemisinin-resistant falciparum in Viet Nam (2017–2018). *Clin Infect Dis*. (2020) 70:2187–95. doi: 10.1093/cid/ciz580

37. Duncan KT, Grant A, Johnson B, Sundstrom KD, Saleh MN, SEJV-B L, et al. Identification of *Rickettsia* Spp. and *Babesia* Conradae in *Dermacentor* Spp. Collected from dogs and cats across the United States. *Vector Borne Zoonotic Dis*. (2021) 21:911–20. doi: 10.1089/vbz.2021.0047

38. Abiodun A. Effect of Artesunate on Haematological and plasma biochemical parameters in female Wistar rats. *Biomed. Pharmacol J*. (2023) 16:1257–62. doi: 10.13005/bpj/2706

39. Soniran O, Idowu O, Ajayi O, Olubi I. Comparative study on the effects of chloroquine and artesunate on histopathological Damages caused by *Plasmodium berghei* in four vital organs of infected albino mice. *Malar Res Treat*. (2012) 2012:960758. doi: 10.1155/2012/960758

40. Zhou X, Suo F, Haslinger K, Quax WJ. Artemisinin-type drugs in tumor cell death: mechanisms, combination treatment with biologics and nanoparticle delivery. *Pharmaceutics*. (2022) 14:395. doi: 10.3390/pharmaceutics14020395

41. Laurindo LF, Santos ARO, Carvalho ACA, Bechara MD, Guiguer EL, Goulart RA, et al. Phytochemicals and regulation of Nf-kb in inflammatory bowel diseases: an overview of in vitro and in vivo effects. *Meta*. (2023) 13:96. doi: 10.3390/metabo13010096

42. Lu H, Wang B, Cui N, Zhang Y. Artesunate suppresses oxidative and inflammatory processes by activating Nrf2 and Ros-dependent P38 Mapk and protects against cerebral ischemia-reperfusion injury. *Mol Med Rep*. (2018) 17:6639–46. doi: 10.3892/mmr.2018.8666

43. De Mast Q, Brouwers J, Syafruddin D, Bousema T, Baidjoe AY, de Groot PG, et al. Is asymptomatic malaria really asymptomatic? hematological, vascular and inflammatory effects of asymptomatic malaria parasitemia. *J Infect*. (2015) 71:587–96. doi: 10.1016/j.jinf.2015.08.005

44. Yang Z-B, Qiu L-Z, Chen Q, Lin J-D. Artesunate alleviates the inflammatory response of ulcerative colitis by regulating the expression of Mir-155. *Pharm Biol*. (2021) 59:95–103. doi: 10.1080/13880209.2020.1867196

45. Park GS, Ireland KF, Opoka RO, John CC. Evidence of endothelial activation in asymptomatic *Plasmodium falciparum* parasitemia and effect of blood group on levels of von Willebrand factor in malaria. *J Pediatric Infect Dis Soc*. (2012) 1:16–25. doi: 10.1093/jpids/pis010

46. Barić Rafaj R, Kuleš J, Selanec J, Vrkić N, Zovko V, Zupančič M, et al. Markers of coagulation activation, endothelial stimulation, and inflammation in dogs with babesiosis. *J Vet Intern Med*. (2013) 27:1172–8. doi: 10.1111/jvim.12146

frontiers | Frontiers in Public Health

TYPE Original Research
PUBLISHED 11 June 2024
DOI 10.3389/fpubh.2024.1362086

Check for updates

OPEN ACCESS

EDITED BY
Mughees Aizaz Alvi,
University of Agriculture,
Faisalabad,
Pakistan

REVIEWED BY
Shahbaz Ul Haq,
Shantou University,
China
Mohammed Dauda Goni,
Universiti Malaysia Kelantan,
Malaysia
Samson Malwa Haumba,
Georgetown University Medical Center,
United States

*CORRESPONDENCE
Teshiwal Deress
teshiwalderess@gmail.com

RECEIVED 27 December 2023
ACCEPTED 30 May 2024
PUBLISHED 11 June 2024

CITATION
Getie M, Belay G, Amare A, Abebe W and Deress T (2024) Burden and factors influencing intestinal parasitic infections among food handlers in Gondar City, Northwest Ethiopia.
Front. Public Health 12:1362086.
doi: 10.3389/fpubh.2024.1362086

COPYRIGHT
© 2024 Getie, Belay, Amare, Abebe and Deress. This is an open-access article distributed under the terms of the Creative Commons Attribution License (CC BY). The use, distribution or reproduction in other forums is permitted, provided the original author(s) and the copyright owner(s) are credited and that the original publication in this journal is cited, in accordance with accepted academic practice. No use, distribution or reproduction is permitted which does not comply with these terms.

Burden and factors influencing intestinal parasitic infections among food handlers in Gondar City, Northwest Ethiopia

Michael Getie[1], Gizeaddis Belay[1], Azanaw Amare[2], Wondwossen Abebe[2] and Teshiwal Deress[3]*

[1]Department of Medical Microbiology, Amhara National Regional State Public Health Institute, Bahir Dar, Ethiopia, [2]Department of Medical Microbiology, School of Biomedical and Laboratory Sciences, College of Medicine and Health Sciences, University of Gondar, Gondar, Ethiopia, [3]Department of Quality Assurance and Laboratory Management, School of Biomedical and Laboratory Sciences, College of Medicine and Health Sciences, University of Gondar, Gondar, Ethiopia

Background: Intestinal parasitic infections pose significant global health challenges, particularly in developing countries. Asymptomatic infections often present a considerable burden with food handlers serving as potential carriers. In Ethiopia, the prevalence of these parasites varies across regions, and accurate data in the study area is lacking. Therefore, this study aimed to investigate the prevalence of intestinal parasites among food handlers working in hotels and restaurants in Gondar City, Northwest Ethiopia.

Methods: A cross-sectional study collected stool samples from food handlers alongside a structured questionnaire gathering socio-demographic and hygiene practice information. Stool specimens were screened for intestinal parasites using direct wet mount and formol-ether concentration techniques. The collected data were checked for completeness, entered into EpiData software version 3.1, and exported to SPSS version 20 for analysis. A multivariable logistic regression analysis was deemed statistically significant if the *p*-value was less than 0.05.

Results: A total of 257 food handlers working in hotels and restaurants in Gondar City participated in the study. Of these, 33.5% (86/257) were found positive for one or more intestinal parasites, with a 95% confidence interval (CI) of 28.0–39.5%. The study identified nine types of intestinal parasites, with *E. histolytica/dispar* (8.2%, 21/257) and Ascaris lumbricoides (6.6%, 17/257) being the predominant parasites, followed by hookworm (3.5%, 9/257) and *S. mansoni* (2.3%, 6/257). The prevalence of mixed infections was 9.3% (24/257). A significant association was observed between intestinal parasitic infection and the educational level of food handlers.

Conclusion: In this study, a high prevalence of intestinal parasites was detected indicating poor hygiene practices of the food handlers at the study site. Even the prevalence of mixed infections was high. Regular training, strict adherence to personal hygiene and food-handling practices, and routine inspections and medical checkups for food handlers are crucial.

KEYWORDS

food handlers, intestinal parasites, food sanitation, Gondar, Ethiopia

Background

Gastrointestinal parasitic infections are globally distributed and have a significant impact on developing nations (1). Certain parasites possess the ability to afflict both humans and animals, posing a severe threat to the well-being of both species (2). Factors such as inadequate personal hygiene, suboptimal environmental sanitation, and various socio-economic, demographic, and health-related behaviors contribute to the transmission of these infections (3, 4). The health status and hygiene practices of food handlers play a vital role in determining the contamination of food and beverages, particularly in regions with weak regulatory frameworks for food hygiene (5–8). Food handlers can act as carriers and disseminators of enteropathogens, directly or indirectly contaminating food and posing a potential threat to consumer health (7, 9, 10). The area beneath fingernails, which is challenging to clean, harbors a high concentration of microorganisms, further increasing the risk of contamination (6, 11–14). Infected food handlers with poor personal hygiene can serve as significant sources of transmission to society. These handlers are often asymptomatic carriers who are unaware of their role in spreading infections, which hampers effective control and elimination efforts (15). Intestinal parasitic infections (IPIs) often do not exhibit clinical signs and symptoms, and they have several potential carriers, such as food handlers, making eradication and control challenging (16).

Poor hand hygiene and the absence of food safety training are significant factors contributing to the high prevalence of IPIs among food handlers (17). Regular medical check-ups and handwashing practices are protective measures that significantly reduce the risk of infection (13, 17). Foodborne intestinal parasitic diseases are the major causes of morbidity and high death rates globally (18). Intestinal parasites impose a substantial global burden, affecting approximately 3.5 billion people annually and causing over 200,000 reported deaths worldwide (19). Developing countries, especially those in Sub-Saharan Africa, bear a higher burden of intestinal parasites compared to developed nations (20). In Ethiopia, approximately 50,000 deaths per year are attributed to intestinal parasites (21). These infections not only cause morbidity and mortality but also have long-term effects on the health, nutritional status, and overall development of affected individuals (22). Gastrointestinal illnesses impose a significant social and economic burden, particularly in low and middle-income countries, where they are among the leading causes of morbidity and mortality (23). The loss of productivity due to illness affects not only individuals but also businesses and economies at large. The financial impact is further exacerbated by the high prevalence of such diseases in developing nations, where many people still consume contaminated water and lack proper sanitation (24). Food handlers play a critical role in the transmission of intestinal parasites, especially when they do not practice proper hand hygiene after using the toilet or before food preparation (13, 25).

In developing countries like Ethiopia, urbanization has led to increased patronage of food service establishments, where the health and hygiene practices of food handlers are critical in preventing food contamination. Unfortunately, food handlers are often employed without screening for infections that can be transmitted due to poor hygiene, such as intestinal parasites (6). Studies conducted in different settings have reported a high prevalence of intestinal parasites among food handlers, ranging from 29 to 63% (11, 13, 26). Studies in different parts of Ethiopia have revealed a wide variability in the prevalence of intestinal parasites among food handlers (27, 28), with rates ranging from 14.5 to 46.3% (6, 17, 19, 21, 29–33). A recent review in Ethiopia found that 33.6% of food handlers in food establishments were infected with *E. histolytica/dispar* and Ascaris lumbricoides (13). The diversity of factors contributing to the spread of intestinal parasites, such as water sources, personal hygiene practices, and environmental sanitation, underscores the complexity of controlling these infections (25). Moreover, the diverse nature of these parasite species continues to influence the strategies employed to reduce and combat the infection (34).

One of the main challenges in implementing effective public health measures to combat IPIs is the lack of comprehensive and up-to-date data. Many studies, including those conducted in Gondar City, have limitations in scope and may not be generalizable to the broader population (25, 35). This lack of data hinders the ability of local health planners to develop and implement appropriate intervention measures tailored to the specific risk factors identified in different populations. Furthermore, given the widespread prevalence of IPIs with regional variations, there is a pressing need for periodic assessments to guide future interventions, particularly among high-risk groups such as food handlers. Therefore, this study aimed to evaluate the prevalence of IPIs and the factors associated with food handlers working in hotels and restaurants in Gondar City, Northwest Ethiopia.

Rationale

The growing popularity of Gondar as a tourist destination has inevitably led to a surge in demand for food services provided by hotels and restaurants. While the burgeoning hospitality industry contributes to the economic vitality of the region, it concurrently raises concerns regarding the potential health risks associated with foodborne illnesses. As the demand for food services escalates, so does the need to scrutinize the factors influencing food safety, particularly in the context of intestinal parasites. Individuals who are directly engaged in food preparation and service play a crucial role in upholding food hygiene. The close interaction between food handlers and the food they prepare makes this group a critical focus for understanding and mitigating the risk of foodborne parasitic infections.

The distinct circumstances of Gondar City underscore the urgency of appraising the prevalence of intestinal parasites among food handlers. The potential impact of parasitic infections on both the local population and the influx of tourists underscores the urgency of this research. By exploring intestinal parasites among food handlers, the research aims to provide empirical data that can inform evidence-based interventions. The findings of this study will help develop targeted measures to enhance food safety practices, thereby safeguarding public health in Gondar City.

Furthermore, the insights gained from this research can contribute to the broader discourse on food safety in Ethiopia, offering valuable lessons and recommendations that may apply to other regions facing similar challenges. The identification of specific risk factors and the development of interventions tailored to the local context can serve as a model for enhancing food safety practices in other cultural and historical centers across the country.

10.3389/fpubh.2024.1362086

Materials and methods

Study area, design, and period

A cross-sectional study was conducted from February to April 2020 in Gondar City. The city is found in the Amhara regional state, approximately 747 kilometers to the northwest of Addis Ababa (the capital city of Ethiopia) and 182 kilometers from Bahir Dar. According to the Central Statistical Agency's 2017 population projection, the city's total population hovers around 360,600, with roughly 176,593 being males (36, 37). The city is administratively divided into 24 'kebeles,' the smallest administrative units. Furthermore, Gondar is divided into several administrative divisions, each playing a significant role in public health and sanitary issues. These divisions include the Gondar City Administration Health Department, the Gondar City Administration, and individual district offices. The Gondar City Administration Health Department is primarily responsible for overseeing health-related initiatives within the city, including the management of health risks associated with food handling. They conduct regular inspections, provide training for food handlers, and implement regulatory measures to ensure food safety. The Gondar City Administration is responsible for the broader governance of the city, including the provision of public services and infrastructure that indirectly relate to public health. They work in close collaboration with the Health Department to address health challenges. Each district office within Gondar City has its administrative roles in managing health-related activities in their respective districts. They are responsible for implementing health initiatives at a district level, collecting data, and reporting to the zonal Health Department office. The exact number of food handlers in each food establishment could not be determined due to high turnover (see Figure 1).

Populations

The source population consisted of all food handlers who worked at hotels and restaurants in Gondar City during the study period. The study population included only those food handlers who met the inclusion criteria, which were: willingness to participate in the study and no intake of anti-parasite drug (s) in the 2 weeks before the start of the study.

Inclusion and exclusion criteria

The inclusion criteria encompass all individuals directly involved in handling, preparing, or serving food within Gondar City Hotels and Restaurants and willing to take part in the study. The exclusion criteria were study participants who took antiparasitic medication within 2 weeks before the data collection period, and those individuals with chronic illnesses affecting the gastrointestinal tract were excluded.

Sample size determination and sampling technique

The minimum sample size for the study was calculated using a single population proportion formula based on the assumption of a 5% expected margin of error (d = 0.05), 95% confidence interval (z = 1.96), and 8.7% prevalence from a previous study conducted in Wolaita Sodo town (39). It is important to note that Wolaita Sodo town, like Gondar city, is a zonal town. We expect the populations of the two towns to be similar, which forms the basis for our sample size estimation.

$$\frac{n_i = (Z\alpha / 2)^2 \, pq}{d^2}$$

$$\frac{n_i = (1.96)^2 \, 0.087(1 - 0.087)}{(0.05)^2}$$

$$n_i \approx 125^* \, 2.$$

$$n_i \approx 250.$$

Since the total number of the source population was less than 10,000, the correction formula was applied to adjust the final sample size (nf):

$$n_f = \left(1 + \frac{\frac{n_i}{(n_i)}}{N} \right) = \left(1 + \frac{\frac{250}{(250)}}{8417} \approx 244 \right)$$

Finally, considering a 10% non-response rate, the final sample size was estimated to be 269 study participants. The participants were selected from five sub-cities using multistage sampling. A complete list of catering establishments was obtained from the Gondar Trade Administration office. The establishments in the selected sub-cities were stratified into hotels and restaurants. The required sample size was then proportionally allocated to each stratum, and a random sampling technique was employed to include the necessary number of participants from each category.

Data data collection

Data about socio-demographic characteristics and other variables were collected using a structured pre-tested questionnaire. The questionnaire contained information on age, gender, marital status, year of service, educational level, previous training, and practice of hand washing of the food handlers.

Stool sample collection and transportation

Stool samples were collected from food handlers using standard procedures. The collection took place in the morning because this time of the day enhances the detection of parasites in the stool. Each participant was provided with a clean, dry, leak-proof, and labeled plastic stool cup for self-collection. The study

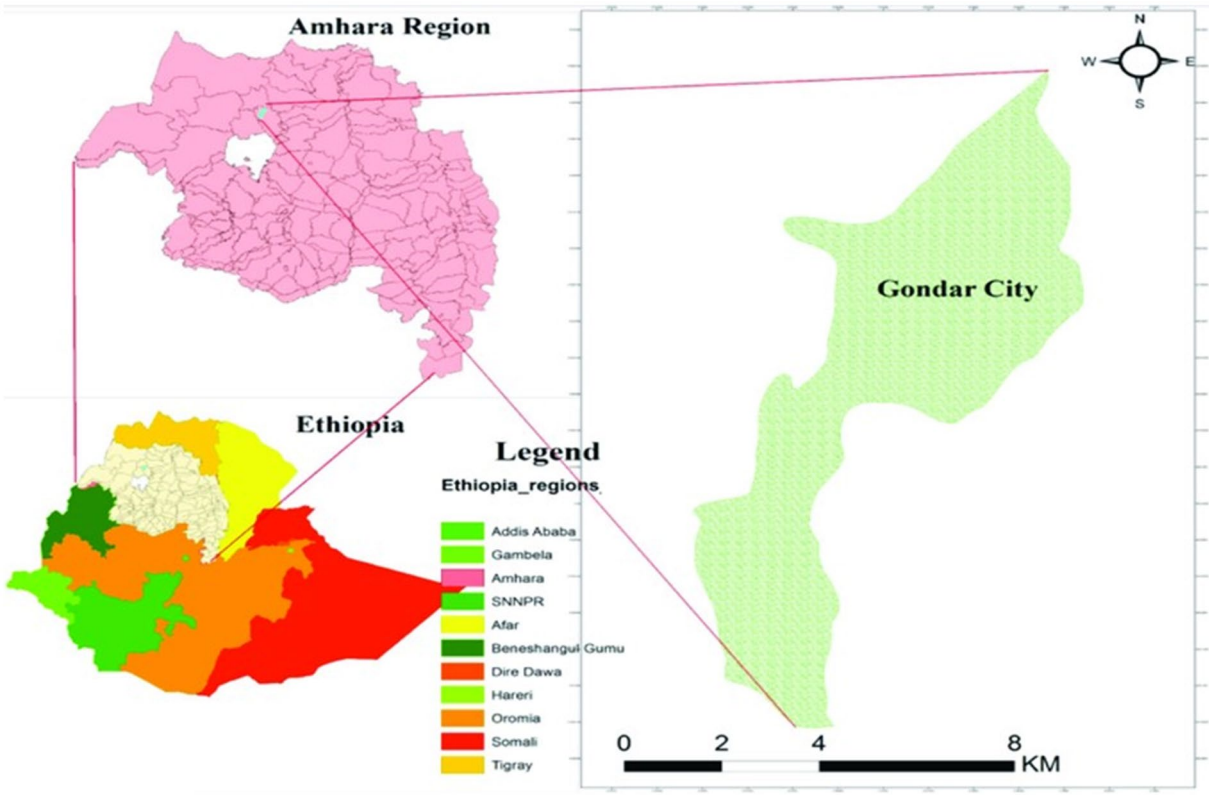

FIGURE 1
Illustrates a visual representation of the study area, Gondar City. Source: Tamiru et al. (38).

participants were instructed to utilize the provided applicator stick to pick up a piece of stool, place it in the clean plastic container provided, and deliver it immediately. A minimum of 10 grams of stool specimens were collected from each study participant. This quantity is necessary to ensure that an adequate amount of the sample is available for diagnostic testing. The containers were tightly closed to prevent leakage and contamination. Then the stool samples were immediately stored in a cold box after labelling them with a code on the outer surface of the plastic cup. The collected samples were then transported at room temperature to the medical parasitology laboratory of the University of Gondar Comprehensive Specialized Hospital within an hour of collection. This rapid transportation minimizes the risk of sample degradation and ensures that the samples reach the laboratory in optimal condition for analysis.

Direct wet mount preparation

A drop of physiological saline was applied to one slide, while the other received Dobell's iodine. Using an applicator stick, a small (equivalent to the size of a matchstick head) quantity of stool specimen was evenly spread over the separate glass slides with physiological saline and iodine. The specimens were then covered with a cover glass and scrutinized for the presence of helminth eggs, larvae, ciliates, cysts, and oocysts under 40× objectives (40).

Formol ether concentration techniques

An estimated 1 g of formed stool sample or 2 mL of watery stool was emulsified in about 4 mL of 10% formol water contained in a screw-cap bottle. Furthermore, 3 mL of 10% formol water was added and mixed well by shaking. The emulsified feces were sieved, and the suspension was transferred to a conical centrifuge tube. About 3 mL of diethyl ether was added, and the tube was mixed for 1 min. Then, the samples were centrifuged at 3000 rpm for 1 min. The tubes were inverted to discard the ether, fecal debris, and formol water, leaving behind the sediment. The bottom of the tubes was taped to re-suspend and mix the sediment. The sediment was transferred to a slide covered with a cover glass and examined microscopically using 40× objective lenses (40).

Data management and analysis

After ensuring completeness, data were entered using EpiData version 3.1 and exported to SPSS 20 for analysis. Descriptive statistics, such as frequencies, percentages, and mean, were used primarily to summarize the findings. Further, bivariate and multivariate logistic regression analyses were performed to investigate the relationships between the predictors and outcome variables. All variables with a p-value of ≤ 0.2 in the bivariate analysis were transferred into the multivariable logistic regression model to

10.3389/fpubh.2024.1362086

adjust for possible confounding variables. Finally, variables with a p-value of <0.05 in the final analysis were considered to indicate significant associations.

Ethical consideration

Ethical clearance was granted by the University of Gondar, School of Biomedical and Laboratory Sciences ethics review committee (SBMLS/870/10), and support letters were written from the North Gondar Hotel and Tourism Management Bureau before data collection. Further permission was obtained from the Zonal Health Department office. A formal letter was also written from the Municipality of the city to food establishments and written informed consent was obtained from each study participant before commencing the data collection. To ensure the privacy of the study participants during interviews, all data collection processes were conducted in an isolated area. Furthermore, participants were informed that all data and samples obtained from them would be kept confidential. Participants who tested positive for intestinal parasitic infection were referred to a nearby health facility for appropriate treatment of the disease.

Results

Socio-demographic data

In this study, a total of 257 food handlers participated in the study with a 96% response rate. From this 91.8% (238) of them were females. The median age of the study participants was 25.71 ± 5.37 years and the majority 74.7% (192) were in the age group of 20–40 years. Nearly one-fourth (63) of the study participants were illiterate, while 47.4% (171) had secondary school education or above.

Hygienic practice of the study participants

The majority (89.1%) of the study participants had worked for less than 5 years. Concerning training, only 23% (59) of them had training certificates on food handling techniques. Slightly higher than three-fourths (200) of the study participants had hand washing practice using water only. Slightly higher than one-third (100) were regularly supervised. The majority 64.6% (166) of the study participants had hair covering practice. Regarding fingernail status, the majority 65.8% (169) of the study participants were observed not clean/ not cut (Table 1).

Prevalence of intestinal parasites

The overall prevalence of IPIs among food handlers in Gondar City was 33.5% (86/257) with a 95% confidence interval (CI) of 28.0–39.5%. Of these, 62 (24.1%) were infected by a single parasite, while 24 (9.3%) had mixed infections (Figure 2).

Nine types of intestinal parasites were found in food handlers' stools. Among these, *E. histolytica/dispar* was the predominant 13.7% (35/257) parasite, followed by *A. lumbricoides* 11% (28/255), hookworms 6.7% (17/255), and *S. mansoni* and *G. lamblia* each accounting for 4.3% (11/257) (Table 2).

TABLE 1 Hygienic practice of study participants in Gondar City, Ethiopia, 2020.

Variables	Variable category	Number (*N*)	%
Training on food handling practice	Yes	59	23.0
	No	198	77.0
Year of service	< 1 year	110	42.8
	1–5 years	119	46.3
	6–10 years	23	8.9
	>11 years	5	1.9
Supervision	Regularly supervised	100	38.9
	Intermittently supervised	118	45.9
	Never supervised	39	15.2
Hair covering practices	Yes	91	35.4
	No	166	64.6
Wearing jewelry	No	177	68.9
	Yes	80	31.1
Hand washing practice	With soap & water	57	22.2
	With water only	200	77.8
Wearing gown	Yes	133	51.8
	No	124	48.2
Fingernail status	Yes, clean and cut	88	34.2
	No, not clean not cut yet	169	65.8
Status of fly infestation during data collection	Not seen	180	70.0
	Seen	77	30.0

Factors associated with intestinal parasitic infections

The bivariate analysis revealed that fingernail status and supervision were marginally associated with intestinal parasitic infections ($p < 0.2$), while educational status and training on food handling were significantly associated with them. The multivariable analysis showed that, after adjusting for potential confounders, illiteracy and having a secondary school education were the key factors contributing to IPIs. Compared to food handlers with college education or above, illiterate food handlers had 7.37 times higher odds of being infected (95% CI: 1.54–35.16), and food handlers with secondary school education had 5.97 times higher odds of being infected (95% CI: 1.31–27.12) ($p < 0.05$) (Table 3).

Discussion

Intestinal parasitic infections pose a significant public health challenge, especially in developing countries. Food handlers, particularly those working in hotels and restaurants, play a crucial role in the transmission of these infections. This study aimed to

10.3389/fpubh.2024.1362086

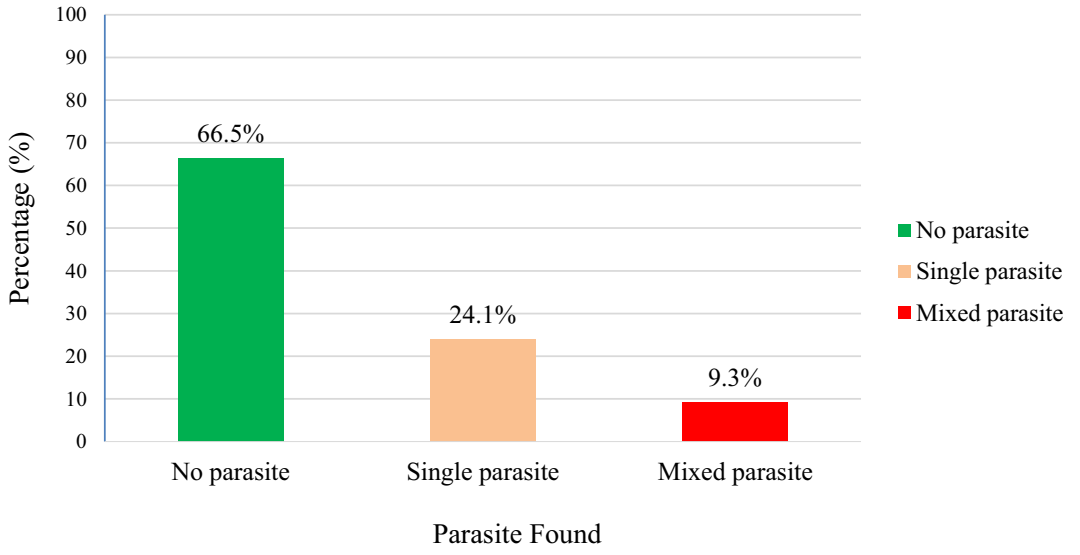

FIGURE 2
Intestinal parasites found from food handlers at Gondar City, Northwest Ethiopia, 2020.

TABLE 2 Types and prevalence of intestinal parasites observed in stool specimens of food handlers in Gondar City, 2020 (*N* = 257).

Type of parasite identified	Number	Prevalence (%)
E. histolytica/dispar	21	8.2
A. lumbricoides	17	6.6
Hookworm species	9	3.5
S. mansoni	6	2.3
E. histolytica/dispar and *A. lumbricoides*	5	1.9
G. lamblia	4	1.6
Taenia species	4	1.6
E. histolytica/dispar and *G. lamblia*	3	1.2
E. histolytica/dispar and *Hookworm species*	3	1.2
A. lumbricoides and *S. mansoni*	3	1.2
Hookworm species and *G. lamblia*	2	0.8
S. mansoni and *E. histolytica/dispar*	2	0.8
G. lamblia and *A. lumbricoides*	2	0.8
Hookworm and *T. trichuira*	2	0.8
E. vermicularis	1	0.4
S. stercoralis and *E. histolytica/dispar*	1	0.4
A. lumbricoides and *Hookworm*	1	0.4

estimate the prevalence of intestinal parasites among food handlers and identify the associated factors.

The overall prevalence of IPIs among food handlers in this study was found to be 33.5%. This finding aligns with systematic review and meta-analysis studies from Ethiopia conducted at different times, which reported prevalence rates of 29.2 and 33.6% (13, 41). Other studies from southern Ethiopia (14, 29, 42), Jimma town (43), Sudan (44), and Kenya (45) reported similar prevalence rates ranging from 29.4 to 39.2%. These results underscore the potential for food handlers to transmit intestinal parasites to consumers, emphasizing the importance of implementing screening and mass drug administration programs to curb the spread of infections within food establishments. However, lower prevalence rates were observed in other studies, ranging from 14.5 to 25.3% in different parts of Ethiopia, Saudi Arabia, Iran, and Sudan (11, 31–33, 46–53). The disparity in prevalence rates across these locations could be influenced by several factors such as the level of awareness regarding intestinal parasites and their transmission, the educational background of food handlers, and the stringency and effectiveness of regulatory enforcement in the food industry could greatly impact the prevalence of such infections. Moreover, the epidemiology of the disease itself could lead to variations in prevalence. The presence of different species of parasites,

10.3389/fpubh.2024.1362086

TABLE 3 Association between intestinal parasite infections and potential factors among food handlers, 2020.

Variables	Variable category	Intestinal parasite		Prevalence of intestinal parasite	
		Yes	No	COR (95% CI)	AOR (95% CI)
Gender	Male	8	13	0.80 (0.32–2.02)	
	Female	78	158	1	–
Age in years	<20	21	36	0.97 (0.21–4.49)	
	20–40	62	130	0.80 (0.18–3.43)	
	>40	3	5	1	
Educational status	Illiterate	28	35	8.40 (1.81–38.92)	7.37 (1.54–35.16)*
	Primary	20	52	4.04 (0.87–18.83)	3.55 (0.74–17.08)
	Secondary	36	63	6.00 (1.33–27.08)	5.97 (1.31–27.12)*
	Collage and above	2	21	1	1
Work experience	<1 year	31	79	0.59 (0.09–3.69)	–
	1–5 years	46	73	0.95 (0.15–5.87)	
	6–10 years	7	16	0.66 (0.09–4.84)	
	>10 years	2	3	1	
Training on food handling	Yes	10	40	1	1
	No	76	129	1.09 (0.59–2.03)	0.61 (0.27–1.38)
Supervision	Regularly	31	69	1	1
	Intermittently	38	80	1.06 (0.60–1.88)	0.89 (0.47–1.66)
	Never	17	22	1.72 (0.80–3.68)	1.44 (0.62–3.33)
Hand washing practice	Using water and soap	67	133	1	
	Using only water	19	38	0.99 (0.53–1.85)	–
Wearing gown	Yes	46	87	1	
	No	40	84	0.90 (0.54–1.51)	
Hair cover	Yes	32	59	1	
	No	54	112	0.89 (0.52–1.52)	–
Jewelry	Yes	26	54	1	
	No	60	117	0.94 (0.54–1.65)	
Fingernail status	Not trimmed	62	107	1.55 (0.88–2.72)	0.70 (0.38–1.30)
	Trimmed	24	64	1	1
Flies	Seen	26	51	0.98 (0.0.56–1.73)	–
	Not seen	60	120	1	

*Statistically significant.

their life cycles, and the local environmental conditions all contribute to this epidemiological complexity (54). Additionally, the methodologies and accuracy of laboratory techniques employed, along with the expertise of the laboratory personnel, are critical factors that determine the reliability of the prevalence figures reported. These multifaceted factors underscore the complexity of controlling IPIs among food handlers.

Significantly higher prevalence rates were observed in various locations, notably in Turkey (59%), Gondar (45.7%), Mettu town (44.6%), south Ethiopia (41%), Addis Ababa University student's cafeteria (45.3%), Pakistan (59.8%), and Nekemte town (52.1%) (17, 21, 55–59). The disparities in prevalence might be attributed to various factors, including differences in laboratory techniques, regional epidemiology, weather conditions, levels of awareness and education among study participants, and variations in regulatory enforcement.

The prevalence of mixed infections of intestinal parasitic infections among food handlers is alarmingly high at 9.3%. This percentage is notably greater than what has been observed in various regions of Ethiopia, such as Tigray, the University of Southern Ethiopia, Southern Ethiopia, Wolaita Sodo, and Addis Ababa, which reported prevalence rates of 3.4, 3.3, 0.6, 0.8, and 3.4%, respectively, (14, 17, 29, 47). This prevalence of mixed infections in the current study is more than double the highest rate seen in these other areas. This data suggests that the problem is not evenly distributed, and that certain populations or areas might be more vulnerable to these parasitic infections than others. There might be various factors contributing to this discrepancy, such as differences in hygiene practices, access to clean water, exposure to contaminated food, or local health policies. The high prevalence rate of mixed infections from the current study is concerning due to the complexity it brings to treatment. This complicates treatment as

different parasites may require different therapeutic approaches. Furthermore, the presence of multiple parasites can exacerbate the severity of the disease and lead to more severe health outcomes. This situation emphasizes the urgent need for intervention.

The current study found that *E. histolytica/dispar* and *A. lumbricoides* were the most identified parasites, with prevalence rates of 8.2 and 6.6%, respectively. These were followed by Hookworm species (3.5%) and *S. mansoni* (2.3%). The prevalence of these parasites is not uniform and shows considerable variation across different geographical locations and study populations. For instance, in Yebu, the prevalence of *A. lumbricoides* was reported to be 17.8%, which is significantly higher than our findings (6). Similarly, in Jimma, both *A. lumbricoides* and *E. histolytica/dispar* were found at 16.0 and 4.3%, respectively (60). In Arba Minch, the prevalence rates for *E. histolytica/dispar* and *A. lumbricoides* were 14 and 9.27%, respectively, which are also higher than our current study results (14). A study from Pakistan reported even higher prevalence rates for *A. lumbricoides* and *E. histolytica/dispar* at 55.8 and 14.2%, respectively (61). Moreover, a staggering 70.8% prevalence of *E. histolytica/dispar* was reported from Addis Ababa (62).

Several factors such as local sanitation practices, the availability of clean water, public health initiatives, and the level of community awareness about parasitic infections can greatly influence the prevalence rates. For example, areas with poor sanitation and hygiene practices are more likely to have higher rates of parasitic infections due to the increased risk of fecal-oral transmission. Additionally, the climate and environmental conditions of a region can affect the lifecycle of parasites and their transmission dynamics, leading to regional differences in prevalence. Furthermore, the methodology of the studies, including the diagnostic techniques used, can also contribute to the variability in reported prevalence rates. Some diagnostic methods may have higher sensitivity and specificity, leading to more accurate detection of parasitic infections.

The study revealed a significant correlation between the educational background of food handlers and the prevalence of intestinal parasites. It was found that food handlers who were illiterate had a risk of 7.37 times greater than that of individuals with a college or higher level of education. Similarly, those with a secondary school education were found to have a 5.97 times higher chance of getting an infection when compared to their counterparts with a college education or above. Interestingly, food handlers with primary education exhibited a lower risk of infection than both their uneducated peers and those with secondary education. This unexpected finding warrants further investigation into the specific factors influencing these relationships. It was evident that, despite having a high level of education, some food handlers were found to be infected with intestinal parasites (63). Despite the complexities, the study highlights the critical role that education plays in fostering proper hygiene practices among food handlers. It underscores the need for educational programs specifically tailored to this group to diminish the prevalence of parasitic infections. Such interventions are crucial, as they not only improve the health standards of the food handlers themselves but also safeguard the well-being of the wider community they serve.

Treatment strategies and future perspectives

Early diagnosis and prompt treatment are key, with screening programs essential for early detection and reducing transmission. Furthermore, due to the increasing drug resistance and limited options for controlling parasitic infections, it is vital to investigate drug efficacy and develop alternative preventive measures (2). Effective management of mixed infections requires customized treatments and in-depth knowledge of parasites by healthcare providers. To tackle IPIs, understanding local factors like awareness and regulations is vital for creating targeted interventions. Regular monitoring of food handlers is important for controlling infection spread and informing policy. Educational programs for food handlers, focusing on hygiene and prevention, are crucial in reducing infections and improving public health.

Strengths

The study demonstrated strength in its methodology by utilizing both direct wet mount preparations and formol-ether concentration techniques for the microscopic examination of stool samples. The incorporation of the concentration technique notably increased the sensitivity of parasite detection, thereby enhancing the precision and reliability of the study's findings. Additionally, the study exhibited a proactive approach to participant welfare by ensuring that individuals who tested positive for intestinal parasitic infections were promptly linked to nearby health facilities for necessary treatment.

Limitations

The study presented several limitations that impacted its findings. Firstly, the cross-sectional design of the study was a significant limitation as it restricted the ability to establish causal relationships between various factors and the outcomes related to intestinal parasitic infections. Secondly, the reliance on self-reported data from the food handlers could have introduced biases such as recall bias and social desirability bias. This is evident in instances where food handlers might have overestimated their frequency of hand-washing or underreported symptoms associated with intestinal parasitic infections. Additionally, the study's methodology of using a single stool sample from each participant may not have accurately represented the true prevalence of intestinal parasitic infections. The intermittent or low shedding rate of some parasites could lead to false negative results, suggesting that repeated stool examinations or more sensitive diagnostic methods might be necessary to verify the food handlers' infection status accurately. Lastly, the study did not evaluate the quality and availability of water and sanitation facilities within the food establishments, which are critical factors that can influence the risk of intestinal parasitic infections. Furthermore, there was no assessment of the food handlers' knowledge, attitude, and practice regarding food safety and hygiene, which are essential components that can affect their behavior and, consequently, their infection status.

Conclusion

The study uncovered a high prevalence of intestinal parasitic infections among food handlers with a notable prevalence of mixed infections. Among the isolated infections, *E. histolytica/dispar* and *A. lumbricoides* were identified as the most commonly prevalent

parasitic infections among study participants. The study also highlighted a significant correlation between educational status and the risk of infection, emphasizing the potential public health threat posed to consumers and the community.

Recommendations

- The Federal Ministry of Health and other stakeholders should implement policies and programs that aim to improve the awareness of food handlers.
- The Federal Ministry of Education should implement policies and programs that aim to improve the educational status of food handlers.
- The Gondar city administration office should design and periodically provide training to food handlers on the modes of transmission, prevention, and treatment of parasitic infections, as well as the importance of personal hygiene and sanitation.
- Zonal health department and city administration offices should conduct periodic screening and treatment of food handlers and enforce strict compliance with regulations and standards.
- Researchers should conduct large-scale studies to explore factors influencing the compliance and adherence of food handlers to preventive measures, along with assessing the cost-effectiveness and feasibility of screening and mass drug administration programs.
- Zonal health departments and city administration offices should conduct periodic inspections to ensure compliance with food safety standards and regulations.

Data availability statement

The original contributions presented in the study are included in the article/supplementary material, further inquiries can be directed to the corresponding author.

Ethics statement

The studies involving humans were approved by University of Gondar, School of Biomedical and Laboratory Sciences Research and Ethics Review comitee. The studies were conducted in accordance with the local legislation and institutional requirements. The participants provided their written informed consent to participate in this study.

Author contributions

MG: Conceptualization, Data curation, Formal analysis, Funding acquisition, Resources, Visualization, Writing – original draft. GB: Conceptualization, Data curation, Writing – original draft. AA: Investigation, Supervision, Writing – review & editing. WA: Conceptualization, Data curation, Supervision, Writing – review & editing. TD: Data curation, Formal analysis, Writing – original draft, Writing – review & editing.

Funding

The author(s) declare that no financial support was received for the research, authorship, and/or publication of this article.

Acknowledgments

The authors gratefully acknowledge the invaluable contributions of the medical laboratory professionals, section heads, and quality officers from the participating hospital laboratories for their willingness to participate and unwavering cooperation in the success of this study. Additionally, we extend our sincere thanks to the University of Gondar for providing material support and allowing us to use their laboratory for the examination of stool samples, which was vital to the completion of this research project. Finally, the authors would like to express their deep appreciation to the data collectors and study participants whose involvement was indispensable to the realization of this project.

Conflict of interest

The authors declare that the research was conducted in the absence of any commercial or financial relationships that could be construed as a potential conflict of interest.

Publisher's note

All claims expressed in this article are solely those of the authors and do not necessarily represent those of their affiliated organizations, or those of the publisher, the editors and the reviewers. Any product that may be evaluated in this article, or claim that may be made by its manufacturer, is not guaranteed or endorsed by the publisher.

References

1. Sinniah B, Hassan A, Sabaridah I, Soe M, Ibrahim Z, Ali O. Prevalence of intestinal parasitic infections among communities living in different habitats and its comparison with one hundred and one studies conducted over the past 42 years (1970 to 2013) in Malaysia. *Trop Biomed*. (2014) 31:190–206.

2. Kandeel M, Rehman TU, Akhtar T, Zaheer T, Ahmad S, Ashraf U, et al. Anti-parasitic applications of nanoparticles: a review. *Pak Vet J*. (2022) 42:135–40. doi: 10.29261/pakvetj/2022.040

3. Norhayati M, Fatmah M, Yusof S, Edariah A. Intestinal parasitic infections in man: a review. *Med J Malays*. (2003) 58:296–305; quiz 306.

4. Saki J. Prevalence of intestinal parasitic infections among food handlers in Khuzestan, southwest of Iran: a 10–year retrospective study. *Afr J Microbiol Res*. (2012) 6:6. doi: 10.5897/AJMR11.1533

5. Pullan RL, Smith JL, Jasrasaria R, Brooker SJ. Global numbers of infection and disease burden of soil transmitted helminth infections in 2010. *Parasit Vectors*. (2014) 7:37. doi: 10.1186/1756-3305-7-37

6. Tefera T, Mebrie G. Prevalence and predictors of intestinal parasites among food handlers in Yebu town, Southwest Ethiopia. *PLoS One*. (2014) 9:e110621. doi: 10.1371/journal.pone.0110621

7. Kibret M, Abera B. The sanitary conditions of food service establishments and food safety knowledge and practices of food handlers in Bahir Dar town. *Ethiop J Health Sci*. (2012) 22:27–35.

8. Bishop J, Tritscher A. Food safety surveillance and response. *Western Pac Surveill Response J*. (2012) 3:1–3. doi: 10.5365/wpsar.2012.3.2.013

9. Derrick J, Hollinghurst P, O'Brien S, Elviss N, Allen DJ, Iturriza-Gómara M. Measuring transfer of human norovirus during sandwich production: simulating the role of food, food handlers and the environment. *Int J Food Microbiol*. (2021) 348:109151. doi: 10.1016/j.ijfoodmicro.2021.109151

10. Hedberg C. Epidemiology of viral foodborne outbreaks: role of food handlers, irrigation water, and surfaces. *Viruses Foods*. (2016):147–63. doi: 10.1007/978-3-319-30723-7_5

11. Zaglool DA, Khodari YA, Othman RA, Farooq MU. Prevalence of intestinal parasites and bacteria among food handlers in a tertiary care hospital. *Niger Med J*. (2011) 52:266–70. doi: 10.4103/0300-1652.93802

12. Kheirandish F, Tarahi MJ, Ezatpour B. Prevalence of intestinal parasites among food handlers in Western Iran. *Rev Inst Med Trop São Paulo*. (2014) 56:111–4. doi: 10.1590/S0036-46652014000200004

13. Yimam Y, Woreta A, Mohebali M. Intestinal parasites among food handlers of food service establishments in Ethiopia: a systematic review and meta-analysis. *BMC Public Health*. (2020) 20:73. doi: 10.1186/s12889-020-8167-1

14. Mama M, Alemu G. Prevalence and factors associated with intestinal parasitic infections among food handlers of southern Ethiopia: cross sectional study. *BMC Public Health*. (2016) 16:105. doi: 10.1186/s12889-016-2790-x

15. Ayeh-Kumi P, Quarcoo S, Kwakye-Nuako G, Kretchy J, Osafo-Kantanka A, Mortu S. Prevalence of intestinal parasitic infections among food vendors in Accra, Ghana. *J Trop Med Parasitol*. (2009) 32:1–8.

16. Andargie G, Kassu A, Moges F, Tiruneh M, Huruy K. Prevalence of bacteria and intestinal parasites among food-handlers in Gondar town, Northwest Ethiopia. *J Health Popul Nutr*. (2008) 26:451–5. doi: 10.3329/jhpn.v26i4.1887

17. Abera W, Gintamo B, Shitemaw T, Mekuria ZN, Gizaw Z. Prevalence of intestinal parasites and associated factors among food handlers in food establishments in the Lideta subcity of Addis Ababa, Ethiopia: an institution-based, cross-sectional study. *BMJ Open*. (2022) 12:e061688. doi: 10.1136/bmjopen-2022-061688

18. Javed K, Alkheraije KA. Cryptosporidiosis: a foodborne zoonotic disease of farm animals and humans. *Pak Vet J*. (2023) 43:213–23. doi: 10.29261/pakvetj/2023.038

19. Hajare ST, Gobena RK, Chauhan NM, Erniso F. Prevalence of intestinal parasite infections and their associated factors among food handlers working in selected catering establishments from Bule hora, Ethiopia. *Biomed Res Int*. (2021) 2021:1–15. doi: 10.1155/2021/6669742

20. Gizaw Z, Addisu A, Gebrehiwot M. Socioeconomic predictors of intestinal parasitic infections among under-five children in rural Dembiya, Northwest Ethiopia: a community-based cross-sectional study. *Environ Health Insights*. (2019) 13:117863021989680. doi: 10.1177/1178630219896804

21. Wondimu H, Mihret M. Prevalence and associated factors of intestinal parasites among food handlers working in food service establishments in Northwest Ethiopia, 2022. *J Parasitol Res*. (2023) 2023:1–6. doi: 10.1155/2023/3230139

22. Haque R. Human intestinal parasites. *J Health Popul Nutr*. (2007) 25:387–91.

23. Sang X-L, Liang X-C, Chen Y, Li J-D, Li J-G, Bai L, et al. Estimating the burden of acute gastrointestinal illness in the community in Gansu Province, Northwest China, 2012–2013. *BMC Public Health*. (2014) 14:787. doi: 10.1186/1471-2458-14-787

24. Payment P, Riley MS. *Resolving the global burden of gastrointestinal illness: a call to action* Washington, DC (2002).

25. Regassa K, Tedla K, Bugssa G, Gebrekirstos G, Gebreyesus H, Shfare MT. Prevalence and factors associated with intestinal parasites among food handlers in Medebay Zana District, north West Tigray, northern Ethiopia. *Trop Dis Travel Med Vaccines*. (2021) 7:2. doi: 10.1186/s40794-020-00123-1

26. Heydari-Hengami M, Hamedi Y, Najafi-Asl M, Sharifi-Sarasiabi K. Prevalence of intestinal parasites in food handlers of Bandar Abbas, southern Iran. *Iran J Public Health*. (2018) 47:111–8.

27. Wegayehu T, Tsalla T, Seifu B, Teklu T. Prevalence of intestinal parasitic infections among highland and lowland dwellers in Gamo area, South Ethiopia. *BMC Public Health*. (2013) 13:151. doi: 10.1186/1471-2458-13-151

28. Takalkar A, Madhekar N, Kumavat A, Bhayya S. Prevalence of intestinal parasitic infections amongst food handlers in hotels and restaurants in Solapur city. *Indian J Public Health*. (2010) 54:47–8. doi: 10.4103/0019-557X.70557

29. Desalegn W, Birke W, Teshome T, Bacha K, Tamene A, Tesfaye L, et al. Intestinal Parasitosis and associated factors among food handlers working in the University of Southern Ethiopia. *Environ Health Insights*. (2022) 16:117863022211284. doi: 10.1177/11786302221128455

30. Dejen T, Yitayew FM, Amlak BT, Birhanie SA, Tiliksew MM, Alemineh TL, et al. Intestinal parasite infection and associated factors among food handlers in Feres bet town, north West Amhara, Ethiopia, 2021. *Heliyon*. (2023) 9:e14075. doi: 10.1016/j.heliyon.2023.e14075

31. Alemnew B, Belay Y, Demis A. Magnitude of intestinal parasitic infections and associated factors among food handlers working at Woldia University student's cafeteria, Northeastern Ethiopia: an institution based cross-sectional study. *BMC Res Notes*. (2019) 12:736. doi: 10.1186/s13104-019-4777-z

32. Alemu AS, Baraki AG, Alemayehu M, Yenit MK. The prevalence of intestinal parasite infection and associated factors among food handlers in eating and drinking establishments in Chagni town, Northwest Ethiopia. *BMC Res. Notes*. (2019) 12:302. doi: 10.1186/s13104-019-4338-5

33. Gezehegn D, Abay M, Tetemke D, Zelalem H, Teklay H, Baraki Z, et al. Prevalence and factors associated with intestinal parasites among food handlers of food and drinking establishments in Aksum town, northern Ethiopia. *BMC Public Health*. (2017) 17:819. doi: 10.1186/s12889-017-4831-5

34. Alvi MA, Alshammari A, Ali RMA, Rashid I, Saqib M, Qamar W, et al. Molecular characterization of Hydatigera taeniaeformis recovered from rats: an update from Pakistan. *Pak Vet J*. (2023) 43:601–5. doi: 10.29261/pakvetj/2023.049

35. Gelaw A, Anagaw B, Nigussie B, Silesh B, Yirga A, Alem M, et al. Prevalence of intestinal parasitic infections and risk factors among schoolchildren at the University of Gondar Community School, Northwest Ethiopia: a cross-sectional study. *BMC Public Health*. (2013) 13:304. doi: 10.1186/1471-2458-13-304

36. Abebe Z, Zelalem Anlay D, Biadgo B, Kebede A, Melku T, Enawgaw B, et al. High prevalence of undernutrition among children in Gondar town, Northwest Ethiopia: a community-based cross-sectional study. *Int J Pediatr*. (2017) 2017:1–9. doi: 10.1155/2017/5367070

37. Takele MD, Sany K, Getie K, Wayessa DI, Jember G, Gobezie M, et al. Prevalence and associated factors of frailty among community dweller older adults living in Gondar town, northwest, Ethiopia: a community based cross-sectional study. *BMC Public Health*. (2023) 23:1309. doi: 10.1186/s12889-023-16201-w

38. Tamiru AT, Rade BK, Taye EB, Azene ZN, Merid MW, Muluneh AG, et al. Community level of COVID-19 information exposure and influencing factors in Northwest Ethiopia. *Risk Manag Healthc Policy*. (2020) 13:2635–44. doi: 10.2147/RMHP.S280346

39. Al-Hindi AI, Elmanama AA, Ashour N, Hassan I, Salamah A. Occurrence of intestinal parasites and hygiene characters among food handlers in Gaza strip, Palestine. *Ann Alquds Med*. (2012) 1433:2–3.

40. Cheesbrough M. *District laboratory practice in tropical countries* Cambridge university press (2006).

41. Girma A, Aemiro A. Prevalence and associated risk factors of intestinal parasites and enteric bacterial infections among selected region food handlers of Ethiopia during 2014–2022: a systematic review and meta-analysis. *Sci World J*. (2022) 2022:1–14. doi: 10.1155/2022/7786036

42. Lette A, Negash G, Kumbi M, Hussen A, Kassim J, Zenbaba D, et al. Predictors of intestinal parasites among food handlers in Goba town, Southeast Ethiopia, 2020. *J Parasitol Res*. (2022) 2022:1–5. doi: 10.1155/2022/3329237

43. Gemechu T, Eshetu T, Kassa T, Jarso H. Assessment of intestinal parasites, enteric bacterial infections, and antimicrobial susceptibility among street food handlers in Jimma town, Southwest Ethiopia. *J Trop Med*. (2022) 2022:1–8. doi: 10.1155/2022/5483367

44. Babiker MA, Ali MS, Ahmed ES. Frequency of intestinal parasites among food-handlers in Khartoum, Sudan. *East Mediterr Health J*. (2009) 15:1098–104. doi: 10.26719/2009.15.5.1098

45. Ogolla JO. Prevalence and factors associated with intestinal protozoan and helminthic infections among certified food handlers in Eldoret town, Uasin Gishu county in Kenya. *Int Clin Pathol J*. (2018) 6:124–8. doi: 10.15406/icpjl.2018.06.00171

46. Kebede E, Seid A, Akele S. Prevalence and associated risk factors of intestinal parasitic infections among asymptomatic food handlers in Wollo university student's cafeteria, Northeastern Ethiopia. *BMC Res Notes*. (2019) 12:139. doi: 10.1186/s13104-019-4182-7

47. Kumma WP, Meskele W, Admasie A. Prevalence of intestinal parasitic infections and associated factors among food handlers in Wolaita Sodo University students caterings, Wolaita Sodo, southern Ethiopia: a cross-sectional study. *Front Public Health*. (2019) 7:140. doi: 10.3389/fpubh.2019.00140

48. Kumalo A, Gambura E, Dodicho T, Ahmed KS, Balcha T, Beshir B, et al. Prevalence of intestinal parasites and *Salmonella typhi* among food handlers working in catering establishments of public institutes found in Dawuro zone, South-Western Ethiopia. *J Parasitol Res*. (2021) 2021:1–10. doi: 10.1155/2021/8889302

49. Kuti KA, Nur RA, Donka GM, Kerbo AA, Roba AE. Predictors of intestinal parasitic infection among food handlers working in Madda Walabu university, Ethiopia: a cross-sectional study. *Interdiscip Perspect Infect Dis*. (2020) 2020:1–8. doi: 10.1155/2020/9321348

50. Kalantan KA, Al-Faris EA, Al-Taweel AA. Pattern of intestinal parasitic infection among food handlers in Riyadh, Saudi Arabia. *J Family Community Med*. (2001) 8:67–72. doi: 10.4103/2230-8229.98065

51. Sharif M, Daryani A, Kia E, Rezaei F, Nasiri M, Nasrolahei M. Prevalence of intestinal parasites among food handlers of sari, northern Iran. *Rev Inst Med Trop São Paulo*. (2015) 57:139–44. doi: 10.1590/S0036-46652015000200007

52. Sharifi-Sarasiabi K, Heydari-Hengami M, Shokri A, HosseyniTeshnizi S. Prevalence of intestinal parasitic infection in food handlers of Iran: a systematic review and meta-analysis. *Vet Med Sci*. (2021) 7:2450–62. doi: 10.1002/vms3.590

53. Gamar TA, Musa HH, Altayb HN, Kabbashi M, Alsayed Y, Abakar AD. Prevalence of intestinal parasites among food handlers attending public health laboratories in Khartoum state, Sudan. *F1000Research*. (2018) 7:681. doi: 10.12688/f1000research.14681.1

54. Almuzaini AM. Flow of zoonotic toxoplasmosis in food chain. *Pak Vet J*. (2023) 43:1–16. doi: 10.29261/pakvetj/2023.010

55. Şahin M, Ödemiş N, Yılmaz H, Beyhan YE. Investigation of parasites in food handlers in Turkey. *Foodborne Pathog Dis*. (2023) 20:381–7. doi: 10.1089/fpd.2023.0016

56. Yeshanew S, Tadege M, Abamecha A. Prevalence and associated factors of intestinal parasitic infections among food handlers in Mettu town, Southwest Ethiopia. *J Trop Med*. (2021) 2021:1–5. doi: 10.1155/2021/6669734

57. Solomon FB, Wada FW, Anjulo AA, Koyra HC, Tufa EG. Burden of intestinal pathogens and associated factors among asymptomatic food handlers in South Ethiopia: emphasis on salmonellosis. *BMC Res Notes*. (2018) 11:502. doi: 10.1186/s13104-018-3610-4

58. Khan W, Arshad S, Khatoon N, Khan I, Ahmad N, Kamal M, et al. Food handlers: an important reservoir of protozoans and helminth parasites of public health importance. *Braz J Biol*. (2021) 82:e238891. doi: 10.1590/1519-6984.238891

59. Eshetu L, Dabsu R, Tadele G. Prevalence of intestinal parasites and its risk factors among food handlers in food services in Nekemte town, West Oromia, Ethiopia. *Res Rep Trop Med*. (2019) 10:25–30. doi: 10.2147/RRTM.S186723

60. Girma H, Getenet B, Zeleke M. Prevalence of intestinal parasites among food handlers at cafeteria of Jimma University specialized hospital, Southwest Ethiopia. *Asian Pac J Trop Dis*. (2017) 7:467–71. doi: 10.12980/apjtd.7.2017D7-20

61. Khan W, Noor-un-Nisa KA. Prevalence and risk factors associated with intestinal parasitic infections among food handlers of swat, Khyber Pakhtunkhwa. *Pak J Food Nutr Res*. (2017) 5:331–6. doi: 10.12691/jfnr-5-5-7

62. Aklilu A, Kahase D, Dessalegn M, Tarekegn N, Gebremichael S, Zenebe S, et al. Prevalence of intestinal parasites, salmonella and shigella among apparently health food handlers of Addis Ababa university student's cafeteria, Addis Ababa, Ethiopia. *BMC Res Notes*. (2015) 8:17. doi: 10.1186/s13104-014-0967-x

63. Alqarni AS, Wakid MH, Gattan HS. Hygiene practices and factors influencing intestinal parasites among food handlers in the province of Belgarn, Saudi Arabia. *PeerJ*. (2023) 11:e14700. doi: 10.7717/peerj.14700

frontiers | Frontiers in Veterinary Science

TYPE Case Report
PUBLISHED 13 June 2024
DOI 10.3389/fvets.2024.1373035

Check for updates

OPEN ACCESS

EDITED BY
Mughees Aizaz Alvi,
University of Agriculture, Pakistan

REVIEWED BY
Zorica D. Dakić,
University of Belgrade, Serbia
Ranju Manoj,
Cornell University, United States
Erica Marchiori,
University of Padua, Italy

*CORRESPONDENCE
Nozomu Yokoyama
y-nozomu@vetmed.hokudai.ac.jp
Nariaki Nonaka
nnonaka@vetmed.hokudai.ac.jp

†These authors have contributed equally to this work and share senior authorship

RECEIVED 19 January 2024
ACCEPTED 03 June 2024
PUBLISHED 13 June 2024

CITATION
Kida I, Hayashi N, Yokoyama N, Nagata N, Sasaoka K, Sasaki N, Morishita K, Nakamura K, Kouguchi H, Yagi K, Nakao R, Takiguchi M and Nonaka N (2024) Case report: *Echinococcus multilocularis* infection in a dog showing gastrointestinal signs in Hokkaido, Japan. *Front. Vet. Sci.* 11:1373035. doi: 10.3389/fvets.2024.1373035

COPYRIGHT
© 2024 Kida, Hayashi, Yokoyama, Nagata, Sasaoka, Sasaki, Morishita, Nakamura, Kouguchi, Yagi, Nakao, Takiguchi and Nonaka. This is an open-access article distributed under the terms of the Creative Commons Attribution License (CC BY). The use, distribution or reproduction in other forums is permitted, provided the original author(s) and the copyright owner(s) are credited and that the original publication in this journal is cited, in accordance with accepted academic practice. No use, distribution or reproduction is permitted which does not comply with these terms.

Case report: *Echinococcus multilocularis* infection in a dog showing gastrointestinal signs in Hokkaido, Japan

Izumi Kida[1], Naoki Hayashi[2], Nozomu Yokoyama[3]*†, Noriyuki Nagata[4], Kazuyoshi Sasaoka[4], Noboru Sasaki[4], Keitaro Morishita[5], Kensuke Nakamura[3], Hirokazu Kouguchi[6], Kinpei Yagi[2], Ryo Nakao[2], Mitsuyoshi Takiguchi[3] and Nariaki Nonaka[2]*†

[1]Division of Risk Analysis and Management, International Institute for Zoonosis Control, Hokkaido University, Sapporo, Japan, [2]Laboratory of Parasitology, Department of Disease Control, Faculty of Veterinary Medicine, Hokkaido University, Sapporo, Japan, [3]Laboratory of Veterinary Internal Medicine, Department of Clinical Sciences, Graduate School of Veterinary Medicine, Hokkaido University, Sapporo, Japan, [4]Veterinary Teaching Hospital, Graduate School of Veterinary Medicine, Hokkaido University, Sapporo, Japan, [5]Laboratory of Molecular Medicine, Department of Disease Control, Faculty of Veterinary Medicine, Hokkaido University, Sapporo, Japan, [6]Department of Infectious Diseases, Hokkaido Institute of Public Health, Sapporo, Hokkaido, Japan

Echinococcus multilocularis is a cestode that causes human alveolar echinococcosis, a lethal zoonotic disease distributed in the northern hemisphere. The life cycle of this parasite is maintained in nature by voles as intermediate hosts and foxes as definitive hosts in Hokkaido, Japan. Although dogs are also susceptible to the parasite, the infection has been considered typically asymptomatic. We report the detection of *E. multilocularis* eggs in the diarrheal feces of a dog with chronic gastrointestinal signs, which disappeared after anthelmintic treatment. The mitochondrial genome sequence constructed by sequencing of the overlapping PCRs using DNA from the eggs was identical to the most predominant haplotype previously reported in red foxes in Hokkaido. This case highlights that *Echinococcus* infection should be considered as a differential diagnosis for diarrheal dogs in the disease endemic areas. Further efforts are needed to accumulate parasite genotypes in domestic dogs as well as humans to assess the risk of human infection from dogs.

KEYWORDS

***Echinococcus multilocularis*, gastrointestinal sign, dog, zoonosis, mitochondrial genome**

Introduction

Alveolar echinococcosis (AE) in humans, a potentially fatal zoonosis if left untreated is caused by the metacestode stage of the parasite *Echinococcus multilocularis*, which is widely distributed in the northern hemisphere. The life cycle of this parasite involves carnivores such as foxes and dogs as definitive hosts and voles as intermediate hosts. A total of 254 AE cases were reported between 2010 and 2020 in Japan, with Hokkaido having the highest burden of the disease (1). The prevalence of *E. multilocularis* infections in foxes was 30–40% in Hokkaido (2). Furthermore, studies of pet dogs in Hokkaido have estimated the infection rates to be 7.1%

in a rural area (3) and 1.9% in an urban area (4). Thus, pet dogs in endemic areas may play an important role in the transmission of the parasite to humans.

The adult cestode resides in the small intestine of the definitive host, and infected hosts typically do not show clinical signs (5). However, there have been two reports of the incidental detection of *E. multilocularis* in dogs that exhibited severe gastrointestinal signs such as vomiting and diarrhea with mild hypoproteinemia (6, 7). Here, we report a case of a pet dog raised in an urban area of Hokkaido that showed intermittent gastrointestinal symptoms and was infected with *E. multilocularis*. When treated with an anthelmintic, the clinical signs of the dog disappeared.

Case description

An 8-year-old female spayed Jack Russell Terrier was presented to Hokkaido University Veterinary Teaching Hospital with a 2-month history of intermittent vomiting, anorexia, and borborygmi. These clinical signs were unresponsive to symptomatic therapy provided by the referring veterinarian in Sapporo, Hokkaido. The dog had no previous clinical history, and was prescribed ivermectin monthly for heartworm prevention. The owner always kept the dog indoors or on a leash when outdoors.

At presentation, the dog's feces were watery, and blood and taeniid eggs were observed on direct fecal smear examination (Figure 1). Physical examination showed no abnormalities. A complete blood count demonstrated mild eosinophilia (1,820 cells/μL, reference range 170–1,570 cells/μL) and serum chemistry revealed no significant abnormalities. Abdominal ultrasonography revealed mild jejunal lymphadenopathy.

The dog was treated with praziquantel (6.4 mg/kg), pyrantel (18.5 mg/kg), and febantel (19.2 mg/kg) (Drontal Plus, Bayer Yakuhin, Osaka, Japan) as an oral single dose for the treatment of intestinal cestodiasis with suspected echinococcosis. The therapeutic response in the dog was carefully monitored, with chronic inflammatory enteritis (CIE) also considered as a differential diagnosis. Gastrointestinal signs resolved markedly within a few days after treatment and did not recur. A follow-up fecal examination with a flotation technique performed 5 days after treatment revealed no parasite eggs.

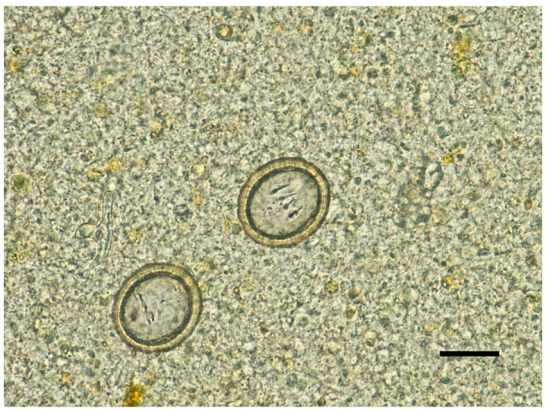

FIGURE 1
Taeniid eggs detected in a dog with gastrointestinal signs. Scale bar = 20 μm.

To identify the taeniid species of the eggs, we performed a multiplex PCR assay (8). DNA was extracted from 0.2 g of the fecal sample, according to the method previously described (9). The PCR performed using this DNA yielded a single band of ~400 bp, which was in accordance with the expected amplicon size for *E. multilocularis*.

We used an amplicon-based next-generation sequencing method to genotype the parasite, targeting mitochondrial protein-coding sequences (CDSs). The whole mitochondrial genome was amplified by overlapping PCRs using four sets of primers as reported previously (10). Illumina sequencing libraries were constructed and sequenced on an Illumina MiSeq platform using the MiSeq reagent kit v3 for 600 cycles (Illumina, Hayward, CA, United States). Read mapping against a reference mitogenome sequence of *E. multilocularis* (GenBank accession no. AB018440) (11) using CLC Genomics Workbench v20.0.4 (Qiagen, Hilden, Germany) generated a complete mitochondrial genome sequence for the parasite (accession no. LC744000). The sequence is 13,738 bp in length and consisted of 12 CDSs, 22 transfer RNA genes, and 2 ribosomal RNA genes as previously reported (10). The network analysis using PopART v1.7 (12) showed that the mitochondrial haplotype based on three complete CDSs (cytochrome *b*, NADH dehydrogenase subunit 2, cytochrome *c* oxidase subunit I) was genotype A4, which is predominantly detected in wild foxes in Hokkaido (Figure 2) (10, 13–16).

Discussion and conclusion

We have reported a rare case of intestinal *E. multilocularis* infection in a pet dog with gastrointestinal signs. Chronic intermittent or persistent diarrhea in dogs is commonly caused by gastrointestinal or extragastrointestinal disorders. The cause of gastrointestinal disorders includes infectious, neoplastic, mechanical, toxic, or noninfectious inflammatory such as CIE. CIE is the most common cause of chronic gastrointestinal disease in dogs (79%), followed by parasitic infection (12%) (17). Given the complete resolution of these signs following anthelmintic therapy, *Echinococcus* infection was thought to be the most likely cause of the disease. In fact, experimental oral infection of *E. multilocularis* protoscoleces into beagle dogs resulted in intermittent diarrhea in two out of four dogs (18). Moreover, upon reinfection all four dogs exhibited frequent diarrhea from the early stages of the infection. These experimental data, together with previous reports of symptomatic echinococcosis in dogs (6, 7), support the assumption that dogs could develop gastrointestinal signs including diarrhea upon *E. multilocularis* infection. Thus, this parasitic disease should be considered as one of the differential diagnoses in dogs with chronic gastrointestinal signs that live in endemic areas.

Although Hokkaido is an endemic region for AE, there are no national regulations for animal deworming. The lack of regulations poses not only the risk of transmission from pet dogs to humans, but also the risk of further expansion of the parasite distribution through animal transportation (10). The case presented here, where the indoor dog became infected, underscores such potential risks of diffusion by pet animals. It would be important to apply appropriate deworming programs for high-risk dogs and to use reliable diagnostic methods.

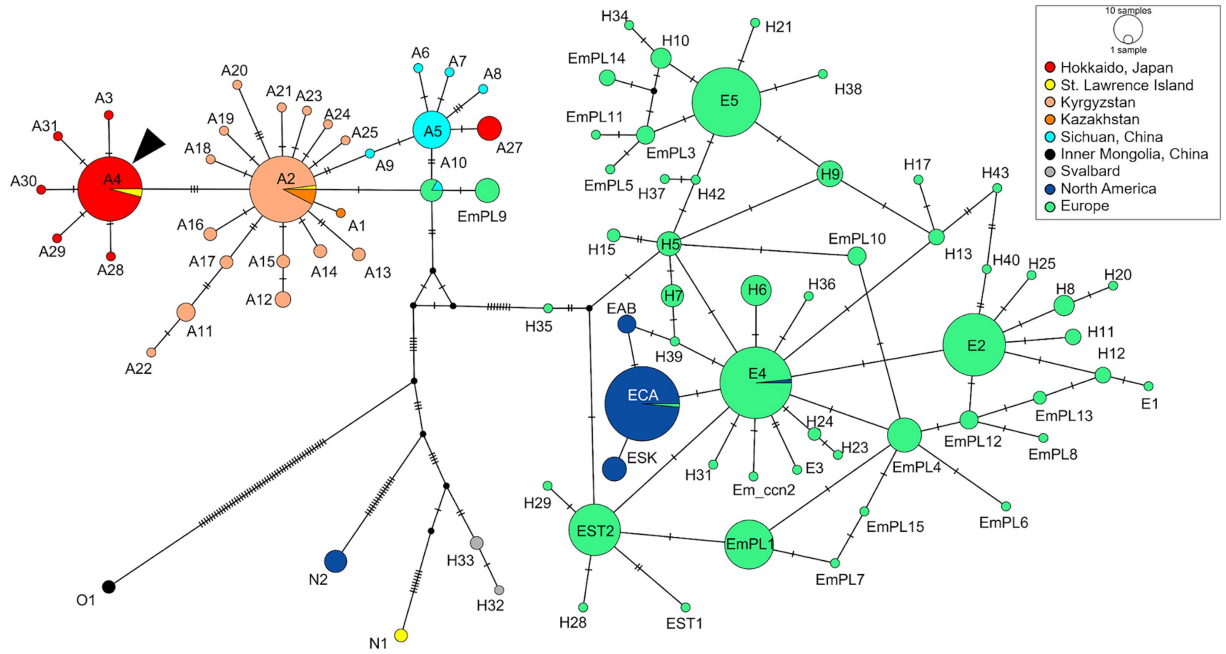

FIGURE 2
Median-joining haplotype network of *Echinococcus multilocularis* based on three mitochondrial protein-coding sequences. The analysis included haplotypes based on three mitochondrial genes (cytochrome *b*, NADH dehydrogenase subunit 2, and cytochrome *c* oxidase subunit I) previously reported in other endemic areas. The arrowhead indicates the haplotype obtained in this case (A4).

In certain areas of Hokkaido, the periodic distribution of praziquantel-containing baits has been provided to reduce the prevalence of *E. multilocularis* in foxes. Field studies have demonstrated the efficacy of anthelmintic baiting in reducing contamination by the eggs, thereby decreasing the risk of infection (19–21). It is worth mentioning here that mass drug administration for controlling malaria has been associated to the emergence of drug-resistant parasites (22–25). Although the drug resistance in *E. multilocularis* has never been reported, a recent study introduced the clinical resistance to praziquantel in another cestode, *Dipylidium caninum* (26). Therefore, it is important to monitor the drug resistance in clinical settings and explore alternative treatment options for canine echinococcosis.

Genotyping parasites is essential for a better understanding the epidemiological status of infectious diseases. For instance, a previous study in Kyrgyzstan found that haplotype A2 was the most common genotype in both humans and dogs, which is pivotal information to analyze the transmission dynamics and pathogenicity of the parasites (16). Previous research has revealed that an Asian haplotype A4 is the most predominant haplotype among red foxes in Hokkaido (10). The genotype detected in the current study was also assigned to the same haplotype, which may indicate that dogs are likely to have the same susceptibility to the genotype as foxes. Given the potential phenotypic differences among genotypes (27, 28), further studies genotyping parasites affecting both pet dogs and humans would be valuable to assess the risk of human infection from dogs.

In the current case, the animal was always kept indoors or on a leash when outdoors, and never observed any hunting behavior. These are contrary to the risk factors for canine echinococcosis, including roaming outdoors unattended and hunting/killing small animals (29, 30). Nevertheless, the dog likely became infected as a result of ingesting infected vole(s) during outdoor activities, such as preying or scavenging. This is supported by the facts that the detected parasite was the most dominant haplotype in Hokkaido, and the dog had no travel history outside Hokkaido. Taken together, this case emphasizes the importance for pet owners and animal care professionals to understand the risk of transmission of *E. multilocularis* even from indoor dogs in the endemic regions. It also highlights the need to employ proper biosafety protocols when handling suspect animals showing gastrointestinal signs.

Data availability statement

The datasets presented in this study can be found in online repositories. The names of the repository/repositories and accession number(s) can be found in the article/supplementary material.

Ethics statement

The requirement of ethical approval was waived by Ethics Screening Committee of Hokkaido University Veterinary Teaching Hospital for the studies involving animals because this is a case report of examinations performed for the purpose of patient treatment, and no action contrary to treatment was performed. The studies were conducted in accordance with the local legislation and institutional requirements. Written informed consent was obtained from the owners of the animals for the publication of this case report.

Author contributions

IK: Funding acquisition, Investigation, Writing – original draft. NH: Formal analysis, Investigation, Methodology, Writing – original draft. NY: Conceptualization, Supervision, Writing – review & editing. NoN: Resources, Writing – review & editing. KS: Resources, Writing – review & editing. NS: Resources, Writing – review & editing. KM: Resources, Writing – review & editing. KN: Resources, Writing – review & editing. HK: Resources, Writing – review & editing. KY: Funding acquisition, Resources, Writing – review & editing. RN: Conceptualization, Supervision, Writing – review & editing. MT: Resources, Supervision, Writing – review & editing. NaN: Conceptualization, Funding acquisition, Supervision, Writing – review & editing.

Funding

The author(s) declare that financial support was received for the research, authorship, and/or publication of this article. This study was supported by the Japan Society for the Promotion of Science KAKENHI (grant no. JP20K06402 and JP23H02369) and JST SPRING (grant no JPMJSP2119).

Conflict of interest

The authors declare that the research was conducted in the absence of any commercial or financial relationships that could be construed as a potential conflict of interest.

Publisher's note

All claims expressed in this article are solely those of the authors and do not necessarily represent those of their affiliated organizations, or those of the publisher, the editors and the reviewers. Any product that may be evaluated in this article, or claim that may be made by its manufacturer, is not guaranteed or endorsed by the publisher.

References

1. National Institute of Infectious Diseases. Infectious diseases weekly report [internet]. (2022). Available at: https://www.niid.go.jp/niid/ja/idwr.html (Accessed February 24, 2024).

2. Kamiya M. Collaborative control initiatives targeting zoonotic agents of alveolar echinococcosis in the northern hemisphere. *J Vet Sci*. (2007) 8:313–21. doi: 10.4142/jvs.2007.8.4.313

3. Irie T, Yamada K, Morishima Y, Yagi K. High probability of pet dogs encountering the sylvatic cycle of *Echinococcus multilocularis* in a rural area in Hokkaido, Japan. *J Vet Med Sci*. (2019) 81:1606–8. doi: 10.1292/jvms.19-0307

4. Irie T, Mukai T, Yagi K. *Echinococcus multilocularis* surveillance using copro-DNA and egg examination of shelter dogs from an endemic area in Hokkaido, Japan. *Vector Borne Zoonotic Dis*. (2018) 18:390–2. doi: 10.1089/vbz.2017.2245

5. Deplazes P, Eckert J. Veterinary aspects of alveolar echinococcosis – a zoonosis of public health significance. *Vet Parasitol*. (2001) 98:65–87. doi: 10.1016/S0304-4017(01)00424-1

6. Jenkins EJ, Kolapo TU, Jarque MP, Ruschkowski C, Frey C. Intestinal infection with *Echinococcus multilocularis* in a dog. *J Am Vet Med Assoc*. (2023) 261:1–3. doi: 10.2460/javma.23.02.0099

7. Kuroki K, Morishima Y, Neil J, Beerntsen BT, Matsumoto J, Stich RW. Intestinal echinococcosis in a dog from Missouri. *J Am Vet Med Assoc*. (2020) 256:1041–6. doi: 10.2460/javma.256.9.1041

8. Trachsel D, Deplazes P, Mathis A. Identification of taeniid eggs in the faeces from carnivores based on multiplex PCR using targets in mitochondrial DNA. *Parasitology*. (2007) 134:911–20. doi: 10.1017/S0031182007002235

9. Irie T, Ito T, Kouguchi H, Yamano K, Uraguchi K, Yagi K, et al. Diagnosis of canine *Echinococcus multilocularis* infections by copro-DNA tests: comparison of DNA extraction techniques and evaluation of diagnostic deworming. *Parasitol Res*. (2017) 116:2139–44. doi: 10.1007/s00436-017-5514-y

10. Hayashi N, Nakao R, Ohari Y, Irie T, Kouguchi H, Chatanga E, et al. Mitogenomic exploration supports the historical hypothesis of anthropogenic diffusion of a zoonotic parasite *Echinococcus multilocularis*. *iScience*. (2023) 26:107741. doi: 10.1016/j.isci.2023.107741

11. Nakao M, Yokoyama N, Sako Y, Fukunaga M, Ito A. The complete mitochondrial DNA sequence of the cestode *Echinococcus multilocularis* (Cyclophyllidea: Taeniidae). *Mitochondrion*. (2002) 1:497–509. doi: 10.1016/S1567-7249(02)00040-5

12. Leigh JW, Bryant D. Popart: full-feature software for haplotype network construction. *Methods Ecol Evol*. (2015) 6:1110–6. doi: 10.1111/2041-210X.12410

13. Santoro A, Santolamazza F, Cacciò SM, La Rosa G, Antolová D, Auer H, et al. Mitochondrial genetic diversity and phylogenetic relationships of *Echinococcus multilocularis* in Europe. *Int J Parasitol*. (2024) 54:233–45. doi: 10.1016/j.ijpara.2024.01.003

14. Nakao M, Xiao N, Okamoto M, Yanagida T, Sako Y, Ito A. Geographic pattern of genetic variation in the fox tapeworm *Echinococcus multilocularis*. *Parasitol Int*. (2009) 58:384–9. doi: 10.1016/j.parint.2009.07.010

15. Bohard L, Lallemand S, Borne R, Courquet S, Bresson-Hadni S, Richou C, et al. Complete mitochondrial exploration of *Echinococcus multilocularis* from French alveolar echinococcosis patients. *Int J Parasitol*. (2023) 53:555–64. doi: 10.1016/j.ijpara.2023.03.006

16. Alvarez Rojas CA, Kronenberg PA, Aitbaev S, Omorov RA, Abdykerimov KK, Paternoster G, et al. Genetic diversity of *Echinococcus multilocularis* and *Echinococcus granulosus sensu lato* in Kyrgyzstan: the A2 haplotype of *E. multilocularis* is the predominant variant infecting humans. *PLoS Negl Trop Dis*. (2020) 14:e0008242. doi: 10.1371/journal.pntd.0008242

17. Volkmann M, Steiner JM, Fosgate GT, Zentek J, Hartmann S, Kohn B. Chronic diarrhea in dogs – retrospective study in 136 cases. *J Vet Intern Med*. (2017) 31:1043–55. doi: 10.1111/jvim.14739

18. Kouguchi H, Irie T, Matsumoto J, Nakao R, Sugano Y, Oku Y, et al. The timing of worm exclusion in dogs repeatedly infected with the cestode *Echinococcus multilocularis*. *J Helminthol*. (2016) 90:766–72. doi: 10.1017/S0022149X15001169

19. Uraguchi K, Irie T, Kouguchi H, Inamori A, Sashika M, Shimozuru M, et al. Anthelmintic baiting of foxes against *Echinococcus multilocularis* in small public area, Japan. *Emerg Infect Dis*. (2022) 28:1677–80. doi: 10.3201/eid2808.212016

20. Inoue T, Nonaka N, Kanai Y, Iwaki T, Kamiya M, Oku Y. The use of tetracycline in anthelmintic baits to assess baiting rate and drug efficacy against *Echinococcus multilocularis* in foxes. *Vet Parasitol*. (2007) 150:88–96. doi: 10.1016/j.vetpar.2007.08.027

21. Hegglin D, Deplazes P. Control of *Echinococcus multilocularis*: strategies, feasibility and cost-benefit analyses. *Int J Parasitol*. (2013) 43:327–37. doi: 10.1016/j.ijpara.2012.11.013

22. Payne D. Spread of chloroquine resistance in *Plasmodium*. *Parasitol Today*. (1987) 3:241–6. doi: 10.1016/0169-4758(87)90147-5

23. Verdrager J. Epidemiology of the emergence and spread of drug-resistant falciparum malaria in South-East Asia and Australasia. *J Trop Med Hyg*. (1986) 89:277–89.

24. Verdrager J. Localized permanent epidemics: the genesis of chloroquine resistance in *Plasmodium falciparum*. *Southeast Asian J Trop Med Public Health*. (1995) 26:23–8.

25. Wernsdorfer WH. The biological and epidemiological basis of drug resistance in malaria parasites. *Southeast Asian J Trop Med Public Health*. (1992) 23:123–9.

26. Chelladurai JJ, Kifleyohannes T, Scott J, Brewer MT. Praziquantel resistance in the zoonotic Cestode *Dipylidium caninum*. *Am J Trop Med Hyg*. (2018) 99:1201–5. doi: 10.4269/ajtmh.18-0533

27. Bartel MH, Seesee FM, Worley DE. Comparison of Montana and Alaska isolates of *Echinococcus multilocularis* in gerbils with observations on the cyst growth, hook characteristics, and host response. *J Parasitol*. (1992) 78:529–32. doi: 10.2307/3283660

28. Davidson RK, Lavikainen A, Konyaev S, Schurer J, Miller AL, Oksanen A, et al. *Echinococcus* across the north: current knowledge, future challenges. *Food Waterborne Parasitol*. (2016) 4:39–53. doi: 10.1016/j.fawpar.2016.08.001

29. Kern P, Ammon A, Kron M, Sinn G, Sander S, Petersen LR, et al. Risk factors for alveolar echinococcosis in humans. *Emerg Infect Dis*. (2004) 10:2088–93. doi: 10.3201/eid1012.030773

30. Stehr-Green JK, Stehr-Green PA, Schantz PM, Wilson JF, Lanier A. Risk factors for infection with *Echinococcus multilocularis* in Alaska. *Am J Trop Med Hyg*. (1988) 38:380–5. doi: 10.4269/ajtmh.1988.38.380

frontiers | Frontiers in Veterinary Science

TYPE Original Research
PUBLISHED 29 August 2024
DOI 10.3389/fvets.2024.1427690

Check for updates

OPEN ACCESS

EDITED BY
Hongbin Yan,
Chinese Academy of Agricultural Sciences, China

REVIEWED BY
Nabil Amor,
Tunis El Manar University, Tunisia
Piyanan Taweethavonsawat,
Chulalongkorn University, Thailand
Ashiq Ali,
Shantou University, China

*CORRESPONDENCE
Quan Zhao
✉ zhaoquan0825@163.com
He Ma
✉ mahe@qau.edu.cn

†These authors have contributed equally to this work

RECEIVED 04 May 2024
ACCEPTED 14 August 2024
PUBLISHED 29 August 2024

CITATION
Gao Z-Q, Wang H-T, Hou Q-Y, Qin Y, Qin S-Y, Zhao Q and Ma H (2024) Wild rodents in three provinces of China exhibit a wide range of *Enterocytozoon bieneusi* diversity. *Front. Vet. Sci.* 11:1427690. doi: 10.3389/fvets.2024.1427690

COPYRIGHT
© 2024 Gao, Wang, Hou, Qin, Qin, Zhao and Ma. This is an open-access article distributed under the terms of the Creative Commons Attribution License (CC BY). The use, distribution or reproduction in other forums is permitted, provided the original author(s) and the copyright owner(s) are credited and that the original publication in this journal is cited, in accordance with accepted academic practice. No use, distribution or reproduction is permitted which does not comply with these terms.

Wild rodents in three provinces of China exhibit a wide range of *Enterocytozoon bieneusi* diversity

Zhen-Qiu Gao[1†], Hai-Tao Wang[2,3†], Qing-Yu Hou[3], Ya Qin[3], Si-Yuan Qin[4], Quan Zhao[2*] and He Ma[3*]

[1]School of Pharmacy, Yancheng Teachers University, Yancheng, China, [2]College of Life Sciences, Changchun Sci-Tech University, Shuangyang, China, [3]College of Veterinary Medicine, Qingdao Agricultural University, Qingdao, China, [4]Center of Prevention and Control Biological Disaster, State Forestry and Grassland Administration, Shenyang, China

Introduction: *Enterocytozoon bieneusi* is one of the most important zoonotic pathogens, responsible for nearly 90% of human infections. Its host spectrum is broad in China, encompassing humans, non-human primates, domestic animals, wildlife, and wastewater. Wild rodents have the potential to act as carriers of *E. bieneusi*, facilitating the parasite's transmission to humans and domestic animals.

Methods: The present study involved the collection of 344 wild rodents, representing nine species, from three provinces in China. The prevalence and genotypes of *E. bieneusi* were determined through amplification of the ITS gene. Evolutionary analysis was conducted using Mega 5.0 with the neighbor-joining method (Kimura 2-parameter model, 1,000 replicates).

Results: Among the sampled wild rodents, 41 (11.92%) were tested positive for *E. bieneusi*. *Rattus flavipectus* exhibited the highest prevalence (11/39), while *Bandicota indica* and *Rattus rattus sladeni* showed no infections (0/39 and 0/5, respectively), highlighting significant differences. Environmental factors strongly influenced *E. bieneusi* infection; rodents residing in lake beaches (10.27%, 15/146) and fields (19.95%, 18/95) were more susceptible compared to those in mountainous areas (7.77%, 8/103). The study identified four known genotypes (D, Type IV, SDD5, PigEBITS7) and five novel genotypes (HNRV-1 to HNRV-3, GXRL-1, GXRL-2) in the investigated wild rodents, with Genotype D exhibiting the highest prevalence.

Discussion: Remarkably, this study reports the presence of *E. bieneusi*, *R. flavipectus*, *M. fortis*, *A. agrarius*, *R. losea*, and *N. lotipes* for the first time. These findings underscore the common occurrence of *E. bieneusi* infection in wild rodents in China, highlighting its diverse nature and significant potential for zoonotic transmission. Hence, it is imperative to conduct a comprehensive epidemiological investigation of rodent infection with *E. bieneusi*, particularly focusing on wild rodents that are closely associated with humans. Additionally, developing appropriate measures and monitoring strategies to minimize the risk of infection is essential.

KEYWORDS

***Enterocytozoon bieneusi*, prevalence, diversity, wild rodents, China**

1 Introduction

Microsporidia encompass nearly 1,700 species distributed across over 220 genera (1). Among them, *Enterocytozoon bieneusi* stands out as a significant microsporidian species, responsible for nearly 90% of human infections (2). *E. bieneusi* was first identified in a Haitian patient with HIV/AIDS in 1985 who experienced severe diarrhea (3). As an emerging infectious agent, *E. bieneusi* is characterized by symptoms such as acute or chronic diarrhea, malabsorption, and/or wasting (1). The spores of *E. bieneusi* infect epithelial cells, undergo a proliferative phase, and are then released as new mature spores during the sporogonic phase, contaminating the environment, including drinking water and wastewater sources, and posing a risk to public health (4). Notably, *E. bieneusi* exhibits a broad host range, infecting various animals including foxes (5), cattle (6), raccoon dogs (7), sika deer (8), and wild rodents (9). Transmission typically occurs through the ingestion of food and water contaminated with spores, serving as the primary route for both humans and animals to acquire infections (2). Additionally, close contact between humans and infected animals or humans constitutes another significant pathway for pathogen transmission (2). Consequently, *E. bieneusi* has been classified as a Category B Priority Pathogen by the United States Environmental Protection Agency (EPA) (10).

Since its initial description in 1985 (11), *E. bieneusi* has seen the identification of 15 phylogenetic groups, encompassing over 500 genotypes, by analyzing sequence polymorphisms of the ribosomal internal transcribed spacer (ITS) and applying standard genotype terminology for classifying sequence variants (1). Among these groups, Group 1 predominantly harbors zoonotic genotypes, commonly detected in both humans and animals (9). While Groups 2–11 are typically regarded as host-adapted groups, occasional reports indicate certain *E. bieneusi* genotypes from these groups, such as Group 2 (I and J), Group 5 (KIN-3), and Group 6 (MAY1 and Nig3), have been observed in humans (1). Notably, more than 70 *E. bieneusi* genotypes have been recognized in wild rodents, including EbpB, D, ESH02, S7, SCC-2, MouseSpEb1, and NESQ1. Of significance, some of these genotypes, such as EbpC, EbpA, and D, have been detected in humans as well (1, 9), indicating a potentially significant zoonotic risk.

Enterocytozoon bieneusi has been reported in a wide range of hosts, including humans (12), non-human primates (13), domestic animals (14), wildlife (8), and wastewater (15), in China. A meta-analysis of *E. bieneusi* infections in China estimated that the prevalence rates in cattle, pigs, goats, and wastewater were 20.0, 45.1, 28.1, and 64.5%, respectively (16). Considering the gravity of this situation, it remains crucial to investigate the prevalence and genotypes of *E. bieneusi* in wild rodents. Consequently, the current study was undertaken to assess the prevalence of *E. bieneusi* in 344 wild rodents across Yunnan Province, Hunan Province, and Guangxi Province, China, employing ITS gene amplification of *E. bieneusi* and subsequent genotype determination. The study findings will furnish vital data for further investigations into *E. bieneusi* distribution and for the prevention and control of *E. bieneusi* infection in both human and animal populations within the surveyed regions.

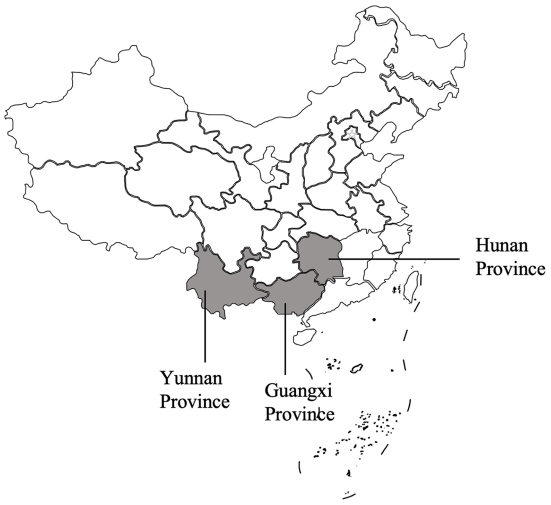

FIGURE 1
Specifc locations where samples were collected in this study.

2 Materials and methods

2.1 Specimen collection and preparation

Between September 2023 and February 2024, a total of 344 wild rodents belonging to nine species were randomly captured from Yunnan Province, Hunan Province, and Guangxi Province in China using mousetraps (refer to Figure 1 and Table 1). Each rodent's rectal fecal sample was collected, and all samples were then transported to the laboratory packed in boxes with dry ice. DNA extraction was performed using the Stool DNA kit (OMEGA, United States), following the manufacturer's instructions meticulously. The extracted DNA was stored at −20°C until PCR amplification. Detailed information regarding the wild rodents can be found in Table 1.

2.2 PCR amplification, sequencing and phylogenetic analyses

Nested PCR was employed to investigate the prevalence and species/genotypes of *E. bieneusi*, utilizing specific primers targeting the ITS genes of *E. bieneusi* (7). The expected amplification product was a 390 bp fragment. The primers were EBITS3 (5'-GGTCATAGGGATGAAGAG-3') and EBITS4 (5'-TTCGAGTTC TTTCGCGCTC-3') as external primers and EBITS1 (5'-GCTCTGA ATATCTATGGCT-3') and EBITS2.4 (5'-ATCGCCGACGGATCC AAGTG-3') as internal primers. Each test included both positive and negative controls to ensure accuracy. The PCR products were visualized under UV light after electrophoresis on 2% agarose gels. All positive products were sequenced based on bidirectional sequencing at the General Biol. Company in Anhui, China. Then, the obtained sequences were blasted in GenBank.[1] For evolutionary analysis, Mega

1 https://blast.ncbi.nlm.nih.gov/Blast.cgi

TABLE 1 Distribution of *Enterocytozoon bieneusi* genotypes and factors associated with its prevalence in wild rodents.

Factors	Category	No. tested	No. positive	% (95%CI*)	*p*-value	OR (95% CI)	Subtypes (No.)
Region	Yunnan Province	88	17	19.32 (11.67–28.29)	0.0525	2.84 (1.16–6.96)	D (*n* = 11), PigEBITS7 (*n* = 3), Type IV (*n* = 3)
	Hunan Province	153	16	10.46 (6.05–15.85)		1.39 (0.57–3.37)	D (*n* = 7), HNRV-1 (*n* = 1), HNRV-2 (*n* = 1), HNRV-3 (*n* = 1), PigEBITS7 (*n* = 2), SDD5 (*n* = 2), Type IV (*n* = 2)
	Guangxi Province	103	8	7.77 (3.26–13.84)		Reference	D (*n* = 1), GXRL-1 (*n* = 2), GXRL-2 (*n* = 1), PigEBITS7 (*n* = 3), Type IV (*n* = 1)
Species	*Rattus flavipectus*	39	11	28.21 (15.03–43.49)	0.0081	3.51 (1.44–8.54)	D (*n* = 6), PigEBITS7 (*n* = 2), Type IV (*n* = 3)
	Mus musculus	13	2	15.38 (0.37–40.99)		1.62 (0.33–8.08)	D (*n* = 1), PigEBITS7 (*n* = 1)
	Apodemus agrarius	14	2	14.29 (0.33–38.41)		1.49 (0.30–7.34)	D (*n* = 1), Type IV (*n* = 1)
	Niviventer lotipes	23	3	13.04 (1.81–30.45)		1.34 (0.35–5.08)	PigEBITS7 (*n* = 3)
	Rattus norvegicus	31	4	12.90 (2.98–27.39)		1.32 (0.40–4.33)	D (*n* = 4)
	Rattus losea	41	5	12.20 (3.64–24.26)		1.24 (0.42–3.68)	D (*n* = 1), GXRL-1 (*n* = 2),GXRL-2 (*n* = 1), Type IV (*n* = 1)
	Microtus fortis	139	14	10.07 (5.55–15.69)		Reference	D (*n* = 6), HNRV-1 (*n* = 1), HNRV-2 (*n* = 1), HNRV-3 (*n* = 1), PigEBITS7 (*n* = 2), SDD5 (*n* = 2), Type IV (*n* = 1)
	Bandicota indica	39	0	0.00 (–)		–	–
	Rattus rattus sladeni	5	0	0.00 (–)		–	–
Season	Autumn	88	17	19.32 (11.67–28.29)	0.0525	2.84 (1.16–6.96)	D (*n* = 11), PigEBITS7 (*n* = 3), Type IV (*n* = 3)
	Summer	153	16	10.46 (6.05–15.85)		1.39 (0.57–3.37)	D (*n* = 7), HNRV-1 (*n* = 1), HNRV-2 (*n* = 1), HNRV-3 (*n* = 1), PigEBITS7 (*n* = 2), SDD5 (*n* = 2), Type IV (*n* = 2)
	Winter	103	8	7.77 (3.26–13.84)		Reference	D (*n* = 1), GXRL-1 (*n* = 2), GXRL-2 (*n* = 1), PigEBITS7 (*n* = 3), Type IV (*n* = 1)
Gender	Female	147	20	13.61 (8.49–19.67)	0.4026	1.32 (0.69–2.54)	D (*n* = 8), GXRL-1 (*n* = 1), HNRV-1 (*n* = 1), HNRV-3 (*n* = 1), PigEBITS7 (*n* = 5), SDD5 (*n* = 1), Type IV (*n* = 3)
	Male	197	21	10.66 (6.70–15.39)		Reference	D (*n* = 11), GXRL-1 (*n* = 1), GXRL-2 (*n* = 1), HNRV-2 (*n* = 1), PigEBITS7 (*n* = 3), SDD5 (*n* = 1), Type IV (*n* = 3)
Environment	Field	95	18	18.95 (11.63–27.51)	0.0530	2.78 (1.18–6.73)	D (*n* = 12), PigEBITS7 (*n* = 3), Type IV (*n* = 3)
	Lakebeach	146	15	10.27 (5.81–15.78)		1.36 (0.55–3.34)	D (*n* = 6), HNRV-1 (*n* = 1), HNRV-2 (*n* = 1), HNRV-3 (*n* = 1), PigEBITS7 (*n* = 2), SDD5 (*n* = 2), Type IV (*n* = 2)
	Mountain	103	8	7.77 (3.26–13.84)		Reference	D (*n* = 1), GXRL-1 (*n* = 2),GXRL-2 (*n* = 1), PigEBITS7 (*n* = 3), Type IV (*n* = 1)
Total		344	41	11.92 (8.71–15.55)			D (*n* = 19), GXRL-1 (*n* = 2), GXRL-2 (*n* = 1), HNRV-1 (*n* = 1), HNRV-2 (*n* = 1), HNRV-3 (*n* = 1), PigEBITS7 (*n* = 8), SDD5 (*n* = 2), Type IV (*n* = 6)

CI*, confidence interval.

10.3389/fvets.2024.1427690

5.0[2] was utilized to construct the phylogenetic tree employing the neighbor-joining (NJ) method with the Kimura 2-parameter model and 1,000 replicates. All representative sequences were submitted into GenBank with accession numbers PP702179-PP702190.

2.3 Statistical analysis

The Chi-square test in SAS (Statistical Analysis System, Version 9.0) was employed to assess variations in *E. bieneusi* prevalence (*y*) across different regions (*x1*), species (*x2*), seasons (*x3*), environments (*x4*), and genders (*x5*) of wild rodents. The analysis also examined the discrepancies between *E. bieneusi* prevalence and each of the risk factors. In the multivariable regression analysis, each of these variables was included in the binary logit model as an independent variable. The best model was judged by Fisher's scoring algorithm (17). All tests were two-sided, and a significance level of $p < 0.05$ indicated a statistically significant difference, with corresponding odds ratios (ORs) and their 95% confidence intervals (95% CIs) provided.

3 Results

3.1 Prevalence of *Enterocytozoon bieneusi*

In this study, PCR analysis of the ITS gene detected *E. bieneusi* in 41 out of 344 wild rodents, resulting in a prevalence of 11.92% (95% CI 8.71–15.55) (Partial results of agarose gel electrophoresis of the PCR amplification products were shown in Figure 2). The prevalence varied among different species groups, ranging from 0 to 28.21% (95% CI 15.03–43.49), with the highest prevalence observed in *Rattus flavipectus* (11/39). Across different regions, the prevalence of *E. bieneusi* in wild rodents from Guangxi, Yunnan, and Hunan was 7.77% (8/103, 95% CI 3.26–13.84), 19.32% (17/88, 95% CI 11.67–28.29), and 10.46% (16/153, 95% CI 6.05–15.85), respectively. The prevalence in wild rodents of different gender groups was 10.66% in males and 13.61% in females. Regarding different environments, the prevalence varied, with rates of 7.77% (8/103, 95% CI 3.26–13.84) in mountain-dwelling rodents, 10.27% (15/146, 95% CI 5.81–15.78) in those residing near lake beaches, and 18.95% (18/95, 95% CI 11.63–27.51) in those inhabiting fields. Furthermore, the prevalence of *E. bieneusi* differed across seasons, with rates of 7.77% (8/103, 95% CI 3.26–13.84) in winter, 19.32% (17/88, 95% CI 11.67–28.29) in autumn, and 10.46% (16/153, 95% CI 6.05–15.85) in summer.

3.2 Risk factors of *Enterocytozoon bieneusi*

Table 1 displays the associations between *E. bieneusi*-positive cases in wild rodents and various factors including regions, species, seasons, environment, and gender, analyzed through univariate analysis. The impact of these factors on *E. bieneusi* infection was further evaluated using forward stepwise logistic regression analysis based on Fisher's scoring technique. Ultimately, only environment was retained in the final model, indicating its significant influence on *E. bieneusi* infection. The equation derived from the regression analysis is expressed as follows: $y = 0.5402 \times 1 + 0.9704$. Notably, environment emerged as a strong determinant of *E. bieneusi* infection in wild rodents, with an odds ratio (OR) of 1.72 (95% CI 1.10–2.68). Specifically, wild rodents inhabiting lake beaches (OR 1.36, 95% CI 0.55–3.34) and fields (OR 2.78, 95% CI 1.18–6.73) exhibited higher susceptibility compared to those dwelling in mountainous regions (see Table 1).

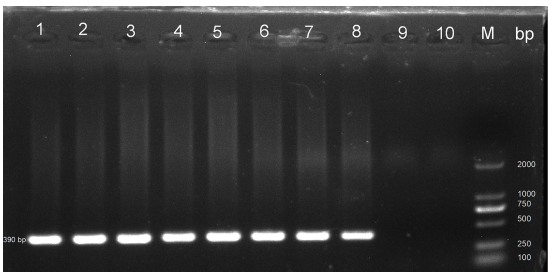

FIGURE 2
Representative agarose gel image showing PCR amplification products of the ITS gene of *E. bieneusi* (expected band size 390 bp). Lanes 1–9: Samples; Lane 10: Negative control; M: DL 2000 DNA marker.

3.3 Distribution of *Enterocytozoon bieneusi* genotypes

In the investigated wild rodents, a total of nine genotypes were identified, comprising four known genotypes (D, Type IV, SDD5, PigEBITS7) and five novel genotypes (HNRV-1 to HNRV-3, GXRL-1, GXRL-2) (refer to Table 1). Furthermore, a total of 24 polymorphic sites were observed among these genotypes (Table 2), resulting in a few amino acid substitutions (refer to Table 3). Among these, genotype D displayed the highest prevalence among the studied rodents, followed by Type IV and PigEBITS7. Notably, Type IV, SDD5, and PigEBITS7 were prevalent across all three provinces, whereas SDD5, HNRV-1, HNRV-2, and HNRV-3 were exclusively detected in Hunan Province, and the remaining genotypes were solely identified in Guangxi Province. Genotype D was observed in six species of wild rodents, followed by PigEBITS7 in five rodent species and Type IV in five rodent species, while the remaining genotypes were only present in one species of wild rodents each. Interestingly, Type IV, PigEBITS7, and D were detected in rodents across all environmental factors, whereas HNRV-1, HNRV-2, HNRV-3, and SDD5 were specifically distributed in rodents from lake beaches. Additionally, GXRL-1 and GXRL-2 were exclusively found in rodents inhabiting mountainous regions.

3.4 Phylogenetic analysis of *Enterocytozoon bieneusi*

Phylogenetic analysis of the ITS region of *E. bieneusi* divided the identified genotypes into two groups (refer to Figure 3). Specifically, out of these nine genotypes, eight (comprising three known and five novel genotypes) were classified into Group 1, comprising D, PigEBITS7, HNRV-1, HNRV-2, and HNRV-3 in 1a, Type IV in 1c, and

2 http://www.megasoftware.net/

TABLE 2 Variations in the ITS nucleotide sequences among genotypes of the *Enterocytozoon bieneusi* in wild rodents.

Genotypes (no.)	Nucleotide at position																								GenBank accession no.
	93	113	114	116	118	121	136	140	160	165	169	176	177	197	201	203	208	221	231	311	318	322	328	330	
D (Reference)	G	T	G	G	T	G	A	G	C	C	G	G	C	C	T	T	G	C	G	G	G	G	C	G	MN704918
D (1)	G	T	G	G	T	G	A	G	C	C	G	G	C	C	T	T	G	C	G	G	G	G	C	G	PP702184
D (1)	G	T	G	G	T	G	A	G	C	C	G	G	C	C	T	T	G	C	G	G	G	G	C	G	PP702189
D (17)	G	T	G	G	T	G	A	G	C	C	G	G	C	C	T	T	G	C	G	G	G	G	C	G	PP702190
Type IV (3)	G	T	G	G	T	G	A	G	C	C	G	G	T	C	G	T	G	C	G	G	G	G	C	G	PP702179
Type IV (3)	G	T	G	G	T	G	A	G	C	C	G	G	T	C	G	T	G	C	G	G	G	G	C	G	PP702182
PigEBITS7 (8)	G	T	A	G	C	G	A	G	C	C	G	G	C	C	T	T	G	C	G	G	G	G	C	G	PP702183
HNRV-1 (1)	G	T	A	G	C	G	A	G	C	C	G	G	C	C	T	C	G	C	G	G	G	G	C	G	PP702185
HNRV-2 (1)	G	T	G	G	T	G	A	G	C	C	G	G	C	C	T	T	G	C	G	A	G	A	C	G	PP702186
HNRV-3 (1)	G	T	G	G	T	G	A	G	C	C	G	G	C	C	T	T	G	C	G	A	A	A	G	A	PP702187
GXRL-1 (2)	G	C	A	G	T	G	A	G	G	T	G	G	T	C	G	T	G	C	G	G	G	G	C	G	PP702180
GXRL-2 (1)	G	T	A	G	T	G	A	G	G	T	G	G	T	C	G	T	G	C	G	G	G	G	C	G	PP702181
SDD5 (2)	A	T	A	C	T	A	G	-	C	T	A	A	T	T	G	T	A	T	A	G	G	G	C	G	PP702188

TABLE 3 Variations in amino acid substitution among genotypes of the *Enterocytozoon bieneusi* in wild rodents.

Genotypes (no.)	Amino acid substitution																	GenBank accession no.
	38	39	40	41	46	54	57	59	66	67	68	70	74	77	104	108	110	
D (Reference)	V	W	~	V	M	R	G	C	A	S	V	D	A	R	R	E	Q	MN704918
D (1)																		PP702184
D (1)																		PP702189
D (17)																		PP702190
Type IV (3)																		PP702179
Type IV (3)																		PP702182
PigEBITS7 (8)			Q															PP702183
HNRV-1 (1)			Q								A							PP702185
HNRV-2 (1)															K	K		PP702186
HNRV-3 (1)															K	K	E	PP702187
GXRL-1 (2)	A					G				R								PP702180
GXRL-2 (1)						G				R								PP702181
SDD5 (2)		S		M	V		S	Y	V	R		N	V	A				PP702188

10.3389/fvets.2024.1427690

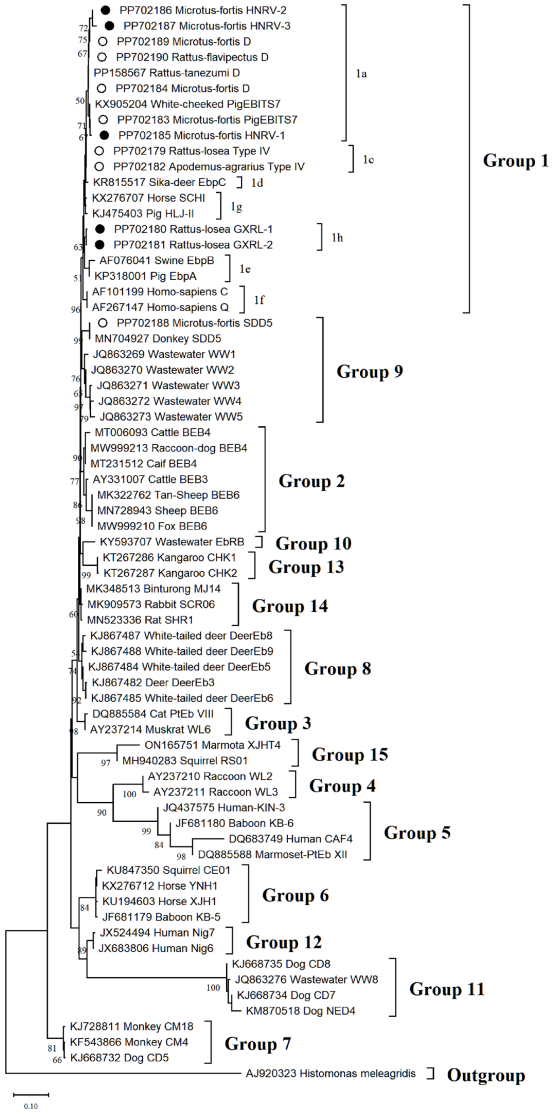

FIGURE 3
The phylogenetic tree was constructed based on the ITS gene of *E. bieneusi* using Neighbor-joining (NJ) methods (Kimura 2-parameter model and 1,000 replicates). Bootstrap values more than 50% are shown. The known *E. bieneusi* genotypes identified in this study are indicated by empty circles, and the novel genotypes are marked as black circle.

GXRL-1 and GXRL-2 in 1 h. The remaining genotype, SDD5, was placed within Group 9.

4 Discussion

Rodents are widely distributed worldwide and frequently carry infectious parasites that pose a threat to human health. Studies have indicated that rodents serve as crucial hosts for parasites such as *Hydatigera taeniaeformis* (18, 19), *Toxoplasma gondii* (20), *Giardia duodenalis* (21), *Blastocystis* (22), and *Enterocytozoon bieneusi* (23). The extensive distribution of rodents enables them to transmit these parasites to other animals and humans via the fecal-oral route through contaminated water and food, thereby contributing to the propagation of infections (24). Among the above-mentioned parasites, *E. bieneusi* is a significant zoonotic pathogen that causes gastrointestinal disorders (1). Since its initial identification, the host spectrum of *E. bieneusi* has significantly broadened, including that of humans (21), foxes (5), cattle (6), goats (25), raccoon dogs (7), sika deer (8), yaks (24), Tibetan pigs (24), and wild rodents (9), accompanied by the documentation of numerous genotypes. Therefore, it is essential to explore the prevalence and genotypes of *E. bieneusi* in wild rodents.

In this investigation, we collected and examined 344 wild rodents to explore the prevalence and genotypic variations of *E. bieneusi*. The overall prevalence of *E. bieneusi* among the examined rodents was 11.92% (41/344), which was lower than the rates previously reported in rodents from southwestern Poland (38.9%, 121/311) (26) and the United States (26.8%, 38/142) (27), but higher than those observed in Iran (8.75%, 14/160) (28), Peru (6.7%, 4/60) (29), and Japan (0%, 0/162) (30). Disparities in *E. bieneusi* prevalence rates across various countries could arise from differences in sample locations, sampling periods, rodent species and populations, levels of environmental contamination, and diagnostic methodologies. It's worth noting that, apart from China and the United States, only one study was conducted in other countries, necessitating further exploration of the factors contributing to the divergent epidemic rates of *E. bieneusi* among these countries.

Considerable variations in prevalence were noted among different species of wild rodents, with the highest occurrence observed in *R. flavipectus* (28.21%, 11/39), whereas *Bandicota indica* and *Rattus rattus sladeni* exhibited no instances of infection (0%, 0/39 and 0%, 0/5 respectively). *E. bieneusi* infection rates have been documented in various other rodent species in China as well, including coypu (*Myocastor coypus*) (41.02%, 127/308) (23), squirrels (19.4%, 61/314) (31), wild rats (11.1%, 41/370) (32), experimental rats (4.8%, 14/291) (33), pet fancy rats (*Rattus norvegicus*) (11.2%, 17/152) (34), marmots (11.8%, 47/399) (35), plateau zokors (*Myospalax baileyi*) (4.1%, 4/98) (36), and bamboo rats (*Rhizomys sinensis*) (5.1%, 22/435) (37), indicating widespread distribution of *E. bieneusi* among rodents in China. The disparities in prevalence rates among different species could be attributed to varying factors such as susceptibility, age distribution, sample size, sampling time, and detection method (38).

Furthermore, wild rodents residing in diverse environments exhibited varying prevalences of *E. bieneusi*, with the highest occurrence recorded in fields (18.95, 95% CI 11.63–27.51), followed by lake beaches (10.27, 95% CI 5.81–15.78), and the lowest in mountainous areas (7.77, 95% CI 3.26–13.84), highlighting statistically significant differences. This was likely due to the presence of numerous infected wild and domestic animals in the areas where the samples were collected. The spores of *E. bieneusi* in the feces of infected animals might have dispersed into fields or onto cultivated vegetables and fruits, and fecal-oral transmission of spores may further elevate the infection rate among wild rodents. These findings suggest extensive ranges of activity among wild rodents, thereby facilitating the dissemination of *E. bieneusi*.

The study found no significant gender-based differences in prevalence rates ($p = 0.4026$), consistent with a prior investigation into *E. bieneusi* infection rates in pet chipmunks in Sichuan Province, China (39). Notably, the prevalence of *E. bieneusi* in rodent feces collected during autumn (19.32%, 17/88) was slightly higher than that

in samples collected during summer (10.46%, 16/153) and winter (7.77%, 8/103). However, the prevalence rates across seasons did not exhibit a significant difference ($p = 0.0525$), aligning with the findings of a meta-analysis on *E. bieneusi* infection rates (40).

Presently, over 500 genotypes of *E. bieneusi* have been cataloged, with the majority exhibiting host-specificity. Among them, at least 143 are capable of infecting humans, while 49 have the potential to infect both humans and animals, posing a zoonotic risk (41, 42). Globally, more than 70 genotypes have been identified in rodents (1, 9). However, only nine genotypes were identified in the current study, comprising four known genotypes (D, PigEBITS7, Type IV, and SDD5) and five novel genotypes (GXRL-1, GXRL-2, HNRV-1, HNRV-2, and HNRV-3). Of these, genotype D emerged as the predominant genotype in *E. bieneusi*, accounting for 46.3% (19/41) of the infected samples. Extensive studies have highlighted genotype D's expansive host range and geographical distribution (40, 41, 43). It has been identified as the most prevalent genotype in humans, particularly among individuals with diarrhea and compromised immune systems (40), as well as in children (21). Moreover, genotype D has been detected in wild and domestic animals worldwide, including cattle (4), donkeys (44), dogs (45), cats (45), golden snub-nosed monkeys (46), raccoon dogs (47), horses (48), pigeons (49), and foxes (47). Its prevalence extends to rodents as well, including bamboo rats, pet chipmunks, brown rats, white-toothed rats, red-bellied tree squirrels, and red squirrels in China (37, 39, 42), along with various small rodents in Poland, along the Switzerland-Germany border (26), and along the Czech Republic-Germany border (50). In this study, *E. bieneusi* was detected across six species of wild rodents, namely *R. flavipectus*, *Microtus fortis*, *Rattus norvegicus*, *Apodemus agrarius*, *Rattus losea*, and *Mus musculus*. These findings underscore the significance of genotype D as one of the most critical zoonotic genotype of *E. bieneusi*, warranting increased attention in forthcoming research endeavors.

In the present study, PigEBITS7 was identified in *R. flavipectus*, *M. fortis*, *M. musculus*, and *N. lotipes*, constituting 19.5% (8/41) of the positive samples. PigEBITS7 was initially detected in pigs in Switzerland, and is one of the most commonly encountered genotypes in domestic pigs and wild boars (27). PigEBITS7 has been identified in AIDS patients in China, Thailand, and India (51–54). It has also been detected in various rodent species, including Asian house rats, brown rats, and Chinese white-bellied rats from Hainan Province, China (42), as well as in two wild rat species collected from Chongqing City and Guangdong Province, China (55). These studies indicate the potential for transmission of PigEBITS7 between wild and domestic animals and humans, thereby posing a zoonotic hazard. Type IV was detected in *R. flavipectus*, *M. fortis*, *A. agrarius*, and *R. losea*, representing 14.6% (6/41) of the positive samples. Research has indicated that Type IV is commonly encountered across various hosts, including humans (21), non-human primates (13), cattle (56), macaques (57), cats (58), dogs (58), and birds (59). Moreover, Type IV has been documented in rodents in the United States (27) and has been identified in rodents from Hainan Province and Zhejiang Province, China (32, 42). The remaining known genotype, SDD5, has been identified in donkeys (33), but has not been found in humans. Its zoonotic potential remains uncertain. These data underscore the frequent detection of zoonotic genotypes D, Type IV, and PigEBITS7 in rodents, suggesting that wild rodents may contribute significantly to the cycling of *E. bieneusi* among humans, livestock, wildlife, and the environment.

The genetic relationships between the *E. bieneusi* genotypes discovered in this study and the previously identified strains were determined through phylogenetic analysis. Eight out of the nine genotypes clustered into Group 1, and the five novel genotypes (GXRL-1, GXRL-2, HNRV-1, HNRV-2, and HNRV-3) were also aligned with Group 1. Group 1 is primarily composed of genotypes derived from humans, characterized by low host specificity, and is notably contagious across diverse species, thus posing a significant potential for zoonotic transmission (9, 41). This suggests that the five novel genotypes may have a wider host range and can infect humans, thereby posing a significant threat to public health. However, further research is required to confirm this hypothesis. The remaining genotype, SDD5, was relatively distantly related to genotype D (MN704918), with 15 nucleotide differences and 10 amino acid substitutions, and was placed within Group 9. Group 9 appeared to have adapted to wild carnivores, rodents, and wastewater (41). This observation suggests that it is crucial to pay close attention to the waterborne transmission routes of *E. bieneusi* contributed by wild rodents to ensure safe consumption of water.

Despite the fact that this study provided significant evidence of *E. bieneusi* infections in rodents, there are certain limitations that need to be acknowledged. The rodent samples obtained in this study were limited to specific geographic areas, which does not offer a comprehensive understanding of the prevalence of *E. bieneusi* infection in rodents throughout China. Additionally, the number of positive samples in this study was limited, which may have led to insufficient representation of the genetic diversity of *E. bieneusi*. To gain a more comprehensive understanding of the prevalence of *E. bieneusi*, it is necessary to expand the sample size and collection area in future studies.

5 Conclusion

The findings of the study highlight the prevalence of *E. bieneusi* infection among wild rodents in China. This research marks the first documentation of *E. bieneusi* presence in *R. favipectus*, *M. fortis*, *A. agrarius*, *R. losea*, and *N. lotipes*, thereby broadening the spectrum of hosts susceptible to *E. bieneusi*. Both species type and environmental factors emerge as significant influencers of *E. bieneusi* infection among wild rodents. Notably, the study identifies genotype D as the predominant strain among the infected samples, while also unveiling, for the first time, the presence of genotypes GXRL-1, GXRL-2, HNRV-1, HNRV-2, and HNRV-3. Moreover, the five novel genotypes uncovered in this investigation are categorized within Group 1, suggesting potential zoonotic implications. This study contributes to an enhanced comprehension of *E. bieneusi* genotypic diversity in wild rodents, shedding light on its extensive variability.

Data availability statement

The datasets presented in this study can be found in online repositories. The names of the repository/repositories and accession number(s) can be found in the article/supplementary material.

Ethics statement

The animal study was approved by the Animal Ethics Committee of Yancheng Teachers University. The study was conducted in accordance with the local legislation and institutional requirements.

Author contributions

Z-QG: Methodology, Software, Writing – original draft. H-TW: Methodology, Software, Writing – original draft. Q-YH: Data curation, Methodology, Writing – review & editing. YQ: Data curation, Resources, Visualization, Writing – review & editing. S-YQ: Data curation, Resources, Visualization, Writing – review & editing. QZ: Conceptualization, Resources, Supervision, Writing – review & editing. HM: Conceptualization, Resources, Supervision, Writing – review & editing.

Funding

The author(s) declare that no financial support was received for the research, authorship, and/or publication of this article.

Acknowledgments

The authors would like to thank Chair Professor Hany Elsheikha, Faculty of Medicine and Health Sciences, University of Nottingham for the valuable comments and constructive feedback.

Conflict of interest

The authors declare that the research was conducted in the absence of any commercial or financial relationships that could be construed as a potential conflict of interest.

Publisher's note

All claims expressed in this article are solely those of the authors and do not necessarily represent those of their affiliated organizations, or those of the publisher, the editors and the reviewers. Any product that may be evaluated in this article, or claim that may be made by its manufacturer, is not guaranteed or endorsed by the publisher.

References

1. Jiang S, Yu S, Feng Y, Zhang L, Santin M, Xiao L, et al. Widespread distribution of human-infective *Enterocytozoon bieneusi* genotypes in small rodents in Northeast China and phylogeny and zoonotic implications revisited. *Acta Trop*. (2024) 253:107160. doi: 10.1016/j.actatropica.2024.107160

2. Karim MR, Rume FI, Li D, Li J, Zhang L. First molecular characterization of *Enterocytozoon bieneusi* in children and calves in Bangladesh. *Transbound Emerg Dis*. (2022) 69:1999–2007. doi: 10.1111/tbed.14187

3. Desportes I, Le Charpentier Y, Galian A, Bernard F, Cochand-Priollet B, Lavergne A, et al. Occurrence of a new microsporidan: *Enterocytozoon bieneusi* n.g., n. sp., in the enterocytes of a human patient with AIDS. *J Protozool*. (1985) 32:250–4. doi: 10.1111/j.1550-7408.1985.tb03046.x

4. Li W, Feng Y, Xiao L. Enterocytozoon bieneusi. *Trends Parasitol*. (2022) 38:95–6. doi: 10.1016/j.pt.2021.08.003

5. Zhang XX, Cong W, Lou ZL, Ma JG, Zheng WB, Yao QX, et al. Prevalence, risk factors and multilocus genotyping of *Enterocytozoon bieneusi* in farmed foxes (*Vulpes lagopus*), Northern China. *Parasit Vectors*. (2016a) 9:72. doi: 10.1186/s13071-016-1356-1

6. Gao H, Liang G, Su N, Li Q, Wang D, Wang J, et al. Prevalence and molecular characterization of *Cryptosporidium* spp., *Giardia duodenalis*, and *Enterocytozoon bieneusi* in diarrheic and non-diarrheic calves from Ningxia, northwestern China. *Animals (Basel)*. (2023) 13, 13:1983. doi: 10.3390/ani13121983

7. Chen M, Wang H, Li X, Guo Y, Lu Y, Zheng L, et al. Molecular epidemiology of *Enterocytozoon bieneusi* from foxes and raccoon dogs in the Henan and Hebei provinces in China. *BMC Vet Res*. (2024) 20:53. doi: 10.1186/s12917-024-03883-6

8. Zhang XX, Cong W, Liu GH, Ni XT, Ma JG, Zheng WB, et al. Prevalence and genotypes of Enterocytozoon bieneusi in sika deer in Jilin province, Northeastern China. *Acta Parasitol*. (2016b) 61:382–8. doi: 10.1515/ap-2016-0050

9. Ni HB, Sun YZ, Qin SY, Wang YC, Zhao Q, Sun ZY, et al. Molecular detection of Cryptosporidium spp. and *Enterocytozoon bieneusi* infection in wild rodents from six provinces in China. *Front Cell Infect Microbiol*. (2021) 11:783508. doi: 10.3389/fcimb.2021.783508

10. Didier ES, Weiss LM. Microsporidiosis: current status. *Curr Opin Infect Dis*. (2006) 19:485–92. doi: 10.1097/01.qco.0000244055.46382.23

11. Wang Y, Li XM, Yang X, Wang XY, Wei YJ, Cai Y, et al. Global prevalence and risk factors of *Enterocytozoon bieneusi* infection in humans: a systematic review and meta-analysis. *Parasite*. (2024) 31:9. doi: 10.1051/parasite/2024007

12. Qi M, Yu F, Zhao A, Zhang Y, Wei Z, Li D, et al. Unusual dominant genotype NIA1 of Enterocytozoon bieneusi in children in southern Xinjiang, China. *PLoS Negl Trop Dis*. (2020) 14:e0008293. doi: 10.1371/journal.pntd.0008293

13. Karim MR, Wang R, Dong H, Zhang L, Li J, Zhang S, et al. Genetic polymorphism and zoonotic potential of *Enterocytozoon bieneusi* from nonhuman primates in China. *Appl Environ Microbiol*. (2014a) 80:1893–8. doi: 10.1128/aem.03845-13

14. Li F, Wang R, Guo Y, Li N, Feng Y, Xiao L. Zoonotic potential of *Enterocytozoon bieneusi* and *Giardia duodenalis* in horses and donkeys in northern China. *Parasitol Res*. (2020) 119:1101–8. doi: 10.1007/s00436-020-06612-8

15. Li N, Xiao L, Wang L, Zhao S, Zhao X, Duan L, et al. Molecular surveillance of *Cryptosporidium* spp., *Giardia duodenalis*, and *Enterocytozoon bieneusi* by genotyping and subtyping parasites in wastewater. *PLoS Negl Trop Dis*. (2012) 6:e1809. doi: 10.1371/journal.pntd.0001809

16. Qiu L, Xia W, Li W, Ping J, Ding S, Liu H. The prevalence of microsporidia in China: a systematic review and meta-analysis. *Sci Rep*. (2019) 9:3174. doi: 10.1038/s41598-019-39290-3

17. Zhang NZ, Zhang XX, Zhou DH, Huang SY, Tian WP, Yang YC, et al. Seroprevalence and genotype of Chlamydia in pet parrots in China. *Epidemiol Infect*. (2015) 143:55–61. doi: 10.1017/S0950268814000363

18. Alvi MA, Alshammari A, Ali RMA, Rashid I, Saqib M, Qamar W, et al. Molecular characterization of *Hydatigera taeniaeformis* recovered from rats: an update from Pakistan. *Pak Vet J*. (2023) 43:601–5. doi: 10.29261/pakvetj/2023.049

19. Alvi MA, Li L, Ohiolei JA, Qamar W, Saqib M, Tayyab MH, et al. *Hydatigera taeniaeformis* in urban rats (*Rattus rattus*) in Faisalabad, Pakistan. *Infect Genet Evol*. (2021) 92:104873. doi: 10.1016/j.meegid.2021.104873

20. Almuzaini AM. Flow of zoonotic toxoplasmosis in food chain. *Pak Vet J*. (2023) 43:1–16. doi: 10.29261/pakvetj/2023.010

21. Lobo ML, Augusto J, Antunes F, Ceita J, Xiao L, Codices V, et al. *Cryptosporidium* spp., *Giardia duodenalis*, *Enterocytozoon bieneusi* and other intestinal parasites in young children in Lobata province, Democratic Republic of São Tomé and Principe. *PLoS One*. (2014) 9:e97708. doi: 10.1371/journal.pone.0097708

22. Gao ZQ, Wang HT, Hou QY, Qin Y, Yang X, Zhao Q, et al. Prevalence and subtypes of Blastocystis in wild rodents from three provinces in China. *Front Vet Sci*. (2024) 11:1432741. doi: 10.3389/fvets.2024.1432741

23. Yu F, Cao Y, Wang H, Liu Q, Zhao A, Qi M, et al. Host-adaptation of the rare *Enterocytozoon bieneusi* genotype CHN4 in *Myocastor coypus* (Rodentia: Echimyidae) in China. *Parasit Vectors*. (2020) 13:578. doi: 10.1186/s13071-020-04436-0

24. Chen X, Saeed NM, Ding J, Dong H, Kulyar MFEA, Bhutta ZA, et al. Molecular epidemiological investigation of *Cryptosporidium* sp., *Giardia duodenalis*, *Enterocytozoon bieneusi* and *Blastocystis* sp. infection in free-ranged yaks and tibetan pigs on the plateau. *Pak Vet J*. (2022) 42:533–9. doi: 10.29261/pakvetj/2022.060

25. Udonsom R, Prasertbun R, Mahittikorn A, Chiabchalard R, Sutthikornchai C, Palasuwan A, et al. Identification of *Enterocytozoon bieneusi* in goats and cattle in Thailand. *BMC Vet Res*. (2019) 15:308. doi: 10.1186/s12917-019-2054-y

26. Perec-Matysiak A, Buńkowska-Gawlik K, Kváč M, Sak B, Hildebrand J, Leśniańska K. Diversity of *Enterocytozoon bieneusi* genotypes among small rodents in southwestern Poland. *Vet Parasitol*. (2015) 214:242–6. doi: 10.1016/j.vetpar.2015.10.018

27. Guo Y, Alderisio KA, Yang W, Cama V, Feng Y, Xiao L. Host specificity and source of *Enterocytozoon bieneusi* genotypes in a drinking source watershed. *Appl Environ Microbiol*. (2014) 80:218–25. doi: 10.1128/aem.02997-13

28. Tavalla M, Mardani-Kateki M, Abdizadeh R, Soltani S, Saki J. Molecular diagnosis of potentially human pathogenic *Enterocytozoon bieneusi* and Encephalitozoon species in exotic birds in southwestern Iran. *J Infect Public Health*. (2018) 11:192–6. doi: 10.1016/j.jiph.2017.07.028

29. Cama VA, Pearson J, Cabrera L, Pacheco L, Gilman R, Meyer S, et al. Transmission of *Enterocytozoon bieneusi* between a child and guinea pigs. *J Clin Microbiol*. (2007) 45:2708–10. doi: 10.1128/jcm.00725-07

30. Tsukada R, Tsuchiyama A, Sasaki M, Park CH, Fujii Y, Takesue M, et al. Encephalitozoon infections in Rodentia and Soricomorpha in Japan. *Vet Parasitol*. (2013) 198:193–6. doi: 10.1016/j.vetpar.2013.08.018

31. Deng L, Chai Y, Luo R, Yang L, Yao J, Zhong Z, et al. Occurrence and genetic characteristics of Cryptosporidium spp. and *Enterocytozoon bieneusi* in pet red squirrels (*Sciurus vulgaris*) in China. *Sci Rep*. (2020) 10:1026. doi: 10.1038/s41598-020-57896-w

32. Zhang T, Yu K, Xu J, Cao W, Wang Y, Wang J, et al. *Enterocytozoon bieneusi* in wild rats and shrews from Zhejiang Province, China: occurrence, genetic characterization, and potential for zoonotic transmission. *Microorganisms*. (2024) 12:811. doi: 10.3390/microorganisms12040811

33. Li J, Jiang Y, Wang W, Chao L, Jia Y, Yuan Y, et al. Molecular identification and genotyping of *Enterocytozoon bieneusi* in experimental rats in China. *Exp Parasitol*. (2020) 210:107850. doi: 10.1016/j.exppara.2020.107850

34. Wang J, Lv C, Zhao D, Zhu R, Li C, Qian W. First detection and genotyping of *Enterocytozoon bieneusi* in pet fancy rats (*Rattus norvegicus*) and guinea pigs (*Cavia porcellus*) in China. *Parasite*. (2020) 27:21. doi: 10.1051/parasite/2020019

35. Xu J, Wang X, Jing H, Cao S, Zhang X, Jiang Y, et al. Identification and genotyping of *Enterocytozoon bieneusi* in wild Himalayan marmots (*Marmota himalayana*) and Alashan ground squirrels (*Spermophilus alashanicus*) in the Qinghai-Tibetan plateau area (QTPA) of Gansu Province, China. *Parasit Vectors*. (2020) 13:367. doi: 10.1186/s13071-020-04233-9

36. Hu B, Wang J, Zhang S, Wang B, Xing Y, Han S, et al. Novel genotypes of *Cryptosporidium* and *Enterocytozoon bieneusi* detected in plateau zokors (*Myospalax baileyi*) from the Tibetan plateau. *Int J Parasitol Parasites Wildl*. (2022) 19:263–8. doi: 10.1016/j.ijppaw.2022.11.002

37. Wang H, Liu Q, Jiang X, Zhang Y, Zhao A, Cui Z, et al. Dominance of zoonotic genotype D of *Enterocytozoon bieneusi* in bamboo rats (*Rhizomys sinensis*). *Infect Genet Evol*. (2019) 73:113–8. doi: 10.1016/j.meegid.2019.04.025

38. Alvi MA, Li L, Bahadur SUK, Saqib M, Ohiolei JA, Ali RMA, et al. First comparative biochemical profile analysis of cystic fluids of *Taenia hydatigena* and *Echinococcus granulosus* obtained from slaughtered sheep and goats. *Pak Vet J*. (2022) 42:215–21. doi: 10.29261/pakvetj/2022.001

39. Deng L, Li W, Zhong Z, Chai Y, Yang L, Zheng H, et al. Molecular characterization and new genotypes of Enterocytozoon bieneusi in pet chipmunks (Eutamias asiaticus) in Sichuan province, China. *BMC Microbiol*. (2018) 18:37. doi: 10.1186/s12866-018-1175-y

40. Ruan Y, Xu X, He Q, Li L, Guo J, Bao J, et al. The largest meta-analysis on the global prevalence of microsporidia in mammals, avian and water provides insights into the epidemic features of these ubiquitous pathogens. *Parasit Vectors*. (2021) 14:186. doi: 10.1186/s13071-021-04700-x

41. Li W, Feng Y, Santin M. Host specificity of *Enterocytozoon bieneusi* and public health implications. *Trends Parasitol*. (2019) 35:436–51. doi: 10.1016/j.pt.2019.04.004

42. Zhao W, Zhou H, Yang L, Ma T, Zhou J, Liu H, et al. Prevalence, genetic diversity and implications for public health of Enterocytozoon bieneusi in various rodents from Hainan Province, China. *Parasit Vectors*. (2020) 13:438. doi: 10.1186/s13071-020-04314-9

43. Taghipour A, Bahadory S, Abdoli A, Javanmard E. A systematic review and meta-analysis on the global molecular epidemiology of microsporidia infection among rodents: a serious threat to public health. *Acta Parasitol*. (2022) 67:18–30. doi: 10.1007/s11686-021-00447-8

44. Yue DM, Ma JG, Li FC, Hou JL, Zheng WB, Zhao Q, et al. Occurrence of *Enterocytozoon bieneusi* in donkeys (*Equus asinus*) in China: a public health concern. *Front Microbiol*. (2017) 8:565. doi: 10.3389/fmicb.2017.00565

45. Zhang Y, Koehler AV, Wang T, Cunliffe D, Gasser RB. Enterocytozoon bieneusi genotypes in cats and dogs in Victoria, Australia. *BMC Microbiol*. (2019) 19:183. doi: 10.1186/s12866-019-1563-y

46. Yu F, Wu Y, Li T, Cao J, Wang J, Hu S, et al. High prevalence of *Enterocytozoon bieneusi* zoonotic genotype D in captive golden snub-nosed monkey (*Rhinopithecus roxellanae*) in zoos in China. *BMC Vet Res*. (2017) 13:158. doi: 10.1186/s12917-017-1084-6

47. Yang Y, Lin Y, Li Q, Zhang S, Tao W, Wan Q, et al. Widespread presence of human-pathogenic *Enterocytozoon bieneusi* genotype D in farmed foxes (*Vulpes vulpes*) and raccoon dogs (*Nyctereutes procyonoides*) in China: first identification and zoonotic concern. *Parasitol Res*. (2015) 114:4341–8. doi: 10.1007/s00436-015-4714-6

48. Deng L, Li W, Zhong Z, Gong C, Liu X, Huang X, et al. Molecular characterization and multilocus genotypes of *Enterocytozoon bieneusi* among horses in southwestern China. *Parasit Vectors*. (2016) 9:561. doi: 10.1186/s13071-016-1844-3

49. da Cunha MJR, Cury MC, Santín M. Molecular identification of *Enterocytozoon bieneusi*, *Cryptosporidium*, and Giardia in Brazilian captive birds. *Parasitol Res*. (2017) 116:487–93. doi: 10.1007/s00436-016-5309-6

50. Sak B, Kváč M, Květoňová D, Albrecht T, Piálek J. The first report on natural *Enterocytozoon bieneusi* and *Encephalitozoon* spp. infections in wild east-European house mice (*Mus musculus musculus*) and west-European house mice (*M. m. Domesticus*) in a hybrid zone across the Czech Republic-Germany border. *Vet Parasitol*. (2011) 178:246–50. doi: 10.1016/j.vetpar.2010.12.044

51. Breitenmoser AC, Mathis A, Bürgi E, Weber R, Deplazes P. High prevalence of *Enterocytozoon bieneusi* in swine with four genotypes that differ from those identified in humans. *Parasitology*. (1999) 118:447–53. doi: 10.1017/s0031182099004229

52. Leelayoova S, Subrungruang I, Suputtamongkol Y, Worapong J, Petmitr PC, Mungthin M. Identification of genotypes of *Enterocytozoon bieneusi* from stool samples from human immunodeficiency virus-infected patients in Thailand. *J Clin Microbiol*. (2006) 44:3001–4. doi: 10.1128/jcm.00945-06

53. Li W, Cama V, Akinbo FO, Ganguly S, Kiulia NM, Zhang X, et al. Multilocus sequence typing of *Enterocytozoon bieneusi*: lack of geographic segregation and existence of genetically isolated sub-populations. *Infect Genet Evol*. (2013) 14:111–9. doi: 10.1016/j.meegid.2012.11.021

54. Wang L, Zhang H, Zhao X, Zhang L, Zhang G, Guo M, et al. Zoonotic Cryptosporidium species and *Enterocytozoon bieneusi* genotypes in HIV-positive patients on antiretroviral therapy. *J Clin Microbiol*. (2013) 51:557–63. doi: 10.1128/jcm.02758-12

55. Gui BZ, Zou Y, Chen YW, Li F, Jin YC, Liu MT, et al. Novel genotypes and multilocus genotypes of *Enterocytozoon bieneusi* in two wild rat species in China: potential for zoonotic transmission. *Parasitol Res*. (2020) 119:283–90. doi: 10.1007/s00436-019-06491-8

56. Sulaiman IM, Fayer R, Yang C, Santin M, Matos O, Xiao L. Molecular characterization of *Enterocytozoon bieneusi* in cattle indicates that only some isolates have zoonotic potential. *Parasitol Res*. (2004) 92:328–34. doi: 10.1007/s00436-003-1049-5

57. Chen L, Li N, Guo Y, Zhao J, Feng Y, Xiao L. Multilocus sequence typing of *Enterocytozoon bieneusi* in crab-eating macaques (*Macaca fascicularis*) in Hainan, China. *Parasit Vectors*. (2020) 13:182. doi: 10.1186/s13071-020-04046-w

58. Karim MR, Dong H, Yu F, Jian F, Zhang L, Wang R, et al. Genetic diversity in *Enterocytozoon bieneusi* isolates from dogs and cats in China: host specificity and public health implications. *J Clin Microbiol*. (2014b) 52:3297–302. doi: 10.1128/jcm.01352-14

59. Zhou K, Liu M, Wu Y, Zhang R, Wang R, Xu H, et al. *Enterocytozoon bieneusi* in patients with diarrhea and in animals in the northeastern Chinese city of Yichun: genotyping and assessment of potential zoonotic transmission. *Parasite*. (2022) 29:40. doi: 10.1051/parasite/2022041

60. Li S, Wang P, Zhu XQ, Zou Y, Chen XQ. Prevalence and genotypes/subtypes of *Enterocytozoon bieneusi* and *Blastocystis* sp. in different breeds of cattle in Jiangxi Province, southeastern China. *Infect Genet Evol*. (2022) 98:105216. doi: 10.1016/j.meegid.2022.105216

frontiers | Frontiers in Veterinary Science

TYPE Original Research
PUBLISHED 08 October 2024
DOI 10.3389/fvets.2024.1443267

Check for updates

OPEN ACCESS

EDITED BY
Hussam Askar,
Al Azhar University, Egypt

REVIEWED BY
Ahmed El-Shamy,
California Northstate University, United States
Shahbaz Ul Haq,
Shantou University, China
Hafeez Faridi,
Chicago State University, United States

*CORRESPONDENCE
Asmaa M. El-kady
✉ asmaa.elkady@med.svu.edu.eg
Majed H. Wakid
✉ mwakid@kau.edu.sa
Hatem A. Elshabrawy
✉ hatem.elshabrawy@shsu.edu

RECEIVED 03 June 2024
ACCEPTED 23 September 2024
PUBLISHED 08 October 2024

CITATION
El-kady AM, Altwaim SA, Wakid MH, Banjar AS, Mohammed K, Alfaifi MS, Elshazly H, Al-Megrin WAI, Alshehri EA, Sayed E and Elshabrawy HA (2024) Prior *Trichinella spiralis* infection protects against *Schistosoma mansoni* induced hepatic fibrosis. *Front. Vet. Sci.* 11:1443267. doi: 10.3389/fvets.2024.1443267

COPYRIGHT
© 2024 El-kady, Altwaim, Wakid, Banjar, Mohammed, Alfaifi, Elshazly, Al-Megrin, Alshehri, Sayed and Elshabrawy. This is an open-access article distributed under the terms of the Creative Commons Attribution License (CC BY). The use, distribution or reproduction in other forums is permitted, provided the original author(s) and the copyright owner(s) are credited and that the original publication in this journal is cited, in accordance with accepted academic practice. No use, distribution or reproduction is permitted which does not comply with these terms.

Prior *Trichinella spiralis* infection protects against *Schistosoma mansoni* induced hepatic fibrosis

Asmaa M. El-kady[1]*, Sarah A. Altwaim[2,3], Majed H. Wakid[3,4]*, Alaa S. Banjar[4,5], Khalil Mohammed[6], Mashael S. Alfaifi[6], Hayam Elshazly[7,8], Wafa Abdullah I. Al-Megrin[9], Eman Abdullah Alshehri[10], Eman Sayed[11] and Hatem A. Elshabrawy[12]*

[1]Department of Medical Parasitology, Faculty of Medicine, South Valley University, Qena, Egypt, [2]Department of Clinical Microbiology and Immunology, Faculty of Medicine, King Abdulaziz University, Jeddah, Saudi Arabia, [3]Special Infectious Agents Unit, King Fahd Medical Research Center, Jeddah, Saudi Arabia, [4]Department of Medical Laboratory Sciences, Faculty of Applied Medical Sciences, King Abdulaziz University, Jeddah, Saudi Arabia, [5]Center of Innovation in Personalized Medicine (CIPM), King Abdulaziz University, Jeddah, Saudi Arabia, [6]Department of Epidemiology and Medical Statistics, Faculty of Public Health and Health Informatics, Umm Al-Qura University, Mecca, Saudi Arabia, [7]Department of Biology, Faculty of Sciences-Scientific Departments, Qassim University, Buraidah, Qassim, Saudi Arabia, [8]Department of Zoology, Faculty of Science, Beni-Suef University, Beni Suef, Egypt, [9]Department of Biology, College of Science, Princess Nourah bint Abdulrahman University, Riyadh, Saudi Arabia, [10]Department of Zoology, College of Science, King Saud University, Riyadh, Saudi Arabia, [11]Department of Parasitology, Faculty of Veterinary Medicine, South Valley University, Qena, Egypt, [12]Department of Molecular and Cellular Biology, College of Osteopathic Medicine, Sam Houston State University, Conroe, TX, United States

Background: Schistosomiasis affects approximately 250 million people worldwide, with 200,000 deaths annually. It has been documented that the granulomatous response to *Schistosoma mansoni* (*S. mansoni*) oviposition is the root cause of progressive liver fibrosis in chronic infection, in 20% of the patients, and can lead to liver cirrhosis and/or liver cancer. The influence of helminths coinfection on schistosomiasis-induced liver pathological alterations remains poorly understood. Therefore, in this study, we investigated the effect of *Trichinella spiralis* (*T. spiralis*) infection on *S. mansoni*-induced hepatic fibrosis.

Materials and methods: Thirty adult male Balb-c mice were divided into three groups. Group 1 was left uninfected; group 2 was infected with *S. mansoni* cercariae and group 3 was orally infected with *T. spiralis* larvae, then 28 days later, this group was infected with *S. mansoni* cercariae. All groups were sacrificed at the end of the 8th week post infection with *S. mansoni to evaluate* the effect of pre-infection with *T. spiralis* on *S. mansoni* induced liver fibrosis was evaluated parasitologically (worm burden and egg count in tissues), biochemically (levels of alanine aminotransferase and aspartate aminotransferase), histopathologically (H&E and MT staining, and immunohistochemical staining for the expression of α-SMA, IL-6, IL-1β, IL-17, IL-23, TNF-α, and TGF-β).

Results: The results in the present study demonstrated marked protective effect of *T. spiralis* against *S. mansoni* induced liver pathology. We demonstrated that pre-infection with *T. spirais* caused marked reduction in the number of *S. mansoni* adult worms (3.17 ± 0.98 vs. 18 ± 2.16, $P = 0.114$) and egg count in both the intestine (207.2 ± 64.3 vs. 8,619.43 ± 727.52, $P = 0.009$) and liver tissues (279 ± 87.2 vs. 7,916.86 ± 771.34; $P = 0.014$). Consistently, we found significant reductions in both number (3.4 ± 1.1 vs. 11.8.3 ± 1.22; $P = 0.007$) and size (84 ± 11 vs. 294.3 ± 16.22; $P = 0.001$) of the hepatic granulomas in mice pre-infected with *T. spiralis* larvae compared to those infected with only *S. mansoni*. Furthermore, pre- infection with *T. spiralis* markedly reduced *S. mansoni*-

induced hepatic fibrosis, as evidenced by decreased collagen deposition, low expression of α-SMA, and significantly reduced levels of IL-17, IL-1B, IL-6, TGF-B, IL-23, and TNF-α compared to mice infected with *S. mansoni* only.

Conclusions: Our data show that pre-infection with *T. spiralis* effectively protected mice from severe schistosomiasis and liver fibrosis. We believe that our findings support the potential utility of helminths for the preventing and ameliorating severe pathological alterations induced by schistosomiasis.

KEYWORDS

***Schistosoma mansoni*, *Trichinella spiralis*, murine model, hepatic fibrosis, fibrosis markers**

1 Introduction

Although helminths are responsible for causing many diseases in animals and humans (1, 2), it has been noted that the lowest frequency of autoimmune and allergic illnesses is correlated with the highest density of helminth infections (3). The "hygiene hypothesis," which was developed in response to this observation, contends that helminth infections can both prevent and shield against the development of aberrant adaptive immune responses to normally non-immunogenic foreign or self-antigens, and that living in an exceptionally clean environment predisposes humans to such conditions (4–8). Supporting data from animal models of inflammatory bowel illness (9) and experimental allergic encephalomyelitis (10, 11), type 1 diabetes (9, 12, 13), experimental asthma (14), and Graves' thyroiditis (15), has significantly supported this theory. Coinfections with helminths, predictably attenuate proinflammatory responses against other pathogens, typically leading to decreased immunopathology overall, though occasionally at the expense of decreased protection (16–22). The ability of helminths to reduce inflammation through the induction of anti-inflammatory Th2-type cells, T-regulatory cells (Treg), and alternatively activated macrophages (AAM) has been linked to the ameliorating effect of these organisms on disease susceptibility or magnitude (23).

Chronic schistosomiasis is considered one of the most serious helminth diseases known to humanity especially in tropical and subtropical regions (24–28). Approximately 250 million people are affected worldwide, with more than 200,000 deaths annually (29). Schistosomiasis causes more than 1.8 million disability-adjusted life years (DALYs) (30, 31). It is estimated that at least 220 million people need preventive treatment (31–33). The granulomatous response to *Schistosoma* oviposition and subsequent progressive liver fibrosis in chronic infection are the main pathological lesions of intestinal schistosomiasis (34). Liver fibrosis results from massive deposition of extracellular matrix in the periportal space, leading to portal vein occlusion and a number of complications such as portal hypertension, splenomegaly, portacaval shunt, gastrointestinal disorders, and varicose veins (35). Previous reports indicated that approximately 20% of schistosomiasis patients develop liver fibrosis (36), which may be a risk factor for liver cirrhosis and/or liver cancer with high mortality (37).

Keeping in view the recent developments in vaccine designing and nano-medicine to curb the prevalence of helminthic infestation (38, 39), there is need to put more efforts to design control and treatment strategies against schistosomiasis. Previous studies have investigated the effect of pre-infection with some parasites on *S. mansoni*-induced liver pathology with different outcomes. Regarding co-infection of *Schistosoma* and protozoan parasites, the researchers demonstrated that mice pre-infected with either *T. gondii* or *T. brucei* before *S. mansoni* infection were protected against *S. mansoni* induced liver pathology (40, 41). On the other hand, pre-infection of *S. mansoni* infected mice with helminth parasites showed varying outcomes. *E. caproni* had no protective effect on *S. mansoni* induced liver pathology (42). However, pre-infection with *H. polygyrus* alleviated the schistosome egg-induced hepatic immunopathology (43).

Trichinosis or trichinellosis is a zoonotic parasitic disease of humans and more than 150 animal species transmitted through the consumption of raw or undercooked pork (28, 44, 45). *T. spiralis* is unique among helminths in that adultworms and larvae live in two different habitats within the same host, namely the small intestine and skeletal muscle, respectively (46–48). Therefore, *T. spiralis* is best considered as an intestinal and tissue parasite. In the intestinal phase, the initial T cell response is Th1 that quickly switches to a strong Th2 response, which is also effective against the skeletal muscle infection (49). This parasite has evolved to suppress the host immune response against itself in order to survive (50), but it also suppresses immune responses to autoantigens and allergens (51, 52) and prevents or attenuates malignant cell development and expansion (53). Many aspects of the inhibitory effect of *T. spiralis* on cancer have been investigated both in animals and *in vitro*. Authors reported the antitumor effects of *T. spiralis* lung cancer, colorectal carcinoma, glioma, esophageal carcinoma and mouse ascitic hepatoma (44, 54, 55). *T. spiralis* had shown a good immunomodulatory effects in autoimmune diseases using either crude muscle larval antigens, excretory products, or infection (13, 56–60). In the case of allergic diseases, the use of ESPs from *T. spiralis* has also shown promising results in animal models of allergic asthma, a chronic inflammatory respiratory disorder (61, 62).

Although it should be borne in mind that *T. spiralis* infection could be followed by adverse effects like downregulation of T cell responses to viral infection, causing its exacerbation (63), it is important to emphasize that Th2 type of immune response induced by helminths may also mitigate tissue damage by reducing harmful inflammation and enhancing tissue repair (64). We believe that understanding the impact of helminth infections on the development of schistosomiasis and the progression of

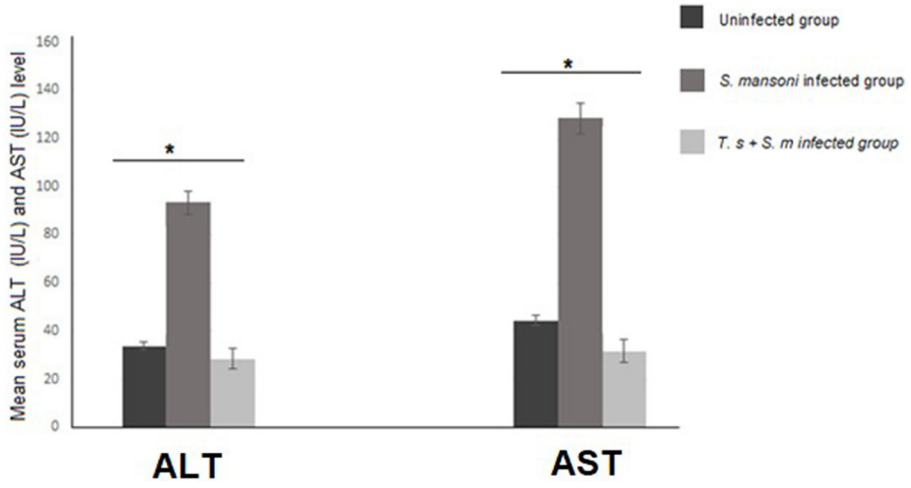

FIGURE 1
ALT and AST serum levels in mice infected with *S. mansoni* compared to uninfected mice and mice that were pre-infected with *T. spiralis*. Values represent mean percentage ± SD, and data were analyzed using ANOVA with Tukey corrections as a *post hoc* test. Asterisks [*] indicate significant difference; $P = 0.007$ for ALT and $P = 0.004$ for AST.

fibrosis could help identify novel therapeutic approaches for schistosomiasis. To the best of our knowledge, there are no studies on the coinfections of *S. mansoni* and *Trichinella spiralis* [*T. spiralis*]. In the present study, we aimed to assess whether the immune response associating *T. spiralis* infection is protective against *S. mansoni* induced liver pathology or not. In our study, using a mouse model, we show that pre-infection with *T. spiralis* mitigated the formation of *S. mansoni* egg granulomas—in comparison to mice infected with *S. mansoni* only- with subsequent alleviation of liver fibrosis.

2 Materials and methods

2.1 Animal experiment

Thirty adult male Balb-c mice, each weighing 18–20 g, were obtained from the Schistosome Biological Supply Program at Theodor Bilharz Research Institute, Imbaba, Giza, Egypt. For *S. mansoni* infection, 20 shedding adult B. alexandrina snails (4–6 mm in diameter) were obtained from the Schistosome Biological Supply Centre, Theodor Bilharz Research Institute, Cairo, Egypt. Snails were allowed to shed under light and the fresh exiting cercariae were used to infect the mice. Briefly, the infected snails were kept in a test tube containing distilled water and then exposed to artificial light at 28°C ± 1 for 2 h to induce shedding of cercariae. The number of cercariae was determined by using a dissecting microscope. Generally; three counts were made and the average was used to calculate the number of cercariae per 0.1 ml of the cercarial suspension. For *T. spiralis* infection, *T. spiralis*-infected BALB/c mice were acquired from the Assiut University's Faculty of Medicine in Assiut, Egypt. As previously mentioned, larvae were extracted from the affected muscles (65). To summarize, the infected muscles were subjected to a 12-h mechanical stirrer immersion in a 1,000 ml saline solution containing 20 mL of HCl and 20 g of pepsin at 37°C. The suspension was centrifuged for 2 min at 1,000 rpm in order to liberate the larvae. The material was centrifuged again after being washed with saline (0.9% NaCl). Hemocytometers were used to count the larvae in order to calculate the size of the inoculum needed to infect mice. For use in the animal trials, the sediment containing the larvae was re-suspended in saline containing 1.5% gelatin.

The mice were divided into three groups, each of 10 mice. Group I mice were kept uninfected, whereas group 2 mice was infected with approximately 60 ± 10 *S. mansoni* cercariae by the paddling method, where mice were immobilized without anesthetics and the tail was exposed and immersed in water containing *S. mansoni* cercaria for 45 min (66). Mice in group 3 were orally infected with *T. spiralis* larvae (300 larvae/mouse) then infected with approximately 60 ± 10 *S. mansoni* cercariae by the paddling method at 28th day post *Trichinella* infection (67). All mice were anesthetized with isoflurane by the inhalation route and euthanized by cervical dislocation at the end of 8th week post infection with *S. mansoni*.

2.2 Parasitological studies

2.2.1 Determination of *S. mansoni* worm burden

Sacrificed mice were subjected to hepato-portomesenteric perfusion technique to collect adult *S. mansoni* worms, detect sex [male/female/copula], determine worm burden, and then calculate the percentage of reduction of total worms, as described previously (68). Briefly, adult worms from each mouse were recovered in a Petri dish. Males and females were differentiated using a dissecting microscope on basis of the size and color of the parasites in addition to the presence of gynaecophoric canal and tubercles, which are characteristics absent in the female. Male adult worms are clear and female adult worms are longer and darker. Then, males and females recovered from each mouse and each group were counted for calculation of the mean number for male/female/copula in each group.

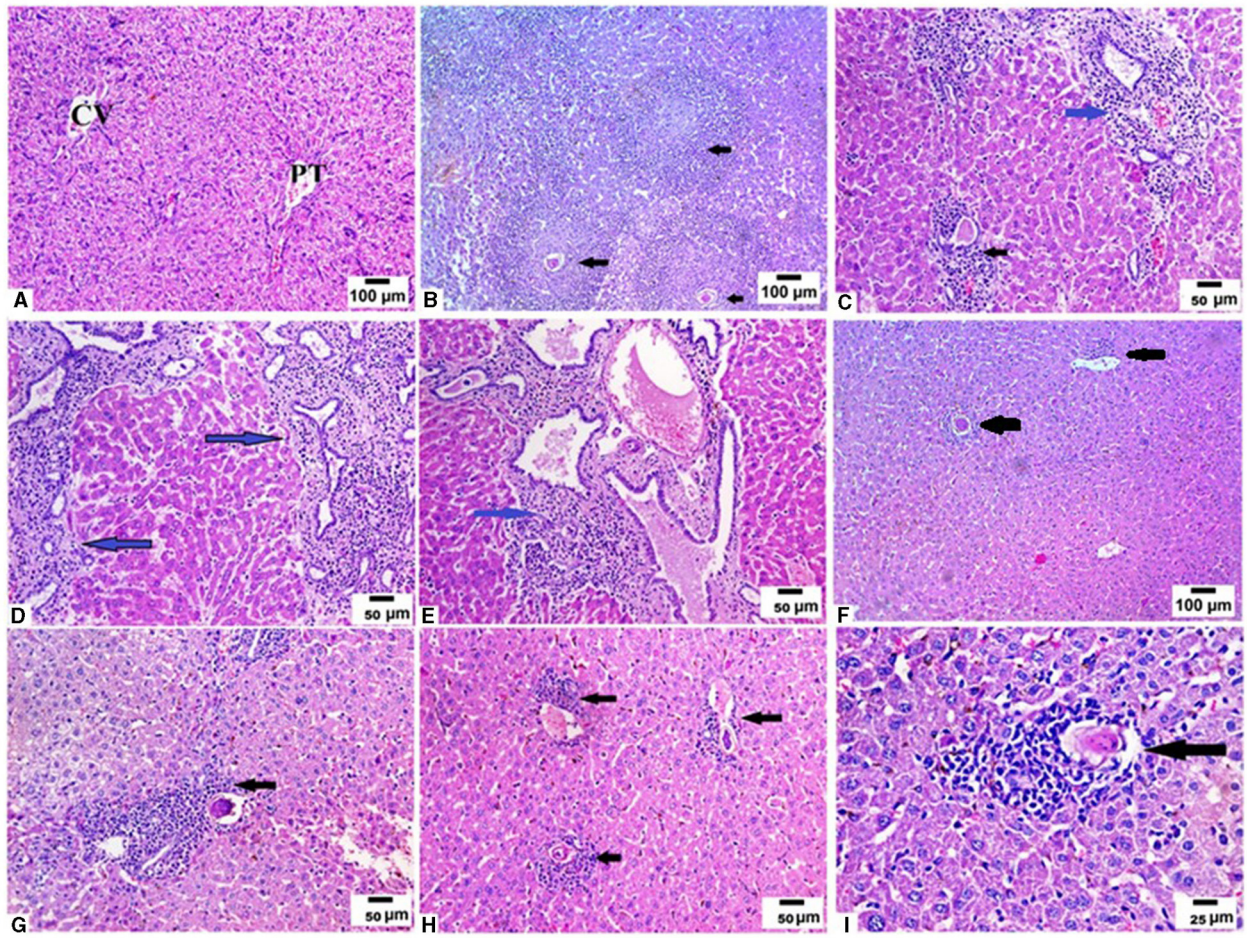

FIGURE 2
Pre-infection with *T. spiralis* reduced the size and number of granulomas in *S. mansoni* infected mice. Liver sections of different animal groups were stained with H&E stain. **(A)** Representative photomicrograph of liver sections of uninfected mice showing preserved hepatic lobular architecture with small portal tracts (PT), central veins (CV), and intact hepatocytes (200x). **(B)** Representative photomicrograph of liver sections of mice infected only with *S. mansoni* showing severe granulomatous inflammation around *S. mansoni* egg (black arrow) (100x). **(C–E)** Representative photomicrographs of liver sections of mice infected only with *S. mansoni* showing thickened portal tracts with mononuclear cellular infiltration (blue arrows) severe granulomatous inflammation around *S. mansoni* egg (black arrow) (200x). **(F)** Representative photomicrographs of liver sections of mice pre-infected with *T. spiralis* followed by *S. mansoni* showing markedly reduced granuloma size (black arrows) (100x). **(G, H)** Representative photomicrographs of liver sections of mice pre-infected with *T. spiralis* followed by *S. mansoni* showing cellular egg granulomas (black arrows) with intact central ova with markedly reduced granuloma size (200x). **(I)** Representative photomicrograph of liver sections of mice pre-infected with *T. spiralis* followed by *S. mansoni* showing mild granulomatous inflammation around *S. mansoni* egg (black arrow) (400x).

2.2.2 Determination of egg count in tissues

Small pieces of hepatic and intestinal tissue were weighted, digested overnight in 5 ml of 5% KOH solution, and three samples (each 50 µl) of the digested tissue were examined microscopically to determine the mean of *S. mansoni* egg count (69). Number of eggs/gram tissue, and the percentage reduction in total eggs/gram tissue were calculated according to Kloetzel (70).

2.3 Biochemical measurements

Blood was obtained by cardiac puncture and was centrifuged at 600 xg for 10 min to obtain the serum. The levels of alanine aminotransferase (ALT) and aspartate aminotransferase (AST) enzymes in mice sera were measured by Hitachi 7080 Chemistry Analyzer (Hitachi Ltd., Tokyo, Japan) using commercial kits from Randox Laboratories Ltd. (Crumlin, Northern Ireland).

2.4 Histopathological studies

2.4.1 Hematoxylin and eosin staining and Masson's trichrome staining

Liver tissue specimens were obtained from all groups of mice and immediately fixed in 10% buffered formalin for 24 h and then dehydrated in increasing concentrations of ethanol and processed for paraffin sectioning. Sections of 4 µm thick were deparaffinized, rehydrated in decreasing concentrations of alcohol, and stained with hematoxylin and eosin (H&E). The H&E staining protocol starting with staining with Harris hematoxylin solution followed by counterstaining with Alcoholic-Eosin solution

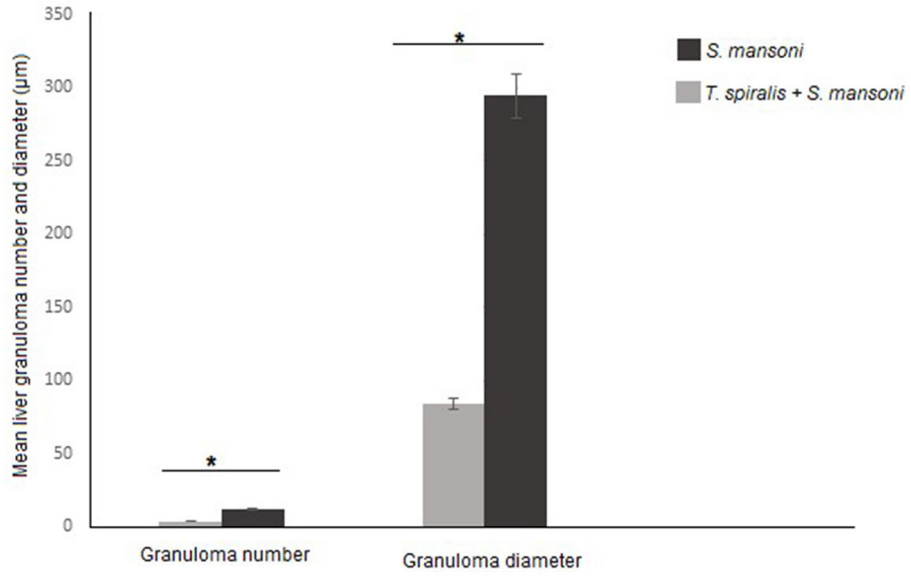

FIGURE 3
Granulomas number and size in livers of mice that were pre-infected with *T. spiralis* followed by *S. mansoni* infection compared to *S. mansoni* monoinfection. Asterisks (*) indicate a statistically significant reduction in the number ($P = 0.014$) and diameter of granulomas ($P = 0.014$).

was strictly followed. Slides were then dehydrated, cleared in Xylene and then mounted and cover slipped. H&E-stained sections were examined for granuloma formation and the associated histopathological changes. The number and sizes of the granulomas in different groups were determined. Mean granuloma number was determined in 10 successive fields of five slides from each mouse, and was accordingly determined in each group (71). Similarly, mean granuloma size in each mouse was calculated by measuring their diameters under the light microscope, equipped with an ocular micrometer. Only granuloma surrounding eggs were measured. The mean diameter was calculated from 10 granuloma, and the mean granuloma size was calculated for each group (71).

For Masson's trichrome (MT), outline steps, such as fixation, grossing, processing, embedding, and sectioning, were performed before MT staining. After deparaffinization and rehydration, the sections were re-fixed in Bouin's solution for 1 h at 56°C to enhance the staining quality. The MT stain procedure includes staining with Weigert's iron hematoxylin, Biebrich scarlet-acid fuchsin, and aniline blue solutions, followed by dehydration in alcohol grades. Then slides were mounted and cover slipped and examined for histopathological evaluation and image analysis.

Using MT staining, paraffin-embedded liver tissue sections were used according to Kiernan (72), to show the density of fibrosis in granulomas. The mean fibrosis area percent in 10 microscopic fields of each specimen was calculated and then the mean percent fibrosis/group was determined and compared between groups.

2.4.2 Immunohistochemical staining

Sections at 4 µm thickness were taken from the previously prepared paraffin-embedded tissue blocks and mounted on glass slides. Sections were then deparaffinized, rehydrated with decreasing concentrations of alcohol, then rinsed with distilled water. Endogenous peroxidase activity was blocked using 0.6% hydrogen peroxide for 10 min. For epitope retrieval, sections were microwaved in citrate buffer (pH 6) for 12 min. Sections were then incubated with anti-α-smooth muscle actin () antibody (α-SMA, ABclonal, catalog no A7248, dilution: 1: 50), interleukin 1 beta (IL 1β, ABclonal, catalog no A16640, dilution: 1: 50), interleukin 6 (IL-6, ABclonal, catalog no A0286, dilution: 1: 50), interleukin 23 (IL-23, ABclonal, catalog no A1613, dilution: 1: 50), tumor necrosis factor-α (TNF-α, ABclonal, catalog no A11534, dilution: 1: 50), transforming growth factor- β (TGF-β, ABclonal, catalog no A16640, dilution: 1: 50), and interleukin 17 (IL-17, ABclonal, catalog no A12454, dilution: 1: 50) for 1 h at room temperature. Sections were washed with TBS containing 0.05% Tween-20 (TBS-T) and were then incubated with HRP-conjugated goat anti-rabbit secondary antibodies (Vivantis Technologies, Malaysia) at a dilution of 1:5,000 for 1 h at 4°C. After washing in TBS-T, the color was developed by incubating sections with 0.05% diaminobenzidine (DAB) and 0.01% H_2O_2 for 3 min. Counterstaining was performed with hematoxylin for 30 seconds, and sections were then examined by light microscopy. Negative controls were obtained by omitting the primary antibody.

Hepatocytes with cytoplasmic reaction to the antibodies were considered positive. Semi-quantitative analysis of positively stained tissue sections was performed through modified Allred scoring system guidelines. The percentage of positive cells was estimated in 3 different fields (200x) and the mean percentage (±SD)/group was calculated. Individual scores of the percentage of positive cells (0–5) and the intensity of cytoplasmic staining (0–3) were summed up to obtain the final scores. The scoring of percentage of positive cells was set as follows: 1: <10% positive cells; 2: 10%−20% positive cells; 3: 20%−50% positive cells; 4: 50%−70% positive cells; and 5: more than 70% positive cells. The scoring of staining intensity was determined as follows: 1: weak; 2: moderate; and 3: strong.

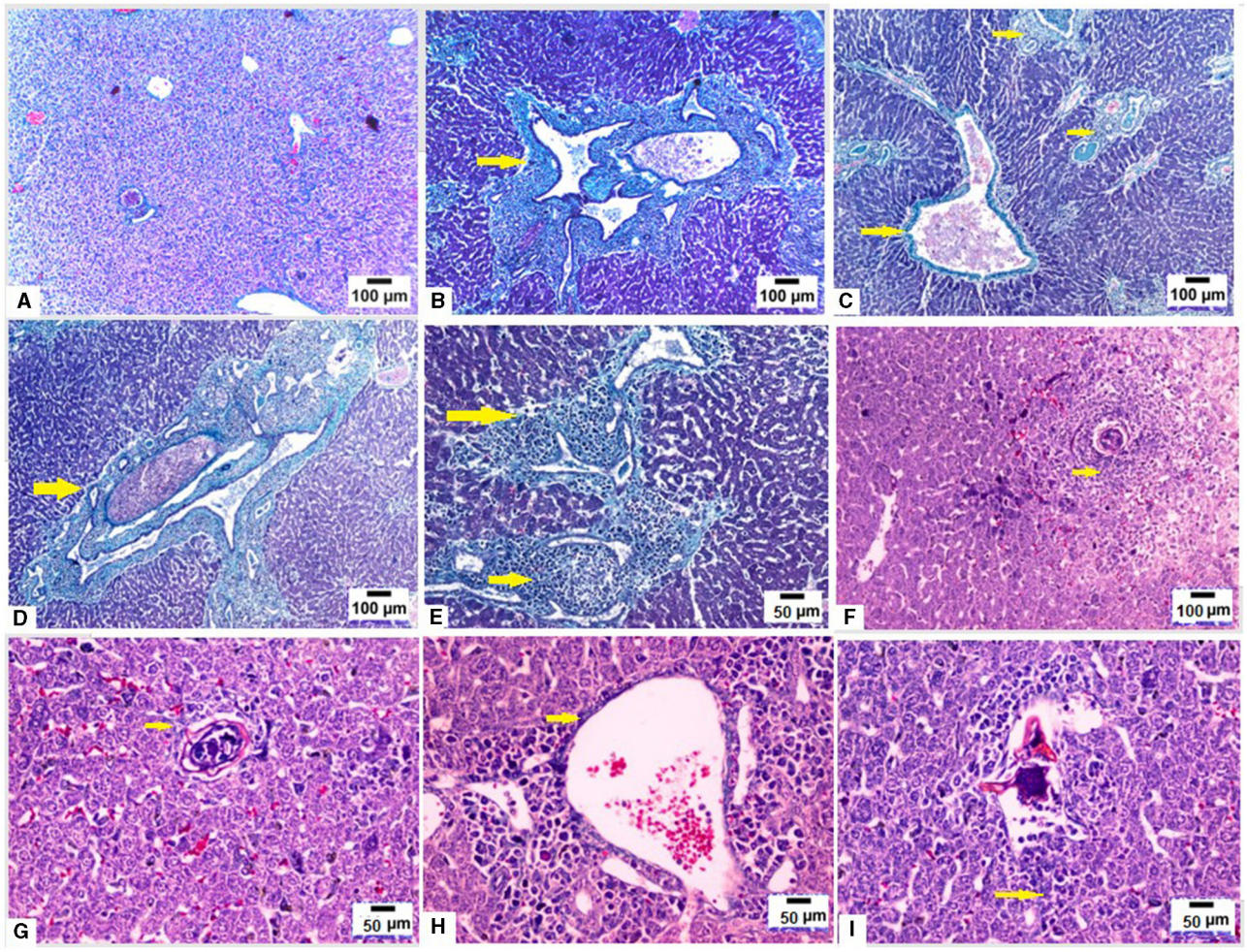

FIGURE 4
Pre-infection with *T. spiralis* reduced hepatic fibrosis due to *S. mansoni* infected mice. Liver sections of different animal groups were stained with Masson's trichrome stain. **(A)** Representative photomicrograph of liver sections of uninfected mice showing no fibrosis (100x). **(B–D)** Representative photomicrographs of liver sections of mice infected only with *S. mansoni* showing marked expansion of portal tracts by fibrous tissue and mononuclear inflammatory cells (yellow arrows) (100x). **(E)** Representative photomicrograph of liver sections of mice infected only with *S. mansoni* showing extensive deposition of fibrous tissue (200x). **(F)** Representative photomicrograph of liver sections of mice pre-infected with *T. spiralis* followed by *S. mansoni* showing cellular granuloma with no evidence of fibrosis (100x). **(G)** Representative photomicrograph of liver sections of mice pre-infected with *T. spiralis* followed by *S. mansoni* showing cellular granuloma with minimal fibrosis (yellow arrows) (200X). **(H, I)** Representative photomicrographs of liver sections of mice pre-infected with *T. spiralis* followed by *S. mansoni* showing minimal delicate fibrosis (yellow arrows) (200x).

2.5 Statistical analysis

The Statistical Package for Social Sciences (SPSS) version 20 for Windows was used to analyze the acquired data. All parameters were shown as mean ± standard deviation (SD). ANOVA (analysis of variance) and Independent sample *T* test were used for statistical comparison between the groups. A *p*-value of < 0.05 was regarded as statistically noteworthy.

3 Results

3.1 Pre- infection with *T. spiralis* reduced adult *S. mansoni* worm count as well as intestinal and hepatic egg burden

Worm burden of *S. mansoni* was determined at the end of the 8th week post *S. mansoni* infection. Mice pre-infected with *T. spiralis* showed statistically significant reduction of the worm count in comparison to mice infected with only *S. mansoni* [R (percent of reduction) = 82.4%, $P = 0.045$ and $P = 0.002$ for males and females adults worms respectively; Supplementary Table 1].

In the same context, there was a statistically significant reduction in the count of eggs per gram of intestine and liver in mice pre-infected with *T. spiralis* compared to those infected with *S. mansoni* alone ($P = 0.009$, $P = 0.014$, $P = 0.009$ for intestinal, liver and total egg count respectively; Supplementary Table 2).

3.2 Pre- infection with *T. spiralis* reduced ALT and AST levels in the sera of *S. mansoni*-infected mice

Next, we measured the levels of serum ALT and AST as markers for liver function. We found that serum ALT and AST levels were

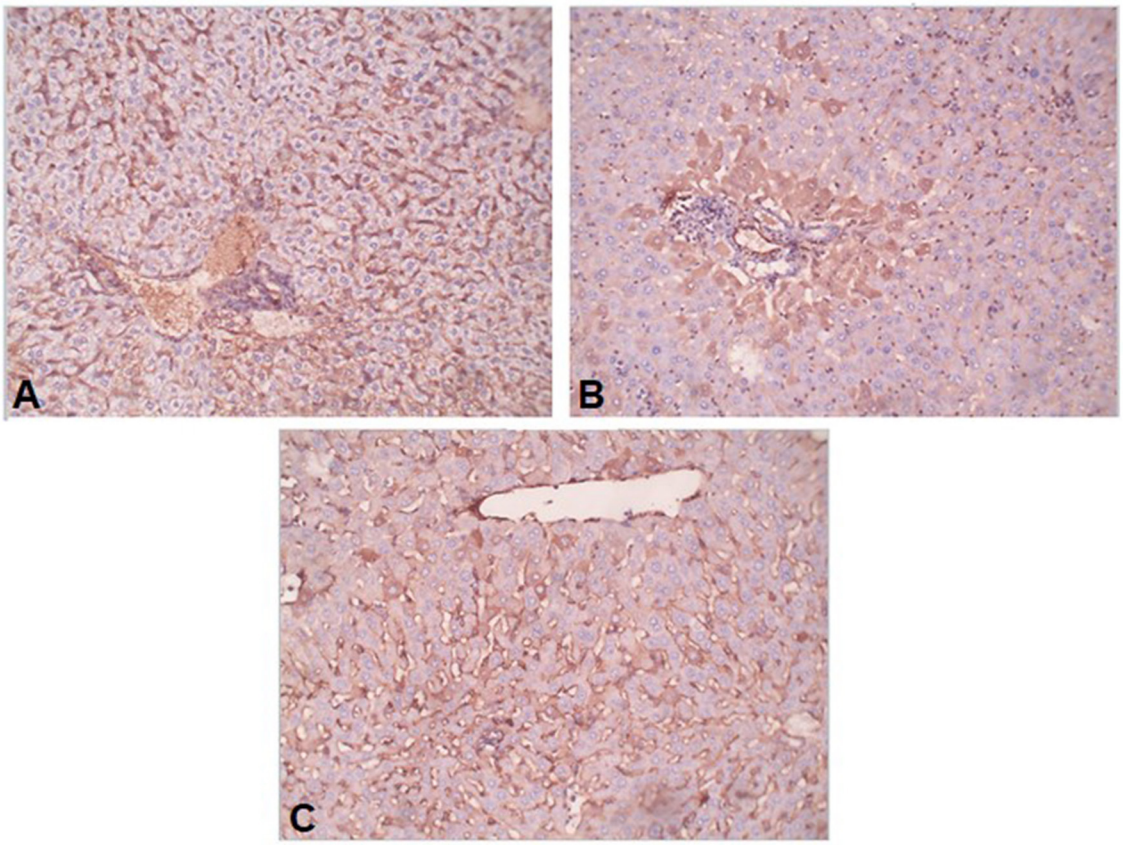

FIGURE 5
Preinfection with *T. spiralis* alleviated the liver fibrosis in *S. mansoni*-infected mice. Representative photomicrographs of liver sections stained for α-SMA: **(A)** Uninfected mice liver section showing weak reaction in sinusoids only, **(B)** *S. mansoni*-infected mice liver section showing focal strong expression of α-SMA in peri-portal hepatocytes, and **(C)** Liver section of mice pre-infected with *T. spiralis* followed by *S. mansoni* infection showing no expression of α-SMA in hepatocytes. Magnification is 200x.

higher in the *S. mansoni*-infected mice than in mice that were pre-infected with *T. spiralis* (with statistical significance $P = 0.007$ and 0.004 for AST and respectively, Figure 1).

3.3 Pre-infection with *T. spiralis* reduced the number and diameter of granulomas in *S. mansoni*-infected mice

We examined the livers extracted from all animal groups using H&E staining. Liver sections of uninfected mice showed normal hepatocytic architecture with no inflammatory cells in between or surrounding the central vein, normal hepatic lobules, and bile ducts (Figure 2A). Infection with *S. mansoni* caused marked granulomatous inflammation (Figure 2B; black arrows). Hepatic granulomas were of two types: fibrocellular (75%) and cellular granulomas (25%). Cellular granulomas were made up of bilharzial ova and adult worms surrounded by lymphocytes, eosinophils, histiocytes, macrophages and plasma cells with altered liver architecture (Figures 2C–E; blue arrows). On the contrary, mice infected with *T. spiralis* prior to *S. mansoni* infection showed alleviation of *S. mansoni*-induced pathological alterations with marked reduction of granuloma size (Figure 2F; black arrows). All granulomas recorded in this group were of the cellular type. Granulomas consisted of lymphocytes, eosinophils, histiocytes, macrophages, and plasma cells surrounding bilharzial ova and adult worms with disrupted liver architecture (Figures 2G–I; black arrows). Pre-infection with *T. spiralis* significantly reduced the number of *S. mansoni* induced hepatic granulomas (mean ± SD = 11.8.3 ± 1.22 in *S. mansoni* only-infected mice vs. 3.4 ± 1.1 in mice priorly infected with *T. spiralis*) (Figure 3). Hepatic granuloma diameters were significantly reduced in mice that were pre-infected with *T. spiralis* compared to *S. mansoni* only-infected mice (mean ± SD = 294.3 ± 16.22) in *S. mansoni* only-infected mice vs. (mean ± SD = 84 ± 11) in mice pre-infected with *T. spiralis* (Figure 3).

3.4 Pre-infection with *T. spiralis* alleviated *S. mansoni* induced liver fibrosis

We used MT stain to evaluate fibrosis in hepatic tissues of mice from different groups. Liver sections from uninfected mice showed normal liver architecture and no fibrosis (Figure 4A). On the other hand, infection with *S. mansoni* resulted in large fibrocellular granulomas with central eggs, marked fibrosis and a significant amount of collagen deposition in concentric manner

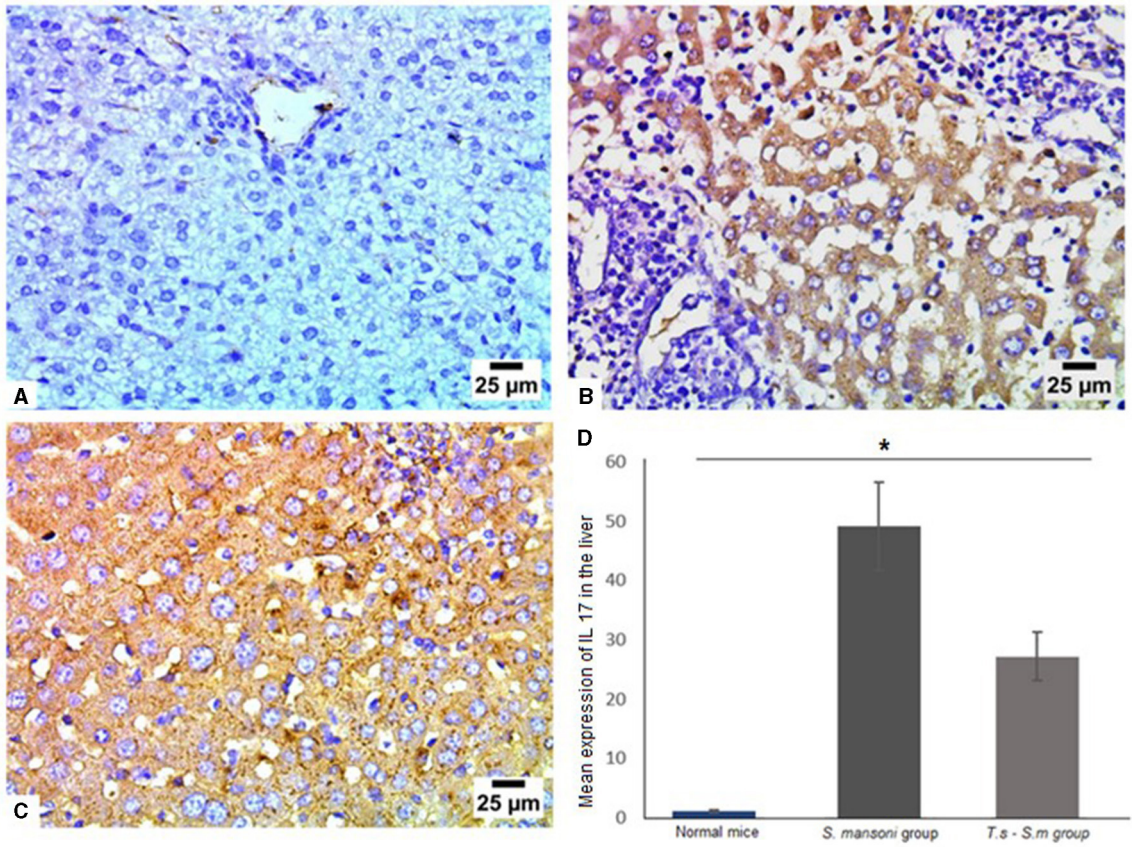

FIGURE 6
Pre-infection with *T. spiralis* reduced IL-17 expression in *S. mansoni*-infected mice. Representative photomicrographs of liver sections stained for IL-17: **(A)** Uninfected mice liver tissue showing negative expression of IL-17, **(B)** liver tissue of *S. mansoni*-infected mice showing intense expression of IL-17 and **(C)** Liver tissue of *T. spiralis*-pre-infected mice showing significant reduction of IL-17 expression. Magnification is 400x. **(D)** Quantification of IL-17 expression in different mice groups. Values represent mean percentage ± SD, and data were analyzed using ANOVA with Tukey corrections as a *post hoc* test. Asterisk (*) indicates a statistically significant difference; $P = 0.012$.

within those granulomas in addition to extensive fibrous collagen deposition between the portal vein and lobules (Figures 4B–E; yellow arrows). On the contrary, pre- infection with *T. spiralis* treatment significantly decreased collagen fiber accumulation, suggesting that *T. spiralis* infection prevented hepatic fibrosis (Figures 4F–I).

Conversion of hepatic stellate cells (HSCs) into fibroblasts is the key event in the process of liver fibrosis. The expression of α-SMA is commonly used as a hallmark of activated HSCs. In our study, the uninfected mice livers showed no expression of α-SMA or low expression that was limited to the walls of the central vein (Figure 5A). In the *S. mansoni*-infected mice, intense α-SMA immunostaining was observed in the central and portal tract areas (Figure 5B). Interestingly, pre-infection with *T. spiralis* reduced α-SMA expression compared to *S. mansoni*-infected mice (Figure 5C), indicating inhibition of HSC activation.

3.5 Pre-infection with *T. spiralis* reduced inflammation in *S. mansoni*-infected mice

Mechanisms underlying the pathology in schistosomiasis are not well-defined. Animal studies identified a moderate type 1 helper [Th1] response to parasite antigens, but a robust Th2 response to egg-derived antigens dominates and promotes fibrogenesis in the liver (73, 74). Th17 cells produce several cytokines, including IL-17, and have demonstrated profibrogenic roles in different experimental models of hepatic, pulmonary, and myocardial fibrosis (75–77). Based on the above findings, we examined the expression of various cytokines in liver tissues of all mice groups (Figures 6A–D). Mice infected with *S. mansoni* only showed high expression of IL-17 (mean percentage = 49 ± 15, Figures 6B and D). There was a marked reduction in IL-17 production in mice that were pre-infected with *T. spiralis* (Figures 6C and D, $P = 0.012$, mean percentage ± SD = 29 ± 13.5).

IL-1β is a significant mediator of tissue damage and plays an essential role in the progression of schistosomiasis (78–81). Therefore, we examined IL-1β levels in livers of mice of different groups (Figures 7A–D). Similar to IL-17, we found that IL-1β was highly expressed in *S. mansoni* only infected mice (Figures 7B and D, mean percentage ± SD = 27.5 ± 11.5). IL-1β was significantly downregulated in the livers of mice that were pre-infected with *T. spiralis* compared to *S. mansoni*-infected mice (Figures 7C and D, mean percentage ± SD = 15± 6.7, $P = 0.005$).

Furthermore, we examined the IL-6 levels in liver tissues of different mice groups since it has been reported as a major

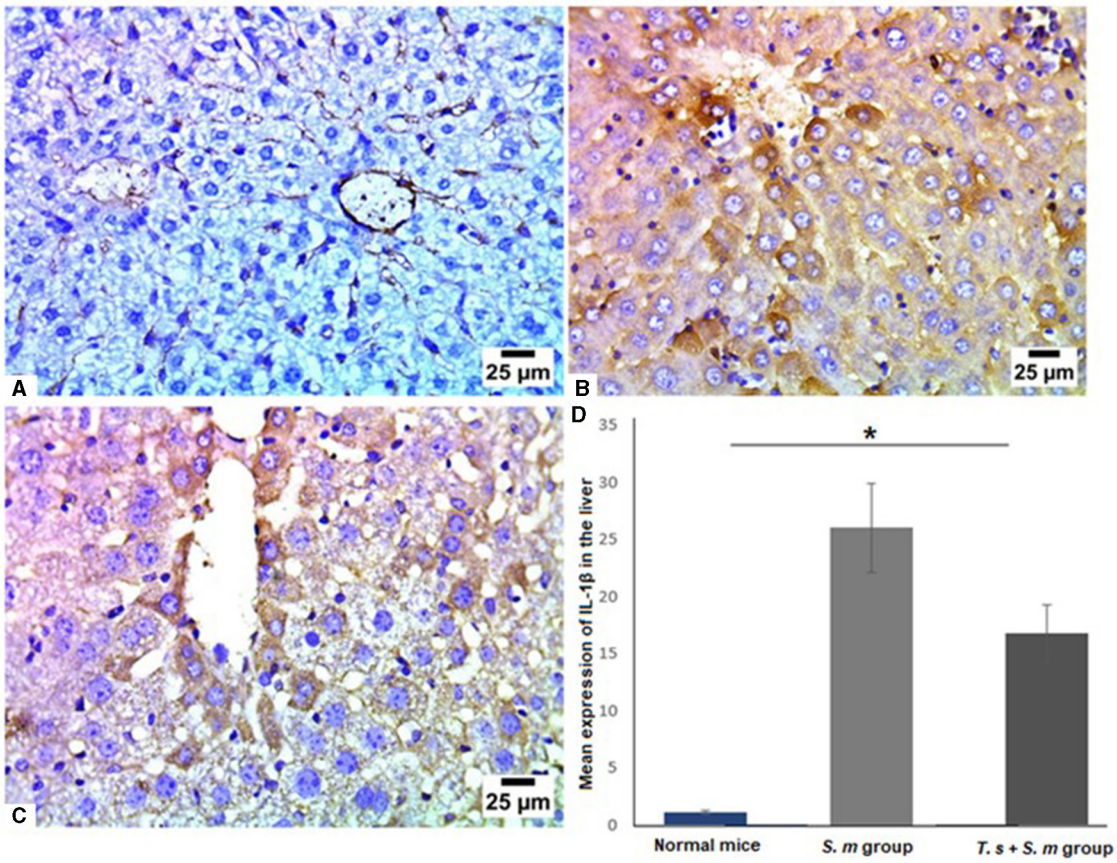

FIGURE 7
IL-1β was significantly reduced in liver tissues of *T. spiralis* pre-infected mice. Representative photomicrographs of liver sections stained for IL-1β: **(A)** Uninfected mice liver tissue showing negative expression of IL-1β, **(B)** *S. mansoni*-infected mice liver tissue showing intense expression of IL-1β and **(C)** Liver tissue of *T. spiralis*- pre-infected mice showing significant reduction of IL-1β expression. Magnification is 400x. **(D)** Quantification of IL-1β expression in different mice groups. Values represent mean percentage ± SD, and data were analyzed using ANOVA with Tukey corrections as a *post hoc* test. Asterisk (*) indicates a statistically significant difference; $P = 0.005$.

fibrogenic agent by regulating neutrophil transport, chemokine production, and leukocyte apoptosis (82–85). Our data show that liver tissues of mice that infected only with *S. mansoni* showed high expression of IL-6 (Figures 8A, B and D, mean percentage ± SD = 24.6 ± 10.3). Meanwhile, mice group which were pre-infected with *T. spiralis* had significantly lower levels of IL-6 compared to mice infected with *S. mansoni* alone (Figures 8C and D, mean percentage ± SD = 16.7 ± 3.5, $P = 0.04$).

Several studies had identified IL-23 as an important pro-inflammatory cytokine involved in inducing Th17 cell differentiation and fibrogenic response (86, 87). Like other cytokines examined in this study, our results showed *S. mansoni* infected mice showed high levels of IL-23 (Figures 9A, B and D, mean percentage ± SD = 22.9 ± 9.7), with a a significant reduction in the expression of IL-23 in *T. spiralis* pre-infected mice compared to mice infected with *S. mansoni* alone (Figures 9C and D, mean percentage ± SD = 14.9 ± 3.2, $P = 0.032$).

Next, we aimed to examine the expression of TNF-α in liver tissue of different mice groups since it is an important mediator of murine granuloma formation and hepatic fibrosis (88). In line with our findings in this study, TNF-α was markedly high in mice infected with *S. mansoni* (Figures 10A, B and D, mean percentage ± SD = 12 ± 1.5). Significant reduction in TNF-α expression in liver tissues of mice that were pre-infected with *T. spiralis* in comparison to mice infected with *S. mansoni* alone (Figures 10C and D, mean percentage ± SD = 9 ± 3.1, $P = 0.031$).

The production of TGF-β may modulate inflammation and regulate fibrogenesis in response to *S. mansoni* eggs. Several investigators indicated that TGF-β is a regulatory cytokine, that is mainly produced by regulatory T cells, which provides an effective mechanism of control of the progression of fibrosis (88, 89). Our data showed that infection of mice with *S. mansoni* increased the level of TGF-β in liver tissues compared to uninfected mice group (Figures 11A, B and D, mean percentage ± SD = 28.7 ± 7.5). However, prior *T. spiralis* infection significantly reduced the production of TGF-β (Figures 11C and D, mean percentage ± SD = 12 ± 2.5, $P = 0.041$). All our findings support the protective role of *T. spiralis* prior infection against the pathological effects of *S. mansoni* infection.

4 Discussion

In the case of infection with schistosomes, there is predictable severe disease in about 5% to 10% of the population (43). Granuloma formation and fibrosis are the major causes of

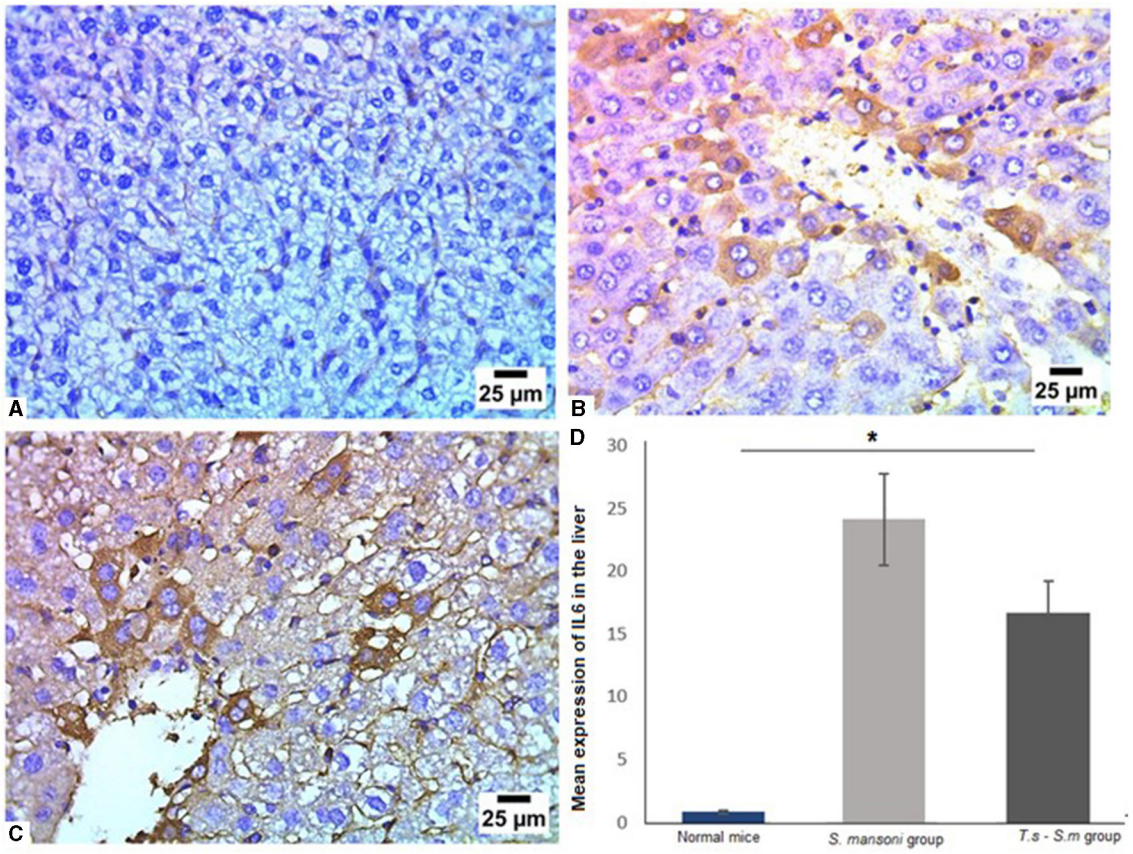

FIGURE 8
Pre-infection with *T. spiralis* significantly reduced IL-6 in liver tissues of *S. mansoni*-infected mice. Representative photomicrographs of liver sections stained for IL-6: **(A)** Uninfected mice liver tissue showing negative expression of IL-6, **(B)** Liver tissue of *S. mansoni*-infected mice showing positive expression of IL-6 and **(C)** Liver tissue of *T. spiralis*-pre-infected mice showing significant reduction of IL-6 expression. Magnification is 400x. **(D)** Quantification of IL-6 expression in different mice groups. Values represent mean percentage ± SD, and data were analyzed using ANOVA with Tukey corrections as a *post hoc* test. Asterisk (*) indicates a statistically significant difference; $P = 0.04$.

morbidity and mortality in association with schistosomiasis. This process may lead to fibrosis with excessive accumulation of collagen and other extracellular matrix proteins in the periportal space (90). The immunopathology in schistosomiasis is mediated by CD4 effector T cells (91).

In this study, we tested the hypothesis that low pathology is at least in part determined by coinfection with intestinal nematodes. Based on the observations that nematode coinfection is prevalent in areas where schistosomiasis is endemic and that nematode infection creates a host immune environment associated with attenuated incidence of CD4 T-cell-dependent autoimmune diseases (5).

Using the murine model of schistosomiasis, we show here that pre-infection with *T. spiralis* parasitic nematode caused a significant reduction in the number of recovered worms, egg count in both the intestine and liver tissues. Regarding *S. mansoni* induced liver pathology, pre-infection with *T. spiralis* caused a significant reduction of both number and size of the hepatic granulomatous inflammation caused by schistosome eggs when compared with *S. mansoni* only infected mice. Moreover, *S. mansoni* induced hepatic fibrosis was markedly reduced in mice pre-infected with *T. spiralis* as manifested with the low deposition of collagen in hepatic sections stained with MT in addition to the low expression of α-SMA antibodies.

The production of fibrosis, which are key signs of both chronic and advanced schistosomiasis, depends on different key cytokines (36). In the present study, the decrease in granulomatous reaction and subsequent fibrosis was accompanied by a marked decrease in the levels of IL-17, IL-1B, IL-6, TGF-β, IL 23, and TNF-α. These cytokines are correlated with the immunopathology of schistosomiasis and its drive (92–95). In particular, the proinflammatory function of IL-17, which induces chemokine-mediated leukocyte recruitment, has also been demonstrated in the context of other infectious and autoimmune diseases (10, 11, 96). IL-17 production is associated with a distinct subset of CD4 T cells, Th17 cells (77, 97), which are variously promoted by an array of innate immunocyte-derived cytokines, including IL-6, TGF-β, IL-23, and IL-1β (98–103).

IL-17 was defined as a main player in the process of fibrosis in different experimental models of hepatic, pulmonary, and myocardial fibrosis (75, 76). IL-17-producing cells contribute to the hepatic granulomatous inflammation and subsequent fibrosis

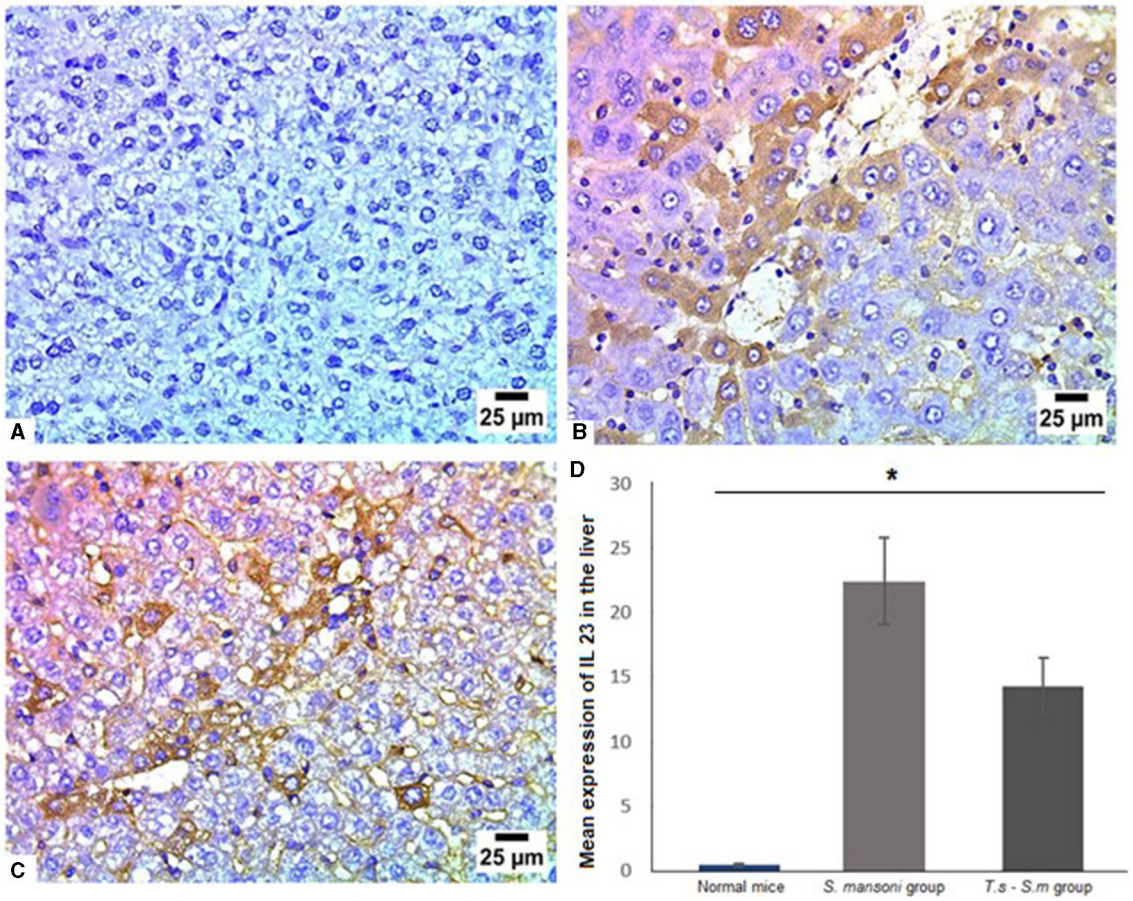

FIGURE 9
IL-23 had significantly lower levels in liver tissues of *S. mansoni*-infected mice that were pre-infected with T. spiralis. Representative photomicrographs of liver sections stained for IL-23: **(A)** Uninfected mice liver tissue showing no expression of IL-23, **(B)** Liver tissue of *S. mansoni*-infected mice showing high expression of IL-23 and **(C)** Liver tissue of *T. spiralis*-pre-infected mice showing significant reduction of IL-23 expression. Magnification is 400x. **(D)** Quantification of IL-23 expression in different mice groups. Values represent mean percentage ± SD, and data were analyzed using ANOVA with Tukey corrections as a *post hoc* test. Asterisk (*) indicates a statistically significant difference; $P = 0.032$.

in addition to the Th1, Th2, and Th17 associated cytokines (104). In the present study, IL-17 was significantly high in mice infected with *S. mansoni* and reduced in mice pre-infected with *T. spiralis*. Similar results have been obtained by previous research which observed that the level of IL-17 was increased in the injured liver compared to control animals (105–107). The increased level of IL-17 facilitates the influx of inflammatory cells, drives the expression of profibrogenic growth factors and activates hepatic stellate cells in the liver (31, 108). The liver infiltrating inflammatory cells in turn induce the production of profibrotic cytokines such as TNF-α, IL-6, IL-1, and TGF-β1 (109). On the other hand, a large body of articles stated that those cytokines involving IL-6, TGF-β, IL-23, and IL-1β are incorporated in the expression of the Th17-specific transcription factor RORγt (98, 99, 101, 110). So, we measured the level of IL-23, it was markedly high in *S. mansoni* only infected mice with significant reduction in mice pre-infected with *T. spiralis*. Our results are in consistency with other authors who reported the role of IL-23 in the immunopathology of schistosomiasis (92, 110).

Regarding IL-6, our results showed that schistosomiasis resulted in high expression of IL-6 which was significantly reduced in mice pre-infected with *T. spiralis*. In line with this result, previous studies have reported high levels of IL-6 in schistosomiasis infected subjects (111–113). Moreover, it has been postulated that the induction of Th17 cells is triggered through simultaneous stimulation with IL-6 (99, 103).

Like IL-6, TGF-β is also a necessary factor for the early differentiation of Th17 cells, and this cytokine induces the expression of the master transcription factor, Foxp3, that is needed for the differentiation of regulatory T cells. So, we examined TGF-β in mice groups. In the current study, infection of mice with *S. mansoni* caused pronounced elevations in serum TGF-β levels, which was reduced in mice pre-infected with *T. spiralis*. Similar results obtained by several studies have reported high level of TGF-β in Schistosomiasis (114, 115). This cytokine is considered a multifunctional cytokine that regulates biological processes such as inflammation, development, and differentiation of many cell types, tissue repair, and tumor genesis. It is also associated with pro-inflammatory responses and immunosuppressive activities (116) and participates in the process of Th17 cells differentiation (117). In the evolution of the granulomatous response to the *S. mansoni* eggs the production of TGF-β may modulate inflammation and

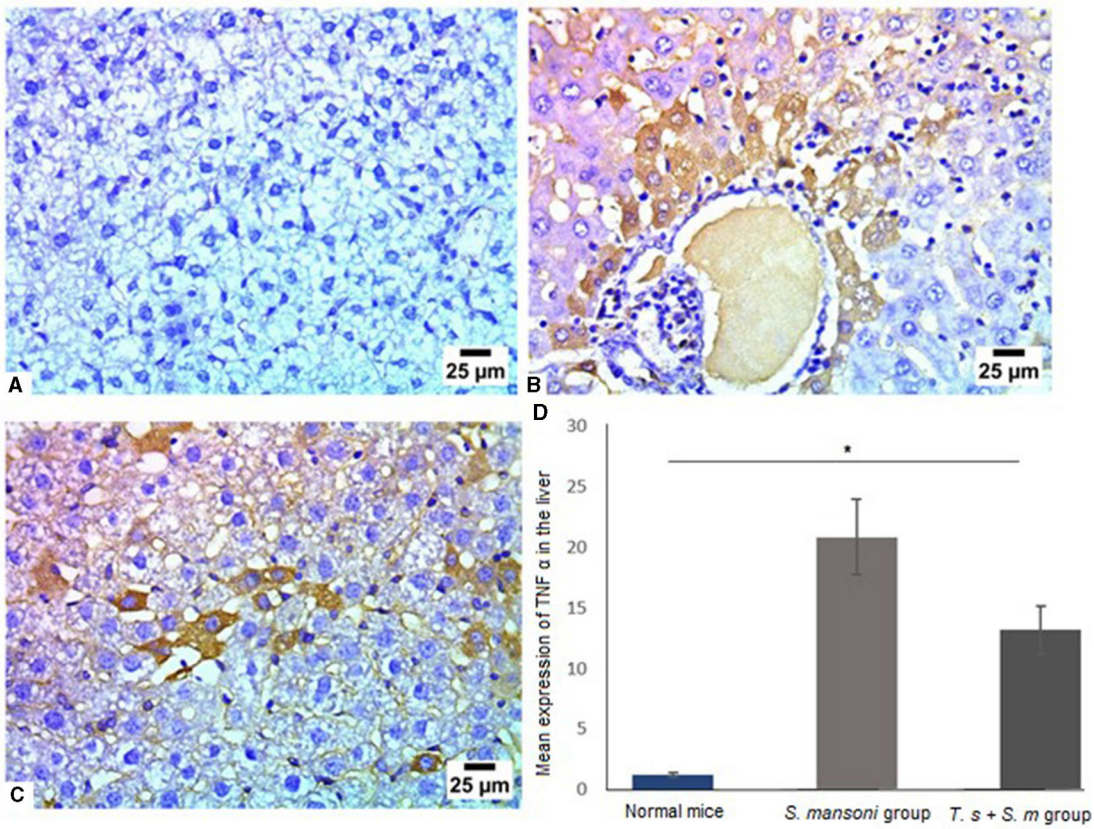

FIGURE 10
Pre-infection with *T. spiralis* significantly reduced TNF-α in liver tissues of *S. mansoni*-infected mice. Representative photomicrographs of liver sections stained for TNF-α: **(A)** Uninfected mice liver tissue showing no expression of TNF-α, **(B)** Liver tissue of *S. mansoni*-infected mice showing positive expression of TNF-α and **(C)** Liver tissue of *T. spiralis*-pre-infected mice showing mild positive expression of TNF-α. Magnification is 400x. **(D)** Quantification of TNF-α expression in different mice groups. Values represent mean percentage ± SD, and data were analyzed using ANOVA with Tukey corrections as a *post hoc* test. Asterisk (*) indicates a statistically significant difference; $P = 0.031$.

regulate fibrogenesis. Several investigators indicated that TGF-β is a regulatory cytokine that is mainly produced by regulatory T cells which provides an effective mechanism of control of the progression of fibrosis (89).

In the same text, IL-1β was reported to promote clonal expansion in an inflammatory environment (102, 118). In the present study, our results demonstrated significant reduction of IL-1β which may also be attributed to reduction of IL-6 level (118). Our results are in accordance with other studies which demonstrated that IL-1β is an important participant, along with other cytokines, and controls the progression from liver injury to fibrogenesis through activation of HSCs (119, 120).

The result of this study showed decreased level of TNF-α after it has been markedly increased due to *S. mansoni* infection in mice. In experimental models, authors attribute to the TNF-α proinflammatory and profibrogenic effects that may aggravate the disease (90). Our results confirmed previously published data that showed that cases of severe portal fibrosis were shown to be associated with high levels of TNF- α (90, 121, 122).

The ameliorating effect of nematode coinfection on the severity of schistosomiasis is similar to that exerted on a variety of autoimmune diseases (9–15, 123), thus offering a collective explanation for the lower incidence of these T-cell-mediated conditions in areas where helminths are endemic. Such an effect of nematodes with relatively little intrinsic pathogenicity appears to be beneficial for the host and is currently being explored as a therapeutic means to control inflammatory bowel disease in humans (124) and possibly other autoimmune diseases (10). On the other hand, the helminths may be detrimental under conditions in which a strong proinflammatory response is necessary to control other infectious agents (20, 125–128).

In summary, pre-exposure to intestinal nematodes effectively protected mice from severe schistosomiasis by downregulation of pathogenic Th1- and Th17-cell-mediated responses. Regardless, a concept supported by our findings is that, as a whole, natural or therapeutic helminth infections can be important elements in the prevention and amelioration of aberrant or excessive CD4 T-cell-mediated disease.

4.1 Study limitations and recommendations

Chronic schistosomiasis is a serious health concern affecting large population worldwide. The present study

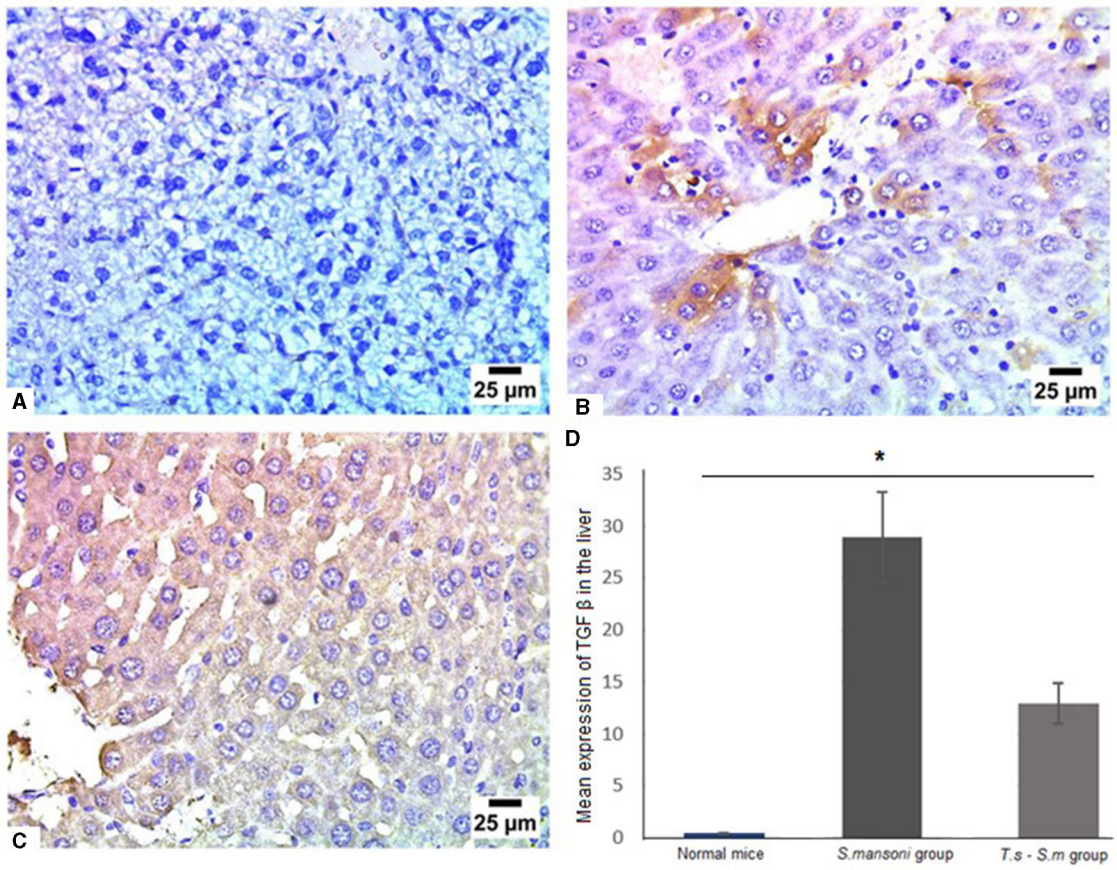

FIGURE 11
TGF-β was markedly reduced in liver tissues of *T. spiralis*-pre-infected mice. Representative photomicrographs of liver sections stained for TGF-β: **(A)** Uninfected mice liver tissue showing no expression of TGF-β, **(B)** Liver tissue of *S. mansoni*-infected mice showing moderate expression of TGF-β and **(C)** Liver tissue of *T. spiralis*-pre-infected mice showing lower expression of TGF-β. Magnification is 400x. **(D)** Quantification of TGF-β expression in different mice groups. Values represent mean percentage ± SD, and data were analyzed using ANOVA with Tukey corrections as a *post hoc* test. Asterisk (*) indicates a statistically significant difference; $P = 0.041$.

investigated the effect of co-infection with *T. spiralis* on *S. mansoni* induced liver pathology. Pre-infection with *T. spiralis* showed a promising protective effect against *S. mansoni* liver fibrosis. Further studies are needed to exactly identify the underlying molecular and immunological basis of either parasitic co-infection or parasitic antigens in the protection against chronic schistosomiasis.

Data availability statement

The original contributions presented in the study are included in the article/Supplementary material, further inquiries can be directed to the corresponding authors.

Ethics statement

All animal experiments were conducted according to the guidelines of the Declaration of Helsinki. The Faculty of Medicine's Institutional Review Board and Ethics Committee at New Valley University, Egypt, approved all animal experiments [NVREC-0232-2024-8]. The study was conducted in accordance with the local legislation and institutional requirements.

Author contributions

AE-k: Conceptualization, Data curation, Formal analysis, Funding acquisition, Investigation, Methodology, Project administration, Resources, Software, Supervision, Validation, Visualization, Writing – original draft, Writing – review & editing. SA: Writing – review & editing. MW: Writing – original draft, Writing – review & editing. AB: Writing – review & editing. KM: Writing – review & editing. MA: Writing – review & editing. HE: Writing – review & editing. WA-M: Writing – review & editing. EA: Writing – review & editing. ES: Writing – review & editing. HE: Conceptualization, Data curation, Formal analysis, Investigation, Resources, Software, Supervision, Validation, Visualization, Writing – review & editing.

Funding

The author(s) declare that financial support was received for the research, authorship, and/or publication of this article.

The authors extend their acknowledgment to Princess Nourah bint Abdulrahman University Researchers Supporting Project number (PNURSP2024R39), Princess Nourah bint Abdulrahman University, Riyadh, Saudi Arabia and Researchers Supporting Project number (RSPD2024R859), King Saud University, Riyadh, Saudi Arabia.

Conflict of interest

The authors declare that the research was conducted in the absence of any commercial or financial relationships that could be construed as a potential conflict of interest.

Publisher's note

All claims expressed in this article are solely those of the authors and do not necessarily represent those of their affiliated organizations, or those of the publisher, the editors and the reviewers. Any product that may be evaluated in this article, or claim that may be made by its manufacturer, is not guaranteed or endorsed by the publisher.

Supplementary material

The Supplementary Material for this article can be found online at: https://www.frontiersin.org/articles/10.3389/fvets.2024.1443267/full#supplementary-material

References

1. Aguilar-Marcelino L, Bautista-Garfias C, Zaheer T, Maqsood A, Salman S, Bamarni I, et al. Potential of anisakiasis in foodborne zoonosis. *Pakistan Veter J.* (2022) 42:80. doi: 10.29261/pakvetj/2022.080

2. Mahmood Q, Younus M, Sadiq S, Iqbal S, Idrees A, Khan S, et al. Prevalence and associated risk factors of cystic echinococcosis in food animals–a neglected and prevailing zoonosis. *Pak Vet J.* (2022) 42:59–64. doi: 10.29261/pakvetj/2022.008

3. Finlay CM, Stefanska AM, Walsh KP, Kelly PJ, Boon L, Lavelle EC, et al. Helminth products protect against autoimmunity via innate type 2 cytokines Il-5 and Il-33, which promote eosinophilia. *J Immunol.* (2016) 196:703–14. doi: 10.4049/jimmunol.1501820

4. Capron A, Dombrowicz D, Capron M. Helminth infections and allergic diseases: from the th2 paradigm to regulatory networks. *Clin Rev Allergy Immunol.* (2004) 26:25–34. doi: 10.1385/CRIAI:26:1:25

5. Dunne DW, Cooke A. A worm's eye view of the immune system: consequences for evolution of human autoimmune disease. *Nat Rev Immunol.* (2005) 5:420–6. doi: 10.1038/nri1601

6. Maizels RM. Infections and allergy - helminths, hygiene and host immune regulation. *Curr Opin Immunol.* (2005) 17:656–61. doi: 10.1016/j.coi.2005.09.001

7. Yazdanbakhsh M, Kremsner PG, van Ree R. Allergy, parasites, and the hygiene hypothesis. *Science (New York, NY).* (2002) 296:490–4. doi: 10.1126/science.296.5567.490

8. Yazdanbakhsh M, Matricardi PM. Parasites and the hygiene hypothesis: regulating the immune system? *Clin Rev Allergy Immunol.* (2004) 26:15–24. doi: 10.1385/CRIAI:26:1:15

9. Cooke A, Tonks P, Jones FM, O'Shea H, Hutchings P, Fulford AJ, et al. Infection with *Schistosoma mansoni* prevents insulin dependent diabetes mellitus in non-obese diabetic mice. *Parasite Immunol.* (1999) 21:169–76. doi: 10.1046/j.1365-3024.1999.00213.x

10. La Flamme AC, Canagasabey K, Harvie M, Bäckström BT. Schistosomiasis protects against multiple sclerosis. *Mem Inst Oswaldo Cruz.* (2004) 99:33–6. doi: 10.1590/S0074-02762004000900006

11. Sewell D, Qing Z, Reinke E, Elliot D, Weinstock J, Sandor M, et al. Immunomodulation of experimental autoimmune encephalomyelitis by helminth ova immunization. *Int Immunol.* (2003) 15:59–69. doi: 10.1093/intimm/dxg012

12. Zaccone P, Fehérvári Z, Jones FM, Sidobre S, Kronenberg M, Dunne DW, et al. *Schistosoma mansoni* antigens modulate the activity of the innate immune response and prevent onset of type 1 diabetes. *Eur J Immunol.* (2003) 33:1439–49. doi: 10.1002/eji.200323910

13. Saunders KA, Raine T, Cooke A, Lawrence CE. Inhibition of autoimmune type 1 diabetes by gastrointestinal helminth infection. *Infect Immun.* (2007) 75:397–407. doi: 10.1128/IAI.00664-06

14. Kitagaki K, Businga TR, Racila D, Elliott DE, Weinstock JV, Kline JN. Intestinal helminths protect in a murine model of asthma. *J immunology.* (2006) 177:1628–35. doi: 10.4049/jimmunol.177.3.1628

15. Nagayama Y, Watanabe K, Niwa M, McLachlan SM, Rapoport B. *Schistosoma mansoni* and alpha-galactosylceramide: prophylactic effect of th1 immune suppression in a mouse model of graves' hyperthyroidism. *J immunology.* (2004) 173:2167–73. doi: 10.4049/jimmunol.173.3.2167

16. Elias D, Britton S, Kassu A, Akuffo H. Chronic helminth infections may negatively influence immunity against tuberculosis and other diseases of public health importance. *Expert Rev Anti Infect Ther.* (2007) 5:475–84. doi: 10.1586/14787210.5.3.475

17. Nacher M, Singhasivanon P, Yimsamran S, Manibunyong W, Thanyavanich N, Wuthisen R, et al. Intestinal helminth infections are associated with increased incidence of *Plasmodium falciparum* malaria in Thailand. *J Parasitol.* (2002) 88:55–8. doi: 10.1645/0022-3395(2002)088[0055:IHIAAW]2.0.CO;2

18. Noland GS, Urban JF, Fried B, Kumar N. Counter-regulatory anti-parasite cytokine responses during concurrent *Plasmodium yoelii* and intestinal helminth infections in mice. *Exp Parasitol.* (2008) 119:272–8. doi: 10.1016/j.exppara.2008.02.009

19. Su Z, Segura M, Morgan K, Loredo-Osti JC, Stevenson MM. Impairment of protective immunity to blood-stage malaria by concurrent nematode infection. *Infect Immun.* (2005) 73:3531–9. doi: 10.1128/IAI.73.6.3531-3539.2005

20. Talaat KR, Bonawitz RE, Domenech P, Nutman TB. Preexposure to live *Brugia malayi* microfilariae alters the innate response of human dendritic cells to *Mycobacterium tuberculosis*. *J Infect Dis.* (2006) 193:196–204. doi: 10.1086/498912

21. Tristão-Sá R, Ribeiro-Rodrigues R, Johnson LT, Pereira FE, Dietze R. Intestinal nematodes and pulmonary tuberculosis. *Rev Soc Bras Med Trop.* (2002) 35:533–5. doi: 10.1590/S0037-86822002000500020

22. Weng M, Huntley D, Huang IF, Foye-Jackson O, Wang L, Sarkissian A, et al. Alternatively activated macrophages in intestinal helminth infection: effects on concurrent bacterial colitis. *J Immunol.* (2007) 179:4721–31. doi: 10.4049/jimmunol.179.7.4721

23. Anthony RM, Rutitzky LI, Urban JF, Stadecker MJ. Gause WC. Protective immune mechanisms in helminth infection. *Nat Rev Immunol.* (2007) 7:975–87. doi: 10.1038/nri2199

24. El-Derbawy MM, Salem HS, Raboo M, Baiuomy IR, Fadil SA, Fadil HA, et al. In vivo evaluation of the anti-schistosomal potential of ginger-loaded chitosan nanoparticles on *Schistosoma mansoni*: histopathological, ultrastructural, and immunological changes. *Life.* (2022) 12:1834. doi: 10.3390/life12111834

25. Nelwan ML. Schistosomiasis: life cycle, diagnosis, and control. *Curr Ther Res Clin Exp.* (2019) 91:5–9. doi: 10.1016/j.curtheres.2019.06.001

26. Salawu OT, Odaibo AB. Maternal schistosomiasis: a growing concern in sub-Saharan Africa. *Pathog Glob Health.* (2014) 108:263–70. doi: 10.1179/2047773214Y.0000000150

27. Mbugi NO, Laizer H, Chacha M, Mbega E. Prevalence of human schistosomiasis in various regions of *Tanzania* mainland and *Zanzibar*: a systematic review and meta-analysis of studies conducted for the past ten Years (2013-2023). *PLoS Negl Trop Dis.* (2024) 18:e0012462. doi: 10.1371/journal.pntd.0012462

28. Dag O, Erez M, Kozan E, Mine A, Irem I. In vitro anthelmintic activity of five different *Artemisia l.* species growing in Türkiye. *Pakistan Veter J.* (2023) 2023:2074–7764. doi: 10.29261/pakvetj/2023.087

29. Fadladdin YAJ. Evaluation of antischistosomal activities of crude aqueous extracts of *Artemisia annua*, *Nigella sativa*, and *Allium sativum* against *Schistosoma mansoni* in hamsters. *Biomed Res Int.* (2022) 2022:5172287. doi: 10.1155/2022/5172287

30. Hay SI, Abajobir AA, Abate KH, Abbafati C, Abbas KM, Abd-Allah F, et al. Global, regional, and national disability-adjusted life-years (dalys) for 333 diseases and injuries and healthy life expectancy (hale) for 195 countries and territories, 1990-2016: a systematic analysis for the global burden of disease study 2016. *Lancet.* (2017) 390:1260–344. doi: 10.1016/S0140-6736(17)32130-X

31. Kahisay M, Birhanie M, Derso A. Prevalence and intensity of *Schistosoma mansoni* infection and its associated risk factors among patients with and without HIV at chuahit health center, Dembia district, Northwest Ethiopia. *Res Rep Trop Med.* (2021) 12:25–32. doi: 10.2147/RRTM.S292899

32. Egbuna C, Akram M, Ifemeje JC. *Neglected Tropical Diseases and Phytochemicals in Drug Discovery.* New York: Wiley Online Library (2021). doi: 10.1002/9781119617143

33. Bekana T, Abebe E, Mekonnen Z, Tulu B, Ponpetch K, Liang S, et al. Parasitological and malacological surveys to identify transmission sites for *Schistosoma mansoni* in Gomma district, south-western Ethiopia. *Sci Rep.* (2022) 12:17063. doi: 10.1038/s41598-022-21641-2

34. Cheever AW. Differential regulation of granuloma size and hepatic fibrosis in schistosome infections. *Memórias do Instituto Oswaldo Cruz.* (1997) 92:689–92. doi: 10.1590/S0074-02761997000500024

35. Gryseels B, Polman K, Clerinx J, Kestens L. Human schistosomiasis. *Lancet.* (2006) 368:1106–18. doi: 10.1016/S0140-6736(06)69440-3

36. Arnaud V, Li J, Wang Y, Fu X, Mengzhi S, Luo X, et al. Regulatory role of interleukin-10 and interferon-γ in severe hepatic central and peripheral fibrosis in humans infected with *Schistosoma japonicum*. *J Infect Dis.* (2008) 198:418–26. doi: 10.1086/588826

37. Takemura Y, Kikuchi S, Inaba Y. Epidemiologic study of the relationship between schistosomiasis due to *Schistosoma japonicum* and liver cancer/cirrhosis. *Am J Trop Med Hyg.* (1998) 59:551–6. doi: 10.4269/ajtmh.1998.59.551

38. Kandeel M, Rehman T, Akhtar T, Zaheer T, Andrabi S, Ashraf U, et al. Anti-parasitic applications of nanoparticles: a review. *Pak Vet J.* (2022) 42:2074–7764. doi: 10.29261/pakvetj/2022.040

39. Rehman T, Elsaid F, Magdalena M, Toledo G, Gentile A, Ahmed Gul R, et al. Fasciolosis: recent update in vaccines development and their efficacy. *Pak Vet J.* (2023) 43:2074–7764. doi: 10.29261/pakvetj/2023.034

40. Hammouda NA, el-Nassery SF, Bakr ME, el-Gebaly WM, Hassan AM. Effect of toxoplasmosis on experimental schistosomiasis. *J Egypt Soc Parasitol.* (1994) 24:395–406.

41. Hammouda NA, el-Nassery SF, Bakr ME, el-Gebali WM, abo el-Nazar SY, Hassan AM. Immunological and histopathological studies on the effect of toxoplasmosis in experimental schistosomiasis. *J Egypt Soc Parasitol.* (1994) 24:429–37.

42. Sirag SB, Christensen NO, Frandsen F, Monrad J, Nansen P. Homologous and heterologous resistance in echinostoma revolutum infections in mice. *Parasitology.* (1980) 80:479–86. doi: 10.1017/S0031182000000949

43. Bazzone LE, Smith PM, Rutitzky LI, Shainheit MG, Urban JF, Setiawan T, et al. Coinfection with the intestinal nematode heligmosomoides polygyrus markedly reduces hepatic egg-induced immunopathology and proinflammatory cytokines in mouse models of severe schistosomiasis. *Infect Immun.* (2008) 76:5164–72. doi: 10.1128/IAI.00673-08

44. Liao C, Cheng X, Liu M, Wang X, Boireau P. *Trichinella spiralis* and tumors: cause, coincidence or treatment? *Anticancer Agents Med Chem.* (2018) 18:1091–9. doi: 10.2174/1871520617666171121115847

45. Gottstein B, Pozio E, Nöckler K. Epidemiology, diagnosis, treatment, and control of trichinellosis. *Clin Microbiol Rev.* (2009) 22:127–45. doi: 10.1128/CMR.00026-08

46. Bruschi F, Dupouy-Camet J. *Helminth Infections and Their Impact on Global Public Health.* Cham: Springer. (2014). doi: 10.1007/978-3-7091-1782-8

47. Gao F, Wang R, Liu M. *Trichinella spiralis*, potential model nematode for epigenetics and its implication in metazoan parasitism. *Front Physiol.* (2014) 4:410. doi: 10.3389/fphys.2013.00410

48. Malone CJ, Oksanen A, Mukaratirwa S, Sharma R, Jenkins E. From wildlife to humans: the global distribution of *Trichinella* species and genotypes in wildlife and wildlife-associated human trichinellosis. *Int J Parasitol.* (2024) 24:100934. doi: doi: 10.1016/j.ijppaw.2024.100934

49. Ilic N, Gruden-Movsesijan A, Sofronic-Milosavljevic L. *Trichinella spiralis*: shaping the immune response. *Immunol Res.* (2012) 52:111–9. doi: 10.1007/s12026-012-8287-5

50. Bruschi F, Gómez-Morales M. Immune response to parasitic infections-immunity to helminths and novel therapeutic approaches. *Clin Infect Dis.* (2014) 60:1734. doi: 10.1093/cid/civ175

51. Park HK, Cho MK, Choi SH, Kim YS Yu HS. *Trichinella spiralis*: infection reduces airway allergic inflammation in mice. *Exp Parasitol.* (2011) 127:539–44. doi: 10.1016/j.exppara.2010.10.004

52. Ashour DS. *Trichinella spiralis* immunomodulation: an interactive multifactorial process. *Expert Rev Clin Immunol.* (2013) 9:669–75. doi: 10.1586/1744666X.2013.811187

53. Wang XL, Fu BQ, Yang SJ, Wu XP, Cui GZ, Liu MF, et al. *Trichinella spiralis*–a potential anti-tumor agent. *Vet Parasitol.* (2009) 159:249–52. doi: 10.1016/j.vetpar.2008.10.052

54. Molinari JA, Ebersole JL. Antineoplastic effects of long-term *Trichinella spiralis* infection on b-16 melanoma. *Int Arch Allergy Appl Immunol.* (1977) 55:444–8. doi: 10.1159/000231956

55. Pocock D, Meerovitch E. The anti-neoplastic effect of trichinellosis in a syngeneic murine model. *Parasitology.* (1982) 84:463–73. doi: 10.1017/S0031182000052768

56. Luo J, Yu L, Xie G, Li D, Su M, Zhao X, et al. Study on the mitochondrial apoptosis pathways of small cell lung cancer H446 cells induced by *Trichinella spiralis* muscle larvae ESPS. *Parasitology.* (2017) 144:793–800. doi: 10.1017/S0031182016002535

57. Gruden-Movsesijan A, Radulović N, Mostarica Stojkovic M, Stosic-Grujicic S, Milic M, Sofronic-Milosavljevic L. *Trichinella spiralis*: modulation of experimental autoimmune encephalomyelitis in da rats. *Exp Parasitol.* (2008) 118:641–7. doi: 10.1016/j.exppara.2007.12.003

58. Gruden-Movsesijan A, Ilic N, Mostarica-Stojkovic M, Stosic-Grujicic S, Milic M, Sofronic-Milosavljevic L. Mechanisms of modulation of experimental autoimmune encephalomyelitis by chronic *Trichinella spiralis* infection in dark agouti rats. *Parasite Immunol.* (2010) 32:450–9. doi: 10.1111/j.1365-3024.2010.01207.x

59. Du L, Tang H, Ma Z, Xu J, Gao W, Chen J, et al. The protective effect of the recombinant 53-kda protein of *Trichinella spiralis* on experimental colitis in mice. *Dig Dis Sci.* (2011) 56:2810–7. doi: 10.1007/s10620-011-1689-8

60. Eissa MM, Mostafa DK, Ghazy AA, El Azzouni MZ, Boulos LM, Younis LK. Anti-arthritic activity of *Schistosoma mansoni* and *Trichinella spiralis* derived-antigens in adjuvant arthritis in rats: role of Foxp3+ Treg Cells. *PLoS ONE.* (2016) 11:e0165916. doi: 10.1371/journal.pone.0165916

61. Sun S, Li H, Yuan Y, Wang L, He W, Xie H, et al. Preventive and therapeutic effects of *Trichinella spiralis* adult extracts on allergic inflammation in an experimental asthma mouse model. *Parasit Vectors.* (2019) 12:326. doi: 10.1186/s13071-019-3561-1

62. Sofronic-Milosavljevic L, Ilic N, Pinelli E, Gruden-Movsesijan A. Secretory products of *Trichinella spiralis* muscle larvae and immunomodulation: implication for autoimmune diseases, allergies, and malignancies. *J Immunol Res.* (2015) 2015:523875. doi: 10.1155/2015/523875

63. Osborne LC, Monticelli LA, Nice TJ, Sutherland TE, Siracusa MC, Hepworth MR, et al. Coinfection virus-helminth coinfection reveals a microbiota-independent mechanism of immunomodulation. *Science (New York, NY).* (2014) 345:578–82. doi: 10.1126/science.1256942

64. Maizels RM, Gause WC. Immunology. How helminths go viral. *Science (New York, NY).* (2014) 345:517–8. doi: 10.1126/science.1258443

65. Gamble HR. Detection of trichinellosis in pigs by artificial digestion and enzyme immunoassay. *J Food Prot.* (1996) 59:295–8. doi: 10.4315/0362-028X-59.3.295

66. Abd El Wahab WM, El-Badry AA, Mahmoud SS, El-Badry YA, El-Badry MA, Hamdy DA. Ginger (*Zingiber officinale*)-derived nanoparticles in *Schistosoma mansoni* infected mice: hepatoprotective and enhancer of etiological treatment. *PLoS Negl Trop Dis.* (2021) 15:e0009423. doi: 10.1371/journal.pntd.0009423

67. Murambiwa P, Silas E, Mdleleni Y, Mukaratirwa S. Chemokine, cytokine and haematological profiles in sprague-dawley rats co-infected with *Plasmodium berghei* anka and *Trichinella zimbabwensis*-a laboratory animal model for malaria and tissue-dwelling nematodes co-infection. *Heliyon.* (2020) 6:e03475. doi: 10.1016/j.heliyon.2020.e03475

68. Duvall RH, DsWitt W. An improved perfusion technique for recovering adult schistosomes from laboratory animals. *Am J Trop Med Hyg.* (1967) 16:483–6. doi: 10.4269/ajtmh.1967.16.483

69. Pellegrino J, Oliveira CA, Faria J, Cunha AS. New approach to the screening of drugs in experimental schistosomiasis mansoni in mice. *Am J Trop Med Hyg.* (1962) 11:201–15. doi: 10.4269/ajtmh.1962.11.201

70. Kloetzel K. A suggestion for the prevention of severe clinical forms of schistosomiasis mansoni. *Bull World Health Organ.* (1967) 37:686.

71. Younis S, Diab R, Eltarahony M, Arafa F. The anti-schistosomal activity of magnetite and zero-valent iron nanoparticles on *Schistosoma mansoni*: an in vivo study. *Parasitologists United J.* (2021) 14:1126. doi: 10.21608/puj.2021.88219.1126

72. Kiernan J. *Histological and Histochemical Methods, Theory and Practice*. Delhi, India: Butter Worth Heinemann Replika Press Pvt Ltd. (1999).

73. Zaalouk T, Abu-Sheishaa G, Aly I. Regulation of liver fibrosis during murine schistosomiasis mansoni. *Egypt J Hospital Med.* (2020) 81:1275. doi: 10.21608/ejhm.2020.112318

74. Pearce EJ, MacDonald AS. The immunobiology of schistosomiasis. *Nat Rev Immunol.* (2002) 2:499–511. doi: 10.1038/nri843

75. Cortez DM, Feldman MD, Mummidi S, Valente AJ, Steffensen B, Vincenti M, et al. Il-17 stimulates mmp-1 expression in primary human cardiac fibroblasts via P38 Mapk- and Erk1/2-Dependent C/Ebp-Beta, Nf-Kappab, and Ap-1 activation. *Am J Physiol Heart Circ Physiol.* (2007) 293:H3356–65. doi: 10.1152/ajpheart.00928.2007

76. Lemmers A, Moreno C, Gustot T, Maréchal R, Degré D, Demetter P, et al. The interleukin-17 pathway is involved in human alcoholic liver disease. *Hepatology.* (2009) 49:646–57. doi: 10.1002/hep.22680

77. Harrington LE, Hatton RD, Mangan PR, Turner H, Murphy TL, Murphy KM, et al. Interleukin 17-producing Cd4+ effector T cells develop via a lineage distinct from the t helper type 1 and 2 lineages. *Nat Immunol.* (2005) 6:1123–32. doi: 10.1038/ni1254

78. Yingchun L, Huihan W, Rong Z, Guojun Z, Ying Y, Zhuogang L, et al. Antitumor activity of asiaticoside against multiple myeloma drug-resistant cancer cells is mediated by autophagy induction, activation of effector caspases, and inhibition of cell migration, invasion, and stat-3 signaling pathway. *Med Sci Monitor.* (2019) 25:1355. doi: 10.12659/MSM.913397

79. Liu S, An J, Qi F, Yang L, Tian Z, Zhao M. Neuroprotective effects of asiaticoside. *Neural Regen Res.* (2014) 9:1275–82. doi: 10.4103/1673-5374.137574

80. Koyama Y, Brenner DA. Liver inflammation and fibrosis. *J Clin Invest.* (2017) 3:55–64. doi: 10.1172/JCI88881

81. Jones SA, Jenkins BJ. Recent insights into targeting the IL-6 cytokine family in inflammatory diseases and cancer. *Nat Rev Immunol.* (2018) 18:773–89. doi: 10.1038/s41577-018-0066-7

82. Ghasemi H. Roles of IL-6 in ocular inflammation: a review. *Ocu. Immunol Inflam.* (2018) 26:37–50. doi: 10.1080/09273948.2016.1277247

83. Tseng Y-J, Dong L, Liu Y-F, Xu N, Ma W, Weng S-Q, et al. Role of autophagy in chronic liver inflammation and fibrosis. *Curr Protein Peptide Sci.* (2019) 20:817–22. doi: 10.2174/1389203720666190305165203

84. Wang J, Li Z, Wang Z, Yu Y, Li D, Li B, et al. Nanomaterials for combinational radio–immuno oncotherapy. *Adv Funct Mater.* (2020) 30:1910676. doi: 10.1002/adfm.201910676

85. Yu L, He P, Xu Y, Kou X, Yu Z, Xie X, et al. Manipulations of DNA four-way junction architecture and DNA modified Fe3O4@ Au nanomaterials for the detection of miRNA. *Sensors Actuat B.* (2020) 313:128015. doi: 10.1016/j.snb.2020.128015

86. Larkin BM, Smith PM, Ponichtera HE, Shainheit MG, Rutitzky LI, Stadecker MJ. Induction and regulation of pathogenic Th17 cell responses in schistosomiasis. In: *Seminars in immunopathology.* Springer (2012). doi: 10.1007/s00281-012-0341-9

87. Duffield JS, Lupher M, Thannickal VJ. Wynn T. Host responses in tissue repair and fibrosis. *Ann Rev Pathol.* (2013) 8:241–76. doi: 10.1146/annurev-pathol-020712-163930

88. El-Sayed NM, Fathy GM, Abdel-Rahman SA, El-Shafei MA. Cytokine patterns in experimental schistosomiasis mansoni infected mice treated with silymarin. *J Parasitic Dis.* (2016) 40:922–9. doi: 10.1007/s12639-014-0606-4

89. Kitani A, Fuss I, Nakamura K, Kumaki F, Usui T, Strober W. Transforming growth factor (Tgf)-beta1-producing regulatory T cells induce smad-mediated interleukin 10 secretion that facilitates coordinated immunoregulatory activity and amelioration of Tgf-beta1-mediated fibrosis. *J Exp Med.* (2003) 198:1179–88. doi: 10.1084/jem.20030917

90. Henri S, Chevillard C, Mergani A, Paris P, Gaudart J, Camilla C, et al. Cytokine regulation of periportal fibrosis in humans infected with *Schistosoma mansoni*: Ifn-gamma is associated with protection against fibrosis and Tnf-alpha with aggravation of disease. *J Immunol.* (2002) 169:929–36. doi: 10.4049/jimmunol.169.2.929

91. Zinn-Justin A, Marquet S, Hillaire D, Dessein A, Abel L. Genome search for additional human loci controlling infection levels by *Schistosoma mansoni*. *Am J Trop Med Hyg.* (2001) 65:754–8. doi: 10.4269/ajtmh.2001.65.754

92. Rutitzky LI, Bazzone L, Shainheit MG, Joyce-Shaikh B, Cua DJ, Stadecker MJ. Il-23 is required for the development of severe egg-induced immunopathology in schistosomiasis and for lesional expression of Il-171. *J Immunol.* (2008) 180:2486–95. doi: 10.4049/jimmunol.180.4.2486

93. Rutitzky LI, Hernandez HJ, Stadecker MJ. Th1-polarizing immunization with egg antigens correlates with severe exacerbation of immunopathology and death in schistosome infection. *Proc Natl Acad Sci U S A.* (2001) 98:13243–8. doi: 10.1073/pnas.231258498

94. Rutitzky LI, Lopes da. Rosa JR, Stadecker MJ. Severe Cd4 T cell-mediated immunopathology in murine schistosomiasis is dependent on Il-12p40 and correlates with high levels of Il-17. *J Immunol.* (2005) 175:3920–6. doi: 10.4049/jimmunol.175.6.3920

95. Qiu W, Guo K, Yi L, Gong Y, Huang L, Zhong W. Resolvin E1 reduces hepatic fibrosis in mice with *Schistosoma japonicum* infection. *Exp Ther Med.* (2014) 7:1481–5. doi: 10.3892/etm.2014.1641

96. Kastelein RA, Hunter CA, Cua DJ. Discovery and biology of Il-23 and Il-27: related but functionally distinct regulators of inflammation. *Annu Rev Immunol.* (2007) 25:221–42. doi: 10.1146/annurev.immunol.22.012703.104758

97. Park H, Li Z, Yang XO, Chang SH, Nurieva R, Wang YH, et al. A distinct lineage of CD4 t cells regulates tissue inflammation by producing interleukin 17. *Nat Immunol.* (2005) 6:1133–41. doi: 10.1038/ni1261

98. Aggarwal S, Ghilardi N, Xie MH, de Sauvage FJ, Gurney AL. Interleukin-23 promotes a distinct CD4 T cell activation state characterized by the production of interleukin-17. *J Biol Chem.* (2003) 278:1910–4. doi: 10.1074/jbc.M207577200

99. Bettelli E, Carrier Y, Gao W, Korn T, Strom TB, Oukka M, et al. Reciprocal developmental pathways for the generation of pathogenic effector Th17 and regulatory T cells. *Nature.* (2006) 441:235–8. doi: 10.1038/nature04753

100. Korn T, Bettelli E, Gao W, Awasthi A, Jäger A, Strom TB, et al. Il-21 initiates an alternative pathway to induce proinflammatory T(H)17 cells. *Nature.* (2007) 448:484–7. doi: 10.1038/nature05970

101. Langrish CL, Chen Y, Blumenschein WM, Mattson J, Basham B, Sedgwick JD, et al. Il-23 drives a pathogenic T cell population that induces autoimmune inflammation. *J Exp Med.* (2005) 201:233–40. doi: 10.1084/jem.20041257

102. Sutton C, Brereton C, Keogh B, Mills KH, Lavelle EC. A crucial role for interleukin (Il)-1 in the induction of Il-17-producing t cells that mediate autoimmune encephalomyelitis. *J Exp Med.* (2006) 203:1685–91. doi: 10.1084/jem.20060285

103. Veldhoen M, Hocking RJ, Atkins CJ, Locksley RM, Stockinger B. Tgfbeta in the context of an inflammatory cytokine milieu supports de novo differentiation of il-17-producing T cells. *Immunity.* (2006) 24:179–89. doi: 10.1016/j.immuni.2006.01.001

104. Wang B, Liang S, Wang Y, Zhu XQ, Gong W, Zhang HQ, et al. Th17 down-regulation is involved in reduced progression of schistosomiasis fibrosis in ICOSL KO mice. *PLoS Negl Trop Dis.* (2015) 9:e0003434. doi: 10.1371/journal.pntd.0003434

105. Franco KGS, de Amorim FJR, Santos MA, Rollemberg CVV, de Oliveira FA, França AVC, et al. Association of Il-9, Il-10, and Il-17 cytokines with hepatic fibrosis in human *Schistosoma mansoni* infection. *Front Immunol.* (2021) 12:779534. doi: 10.3389/fimmu.2021.779534

106. Shainheit MG, Lasocki KW, Finger E, Larkin BM, Smith PM, Sharpe AH, et al. The pathogenic th17 cell response to major schistosome egg antigen is sequentially dependent on il-23 and Il-1β. *J immunology.* (2011) 187:5328–35. doi: 10.4049/jimmunol.1101445

107. Kalantari P, Morales Y, Miller EA, Jaramillo LD, Ponichtera HE, Wuethrich MA, et al. Cd209a synergizes with dectin-2 and mincle to drive severe th17 cell-mediated schistosome egg-induced immunopathology. *Cell Rep.* (2018) 22:1288–300. doi: 10.1016/j.celrep.2018.01.001

108. Meng F, Wang K, Aoyama T, Grivennikov SI, Paik Y, Scholten D, et al. Interleukin-17 signaling in inflammatory, kupffer cells, and hepatic stellate cells exacerbates liver fibrosis in mice. *Gastroenterology.* (2012) 143:765–76.e3. doi: 10.1053/j.gastro.2012.05.049

109. Ramani K, Biswas PS. Interleukin-17: friend or foe in organ fibrosis. *Cytokine.* (2019) 120:282–8. doi: 10.1016/j.cyto.2018.11.003

110. Shainheit MG, Smith PM, Bazzone LE, Wang AC, Rutitzky LI, Stadecker MJ. Dendritic cell Il-23 and Il-1 production in response to schistosome eggs induces th17 cells in a mouse strain prone to severe immunopathology. *J Immunol.* (2008) 181:8559–67. doi: 10.4049/jimmunol.181.12.8559

111. do Nascimento WR, Nóbrega CG, Fernandes ED, Santos PD, Melo FL, Albuquerque MC, et al. *Schistosoma mansoni* infection decreases il-33-mrna expression and increases cxcl9 and cxcl10 production by peripheral blood cells. *Med Microbiol Immunol.* (2022) 211:211–8. doi: 10.1007/s00430-022-00745-6

112. Koch DT, Koliogiannis D, Drefs M, Schirren M, von Ehrlich-Treuenstätt V, Nieß H, et al. Baseline interleukin-6 as a preoperative biomarker for liver fibrosis. *Visceral Med.* (2024) 39:184–92. doi: 10.1159/000535627

113. Li Y, Zhao J, Yin Y, Li K, Zhang C, Zheng Y. The role of il-6 in fibrotic diseases: molecular and cellular mechanisms. *Int J Biol Sci.* (2022) 18:5405–14. doi: 10.7150/ijbs.75876

114. Seki E, De Minicis S, Osterreicher CH, Kluwe J, Osawa Y, Brenner DA, et al. Tlr4 enhances Tgf-beta signaling and hepatic fibrosis. *Nat Med.* (2007) 13:1324–32. doi: 10.1038/nm1663

115. Dewidar B, Meyer C, Dooley S, Meindl-Beinker AN. TGF-β in hepatic stellate cell activation and liver fibrogenesis-updated 2019. *Cells.* (2019) 8:1419. doi: 10.3390/cells8111419

116. Li MO, Wan YY, Sanjabi S, Robertson A-KL, Flavell RA. Transforming growth factor-β regulation of immune responses. *Annu Rev Immunol.* (2006) 24:99–146. doi: 10.1146/annurev.immunol.24.021605.090737

117. Tallima H, Salah M, Guirguis FR, El Ridi R. Transforming growth factor-β and th17 responses in resistance to primary murine schistosomiasis mansoni. *Cytokine.* (2009) 48:239–45. doi: 10.1016/j.cyto.2009.07.581

118. Gulen MF, Kang Z, Bulek K, Youzhong W, Kim TW, Chen Y, et al. The receptor Sigirr suppresses Th17 cell proliferation via inhibition of the interleukin-1 receptor pathway and MTOR kinase activation. *Immunity.* (2010) 32:54–66. doi: 10.1016/j.immuni.2009.12.003

119. Gieling RG, Wallace K, Han YP. Interleukin-1 participates in the progression from liver injury to fibrosis. *Am J Physiol Gastroint Liver Physiol.* (2009) 296:G1324–31. doi: 10.1152/ajpgi.90564.2008

120. Mancini R, Benedetti A, Jezequel AM. An interleukin-1 receptor antagonist decreases fibrosis induced by dimethylnitrosamine in rat liver. *Virchows Archiv.* (1994) 424:25–31. doi: 10.1007/BF00197389

121. Booth M, Vennervald BJ, Butterworth AE, Kariuki HC, Amaganga C, Kimani G, et al. Exposure to malaria affects the regression of hepatosplenomegaly after

treatment for *Schistosoma mansoni* infection in kenyan children. *BMC Med.* (2004) 2:36. doi: 10.1186/1741-7015-2-36

122. de Jesus AR, Magalhães A, Miranda DG, Miranda RG, Araújo MI, de Jesus AA, et al. Association of type 2 cytokines with hepatic fibrosis in human *Schistosoma mansoni* infection. *Infect Immun.* (2004) 72:3391–7. doi: 10.1128/IAI.72.6.3391-3397.2004

123. Elliott DE, Setiawan T, Metwali A, Blum A, Urban JF, Weinstock JV. Heligmosomoides polygyrus inhibits established colitis in il-10-deficient mice. *Eur J Immunol.* (2004) 34:2690–8. doi: 10.1002/eji.200324833

124. Summers RW, Elliott DE, Urban JF, Thompson R, Weinstock JV. *Trichuris suis* therapy in Crohn's disease. *Gut.* (2005) 54:87–90. doi: 10.1136/gut.2004.041749

125. Dunne DW, Riley EM. Immunity, morbidity and immunoepidemiology in parasite infections. *Parasite Immunol.* (2004) 26:425–8. doi: 10.1111/j.0141-9838.2004.00737.x

126. Helmby H, Kullberg M, Troye-Blomberg M. Altered immune responses in mice with concomitant *Schistosoma mansoni* and *Plasmodium chabaudi* infections. *Infect Immun.* (1998) 66:5167–74. doi: 10.1128/IAI.66.11.5167-5174.1998

127. Khan IA, Hakak R, Eberle K, Sayles P, Weiss LM, Urban JF. Coinfection with heligmosomoides polygyrus fails to establish Cd8+ T-cell immunity against *Toxoplasma gondii*. *Infect Immun.* (2008) 76:1305–13. doi: 10.1128/IAI.01236-07

128. Legesse M, Erko B, Balcha F. Increased parasitaemia and delayed parasite clearance in *Schistosoma mansoni* and *Plasmodium berghei* co-infected mice. *Acta Trop.* (2004) 91:161–6. doi: 10.1016/j.actatropica.2004.04.002

frontiers | Frontiers in Veterinary Science

TYPE Original Research
PUBLISHED 05 November 2024
DOI 10.3389/fvets.2024.1387352

Check for updates

OPEN ACCESS

EDITED BY
Sirikachorn Tangkawattana,
Khon Kaen University, Thailand

REVIEWED BY
Dean Konjević,
University of Zagreb, Croatia
Mughees Aizaz Alvi,
University of Agriculture, Faisalabad, Pakistan

*CORRESPONDENCE
Kohei Makita
✉ kmakita@rakuno.ac.jp

RECEIVED 17 February 2024
ACCEPTED 30 September 2024
PUBLISHED 05 November 2024

CITATION
Fukui M, Uraguchi K, Numa H, Suzuki T, Karasawa M, Maita K, Yokozawa T, Hayama Y and Makita K (2024) Ecological factors associated with fox feces density in an *Echinococcus multilocularis* endemic zone in Japan.
Front. Vet. Sci. 11:1387352.
doi: 10.3389/fvets.2024.1387352

COPYRIGHT
© 2024 Fukui, Uraguchi, Numa, Suzuki, Karasawa, Maita, Yokozawa, Hayama and Makita. This is an open-access article distributed under the terms of the Creative Commons Attribution License (CC BY). The use, distribution or reproduction in other forums is permitted, provided the original author(s) and the copyright owner(s) are credited and that the original publication in this journal is cited, in accordance with accepted academic practice. No use, distribution or reproduction is permitted which does not comply with these terms.

Ecological factors associated with fox feces density in an *Echinococcus multilocularis* endemic zone in Japan

Megumi Fukui[1], Kohji Uraguchi[2], Himika Numa[1], Toru Suzuki[3], Michiko Karasawa[1], Kaoruko Maita[1], Terumi Yokozawa[1], Yoko Hayama[4] and Kohei Makita[1]*

[1]Veterinary Epidemiology Unit, Department of Veterinary Medicine, School of Veterinary Medicine, Rakuno Gakuen University, Ebetsu, Hokkaido, Japan, [2]Hokkaido Institute of Public Health, Sapporo, Hokkaido, Japan, [3]Department of Environmental and Symbiotic Sciences, College of Agriculture, Food and Environmental Sciences, Rakuno Gakuen University, Ebetsu, Hokkaido, Japan, [4]Division of Transboundary Animal Disease Research, National Institute of Animal Health, National Agriculture and Food Research Organization, Tsukuba, Ibaraki, Japan

Introduction: Human alveolar echinococcosis caused by *Echinococcus multilocularis* is an important zoonotic disease in the northern hemisphere. The life cycle of *E. multilocularis* is maintained primarily in wild animals and requires an intermediate host (mainly small mammals). Human can become an intermediate host through accidental ingestion of *E. multilocularis* eggs. Hokkaido Prefecture is the only area of Japan in which human alveolar echinococcosis is endemic. The purposes of this study were to elucidate the land use ecological factors associated with the density of red fox feces along paved roads and the relationship between the distributions of red fox (*Vulpes vulpes*) populations and fox feces, which determine the level of hazard from eggs.

Methods: A series of surveys was conducted in the central part of the Nemuro Peninsula of Hokkaido, excluding urban areas, over a total of 4 years in May–June in 2014 and 2016–2018 when red foxes remain with their cubs around the dens. Transects of 500 m were set up on paved roads, and feces within the transects were counted. Univariable and multivariable analyses were performed to examine ecological factors including the principal components (PCs) of five land use–type occupancy proportions within 500 m and 1 km, respectively, as explanatory fixed-effect variables. The number of feces in each transect was examined as the response variable using integrated nested Laplace approximation with negative binomial errors with a spatio-temporal autocorrelations structure to separate the effects of similarities of neighboring locations and annual variation. The multivariable models with the lowest widely applicable information criterion values were selected.

Results: The feces density was explained by the PC of the 500- m buffer (−0.27, 2.5th and 97.5th percentiles: −0.44, −0.10) characterized by mixed forests (−0.82) and scarcity of residential areas (0.29) and the proximity to the nearest livestock farm house (−0.35, 2.5th and 97.5th percentiles: −0.53, −0.17). This suggested that foxes defecate in the areas where prey is abundant, avoiding humans.

Discussion: Policy discussions regarding bait distribution design targeting these conditions should be initiated.

KEYWORDS

echinococcosis, feces count, red fox, INLA, spatio-temporal autocorrelation

10.3389/fvets.2024.1387352

1 Introduction

Human alveolar echinococcosis caused by *Echinococcus multilocularis* is an important zoonotic disease in the northern hemisphere and a neglected zoonotic disease according to the World Health Organization (1). Genus *Echinococcus* taxonomically belongs to phylum Platyhelminthes, class Cestoda, order Cyclophyllidea, family Taenidae (2). *Echinococcus* had a long history of taxonomic and nomenclatural confusion, but recent application of molecular tools in addition to morphological and ecological criteria brought widespread agreement that *Echinococcus* should be split into 10 species. According to the criteria, *E. multilocularis* is the only species which causes alveolar echinococcosis in humans (3). The life cycle of *E. multilocularis* involves foxes as the definitive host and to a lesser extent dogs, cats, coyotes, and wolves and their rodent prey (intermediate hosts) in ecosystems generally separate from humans (4).

Hokkaido Prefecture is the only area of Japan in which human alveolar echinococcosis is endemic (Figure 1). In this prefecture, the life cycle of *E. multilocularis* is maintained between the final host, the red fox (*Vulpes vulpes schrencki*), and the intermediate host, voles (*Myodes rufocanus bedfordiae*) (5). The definitive host ingests larvae through predation of intermediate hosts that became infected via ingestion of eggs excreted by the final host. In the intermediate host, larval growth continues indefinitely in the liver in the proliferative stage (4). Humans, as aberrant intermediate hosts, become infected following the accidental ingestion of *E. multilocularis* eggs (6). After a period of slow larval growth, the numerous tiny cysts within the liver can cause a lethal pathophysiology similar to liver carcinoma. Unfortunately, early diagnosis of alveolar echinococcosis is very difficult because of the long latent or asymptomatic period, which can span as long as 20 years (7). The only effective treatment for alveolar echinococcosis is surgical resection, and > 90% of patients die if the disease is left untreated (8). Moreover, helminths are known to regulate host immunity (9) and to hinder any vaccines from providing optimal protection (10). The disease burden in humans may be therefore greater than that directly observed in the case counts.

Incursion of human alveolar echinococcosis into Hokkaido Prefecture has been reported twice. The first incursion occurred in 1937 on Rebun Island (Figure 1) (11). The disease was successfully eliminated in the island by 1970. The second incursion was reported

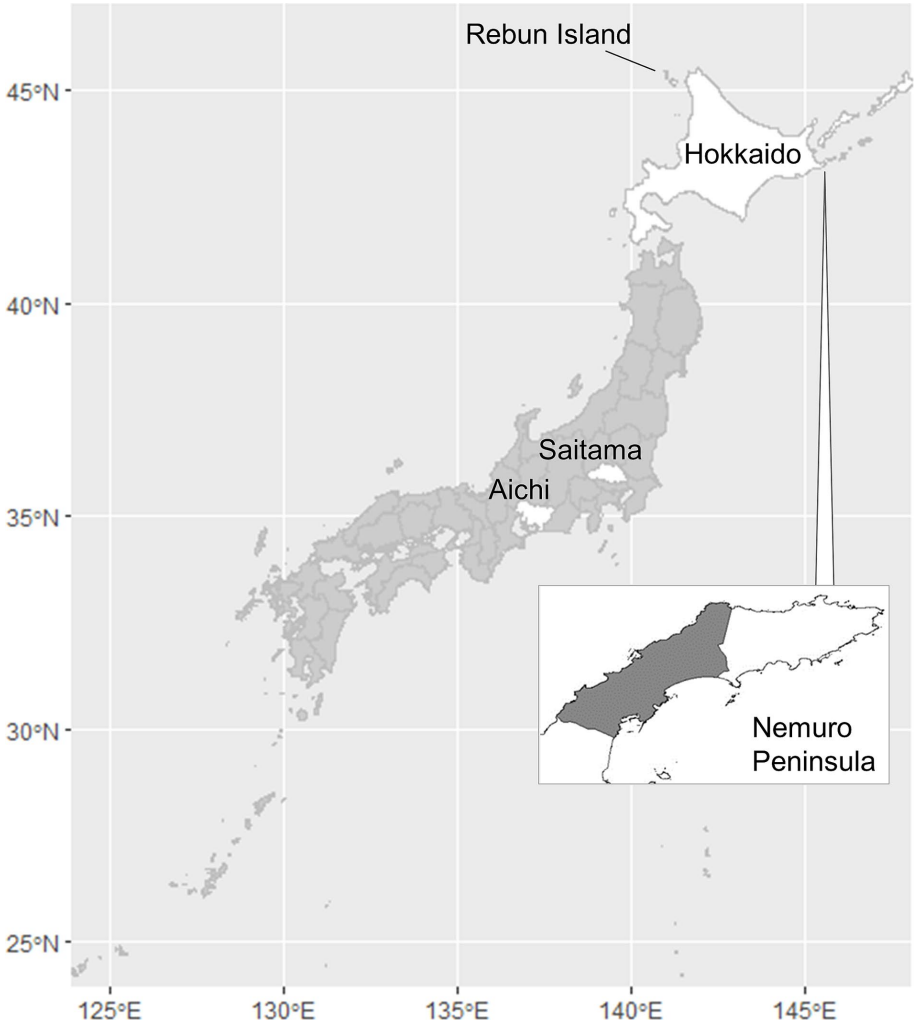

FIGURE 1
Map of Japan indicating the locations of Aichi, Hokkaido, and Saitama Prefectures, the Nemuro Peninsula, and Rebun Island. The shaded portion of the Nemuro Peninsula represents the study area.

in the Nemuro Peninsula, the study site in this paper, in 1965 (12). Human cases of the disease were restricted within this region until 1979, but thereafter, the geographic distribution of cases expanded to cover all of Hokkaido (13). This geographic expansion of the disease in humans was accompanied by a gradual increase in the prevalence in red foxes, reaching 57.4% in 1998 (Figure 2) before stabilizing at approximately 40% in the early 2000s according to the monitoring of Hokkaido Prefectural Government (8, 14). Human cases also increased and since 2000, approximately 20 new human cases have been reported annually in Hokkaido Prefecture (15). The age of the infected individuals has ranged between 7 and 81 years, with the highest frequency in those 40–60 years old (16). Important risk factors in Hokkaido Prefecture include livestock farming (cattle and pigs) and the use of well water (17). Moreover, dairy farmers, fishermen, civil engineering workers, and individuals involved in outdoor jobs are at higher risk of infection (6). In recent years, cases of canines infected with *E. multilocularis* have been reported in Saitama (18) and Aichi Prefectures (19) on Honshu, the main island of Japan (Figure 1). The geographical expansion of *E. multilocularis* has been observed in Europe in different contexts. In addition to foxes, wild invaders such as racoon dog play increasingly important roles in transmission (20, 21). The urbanization of *E. multilocularis* has emerged in Europe, and fox density can be larger in urban than in rural areas, suggesting enhanced chance of contact between humans and infected fox feces (21, 22). In Hokkaido, Japan, the increase of urban foxes has been recognized (23), and racoon dogs are already known to be infected with *E. multilocularis* (24).

For zoonotic helminths including echinococcosis, establishing diagnostic capability, understanding epidemiology including transmission and wildlife habitat dynamics, border security and surveillance, understanding culture are important (21). The key strategy for reduction of prevalence in red foxes is currently anthelmintic bait distribution (23). Vaccine development against helminths is challenging, primary due to economic reason (21), but also the accessibility of the tissues in which the helminths reside (9). However, new technologies such as organoids and single-cell sequencing may facilitate development of helminth vaccines (9). Even though such new tools may become available, the effective control of echinococcosis must take One Health approach (21, 25, 26).

Regarding the disease control, the Hokkaido Prefectural Government established the Hokkaido Prefecture Echinococcosis Control Council, which provides services such as hygiene education and medical examinations, development and dissemination of early detection techniques (serum diagnosis), improvements to the water supply, and implementation of measures to control host animals. With regard to measures to control host animals, the Hokkaido Institute of Public Health supervises the distribution of anthelmintic-containing bait for foxes and has conducted effectiveness tests of baits prepared by the local municipalities since 1999 (27, 28). In the effective tests conducted in Nemuro Peninsula, baits were distributed in a density of 15/km^2 at an average frequency of 4.3 rounds per year, and prevalence in foxes decreased from 49.4% in 1999 to 15.8% in 2006 (27). However, bait distribution in red foxes is not mandatory in the local municipalities in Hokkaido Prefecture. In 2004, a limited liability company known as the Forum on Environment and Animals was established to conduct *Echinococcus* antigen ELISA and egg examinations for pet animals, in addition to providing advice regarding bait distribution and educational programs on zoonosis

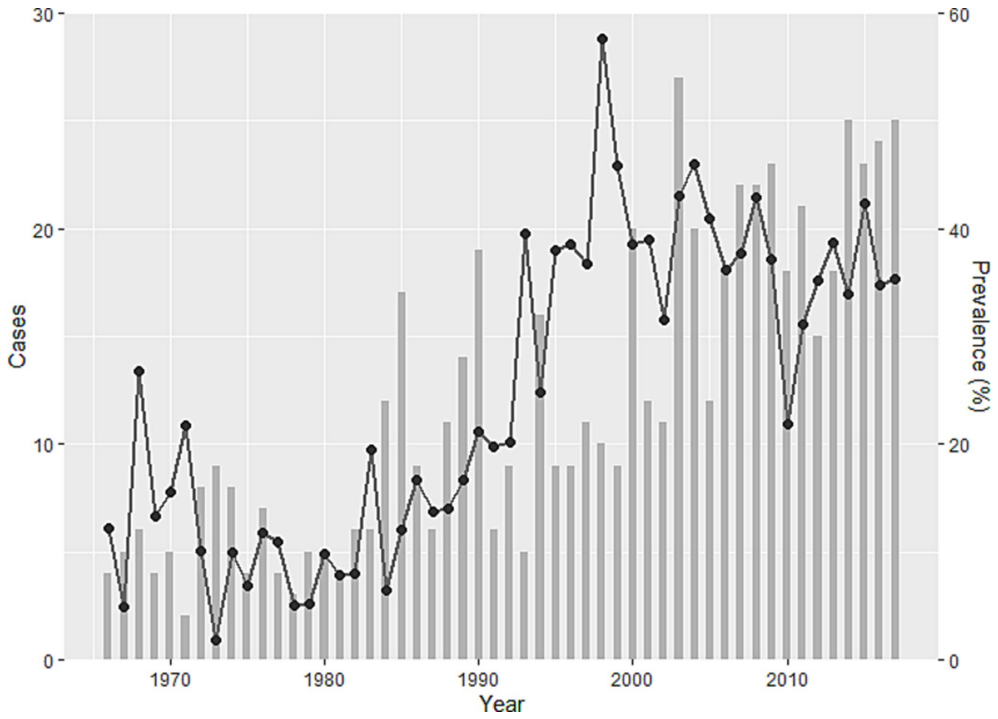

FIGURE 2
Trends in human alveolar echinococcosis cases (bar chart) and prevalence of *Echinococcus multilocularis* in foxes (line) in Hokkaido Prefecture between 1966 and 2017 (15). The bar chart shows cases, and the line shows the temporal change of prevalence.

(29). The guidance and support of the Hokkaido Institute of Public Health and the Forum on Environment and Animals have resulted in a gradual increase in the number of municipalities participating in bait distribution programs. As of 2017, 13 of 185 municipalities in the prefecture participated in bait distribution (28). The Hokkaido Institute of Public Health also monitors red foxes inhabiting Nemuro Peninsula, an area once heavily infected with *E. multilocularis*. In addition, in 2019, Hokkaido Prefectural Government published a handbook of small-area bait distribution to reduce the risks in parks, universities, and zoos in urban areas, suggesting to distribute a bait each in a 100 m grid square (30).

In order to revitalize echinococcosis control efforts targeting red foxes, local municipalities must be provided with up-to-date scientific knowledge to facilitate evidence-based policy discussions. Potentially useful information for policy discussions includes predictions of red fox populations and fox feces densities. Currently baits are distributed at a same interval on a paved road to achieve a target density in a unit area (27, 30). Various methods have been developed to estimate red fox populations, including determination of the number of breeding dens, the frequency of sightings, footprint density, and feces counting (31, 32). Of these methods, counting feces on paved roads is often employed because it can be done by local municipality officers and serves as a valuable indicator of the risk to humans from exposure to infected feces. However, published methods for feces counting require walking deep inside forested areas (33), which carries the risk of encountering bears. This study was conducted to elucidate the ecological factors associated with the density of red fox feces along paved roads and the relationship between the distributions of red fox populations and fox feces. These data may be useful in designing new echinococcosis control strategies by targeted bait distribution.

2 Materials and methods

2.1 Study area

The study area was in the central part of Nemuro Peninsula in Hokkaido, Japan, and encompassed approximately 73 km^2 (Figure 1). The average annual temperature in the study area is 6.6°C, with highest and lowest average temperatures of 17.4°C and −3.8°C in August and February, respectively. The average annual rainfall over a 30-year period (1991–2020) is 1,040 mm (34). The land is primarily flat, with a highest elevation of 55 m above sea level; the dominant vegetation in the area is pastures, natural grass, and forests (35). Precise geographical locations of fox dens are available only in this area in Hokkaido. Hokkaido Prefecture has the largest number of dairy cattle among 47 prefectures of Japan, which accounted for 59.6% of total dairy cattle population (36). The vegetation is therefore representative of dairy farming areas of the prefecture.

2.2 Feces count surveys

Feces count surveys were conducted for a total of 4 years: in 2014, 2016, 2017, and 2018. Each year's survey consisted of two field projects: cleaning of transects, and counting of feces 2 weeks later to quantify the number of feces accumulated in the transects during the period. Prior to the surveys, all field workers were trained for distinguishing fox feces from other animal feces morphologically and by feeding habit at the Hokkaido Institute of Public Health using photographs and field visits. The photographs of all the feces were taken with identification numbers and geo-coordinates, and doubtful images were checked by the experts. Feces counting was conducted on 1–3 June 2014, 2–3 June 2016, 15–16 May 2017, and 12–13 May 2018, during the season in which red foxes remain with their cubs around the den to ensure a controlled assessment of hazards associated with the most restricted movement pattern of adult foxes during the year. After this season, juveniles, as well as both adult males and females increase range size (37), and it would not be possible to associate feces density data with dens.

Urban foxes, defined as foxes for which part or all of their territory includes urban areas (38), are known to exhibit different behavioral patterns than rural foxes (39–42). In this study, red foxes in suburban and rural areas were targeted, and urban areas were excluded from the surveys.

For setting of the transects, random points were generated using a shapefile, which is a geographical data, of the paved roads, downloaded from the Basic Geospatial Information (43) database using ArcGIS version 10.6.1 (ESRI Japan, Tokyo). Only paved roads were selected for three reasons: (1) foxes mark linear boundaries such as roads and hedges (33), (2) overlooking of feces is more easily avoided, and (3) the risk of encountering bears is lower. The number of random points to be generated was determined by the research team each year so that each survey could be completed within 2 days.

Just before cleaning of feces, both ends of the transect, each of which was 250 m away from the central point in opposite directions along the paved road, were marked with colored spray on the sides of the road. A total length of 500 m along the road both sides was carefully surveyed, and old animal feces were removed. When a length of 500 m was not possible due to factors such as the road being unpaved or damaged, the transects were excluded from the survey.

Two weeks after the initial survey, the transects were revisited using a hand-held GPS device (GPSMAP62SJ, eTrex10J, eTrex30J, eTrex20x, GARMIN), and feces counting was conducted according to the marks previously indicated. The survey range for fox feces was up to 1 m from the edge of and on the pavement. All field investigators were trained in advance to identify fox feces by an expert from the Hokkaido Institute of Public Health. The locations of fox feces were recorded using the hand-held GPS device, and total number of feces in each transect was recorded. The fox feces and the surrounding environment of the transect were also photographed. All recorded feces were regarded as those of adults, as cubs should have stayed around the den. The total number of transects set in 2014, 2016, 2017, and 2018 was 22, 25, 44, and 30, respectively.

2.3 Collections of spatial data

The geo-coordinates of fox dens in the study years were obtained from the annual monitoring data for Nemuro Peninsula by the Hokkaido Institute of Public Health. The land use data used in this study were downloaded from the National Land Numerical Information website (44). The land use categories for the 100-m grid squares in the study areas included farm land, mixed forest, wasteland, residential areas, and rivers, ponds, and lakes (Figure 3). The degree of slope used for calculations in this study was the value for the 10-m grid square. In the study area, most

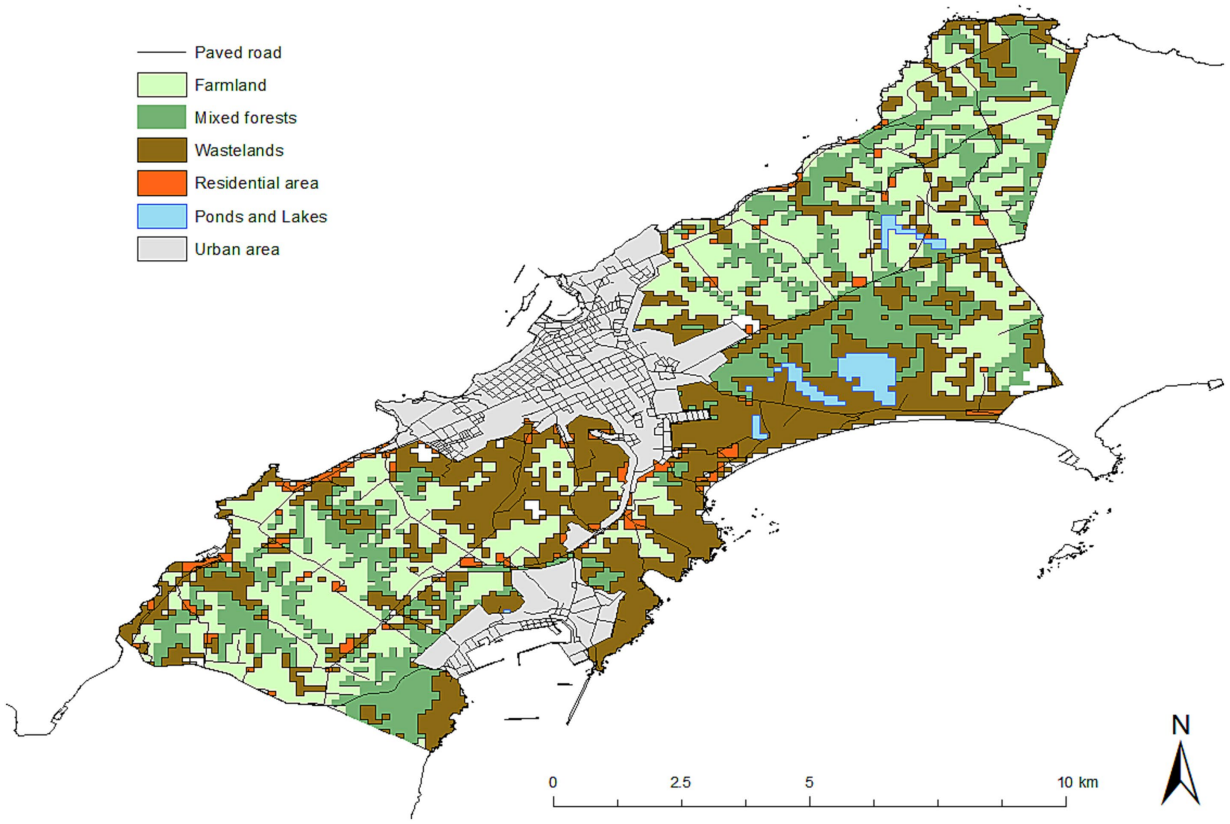

FIGURE 3
Map of land use categories in the study area.

farm lands are dairy pastures, and based on the vegetation data (45), we refer to dairy farming areas as 'pasture' throughout this manuscript. Also, 'building sites' are referred to as residential areas in this manuscript to indicate human settlements, as compared to potential territories of foxes. Wastelands included wasteland, cliffs, and rocks.

The Euclidean distances—shortest distances—from a transect to the nearest river, human settlement, livestock farm house (type of animals could not be determined), pasture, and used dens, the distances from used dens to the nearest rivers, and the distances between used dens in the year were calculated using Spatial Analyst in ArcGIS. ArcGIS was also used to calculate the occupancy proportion of each pasture, mixed forest, wasteland, residential area, pond/lake, and steep slope suitable for den sites (35) (slope > 13° within radii of 1 km and 500 m) from the central point of each transect. A slope of >13° was selected based on previous epidemiologic factors evaluated by the authors; the proportion of area > 13° of a circle with 1 km radii was the most positively associated with the number of dens within the circle, using 10 m grid square data for elevation (46) (unpublished). The areas adjacent to each transect were classified ecologically as pasture, mixed forest, wasteland, or residential area (a transect was sometimes adjacent to areas encompassing several different ecological categories). No transect was located by a pond/lake. A residential area for the adjacent ecology of a transect was defined as an area with three or more residential buildings. The adjacent ecological condition of each transect was identified based on satellite images from Google Earth Pro, version 7.3.2.5776 (Google LLC, Mountain View, California) and photographs taken during fieldwork. The number of dens within a 1-km radius from the transect was also calculated using ArcGIS.

2.4 Descriptive epidemiology

Spatial distributions of the transects with feces counts and dens used in each year were indicated on a map using ArcGIS. The mean number of feces counted and number of used dens were summarized by year. The shortest distance between used dens was calculated for each year but summarized using 4 years of data.

2.5 Ecological factors related to building dens

To characterize the ecological factors related to den building, fox dens were compared with artificially generated control sites. For 131 points where a fox den existed, 262 points were randomly generated using Create Random Points in Geoprocessing in ArcGIS and used as controls. The distance from each point to the river (m), the distance to the road (m), and the slope (degrees) of each point were compared using the Wilcoxon rank-sum test. All shapefiles were downloaded from Basic Geospatial Information (43).

10.3389/fvets.2024.1387352

2.6 Ecological factor analysis for predicting fox feces counts

Data collected over a 4-year period were used to analyze the ecological factors associated with fox feces counts. Based on Akaike's information criterion, the error structure, negative binomial error, was selected for fox feces counts from Poisson, negative binomial, zero-inflated Poisson, and zero-inflated negative binomial errors using generalized linear models in the null model.

To generate a variable that was representative of the ecological conditions surrounding the transects, principal component analysis (PCA) was performed to examine the occupancy proportions of the five land use categories within 1 km or 500 m radii from the transects, which were mutually exclusive, using 4 years of accumulated data. The standard deviation, Eigen values, proportion and cumulative proportions of variance of the principal components (PCs) were also calculated. The first PC explains the most variance, and the second PC takes the orthogonal direction to the fist PC which maximizes the remained variance to explain, and so forth. The 1-km and 500-m buffers were selected based on the calculated shortest distances between used dens in a given year (see Results).

Univariable analysis was conducted using continuous domain stochastic partial differential equation (SPDE) in an Integrated Nested Laplace Approximation (INLA) with negative binomial errors. SPDE is a basis-penalty smoother based on the idea that quantities that occur closer together are more similar than those further apart (47), and is applied for point data (48, 49). The residual autoregressive correlation of order 1 (AR1) was selected for the temporal portion to take spatio-temporal autocorrelations into account. AR1 separates the annual variation in fox feces count as random effect from the fixed-effect variables of interest (48, 49). In the analyses, feces count on a transect was selected as the response variable, and ecological factors potentially associated with prey abundance, water availability, den, and human avoidance, such as the principal components for both the 1-km and 500-m buffers, transect ecological category, land use occupancy proportions and slopes >13° degrees within a 1-km radius, and distances from each transect to the nearest river, human settlement, livestock farm house (type of animals was not identifiable), pasture, and used dens were selected as explanatory fixed-effect variables.

Factors with a 95% credible interval (CI) not including zero in the univariable analyses were selected for the multivariable analysis. Collinearity between continuous variables was checked using the variance inflated factor (VIF) to avoid reduced reliability of the model, and there was no pair with a VIF >2. Multivariable SPDE-INLA AR1 models with negative binomial errors were prepared for all combinations of explanatory fixed-effect variables, selecting the feces count on a transect as the response variable. Continuous fixed-effect variables were standardized by dividing their standard deviations. However, inclusion of the PCs from both the 1-km and 500-m buffers in a single model was avoided. The multivariable models were compared based on widely applicable information criteria (WAIC). The R package "INLA" (50) in the statistical software R, version 4.3.0 (51), was used for the analyses.

3 Results

3.1 Descriptive epidemiology

Table 1 shows the numbers of transects and feces studied, the average number of feces per transect, and used dens over the 4-year study period. The mean and median shortest distances between used dens were 1,347 and 1,368 m, respectively (range: 64–2,919 m; inter-quartile range: 975–1,663 m).

Figure 4 shows the spatial distributions of fox feces, with the number of feces in a transect indicated by the size of the circle. Variation between years was observed, but the higher number of feces in a transect was observed in mixed forests and farm land (pasture) (Figures 3, 4).

3.2 Ecological factors related to den building

Table 2 shows a Wilcoxon rank-sum test comparison of the geographic features of dens and controls. The results suggested that red foxes prefer to build dens close to a river ($p = 0.019$), far from roads ($p = 0.019$), and locations with steep terrain ($p < 0.010$).

3.3 Ecological factor analysis for predicting fox feces counts

Tables 3, 4 show the results of PCA of the 1-km and 500-m transect buffers, respectively. For the 1-km buffer, the cumulative variance exceeded 70% at PC2, whereas for the 500-m buffer, the cumulative variance exceeded 70% at PC3. Similarly, the Eigen value exceeded 1 in PCs 1 and 2 for the 1-km buffer, and in PCs 1 to 3 for the 500-m buffer. The loading with greater absolute values in both signs (positive or negative) explains the PC more. PC1 of the 1-km buffer was characterized by negative values of loading for pastures and mixed forests. Negative values in PC2 of the 1-km buffer suggested human activities, dairy farming for pastures and human settlements, whereas positive values were associated with natural resources.

The pattern of PC1 of the 500-m buffer was similar to that of the 1-km buffer (i.e., negative values for pastures and mixed forests). PC2 of the 500-m buffer exhibited a strong positive load for human settlement (0.72). PC3 of the 500-m buffer was characterized by a low load of mixed forests (−0.82).

TABLE 1 Numbers of transects, feces, and used dens in 2014–2018.

Year	Transects	Feces count	Mean number of feces	Number of used dens
2014	22	63	2.86	14
2016	25	74	2.96	11
2017	44	143	3.25	13
2018	30	96	3.20	11
Total	121	376	3.11	39*

*Overlapped dens used in preceded years were excluded.

10.3389/fvets.2024.1387352

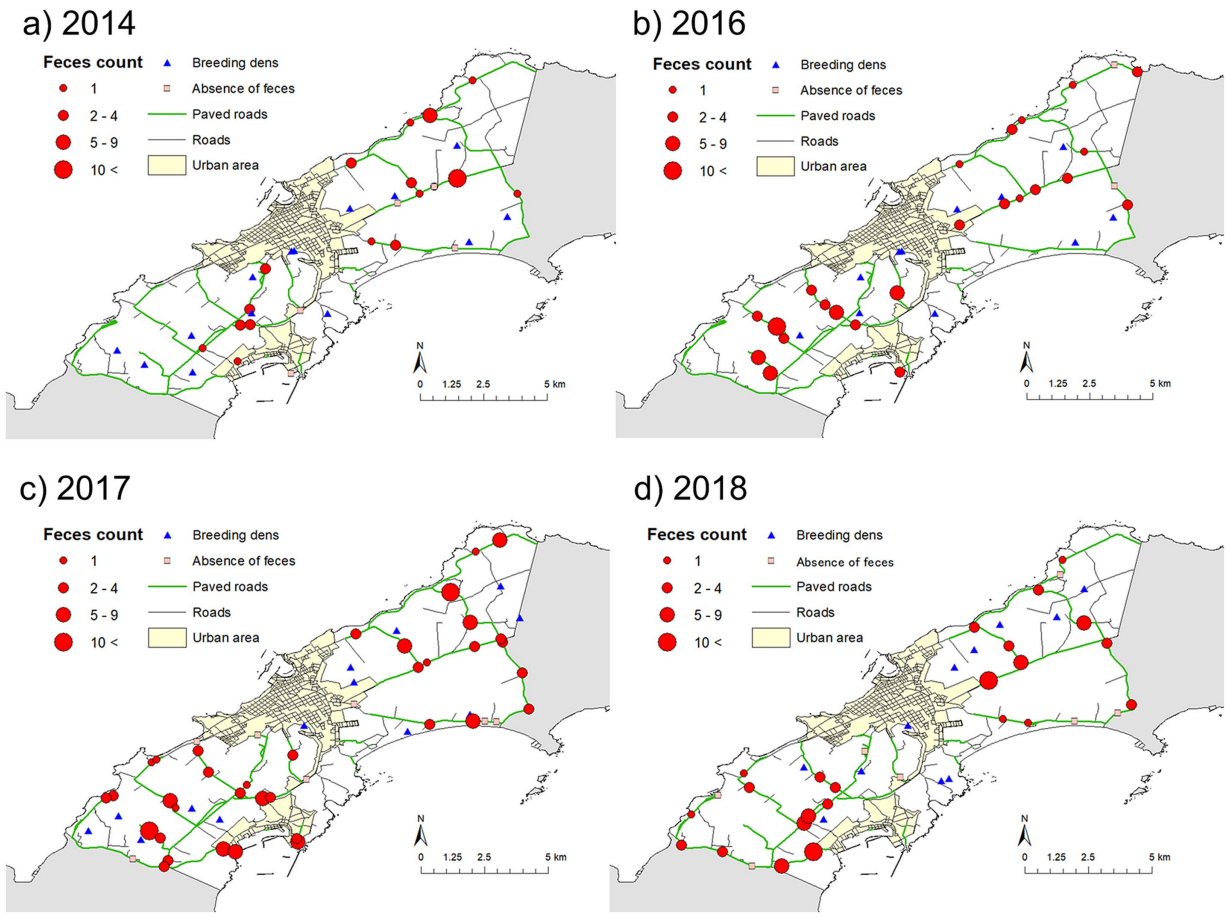

FIGURE 4
Maps showing the distributions of fox feces counts and used dens. Maps (a–d) show the distributions in 2014, 2016, 2017, and 2018, respectively.

TABLE 2 Wilcoxon rank-sum test comparison of geographic features of dens and controls.

	Mean		*p*-value
	Dens ($n = 131$)	Control ($n = 262$)	
Distance from nearest river (m)	228	282	0.019
Distance from nearest roads (m)	258	204	<0.010
Slope (degree)	6.76	5.61	<0.010

Table 5 shows the results of univariable analysis of the factors associated with fox feces counts. The PC1 values for both the 1-km and 500-m buffers (mean estimates = −0.29 and − 0.33, respectively), which were associated with negative loads for pastures and mixed forests in the PCAs, exhibited negative associations with fox feces count (95% CIs did not include zero). PC3 of the 500-m buffer (mean estimate = −0.24), which was associated with negative loads for mixed forests, was also negatively associated with fox feces count. This suggested that, similarly to PC1, mixed forest occupancy is positively associated with fox feces count.

Significant positive relationships were observed between fox feces count and the categories of transects, pastures, and mixed forests (mean estimates = 0.38 and 0.55, respectively), and feces count was negatively associated with distance to the nearest livestock farm house (−0.33), transects along wastelands (−0.46), and human settlements (−0.43).

Table 6 shows the best five models with the lowest WAIC. No multivariable model including PC1 of the 1-km buffer remained among the 10 models with the lowest WAIC. All five of the best models included PC3 of the 500-m buffer and distance from the nearest livestock farm house. Models 2, 3, and 5 included adjacent ecological categories of the transects; however, none of these ecological categories was significant (95% CIs included zero).

The best model with the lowest WAIC showed that the density of fox feces was significantly negatively associated with PC3 of the 500-m buffer and distance from the nearest farm house (Tables 6, 7). The random-effects model showed a strong spatial autocorrelation (low standard deviation) and weak temporal autocorrelation (Table 7).

10.3389/fvets.2024.1387352

TABLE 3 Results of principal component analysis of 1-km buffers.

Land use types	PC1	PC2	PC3
Pasture	−0.52	−0.13	−0.58
Mixed forests	−0.42	0.19	0.78
Wastelands	0.58	0.12	0.01
Human settlements	0.42	−0.56	0.14
Ponds and lakes	0.23	0.79	−0.18
Standard deviation	1.61	1.09	0.91
Eigen value	2.59	1.19	0.84
Proportion of variance	52.1%	23.7%	16.7%
Cumulative proportion	52.1%	75.7%	92.4%

TABLE 4 Results of principal component analysis of 500-m buffers.

Land use types	PC1	PC2	PC3
Pasture	−0.56	−0.26	0.42
Mixed forests	−0.29	0.30	−0.82
Wastelands	0.64	−0.05	0.04
Human settlements	0.25	0.72	0.29
Ponds and lakes	0.37	−0.57	−0.27
Standard deviation	1.50	1.09	1.03
Eigen value	2.25	1.19	1.06
Proportion of variance	44.8%	23.6%	21.1%
Cumulative proportion	44.8%	68.4%	89.5%

4 Discussion

This study was conducted to characterize the ecological factors associated with the density of fox feces along paved roads and the relationship between the distributions of red fox populations and fox feces. The final multivariable model indicated that the density of fox feces could be explained by the surrounding environment within a 500-m radius (i.e., PC3 of 500-m buffers), which was associated with food availability and avoidance of humans. PCA results showed that PC3 of the 500-m buffers was associated with strong negative loading of mixed forests and weak positive loading of human settlements. The negative association between fox feces density and PC3 in the final model suggested that fox feces density is high in areas with high occupancy of mixed forests and few human settlements. The data suggested that red foxes use mixed forests as places to search for food because these areas are inhabited by voles (*Myodes rufocanus bedfordiae*), the main prey of red foxes (35). Red foxes reportedly defecate more in areas in which they spend more time hunting for prey, and they also use feces for scent-marking. A previous study in Spain reported that the density of feces is highest at sites with higher rabbit (prey) population densities, but the locations of feces are associated with landmarks (52). A report on the daily activity patterns in red foxes in Spain found that fox activity is positively associated with prey abundance, and negatively associated with the distance from human settlements, particularly in twilight (after sunrise and before sunset). These relationships are weaker at night (53). Although red foxes are not active during daytime, they exhibit even greater reductions in activity in daytime in areas in which intense fox control measures are implemented (54). Hokkaido Prefecture conducts echinococcosis vector animal epidemiologic surveys (14) particularly in Nemuro Peninsula, and citizens are generally aware of the risk of echinococcosis. Red foxes in the study area may fear human activities, which is commonly seen in many mammalian species (54, 55). Although the transect along human settlements did not remain in the best model in the present study, red fox avoidance of humans could be explained in other alternative models with low WAIC, and the type of environment of the transect is likely associated with feces density. Both prey search and avoidance of humans should be directly associated with survival of red foxes. The animal species of prey for red foxes are different according to the geographical and ecological settings (4); however, dependence of red foxes in their maintenance on prey and human avoidance may be universal.

The PC of the 500-m buffer was an important predictor of feces density, as it was a significant factor in the final multivariable model, whereas the PC of the 1-km buffer was not. This discrepancy can be explained by the mean distance between the nearest used dens, 1,347 m. This suggested that the radius of the home range would be approximately half that distance, or 674 m, slightly above 500 m. Red foxes are territorial animals, with a home range varying from a few hectares to as much as 20–30 km^2, and overlap of home ranges between fox families is more common among fox species with large ranges than those with small ranges (56). According to a study conducted in the Ashio Mountains in central Japan, the home range of red foxes in the denning period is 108.7 ha (37). Assuming that the home range is circular, the calculated radius in Ashio Mountains would be 588.4 m, which is again comparable to 500 m. This suggests that a home range may be similar in different ecological settings, as parent foxes need to feed cubs in dens. However, caution should be exercised in extrapolations using a 500-m buffer in predicting feces density in the denning period in other areas, as a home range may be influenced by fox population density even in the period.

The density of fox feces was also significantly higher in areas in which the distance to the nearest farm house was shorter. Foxes commonly enter cattle sheds to forage on potential various food sources, including cattle placenta, and the bait application around livestock farms with a caution to avoid accidental ingestion of bait by farm animals has been recommended by the Hokkaido Prefectural Government (57). Other studies have also reported the behavior of red foxes foraging cattle placenta or post-calving discharges, which was associated with the infection with *Mycobacterium bovis* in France (58) and *Neospora caninum* in the United States (59). Cattle placenta can be a favorable prey as less effort is needed to capture than live preys in any country settings.

In the present study, fox dens were characterized as being located close to rivers, far from roads, and on steep terrain. In a previous field study conducted in the same area between June 1986 and May 1987, fox dens were characterized as being located on slopes in woodlands near open spaces and streams but far from human settlements (35). These results suggest that the pattern of den making has not changed in this area.

According to INLA univariable analyses, the distance from the nearest den and the proportion of grid squares with a slope > 13° were

10.3389/fvets.2024.1387352

not associated with fox feces density. From beginning to mid-May, when the field surveys were conducted, feces were concentrated around den sites, because the fox cubs, which on average are born approximately four cubs per belly, defecate there (60). Transects that were very close to fox dens might have a high density of feces, including those of adult foxes, due to the high amount of time spent near the den to care for the cubs. However, because dens are located far from roads, as demonstrated in this study, counting feces along paved roads may not be sufficiently sensitive to indicate the location of dens. Mesopredators are reported to often travel along roads in winter to conserve energy (61), and red fox in Nemuro Peninsula may also use roads for traveling. There is a report from Spain that the number of red fox feces deposited in clearings was significantly higher than on roads (52), suggesting that the intensity of road use by red foxes is not that high.

TABLE 5 Results of univariable analysis of factors associated with fox feces count.

Variables	Mean	95%CI	WAIC
PC1 (1 km buffer)	−0.29	−0.47, −0.11*	592.2
PC2 (1 km buffer)	0.12	−0.10, 0.37	600.2
PC1 (500 m buffer)	−0.33	−0.52, −0.15*	590.1
PC2 (500 m buffer)	−0.05	−0.27, 0.16	601.0
PC3 (500 m buffer)	−0.24	−0.42, −0.06*	593.3
Distance from nearest river	−0.05	−0.21, 0.13	600.7
Distance from nearest used den	−0.01	−0.19, 0.17	601.2
Distance from nearest human settlements	−0.01	−0.19, 0.19	601.6
Distance from nearest livestock farm house	−0.33	−0.51, −0.14*	590.7
Distance from nearest pasture	−0.05	−0.22, 0.12	600.7
Transect along pasture	0.38	0.02, 0.75*	597.8
Transect along mixed forest	0.55	0.20, 0.91*	593.1
Transect along wasteland	−0.46	−0.94, −0.01*	597.5
Transect along human settlements	−0.43	−0.78, −0.08*	596.4
Proportion of steep area > 13 degree	0.11	−0.05, 0.28	599.6

*95% credible interval does not include zero.

Identifying all used dens in the breeding season in a target area would allow estimation of the red fox population, which would be of interest to local public health authorities. Although foxes are more active in areas they densely populate (53), defecation depends on prey seeking, marking (52), and avoidance of disturbances associated with human activities (62). Therefore, precisely estimating red fox populations by counting feces along paved roads may not be achievable. Recently, spatial capture-recapture modeling of non-invasive genetic sampling (NGS) data has been applied to estimate the red fox density in Norway (63). NGS can identify individuals and even sex of red foxes, and that is why biological samples collected in the field can estimate the range sizes of them. Recent molecular researches characterize genetic diversity of *E. multilocularis* and other helminths (64, 65). Integrated spatial analysis of genetic information of foxes and *E. multilocularis* may increase understanding of fox population and infection dynamics of *E. multilocularis*.

The present study provided information useful for reducing the risk of echinococcosis in the study area. Praziquantel bait distribution may be targeted at livestock farms and mixed forests. As the incidence of alveolar echinococcosis is high among dairy farmers and agriculturalists (6), considering the potentially significant land coverage of mixed forests, targeting bait distribution to livestock farms may be an effective public health strategy with high economic efficacy. As red foxes are highly mobile, such targeted bait distribution may result in a reduction in the risk of echinococcosis in peri-urban dwellers as well. The Nemuro City Council follows the guideline for deworming foxes published by Hokkaido Prefecture (57). In practice, baits are distributed along roads at the intervals of either 100 m, 150 m, or 200 m, so that the density of bait exceeds 15 baits per km^2, avoiding the following areas: (1) where livestock may feed, such as pastures, (2)

TABLE 6 Multivariable models exhibiting the lowest WAIC.

Model	PC1 (500 m)	PC3 (500 m)	Distance from farm house	Transects along pasture	Transects along mixed forests	Transects along human settlements	Transects along wastelands	WAIC
1		−0.27 (−0.44, −0.10)	−0.35 (−0.53, −0.17)					582.26
2		−0.26 (−0.43, −0.08)	−0.33 (−0.52, −0.14)				−0.29 (−0.73, 0.16)	583.01
3		−0.23 (−0.41, −0.05)	−0.34 (−0.52, −0.15)			−0.24 (−0.59, 0.11)		583.20
4	−0.13 (−0.41, 0.13)	−0.26 (−0.44, −0.08)	−0.25 (−0.52, 0.03)					583.55
5		−0.23 (−0.42, −0.04)	−0.32 (−0.52, −0.12)		0.17 (−0.22, 0.57)			584.07

TABLE 7 Final results of the multivariable analysis.

Variables	Mean	2.5th	97.5th
Intercept	1.19	−1.30	3.44
Fixed effects			
PC3 (500 m)	−0.27	−0.44	−0.10
Distance from the nearest farm house	−0.35	−0.53	−0.17
Random effects			
Standard deviation for spatial effect	0.08	0.01	0.42
Rho of temporal effect	0.25	−0.98	0.99

where agricultural products may be affected, and (3) near natural water sources such as springs, ponds, rivers, and lakes. The current guideline considers even distribution of baits in a target area. To apply the study findings, baits may be distributed at shorter intervals in mixed forest areas, longer in human settlements, and at livestock farms, targeting the areas where red foxes seek prey. Of course, care should be taken in the bait distribution at livestock farms. Moreover, fox dens can be targeted, by choosing the areas with steepness.

This study has three limitations. First, the spatial model used for predicting fox feces counts may not be suitable for other areas in Hokkaido Prefecture or other countries. Red fox is a species highly adapted to diverse ecological conditions (53), and predictive ecological factors may differ in different settings. However, the approach of targeting fox feces can be applied for echinococcosis hazard control considerations in any fox habitat. The most likely difference that may be observed in the statistical results is the PCs significantly associated with fox feces count. In a different climatic or ecological condition, foxes may depend on different animal species or other available foods for prey. Then the loadings of the significant PCs may exhibit ecological characteristics suitable for such prey. Therefore, when this approach is used in the other country or region, it is important to plan how the data representing prey abundance and human avoidance which are suitable for the ecological condition are collected. The second limitation is that this study did not consider urban fox populations. Increased invasion of foxes into urban areas has been reported in several countries (66, 67) and can increase the risk of infection with *Echinococcus* among domestic dogs and, of course, pet owners (68). Food sources associated with households, gardens, and public areas can feed a high number of urban foxes (69). Hegglin et al. (70) reported the successful reduction of *E. multilocularis* coproantigen prevalence in fox feces by targeting bait distribution to sites in which foxes had been seen. As urban areas were excluded in this analysis, the factor associated with fox feces count, mixed forest, would not be a suitable predictor in such areas. Future studies should examine urban risks in greater detail. Spatial analysis can be applied to understand the favorable conditions to make fox dens, prey seeking such as garbage dumping area, and feces count in higher precision. Such information will be helpful in designing small public area bait distribution (23), monitoring *E. multilocularis* prevalence in feces, and evaluation of the disease control. The third limitation is that the level of hazard from infected feces of other mammals such as raccoon dogs is not studied. Raccoon dogs are known to make a pile of feces (71), and pairs can use the same latrines. The method of counting feces on paved roads developed in this study is not applicable to raccoon dogs. Future study for raccoon dogs is needed with new study design.

Although the distribution of praziquantel bait reduces the prevalence of *E. multilocularis*–contaminated fox feces, it has the potential to recover, as a trial of over 1.5 years in an urban area showed failure of complete interruption of the life cycle of *E. multilocularis* (70). Control strategies for maintaining a low prevalence of *E. multilocularis*–contaminated fox feces are thus important. The present study provides a risk-based approach for the control of *E. multilocularis*, which should be practically applied under One Health collaboration (25, 26) between different stakeholders.

Data availability statement

The raw data supporting the conclusions of this article will be made available by the authors, without undue reservation.

Author contributions

MF: Formal analysis, Investigation, Visualization, Writing – original draft. KU: Conceptualization, Funding acquisition, Investigation, Methodology, Writing – review & editing. HN: Formal analysis, Writing – review & editing. TS: Formal analysis, Writing – review & editing. MK: Investigation, Methodology, Writing – review & editing. KaM: Formal analysis, Investigation, Writing – review & editing. TY: Investigation, Methodology, Writing – review & editing. YH: Methodology, Writing – review & editing. KoM: Conceptualization, Data curation, Formal analysis, Funding acquisition, Investigation, Methodology, Project administration, Supervision, Validation, Visualization, Writing – original draft, Writing – review & editing.

Funding

The author(s) declare financial support was received for the research, authorship, and/or publication of this article. The fox den survey was conducted under the annual program of the Hokkaido Institute of Public Health. The discussions with experts were supported by the Hokkaido Prefecture Echinococcosis Control Council. The field surveys of fox feces count were funded by the Graduate School of Veterinary Medicine and School of Veterinary Medicine, Rakuno Gakuen University.

Acknowledgments

Some analyses in this study were carried out by the Hokkaido Prefecture Echinococcosis Control Council. We thank members of the Veterinary Epidemiology Unit, Rakuno Gakuen University, for helping with field surveys between 2014 and 2020.

Conflict of interest

The authors declare that the research was conducted in the absence of any commercial or financial relationships that could be construed as a potential conflict of interest.

Publisher's note

All claims expressed in this article are solely those of the authors and do not necessarily represent those of their affiliated organizations, or those of the publisher, the editors and the reviewers. Any product that may be evaluated in this article, or claim that may be made by its manufacturer, is not guaranteed or endorsed by the publisher.

References

1. WHO. Neglected zoonotic tropical diseases. World Health Organization. (2015). Available at: https://www.who.int/news-room/facts-in-pictures/detail/neglected-zoonotic-tropical-diseases (Accessed January 14, 2024).

2. Thaenkham U, Chaisiri K, Hui En Chan A. Parasitic helminths of medical and public health importance In: Molecular systematics of parasitic helminths. Singapore: Springer (2022)

3. Thompson RCA. The molecular epidemiology of *Echinococcus* infections. *Pathogens*. (2020) 9:453. doi: 10.3390/pathogens9060453

4. Moro P, Schantz PM. Echonococcosis: a review. *Int J Infect Dis*. (2009) 13:125–33. doi: 10.1016/j.ijid.2008.03.037

5. Takahashi K, Uraguchi K, Kudo S. The epidemiological status of *Echinococcus multilocularis* in animals in Hokkaido, Japan. *Mammal Study*. (2005) 30:S101–5. doi: 10.3106/1348-6160(2005)30[101:TESOEM]2.0.CO;2

6. Sato N, Uchino J, Ogasawara K, Todo S, Furuya K. Pathophysiology and prevention of alveolar echinococcosis from the perspective of the relationship with occupation. *JJOMT*. (2003) 51:17–23.

7. Konno K, Oku Y, Tamashiro H. Prevention of alveolar echinococcosis—ecosystem and risk management perspectives in Japan. *Acta Trop*. (2003) 89:33–40. doi: 10.1016/j.actatropica.2003.09.001

8. Kamiya M. Towards the risk management of echinococcosis - current status and strategies (in Japanese). *J Jpn Vet Med Assoc*. (2004) 57:605–11.

9. Loke P, Lee SC, Oyesola OO. Effects of helminths on the human immune response and the microbiome. *Mucosal Immunol*. (2022) 15:1224–33. doi: 10.1038/s41385-022-00532-9

10. Natukunda A, Zirimenya L, Nassuuna J, Nkurunungi G, Cose S, Elliot AM, et al. The effect of helminth infection on vaccine responses in humans and animal models: A systematic review and meta-analysis. *Parasite Immunol*. (2022) 44:e12939. doi: 10.1111/pim.12939

11. Tsunoda I, Mikami J, Aoki T. On a case of typical alveolar echinococcosis found recently in Japan. (in Japanese). *Grenzgebiet*. (1937) 11:1093–100.

12. Kasai Y, Koshino I, Kawanishi N, Sakamoto H, Sasaki E, Kumagai M. Alveolar echinococcosis of the liver; studies on 60 operated cases. *Ann Surg*. (1980) 191:145–52. doi: 10.1097/00000658-198002000-00003

13. Minagawa T. Survey of echinococcosis in Hokkaido and measure against it. (in Japanese). *Hokkaido Igaky Zasshi*. (1997) 72:569–81.

14. Hokkaido Prefectural Government. Echinococcosis vector animals. Overview of food and livelihood hygiene administration (in Japanese). Food Safety Division, Health Bureau, Department of Health and Welfare. (2019). Available at: https://www.pref.hokkaido.lg.jp/hf/kse/gyoseigaiyo.html (Accessed April 10, 2023).

15. Hokkaido Infectious Disease Surveillance Center. Echinococcosis data (in Japanese). (2019). Available at: https://www.iph.pref.hokkaido.jp/kansen/402/data.html (Accessed February 5, 2024).

16. Eckert J, Gemmell MA, Meslin FX, Pawlowski ZS. WHO/OIE manual on echinococcosis in humans and animals: a public health problem of global concern. Paris, France: World Organisation for Animal Health (2001).

17. Yamamoto N, Kishi R, Katakura Y, Miyake H. Risk factors for human alveolar echinococcosis: a case-control study in Hokkaido, Japan. *Ann Trop Med Parasitol*. (2001) 95:689–96. doi: 10.1080/00034980120103252

18. Yamamoto N, Morishima Y, Kon M, Yamaguchi M, Tanno S, Koyama M, et al. The first reported case of a dog infected with *Echinococcus multilocularis* in Saitama Prefecture, Japan. *Jpn J Infect Dis*. (2006) 59:351–2. doi: 10.7883/yoken.JJID.2006.351

19. Morishima Y, Tomaru Y, Fukumoto S, Sugiyama H, Yamasaki H, Hashimoto C, et al. Canine echinococcosis due to *Echinococcus multilocularis*: a second notifiable case from mainland Japan. *Jpn J Infect Dis*. (2016) 69:448–9. doi: 10.7883/yoken.JJID.2015.573

20. Bagrade G, Deksne G, Ozolina Z, Howlett SJ, Interisano M, Casulli A, et al. *Echinococcus multilocularis* in foxes and raccoon dogs: an increasing concern for Baltic countries. *Parasit Vectors*. (2016) 9:615. doi: 10.1186/s13071-016-1891-9

21. Thompson RCA. Zoonotic helminths – why the challenge remains. *J Helminthol*. (2023) 97:1–15. doi: 10.1017/S0022149X23000020

22. Mackenstedt U, Jenkins D, Romig T. The role of wildlife in the transmission of parasitic zoonoses in peri-urban and urban areas. *Int J Parasitol Parasites Wildl*. (2015) 4:71–9. doi: 10.1016/j.ijppaw.2015.01.006

23. Uraguchi K, Irie T, Kouguchi H, Inamori A, Sashika M, Shimozuru M, et al. Anthelmentic baiting of foxes against *Echinococcus multilocularis* in small public area, Japan. *Emerg Infect Dis*. (2022) 28:1677–80. doi: 10.3201/eid2808.212016

24. Hidaka M, Matsuyama H, Uraguchi K, Kouguchi H. Recent cases of *Echinococcus multilocularis* parasitism in raccoon dogs (*Nyctereutes procyonoides*) in Hokkaido, Japan (in Japanese). *Rep Hokkaido Inst Pub Health*. (2022) 72:33–6.

25. Schwabe CW. Veterinary medicine and human health. *2nd* ed. Baltimore: Williams and Wilkins. 713 p.

26. Zinsstag J, Schelling E, Walter-Toews D, Tanner M. From 'one medicine' to 'one health' and systemic approaches to health and well-being. *Prev Vet Med*. (2011) 101:148–56. doi: 10.1016/j.prevetmed.2010.07.003

27. Takahashi K, Uraguchi K, Hatakeyama H, Giraudoux P, Roming T. Efficacy of anthelmintic baiting of foxes against *Echinococcus multilocularis* in northern Japan. *Vet Parasitol*. (2013) 198:122–6. doi: 10.1016/j.vetpar.2013.08.006

28. Yagi K. The control measures of alveolar echiococcosis conducted by Hokkaido local government(in Japanese). Report of Hokkaido Institute of Public Health *67* (2017) 1–7.

29. Forum on Environment and Animals. Forum on Environment and Animals website. (2003). Available at: https://www.fea-echino.com/ (Accessed January 15, 2024).

30. Hokkaido Prefectural Government. A handbook pf small-area anthelmintic bait distribution for red foxes (in Japanese). Food Safety Division, Health Bureau, Department of Health and Welfare. (2019) Available at: https://www.pref.hokkaido.lg.jp/hf/kse/nik/eki/102758.html (Accessed September 15, 2024).

31. Sargeant AB, Pfeifer WK, Allen SH. A spring aerial census of red foxes in North Dakota. *J Wildl Manag*. (1975) 39:30–9. doi: 10.2307/3800462

32. Harris S. An estimation of the number of foxes (*Vulpes vulpes*) in the city of Bristol, and some possible factors affecting their distribution. *J Appl Ecol*. (1981) 18:455–65. doi: 10.2307/2402406

33. Webbon C, Baker P, Harris S. Faecal density counts for monitoring changes in red fox numbers in rural Britain. *J Appl Ecol*. (2004) 41:768–79. doi: 10.1111/j.0021-8901.2004.00930.x

34. Japan Meteorological Agency. Past meteorological data search. Ministry of Land, Transport and Tourism. (2024). Available at: https://www.jma.go.jp/jma/index.html (Accessed on January 5, 2024).

35. Uraguchi K, Den Takahashi K. Site selection and utilization by the red fox in Hokkaido, Japan. *Mammal Study*. (1998) 23:31–40. doi: 10.3106/mammalstudy.23.31

36. Ministry of Agriculture, Forestry, and Fisheries. Livestock statistics (dairy and beef) (in Japanese). Available at: https://www.maff.go.jp/j/tokei/kouhyou/tikusan/ (Accessed September 16, 2024).

37. Takeuchi M, Koganezawa M. Home range and habitat utilisation of the red fox *Vulpes vulpes* in the Ashio Mountains, Central Japan. *J Mamm Soc Japan*. (1992) 17:95–110. doi: 10.11238/jmammsocjapan.17.95

38. Uraguchi K. Population estimate of urban fox (in Japanese). *Honyurui Kagaku*. (2004) 44:87–90.

39. Trewhella WJ, Harris S, Smith GC, Nadian AK. A field trial evaluating bait uptake by an urban fox (*Vulpes vulpes*) population. *J Appl Ecol*. (1991) 28:454–6. doi: 10.2307/2404561

40. Baker PJ, Funk SM, Harris S, White PCL. Flexible spatial organization of urban foxes, *Vulpes vulpes*, before and during an outbreak of sarcoptic mange. *Anim Behav*. (2000) 59:127–46. doi: 10.1006/anbe.1999.1285

41. Bateman PW, Fleming PA. Big city life: carnivores in urban environments. *J Zool*. (2012) 287:1–23. doi: 10.1111/j.1469-7998.2011.00887.x

42. Gil-Fernández M, Harcourt R, Newsome T, Towerton A, Carthey A. Adaptations of the red fox (*Vulpes vulpes*) to urban environments in Sydney, Australia. *J Urban Ecol*. (2020) 6:1–9. doi: 10.1093/jue/juaa009

43. Geospatial Information Authority of Japan. Basic Geospatial Information. (2021). Available at: https://www.gsi.go.jp/kiban/index.html (Accessed August 20, 2021).

44. Ministry of Land, Infrastructure, Transport and Tourism. Land utilization tertiary mesh data. National Land Numerical Information. (2021). Available at: https://nlftp.mlit.go.jp/ksj/ (Accessed August 20, 2021).

45. Biodiversity Center of Japan. Vegetation data of Vegetation Survey on 6th and 7th National Basic Survey on Natural Environment. Ministry of the Environment. (2021). Available at: https://www.biodic.go.jp/index_e.html (Accessed September 5, 2021).

46. Geospatial Information Authority of Japan. Basic map information (numerical elevation model). (2014) Available at: https://fgd.gsi.go.jp/download/ref_dem.html (Accessed November 1, 2014).

47. Lindgren F, Rue H, Lindstrm J. An explicit link between Gaussian felds and Gaussian Markov random felds: the stochastic partial differential equation approach. *J R Stat Soc Ser B Methodol*. (2011) 73:423–98. doi: 10.1111/j.1467-9868.2011.00777.x

48. Blangiardo M, Cameletti M. Spatial and spatio-temporal Bayesian models with R-INLA. Chichester, West Sussex, United Kingdom: John Wiley & Sons, Ltd (2015).

49. Zuur A, Ieno EN, Saveliev AA. Beginner's guide to spatial, temporal and spatial-temporal ecological data analysis with R-INLA. Volume I: Using GLM and GLMM. Newburgh, United Kingdom: Highland Statistics Ltd (2017).

50. Rue H, Martino S, Chopin N. Approximate Bayesian inference for latent Gaussian models by using integrated nested Laplace approximations. *J R Stat Soc Series B Stat Methodol*. (2009) 71:319–92. doi: 10.1111/j.1467-9868.2008.00700.x

51. R Core Team. R: A language and environment for statistical computing. Vienna, Austria: R Foundation for Statistical Computing (2021).

52. Monclús R, Arroyo M, Valencia A, de Miguel FJ. Red foxes (*Vulpes vulpes*) use rabbit (*Oryctolagus cuniculus*) scent marks as territorial marking sites. *J Ethol*. (2009) 27:153–6. doi: 10.1007/s10164-008-0098-8

53. Díaz-Ruiz F, Caro J, Delibes-Mateos M, Arroyo B, Ferras P. Drivers of red fox (*Vulpes vulpes*) daily activity: prey availability, human disturbance or habitat structure? *J Zool*. (2015) 298:128–38. doi: 10.1111/jzo.12294

54. Martin J, Basille M, van Moorter B, Kindberg J, Allaine D, Swenson JE. Coping with human disturbance: spatial and temporal tactics of the brown bears (*Ursus arctos*). *Can J Zool*. (2010) 88:875–83. doi: 10.1139/Z10-053

55. Belotti E, Heurich M, Kreisinger J, Sustr P, Bufka L. Influence of tourism and traffic on the Eurasian lynx hunting activity and daily movements. *Anim Biodivers Conserv*. (2012) 35:235–46. doi: 10.32800/abc.2012.35.0235

56. Goszczyński J. Home ranges in red fox: territoriality diminishes with increasing area. *Acta Theriol*. (2002) 47:103–14. doi: 10.1007/BF03192482

57. Hokkaido Prefecture. Guideline for dewarming foxes. For controling echinococcosis. (in Japanese). *Food Hygiene Division*. (2007) 1–10.

58. Richomme C, Réveillaud E, Moyen JL, Sabatier P, De Cruz K, Michelet L, et al. *Mycobacterium bovis* infection in red foxes in four animal tuberculosis endemic areas in France. *Microorganisms*. (2020) 8:1070. doi: 10.3390/microorganisms8071070

59. Barling KS, Sherman M, Peterson MJ, Thompson JA, McNeill JW, Craig TM, et al. Spatial associations among density of cattle, abundance of wild canids, and seroprevalence to *Neospora caninum* in a population of beef calves. *J Am Vet Med Assoc*. (2000) 217:1361–5. doi: 10.2460/javma.2000.217.1361

60. Tsukada H, Okada H, Yamanaka M, Nonaka N, Oku Y. Foraging behavior of red foxes and echinococcosis. (In Japanese). *Honyurui Kagaku*. (2005) 45:91–8.

61. Crête M, Larivière S. Estimating the costs of locomotion in snow for coyotes. *Can J Zool*. (2003) 81:1808–14. doi: 10.1139/z03-182

62. Baker PJ, Dowding CV, Molony SE, White PCL, Harris S. Activity patterns of urban red foxes (*Vulpes vulpes*) reduce the risk of traffic-induced mortality. *Bihav Ecol*. (2007) 18:716–24. doi: 10.1093/beheco/arm035

63. Lindsø LK, Dupont P, Rød-Eriksen L, Andersskog IPØ, Ulvund KR, Flagstad Ø, et al. Estimating red fox density using non-invasive genetic sampling and spatial capture-recapture modelling. *Oecologia*. (2022) 198:139–51. doi: 10.1007/s00442-021-05087-3

64. Alshammari A, Subhani MI, Wakid MH, Alkhaldi AAM, Hussain S, Malik MA, et al. Genetic diversity and population structure of *Echinococcus multilocularis*: an in-silico global analysis. *J Adv Vet Anim Res*. (2024) 11:264–74. doi: 10.5455/javar.2024.k772

65. Alvi MA, Khalid A, Ali RMA, Saqib M, Qamar W, Li L, et al. Genetic variation and population structure of *Fasciola hepatica*: an in silico analysis. *Parasitol Res*. (2023) 122:2155–73. doi: 10.1007/s00436-023-07917-0

66. Adkins CA, Stott P. Home ranges, movements and habitat associations of red foxes *Vulpes vulpes* in suburban Toronto, Ontario, Canada. *J Zool*. (2006) 244:335–46. doi: 10.1111/j.1469-7998.1998.tb00038.x

67. Gloor S, Bontadina F, Hegglin D, Deplazes P, Breitenmoser U. The rise of urban fox populations in Switzerland. *Mamm Biol*. (2001) 66:155–64. doi: 10.5167/uzh-141504

68. Deplazes P, Hegglin D, Gloor S, Romig T. Wilderness in the city: the urbanization of *Echinococcus multilocularis*. *Trends Parasitol*. (2004) 20:77–84. doi: 10.1016/j.pt.2003.11.011

69. Contesse P, Hegglin D, Gloor S, Bontadina F, Deplazes P. The diet of urban foxes (*Vulpes vulpes*) and the availability of anthropogenic food in the city of Zürich, Switzerland. *Mamm Biol*. (2004) 69:81–95. doi: 10.1078/1616-5047-00123

70. Hegglin D, Ward PI, Deplazes P. Anthelmintic baiting of foxes against urban contamination with *Echinococcus multilocularis*. *Emerg Infect Dis*. (2003) 9:1266–72. doi: 10.3201/eid0910.030138

71. Tuomikoski E, Selonen V, Merimaa K, Laaksonen T. Diet of the raccoon dog, an invasive mesopredator, during the breeding season of declining waterbird populations. *Glob Ecol Conserv*. (2024) 51:e02917. doi: 10.1016/j.gecco.2024.e02917

frontiers | Frontiers in Veterinary Science

TYPE Original Research
PUBLISHED 19 December 2024
DOI 10.3389/fvets.2024.1498682

Check for updates

OPEN ACCESS

EDITED BY
Hongbin Yan,
Chinese Academy of Agricultural Sciences, China

REVIEWED BY
Houqiang Luo,
Wenzhou Vocational College of Science and Technology, China
František Zigo,
University of Veterinary Medicine and Pharmacy in Košice, Slovakia

*CORRESPONDENCE
Naimat Ullah Khan
✉ naimatullahkhan19@yahoo.com
Farhad Badshah
✉ farhadbadshah999@gmail.com

RECEIVED 19 September 2024
ACCEPTED 09 December 2024
PUBLISHED 19 December 2024

CITATION
Rafiq M, Khan NU, Khan I, Ahmad M, Bibi A, Ben Said M, Belkahia H, Tariq M, Saeed S, Abdel-Maksoud MA, El-Tayeb MA, Fatima S, Kiani BH, Alfuraydi AA and Badshah F (2024) Evaluating prevalence, risk factors, and diagnostic techniques for *Cryptosporidium* infection in goats and surrounding water sources.
Front. Vet. Sci. 11:1498682.
doi: 10.3389/fvets.2024.1498682

COPYRIGHT
© 2024 Rafiq, Khan, Khan, Ahmad, Bibi, Ben Said, Belkahia, Tariq, Saeed, Abdel-Maksoud, El-Tayeb, Fatima, Kiani, Alfuraydi and Badshah. This is an open-access article distributed under the terms of the Creative Commons Attribution License (CC BY). The use, distribution or reproduction in other forums is permitted, provided the original author(s) and the copyright owner(s) are credited and that the original publication in this journal is cited, in accordance with accepted academic practice. No use, distribution or reproduction is permitted which does not comply with these terms.

Evaluating prevalence, risk factors, and diagnostic techniques for *Cryptosporidium* infection in goats and surrounding water sources

Manahil Rafiq[1], Naimat Ullah Khan[2]*, Imad Khan[2], Mansoor Ahmad[1], Aiman Bibi[3], Mourad Ben Said[4,5], Hanène Belkahia[5], Muhammad Tariq[6], Silwat Saeed[7], Mostafa A. Abdel-Maksoud[8], Mohamed A. El-Tayeb[8], Sabiha Fatima[9], Bushra Hafeez Kiani[10], Akram A. Alfuraydi[8] and Farhad Badshah[1,11,12]*

[1]Department of Zoology, Abdul Wali Khan University, Mardan, Pakistan, [2]College of Veterinary Sciences and Animal Husbandry, Abdul Wali Khan University, Mardan, Pakistan, [3]Department of Chemistry, Hazara University Mansehra, Mansehra, Pakistan, [4]Department of Basic Sciences, Higher Institute of Biotechnology of Sidi Thabet, University of Manouba, Manouba, Tunisia, [5]Laboratory of Microbiology, National School of Veterinary Medicine of Sidi Thabet, University of Manouba, Manouba, Tunisia, [6]College of Animal Science and Technology, Nanjing Agricultural University, Nanjing, China, [7]Institute of Animal Sciences, Chinese Academy of Agricultural Sciences, Beijing, China, [8]Botany and Microbiology Department, College of Science, King Saud University, Riyadh, Saudi Arabia, [9]Department of Clinical Laboratory Science, College of Applied Medical Sciences, King Saud University, Riyadh, Saudi Arabia, [10]Department of Biology and Biotechnology, Worcester Polytechnic Institute, Worcester, MA, United States, [11]Shenzhen Branch, Guangdong Laboratory of Lingnan Modern Agriculture, Key Laboratory of Livestock and Poultry Multi-Omics of MARA, Agricultural Genomics Institute at Shenzhen, Chinese Academy of Agricultural Sciences, Shenzhen, China, [12]State Key Laboratory of Animal Biotech Breeding, Institute of Animal Sciences, Chinese Academy of Agricultural Sciences, Beijing, China

Background: *Cryptosporidium* spp. are protozoan parasites that infect the gastrointestinal tract of various animals, including goats, and can also contaminate water sources, posing a significant public health risk. Detecting *Cryptosporidium* oocysts in fecal and water samples is critical for understanding the epidemiology of cryptosporidiosis and implementing appropriate control measures. Various staining methods, such as the Modified Ziehl-Neelsen (ZN) and Kenyon's Acid-Fast (KAF) staining techniques, are employed to identify these oocysts. This study compared the effectiveness of these two staining methods in detecting *Cryptosporidium* oocysts in goat feces and water samples across different geographic regions in district of Mardan, Khyber Pakhtunkhwa, Pakistan, and other factors such as genders, age groups, diarrheal statuses, and feeding regimes.

Methods: A total of 300 fecal and 300 water samples were collected from goats and water sources in four geographic regions: Tehsil Katlang, Tehsil Takhtbhai, Tehsil Mardan, and Tehsil Lundkhwarh. Samples were categorized based on gender, age group (<1 year, 1–2 years, and >2 years), diarrheal status, and feeding regime (stall feeding, grazing). The two staining methods, ZN and KAF staining, were employed to detect *Cryptosporidium* oocysts. The detection rates were calculated, and statistical analyses were performed to compare the effectiveness of the two methods across different categories.

Results: The overall detection rates of *Cryptosporidium* oocysts for fecal samples were 61.00% (95% CI: 55.22–66.55%) using the ZN method and 63.33% (95% CI: 57.60–68.79%) using KAF method, with no significant difference ($p > 0.05$). The highest detection rate was observed in Tehsil Katlang (70.66%) with the ZN method and in both Tehsil Katlang and Takhtbhai (66.66%) with the KAF staining method, having no significant difference ($p > 0.05$). Gender-wise analysis in fecal samples showed similar detection rates for males and females, with no significant differences. Age-wise, the highest detection rates were found in the youngest age group (<1 year) using the ZN method, and in the oldest age group (>2 years) using KAF staining, with no significant differences between age groups. Diarrheal status analysis indicated higher detection rates in diarrheic goats for both methods, with the highest detection rate in the diarrheic group of Tehsil Katlang (84.61%) using the ZN method. Feeding regime analysis showed no significant differences between stall-fed and grazing goats. For water samples, the detection rates of *Cryptosporidium* oocysts were significantly different between the two methods. The ZN technique had a significantly higher overall detection rate of 16.00% (95% CI: 12.03–20.64%) compared to 1.00% (95% CI: 0.20–2.89%) for KAF staining ($p < 0.001$). The performance of the two staining methods for the detection of *Cryptosporidium* oocysts in contaminated water samples from different geographic regions was also presented.

Conclusion: Both ZN and KAF staining methods are effective for detecting *Cryptosporidium* oocysts in goat feces. However, in water samples, the ZN method showed a significantly higher detection rate compared to KAF staining method, suggesting its suitability for environmental surveillance. These findings highlight the importance of integrating reliable diagnostic techniques with public health interventions to mitigate the zoonotic risks of cryptosporidiosis.

KEYWORDS

cryptosporidiosis, *Cryptosporidium* oocysts, goats, water sources, risk factors, Pakistan

1 Introduction

Cryptosporidium is a significant enteric protozoan parasite that can infect a wide range of hosts, including humans, livestock, and wildlife (1). This apicomplexan parasite is the causative agent of cryptosporidiosis, a diarrheal disease that can be particularly severe in immunocompromised individuals (2). *Cryptosporidium* species have a complex life cycle, with both asexual and sexual stages, which allows them to effectively colonize and persist within the gastrointestinal tract of their hosts (3).

Cryptosporidial infections in goats can lead to diarrhea, weight loss, and reduced productivity, posing a threat to goat farming and the livelihoods of small-scale farmers (3, 4). Goats are considered important reservoirs of *Cryptosporidium*, as they can harbor both host-adapted and zoonotic species of the parasite (4, 5). Infected goats can shed large numbers of *Cryptosporidium* oocysts in their feces, which can contaminate the environment and serve as a source of infection for other animals and humans (1).

The prevalence of *Cryptosporidium* infection in goats can vary widely, depending on the geographical region, management practices, and other factors (6). Understanding the epidemiology of *Cryptosporidium* in goats, including the identification of risk factors associated with infection, is crucial for the development of effective control and prevention strategies (5, 7). Studies like Peng et al. (8) have shown how farm management practices, age, and health status significantly influence *Cryptosporidium* prevalence in yaks, emphasizing similar risk factors observed in goats. Additionally, molecular characterization studies such as Shehata et al. (9) demonstrate the value of using genotyping to identify zoonotic *Cryptosporidium* strains in livestock and their impact on host health. For instance, a recent meta-analysis highlighted that infections in livestock often reflect regional variations in climate and water management practices, making localized studies essential for effective parasite control (10).

The zoonotic potential of *Cryptosporidium* species poses a public health concern, as infected animals can serve as a reservoir for transmission to humans (1, 5). Similarly, other zoonotic pathogens, such as Toxoplasma gondii, have demonstrated significant flow within the food chain, necessitating robust surveillance measures in livestock (11). *Cryptosporidium* is considered an important zoonotic pathogen, with several species and genotypes capable of infecting both humans and animals (12, 13). Outbreaks of cryptosporidiosis have been linked to direct contact with infected livestock, as well as the consumption of contaminated water or food (6, 14). Recent research shows that children, elderly, and immunocompromised individuals are particularly vulnerable to severe cryptosporidiosis when exposed to contaminated water or animal environments (15).

Contaminated water sources, such as surface water, groundwater, and drinking water, can also be a source of *Cryptosporidium* transmission, contributing to the spread of the parasite in both human and animal populations (6, 16). Recent investigations, conducted by Hussain et al. (17), highlight the diversity of aquatic parasites in

pristine water sources. They demonstrate that even minimally disturbed ecosystems can harbor a wide range of protozoan pathogens, including *Cryptosporidium*, which poses significant zoonotic risks. Water-borne cryptosporidiosis outbreaks have been reported worldwide, highlighting the importance of monitoring water quality for the presence of *Cryptosporidium* (18, 19). The environmental persistence and chlorine resistance of *Cryptosporidium* oocysts make them a significant challenge for water treatment and disinfection processes (7, 20). This resilience is emphasized in recent studies on waterborne outbreaks in low-resource areas, where limited water treatment facilities compound the risk of zoonotic transmission (21).

Cryptosporidiosis is an emerging zoonotic disease with significant implications for both human and animal health. Recent studies emphasize the role of livestock as primary reservoirs for *Cryptosporidium*, contributing to environmental contamination and waterborne transmission risks. For instance, research by Javed and Alkheraije (22), highlights the spread of *Cryptosporidium* via contaminated food and water, underscoring the importance of farm hygiene and water quality management in mitigating zoonotic risks. Studies conducted in diverse geographic settings illustrate the widespread nature of *Cryptosporidium* transmission across agricultural regions. A study from Mexico demonstrated substantial prevalence of *Cryptosporidium* in both domestic and wild animals, reinforcing the need for rigorous monitoring of animal and environmental contamination (23). Similarly, research on free-ranging livestock in Tibet found that shared water sources substantially heighten infection risks, illustrating how environmental factors can influence the spread of *Cryptosporidium* (24). These insights underscore the necessity of surveillance efforts, especially in agricultural regions where water contamination poses public health risks.

Accurate diagnosis and understanding the prevalence and risk factors associated with *Cryptosporidium* infections in goats and contaminated water sources are crucial for the development of effective control and prevention strategies (7). Robust diagnostic techniques, such as microscopy, immunoassays, and molecular methods, are necessary to accurately identify *Cryptosporidium* species and genotypes, which can have different host specificities and pathogenic potential (12, 25). Epidemiological studies investigating the prevalence and distribution of *Cryptosporidium* in goats and water sources can provide valuable insights into the transmission dynamics and risk factors associated with these infections (26, 27).

Limited research has been conducted on the epidemiology of *Cryptosporidium* infections in goats and the contamination of water sources in Pakistan (12, 13). Previous studies in the country have primarily focused on human cryptosporidiosis, with limited data available on the situation in livestock and the environment. This knowledge gap highlights the need for more comprehensive investigations into the prevalence and risk factors associated with *Cryptosporidium* infections in the Pakistani context, particularly in the important agricultural sector of goat farming.

This study represents the first comprehensive investigation in Pakistan to evaluate the prevalence of *Cryptosporidium* infection in goats within the Mardan district, Khyber Pakhtunkhwa. It aims to identify associated risk factors, detect *Cryptosporidium* in surrounding water sources, and assess the performance of diagnostic techniques, with a novel emphasis on comparing the efficacy of the Modified Ziehl-Neelsen (ZN) and Kenyon's Acid-Fast (KNKAF) staining methods for detecting *Cryptosporidium* in both fecal and water samples.

2 Materials and methods

2.1 Sampling area

The study was conducted in the district of Mardan, located in KP, Pakistan, at coordinates 34.19860N and 72.04040E (Figure 1). Mardan is situated in the southwest of the district at an altitude of 283 meters (928 ft). The district comprises five different Tehsils, of which four were selected: Katlang, Takht Bahi, Mardan, and Lund-Khwarh. Within these Tehsils, five villages were randomly selected for sampling in each Tehsil. The coordinates and elevations of the selected Tehsils are as follows: Katlang (34°21′7.41″N, 72°4′35.2″E, 375.14 m), Takht Bahi (34°19′9.00″N, 71°56′26.99″E, 416 m), Mardan (34°12′7.02″N, 72°03′9.14″E, 337 m), and Lund-Khwarh (34°22′59.99”N, 71°58′59.99″E, 371 m). These locations were chosen to represent the diverse geographic and environmental conditions within the district.

2.2 Questionnaire

A detailed questionnaire was designed to systematically collect all relevant data related to the host and environmental conditions for this study on *Cryptosporidium* spp. in goats and water sources. Information such as age, geographic area, sex, feeding habits, and disease conditions, among other variables, were recorded prior to sample collection. This data collection was essential for understanding the epidemiology of cryptosporidiosis and implementing appropriate control measures. Participation of the goat owners was mandatory during the filling of the questionnaire to ensure the accuracy and completeness of the information. Owners provided detailed insights about each animal and water source, allowing for a thorough analysis of factors potentially influencing the prevalence of *Cryptosporidium* infections.

2.3 Sample collection, filtration, and preservation

2.3.1 Fecal sample collection and preservation

A total of 300 fecal samples were randomly collected from goat farms and home-kept goats with different feeding habits, such as stall feeding and grazing. Samples were gathered from goats of various age groups: less than 1 year (G1), 1–2 years (G2), and 3–5 years (G3). All samples came from flocks owned by private owners. Each farm typically had about 200–250 goats, while home-kept goats ranged from 3 to 10 or more. About 5–10 grams of feces were collected in sterile plastic bottles using appropriate techniques and protective measures, including gloves, forceps, and water-resistant tags. Fecal samples were collected in two ways: from freshly passed feces and directly from the rectum. After collection, formalin was added to preserve the samples. Before further processing, the samples were stored in a refrigerator at −60°C.

2.3.2 Collection and preservation of water samples

Water samples (n = 300) of approximately 100 ml were collected in sterilized plastic bottles from various sources, including surface water,

FIGURE 1
Map of the Mardan District, Khyber Pakhtunkhwa, Pakistan.

groundwater (tubewells), wells, canals, and tap water. Samples were collected from a depth of about 20–30 cm below the surface. The samples were then filtered through gauze or filter cartridges with a pore size of 0.4–1 μm (28, 29). The filtered samples were stored in a refrigerator at 1–10°C and delivered to the laboratory within 96 h. For further analysis, including staining, a volume of 10 μl (one drop) was used (28, 30, 31).

2.4 *Cryptosporidium* oocytes identification

Cryptosporidium oocysts were detected in both freshwater and fecal samples using two diagnostic techniques: (i) Ziehl-Neelsen acid-fast staining (ZN) and (ii) Kenyon's acid-fast staining (KAF) (32). Prepared slides were properly stained and examined under a microscope. Oocysts were identified based on their distinctive size, shape, and staining characteristics.

2.5 Prevalence calculation

The prevalence rate of *Cryptosporidium* in goat and water samples was calculated using the following formula:

Prevalence rate (%) = (total number of positive samples/total number of examined samples) × 100.

2.6 Statistical analysis

The collected data was analyzed using various software tools. Microsoft Excel was used to organize and store data for further analysis. Exact confidence intervals (CI) for prevalence rates at the 95% level were calculated. to compare differences in prevalence rates among various variables of each related risk factor, chi square test or Fisher's exact test were performed using Epi Info 6.01 (CDC, Atlanta, USA) with a cut-off value of 0.05.

3 Results

3.1 *Cryptosporidium* oocyst detection in goat feces

Overall, the detection rate of *Cryptosporidium* oocysts was 61.00% (95% CI: 55.22–66.55%) for the ZN method and 63.33% (95% CI: 57.60–68.79%) for the KAF staining method (Table 1). The highest detection rate of oocysts by the ZN method was observed in the Tehsil Katlang region, reaching 70.66% (95% CI: 59.02–80.61%), while the lowest rate was recorded in the Tehsil Takhtbhai and Tehsil Lundkhwarh regions, with 56.00% (95% CI: 44.05–67.45%) in both cases. The statistical analysis revealed no significant difference

between the two staining methods ($p > 0.05$). Regarding the KAF staining method, the highest rate was observed in the Tehsil Katlang and Tehsil Takhtbhai regions, with 66.66% (95% CI: 54.83–77.13%) in both cases, while the lowest rate was recorded in the Tehsil Lundkhwarh region, with 57.33% (95% CI: 45.37–68.69%; Table 1).

3.2 *Cryptosporidium* oocyst detection by gender across geographic regions

The total detection rates using the ZN staining method were 63.80% (95% CI: 53.85–72.96%) in males and 65.07% (95% CI: 56.07–73.35%) in female. For the KAF staining method, the total detection rates were 64.86% (95% CI: 55.22–73.68%) for males and 67.52% (95% CI: 58.24–75.88%) for females. For the ZN staining method, the highest detection rate was observed in the Tehsil Katlang region for both males (70.37, 95% CI: 49.81–86.24%) and females (69.69, 95% CI: 51.28–84.40%). The lowest rate was recorded in the Tehsil Lundkhwarh region for males (59.00, 95% CI: 36.35–79.29%) and in the Tehsil Takhtbhai region for females (54.83, 95% CI: 36.03–72.68%). The statistical analysis showed no significant difference in the detection rates between males and females across all regions ($p > 0.05$; Table 2). Regarding the KAF staining method, the highest detection rate was observed in the Tehsil Takhtbhai region for both males (70.83, 95% CI: 48.90–87.38%) and females (70.37, 95% CI: 49.81–86.24%). The lowest rate was recorded in the Tehsil Lundkhwarh region for males (60.71, 95% CI: 40.57–78.49%) and in the Tehsil Mardan region for females (69.23, 95% CI: 48.21–85.67%). Similarly, the statistical analysis revealed no significant difference in the detection rates between males and females across all regions ($p > 0.05$; Table 2).

3.3 *Cryptosporidium* oocysts detection in goat feces across age groups and geographic regions

For the ZN staining method, the highest detection rate was observed in the youngest age group (< 1 year), with 66.00% (95% CI: 55.84–75.17%). The lowest rate was seen in the oldest age group (> 2 years), with 57.00% (95% CI: 46.71–66.86%). However, the differences between the age groups were not statistically significant ($p = 0.353$). For KAF staining method, the highest detection rate was observed in the oldest age group (> 2 years), with 67.00% (95% CI: 56.88–76.08%). The lowest rate was seen in the middle age group (1–2 years), with 59.00% (95% CI: 48.71–68.73%). Again, the differences between the age groups were not statistically significant ($p = 0.472$). The highest detection rate by the ZN staining method was observed in age groups 1 and 2 of the Mardan tehsil, with a rate of 80.00% (95% CI: 59.29–93.16%). The lowest rate was observed in

TABLE 1 Comparison of ZN and KAF methods for the Detection of *Cryptosporidium* oocysts in goat feces.

Geographic region	ZN staining		KAF staining	
	Positive/total, rate (%, C.I.[1])	*p* value	Positive/total, rate (%, C.I.[1])	*p* value
Tehsil Katlang	53/75 (70.66, 59.02–80.61)	0.210	50/75 (66.66, 54.83–77.13)	0.594
Tehsil Takhtbhai	42/75 (56.00, 44.05–67.45)		50/75 (66.66, 54.83–77.13)	
Tehsil Mardan	46/75 (61.33, 49.37–72.36)		47/75 (62.66, 50.73–73.56)	
Tehsil Lundkhwarh	42/75 (56.00, 44.05–67.45)		43/75 (57.33, 45.37–68.69)	
Total	183/300 (61.00, 55.22–66.55)		190/300 (63.33, 57.60–68.79)	

The statistical analysis revealed no significant difference between the two staining methods ($p > 0.05$).
[1]C.I.: 95% confidence interval.

TABLE 2 Comparison of ZN and KAF Staining for the detection of *Cryptosporidium* oocysts in goat feces by gender.

Geographic region	ZN staining			KAF staining		
	Positive/total, rate (% ± C.I.[1])		*p* value	Positive/total, rate (% ± C.I.[1])		*p* value
	Male	Female		Male	Female	
Tehsil Katlang	19/27 (70.37, 49.81–86.24)	23/33 (69.69, 51.28–84.40)	0.955	18/27 (66.66, 46.03–83.48)	18/26 (69.23, 48.21–85.67)	0.843
Tehsil Takhtbhai	18/30 (60.00, 40.60–77.34)	17/31 (54.83, 36.03–72.68)	0.881	17/24 (70.83, 48.90–87.38)	19/27 (70.37, 49.81–86.24)	0.971
Tehsil Mardan	17/26 (65.38, 44.33–82.78)	23/32 (71.87, 53.25–86.25)	0.805	20/32 (62.50, 43.69–78.89)	18/26 (69.23, 48.21–85.67)	0.795
Tehsil Lundkhwarh	13/22 (59.00, 36.35–79.29)	19/30 (63.33, 43.85–80.07)	0.982	17/28 (60.71, 40.57–78.49)	24/38 (63.15, 45.99–78.18)	0.840
Total	67/105 (63.80 ± 53.85–72.96)	82/126 (65.07, 56.07–73.35)	0.949	72/111 (64.86, 55.22–73.68)	79/117 (67.52, 58.24–75.88)	0.776

[1]C.I.: 95% confidence interval.

age group 3 of the Lundkhwarh tehsil, with 48.00% (95% CI: 27.79–68.69%). No statistically significant difference was observed between the age groups for this method ($p = 0.353$). For the Kenyon acid-fast staining method, the highest detection rate was observed in age group 3 of the Takhtbhai tehsil, with 80.00% (95% CI: 59.29–93.16%). The lowest rate was observed in age group 2 of the Takhtbhai tehsil, with 52.00% (95% CI: 31.30–72.20%). No statistically significant difference was observed between the age groups for this method ($p = 0.472$). In the Mardan tehsil, the detection rate of *Cryptosporidium* oocysts by the ZN staining method was the highest in age group 1, with 80.00% (95% CI: 59.29–93.16%). This rate decreased significantly in the higher age groups, reaching 64.00% (95% CI: 42.52–82.02%) in age group 2 and only 40.00% (95% CI: 21.12–61.33%) in age group 3 (Table 3). The statistical analysis revealed a significant difference between the age groups ($p = 0.013$), indicating that the age of the goats has a significant impact on the detection of *Cryptosporidium* oocysts by this staining method in the Mardan tehsil (Table 4).

3.4 Detection of *Cryptosporidium* oocysts by diarrheal status

The overall results show that the ZN staining method had a higher detection rate for *Cryptosporidium* oocysts in goat feces compared to KAF staining method. The total positive rate for the ZN method was 73.46% (95% CI: 58.91–85.05%) in the diarrheic group and 57.76% (95% CI: 51.39–63.95%) in the non-diarrheic group, with no statistically significant difference between the two groups ($p = 0.058$). For KAF staining method, the total positive rate was 69.38% (95% CI: 54.58–81.74%) in the diarrheic group and 61.75% (95% CI: 55.43–67.79%) in the non-diarrheic group, with no statistically significant difference between the two groups ($p = 0.394$). The highest detection rate for the ZN method was observed in the diarrheic group of the Katlang tehsil, with 84.61% (95% CI: 65.13–95.64%). The lowest rate for this method was seen in the non-diarrheic group of the Lundkhwarh tehsil, with 50.72% (95% CI: 38.40–62.97%). For KAF staining method, the highest detection rate was observed in the non-diarrheic group of the Takhtbhai

TABLE 3 Comparison of ZN and KAF staining for the detection of *Cryptosporidium* oocysts in goat feces by age group.

Geographic region	ZN staining				KAF staining			
	Positive/total (Rate %, C.I.[1])			*p* value	Positive/total (Rate %, C.I.[1])			*p* value
	Age group 1	Age group 2	Age group 3		Age group 1	Age group 2	Age group 3	
Tehsil Katlang	20/25 (80.00, 59.29–93.16)	18/25 (72.00, 50.61–87.92)	15/25 (60.00, 38.66–78.87)	0.294	18/25 (72.00, 50.61–87.92)	17/25 (68.00, 46.49–85.05)	16/25 (64.00, 42.52–82.02)	0.832
Tehsil Takhtbhai	14/25 (56.00, 34.92–75.59)	14/25 (56.00, 34.92–75.59)	19/25 (76.00, 54.87–90.64)	0.240	17/25 (68.00, 46.49–85.05)	13/25 (52.00, 31.30–72.20)	20/25 (80.00, 59.29–93.16)	0.108
Tehsil Mardan	20/25 (80.00, 59.29–93.16)	16/25 (64.00, 42.52–82.02)	10/25 (40.00, 21.12–61.33)	0.013*	17/25 (68.00, 46.49–85.05)	13/25 (52.00, 31.30–72.20)	17/25 (68.00, 46.49–85.05)	0.401
Tehsil Lundkhwarh	12/25 (48.00, 27.79–68.69)	17/25 (68.00, 46.49–85.05)	13/25 (52.00, 31.30–72.20)	0.320	13/25 (52.00, 31.30–72.20)	16/25 (64.00, 42.52–82.02)	14/25 (56.00, 34.92–75.59)	0.682
Total	66/100 (66.00, 55.84–75.17)	65/100 (65.00, 54.81–74.27)	57/100 (57.00, 46.71–66.86)	0.353	65/100 (65.00, 54.81–74.27)	59/100 (59.00, 48.71–68.73)	67/100 (67.00, 56.88–76.08)	0.472

All samples were collected from different age groups, i.e., group 1 = < 1 year, group 2 = 1–2 years, and group 3= > 2 years.
[1]C.I.: 95% confidence interval.
*Statistically significant test.

TABLE 4 Comparison of ZN and KAF Staining for the Detection of *Cryptosporidium* oocysts in goat feces by Diarrheal Status.

Geographic region	ZN staining			KAF staining		
	Positive/total, rate (% ± C.I.[1])		*p* value	Positive/total, rate (% ± C.I.[1])		*p* value
	Diarrheic	Non-diarrheic		Diarrheic	Non-diarrheic	
Tehsil Katlang	22/26 (84.61, 65.13–95.64)	31/49 (63.26, 48.28–76.57)	0.095	19/26 (73.07, 52.21–88.42)	31/49 (63.26, 48.28–76.57)	0.548
Tehsil Takhtbhai	6/11 (54.54, 23.37–83.25)	36/64 (56.25, 43.27–68.62)	0.916	6/11 (54.54, 23.37–83.25)	43/64 (93.47, 54.31–78.41)	0.637
Tehsil Mardan	4/6 (66.66, 22.27–95.67)	43/69 (62.31, 49.83–73.70)	0.833	5/6 (83.33, 35.87–99.57)	42/69 (60.86, 48.37–72.40)	0.514
Tehsil Lundkhwarh	4/6, (66.66, 22.27–95.67)	35/69 (50.72, 38.40–62.97)	0.746	4/6 (66.66, 22.27–95.67)	39/69 (56.52, 38.40–62.97)	0.746
Total	36/49 (73.46, 58.91–85.05)	145/251 (57.76, 51.39–63.95)	0.058	34/49 (69.38, 54.58–81.74)	155/251 (61.75, 55.43–67.79)	0.394

[1]C.I.: 95% confidence interval.

10.3389/fvets.2024.1498682

tehsil, with 93.47% (95% CI: 54.31–78.41%). The lowest rate for this method was seen in the diarrheic group of the Takhtbhai tehsil, with 54.54% (95% CI: 23.37–83.25%; Table 4).

3.5 Detection of *Cryptosporidium* oocysts by feeding regime

Overall, the results show that the ZN staining method has a higher detection rate for *Cryptosporidium* oocysts in goat feces compared to KAF staining, particularly in the stall-feeding group. However, the differences between the feeding regimes were not statistically significant for the majority of the tehsils. For the ZN staining method, the highest detection rate was observed in the Tehsil Mardan region among goats under stall feeding, with a 100% (95% CI: 84.56–100%) positive rate. This was significantly higher than the detection rate in the grazing group of the same tehsil, which was 63.33% (95% CI: 43.85–80.07%; $p = 0.004$). In contrast, the lowest detection rate for the ZN method was seen in the grazing group of the Tehsil Lundkhwarh, with a rate of 44.44% (95% CI: 21.53–69.24%). The detection rate in the stall-feeding group of the same tehsil was higher at 64.28% (95% CI: 35.13–87.24%), but the difference was not statistically significant ($p = 0.448$). For KAF staining method, the highest detection rate was observed in the grazing group of the Tehsil Katlang, with a rate of 72.00% (95% CI: 50.61–87.92%). The lowest rate for this method was seen in the stall-feeding group of the Tehsil Lundkhwarh, with a rate of 55.55% (95% CI: 35.32–74.52%). However, the differences in detection rates between the feeding regimes were not statistically significant for any of the tehsils ($p > 0.05$; Table 5).

3.6 Detection of *Cryptosporidium* oocysts in contaminated water samples by geographic region

When comparing the two staining methods, the ZN technique had a significantly higher overall detection rate of 16.00% (95% CI: 12.03–20.64%) compared to 1.00% (95% CI: 0.20–2.89%) for KAF staining ($p < 0.001$). For the ZN staining method, the highest detection rate was observed in Tehsil Katlang, with a positive rate of 24.00% (95% CI: 14.88–35.25%), which was not significantly different from the detection rates in the other tehsils ($p > 0.05$). The lowest detection rate for this method was observed in Tehsil Lundkhwarh, with a positive rate of 9.33% (95% CI: 3.83–18.28%). In contrast, KAF staining method showed much lower detection rates overall. The highest rate was observed in Tehsil Katlang, with a positive rate of 2.66% (95% CI: 0.32–9.30%), which was not significantly different from the other tehsils ($p > 0.05$). The Tehsil Takhtbhai and Tehsil Mardan had the lowest detection rates, with 0% positive samples (Table 6).

TABLE 5 Comparison of ZN and KAF staining for the detection of *Cryptosporidium* oocysts in goat feces by feeding regime.

Geographic region	ZN staining			KAF staining		
	Positive/total, rate (% ± C.I.[1])		*p* value	Positive/total, rate (% ± C.I.[1])		*p* value
	Stall feeding	Grazing		Stall feeding	Grazing	
Tehsil Katlang	15/22 (68.18, 45.12–86.13)	19/25 (76.00, 54.87–90.64)	0.786	12/20 (60.00, 36.05–80.88)	18/25 (72.00, 50.61–87.92)	0.595
Tehsil Takhtbhai	17/29 (58.62, 38.93–76.47)	13/22 (59.09, 36.35–79.29)	0.973	17/25 (68, 46.49–85.05)	15/23 (65.21, 42.73–83.62)	0.839
Tehsil Mardan	22/22 (100, 84.56–100)	19/30 (63.33, 43.85–80.07)	0.004*	16/27 (59.25, 38.79–77.61)	19/28 (67.85, 47.64–84.12)	0.702
Tehsil Lundkhwarh	9/14 (64.28, 35.13–87.24)	8/18 (44.44, 21.53–69.24)	0.448	15/27 (55.55, 35.32–74.52)	13/19 (68.42, 43.44–87.42)	0.566
Total	63/87 (72.41, 61.78–81.45)	59/95 (62.10, 51.57–71.86)	0.186	60/99 (60.60, 50.27–70.28)	65/95 (72.63, 58.07–77.57)	0.323

[1]C.I.: 95% confidence interval.
*Statistically significant test.

TABLE 6 Comparison of ZN and KAF staining for the detection of *Cryptosporidium* oocysts in water samples.

Geographic region	ZN staining		KAF staining	
	Positive/total, rate (% ± C.I.[1])	*p* value	Positive/total, rate (% ± C.I.[1])	*p* value
Tehsil Katlang	18/75 (24.00, 14.88–35.25)	0.087	2/75 (2.66, 0.32–9.30)	0.295
Tehsil Takhtbhai	13/75 (17.33, 9.56–27.81)		0/75 (0)	
Tehsil Mardan	10/75 (13.33, 6.58–23.15)		0/75 (0)	
Tehsil Lundkhwarh	7/75 (9.33, 3.83–18.28)		1/75 (1.33, 0.03–7.20)	
Total	48/300 (16.00, 12.03–20.64)		3/300 (1.00, 0.20–2.89)	

[1]C.I.: 95% confidence interval.

3.7 Detection of *Cryptosporidium* oocysts in different water sources

Overall, the ZN staining method showed a significantly higher detection rate of 33.33% (95% CI: 23.05–44.91%) compared to 7.69% (95% CI: 2.87–15.99%) for the KAF staining method ($p = 0.006$). The ZN staining method showed the highest detection rate of 51.51% (95% CI: 33.54–69.20%) in stream water samples from the Tehsil Takhtbhai region, which was significantly higher than the detection rates in other water sources and regions ($p < 0.001$). In contrast, the ZN method had the lowest detection rate of 0% in well and tubewell water samples from the Tehsil Lundkhwarh and Tehsil Mardan regions. For the KAF staining method, the highest detection rate was 16.66% (95% CI: 2.08–48.41%) in stream water samples from the Tehsil Katlang region, which was not significantly different from the other water sources and regions ($p = 0.081$). The KAF staining method had the lowest detection rate of 0% in well and tubewell water samples from the Tehsil Lundkhwarh and Tehsil Mardan regions (Table 7).

4 Discussion

In this study, we examined *Cryptosporidium* spp. infection in goats as well as in different water sources in four tehsils of Mardan district, Pakistan. Several risk factors such as age, sex, personal hygiene, poor sanitation system, diarrheic and non-diarrheic conditions, and the use of various water sources for drinking were studied. These factors may increase the risk of outbreaks worldwide or be a major cause of cryptosporidiosis, often neglected (33, 34). In our current study, fecal samples from symptomatic and asymptomatic goats were collected and examined for the presence of the suspected parasite.

The overall detection rates of *Cryptosporidium* oocysts were similar between the two methods, with 61.00% for the ZN method and 63.33% for the KAF staining method. No statistically significant difference was observed between the two staining methods, suggesting that both methods are equally effective for the detection of *Cryptosporidium* oocysts in goat feces. The consistency in the performance of these two methods indicates that they can be used interchangeably for the diagnosis of *Cryptosporidium* infection in goats. The high detection rates observed with both staining methods suggest a significant prevalence of *Cryptosporidium* infection in the goat population within the study area. The findings highlight the importance of implementing effective diagnostic techniques and control measures to reduce the impact of *Cryptosporidium* infection in goats, which can have implications for animal health, productivity, and potentially human health through zoonotic transmission (34). Additionally, advancements in vaccination strategies against zoonotic pathogens like Toxoplasma gondii provide a framework for improving livestock health and mitigating zoonotic risks (35). Similarly, a study conducted by Nemat et al. (36) on diarrheic sheep in Pakistan found that ZN and modified Ziehl-Neelsen (mZN) staining methods yielded comparable detection rates, indicating high prevalence levels in livestock. The consistency across these methods highlights their reliability as practical diagnostic tools in resource-limited settings. Our findings also emphasize the high prevalence of *Cryptosporidium* in the goat population in Mardan, supporting the need for effective diagnostic practices to manage

TABLE 7 Comparison of ZN and KAF staining for the detection of *Cryptosporidium* oocysts in different water sources.

Geographic region	ZN staining					KAF staining				
	Positive/total, rate (% ± C.I.[1])				*p* value	Positive/total, rate (% ± C.I.[1])				*p* value
	Well	Tubewell	Stream	River		Well	Tubewell	Stream	River	
Tehsil Katlang	1/19 (5.26, 0.13–26.02)	3/23 (13.04, 2.77–33.58)	6/12 (50.00, 21.09–78.90)	9/20 (45.00, 23.05–68.47)	0.003*	0/19 (0)	0/23 (0)	2/12 (16.66, 2.08–48.41)	1/20 (5.00, 0.12–24.87)	0.081
Tehsil Takhtbhai	1/23 (4.34, 0.11–21.94)	1/35 (2.87, 0.07–14.91)	5/6 (83.33, 35.87–99.57)	6/12 (50.00, 2.09–78.90)	0.000*	2/23 (8.69, 1.07–28.03)	1/35 (2.85, 0.07–14.91)	2/6 (33.33, 4.32–77.72)	2/12 (16.66, 2.08–48.41)	0.083
Tehsil Mardan	0/34 (0)	1/19 (5.26, 0.13–26.02)	3/8 (37.50, 8.52–75.51)	6/15 (40.00, 16.33–67.71)	0.000*	1/34 (2.94, 0.07–15.32)	0/19 (0)	1/8 (12.5, 0.31–52.65)	2/15 (13.33, 1.65–40.46)	0.238
Tehsil Lundkhwarh	0/14 (0)	0/22 (0)	3/7 (42.85, 9.89–81.59)	5/31 (16.12, 5.45–33.72)	0.005*	0/14 (0)	0/22 (0)	0/7 (0)	1/31 (3.22, 0.08–16.70)	0.704
Total	2/90 (2.22, 0.27–7.79)	5/99 (5.05, 1.65–11.39)	17/33 (51.51, 33.54–69.20)	26/78 (33.33, 23.05–44.91)	0.000*	3/90 (3.33, 0.69–9.43)	1/99 (1.01, 0.02–5.49)	5/33 (15.15, 5.10–31.89)	6/78 (7.69, 2.87–15.99)	0.006*

[1]C.I.: 95% confidence interval.
*Statistically significant test.

infection and mitigate zoonotic transmission risks in regions with close human-animal contact.

The ZN method showed the highest detection rate (70.66%) in the Tehsil Katlang region, while the lowest rates (56.00%) were observed in the Tehsil Takhtbhai and Tehsil Lundkhwarh regions. For the KAF staining method, the highest detection rates (66.66%) were found in the Tehsil Katlang and Tehsil Takhtbhai regions, while the lowest rate (57.33%) was recorded in the Tehsil Lundkhwarh region. These geographical variations in the detection rates of *Cryptosporidium* oocysts may be influenced by factors such as climate, management practices, or other environmental conditions in the different regions (37).

Our data shows that the prevalence of cryptosporidiosis is generally higher in females than in males. In this study, the infection rate in females was 62.87% on ZN staining and 63.47% on KAF staining, compared to 58.01% on ZN and 62.59% on KAF in males. However, another study conducted in Iraq reported a higher infection rate in males (88.4%) than in females (85.5%), with no statistically significant difference ($p > 0.05$) (13). In contrast a study from Kirkuk province showed a higher infection rate in females (63.35%) than in males (58.75%) in Irak (7).

The prevalence of *Cryptosporidium* spp. infection in goats varies across different age groups. Age-wise, the highest detection rates were found in the youngest age group (<1 year) using the ZN method, and in the oldest age group (>2 years) using KAF staining, with no significant differences between age groups. These findings are consistent with other studies. For instance, a study from Pakistan reported that *Cryptosporidium* was most prevalent in goats aged 1 year (20.46%), followed by 1–2 years (13.73%) and 2–3 years (8.27%) (38). Similarly, a study from Serbia found that kids aged 5–21 days had higher mortality (40–50%) and morbidity (75–100%) rates due to *Cryptosporidium* infection compared to older animals (10). Further, a study in China reported an average *Cryptosporidium* prevalence of 2.23% in goats (16), while a Korean study observed the highest prevalence in goats under 2 months of age (5). In children, a study from Kirkuk Province, Iraq found the highest prevalence of *Cryptosporidium* infection in those under 1 and 2 years of age (32.35 and 26.24%, respectively) compared to older children (7). Additionally, *Cryptosporidium* infection has been reported in pre-weaned calves, with one study in Kuwait finding a prevalence of 33.1% in calves less than 1 month old with poor hygiene (18). Differences in detection across age groups could be attributed to immunological maturity and exposure levels. Younger goats might shed more oocysts detectable by ZN, while KAF may better visualize mature oocysts in older goats. These findings highlight the importance of age as a risk factor for *Cryptosporidium* infection in small ruminants and calves, with younger animals generally more susceptible to the parasite.

Our study found that the total prevalence of *Cryptosporidium* spp. in diarrheic goats in the Mardan district was 73.46% when using the ZN staining method. The prevalence in non-diarrheic goats was lower at 57.76%. When using the Kenyon acid-fast (KAF) staining method, the prevalence in diarrheic goats was 69.38%, while in non-diarrheic goats it was 61.75%. These findings align with other studies that have reported *Cryptosporidium* as a significant pathogen causing neonatal diarrhea in small ruminants such as goats, sheep, and calves. For instance, a study by Ali et al. (31) found that diarrhea, after malaria, is the second most crucial disease in livestock, accounting for 17% of cases. They documented a prevalence of 37.74% in non-diarrheic kids and 62.26% in diarrheic kids. Additionally, a study in Algeria by Bennadji et al. (25) reported a *Cryptosporidium* spp. infection rate of 25% in diarrheic goats and sheep. These results highlight the importance of *Cryptosporidium* as a major contributor to diarrheal disease in young small ruminants. The higher prevalence observed in diarrheic animals compared to non-diarrheic ones underscores the pathogenic role of this parasite in causing clinical disease.

Using KAF staining, the prevalence in grazing goats was 72.63%, while in stall-fed goats it was 60.60%. Using the ZN staining, the prevalence in grazing goats was 62.10%, compared to 72.41% in stall-fed goats. These findings align with several recent studies that have reported *Cryptosporidium* infections in children associated with different feeding practices. For instance, the prevalence of *Cryptosporidium* in stool samples was 16.93% in breastfed children, 59.63% in children who drank sterile/mineral water, and 35.79% in those who drank water from tanks, compared to only 4.58% in children using municipal water (7). In the present study, the researchers used both mZN and Kinyoun's acid-fast stains to detect *Cryptosporidium* spp. in stool samples collected from goats in the Mardan district. They also detected *Cryptosporidium* in various water samples from the same locality, which may have been used by the host animals. Similar staining techniques, such as the ZN stain, have been used by other researchers for the detection of *Cryptosporidium* in stool samples (7, 12). Felefel et al. from Iraq reported *Cryptosporidium* spp. infection rate of 26.66% using the ZN stain, while the frequency was different when using other diagnostic methods, such as ELISA and PCR (12). These findings highlight the importance of considering management practices, such as grazing versus stall-feeding, in the epidemiology and control of *Cryptosporidium* infections in small ruminants. Water is an essential nutrient and a basic component of the diet, with no calories but important structural roles in cells. It is therefore crucial to investigate the influence of contaminated water in the transmission of *Cryptosporidium*, a zoonotic pathogen, to different animals. Ensuring the safety and security of drinking water is important for public health, and water used in farming raw vegetables can also be an indirect route of transmission for waterborne protozoa. Surveillance of various water sources in the study area revealed that, for the ZN staining method, detection rates varied significantly across water sources: 51.51% in streams, 33.33% in rivers, 5.05% in tubewells, and 2.22% in wells ($p < 0.001$). For Kenyon's acid-fast staining, detection rates were 15.15% in streams, 7.69% in rivers, 3.33% in wells, and 1.01% in tubewells ($p = 0.006$). These findings align with a previous study by Abbas et al. from Pakistan (26), which reported an overall *Cryptosporidium* prevalence of 11.5% in water bodies, raw vegetables, and soil. The study emphasized that the frequency of *Cryptosporidium* was highest in sewage water (13%), followed by municipal water (10%) and canal water (9.5%). They highlighted that poor hygiene is a significant risk factor affecting the prevalence of *Cryptosporidium* and other parasites. Another study conducted in Igdir, Turkey, on water samples collected from springs found the prevalence of *Cryptosporidium* to be 10.1% by direct examination, 11.6% by nested PCR, and 7.2% by modified acid-fast staining (27). The study did not observe any significant differences in the physicochemical parameters of the water samples, such as pH, salinity, altitude, pressure, and temperature. These results highlight the importance of monitoring water sources and addressing issues related to water contamination and hygiene practices to reduce the transmission of *Cryptosporidium* and other waterborne pathogens to both animals and humans (39).

5 Conclusion

The findings from this study on evaluating the prevalence, risk factors, and diagnostic techniques for *Cryptosporidium* infection in goats and contaminated water sources underscores the critical need for integrated approaches to address this significant public health challenge. The high prevalence of *Cryptosporidium* detected in goat samples and the occurrence of this parasite in water samples highlights the zoonotic nature of this pathogen and the role of contaminated water sources in its transmission. Implementing effective surveillance, water quality monitoring, and targeted interventions to improve hygiene and sanitation practices are essential to reduce the spread of *Cryptosporidium* among animal and human populations. To enhance these efforts, we recommend adopting ZN staining as a reliable method for water surveillance and combining it with targeted educational campaigns for farmers to promote awareness and prevention of *Cryptosporidium* infections. Additionally, future studies should incorporate molecular diagnostic methods to complement staining techniques, enabling more precise identification and characterization of *Cryptosporidium* species. By adopting a One Health perspective that considers the interconnections between animal, human, and environmental health, researchers and public health authorities can work collaboratively to develop comprehensive strategies to reduce the burden of cryptosporidiosis. Continued research to optimize diagnostic techniques and inform evidence-based risk assessment and management will be crucial in safeguarding the health and well-being of both goats and human communities reliant on shared water resources.

Data availability statement

The raw data supporting the conclusions of this article will be made available by the authors, without undue reservation.

Ethics statement

The animal studies were approved by the ethical approval council of the Abdul Wali Khan University, Pakistan, ethically approved this research study (Approval No. AWKUM/ZOO/2022/8005). The studies were conducted in accordance with the local legislation and institutional requirements. Written informed consent was obtained from the owners for the participation of their animals in this study.

Author contributions

MR: Conceptualization, Data curation, Formal analysis, Methodology, Resources, Software, Validation, Visualization, Writing – original draft, Writing – review & editing, Project administration. NK: Conceptualization, Data curation, Formal analysis, Resources, Software, Validation, Visualization, Writing – original draft, Writing – review & editing, Investigation, Supervision. IK: Data curation, Formal analysis, Resources, Software, Writing – review & editing. MA: Data curation, Formal analysis, Writing – review & editing, Visualization. AB: Data curation, Formal analysis, Visualization, Writing – review & editing. MB: Data curation, Formal analysis, Visualization, Writing – review & editing, Investigation, Software, Validation. HB: Data curation, Formal analysis, Software, Writing – review & editing, Resources. MT: Data curation, Formal analysis, Writing – review & editing, Validation. SS: Data curation, Writing – review & editing, Software. MA-M: Data curation, Software, Writing – review & editing, Formal analysis, Funding acquisition, Resources, Visualization. ME-T: Data curation, Formal analysis, Funding acquisition, Software, Visualization, Writing – review & editing, Project administration. SF: Data curation, Project administration, Software, Writing – review & editing, Resources. BK: Data curation, Project administration, Software, Writing – review & editing, Formal analysis. AA: Data curation, Formal analysis, Software, Writing – review & editing, Resources, Visualization. FB: Data curation, Formal analysis, Resources, Software, Visualization, Writing – review & editing, Conceptualization, Investigation, Methodology, Validation, Writing – original draft.

Funding

The author(s) declare that financial support was received for the research, authorship, and/or publication of this article. The authors extend their appreciation to the Researchers Supporting Project number (RSPD2024R678) King Saud University, Riyadh, Saud Arabia.

Conflict of interest

The authors declare that the research was conducted in the absence of any commercial or financial relationships that could be construed as a potential conflict of interest.

Publisher's note

All claims expressed in this article are solely those of the authors and do not necessarily represent those of their affiliated organizations, or those of the publisher, the editors and the reviewers. Any product that may be evaluated in this article, or claim that may be made by its manufacturer, is not guaranteed or endorsed by the publisher.

References

1. Lang J, Han H, Dong H, Qin Z, Fu Y, Qin H, et al. Molecular characterization and prevalence of *Cryptosporidium* spp. in sheep and goats in western Inner Mongolia, China. *Parasitol Res*. (2023) 122:537–45. doi: 10.1007/s00436-022-07756-5

2. Hao Y, Liu A, Li H, Zhao Y, Yao L, Yang B, et al. Molecular characterization and zoonotic potential of *Cryptosporidium* spp. and Giardia duodenalis in humans and domestic animals in Heilongjiang Province, China. *Parasit Vectors*. (2024) 17:155. doi: 10.1186/s13071-024-06219-3

3. Kabir MHB, Ceylan O, Ceylan C, Shehata AA, Bando H, Essa MI, et al. Molecular detection of genotypes and subtypes of *Cryptosporidium* infection in diarrheic calves, lambs, and goat kids from Turkey. *Parasitol Int*. (2020) 79:102163. doi: 10.1016/j.parint.2020.102163

4. Cheng C, Fan Z, Cheng D, Tao J. Prevalence of *Cryptosporidium* spp. in sheep and goats in Jiangsu, China. Veterinary. *Science*. (2024) 11:144. doi: 10.3390/vetsci11040144

5. Kim A-Y, Alkathiri B, Lee S, Min K-D, Kim S, Lee S-M, et al. Outbreak of severe diarrhea due to zoonotic *Cryptosporidium* parvum and C. Xiaoi in goat kids in Chungcheongbuk-do, Korea. *Parasitol Res*. (2023) 122:2045–54. doi: 10.1007/s00436-023-07904-5

6. Celi K, Guzmán L, Rey-Valeirón C. Apicomplexans in goat: prevalence of Neospora caninum, toxoplasma gondii, *Cryptosporidium* spp., Eimeria spp. and risk factors in farms from Ecuador. *Animals*. (2022) 12:2224. doi: 10.3390/ani12172224

7. Askar HK, Salman YJ, Mohiemeed AA. Some Epidemiological Aspects of Cryptosporidium parvum Among Children Below Five Years in Kirkuk Province. *J. Popul. Ther. Clin. Pharmacol*. (2023) 30:378–389. doi: 10.47750/jptcp.2023.30.08.041

8. Peng S, Xu C, Saleem MU, Babar W, Idrees A, Li K. Epidemiological investigation of *Cryptosporidium* infection in yaks in Chamdo, China. *Pak Vet J*. (2024) 44, 535–538. doi: 10.29261/pakvetj/2024.170

9. Shehata AA, El-Emam A, Mohamed M, Gouda H, El-Said BM, Salman MB, et al. Molecular characterization of *Cryptosporidium* infection and analysis of hematological and biochemical changes in diarrheic pre-weaned calves in Egypt. *Pak Vet J*. (2024) 44, 135–140. doi: 10.29261/pakvetj/2023.071

10. Li X-M, Geng H-L, Wei Y-J, Yan W-L, Liu J, Wei X-Y, et al. Global prevalence and risk factors of *Cryptosporidium* infection in Equus: A systematic review and meta-analysis. *Front Cell Infect Microbiol*. (2022) 12:1072385. doi: 10.3389/fcimb.2022.1072385

11. Almuzaini AM. Flow of zoonotic toxoplasmosis in food chain. *Pak Vet J*. (2023) 43, 1–16. doi: 10.29261/pakvetj/2023.010

12. Felefel WI, Abdel-Rady A, El-Rahim A, Elkamshishi MM, Mostafa W. Detection of *Cryptosporidium parvum* in calf feces using microscopical, serological, and molecular methods. *Iraqi J Vet Sci*. (2023) 37:383–9. doi: 10.33899/ijvs.2022.134661.2390

13. Saeed MS, Randhawa UA, Ahmad I, Ullah MI, Gul ST, Hassan MM, et al. Seroprevalence and risk factors of toxoplasmosis in beetal goats in district Faisalabad and its association with reproductive problems. *Pak J Agric Sci*. (2021) 58. doi: 10.21162/PAKJAS/21.1555

14. Pavlović I, Ivanović S, Petrović MP, Caro Petrović V, Ružić-Muslić D, Bojkovski J, et al. *Cryptosporidium* infection in goats in Serbia. *Bullet UASVM Vet Med*. (2020) 77:101–5. doi: 10.15835/buasvmcn-vm:2020.0027

15. Helmy YA, Hafez HM. Cryptosporidiosis: from prevention to treatment, a narrative review. *Microorganisms*. (2022) 10:2456. doi: 10.3390/microorganisms10122456

16. Pacheco FTF, De FHF, Silva RKNR, De CSS, Martins AS, Menezes JF, et al. *Cryptosporidium* diagnosis in different groups of children and characterization of parasite species. *Rev Soc Bras Med Trop*. (2022) 55:e0041–2022. doi: 10.1590/0037-8682-0041-2022

17. Hussain A, Khan H, Rasool A, Rafiq N, Badshah F, Tariq M, et al. Diversity of aquatic parasites in pristine spring waters in tehsil Babuzai, swat, Pakistan. *Braz J Biol*. (2024) 84:e282008. doi: 10.1590/1519-6984.282008

18. Majeed QA, AlAzemi MS, Al-Sayegh MT, Abdou N-EM. Epidemiological and molecular study of *Cryptosporidium* in preweaned calves in Kuwait. *Animals*. (2022) 12:1805. doi: 10.3390/ani12141805

19. Shahoi HIA, Meroa WMS, Mohammeda AB. Prevalence of cryptosporidiosis and its associated risk factors among human population in Zakho district, Duhok province, Kurdistan region, Iraq. *Sci J Univ Zakho*. (2022) 10, 153–158. doi: 10.25271/sjuoz.2022.10.4.970

20. Ali M, Al-Herrawy A, El-Hawaary S. Detection of enteric viruses, Giardia and *Cryptosporidium* in two different types of drinking water treatment facilities. *Water Res*. (2004) 38:3931–9. doi: 10.1016/j.watres.2004.06.014

21. Chalmers RM. Waterborne outbreaks of cryptosporidiosis. *Annali dell'Istituto superiore di sanita*. (2012) 48:429–46. doi: 10.4415/ANN_12_04_10

22. Javed K, Alkheraije KA. Cryptosporidiosis: A foodborne zoonotic disease of farm animals and humans. *Pak Vet J*. (2023) 43:213–23. doi: 10.29261/pakvetj/2023.038

23. Antonio M, Jovana J, Melina M, Arturo S-S. Frequency of Giardia spp. and *Cryptosporidium* spp. in domestic and captive wild animals in the north of Veracruz, Mexico. *Pak Vet J*. (2023) 43, 814–818. doi: 10.29261/pakvetj/2023.102

24. Chen X, Saeed NM, Ding J, Dong H, Kulyar MF-A, Bhutta ZA, et al. Molecular epidemiological investigation of *Cryptosporidium* sp., Giardia duodenalis, Enterocytozoon bieneusi and Blastocystis sp. infection in free-ranged yaks and Tibetan pigs on the plateau. *Pak Vet J*. (2022) 42:533–9. doi: 10.29261/pakvetj/2022.060

25. El Amine BM, Mimoune N, Khalef D, Oumouna M. Prevalence of cryptosporidiosis in goats in Central Algeria. *Veterinarska stanica*. (2022) 53:573–81. doi: 10.46419/vs.53.5.2

26. Abbas Z, Khan MK, Abbas RZ, Sindhu Zud D, Sajid MS, Munir A, et al. Molecular epidemiology of *Cryptosporidium* parvum and *Giardia lamblia* in different water bodies, soil, and vegetables in Pakistan. *Health Secur*. (2022) 20:308–20. doi: 10.1089/hs.2021.0118

27. Akkaş Ö, Gürbüz E, Aydemir S, Şahin M, Ekici A. (2023). Investigation of *Giardia* spp., *Cryptosporidium* spp. and *Cyclospora cayetanensis* in samples collected from different spring waters Iğdır, Türkiye Farklı Kaynak Sularından Alınan Örneklerde *Giardia* spp., *Cryptosporidium* spp. ve *Cyclospora cayetanensis*' in Araştırılması Iğdır, Türkiye. Turkiye Parazitoloji Dergisi 47.doi: 10.4274/tpd.galenos.2023.74936

28. Medema G, Schijven J. Modelling the sewage discharge and dispersion of *Cryptosporidium* and Giardia in surface water. *Water Res*. (2001) 35:4307–16. doi: 10.1016/S0043-1354(01)00161-0

29. Haseeb A, Rehman HU, Zakir M, Iqbal N, Ullah I, Rasheed F, et al. Comparative study of different types of parasites present in water sources of district DI Khan. *J Entomol Zool Stud*. (2017) 5:1013–6.

30. Karanis P, Kourenti C, Smith H. Waterborne transmission of protozoan parasites: a worldwide review of outbreaks and lessons learnt. *J Water Health*. (2007) 5:1–38. doi: 10.2166/wh.2006.002

31. Ali S, Metlo M, Ahmed Z, Ali S, Ahmed S, Zafar N, et al. Prevalence of water borne diseases in flood affected areas of district Khairpur Mirs, Pakistan. *Pakist J Med Health Sci*. (2023) 17:599–601. doi: 10.53350/pjmhs2023173599

32. Garcia LS, Procop G. Diagnostic medical parasitology. Manual of commercial methods in clinical microbiology In: A. L. Truant, Y-W. Tang, K. B. Waites, C. Bébéar, R. P. Rennie. Manual of Commercial Methods in Clinical Microbiology (2014). 284–308.

33. Kooh P, Thébault A, Cadavez V, Gonzales-Barron U, Villena I. Risk factors for sporadic cryptosporidiosis: A systematic review and meta-analysis. *Microb Risk Anal*. (2021) 17:100116. doi: 10.1016/j.mran.2020.100116

34. Utaaker KS, Chaudhary S, Kifleyohannes T, Robertson LJ. Global goat! Is the expanding goat population an important reservoir of *Cryptosporidium*? *Front Vet Sci*. (2021) 8:648500. doi: 10.3389/fvets.2021.648500

35. Chen R, Jia Peng J, Mohsin M, Huang X, Lin X, Aguilar-Marcelino L, et al. Construction and evaluation of the *Toxoplasma gondii* DNA vaccine targeting DEC-205. *Pak Vet J*. (2022) 42, 256–260.

36. Khan NU, Usman T, Sarwar MS, Ali H, Gohar A, Asif M, et al. The prevalence, risk factors analysis and evaluation of two diagnostic techniques for the detection of *Cryptosporidium* infection in diarrheic sheep from Pakistan. *PLoS One*. (2022) 17:e0269859. doi: 10.1371/journal.pone.0269859

37. Young I, Smith BA, Fazil A. A systematic review and meta-analysis of the effects of extreme weather events and other weather-related variables on *Cryptosporidium* and Giardia in fresh surface waters. *J Water Health*. (2015) 13:1–17. doi: 10.2166/wh.2014.079

38. Khan NU, Saleem MH, Durrani AZ, Ahmad N, Shafee M, Hassan A, et al. Prevalence and chemotherapy of cryptosporidiosis in goats using different herbal and allopathic drugs in southern Khyber Pakhtunkhwa, Pakistan. *Pakist J Zool*. (2021) 53:1–4. doi: 10.17582/journal.pjz/20171007121024

39. Rose JB, Huffman DE, Gennaccaro A. Risk and control of waterborne cryptosporidiosis. *FEMS Microbiol Rev*. (2002) 26:113–23. doi: 10.1111/j.1574-6976.2002.tb00604.x

frontiers | Frontiers in Veterinary Science

TYPE Original Research
PUBLISHED 23 December 2024
DOI 10.3389/fvets.2024.1500930

Check for updates

OPEN ACCESS

EDITED BY
Mughees Aizaz Alvi,
University of Agriculture, Faisalabad, Pakistan

REVIEWED BY
Hafiz Ishfaq Ahmad,
University of Veterinary and Animal Sciences, Pakistan
Jose Reck,
Desidério Finamor Veterinary Research Institute (IPVDF), Brazil

*CORRESPONDENCE
Abid Ali
✉ uop_ali@yahoo.com
Tetsuya Tanaka
✉ tetsuya.tanaka.a3@tohoku.ac.jp

RECEIVED 24 September 2024
ACCEPTED 15 November 2024
PUBLISHED 23 December 2024

CITATION
Ullah Z, Liaqat I, Khan M, Alouffi A, Almutairi MM, Apanaskevich DA, Tanaka T and Ali A (2024) Investigation of *Hyalomma turanicum* and *Hyalomma asiaticum* in Pakistan, with notes on the detection of tickborne Rickettsiales.
Front. Vet. Sci. 11:1500930.
doi: 10.3389/fvets.2024.1500930

COPYRIGHT
© 2024 Ullah, Liaqat, Khan, Alouffi, Almutairi, Apanaskevich, Tanaka and Ali. This is an open-access article distributed under the terms of the Creative Commons Attribution License (CC BY). The use, distribution or reproduction in other forums is permitted, provided the original author(s) and the copyright owner(s) are credited and that the original publication in this journal is cited, in accordance with accepted academic practice. No use, distribution or reproduction is permitted which does not comply with these terms.

Investigation of *Hyalomma turanicum* and *Hyalomma asiaticum* in Pakistan, with notes on the detection of tickborne Rickettsiales

Zafar Ullah[1,2], Iram Liaqat[1], Mehran Khan[2], Abdulaziz Alouffi[3], Mashal M. Almutairi[4], Dmitry A. Apanaskevich[5,6], Tetsuya Tanaka[7]* and Abid Ali[2]*

[1]Microbiology Lab, Department of Zoology, Government College University, Lahore, Punjab, Pakistan, [2]Department of Zoology, Abdul Wali Khan University Mardan, Mardan, Khyber Pakhtunkhwa, Pakistan, [3]King Abdulaziz City for Science and Technology, Riyadh, Saudi Arabia, [4]Department of Pharmacology and Toxicology, College of Pharmacy, King Saud University, Riyadh, Saudi Arabia, [5]United States National Tick Collection, The James H. Oliver Jr. Institute for Coastal Plain Science, Georgia Southern University, Statesboro, GA, United States, [6]Department of Biology, Georgia Southern University, Statesboro, GA, United States, [7]Laboratory of Animal Microbiology, Graduate School of Agricultural Science/Faculty of Agriculture: Tohoku University, Aoba-ku, Sendai, Japan

There is limited information on the occurrence of *Hyalomma turanicum* and *Hyalomma asiaticum* ticks, as well as associated *Rickettsia, Anaplasma,* and *Ehrlichia* species in Pakistan. Addressing this knowledge gap, the current study aimed at morphomolecular confirmation of these ticks and molecular assessment of associated Rickettsiales bacteria (*Rickettsia, Anaplasma*, and *Ehrlichia* spp.) in Balochistan, Pakistan. A total of 314 ticks were collected from 74 of 117 (63.2%) hosts, including 41 of 74 (55.4%) goats and 33 of 74 (44.5%) sheep. Subsequently, a subset of microscopically identified ticks was subjected to DNA extraction and PCR to amplify 16S rDNA and *cox1* fragments. Additionally, *gltA*, *ompA,* and *ompB* fragments were targeted for *Rickettsia* spp. and 16S rDNA fragments for both *Anaplasma* and *Ehrlichia* spp. The 16S rDNA and *cox1* sequences of *Hy. turanicum* demonstrated 100% identity with those of the same species previously reported from Pakistan. The 16S rDNA and *cox1* sequences of *Hy. asiaticum* exhibited 99.52 and 100% identities, respectively, with corresponding species reported from China, Kazakhstan, and Turkey. The *gltA, ompA,* and *ompB* fragments associated with *Hy. turanicum* showed 100% identities with *Rickettsia aeschlimannii* reported from Egypt, Italy, Kazakhstan, Kenya, Pakistan, and Senegal. The 16S rDNA sequences of *Anaplasma* sp. and *Ehrlichia* sp. associated with both *Hy. asiaticum* and *Hy. turanicum* exhibited 99.67 and 100% identities with unknown *Anaplasma* sp. and *Ehrlichia* sp. reported from Morocco and Pakistan, respectively. In the 16S rDNA and *cox1* phylogenetic trees of ticks, *Hy. turanicum* and *Hy. asiaticum* from the current study clustered with their respective species. Similarly, in *gltA, ompA,* and *ompB* phylogenetic trees of *Rickettsia*, *R. aeschlimannii* of the present study clustered with the same species, whereas *Anaplasma* sp. and *Ehrlichia* sp. of this study clustered with undetermined *Anaplasma* spp. and *Ehrlichia* spp. in the 16S rDNA phylogenetic tree of Anaplasmataceae. Among the DNA samples from the screened ticks, a coinfection rate of *R. aeschlimannii*, *Anaplasma* sp., and *Ehrlichia* sp. (2 of 80, 2.5%) was observed in *Hy. turanicum*, whereas individual infection rates were noted as follows: *R. aeschlimannii* (8 of 80, 10%), *Anaplasma* sp. (5 of 80, 6.3%), and *Ehrlichia* sp. (5 of 80, 6.3%). This study marks the first record of molecular characterization of *Hy. turanicum* and *Hy. asiaticum* as well

as the detection of associated *R. aeschlimannii*, *Anaplasma* sp., and *Ehrlichia* sp. in Balochistan, Pakistan.

KEYWORDS

***Hyalomma turanicum*, *Hyalomma asiaticum*, *Rickettsia aeschlimannii*, *Anaplasma* sp., *Ehrlichia* sp., coinfection, phylogeny**

1 Introduction

Ticks are hematophagous ectoparasites and leading vectors of important tickborne pathogens that affect all classes of terrestrial and semi-terrestrial animals, including livestock. Losses due to tick infestation could be either direct or indirect and are affected by certain climatic factors, including fluctuation in temperature, humidity, photoperiod, and vegetation, as well as host availability (1–3). The *Hyalomma* genus is among the prominent genus of ticks found in Asia, Africa, and Southern Europe with 27 reported species (4), while in Pakistan, 14 species of this genus have been reported (5–7). The several species complexes in this genus share many morphological traits, making accurate identification challenging. Within *Hyalomma* (*Euhyalomma*) *marginatum* complex, *Hyalomma glabrum* Delpy 1949, *Hyalomma isaaci* Sharif 1928, *Hy. marginatum* Koch 1844, *Hyalomma rufipes* Koch 1844, and *Hyalomma turanicum* Pomerantzev 1946 are closely related species (8). Of these species, *Hy. turanicum* is found in Africa and Asia (Afghanistan, Bahrain, China, Egypt, India, Iran, Iraq, Israel, Jordan, Kazakhstan, Kyrgyzstan, Nepal, Oman, Pakistan, Qatar, Saudi Arabia, Syria, Tajikistan, Turkmenistan, Uzbekistan, and Yemen) (9, 10). Within *Hyalomma* (*Euhyalomma*) *asiaticum* complex, *Hyalomma asiaticum* Schulze & Schlottke 1929, *Hyalomma dromedarii* Koch 1844, *Hyalomma impeltatum Schulze* & Schlottke 1929, *Hyalomma schulzei* Olenev 1931, and *Hyalomma somalicum* Tonelli Rondelli 1935 are closely related (8, 11). Among these species, *Hy. asiaticum* is limited to Asia (Afghanistan, Armenia, Azerbaijan, China, Georgia, Iran, Iraq, Kazakhstan, Kyrgyzstan, Mongolia, Pakistan, Russia, Syria, Tajikistan, Turkey, Turkmenistan, and Uzbekistan) (9, 10). Key morphological features of these species are adanal plates, spiracular plates, setae, genital aperture, and scutum/conscutum (12, 13).

Morphological-based identification of *Hyalomma* species creates more challenges, which resulted in the re-description of its several species (14, 15). Recent studies of molecular identification have improved our understanding of the inter- and intra-specific diversity of *Hyalomma* ticks, which may help in understanding its taxonomy and epidemiology (9, 16, 17).

Within the order Rickettsiales, the genus *Rickettsia* consists of obligate intracellular *Gram*-negative bacteria that affect veterinary and human health by causing various diseases such as Rocky Mountain spotted fever (18, 19). In this order, *Ehrlichia* species have unique cell tropisms within the vertebrate hosts and are causative agents of tickborne fever in ruminants, while *Anaplasma* species cause human granulocytic anaplasmosis (20, 21). Several *Rickettsia*, *Anaplasma*, and *Ehrlichia* species of medical importance are vectored by *Hyalomma* ticks, including *Hy. turanicum* and *Hy. asiaticum* (22, 23). Moreover, these tick species are also competent vectors of various viruses, including the Crimean–Congo hemorrhagic fever (CCHF) viruses (24). In Pakistan, *Hyalomma* ticks are expected to be associated with tickborne diseases such as babesiosis, theileriosis, rickettsiosis, and CCHF (7, 25–27). Pakistan's economy is mostly based on agriculture, which contributes ≈ 24% to its gross domestic product and employs ≈ 40% of its labor force (53). Consequently, these TBDs can cause significant damage to the country's economy.

Though *Hyalomma* ticks are highly important in both veterinary and medical aspects, morphomolecular studies of *Hy. turanicum* and *Hy. asiaticum* in Pakistan in general and in Balochistan province in particular are limited. Additionally, *Hy. turanicum* and *Hy. asiaticum* ticks from Pakistan have been largely overlooked in terms of pathogen research, including *Rickettsia*, *Anaplasma,* and *Ehrlichia* spp. Therefore, the study represents the first attempt to investigate the occurrence of *Hy. turanicum* and *Hy. asiaticum* ticks and Rickettsiales bacteria associated with these tick species. This study specifically aims to determine whether *Hy. turanicum* and *Hy. asiaticum* are associated with *Rickettsia*, *Anaplasma*, and *Ehrlichia* spp. in the study region.

2 Materials and methods

2.1 Ethical consideration

Prior to performing this study, approval was given by the Advanced Studies and Research Board (REG-ACAD-ASRB-55/23/035) of the Government College University, Lahore, Pakistan. All animal or herd owners were verbally informed, and permission was taken from them.

2.2 Study area

The present study was executed in five districts of the Balochistan province, Pakistan: Musakhail (30°50′52.1″N 69°57′18.0″E), Nushki (29°28′27.1″N 65°39′57.2″E), Pishin (30°44′17.9″N 67°17′05.3″E), Quetta (30°10′47.6″N 67°05′38.8″E), and Sherani (29°46′60″ N 68°31′0″ E). For creating a map (Figure 1) using ArcGIS v. 10.3.1, the coordinates of the above-collected sites were documented using the Global Positioning System. The choice of these districts was strategic because they share borders with neighboring countries (Afghanistan and Iran), making them key areas for cross-border animal movement and trade. Additionally, Quetta, as the provisional capital, serves as a major hub for the transportation of livestock, further increasing the importance of these districts. Livestock, particularly sheep and goats, are more prevalent in these areas, forming the backbone of the local economy.

2.3 Collection and preservation of ticks

Ticks were collected from goats and sheep from April 2023 to April 2024 in the specified districts of Balochistan. To minimize

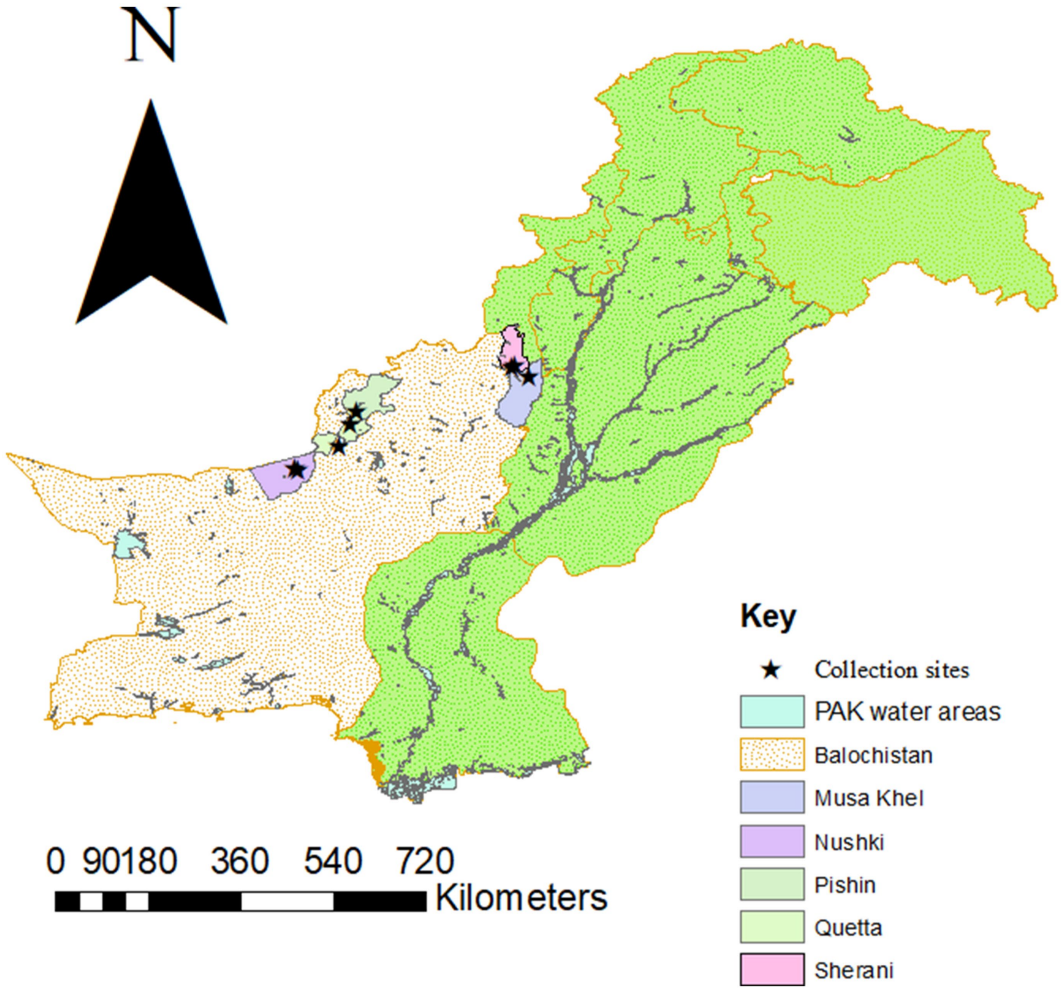

FIGURE 1
Map summarizing the study area.

potential damage to the specimens, a meticulous approach was employed, delicately detaching ticks from the skin of hosts using forceps. The collected specimens underwent a thorough cleaning process with distilled water prior to washing with 70% absolute ethanol. For preservation and further analysis, the ticks were stored in a solution made of 95% ethanol, 4% distilled water, and 1% glycerol.

2.4 Morphological identification

Tick specimens were meticulously examined under a stereo-zoom microscope (Luxeo 6Z, LABOMED, USA). Morphological identification was carried out at both the life stage and species level, with the help of established morphological identification keys specified to *Hyalomma* species (12, 15).

2.5 DNA extraction and PCR

A total of 80 morphologically identified ticks were randomly selected for molecular analysis, including four males and four females of each species per host per district. Subsequently, the homogenized specimens were incubated until dry, involving dissection and grinding with sterile scissors. DNA extraction followed the standard phenol–chloroform method with minor adjustments (28). After extraction, DNA was quantified using a NanoDrop spectrophotometer (NanoQ, Optizen, Daejeon, South Korea) and stored at −20°C for further analysis.

Conventional PCRs (GE-96G, BIOER, Hangzhou, China) were performed to amplify partial fragments of 16S ribosomal DNA and *cox1* genes of ticks from the extracted DNA (Table 1). Additionally, the extracted genomic DNA was molecularly assessed for rickettsial citrate synthase (*gltA*), outer membrane protein A and B (*ompa* and *ompB*), and Anaplasmataceae 16S rDNA (Table 1).

Each PCR was performed in a 20 μL volume, including 1 μL forward and reverse primers each (concentration of 10 μM), 4 μL of "nuclease-free" PCR water, 2 μL of genomic DNA (100 ng/μL), and 12 μL of Dream*Taq* MasterMix (2X) (Thermo Fisher Scientific, Inc., Waltham, MA, USA). The primers and thermocycling conditions used in this study are listed in Table 1. To ensure the reliability of the PCRs, positive control samples containing DNA of *Hyalomma anatolicum* (for ticks) and DNA of *Rickettsia massiliae* (for bacterial species), and

TABLE 1 List of primers and PCR conditions that were used for the molecular identification of ticks and pathogens.

Organisms	Genes	Primer name: Primers Sequences (5′–3′)	Amplicons size	PCR conditions	References
Ticks	16S rDNA	16S + 1: CCGGTCTGAACTCAGATCAAGT 16S-1: GCTCAATGATTTTTTAAATTGCTG	460 bp	94°C—2 min, 34× (94°C—30 s, 55°C—30 s, 72°C—45 s), 72°C—7 min	(49)
	cox1	HCO2198: TAAAC TTCAGGGTG ACCAAAAAATCA LCO1490: GGTCAACAAATCATAAAGATATTGG	710 bp	95°C—5 min, 40× (94°C—40 s, 48°C—60 s, 72°C—1 min),	(50)
Rickettsia	*gltA*	CS-78: GCAAGTATCGGTGTGAGGATGTAAT CS-232: GCTTCCTTAAAATTCAATAAATCAGGAT	401 bp	95°C—3 min, 40 × (95°C—15 s, 56°C—30 s, 72°C—30 s) 72°C—7 min	(42)
	ompA	Rr190.70: ATGGCGAATATTTCTCCAAAA Rr190.701: AGTGCAGCATTCGCTCCCCCT	532 bp	95°C—3 min, 35 × (95°C—20 s, 55°C—30 s, 60°C—2 min) 72°C—7 min	(51)
	ompB	120-M59: CCGCAGGGTTGGTAACTGC 120–807: CCTTTTAGATTACCGCCTAA	862 bp	95°C—3 min, 40 × (95°C—30 s, 50°C—30 s, 68°C—1 min 30 s),	(41)
Anaplasma/Ehrlichia spp.	16S rDNA	EHR16SD: GGTACCYACAGAAGAAGTCC EHR16SR: TAGCACTCATCGTTTACAGC	344 bp	95°C—3 min, 35× (95°C—30 s, 55°C—30 s, 72°C—1 min), 72°C—7 min	(52)

a negative control sample consisting of PCR water (nuclease-free), were part of each PCR. The amplified products of the tick and its pathogen from the PCRs were run on a gel made of 2% agarose. After PCR, the obtained bands were made visible under through UV from a Gel Documentation system (BioDoc-It™ Imaging Systems, UVP, LLC).

2.6 DNA sequencing and phylogenetic analyses

PCR-positive amplified products of the expected size were purified using the DNA Clean and Concentrator Kit (Zymo Research, Irvine, CA, USA) and submitted for bidirectional sequencing (Macrogen Inc., Seoul, South Korea) using the Sanger sequencing method. The resulting sequences were proceeded and purified through SeqMan v. 5 (DNASTAR, Inc., Madison, WI, USA) to remove low-quality and contaminated regions. Trimmed and consensus sequences were then analyzed using the Basic Local Alignment Search Tool (BLAST) at the National Center for Biotechnology Information (NCBI)[1] (29). Sequences with high homology were downloaded in FASTA format. The downloaded sequences, along with an outgroup, were aligned using ClustalW (30) in the BioEdit alignment editor V.7.0.5 tool (Raleigh, NC, USA) (31).

Phylogenetic trees were constructed using MEGA-X (32) with the following specifications: Neighbor-Joining method, Tamura–Nei model, and 1,000 bootstrap replicates. Additionally, coding sequences were aligned using the MUSCLE alignment method (33).

1 https://www.ncbi.nlm.nih.gov/

3 Results

3.1 Morphological identification

Morphologically, *Hy. turanicum* was identified based on different features. The conscutum exhibited a yellow–brown color, with large punctations being rare, while medium- and small-sized punctations were relatively dense and covered the entire conscutum. The perforated portion of dorsal prolongation of the spiracular plate is relatively narrow; circumspiracular setae moderately dense; proximally moderately sized dorsal ivory-colored enamel spot (Figures 2C, D). While the scutum of the female was dark, ranging from reddish brown to nearly black, the genital aperture was wide, deep, and rounded (U-shaped), with the vestibular portion of the vagina bulging to some extent.

The *Hy. asiaticum* tick was morphologically identified based on different features. The conscutum exhibited a yellow to red–brown coloration. The cervical grooves were remarkably deep, while the marginal grooves were short. The adanal plates were long, narrow, and nearly straight, tapering slightly posteriorly from the median projection. (Figures 2A, B). While the scutum of the female was yellow– to red–brown, the genital aperture was narrow, U-shaped with the vestibular portion of the vagina distinctly bulging.

3.2 Hosts and ticks

Altogether, 314 ticks were collected from five districts of Balochistan; Musakhail, Nushki, Pishin, Quetta, and Sherani. These ticks included 165 (56.18%) *Hy. asiaticum*, comprising 104 (53.07%) females and 61 (32.03%) males, as well as 149 (43.81%) *Hy. turanicum*, including 96 (54.77%) females and 53 (31.12%) males. All these ticks were collected from 74 of the 117 examined hosts, demonstrating an overall prevalence of infestation of 63.2%. Moreover, goats exhibited

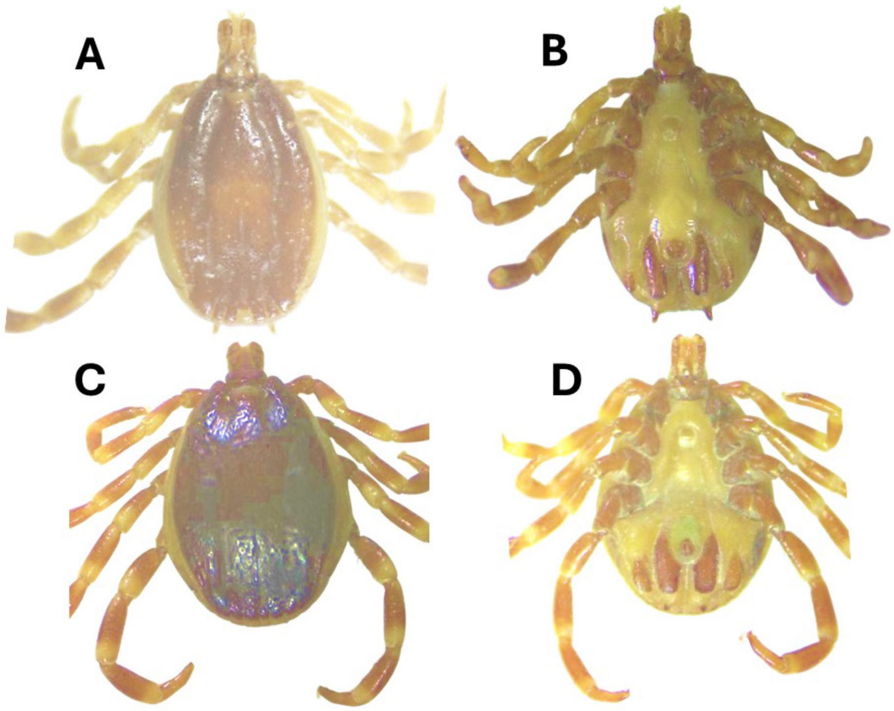

FIGURE 2
Hyalomma asiaticum male [**(A)** dorsal, **(B)** ventral] and *Hyalomma turanicum* male [**(C)** dorsal and **(D)** ventral] were collected in this study.

a high prevalence of infestation (41 of 74, 55.4%) compared to sheep (33 of 74, 44.5%). Detailed results about ticks, small ruminants, and Rickettsiales bacteria are summarized in Table 2.

3.3 Molecular outcomes

DNA was extracted from 80 ticks, including 40 *Hy. turanicum* and 40 *Hy. asiaticum*. Altogether, 53 bidirectional sequences were obtained, including at least one 16S rDNA and one *cox1* for each female and male of each tick species per district. Consensus sequences of ticks were obtained as follows: 16S rDNA for *Hy. turanicum* (410 bp), 16S rDNA for *Hy. asiaticum* (420 bp), *cox1* for *Hy. turanicum* (531 bp), and *cox1* for *Hy. asiaticum* (611 bp). Considering the closest identity, 16S rDNA and *cox1* sequences for *Hy. turanicum* were 100% identical with the corresponding species reported from Pakistan. Similarly, the 16S rDNA sequences for *Hy. asiaticum* showed a maximum identity of 99.52%, while its *cox1* sequences revealed a maximum identity of 100% with conspecific from China, Kazakhstan, and Turkey.

For each amplified fragment of *Rickettsia* spp., bidirectional sequences were obtained, which gave consensus sequences as follows: *gltA* (369 bp), *ompA* (471 bp), and *ompB* (790 bp) genes. The obtained sequences showed 100% identity with *R. aeschlimannii* reported from Egypt, Italy, Kazakhstan, Kenya, Pakistan, and Senegal.

Among the Anaplasmataceae, 8 of 80 (9.52%) samples were positive for 16S rDNA, including four *Hy. turanicum* and four *Hy. asiaticum* ticks. From the amplified fragments of Anaplasmataceae, bidirectional sequences were obtained, which resulted in the following consensus sequences: 16S rDNA (301 bp) for *Anaplasma* sp. and 16S rDNA sequence (333 bp) for *Ehrlichia* sp. The former sequence showed 99.67% identity with unknown *Anaplasma* sp. reported from Morocco, while the latter sequence revealed 100% identity with an undetermined *Ehrlichia* sp. reported from Pakistan.

The overall detection rates were as follows: 10% (8 of 80) for *R. aeschlimannii* associated with *Hy. turanicum*, 6.3% (5 of 80) for *Anaplasma* sp., and 6.3% (5 of 80) for *Ehrlichia* sp. associated with both *Hy. turanicum* and *Hy. asiaticum*. Additionally, coinfection with *R. aeschlimannii*, *Anaplasma* sp., and *Ehrlichia* sp. was found in 2 of 80 (2.5%) *Hy. turanicum* ticks. Detailed information about the infection rates of *R. aeschlimannii*, *Anaplasma* spp., and *Ehrlichia* spp. is shown in Table 2.

Following are the GenBank accession numbers of all consensus sequences of this study: 16S rDNA of *Hy. turanicum* (PQ218624) and *Hy. asiaticum* (PQ218629), *cox1* of *Hy. turanicum* (PQ218744), and *Hy. asiaticum* (PQ218788). *R. aeschlimannii*, *gltA* (PQ221477), *ompA* (PQ227817), and *ompB* (PQ227818), 16S rDNA for *Anaplasma* sp. (PQ213859), and *Ehrlichia* sp. (PQ214321).

3.4 Phylogenetic outcomes

The phylogenetic tree constructed 16S rDNA sequences revealed that *Hy. turanicum* clustered with the same species recorded from Iraq and Pakistan (KU130480, KU130482, and KU130483), while *Hy. asiaticum* grouped with the corresponding species reported from China and Kazakhstan (JX051085 MK530106, OR486026, and OR486010) (Figure 3A). The phylogenetic tree constructed for the *cox1* sequences showed that *Hy. turanicum* clustered with the related species from Saudi Arabia, Pakistan, and Iraq (OQ799122, PP716472,

TABLE 2 Collection sites of collected specimens and their molecular characterization with infection rate.

Collection sites	Hosts		Morphologically identified ticks				Tick subjected to PCR	PCR for pathogens							
	Name	Number of infested hosts/ total		F	M	Total ticks		*R. aeschlimannii*				*Anaplasma* spp.		*Ehrlichia* spp.	
								gltA	*ompA*	*ompB*	Infection rate %	16S rDNA	Infection rate %	16S rDNA	Infection rate %
Musakhail	Goats, Sheep	9/11	*Hy. asiaticum*	23	14	37	4M, 4F	0	0	0	0	1M	1 (1.25)	1M	1 (1.25%)
	Goats, Sheep	6/7	*Hy. turanicum*	18	9	27	4M, 4F	1 M, 2F	1 M, 2F	1 M, 2F	3 (3.8)	2F	2 (2.5)	2F	2 (2.5%)
Nushki	Goats, Sheep	4/5	*Hy. asiaticum*	16	8	24	4M, 4F	0	0	0	0	0	0	0	0
	Goats, Sheep	6/8	*Hy. turanicum*	17	11	28	4M, 4F	1 M, 1F	1 M, 1F	1 M, 1F	2 (2.5)	0	0	0	0
Pishin	Goats, Sheep	12/13	*Hy. asiaticum*	18	8	26	4M, 4F	0	0	0	0	1F	1 (1.25)	1F	1 (1.25%)
	Goats, Sheep	8/11	*Hy. turanicum*	19	10	29	4M, 4F	0	0	0	0	0	0	0	0
Quetta	Goats, Sheep	13/17	*Hy. asiaticum*	26	17	43	4M, 4F	0	0	0	0	1F	1 (1.25)	1F	1 (1.25%)
	Goats, Sheep	11/16	*Hy. turanicum*	23	12	35	4M, 4F	0	0	0	0	0	0	0	0
Sherani	Goats, Sheep	9/11	*Hy. asiaticum*	21	14	35	4M, 4F	0	0	0	0	0	0	0	0
	Goats, Sheep	8/18	*Hy. turanicum*	19	11	30	4M, 4F	2 M, 1F	2 M, 1F	2 M, 1F	3 (3.8)	0	0	0	0
Total		74/117		200	114	314	80	8	8	8	8 (10)	5	5 (6.3)	5	5 (6.3)
Total infection rate (mean ± SD) (%)								20.1 (1.83 ± 2.99)				12.55 (1.14 ± 1.82)		12.55 (1.14 ± 1.82)	
Chi-square value (*p*-value)								2.97 (0.27)							

M, male; F, female.

10.3389/fvets.2024.1500930

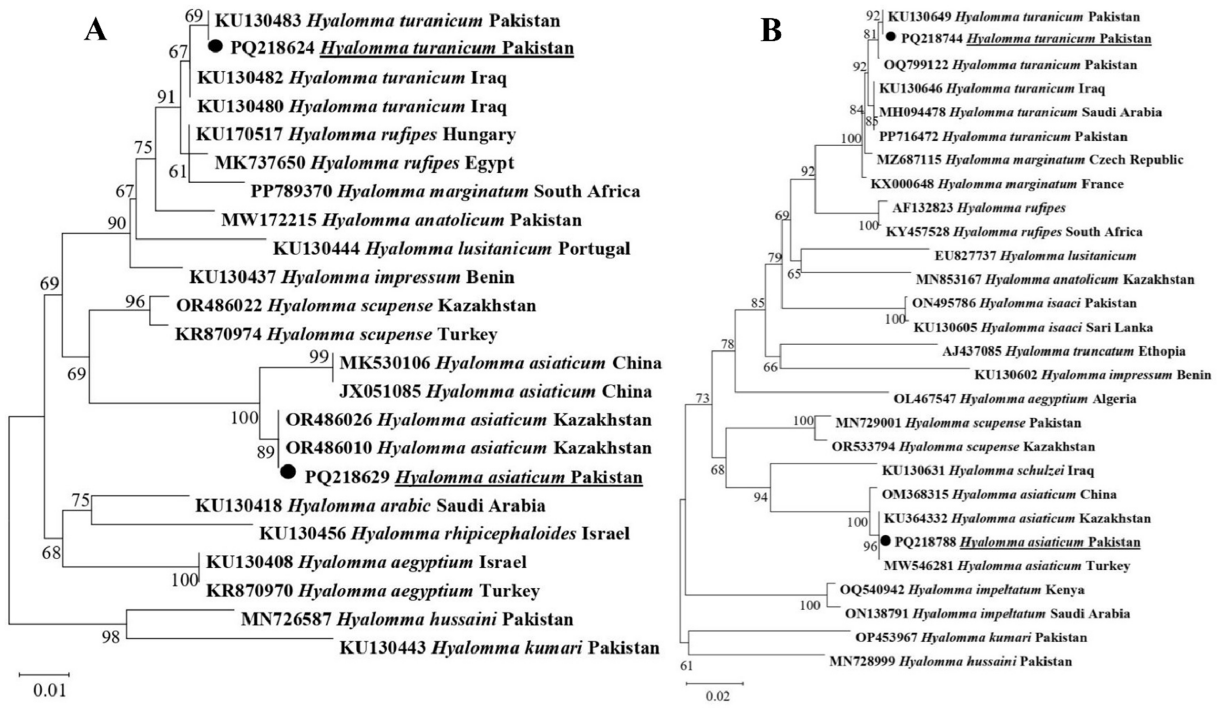

FIGURE 3
Phylogenetic tree constructed for *Hyalomma* spp. based on 16S rDNA **(A)** and *cox1* **(B)** sequences. Each sequence was identified by accession number, species name, and origin country. Sequences of *Hyalomma hussaini* and *Hyalomma kumari* were used as an outgroup. The acquired sequences have been highlighted.

KU130649, KU130646, and MH094478), while *Hy. asiaticum* grouped with the related species described from Kazakhstan, China, and Turkey (OM368315, KU364332, and MW546281) (Figure 3B).

In a phylogenetic tree developed for rickettsial *gltA*, *R. aeschlimannii* was detected in *Hy. turanicum* grouped with the sequences of the corresponding species described from Egypt, Kenya, and Senegal (HQ335148, KX227772, KX227768, and HM050285) (Figure 4A). In a phylogenetic developed for rickettsial *ompA*, *R. aeschlimannii* clustered with the sequences of the same species recorded from Italy and Pakistan (JN944634 and OQ632790) (Figure 4B). Additionally, in the phylogenetic tree obtained for rickettsial *ompB*, *R. aeschlimannii* grouped with the corresponding species reported from Italy, Kazakhstan, and Pakistan (MH532261, MW430414, and OR351961) (Figure 4C).

In the phylogenetic tree for Anaplasmataceae 16S rDNA sequences, *Anaplasma* sp. associated with *Hy. asiaticum* and *Hy. turanicum* was clustered with an undetermined *Anaplasma* sp. described from Morocco (OK606072) (Figure 5). In the same phylogenetic tree, *Ehrlichia* sp. recorded in the same ticks was grouped with an undermined *Ehrlichia* sp. previously reported from Pakistan (MH250197) (Figure 5).

4 Discussion

Sheep and goats are commonly raised animals in Pakistan, particularly in rural areas where these domestic animals serve as a significant source of income (34, 35). Despite the diverse range of ticks and TBDs, which cause significant economic losses in the livestock sector in rural areas of Pakistan, there is limited knowledge about the occurrence of *Hy. turanicum* and *Hy. asiaticum* ticks, as well as the pathogens associated with them. Few studies have been conducted to characterize *Hyalomma* ticks and/or associated pathogens from different regions of Pakistan (5–7, 9, 17). Herein, we morphologically and molecularly characterized two *Hyalomma* species, *Hy. turanicum* and *Hy. asiaticum,* for the first time from Balochistan, Pakistan. Additionally, this research also detected *R. aeschlimannii* in *Hy. turanicum* and undetermined *Anaplasma* sp. and *Ehrlichia* sp. in both *Hy. turanicum* and *Hy. asiaticum*.

Morphological identification of *Hyalomma* ticks, including *Hy. turanicum* and *Hy. asiaticum*, presents challenges (12, 15). In addition to morphological comparisons within their species, *Hy. turanicum* and *Hy. asiaticum* were also compared to their closest relatives within their respective complexes. *Hyalomma turanicum* was distinguished from *Hy. marginatum* by the presence of dense punctations on the conscutum or scutum, moderately narrow dorsal prolongation of the spiracular plate, and denser circumspiracular setae (12). Similarly, *Hy. asiaticum* was differentiated from *Hy. dromedarii* by characteristics such as: in males, a posteromedian groove that does not reach the parma and straighter adanal plates; and in females, a more U-shaped genital operculum and bulging preatrial fold (15).

To validate the morphological identification of ticks and ascertain the presence of a diverse array of pathogens, molecular confirmation holds significance (36, 37). Comprehensive molecular studies on the *Hyalomma* ticks have been conducted using the genetic markers; 16S rDNA and *coxI* (6, 7). In addition to clustering with the same species

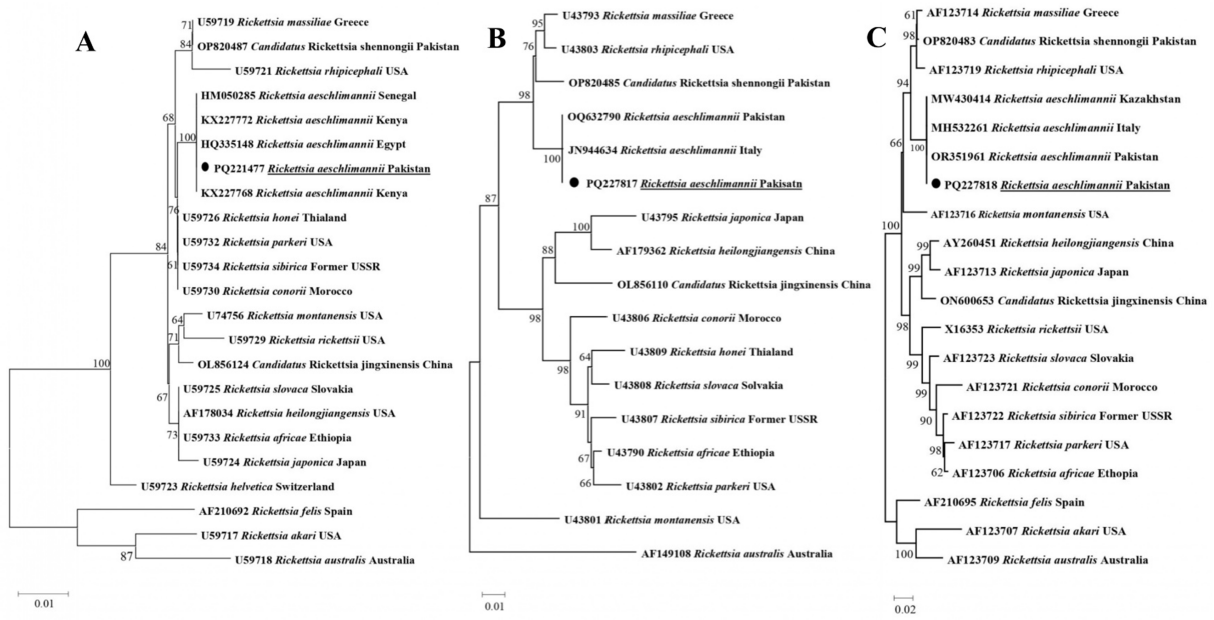

FIGURE 4
Phylogenetic tree constructed for *Rickettsia* spp. based on *gltA* **(A)**, *ompA* **(B)**, and *ompB* **(C)**. Each sequence was identified by accession number, species name, and origin country. *Rickettsia akari* and *Rickettsia australis* were jointly used as outgroups, and the acquired sequence has been highlighted.

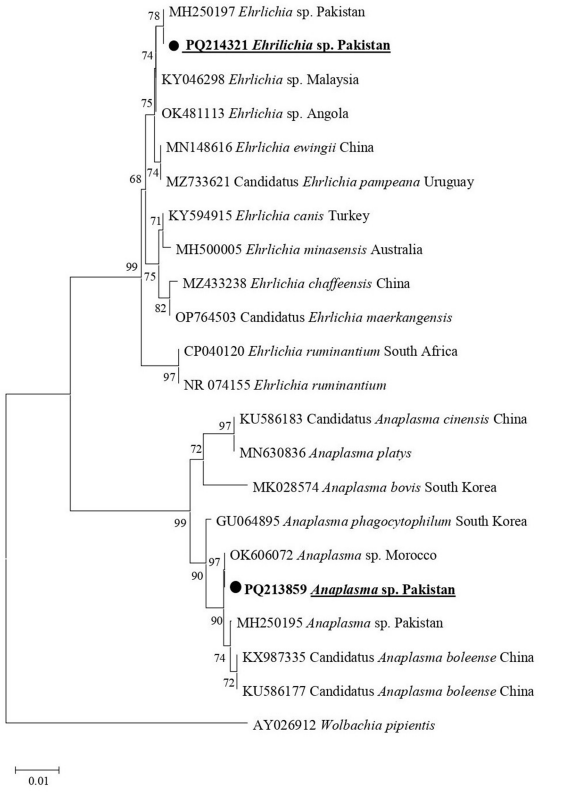

FIGURE 5
Phylogenetic tree constructed for 16S rDNA sequences of *Anaplasma* spp. and *Ehrlichia* spp. Each sequence was identified by providing the accession number, species name, and origin country. The sequence of *Wolbachia pipientis* was used as an outgroup, and the acquired sequences have been highlighted.

in the monophyletic clade, *Hy. turanicum* in the current study formed a sister clade with *Hy. marginatum* and *Hy. rufipus* within the subgenus *Euhyalomma* (38), corroborating previous studies that categorize them as members of the *Hy. marginatum* complex based on both morphological and genetic data (12, 38). Similarly, *Hy. asiaticum* clustered with the same species in the monophyletic clade and formed a sister clade with *Hyalomma schulzei* within the subgenus *Euhyalomma*, consistent with earlier studies that identify them as members of the *Hy. asiaticum* group, supported by morphological and genetic data (15, 38).

Rickettsia spp., including *R. aeschlimannii,* are zoonotic pathogens carried by different arthropod vectors, including *Hyalomma* ticks (18, 26, 39). The detection of *Rickettsia* spp. in ticks is significant not only for recognizing infected ticks but also for assessing the risk of transmission to humans (40). Considering suitability (41, 42), genetic markers such as *gltA*, *ompA*, and *ompB* were employed in this study to detect and phylogenetically analyze *Rickettsia* spp. in *Hyalomma* ticks. Previously, *R. aeschlimannii* has been detected in *Hy. turanicum*, *Ha. bispinosa*, and *Ha. montgomeryi* in Pakistan (43). This study further expanded the range of competent tick hosts and the geographical distribution of *R. aeschlimannii* in Pakistan by detecting it in *Hy. turanicum* in the Balochistan province. Transmission from animals to humans occurs through the bite of an infected tick, resulting in Mediterranean spotted fever (39). Additionally, *Rickettsia amblyommii*, *R. massiliae*, *Rickettsia conorii*, and *Rickettsia hoogstraalii* have been detected in other *Hyalomma* ticks, including *Hy. hussaini*, *Hy. anatolicum*, *Hy. dromedarii*, *Hy. Turanicum*, and *Hy. kumari* (7, 25, 44, 45). By clustering *R. aeschlimannii* with identical species from various regions within the spotted fever group, all three phylogenetic trees mutually validated each other. *Anaplasma* and *Ehrlichia* spp. are primarily transmitted by ticks and can cause diseases in humans and animals (46, 47). Partial fragments of 16S rDNA, widely acknowledged as a reliable molecular marker for characterizing

tick-associated *Anaplasma* and *Ehrlichia* spp. (20), were utilized in this study. The detection of *Anaplasma* and *Ehrlichia* spp. in *Hyalomma* ticks in the present study, as well as *Anaplasma marginale*, *Anaplasma ovis*, and *Anaplasma centrale*, in other *Hyalomma* ticks, including *Hy. anatolicum* and *Hyalomma scupense,* and undetermined *Ehrlichia* spp. in *Hyalomma* ticks, including *Hy. dromedarii* and *Hy. anatolicum*, suggests a greater diversity of these tickborne microorganisms in Pakistan. Herein, *Anaplasma* sp. shared phylogenetic similarities with *Candidatus* Anaplasma boleense, and *Ehrlichia* sp. with *Ehrlichia ewingii*, indicating potential zoonotic implications. The detection of *R. aeschlimannii*, *Anaplasma* sp., and *Ehrlichia* sp. in *Hyalomma* ticks in the study region indicates risks to livestock workers and farmers, especially in rural areas. In addition, it may be associated with economic losses and food security by affecting livestock. Therefore, understanding various aspects of these bacteria, such as their ecology, genetic diversity, and pathogenicity, is necessary to mitigate the associated risks in Pakistan.

The presence of *Hy. turanicum* and *Hy. asiaticum*, along with their notable abundance in the Balochistan province of Pakistan, may be attributed to nomadic migration, resulting in the uncontrolled movement of domestic animals between Balochistan, Afghanistan, and Iran (48). Other factors contributing to the prevalence of these tick species could include the presence of suitable hosts and the arid or semi-arid climate of the study area (6, 26). Alternative approaches implemented in the study area, such as cohabiting with diverse hosts in shared habitats, managing densely populated herds, and employing mixed grazing methods, may positively impact the presence of these ticks. Additionally, these conditions may influence the association between *Hyalomma* ticks and bacterial species. As the present study is based on relatively a small size sample size and is restricted to the Balochistan province of Pakistan, future studies should aim to increase the sample size, expand the geographic coverage, and investigate the vector competence of *Hyalomma* species for associated bacteria.

5 Conclusion

This study addresses a significant knowledge gap concerning *Hy. turanicum* and *Hy. asiaticum*, which were morphologically and genetically characterized for the first time in Balochistan, Pakistan. Additionally, the study molecularly assessed *R. aeschlimannii* in *Hy. turanicum,* as well as *Anaplasma* sp. and *Ehrlichia* sp. in both *Hy. turanicum* and *Hy. asiaticum*. Notably, it records the coinfection of all these three bacterial species in *Hy. turanicum*. This study may help to understand the identity, molecular epidemiology, and geographic distribution of *Hyalomma* ticks and associated pathogens. The findings of the present study indicate that public awareness and surveillance of tick-borne diseases in the region are needed, which may mitigate the risks to public health and livestock.

Data availability statement

The datasets presented in this study can be found in online repositories. The names of the repository/repositories and accession number(s) can be found in the article/supplementary material.

Ethics statement

The animal studies were approved by the Advanced Studies and Research Board (REG-ACAD-ASRB-55/23/035) of the Government College University, Lahore, Pakistan. All animal or herds owners were verbally informed, and permission was taken from them. The studies were conducted in accordance with the local legislation and institutional requirements. Written informed consent was obtained from the owners for the participation of their animals in this study.

Author contributions

ZU: Formal analysis, Investigation, Methodology, Writing – original draft, Writing – review & editing. IL: Formal analysis, Investigation, Methodology, Software, Writing – original draft, Writing – review & editing. MK: Investigation, Methodology, Validation, Visualization, Writing – original draft, Writing – review & editing. AbdA: Funding acquisition, Investigation, Methodology, Project administration, Writing – original draft, Writing – review & editing. MA: Funding acquisition, Investigation, Methodology, Project administration, Resources, Writing – original draft, Writing – review & editing. DA: Formal analysis, Investigation, Methodology, Writing – original draft, Writing – review & editing. TT: Funding acquisition, Investigation, Methodology, Resources, Writing – original draft, Writing – review & editing. AbiA: Conceptualization, Funding acquisition, Investigation, Methodology, Project administration, Resources, Supervision, Writing – original draft, Writing – review & editing.

Funding

The author(s) declare that financial support was received for the research, authorship, and/or publication of this article. The authors acknowledge the financial support provided by the Higher Education Commission (HEC), Pakistan, Pakistan Science Foundation (PSF). The researchers supporting project number (RSP2024R494), King Saud University, Riyadh, Saudi Arabia. This work was supported by JSPS KAKENHI Grant Numbers JP20KK0154, JP22H02522, JP23K23787, JSPS Bilateral Program Grant Number JPJSBP120239937, SHONOGI INFECTIOUS DISEASE RESEARCH PROMOTION FOUNDATION, Japan Association for Livestock New Technology Research Foundation, and Kieikai Research Foundation.

Conflict of interest

The authors declare that the research was conducted in the absence of any commercial or financial relationships that could be construed as a potential conflict of interest.

Publisher's note

All claims expressed in this article are solely those of the authors and do not necessarily represent those of their affiliated organizations, or those of the publisher, the editors and the reviewers. Any product that may be evaluated in this article, or claim that may be made by its manufacturer, is not guaranteed or endorsed by the publisher.

References

1. Ali A, Zahid H, Zeb I, Tufail M, Khan S, Haroon M, et al. Risk factors associated with tick infestations on equids in Khyber Pakhtunkhwa, Pakistan, with notes on *Rickettsia massiliae* detection. *Parasit Vectors*. (2021) 14:363–12. doi: 10.1186/s13071-021-04836-w

2. Cvek M, Broznić D, Puškadija D, Blagonić B, Kirin I, Pustijanac E, et al. Investigation and spatial distribution of hard ticks by geographical information system (gis) in the region of Istria, Croatia. *J Appl Sci*. (2023) 13:9483. doi: 10.3390/app13169483

3. Younas M, Ashraf K, Rashid MI, Ijaz M, Suleman M, Chohan TA. Expression and purification of recombinant multi-epitope protein of *Rhipicephalus microplus* tick and its antigenicity in the rabbit model. *Pak Vet J*. (2023):43. doi: 10.29261/pakvetj/2023.086

4. Hekimoglu O, Ozer AN. Distribution and phylogeny of Hyalomma ticks (Acari: Ixodidae) in Turkey. *Exp Appl Acarol*. (2017) 73:501–19. doi: 10.1007/s10493-017-0192-0

5. Ali A, Khan MA, Zahid H, Yaseen PM, Qayash Khan M, Nawab J, et al. Seasonal dynamics, record of ticks infesting humans, wild and domestic animals and molecular phylogeny of *Rhipicephalus microplus* in Khyber Pakhtunkhwa Pakistan. *Front Physiol*. (2019) 10:793. doi: 10.3389/fphys.2019.00793

6. Alam S, Khan M, Alouffi A, Almutairi MM, Ullah S, Numan M, et al. Spatio-temporal patterns of ticks and molecular survey of *Anaplasma marginale*, with notes on their phylogeny. *Microorganisms*. (2022) 10:1663. doi: 10.3390/microorganisms10081663

7. Ullah S, Alouffi A, Almutairi MM, Islam N, Rehman G, Ul Islam Z, et al. First report of *Rickettsia conorii* in *Hyalomma kumari* ticks. *Animals*. (2023) 13:1488. doi: 10.3390/ani13091488

8. Apanaskevich DA, Schuster AL, Horak IG. The genus *Hyalomma*: VII. Redescription of all parasitic stages of *H*.(Euhyalomma) *dromedarii* and H.(E.) schulzei (Acari: Ixodidae). *J Med Entomol*. (2008) 45:817–31. doi: 10.1093/jmedent/45.5.817

9. Sands AF, Apanaskevich DA, Matthee S, Horak IG, Harrison A, Karim S, et al. Effects of tectonics and large scale climatic changes on the evolutionary history of *Hyalomma* ticks. *Mol Phyl Evol*. (2017) 114:153–65. doi: 10.1016/j.ympev.2017.06.002

10. Guglielmone AA, Nava S, Robbins RG. Geographic distribution of the hard ticks (Acari: Ixodida: Ixodidae) of the world by countries and territories. *Zootaxa*. (2023) 5251:1–274. doi: 10.11646/zootaxa.5251.1.1

11. Apanaskevich DA, Horak IG. The genus *Hyalomma* Koch, 1844. IX. Redescription of all parasitic stages of *H*.(Euhyalomma) *impeltatum* Schulze & Schlottke, 1930 and *H*.(E.) *somalicum* Tonelli Rondelli, 1935 (Acari: Ixodidae). *Syst Parasitol*. (2009) 73:199–218. doi: 10.1007/s11230-009-9190-x

12. Apanaskevich DA, Horak IG. The genus *Hyalomma* Koch, 1844: V. Re-evaluation of the taxonomic rank of taxa comprising the *H*.(Euhyalomma) *marginatum* Koch complex of species (Acari: Ixodidae) with redescription of all parasitic stages and notes on biology. *Int J Acarol*. (2008) 34:13–42. doi: 10.1080/01647950808683704

13. Apanaskevich DA, Filippova NA, Horak IG. The genus *Hyalomma* Koch, 1844. X. Redescription of all parasitic stages of *H*.(Euhyalomma) *scupense* Schulze, 1919 (= *H. Detritum* Schulze)(Acari: Ixodidae) and notes on its biology. *Folia Parasitol (Praha)*. (2010) 57:69–78. doi: 10.14411/fp.2010.009

14. Apanaskevich D, Horak I. The genus *Hyalomma* Koch, 1844. I. Reinstatement of *Hyalomma* (Euhyalomma) *glabrum* Delpy, 1949 (Acari, Ixodidae) as a valid species with a redescription of the adults, the first description of its immature stages and notes on its biology. *Onderstepoort J Ve*. 73:1–12. doi: 10.4102/ojvr.v73i1.164

15. Apanaskevich DA, Horak IG. The genus *Hyalomma*. XI. Redescription of all parasitic stages of *H*.(Euhyalomma) *asiaticum* (Acari: Ixodidae) and notes on its biology. *Exp Appl Acarol*. (2010) 52:207–20. doi: 10.1007/s10493-010-9361-0

16. Khan M, Islam N, Khan A, Islam ZU, Muñoz-Leal S, Labruna MB, et al. New records of *Amblyomma gervaisi* from Pakistan, with detection of a reptile-associated *borrelia* sp. *Ticks Tick-Borne Dis*. (2022) 13:102047. doi: 10.1016/j.ttbdis.2022.102047

17. Jabeen F, Mushtaq M, Qayyum M, Hasan M, Zafar MA, Riaz A, et al. Tick taxonomy and nucleotide sequence analysis by internal transcribed spacer 2 (ITS 2) in large ruminants of Pothohar, Pakistan. *Pak Vet J*. (2022) 42:554–60. doi: 10.29261/pakvetj/2022.063

18. Davison HR, Pilgrim J, Wybouw N, Parker J, Pirro S, Hunter-Barnett S, et al. Genomic diversity across the *rickettsia* and '*Candidatus Megaira*'genera and proposal of genus status for the Torix group. *Nat Commun*. (2022) 13:2630. doi: 10.1038/s41467-022-30385-6

19. Hussain S, Saqib M, Ashfaq K, Sindhu ZUD. First molecular evidence of *Coxiella burnetii* in ticks collected from dromedary camels in Punjab, Pakistan. *Pak Vet J*. (2021):10. doi: 10.29261/pakvetj/2021.073

20. Battilani M, De Arcangeli S, Balboni A, Dondi F. Genetic diversity and molecular epidemiology of *Anaplasma*. *Infect Genet Evol*. (2017) 49:195–211. doi: 10.1016/j.meegid.2017.01.021

21. Barradas PF, Mesquita JR, Ferreira P, Gärtner F, Carvalho M, Inácio E, et al. Molecular identification and characterization of *rickettsia* spp. and other tick-borne pathogens in cattle and their ticks from Huambo, Angola. *Ticks Tick-Borne dis*. (2021) 12:101583. doi: 10.1016/j.ttbdis.2020.101583

22. Parola P, Paddock CD, Raoult D. Tick-borne rickettsioses around the world: emerging diseases challenging old concepts. *Clin Microbiol Rev*. (2005) 18:719–56. doi: 10.1128/CMR.18.4.719-756.2005

23. Yu Z, Wang H, Wang T, Sun W, Yang X, Liu J. Tick-borne pathogens and the vector potential of ticks in China. *Parasites Vectors*. (2015) 8:24–8. doi: 10.1186/s13071-014-0628-x

24. de la Fuente J, Ghosh S, Lempereur L, Garrison A, Sprong H, Lopez-Camacho C, et al. Interventions for the control of Crimean-Congo hemorrhagic fever and tick vectors. *npj Vaccines*. (2024) 9:181. doi: 10.1038/s41541-024-00970-5

25. Karim S, Budachetri K, Mukherjee N, Williams J, Kausar A, Hassan MJ, et al. A study of ticks and tick-borne livestock pathogens in Pakistan. *PLoS Negl Trop Dis*. (2017) 11:e0005681. doi: 10.1371/journal.pntd.0005681

26. Khan M, Almutairi MM, Alouffi A, Tanaka T, Chang S-C, Chen C-C, et al. Molecular evidence of *borrelia theileri* and closely related *borrelia* spp. in hard ticks infesting domestic animals. *Front Vet Sci*. (2023) 10:1297928. doi: 10.3389/fvets.2023.1297928

27. Ullah Z, Khan M, Liaqat I, Kamran K, Alouffi A, Almutairi MM, et al. Unveiling misconceptions among small-scale farmers regarding ticks and tick-borne diseases in Balochistan, Pakistan. *J Vet Sci*. (2024) 11:497. doi: 10.3390/vetsci11100497

28. Sambrook J. Molecular cloning: a laboratory manual Cold Spring Habor Laboratory USA, New York. (1989).

29. Altschul SF, Gish W, Miller W, Myers EW, Lipman DJ. Basic local alignment search tool. *J Mol Biol*. (1990) 215:403–10. doi: 10.1016/S0022-2836(05)80360-2

30. Thompson JD, Higgins DG, Gibson TJ. CLUSTAL W: improving the sensitivity of progressive multiple sequence alignment through sequence weighting, position-specific gap penalties and weight matrix choice. *Nucleic Acids Res*. (1994) 22:4673–80. doi: 10.1093/nar/22.22.4673

31. Hall T, Biosciences I, Carlsbad C. BioEdit: an important software for molecular biology. *GERF Bull Biosci*. (2011) 2:60–1.

32. Kumar S, Stecher G, Li M, Knyaz C, Tamura K. MEGA X: molecular evolutionary genetics analysis across computing platforms. *Mol Biol Evol*. (2018) 35:1547–9. doi: 10.1093/molbev/msy096

33. Edgar RC. MUSCLE: multiple sequence alignment with high accuracy and high throughput. *Nucleic Acids Res*. (2004) 32:1792–7. doi: 10.1093/nar/gkh340

34. Fao F. Food and agriculture organization of the United Nations. Rome (2018):403. Available at: http://faostat.fao.org (Accessed July 11 2024).

35. Tila H, Khan M, Almutairi MM, Alouffi A, Ahmed H, Tanaka T, et al. First report on detection of Hepatozoon ayorgbor in *Rhipicephalus haemaphysaloides* and *Hepatozoon colubri* in *Haemaphysalis sulcata* and *Hyalomma anatolicum*: risks of spillover of *Hepatozoon* spp. from wildlife to domestic animals. *Front Vet Sci*. (2023) 10:1255482. doi: 10.3389/fvets.2023.1255482

36. Lv J, Wu S, Zhang Y, Chen Y, Feng C, Yuan X, et al. Assessment of four DNA fragments (COI, 16S rDNA, ITS2, 12S rDNA) for species identification of the Ixodida (Acari: Ixodida). *Parasit Vectors*. (2014) 7:1–11. doi: 10.1186/1756-3305-7-93

37. Mans BJ, Chitimia-Dobler L, Pienaar R, de Castro M, Khan M, Almutairi MM, et al. Mitochondrial genome and nuclear ribosomal RNA analysis place *Alveonasus lahorensis* within the Argasinae and suggest that the genus *Alveonasus* is paraphyletic. *Parasitology*. (2024):1–10. doi: 10.1017/S0031182024000441

38. Uiterwijk M, Ibáñez-Justicia A, van de Vossenberg B, Jacobs F, Overgaauw P, Nijsse R, et al. Imported *Hyalomma* ticks in the Netherlands 2018–2020. *Parasit Vectors*. (2021) 14:244. doi: 10.1186/s13071-021-04738-x

39. Parola P, Paddock CD, Socolovschi C, Labruna MB, Mediannikov O, Kernif T, et al. Update on tick-borne rickettsioses around the world: a geographic approach. *Clin Microbiol Rev*. (2013) 26:657–702. doi: 10.1128/CMR.00032-13

40. Parola P, Raoult D. Ticks and tickborne bacterial diseases in humans: an emerging infectious threat. *Clin Infect Dis*. (2001) 32:897–928. doi: 10.1086/319347

41. Roux V, Raoult D. Phylogenetic analysis of members of the genus *rickettsia* using the gene encoding the outer-membrane protein rOmpB (ompB). *Int J Syst Evol Microbiol*. (2000) 50:1449–55. doi: 10.1099/00207713-50-4-1449

42. Labruna MB, Whitworth T, Horta MC, Bouyer DH, McBride JW, Pinter A, et al. *Rickettsia* species infecting *Amblyomma cooperi* ticks from an area in the state of Sao Paulo, Brazil, where Brazilian spotted fever is endemic. *J Clin Microbiol*. (2004) 42:90–8. doi: 10.1128/JCM.42.1.90-98.2004

43. Majid A, Almutairi MM, Alouffi A, Tanaka T, Yen T-Y, Tsai K-H, et al. First report of spotted fever group *Rickettsia aeschlimannii* in *Hyalomma turanicum, Haemaphysalis bispinosa*, and *Haemaphysalis montgomeryi* infesting domestic animals: updates on the epidemiology of tick-borne *Rickettsia aeschlimannii*. *Front Microbiol*. (2023) 14:1283814. doi: 10.3389/fmicb.2023.1283814

44. Ghafar A, Cabezas-Cruz A, Galon C, Obregon D, Gasser RB, Moutailler S, et al. Bovine ticks harbour a diverse array of microorganisms in Pakistan. *Parasit Vectors*. (2020) 13:1–15. doi: 10.1186/s13071-019-3862-4

45. Aneela A, Almutairi MM, Alouffi A, Ahmed H, Tanaka T, da Silva VI, et al. Molecular detection of *Rickettsia hoogstraalii* in *Hyalomma anatolicum* and *Haemaphysalis sulcata*: updated knowledge on the epidemiology of tick-borne *Rickettsia hoogstraalii*. *J Vet Sci*. (2023) 10:605. doi: 10.3390/vetsci10100605

46. Dahlgren FS, Heitman KN, Drexler NA, Massung RF, Behravesh CB. Human granulocytic anaplasmosis in the United States from 2008 to 2012: a summary of national surveillance data. *Am J Trop Med Hyg*. (2015) 93:66–72. doi: 10.4269/ajtmh.15-0122

47. Abbas SN, Ijaz M, Abbas RZ, Saleem MH, Mahmood AK. Molecular characterization, risk factor analysis and hematological alterations associated with *Anaplasma phagocytophilum* in domestic cats of Pakistan. *Pak Vet J*. (2023) 43:493–9. doi: 10.29261/pakvetj/2023.082

48. Pourhossein B, Irani AD, Mostafavi E. Major infectious diseases affecting the Afghan immigrant population of Iran: a systematic review and meta-analysis. *Epidemiol Health*. (2015):37. doi: 10.4178/epih/e2015002

49. Mangold A, Bargues M, Mas-Coma S. Mitochondrial 16S rDNA sequences and phylogenetic relationships of species of *Rhipicephalus* and other tick genera among Metastriata (Acari: Ixodidae). *J Parasitol Res*. (1998) 84:478–84. doi: 10.1007/s004360050433

50. Folmer R, Nilges M, Folkers P, Konings R, Hilbers C. A model of the complex between single-stranded DNA and the single-stranded DNA binding protein encoded by gene V of filamentous bacteriophage M13. *J Mol Biol*. (1994) 240:341–57. doi: 10.1006/jmbi.1994.1449

51. Regnery RL, Spruill CL, Plikaytis B. Genotypic identification of rickettsiae and estimation of intraspecies sequence divergence for portions of two rickettsial genes. *J Bacteriol*. (1991) 173:1576–89. doi: 10.1128/jb.173.5.1576-1589.1991

52. Inokuma H, Raoult D, Brouqui P. Detection of *Ehrlichia platys* DNA in brown dog ticks (*Rhipicephalus sanguineus*) in Okinawa Island, Japan. *J Clin Microbiol*. (2000) 38:4219–21. doi: 10.1128/JCM.38.11.4219-4221.2000

53. PES. (2024). Available at: https://finance.gov.pk/survey_2024.html (Accessed 16 July 2024).

frontiers | Frontiers in Veterinary Science

TYPE Brief Research Report
PUBLISHED 15 January 2025
DOI 10.3389/fvets.2024.1463046

Check for updates

OPEN ACCESS

EDITED BY
Hongbin Yan,
Chinese Academy of Agricultural Sciences, China

REVIEWED BY
Luis Garcia Prieto,
National Autonomous University of Mexico, Mexico
Qaisar Tanveer,
University of Edinburgh, United Kingdom

*CORRESPONDENCE
Supaphen Sripiboon
✉ ssripiboon@gmail.com
✉ supaphen.s@ku.th

RECEIVED 11 July 2024
ACCEPTED 05 December 2024
PUBLISHED 15 January 2025

CITATION
Maneepairoj N, Lekcharoen P, Chaisiri K and Sripiboon S (2025) Murine-related helminthiasis: a public health concern at solid waste sites around forest- adjacent communities in Thailand.
Front. Vet. Sci. 11:1463046.
doi: 10.3389/fvets.2024.1463046

COPYRIGHT
© 2025 Maneepairoj, Lekcharoen, Chaisiri and Sripiboon. This is an open-access article distributed under the terms of the Creative Commons Attribution License (CC BY). The use, distribution or reproduction in other forums is permitted, provided the original author(s) and the copyright owner(s) are credited and that the original publication in this journal is cited, in accordance with accepted academic practice. No use, distribution or reproduction is permitted which does not comply with these terms.

Murine-related helminthiasis: a public health concern at solid waste sites around forest- adjacent communities in Thailand

Nattapon Maneepairoj[1], Paisin Lekcharoen[2], Kittipong Chaisiri[3] and Supaphen Sripiboon[1]*

[1]Department of Large Animal and Wildlife Clinical Sciences, Faculty of Veterinary Medicine, Kasetsart University, Bangkok, Thailand, [2]Department of Veterinary Public Health, Faculty of Veterinary Science, Chulalongkorn University, Bangkok, Thailand, [3]Department of Helminthology, Faculty of Tropical Medicine, Mahidol University, Bangkok, Thailand

Murine-related helminthiasis is a frequently overlooked zoonotic disease with significant public health implications. The role of murine rodents in transmitting these infections to other animals remains under-researched. This study aimed to investigate murine-related helminth infections at solid waste sites, particularly in forest-adjacent communities where murine rodent populations are high and multi-host interactions are possible. During a 5-day trapping session, 36 live traps were deployed across different habitats during both wet and dry seasons. Trapped murine rodents and their gastrointestinal (GI) parasites were morphologically evaluated for species identification. The results revealed that a total of 380 murine rodents were captured, with an overall GI helminth infection prevalence of 86.8% (330/380). The adult male murine rodents exhibited higher prevalence, abundance, and species richness of helminths compared to juvenile and female murine rodents. A total of 16 helminth species were identified, with *Trichostrongylus* morphotype A showing the highest infection prevalence (53.2%). Six zoonotic species were also detected, including *Syphacia obvelata* (22.4%), *Syphacia muris* (12.4%), *Raillietina* spp. (10.8%), *Hymenolepis diminuta* (10.3%), *Vampirolepis nana* (10%), and *Cyclodontostomum purvisi* (2.4%). Increased population of murine rodents was observed at the solid waste sites, as indicated by higher trap success (TS) rates. Forest murine rodents exhibited a significant prevalence of helminth infections and high species diversity. These findings suggest that solid waste sites adjacent to forests may pose a heightened risk for disease transmission, warranting further attention.

KEYWORDS

helminth, helminthiasis, murine rodent, solid waste site, Thailand, zoonotic helminth

Introduction

The exponential increase in global municipal solid waste generation, projected to reach 3.40 billion tons by 2050 (1), poses significant threats to public health and environmental sustainability. The World Health Organization (WHO) emphasizes the complex relationship between poor waste management and the contamination of soil, water, and air (2), which creates substantial health hazards for communities (3, 4). Moreover, inadequate waste management transforms solid waste sites into foraging grounds for a diverse range of animals,

including humans. This phenomenon disrupts natural movement patterns and fosters interspecies interactions, potentially increasing the transmission of diseases (4, 5). The cohabitation of diverse species within these environments creates optimal conditions for zoonotic diseases such as leptospirosis, rabies, dengue, and influenza (6), highlighting the urgent need for comprehensive waste management strategies.

Murine rodents (family *Muridae*), including rats and mice, thrive in diverse habitats, particularly human-modified environments such as solid waste sites (7, 8). Murine rodents are not only considered agricultural pests but also serve as reservoirs for numerous zoonotic diseases, including leptospirosis, hantavirus, and several parasitic infections (9–18). Waste sites, with their abundant food resources, may contribute to increased populations of murine rodent and amplify the risk of disease transmission. Although zoonotic diseases in murine rodents have been extensively studied in agricultural and community settings, research specific to solid waste sites is lacking. Addressing this gap is crucial not only for public health but also for mitigating disease transmission to other areas and species (19, 20).

In Thailand, murine rodents are widespread in urban and rural areas, serving as reservoirs for numerous pathogens. Studies have identified murine rodents positive for various microparasites such as *Leptospira* spp., *Orientia* spp., *Bartonella* spp., Hantavirus, Herpes virus, lymphocytic choriomeningitis virus (LCMV), Rabies virus, *Toxoplasma gondii*, *Trypanosoma* spp., and *Babesia* spp. (21–23). Studies on macroparasites have documented ectoparasites such as mites (e.g., *Leptotrombidium* spp. and *Blankaartia* spp.), ticks (e.g., *Dermacentor* spp., *Haemaphysalis* spp., *Ixodes glanulatus,* and *Rhipicephalus sanguieus*), and fleas (e.g., *Xenopsylla cheopis* and *Nosopsyllus fasciatus*). Parasitic nematodes (e.g., *Angiostrongylus cantonensis*, *Calodium hepatium*, *Cyclodontostomum purvisi*, and *Trichuris muris*), cestodes (e.g., *Raillietina* spp., *Hymenolepis diminuta*, *Vampirolepis nana* (syn. *Hymenolepis nana*), and *Hydratigera taeniaeformis*), and trematodes (e.g., *Echinostoma malayanum*) have also been reported (23–33). However, there remains a notable gap in research on gastrointestinal (GI) helminths in murine populations specifically within solid waste sites. These sites could serve as hotspots for parasitic transmission, posing significant risks to public health and ecosystem integrity.

As outlined earlier, solid waste sites represent unique habitat where human activities alter ecological dynamics, including zoonotic disease transmission. Murine rodents frequently inhabit these sites, interacting with multiple species and environmental pathogens. Given their adaptability and close association with human settlements, murine rodents are of particular interest as potential reservoirs of zoonotic diseases. This study aims to fill this gap by investigating the role of murine rodents as potential reservoirs for GI helminths, comparing their abundance and diversity between waste sites and other habitats. In addition, seasonal variations in GI helminth prevalence are explored to better understand parasitic transmission in these understudied environments.

Materials and methods

Study sites and sampling locations

To investigate the abundance and diversity of murine hosts and their GI helminths, three study sites were selected in Nakhon Ratchasima Province, Thailand: Soengsang District (*S1*; 14.3593, 102.4172), Khonburi District (*S2*; 14.4651, 102.1621), and Wangnamkhieo District (*S3*; 14.4372, 101.8155). All three study sites (S1-S3) are situated near the Dong Phayayen–Khao Yai Forest Complex. These study sites encompass four distinct habitat types: (1) solid waste sites (SWS); (2) natural forests (NF), including either dipterocarps or secondary forests; (3) dense understory lands (DUL), characterized by abundant and tightly packed vegetation in the understory, creating a dense cover that provides ideal concealment for small mammals (e.g., corn and cassava crop); and (4) sparse understory lands (SUL), characterized by reduced vegetation density in the understory, offering a less extensive cover (e.g., perennial crop and orchards). Each study site contained an SWS and the other three habitats, which were located within a 2×2 km-square area. This study conducted in 3 study sites, in each sites we selected 5 habitats (from any of 4 types of habitats - SWS, NF, DUL, SUL). A map of the sampling locations is shown in Supplementary Figure S1.

Sampling strategies

During the period 2022–2023, a 5-day trapping session was conducted biannually during the dry season (November to April) and the wet season (May to October). Wild murine rodents were trapped using locally modified wire live traps measuring 12 cm (in width) × 28 cm (in length) × 12 cm (in height). These traps were baited with fresh corn. A total of 36 traps were strategically positioned in each sampling location according to a predefined grid line, with a set distance of 20 meters between each trap. Since murine rodents are nocturnal (9), the traps were deployed in the evening (between 3 and 6 PM) and checked for captures the following morning (between 5 and 8 AM). Animals other than murine rodents were released at the sampling location. Only the trapped murine rodent species were transported to the field stations for further investigation.

The rodents were euthanized through inhalation of an isoflurane overdose in a closed transparent chamber, following the ethical guideline established by Herbreteau et al. (34). Data including body weight, head-to-body length, ear length, hind foot length, tail length, the color of incisor, fur, and tail, and the number of mammae of female rodents were recorded to be used as a key for species identification (9). Initially, body weight and head-to-body length were used to classify specimens as rats or mice, followed by other parameters for accurate species identification. Genital appearance, as described by Herbreteau et al. (34), was used to determine sex and age class (juvenile or adult), with rodents showing underdeveloped genitalia classified as indeterminate. Murine rodent species were identified morphologically using biological measurements and identification keys (9, 35, 36). Subsequently, the rodents were dissected, and their gastrointestinal tracts were collected aseptically, preserved in 95% ethanol, and stored at 4°C until helminthological examination was conducted within 3 months.

Helminthological examination and identification

Helminths were identified through the examination of the gastrointestinal tracts, with dissections conducted under a

stereomicroscope (1.2X–1.4X) to provide detailed insights into their morphology. At this stage, the helminths were initially classified into nematodes, trematodes, and cestodes. For further taxonomic identification, the nematodes were cleared in lactophenol and mounted on temporary slides, while the cestodes and trematodes were stained with Semichon's carmine. The morphological structure, including the mouthparts, tail features, and internal organs, was examined using a light microscope (4X–40X), and the species were identified based on established taxonomic keys (37–39). To obtain quantitative data, a comprehensive count of each helminth species within the individual murine hosts was conducted to assess the abundance of infection.

Statistical analysis

The trap success (TS) rate served as a proxy for estimating the abundance of murine rodents, minimizing bias from unequal trap distributions across the habitats. The trap success rate was calculated using the following formula: Trap Success $(TS) = \frac{number\ animal\ caught}{number\ of\ trap\ efforts} \times 100$ (9).

A chi-squared test was used to assess helminth infection prevalence across the habitats, seasons (dry vs. wet), groups of murine rodents (rat vs. mouse), sex (male vs. female), and age class (juvenile vs. adult). The Kruskal–Wallis test was used to evaluate the effect of habitat type on GI helminth abundance, while the Mann–Whitney U test was employed to compare the influence of age class, sex, groups of murine rodents, and seasons on GI helminths abundance.

The Chao and Jackknife indices were used to estimate true parasite species richness, addressing the under-sampling often observed in cryptic parasite communities. The Chao index predicts unobserved species based on the presence of rare species in the sample, while the Jackknife index estimates richness by systematically omitting parts of the dataset (40, 41). The Shannon index was used to quantify GI helminth species diversity, comparing the variations in abundance and species richness across the habitats and murine rodent species. All analyses were performed in Rstudio version 2024.04.2 + 764 "vegan" and "BiodiversityR" packages (42–44).

Results

Community structure of the murine rodents (trap success rate and species diversity)

A total of 380 murine rodents were trapped from 2,755 trap nights, yielding an overall trap success rate of 13.8%. Of the 380 trapped murine rodents, 59.7% (227/380) were male, while 39.7% (151/380) were female. The sex of two murine rodents could not be identified due to the underdevelopment of their genital organs. In terms of age class, 77.1% (293/380) were adults and the remaining were juveniles. Seasonality had an impact on the murine populations, with a higher number of trapped murine rodents and a higher trap success rate in the dry season compared to the wet season. Variation in the number of trapped murine rodents across the different types of habitats was observed. In addition, the forest habitat showed the highest number of trapped murine rodents ($n = 124$), while the solid waste sites revealed the highest trap success rate (17.6%), indicating the potential for high relative abundance of murine rodent populations in these two habitats. Details of the trapped murine rodents in this study are shown in Table 1.

According to the morphological keys, eight murine species were identified. Among all trapped murine rodents, *Mus cervicolor* ($n = 214$) and *Rattus rattus* complex ($n = 80$) were the most abundant species, with trap success rates of 7.8 and 2.9, respectively. *Mus cervicolor* was the numerically dominant species in all habitat types, especially in the dense understory lands (DUL). In addition, the composition of the murine species varied in each type of the habitat. For example, the agricultural habitat types (DUL and SUL) showed a higher proportion (>75% of the total murine population) of *Mus* spp., including *M. cervicolor, M. caroli, and M. pahari,* compared to the other habitat types. On the other hand, *Maxomys surifer* was the second most abundant murine rodent species in the NF, while none were found in the other habitat types. In addition, a large proportion of *Rattus* spp. were found in the SWS. Details of the murine species composition in each type of the habitat are shown in Figure 1. The Shannon index was used to reveal the distinct murine diversity in the natural forests (1.35), SUL (1.32), SWS (1.17), and DUL (0.49), respectively.

Prevalence of gastrointestinal helminth infection

Of the 380 trapped murine rodents, gastrointestinal helminths were found in 330, resulting in a prevalence of gastrointestinal helminth infection of 86.8%. An investigation into the relationship between the prevalence of gastrointestinal helminth infection and factors, (habitat type, season, age, sex, and murine species), revealed distinctive patterns. All habitats showed high prevalence of the infection, affecting more than 70% of the total population. The highest prevalence of the infection was observed in the SUL (95.56%), whereas the lowest prevalence was recorded in the SWS (74.51%). Habitat was the only exogenous factor that had a statistically significant relationship with the prevalence of the infection ($\chi^2 = 19.394$, $p < 0.01$). The prevalence of the infection was not significantly different ($\chi^2 = 1.7919$, $p = 0.1807$) between the seasons, although the prevalence of the infection in the wet season (89.66%) was slightly higher than that in the dry season (84.47%). The endogenous characteristics, including age Class ($\chi^2 = 12.362$, $p < 0.01$) and sex ($\chi^2 = 5.4426$, $p = 0.01965$), were found to affect the prevalence of the infection with statistical significance, with the adult and male murine rodents showing higher prevalence (Table 1).

Abundance and intensity of the gastrointestinal helminths

In this study, a total of 13,740 individual gastrointestinal helminths were quantified from 380 trapped murine rodent hosts, resulting in a mean abundance (MA) of 36.2 helminths per host and a mean intensity (MI) of 41.6 helminths per host. The mean abundance and mean intensity of helminth infection varied by

TABLE 1 Number of trapped murine rodent hosts, trap success rate (%), prevalence of gastrointestinal helminth infection (%), mean abundance (MA), mean intensity (MI), parasite species richness (PSR) indices, and diversity index divided into types of habitat, season, age class, and sex.

	Total number of murine rodents	Trap success rate (%)	Prevalence of infection (%)	Mean Abundance (number of helminths per host ± SE)	Mean intensity (number of helminths per infected host ± SE)	Parasite Species Richness (PSR)			Diversity index (Shannon)
						Observed PSR	Estimated PSR (Chao)	Estimated PSR (Jackknife)	
Habitat									
Solid waste sites	102	17.6	74.5	35.5 ± 7.9	47.6 ± 10.2	12	13.98	13.98	1.38
Natural forests	124	12.8	90.3	40.6 ± 6.5	45.0 ± 7.1	14	14.49	14.99	1.63
Dense understory lands (DUL)	109	15.3	90.8	30.9 ± 4.9	34.0 ± 5.3	12	13.98	13.98	1.52
Sparse understory lands (SUL)	45	9.1	95.6	38.2 ± 12.8	39.9 ± 13.4	11	16.87	14.91	1.53
Season									
Wet	174	12.0	89.7	50.9 ± 7.1	56.8 ± 7.8	14	14.99	15.99	1.64
Dry	206	15.7	84.5	23.7 ± 4.3	28.1 ± 3.0	15	16.99	16.99	1.65
Age class*									
Adult	293	10.6	89.8	38.9 ± 4.2	43.3 ± 4.6	16	18.99	18.99	1.70
Juvenile	75	2.7	73.33	19.9 ± 4.1	27.1 ± 5.3	11	12.97	12.97	1.49
Sex*									
Male	227	8.3	90.31	45.1 ± 5.3	49.9 ± 5.7	15	16.99	16.91	1.66
Female	151	5.5	81.5	23.2 ± 4.4	28.5 ± 5.2	14	15.99	15.99	1.73
Murine species									
Bandicota indica	4	0.1	75.0	55.8 ± 35.2	74.3 ± 42.3	6	13.50	9.75	0.87
Bandicota savilei	5	0.2	100	42.0 ± 24.9	42.0 ± 24.9	6	12.40	9.20	0.38
Maxomys surifer	30	1.1	90.0	36.3 ± 8.1	40.4 ± 8.6	4	4.00	4.96	0.90
Rattus rattus complex	80	2.9	92.5	69.7 ± 13.9	75.4 ± 14.8	12	12.25	12.99	1.13
Rattus exulans	9	0.3	11.1	1.8 ± 1.8	16	1	1.00	1.89	NA
Mus cervicolor	214	7.8	86.0	25.5 ± 2.9	29.7 ± 3.3	13	13.25	13.99	1.41
Mus caroli	37	1.3	94.6	31.3 ± 7.6	33.1 ± 8.0	9	9.97	10.94	1.12
Mus pahari	1	0.1	100	1	1	1	1.00	1.00	NA

The solid waste sites had the highest trap success rate and the lowest prevalence of the infection, but the highest mean intensity. In contrast, the natural forests exhibited the highest species richness and diversity. *Mus cervicolor* was the dominant species captured, showing the highest parasite richness and diversity.

*Age could not be classified in 12 murine rodents, and sex could not be identified in two murine rodents.

10.3389/fvets.2024.1463046

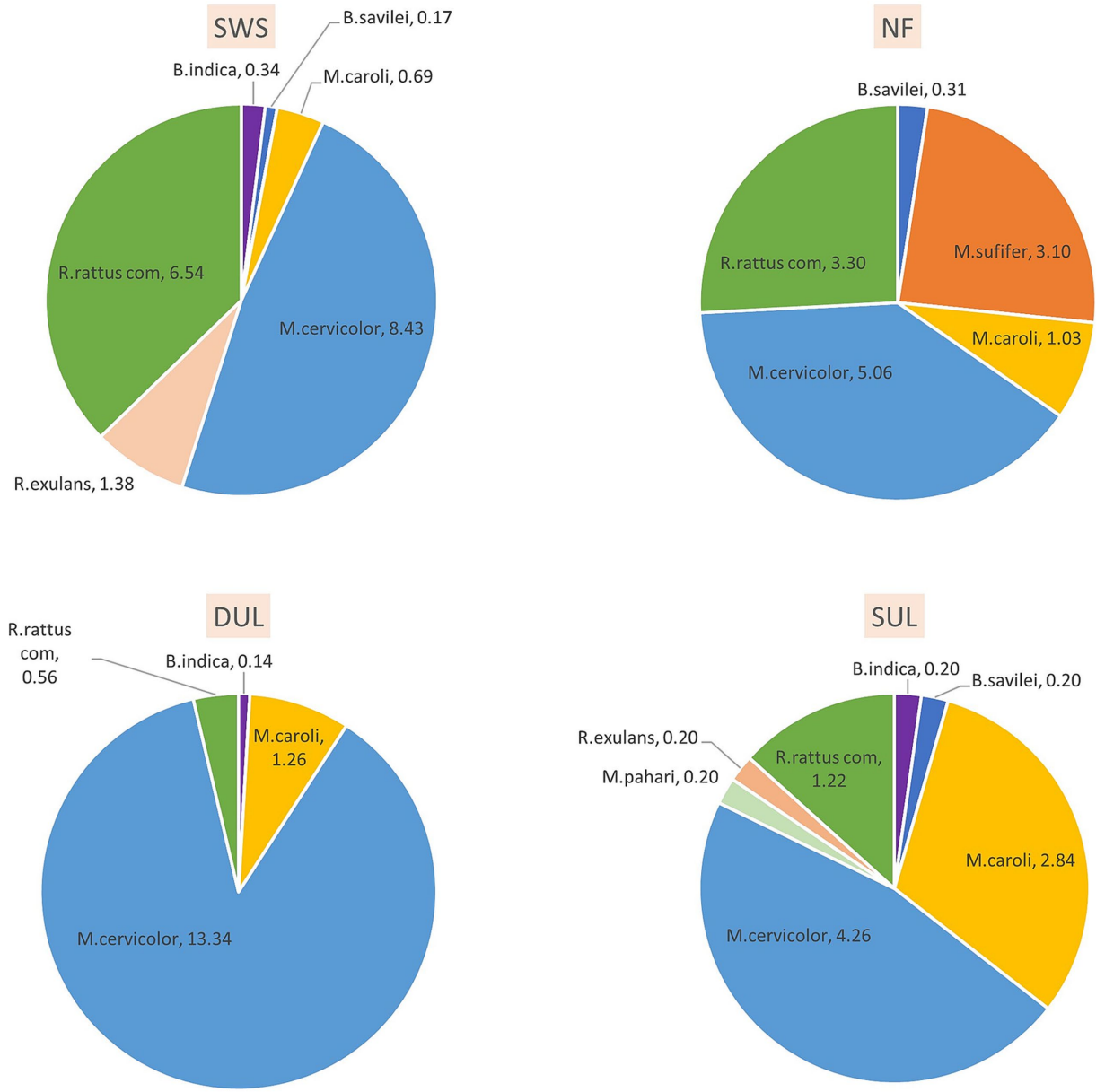

FIGURE 1
The composition of murine rodents varied across different habitats, reflecting the differing habitat suitability for each species. *Mus cervicolor* (the fawn-colored mouse) was dominant in all habitat types observed in this study, especially in the agricultural areas, while *Maxomys surifer* (the red spiny rat) was found exclusively in the forest habitat, where it had the second-highest abundance. SWS, solid waste sites; NF, natural forests; DUL, dense understory lands; SUL, sparse understory lands.

habitat, but there was no significant difference (Kruskal–Wallis chi-squared = 105.1, $p = 0.344$). In addition, the highest mean abundance was observed in the murine rodents from the natural forests (MA = 40.6 ± 6.5), while the SWS exhibited the highest mean intensity of helminth infection at 47.6 ± 10.2. Significant variations in gastrointestinal helminth abundance/intensity between the seasons were observed, with the wet season showing higher helminth abundance/intensity than the dry season (Mann–Whitney U test, W = 13,230, $p < 0.01$). Age, sex, and murine species also significantly impacted ($p < 0.01$) the abundance and intensity of gastrointestinal helminth infection in the murine rodents; see details in Table 1.

Species richness and diversity of the gastrointestinal helminths

A total of 16 species (or taxa) of the gastrointestinal helminths were morphologically identified in this study. *Trichostrongylidae* gen. sp. exhibited the highest population ($n = 6,480$), followed by *Syphacia muris* ($n = 3,573$) and *Syphacia obvelata* ($n = 2,521$). Based on the tail morphology, *Trichostrongylidae* gen. sp. was categorized into three morphotypes: morphotype A ($n = 3,676$), morphotype B ($n = 2,796$), and morphotype C ($n = 8$; Supplementary Figure S2). The total number and prevalence of infection of each helminth are shown in Figure 2 and Supplementary Table S1. Parasite species

richness (PSR) was determined through microscopic examination, and the estimated true PSR was calculated using the Chao and Jackknife indices, revealing that the murine rodents living in the natural forest exhibited the highest PSR, with 14 identified species (or distinct taxa), followed by the murine rodents in the SWS and DUL, which hosted 12 species of GI helminths (Table 1). Of the 16 identified GI helminth species, 9 species were consistently found in every type of habitat, including *Ascaridae* gen. sp., *Protospirura siamensis*, *Syphacia obvelata*, *Capillaria gastrica*, *Trichostrongylus* morphotype A, Trichostrongylus morphotype B, *Hymenolepis diminuta*, *Vampirolepis nana*, and *Raillietina* spp. In contrast, *Notocotylus loeiensis* was only found in one murine rodent among the total of 380 murine rodents (Figure 2). GI helminth diversity was assessed using PSR, and the abundance across the habitats was determined using the Shannon–Wiener index, demonstrated varying values for each habitat: 1.63 for the natural forests, 1.52 for the dense understory lands, 1.53 for the sparse understory lands, and 1.38 for the solid waste sites.

Zoonotic gastrointestinal helminths

Among the 16 species of gastrointestinal helminths investigated in this study, 6 were identified as zoonotic parasites. Notably, three of these parasites were cestodes, including *Raillietina* spp., *Hymenolepis diminuta*, and *Vampirolepis nana*, while the remaining three were nematodes, including *Syphacia obvelata*, *Syphacia muris,* and *Cyclodontostomum purvisi*. The prevalence of the infection for each zoonotic parasite was 10.8, 10.3, 10, 22.4, 12.4, and 2.4%, respectively. The prevalence of zoonotic helminth infection was notably higher and showed significant differences in the surrounding habitats compared to the SWS ($\chi^2 = 24.638$, $p < 0.01$; Table 2). The overall prevalence of the infection was quite similar between the seasons, with 56.3% in the wet season and 50.9% in the dry season ($\chi^2 = 0.88102$, $p = 0.3479$). Furthermore, a significantly higher prevalence of zoonotic helminth infection was observed in the adult ($\chi^2 = 4.7984$, $p = 0.028$) and male ($\chi^2 = 15.643$, $p < 0.01$) rodents (Table 2).

When only zoonotic parasites were considered, a total of 6,343 worms were quantified, with a mean abundance (MA) of 16.7 ± 2.8. The murine rodents from the natural forests (Kruskal–Wallis chi-squared = 77.711, $p = 0.07318$) demonstrated the highest mean abundance and mean intensity, with values of 22.8 and 36.2, respectively. The seasonal effect still showed higher mean abundance of zoonotic helminths in the wet season compared to the dry season (W = 17,379, $p = 0.59$). While the mice population (W = 14,275, $p = 0.053$) had 2,661 individual zoonotic parasites (MA = 10.6), the rat population exhibited 3,682 individual zoonotic parasites (MA = 28.8). Although these differences were not statistically significant, the patterns aligned with the overall gastrointestinal helminth prevalence trends, as detailed in Table 2. Zoonotic parasite species richness (ZPSR) was defined as the count of species, indicating that the natural forests, sparse understory lands, and solid waste sites exhibited the highest ZPSR, each hosting a total of six identified species. In contrast, the dense understory lands accommodated four parasite species each. Zoonotic helminth diversity, assessed using the Shannon–Wiener index, showed varying values, with the highest index found in the natural forests (Table 2).

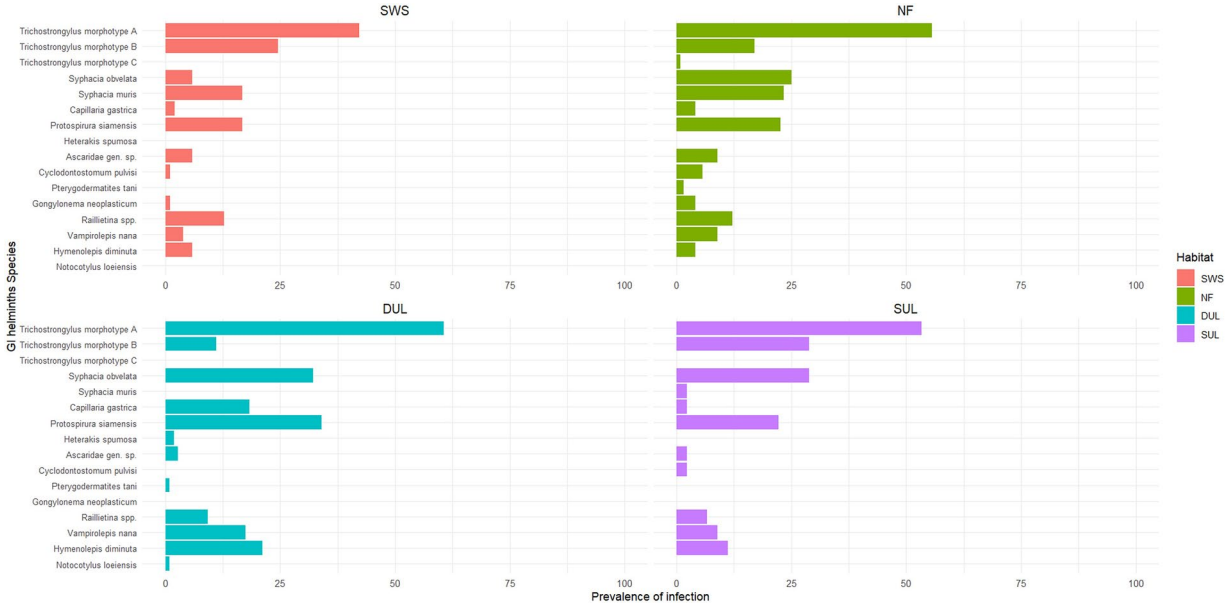

FIGURE 2
The prevalence of gastrointestinal helminth infections (%) varied across different habitat types. *Trichostrongylus* morphotype A was the most common helminth found in this study, while *Trichostrongylus* morphotype C was exclusively found in natural forests. The prevalence of the infection was also linked to the presence of specific host species, which varied by habitat. SWS, solid waste sites; NF, natural forests; DUL, dense understory lands; SUL, sparse understory lands.

TABLE 2 Prevalence of the infection, total abundance, mean abundance, mean intensity, zoonotic parasite species richness (ZPSR), and parasite diversity of the zoonotic parasites found in this study, divided into types of habitat, season, age, class, sex, and murine group.

	Prevalence of zoonotic parasite (%)	Total abundance of zoonotic parasites	Mean Abundance (MA) of zoonotic parasite	Mean Intensity (MI) of zoonotic parasite	Observed ZPSR	Estimated ZPSR (Chao)	Estimated ZPSR (Jackknife)	Diversity index (Shannon)
Habitat								
Solid waste sites	33.3	1,731	17.0 ± 5.7	17 ± 5.7	6	6.00	6.99	0.53
Natural forests	62.9	2,827	22.8 ± 5.5	36.2 ± 8.4	6	6.00	6.00	0.82
Dense understory lands (DUL)	62.4	925	8.5 ± 2.6	13.6 ± 4.0	4	4.00	4.00	0.43
Sparse understory lands (SUL)	51.1	860	19.1 ± 11.6	37.4 ± 22.3	6	6.98	7.96	0.80
Season								
Wet	56.3	3,790	21.8 ± 5.7	38.7 ± 9.7	6	6.00	6.00	0.75
Dry	50.9	2,553	12.4 ± 2.1	24.3 ± 3.8	6	6.00	6.00	0.86
Age class								
Adult	56.3	4,843	16.5 ± 3.0	29.4 ± 5.3	6	6.00	6.00	0.88
Juvenile	41.3	789	10.5 ± 3.4	25.4 ± 7.6	6	6.49	6.99	0.69
Sex								
Male	61.7	4,713	20.8 ± 3.9	33.7 ± 6.0	6	6.00	6.00	0.83
Female	40.4	1,626	10.8 ± 4.1	26.7 ± 9.8	6	6.00	6.00	0.90
Murine group								
Bandicota indica	50.0	117	29.3 ± 28.9	58.5 ± 57.5	3	5.25	5.25	0.14
Bandicota savilei	40.0	5	1 ± 0.6	2.5 ± 0.5	3	5.40	5.40	1.05
Maxomys surifer	53.6	676	24.1 ± 6.9	45.1 ± 10.3	1	1.00	1.00	NA
Rattus rattus complex	67.1	2,274	28.8 ± 9.6	42.9 ± 13.9	5	5.00	5.99	0.18
Rattus exulans	11.1	16	1.8 ± 1.8	16	1	1.00	1.89	NA
Mus cervicolor	50.0	1,888	9.2 ± 1.8	18.3 ± 3.5	5	5.00	5.00	0.31
Mus caroli	54.3	655	18.7 ± 7.1	34.5 ± 12.0	4	4.97	5.95	0.11
Mus pahari	NA	NA	NA	NA	NA	NA	NA	NA

The natural forests posed a potential risk for zoonotic GI helminths, showing the highest prevalence of the infection and mean abundance, with relatively high parasite richness and diversity compared to the other habitats.

Discussion

This study was the first to assess the potential threats of GI helminths in murine rodents captured from solid waste sites and forest-adjacent areas in Nakhon Ratchasima Province, northeastern Thailand. A total of 380 murine rodents were trapped across four habitat types and examined for GI helminths using morphological keys. High trap success rates were observed

in all habitats except the spare understory lands, indicating that this habitat is unsuitable for murine rodents due to the lack of hiding places at ground level (9, 45). On the contrary, the highest trap success rate was noted at the solid waste sites, indicating a potential breeding ground for murine rodents. In addition, the trap success rate was higher during the dry season, likely due to reduced food availability, which led the murine rodents to be more attracted to the bait (46).

Eight murine species were identified, with *Mus cervicolor* being the most predominantly trapped species in this study. This finding is consistent with those of previous studies (9, 34, 47). Its adaptability to various environments highlights its potential role in pathogen transmission (8, 48, 49). Moreover, *Mus cervicolor* was one of the two species carrying the zoonotic parasite, *Syphacia obvelata*, which showed high prevalence of infection in this study. This finding underscores the need for monitoring *S. obvelata* infection in humans within this area. Another notable finding was *Maxomys surifer*, which was exclusively found in the forested area, carrying four helminth species: *Syphacia muris* and three Trichostrongylus morphotypes (A, B, and C). The exclusive presence of this murine species in the forested area, in contrast to earlier research (50, 51), highlights a potential habitat shift due to human disturbances (52, 53), which can potentially facilitate parasite spillback or spillover into new hosts.

The overall prevalence of GI helminth infection in this study was 86.8%, which was notably higher than the prevalence reported from northern and northeastern Thailand, ranging from 55.1 to 71.54% (51, 54). One factor contributing to this higher prevalence is the inclusion of multiple murine rodent species in our study, compared to earlier research that focused on a single murine species. This broader sampling likely captured a wider range of host–parasite dynamics and interactions, increasing the observed prevalence. Seasonal differences also influenced the helminth dynamics, with higher infection prevalence and abundance observed during the wet season (55, 56), likely due to favorable environmental humidity for helminth eggs to hatch and infect hosts (26, 57). The differences in location, season, habitat characteristics, and trapping strategies could have influenced the variations in the prevalence of the infection (58, 59). These findings emphasize the importance of ecological factors in shaping parasite communities and highlight the value of examining diverse host populations to gain a better understanding of infection dynamics.

The factors associated with the prevalence and abundance of GI helminth infection included sex, age, and species. The adult male murine rodents exhibited higher prevalence and abundance of helminths, likely due to their larger body size, which can accommodate more helminths (51, 60–63). Similarly, the rats, with their larger body size, showed higher parasite abundance than the mice (64, 65). This suggests that habitats dominated by rats, such as solid waste sites and forests, may exhibit greater helminth burden. In-depth habitat analysis is further recommended to evaluate the ecological factors linked to the presence of murine rodents and their GI helminths.

Parasitic infections in murine rodents are potentially influenced by ecological factors, differing significantly between natural and human-modified habitats (58, 66). Natural forests provide stable ecosystems that support diverse parasite life cycles and interspecies interactions, which can regulate or promote parasite diversity and infection rates. This study observed moderate to high parasite prevalence and diversity in the murine rodents from the forest habitats compared to those from the solid waste sites. In contrast, human-modified habitats may disrupt parasite life cycles, particularly those requiring intermediate hosts, while favoring parasites with simpler life cycles that can adapt and thrive (66). In addition, changes in diet can influence parasite exposure; for instance, rodents in solid waste sites often forage on anthropogenic food sources, altering their exposure to helminth infective stages. Moreover, intensive agriculture and monoculture practices, often associated with high population of murine rodents, can facilitate parasite transmission by increasing contact between hosts (8, 67, 68), as observed in this study.

Among the 16 species of gastrointestinal helminths examined, *Trichostrongylus* morphotype A emerged as the predominant GI helminth, with high prevalence and abundance across all habitat types. In addition, both *Trichostrongylus* morphotypes A and B were consistently present in each habitat (Figure 2), consistent with the findings from previous studies (50, 51, 69, 70). Due to its direct life cycle and the adaptability of its larvae to various environmental conditions (71), it is therefore common to find this *Trichostrongylidae* gen. sp. in most areas where hosts are present. *Trichostrongylidae* gen. sp. is a gastrointestinal helminth in ruminants, rodents, pigs, horses, birds, and humans, with a worldwide distribution (39). Although *Trichostrongylidae* gen. sp. in rodents has not been reported as zoonotic, it can still affect the well-being of both host and non-host species, potentially causing symptoms such as mild abdominal discomfort and diarrhea (72, 73). In addition, due to its small size and morphological variation, individual identification of this parasitic taxon at the species level was not feasible. It is recommended that future research utilize molecular techniques for more accurate identification of these organisms. This approach will help elucidate its specific taxonomy (38, 74), examine host preferences, and assess potential impact on host populations.

Six zoonotic parasites were identified in this study, all previously documented as zoonotic in Thailand or other countries. While these parasites may remain asymptomatic at low infection levels, they can still cause illness in humans (75), presenting symptoms such as abdominal pain, vomiting, diarrhea, and malnutrition, particularly in children and immunocompromised individuals (26, 42, 76–84). Among them, *Syphacia* spp. are of particular concern as they are capable of infecting humans and causing abdominal pain and eosinophilia (75, 80). *Syphacia obvelata,* reported to be exclusively detected in mouse species (71), was the most prevalent zoonotic helminth observed in this study, with *Mus cervicolor* and *Mus caroli* identified as its primary hosts. Therefore, reducing specific murine rodent populations that serve as helminth reservoirs is considered a key strategy for minimizing the risk of human exposure to these zoonotic parasites (75). In addition, addressing public health concerns, improving sanitation and hygiene, and employing anthelmintic treatments are the recommended measures. To mitigate the issue of anthelmintic resistance, exploring herbal deworming as a sustainable alternative for parasite control could be a promising area for future research (85, 86).

This study found that approximately 8.5% of the murine rodents carried more than one hundred individual parasites without exhibiting visible clinical signs or disorders at the time of

capture. This resilience may be attributed to the hosts' robust immune response and overall health status. Within the gastrointestinal tract, cytokines such as IL-4 and IL-13 stimulate goblet cells, enhancing mucosal defense and reducing parasite-induced damage (87). Macrophages and eosinophils also play a pivotal role by secreting anti-inflammatory molecules that limit tissue damage and regulate the number of parasite species, contributing to the host ability to tolerate high parasite burden (88). These responses aim to contain parasites while minimizing harm to the host. Further research should delve deeper into the mechanisms underlying this balance, including investigations into blood parameters and species-specific immune responses.

In conclusion, the presence of murine rodents across all the habitat types, coupled with a high trap success rate, highlights their significant role in the transmission of zoonotic diseases, including the often-overlooked helminthiasis. The high prevalence of GI helminth infections, including six zoonotic species observed across the habitats, highlights the urgent need for comprehensive investigations into transmission dynamics. Solid waste sites, with the highest trap success rate, were identified as critical hotspots for multi-species interactions that may facilitate the spread of diseases. These sites also create an ideal environment for murine rodents due to abundant food sources, resulting in the highest number of trapped animals, thereby potentially amplifying the risk of disease transmission to humans and other species. To address this issue, it is essential to implement comprehensive waste management practices and establish effective monitoring programs to mitigate risks to public and veterinary health.

Data availability statement

The original contributions presented in the study are included in the article/Supplementary material, further inquiries can be directed to the corresponding author.

Ethics statement

The animal study was approved by Institutional Animal Care and Use Committee (IACUC) of the Faculty of Veterinary Medicine, Kasetsart University. The study was conducted in accordance with the local legislation and institutional requirements.

Author contributions

NM: Conceptualization, Data curation, Formal analysis, Investigation, Methodology, Writing – original draft. PL: Conceptualization, Investigation, Resources, Validation, Writing – review & editing. KC: Investigation, Methodology, Resources, Validation, Writing – review & editing. SS: Funding acquisition, Investigation, Project administration, Resources, Supervision, Writing – review & editing.

Funding

The author(s) declare that financial support was received for the research, authorship, and/or publication of this article. This study was funded by the SEAOHUN Small Grant, grant number (NG22-3-133), and partially supported by the Faculty of Veterinary Medicine at Kasetsart University.

Acknowledgments

The authors would like to thank the Department of Large Animal and Wildlife Clinical Science, Faculty of Veterinary Medicine, Kasetsart University, and the Department of Helminthology, Faculty of Tropical Medicine, Mahidol University, for supporting the facilities and equipment for this research. The authors used ChatGPT (OpenAI, GPT-4, 2024 version) for grammar corrections and minor language refinements.

Conflict of interest

The authors declare that the research was conducted in the absence of any commercial or financial relationships that could be construed as a potential conflict of interest.

Publisher's note

All claims expressed in this article are solely those of the authors and do not necessarily represent those of their affiliated organizations, or those of the publisher, the editors and the reviewers. Any product that may be evaluated in this article, or claim that may be made by its manufacturer, is not guaranteed or endorsed by the publisher.

Supplementary material

The Supplementary material for this article can be found online at: https://www.frontiersin.org/articles/10.3389/fvets.2024.1463046/full#supplementary-material

SUPPLEMENTARY FIGURE S1
Geographical location of each sampling locations deployed in this study. S1–S3 refered to three study sites that located near the Dong Phayayen-Khao Yai Forest Complex. Each study site consisted of at four different sampling locations including solid waste sites (SWS), natural forest (NF), dense understory lands (DUL), and sparse understory lands (SUL).

SUPPLEMENTARY FIGURE S2
The three Trichostrongyles morphotypes identified in this study were distinguished based on the structure of the caudal bulb at the tail structure. Morphotype A had a long and pointed caudal bulb, Morphotype B had a short and pointed caudal bulb, and Morphotype C had a short and blunt caudal bulb.

SUPPLEMENTARY TABLE S1
The prevalence of infection and total abundance of each gastrointestinal helminths found in this study.

References

1. Kaza S, Yao LC, Bhada-tata P, van Woerden F. What a waste 2.0: A global snapshot of solid waste management to 2050. World Bank, Washington, DC. (2018). Available at: http://hdl.handle.net/10986/30317 (Accessed June 1, 2023).

2. World Health Organization. Waste and human health: Evidence and needs, WHO meeting report. World Health Organization, Bonn. (2015).

3. Katiyar M. Solid waste management. *Int J Sci Eng Techno*. (2016) 3:117–124. doi: 10.5958/2395-3381.2016.00015.0

4. Vinti G, Bauza V, Clasen T, Medlicott K, Tudor T, Zurbrügg C, et al. Municipal solid waste management and adverse health outcomes: a systematic review. *Int J Environ Res Public Health*. (2021) 18:1–26. doi: 10.3390/ijerph18084331

5. Katlam G, Prasad S, Aggarwal M, Kumar R. Trash on the menu: patterns of animal visitation and foraging behaviour at garbage dumps. *Curr Sci*. (2018) 115:2322–6. doi: 10.18520/cs/v115/i12/2322-2326

6. Krystosik A, Njoroge G, Odhiambo L, Forsyth JE, Mutuku F, LaBeaud AD. Solid wastes provide breeding sites, burrows, and food for biological disease vectors, and urban zoonotic reservoirs: a call to action for solutions-based research. *Front Public Health*. (2020) 7:1–17. doi: 10.3389/fpubh.2019.00405

7. Schroder GD, Hulse M. Survey of rodent populations associated with an urban landfill. *Am J Public Health*. (1979) 69:713–5. doi: 10.2105/AJPH.69.7.713

8. Pitt WC, Beasley J, Witmer GW. Ecology, impacts, and management of invasive rodents in the United States. Ecology and management of terrestrial vertebrate invasive species in the United States. Boca Raton, FL: CRC Press (2017). 193–220.

9. Aplin KP, Brown PR, Jacob J, Krebs CJ, Singleton GR. Field methods for rodent studies in Asia and the indo-Pacific. Australian Centre for International Agricultural Research (ACIAR): Canberra (2003).

10. Douangboupha B, Brown PR, Khamphoukeo K, Aplin KP, Singleton GR. Population dynamics of rodent pest species in upland farming systems of Lao PDR. *Kasetsart J (Nat Sci)*. (2009) 43:125–31.

11. Morand S, Bordes F, Chen HW, Claude J, Cosson JF, Ribas A, et al. Global parasite and *Rattus* rodent invasions: the consequences for rodent-borne diseases. *Integr Zool*. (2015) 10:409–23. doi: 10.1111/1749-4877.12143

12. Villafañe IEG, Cavia R, Vadell MV, Suárez OV, Busch M. Differences in population parameters of *Rattus norvegicus* in urban and rural habitats of Central Argentina. *Mammalia*. (2013) 77:187–93. doi: 10.1515/mammalia-2012-0075

13. Yu H, Jamieson A, Hulme-Beaman A, Conroy CJ, Knight B, Speller C, et al. Palaeogenomic analysis of black rat (*Rattus rattus*) reveals multiple European introductions associated with human economic history. *Nat Commun*. (2002) 13:2399. doi: 10.1038/s41467-022-30009-z

14. Claveria FG, Causapin J, de Guzman MA, Toledo MG, Salibay C. Parasite biodiversity in *Rattus* spp. caught in wet markets. *Southeast Asian J Trop Med Public Health*. (2005) 36 Suppl 4:146–8.

15. Hwang K, Chen E. Clinical studies on angiostrongyliasis Cantonese among children in Taiwan. *Southeast Asian J Trop Med Public Health*. (1991) 22:194–9.

16. Kandi V, Koka SS, Bhoomigari MR. Hymenolepiasis in a pregnant woman: a case report of *Hymenolepis nana* infection. Cureus (2019) 11:1–e3815, doi: 10.7759/cureus.3810, e3810

17. Mustapha T, Daskum AM, Majid RA, Unyah NZ. A review on rodent-borne parasitic zoonosis: public health risk to humans. *South Asian J Parasitol*. (2019) 3:1–15.

18. Otto GM, Franklin CL, Clifford CB. Biology and diseases of rats In: JG Fox, LC Anderson, GM Otto, KR Pritchett-Corning and MT Whary, editors. Laboratory animal medicine. *3rd* ed. Cambridge, MA: Academic Press (2015). 151–207.

19. Duh D, Hasic S, Buzan E. The impact of illegal waste sites on a transmission of zoonotic viruses. *Virol J*. (2017) 14:1–7. doi: 10.1186/s12985-017-0798-1

20. Priyanto D, Ningsih DP. Identification of endoparasites in rats of various habitats. *Health Sci Indones*. (2014) 5:49–53.

21. Herbreteau V, Bordes F, Jittapalapong S, Supputamongkol Y, Morand S. Rodent-borne diseases in Thailand: targeting rodent carriers and risky habitats. *Infect Ecol Epidemiol*. (2012) 2:18637. doi: 10.3402/iee.v2i0.18637

22. Hulin MS, Quinn R. Wild and black rats In: MA Suckow, SH Weisbroth and CL Franklin, editors. The laboratory rat. *2nd* ed. Cambridge, MA: Academic Press (2006). 865–82.

23. Terashima M, Suyanto A, Tsuchiya K, Moriwaki K, Jin ML, Suzuki H. Geographic variation of *Mus caroli* from east and Southeast Asia based on mitochondrial cytochrome b gene sequences. *Mammal Study*. (2003) 28:67–72. doi: 10.3106/mammalstudy.28.67

24. Baker DG. Parasitic diseases In: MA Suckow, CL Franklin and SH Weisbroth, editors. The laboratory rat. *2nd* ed. Cambridge, MA: Academic Press (2003). 453–78.

25. Betterton C. The intestinal helminths of small mammals in the Malaysian tropical rain forest: patterns of parasitism with respect to host ecology. *Int J Parasitol*. (1979) 9:313–20. doi: 10.1016/0020-7519(79)90080-8

26. Chaisiri K, Siribat P, Ribas A, Morand S. Potentially zoonotic helminthiases of murid rodents from the indo-Chinese peninsula: impact of habitat and the risk of human infection. *Vector Borne Zoonotic Dis*. (2015) 15:73–85. doi: 10.1089/vbz.2014.1619

27. Chenchittikul M, Daengpium S, Hasegawa M, Itoh T, Phanthumachinda B. A study of commensal rodents and shrews with reference to the parasites of medical importance in Chanthaburi Province, Thailand. *Southeast Asian J Trop Med Public Health*. (1983) 14:255–9.

28. Lerdthusnee K, Nigro J, Monkanna T, Leepitakrat W, Leepitakrat S, Insuan S, et al. Surveys of rodent-borne disease in Thailand with a focus on scrub typhus assessment. *Integr Zool*. (2008) 3:267–73. doi: 10.1111/j.1749-4877.2008.00100.x

29. Namue C, Wongsawad C. A survey of helminth infection in rats (*Rattus* spp) from Chiang Mai moat. *Southeast Asian J Trop Med Public Health*. (1997) 28 Suppl 1:179–83.

30. Rahdar M, Elham-Al-Sadat R, Vazirianzadeh B, Alborzi A. Study of internal parasites of rodents in Ahvaz, south-west of Iran. *Jundishapur J Health Sci*. (2016) 9:1–5. doi: 10.17795/jjhs-29067

31. Ribas A, Saijuntha W, Agatsuma T, Thongjun C, Lamsan K, Poonlaphdecha S. Helminths in rodents from wet markets in Thailand. *Helminthologia*. (2016) 53:326–30. doi: 10.1515/helmin-2016-0036

32. Tijjani M, Majid RA, Abdullahi SA, Unyah NZ. Detection of rodent-borne parasitic pathogens of wild rats in Serdang, Selangor, Malaysia: a potential threat to human health. *Int J Parasitol*. (2020) 11:174–82. doi: 10.1016/j.ijppaw.2020.01.008

33. Vitta A, Polseela R, Nateeworanart S, Tattiyapong M. Survey of *Angiostrongylus cantonensis* in rats and giant African land snails in Phitsanulok province, Thailand. *Asian Pac J Trop Med*. (2011) 4:597–9. doi: 10.1016/S1995-7645(11)60154-5

34. Herbreteau V, Jittapalapong S, Rerkamnuaychoke W, Chaval Y, Cosson JF, Morand S. (2011). Protocols for field and laboratory rodent studies. Available at: http://www.ceropath.org/FichiersComplementaires/Herbreteau_Rodents_protocols_2011.pdf (Accessed June 1, 2023).

35. Marshall JT. Family Muridae: rats and mice In: B Lekagul and JA McNeely, editors. Mammals of Thailand. *2nd* ed. Bangkok: Association for the conservation of wildlife (1998). 397–487.

36. Waengsothorn S, Kenthao A, Latinne A, Hugot JP. Rodents within the Centre for Thai national reference collections (CTNRC): past, present and future. *Kasetsart J*. (2009) 43:118–24.

37. Anderson R, Chabaud A, Willmot S. Keys to the nematode parasites of vertebrates: Archival volume. Wallingford: CABI Publishing (2009).

38. Taylor MA, Coop RL, Wall RL. Veterinary helminthology In: Veterinary parasitology. *4th* ed. Chichester: Wiley-Blackwell (2015). 1–109.

39. Schmidt GD, Roberts LS, Janovy J. Foundations of parasitology. *8th* ed. Boston: McGraw-Hill Higher Education (2009).

40. Magurran AE. Measuring biological diversity. *J Torrey Bot Soc*. (2004) 131:277–7. doi: 10.2307/4126959

41. Walther BA, Morand S. Comparative performance of species richness estimation methods. *Parasitology*. (1998) 116:395–405. doi: 10.1017/S0031182097002230

42. Kindt R, Coe R. BiodiversityR: a package for community ecology and suitability analysis. R package version 2.14-3. (2005). Available at: http://www.worldagroforestry.org/output/tree-diversity-analysis (Accessed May 15, 2023).

43. Oksanen J, Blanchet FG, Friendly M, Kindt R, Legendre P, McGlinn D, et al. Vegan: community ecology package. R package version 2.4-3. (2017). Available at: https://CRAN.R-project.org/package=vegan (Accessed May 15, 2023).

44. Bush AO, Lafferty KD, Lotz JM, Shostak AW. Parasitology meets ecology on its own terms: Margolis et al. revisited. *J Parasitol*. (1997) 83:575–83. doi: 10.2307/3284227

45. Schweinfurth MK. The social life of Norway rats (*Rattus norvegicus*). *eLife*. (2020) 9:1–26. doi: 10.7554/eLife.54020

46. Boonsong P, Hongnark S, Suasa-ard K, Khoprasert Y, Promkerd P, Hamarit G, et al. Rodent management in Thailand In: GR Singleton, LA Hinds, H Leirs and Z Zhang, editors. Ecologically-based rodent management. Bruce: ACIAR (1999). 338–57.

47. Kishimoto M, Kato M, Suzuki H. Morphological and molecular recharacterization of the rodent genus *Mus* from Nepal based on museum specimens. *Mammal Study*. (2021) 46:297–308. doi: 10.3106/ms2020-0065

48. Pilosof S, Fortuna MA, Cosson JF, Galan M, Chaisiri K, Ribas A, et al. Host-parasite network structure is associated with community-level immunogenetic diversity. *Nat Commun*. (2014) 5:1–9. doi: 10.1038/ncomms6172

49. Shiels AB, Pitt WC, Sugihara RT, Witmer GW. Biology and impacts of pacific island invasive species. 11. *Rattus rattus*, The black rat (Rodentia: Muridae). *Pac Sci*. (2014) 68:145–84. doi: 10.2984/68.2.1

50. Chaisiri K, Chaeychomsri W, Siruntawineti J, Ribas A, Herbreteau V, Morand S. Gastrointestinal helminth fauna in rodents from Loei province, Thailand. *SWU Sci J*. (2010) 26:111–26.

51. Chaisiri K, Chaeychomsri W, Siruntawineti J, Ribas A, Herbreteau V, Morand S. Diversity of gastrointestinal helminths among murid rodents from northern and northeastern Thailand. *Southeast Asian J Trop Med Public Health*. (2012) 43:21–8.

52. Balakirev AE, Abramov AV, Rozhnov VV. The phytogeography of red spiny rats *Maxomys surifer* (Rodentia, Muridae) in Indochina with comments on taxonomy and description of new subspecies. *Zool Stud*. (2017) 56:1–19. doi: 10.6620/ZS.2017.56-06

53. Pimsai U, Pearch MJ, Satasook C, Bumrungsri S, Bates PJJ. Murine rodents (Rodentia: Murinae) of the Myanmar-Thai-Malaysian peninsula and Singapore: taxonomy, distribution, ecology, conservation status, and illustrated identification keys. *Bonn Zool Bull*. (2014) 63:15–114.

54. Chaisiri K, Herbreteau V, Ribas A, Morand S. A study of great bandicoot (*Bandicota indica*) and their gastrointestinal helminths from northern and northeastern Thailand. *Adv Sci J*. (2010) 10:163–71.

55. Alvi MA, Alshammari A, Ali RMA, Rashid I, Saqib M, Qamar W, et al. 2023. Molecular characterization of *Hydatigera taeniaeformis* recovered from rats: an update from Pakistan. *Pak Vet J*. (2023) 43:601–5. doi: 10.29261/pakvetj/2023/049

56. Alvi MA, Li L, Ohiolei JA, Qamar W, Saqib M, Tayyab MH, et al. *Hydatigera taeniaeformis* in urban rats (*Rattus rattus*) in Faisalabad, Pakistan. *Infect Genet Evol*. (2021) 92:104873. doi: 10.1016/j.meegid.2021.104873

57. O'Connor LJ, Kahn LP, Walkden-Brown SW. Moisture requirements for the free-living development of *Haemonchus contortus*: quantitative and temporal effects under conditions of low evaporation. *Vet Parasitol*. (2007) 150:128–38. doi: 10.1016/j.vetpar.2007.07.021

58. Archer CE, Appleton CC, Mukaratirwa S, Lamb J, Corrie SM. Endoparasites of public health importance recovered from rodents in the Durban metropolitan area, South Africa. *S Afr J Infect Dis*. (2017) 32:57–66. doi: 10.1080/23120053.2016.1262579

59. Mohd Zain SN, Behnke JM, Lewis JW. Helminth communities from two urban rat populations in Kuala Lumpur, Malaysia. *Parasit Vectors*. (2012) 5:47. doi: 10.1186/1756-3305-5-47

60. Muñoz M, Robles MR, Milano F, Navone G. Helminth infection levels on *Rattus rattus* (Rodentia: Muridae) from Corrientes city, Argentina. *Mastozool Neotrop*. (2018) 25:221–7. doi: 10.31687/saremMN.18.25.1.0.18

61. Grandón-Ojeda A, Moreno L, Garcés-Tapia C, Figueroa-Sandoval F, Beltrán-Venegas J, Serrano-Reyes J, et al. Patterns of gastrointestinal helminth infections in *Rattus rattus*, *Rattus norvegicus*, and *Mus musculus* in Chile. *Front Vet Sci*. (2022) 9:1–9. doi: 10.3389/fvets.2022.929208

62. Kataranovski M, Mirkov I, Belij S, Popov A, Petrović Z, Gačić Z, et al. Intestinal helminths infection of rats (*Rattus norvegicus*) in the Belgrade area (Serbia): the effect of sex, age and habitat. *Parasite*. (2011) 18:189–96. doi: 10.1051/parasite/2011182189

63. Omondi C, Ogolla FO, Odhiambo C. Assessment of wild rodents endoparasites in Kirimiri forest in Embu County, Kenya. *Int J Adv Res Pub*. (2019) 4:31–7.

64. Arneberg P. Host population density and body mass as determinants of species richness in parasite communities: comparative analyses of directly transmitted nematodes of mammals. *Ecography*. (2002) 25:88–94. doi: 10.1034/j.1600-0587.2002.250110.x

65. Paladsing Y, Boonsri K, Saesim W, Changsap B, Thaenkham U, Kosoltanapiwat N, et al. Helminth fauna of small mammals from public parks and urban areas in Bangkok metropolitan with emphasis on community ecology of infection in synanthropic rodents. *Parasitol Res*. (2020) 119:3675–90. doi: 10.1007/s00436-020-06897-9

66. Cable J, Barber I, Boag B, Ellison AR, Morgan ER, Murray K, et al. Global change, parasite transmission and disease control: lessons from ecology. *Philos Trans R Soc Lond Ser B Biol Sci*. (2017) 372:20160088. doi: 10.1098/rstb.2016.0088

67. Heroldova M, Bryja J, Zejda J, Tkadlec E. Structure and diversity of small mammal communities in agriculture landscape. *Agric Ecosyst Environ*. (2007) 120:206–10. doi: 10.1016/j.agee.2006.09.007

68. Singleton GR, Lorica RP, Htwe NM, Stuart AM. Rodent management and cereal production in Asia: balancing food security and conservation. *Pest Manag Sci*. (2021) 77:4249–61. doi: 10.1002/ps.6462

69. Coomansingh C, Pinckney RD, Bhaiyat MI, Chikweto A, Bitner S, Baffa A, et al. Prevalence of endoparasites in wild rats in Grenada. *West Indian Vet J*. (2009) 9:17–21.

70. Nursyazana MT, Mohdzain SN, Jeffery J. Biodiversity and macroparasitic distribution of the wild rat population of Carey Island, Klang. *Trop Biomed*. (2013) 30:199–210.

71. Marchiondo AA, Cruthers LR, Reinemeyer CR. Nematoda In: AA Marchiondo, LR Cruthers and JJ Fouries, editors. Parasiticide screening: In vitro and in vivo tests with relevant parasite rearing and host infection/infestation methods, volume 2. Cambridge, MA: Academic Press (2019). 135–355.

72. Farrar J, Garcia P, Hotez P, Junghanss T, Kang G, Lalloo D, et al. Soil-transmitted helminths (Geohelminths) In: Manson's tropical diseases. 24th ed. Amsterdam: Elsevier. (2024). 772–96.

73. Gutierrez Y. Other tissue nematode infections In: Tropical infectious diseases: Principles, pathogens, & practice, vol. 2. 2nd ed. Philadelphia: Saunders. (2006). 1231–47.

74. Gibbons LM, Khalil LF. A key for the identification of genera of the nematode family Trichostrongylidae Leiper, 1912. *J Helminthol*. (1982) 56:185–233. doi: 10.1017/S0022149X00034581

75. King CH. Helminthiasis epidemiology and control: scoring successes and meeting the remaining challenges. in *Adv Parasitol*. ed. N. J. Keiser Cambridge, MA: Academic Press. (2019) 103:11–30.

76. Hasegawa H, Syafruddin. *Cyclodontostomum purvisi* (Syn. *Ancistronema coronatum*) (Nematoda: Strongyloidea: Chabertiidae) from rats of Kalimantan and Sulawesi, Indonesia. *J. Parasitol*. (1994) 80:657–60. doi: 10.2307/3283208

77. Bhaibulaya M, Indrangarm S. Man, an accidental host of *Cyclodontostomum purvisi* (Adams, 1933), and the occurrence in rats in Thailand. *Southeast Asian J Trop Med Public Health*. (1975) 6:391–4.

78. Bogitsh BJ, Carter CE, Oeltmann TN. Intestinal tapeworms In: BJ Bogitsh, CE Carter and TN Oeltmann, editors. Human parasitology. *1st editor* ed. Cambridge, MA: Academic Press (2013). 237–49.

79. Jarošová J, Antolová D, Zalesny G, Halán M. Oxyurid nematodes of pet rodents in Slovakia- a neglected zoonotic threat. *Braz J Vet Parasitol*. (2020) 29:e014319. doi: 10.1590/s1984-29612019072

80. Sapp SGH, Bradbury RS. The forgotten exotic tapeworms: a review of uncommon zoonotic Cyclophyllidea. *Parasitolology*. (2020) 147:533–58. doi: 10.1017/S003118202000013X

81. Sinniah B, Sinniah D, Singh M, Poon GK. Prevalence of parasitic infections in Malaysian oil palm estate workers. *Southeast Asian J Trop Med Public Health*. (1978) 9:272–6.

82. Sirivichayakul C, Radomyos P, Praevanit R, Pojjaroen-Anant C, Wisetsing P. *Hymenolepis nana* infection in Thai children. *J Med Assoc Thail*. (2000) 83:1035–8.

83. Stone WB. Potential helminth infections in humans from pet or laboratory mice and hamsters. *Public Health Rep*. (1966) 81:647–53. doi: 10.2307/4592796

84. William RA. A mouse oxyurid, *Syphacia obvelata*, as a parasite of man. *J Parasitol*. (1919) 6:89–93. doi: 10.2307/3270899

85. Qamar W, Alkheraije KA. Anthelmintic resistance in *Haemonchus contortus* of sheep and goats from Asia–a review of in vitro and in vivo studies. *Pak Vet J*. (2023) 43:376–87. doi: 10.29261/pakvetj/2023.088

86. Al-Saeed FA, Bamarni SSI, Iqbal KJ, Rehman TU, Faruk AZ, Mahmood S, et al. In vitro anthelmintic efficacy of *Haloxylon salicornicum* leaves extract using adult *Heamonchus contortus* worms. *Pak Vet J*. (2023) 43:91–6. doi: 10.29261/pakvetj/2022.091

87. Rückerl D. Characterizing activation, proliferation, and ontogeny of murine macrophages in parasitic helminth infections. *Methods Mol Biol*. (2018) 2018:225–41. doi: 10.1007/978-1-4939-7837-3-21

88. Vacca F, Le Gros G. Tissue-specific immunity in helminth infections. *Mucosal Immunol*. (2022) 15:1212–23. doi: 10.1038/s41385-022-00531-w

frontiers | Frontiers in Veterinary Science

TYPE Original Research
PUBLISHED 16 January 2025
DOI 10.3389/fvets.2024.1506532

Check for updates

OPEN ACCESS

EDITED BY
Hongbin Yan,
Chinese Academy of Agricultural Sciences, China

REVIEWED BY
Siju Susan Jacob,
Indian Council of Agricultural Research (ICAR), India
Asad Murtaza,
UiT The Arctic University of Norway, Norway

*CORRESPONDENCE
Sara Salah Abdel-Hakeem
sara_assiut86@aun.edu.eg

RECEIVED 05 October 2024
ACCEPTED 12 December 2024
PUBLISHED 16 January 2025

CITATION
Abdel-Hakeem SS, Megahed G, Al-Hakami AM, Tolba MEM and Karar YFM (2025) Impact of trypanosomiasis on male camel infertility. *Front. Vet. Sci.* 11:1506532. doi: 10.3389/fvets.2024.1506532

COPYRIGHT
© 2025 Abdel-Hakeem, Megahed, Al-Hakami, Tolba and Karar. This is an open-access article distributed under the terms of the Creative Commons Attribution License (CC BY). The use, distribution or reproduction in other forums is permitted, provided the original author(s) and the copyright owner(s) are credited and that the original publication in this journal is cited, in accordance with accepted academic practice. No use, distribution or reproduction is permitted which does not comply with these terms.

Impact of trypanosomiasis on male camel infertility

Sara Salah Abdel-Hakeem [1]*, Gaber Megahed[2], Ahmed M. Al-Hakami[3], Mohammed E. M. Tolba[3] and Yasser F. M. Karar[4]

[1]Parasitology Laboratory, Department of Zoology and Entomology, Faculty of Science, Assiut University, Asyut, Egypt, [2]Department of Veterinary Theriogenology, Faculty of Veterinary Medicine, Assiut University, Asyut, Egypt, [3]Department of Clinical Microbiology and Parasitology, College of Medicine, King Khalid University, Abha, Saudi Arabia, [4]Zoology and Entomology Department, Faculty of Science, New Valley University, El-Kharga, Egypt

Introduction: Blood parasitism is a significant clinical disease that silently undermines the livestock industry, particularly affecting camels. This study aimed to assess the prevalence of *Trypanosoma evansi* in Arabian camels (*Camelus dromedarius*) and its impact on infertility by examining serum protein fractions, lipids, reproductive indices, and the expression of heat shock protein (HSP70) during breeding season.

Methods: A total of 107 male post-pubertal camels, aged between 5 and 10 years, were collected randomly from slaughtering house in Assiut Governorate, Egypt.

Results: Microscopic and serological examinations revealed that 23.4% (25/107) of the camels were infected with *T. evansi.* Infected camels exhibited a highly significant increase in total serum protein. The assessment of dyslipidemia, measure as binary variables for lipid profiles (cholesterol, triglycerides, HDL, and LDL), indicated a nonsignificant increase in risk of dyslipidemia in infected camels compared to healthy camels. Proteomic analysis identified four major protein fractions in the infected camels compared to healthy camels with molecular weights of 181.72, 87.59, 30.5, and 19.5 kDa using SDS electrophoresis. Testicular tissue of the infected camels showed degeneration and necrotic changes in seminiferous tubules and interstitial tissue, along with edema and congestion. There was a significant reduction in the diameter of seminiferous tubules and germinal epithelium height. A marked reduction in testosterone levels and a high expression of HSP70 in spermatogonia, spermatocytes, Sertoli cells, and Leydig cells were observed.

Discussion: Consequently, a combination of physiological and hormonal analyses may serve as a reliable indicator of *Trypanosoma* infection.

KEYWORDS

Camelus dromedarius*, fertility, HSP70, proteomic, testicular lesion, *Trypanosoma evansi

1 Introduction

The Arabian one-humped camel (*Camelus dromedarius* Linnaeus) is a remarkable mammal that is adapted to extreme heat and harsh desert conditions. These animals play a crucial socio-economic role, being extensively utilized across Africa and Asia for transportation, milk, wool, and meat. In Egypt, *C. dromedarius* is predominantly imported from Sudan (1). However, its reproductive inefficiency poses a significant challenge, with factors such as prolonged calving intervals, a short breeding season, delayed first service, nutritional deficiencies, pathological conditions, and low fertility rates contributing to this issue (2). Disruption in blood protein levels can adversely affect hormone secretion and gonadal function, leading to reproductive impairment (3). Therefore, regular examinations

for blood parasites are essential, as severe infections can delay puberty, reduce semen quality and quantity, and reduce overall fertility.

Previous literature has identified several blood parasites in camels, including *Trypanosoma, Theileria, Babesia, Anaplasma*, and *Filaria,* all of which significantly impact productivity by reducing fertility rates and increasing mortality in heavily parasitized animals (1, 4–8). These parasites can also affect productivity indirectly by limiting food intake, weight gain, and milk production (9). Furthermore, blood parasites are recognized as common causes of infertility in male camels (6, 10, 11) and abortion in female camels (9).

Among these, trypanosomiasis, particularly caused by *Trypanosoma evansi* (Steel), is one of the most dangerous parasitic diseases affecting camels. It presents with clinical symptoms such as lethargy, loss of appetite, and poor body condition (12) and is characterized by various pathological and immunosuppressive effects (13). Recent studies have shown a strong association between trypanosomiasis, hormonal alterations, and testicular lesions (10, 11, 14). However, there is limited data regarding the impact of parasitism on serum proteins, lipid profiles, and the expression of heat shock proteins (HSPs), which are crucial for cellular protection against environmental stresses, infections, physiological disturbances, and oxidative damage (15).

HSP70, in particular, is linked to germ cell development and reproductive capacity (16), exhibiting positive expression in cellular cytoplasm, nuclei, and organelles such as mitochondria (17). Despite its importance, little is known about the relationship between HSP70 expression in the testes of *T. evansi*-infected Arabian camels and serum protein fractions.

Given these gaps in knowledge, our focus was to investigate blood protein fractions and lipid profiles in relation to hormonal disruption and testicular pathogenesis in male camels infected with *T. evansi*. Additionally, this research highlights the significance of parasitic infections as a cause of infertility by examining the expression of HSP70 in testicular tissue.

2 Materials and methods

2.1 Ethical approval

This research received ethical approval from the Faculty of Science Research Ethics Committee (FSREC) at Assiut University, Egypt, in compliance with applicable Egyptian laws regarding research and publication, under approval number (01/2023/0001). All procedures were carried out in conformity with the applicable rules and regulations. The study was conducted in accordance with the ARRIVE (Animals in Research: Reporting *In Vivo* Experiments) criteria (18).

2.2 Animals

A total of 107 male post-pubertal camels, aged between 5 and 10 years, were randomly selected from slaughtering house in the Bani-Adi district, Assiut Governorate, Egypt. In Assiut, camels are primarily processed at the Beni Adi slaughterhouse, with occasional slaughtering at Elhamamyah. To ensure representativeness and minimize selection bias, camels were chosen without prior knowledge of their health status or infection history. This involved selecting every nth animal presented for slaughter during the period of study. The selection of male post-pubertal camels aged 5–10 years was based on regional practices and high frequently of infection. The selected animals were examined for *Trypanosoma* infection based on clinical examinations, including general health condition, rectal temperature, and scrotal contents evaluations. Fresh blood samples were collected during the breeding season, from December 2020 to April 2021. Negative samples based on parasitological and serological examinations were used as controls with no clinical signs. It was difficult to get the owner's consent to collect a testicular Tru cut biopsy, so we had to collect samples from slaughtered animals. The testicular samples were isolated from all camels for histopathology and immunohistochemical analysis.

2.3 Blood collection

Five milliliters of blood were collected via jugular venipuncture using a disposable plastic syringe and a 19G needle. One portion of the blood was collected into a tube containing anticoagulant for parasitological analysis (1). The other portion was collected in tubes without anticoagulant for serum collection at room temperature until clotting occurred. Samples were transported directly on ice to the Parasitology Laboratory, Zoology Department, Faculty of Science, Assiut University, Egypt. Serum samples were collected by centrifuging the blood at 5,000 rpm for 15 min, aliquoted into dry, clean Eppendorf tubes, and stored at −80°C for further analysis.

2.4 Parasitological examination

Five thin blood smears were immediately prepared from each camel's blood sample, dried, and fixed with methyl alcohol. The smears were stained with diluted Giemsa and examined at high power (×400) with oil immersion objectives using a light microscope (OPTICA, Italy). Parasite morphological identification followed the keys of Soulsby (19).

2.5 Serological examination

Sera samples were tested for the presence of anti-*T. evansi* antibodies using the card agglutination test for *T. evansi* (CATT/*T. evansi*), following the manufacturer's protocol (Institute of Tropical Medicine, Antwerp, Belgium). Approximately 45 μl of the antigen was transferred onto the test card and mixed with an equal amount of test serum diluted 1:4 with PBS (pH 7.2). The reaction mixture was agitated with a stirring rod and allowed to react on a card test rotator. Agglutination patterns were scored as negative (−), weakly positive (±), positive (+), or strongly positive (++ or +++) (20). Negative and positive controls were used for each test.

2.6 Quantitative analysis of serum testosterone

The concentration of serum testosterone was assessed using a commercial Enzyme-Linked Immunosorbent Assay (ELISA) kit (Human Gesellschaft für Biochemica und Diagnostica, Wiesbaden, Germany). The sensitivity and intra- and inter-assay coefficients of variation were 11% and 13%, respectively, for total testosterone concentration (21, 22).

2.7 Lipid profile and total protein quantification

Serum total lipids (TP), total cholesterol (TC), high-density lipoproteins (HDL-C), low-density lipoproteins (LDL-C), and triglycerides (TG) were determined using reagent tests from commercial kits (Bio Diagnostic, Egypt) and measured using a colorimetric Spectrophotometer in the Department of Zoology, Faculty of Science, Assiut University, Egypt. Total proteins were determined using a modified Bradford protein quantification assay (23). A standard curve was prepared using commercially available ovalbumin (Sigma, St. Louis, MO, USA). Each sample (100 μL) was mixed with Bradford reagent (1 mL) in a 1.5 mL microcentrifuge tube. The absorbance was measured at 595 nm using a UV spectrophotometer.

2.8 Proteomic analysis

Protein fractionation was evaluated by sodium dodecyl sulfate-polyacrylamide gel electrophoresis (SDS-PAGE) of *T. evansi* whole-cell antigen analysis in 12% polyacrylamide gel under reducing conditions, following the method of Laemmli (24). Briefly, 6.5 μL of each sample, 1.0 μL of reducing agent, and 2.5 μL of sample buffer were denatured in boiling water. The sample buffer contained 70% glycerol, 2% SDS, 70 mM Tris-HCl (pH 6.8), and 0.02% bromophenol blue. After gel solidification, 10 μL of the protein ladder (25–250 kDa, Sigma, Saint Louis, USA) and uninfected and infected samples were loaded into separate wells. The gel was run using an electrophoretic setup. After fractionation, the gel was stained with Coomassie brilliant blue G-250, followed by 7% acetic acid to remove excess dye, then digitized using a UV trans-illuminator (25). The size and quantities of proteins were automatically detected using the GelPro Analyser software package (version 6.3).

2.9 Paraffin tissue embedding

The present study was carried out on 10 representative samples of testes from infected and control animals. The testes were progressively perfused with a small amount of 10% neutral buffered formalin to prevent testicular vascular expansion. Afterwards, small blocks (1 × 1 cm) were immediately immersed in a formalin alcohol fixative for histological processing (26, 27). The fixed specimens were washed with 70% ethyl alcohol to remove remnants of the fixative and dehydrated in a graded series of ethyl alcohol [80%, 90%, 100% (I and II), 30 min each]. Dehydrated specimens were then cleared in xylene, infiltrated with paraffin, and embedded in Paraplast (Sigma Aldrich, USA). Serial 4-5 μm transverse sections were cut using a Richert Leica Microtome (RM 2125, Microsystems, Wetzlar, Germany) and incubated at 40°C to maintain dryness (28). The sections were mounted on clean glass slides, stained with Hematoxylin and Eosin, and examined using a light microscope equipped with a digital-colored camera (OPTICA 4083, Italy).

2.10 Morphometric analysis of testes

The average diameter of the seminiferous tubules and the height of the germinal epithelium were assessed using Image J software (29). Stained testicular sections were examined using an OPTICA light microscope and categorized by a pathologist according to the degree of degeneration. Ten fields from each slide (3 animals per group) were evaluated. Only round seminiferous tubes were randomly selected, and their diameters were measured, averaged, and expressed in micrometers. At least three measurements of the germinal height were taken in each tube, averaged, and expressed in micrometers.

2.11 Immunohistochemical staining of heat shock protein 70 (HSP70)

Testis from control and infected animals were subjected to immunohistochemical analysis of HSP70 according to Alnasser et al. (29). A two-step DAKO EnVisionTM+ Single reagent (Horseradish peroxidase Mouse (HRP), Agilent Technologies, Inc., Santa Clara, USA) was utilized. Section thickness of 4–5 μm sections underwent dewaxing, rehydration in descending grades of ethanol, and washing three times in phosphate buffer saline (PBS, pH 7.4) for 5 min each. A mixture of absolute methanol and drops of hydrogen peroxide (3%) was applied to sections and allowed to dry for 20 min at room temperature. The slides were washed for an additional 10 min under running water to reduce the activity of endogenous peroxidase. For antigen retrieval, the slides were immersed in a sodium citrated buffer (pH 6.0) and heated in a water bath at temperature 95–98°C for 20 min. Then, the slides were allowed to cool at room temperature for 30 min and washed three times in PBS (pH 7.4) for 5 min each. Monoclonal anti-HSP70 primary antibody (Santa Cruz Biotechnology, Cat. No. sc-32239) were applied to the slides at a dilution 1:200 for 30 min at room temperature. A ready to use Goat Anti-Mouse IgG (Abcam, Cat. No. 6789 + TM System Horseradish Peroxidase Labeled Polymer; DAKO) was applied at a dilution at 1:2,000 for 1 h at room temperature. Then, the slides were washed three times for 5 min each with PBS (pH 7.4) and treated with liquid DAB substrate chromogen system (3-amino-9-ethylcarbazole/substrate-chromogen) for 10 min at room temperature to develop a brown color at antigen sites. Sections were counterstained with Harries Hematoxylin for 30 s, dehydrated two rounds of ethanol (90% and 100%), cleared in xylene, and mounted using DPX. The immunohistochemical staining was analyzed using an OLYMPUS

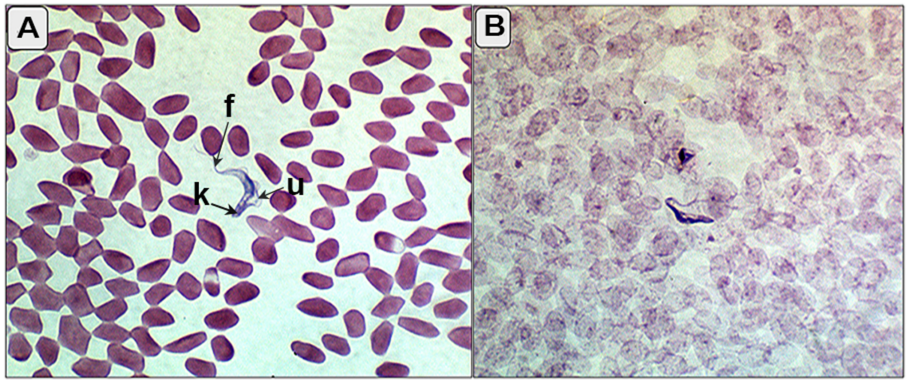

FIGURE 1
(A, B) Blood smear of the infected camels showing trypomastigotes (*T. evansi*) between red blood corpuscles with characterized kinetoplast (k), undulating membrane (u), and free flagella (f).

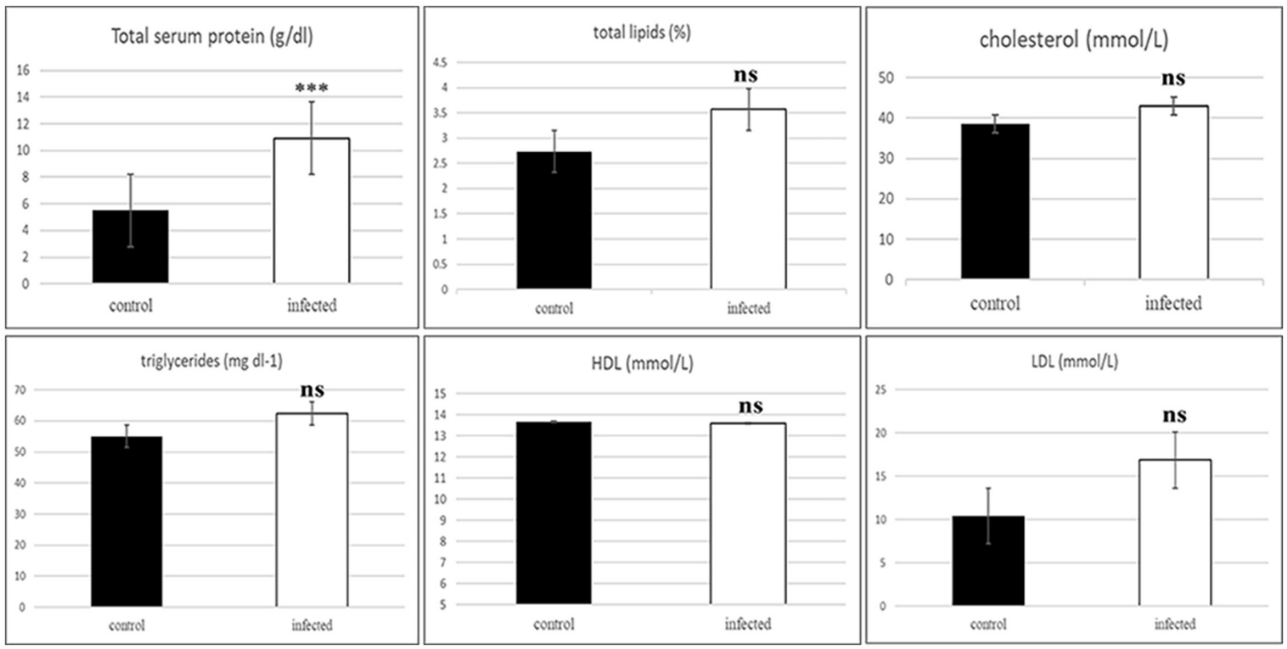

FIGURE 2
Histogram of the serum protein and binary variables for lipid profile of the healthy and infected camels showing significant increase in the total protein and non-significant in the serum lipids includes total lipids, cholesterol, triglycerides, cholesterol-HDL, and cholesterol-LDL in the infected animals. ***Indicates highly significant ($P < 0.001$), ns, indicates non-significant difference).

BX51 light microscope equipped with a digital video camera (OLYMPUS, DP72). Negative control samples were developed using an adapted standard control that excluded the use of primary antibodies.

2.12 CMEIAS color segmentation

CMEIAS Color Segmentation, a free, enhanced computer tool, was used to process negative photos (Supplementary material). Briefly, open image from file menu in CMEIAS Color Segmentation program, pick "Process" from the menu, and then click "Negative image" (30).

2.13 Statistical analysis

Data were normalized using GraphPad prism 9. The normalized data were then analyzed using SPSS version 20 (IBM, Chicago, IL, USA) and summarized by descriptive statistics for the prevalence rate. The Pearson's chi-squared test was applied to analyze the lipid profile in healthy and infected animals.

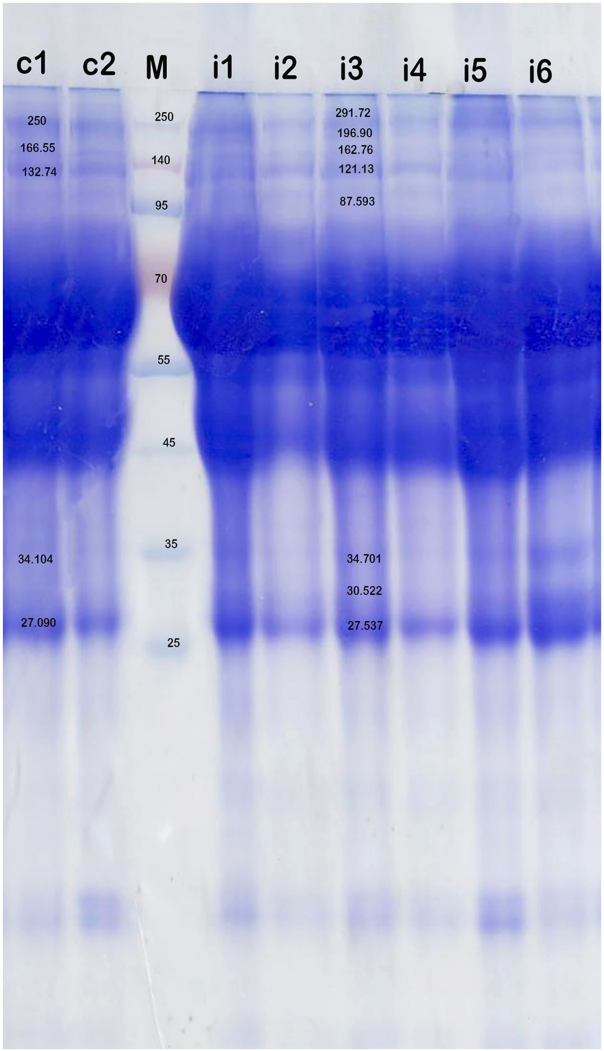

FIGURE 3
SDS-PAGE analysis of serum proteins in the health camels (c1-c2) and camels infected with *T. evansi* (i1-i6) by native gel electrophoresis (12% polyacrylamide gel) and stained with Coomassie brilliant blue. High molecular weight (>95 kDa) antigens are predominantly recognized in the infected animals. M is a protein marker.

One-way ANOVA followed by Duncan as *post-hoc* test, as well as independent t- test, were used to compare protein analysis and morphometric measurements between healthy and infected with 95% confidence intervals at a statistically significant level at $P \leq 0.05$. Data were expressed as mean ± standard deviation (SD).

3 Results

3.1 Prevalence and diagnosis of *T. evansi*

Out of 107 camels, 25 (23.4%) tested positive for *T. evansi* infection using the card agglutination test for *T. evansi* (CATT/*T. evansi*), whereas only 5 camels (4.6%) were positive in blood smear examinations (Figure 1).

3.2 Lipid profile

Infected camels showed a significant increase in total serum protein ($P = 0.000$). The assessment of dyslipidemia, measured as binary variables for lipid profiles (cholesterol, triglycerides, HDL, and LDL), indicated no significant increase in the risk of dyslipidemia in camels infected with *T. evansi* compared to healthy camels. The Pearson Chi-square results were as follows: cholesterol ($\chi^2 = 6.0$, df = 5, $P = 0.306$), triglycerides ($\chi^2 = 6.0$, df = 5, $P = 0.306$), HDL-cholesterol ($\chi^2 = 6.0$, df = 3, $P = 0.112$), and LDL-cholesterol ($\chi^2 = 4.0$, df = 4, $P = 0.406$).

3.3 SDS-PAGE proteomic analysis

A statistically significant increase in total serum protein levels was observed between *T. evansi*-infected and uninfected camels ($t = 10.56$, $P = 0.0001$, Figure 2). Electrophoretic analysis of serum proteins revealed eight major proteins bands with molecular weights (MW) ranging from 25 to 250 kDa. Of these, four major protein peaks were identified in the serum of infected camels, corresponding to MWs of 181.72 kDa (L2), 87.59 kDa (L6), 30.5 kDa (L12), and 19.5 kDa (L14), which were less prominent or absent in the serum of uninfected camels (Table 1). The high molecular weight protein (87.59 kDa) was particularly noteworthy in the serum of infected camels (Figure 3), suggesting the presence of infection-related biomarkers that may correspond to heat shock proteins (HSPs), which are known to play critical roles in thse host response to stress and infection. Conversely, a major peak at 109.5 kDa was more prominent in all serum samples of uninfected camels, representing a potential baseline protein expressed under healthy physiological conditions.

3.4 Serum testosterone levels

The serum testosterone concentration was significantly reduced in infected camels (2.675 ± 1.47 ng/mL) compared to uninfected camels (4.763 ± 0.65 ng/mL), indicating hormonal disruption.

3.5 Morphopathological lesions of testes

Grossly, most examined testes appeared normal, though some displayed congestion. Microscopically, normal camel testes comprise numerous seminiferous tubules enclosed by a basal lamina and myoid cells (Figures 4A, B). Each seminiferous tubule is lined with germinal epithelium containing Sertoli cells and various spermatogenic cells at all stages of development, including spermatogonia, spermatocytes, and spermatids, with abundant

10.3389/fvets.2024.1506532

TABLE 1 Protein fractions (in percent) identified in the uninfected (control) and infected camels with *Trypanosoma evansi*.

Groups / Lanes	Control			Infected						
Protein fractions	%									
r1	4.642637	2.05181	3.415877	5.085117	2.778363	2.888836	2.603671	2.616368	0.153649	0.829235
r2				0.962917	1.073134	1.118106	1.015828	1.562897	2.126265	1.470695
r3	1.584957	0.602417	1.591802		3.912877	2.333664	2.274419	3.74621	1.128755	
r4	3.305347	2.284116	4.331515	4.504949			2.164368			1.530945
r5	77.69924	41.37302	78.32124	2.68233	2.861337	2.073865				
r6				71.83379	73.67374	73.3485	82.07152	74.04509	76.57968	76.79526
r7										
r8										
r9										
r10	3.590892	48.24708	1.577927	3.457715	2.569757	4.682743		3.229021	5.952108	4.438909
r11										2.947883
r12				1.713205	2.863784	1.998405		2.244684	4.170101	10.00405
r13	9.175956	4.909137	7.383255	7.532176	8.715068	9.665172	8.348003	8.534352	8.461199	
r14				1.123549				1.463236		
r15			1.115924			0.43809		0.564428		1.982819
r16		0.532675	2.263094	1.104576	1.551726	1.452395	1.521712	1.993328	1.428383	

spermatocytes in the lumen (Figure 4C). Interstitial spaces contain numerous oval Leydig cells surrounding the seminiferous tubule (Figure 4D).

In infected camels, histological changes ranged from mild to moderate degeneration of seminiferous tubules and germinal epithelium (Figures 5, 6). Mild degeneration was characterized by disorganized and convoluted seminiferous tubules (Figure 5A) and inactive spermatogenesis (Figures 5A–C). The interstitial edema of endothelial cell were observed, indicating fluid accumulation due to inflammatory reaction. Moreover, pyknosis of Leydig cells, characterized by condensation and fragmentation of the cell nucleus, often indication cell death (Figure 5D).

Moderate degeneration involved significant loss of germinal cells and incomplete spermatogenesis (Figures 6A, B) and was associated with depletion of the spermatogenic epithelium, desquamation of spermatogenic cells, and necrosis in the germinal epithelium (Figure 6C). Sertoli cells appeared enlarger, with enlarged nuclei and light eosinophilic cytoplasm, often accompanied by azoospermia (Figure 6C). Additional features of moderate degeneration include interstitial edema with mononuclear inflammatory cell infiltration (Figures 6D, E), multinucleated giant cell formation (Figure 6A), prominent peritubular edema, necrotic degeneration, and nuclear pyknosis (Figure 6F).

Morphometric analysis revealed a non-significant reduction in the diameter of seminiferous tubules during mild degeneration (ANOVA, $P = 0.139$), while a significant reduction (ANOVA, $F = 56.15$, $P < 0.0001$) was observed in moderate degeneration (Figure 7). Both mild and moderate degeneration were associated with a highly significant decrease (ANOVA, $F = 76.01$, $P < 0.0001$) in germinal heights (Figure 7).

3.6 Expression of anti HSP70 in testes of infected camels

Tissue expression of HSP70 was positive in all examined samples, with immunoreactivity indicated by a brown color localized mainly in the membrane and cytoplasm of cells. Mild and focal positive expressions were observed in spermatogonia and interstitial tissue in the testes of some uninfected camels (Figures 8A, B). Infected camels exhibited increased HSP70 expression, particularly in spermatogenic cells and Sertoli cells in mildly degenerative testes (Figure 8C). Leydig cells in the interstitial tissue showed faint membranous HSP70 immunoreactivity (Figure 8D). In moderately degenerative testes, strong immunostaining for HSP70 was observed in spermatogonia, spermatocytes, Sertoli cells, and Leydig cells (Figures 8E, F).

4 Discussion

Trypanosoma evansi is a pathogen that silently cripples Egypt's livestock industry. Trypanosomiasis, a zoonotic disease, is often correlated with bacterial infections transmitted by biting flies and hard ticks (31). In the present study, the prevalence of *T. evansi* infection in the examined camels using Giemsa smear examination 4.65%, which lower than those recently reported in Egypt (8.3%) (32), Saudi Arabia (33), Sudan (34), Kenya (35), Algeria (36), and Nigeria (37). Using CATT technique, 23.4% of examined camels were positive, suggesting high specificity and sensitivity of molecular analysis. These findings align with the previous records in different regions in Egypt (5, 8, 12, 13, 31), though high incidence

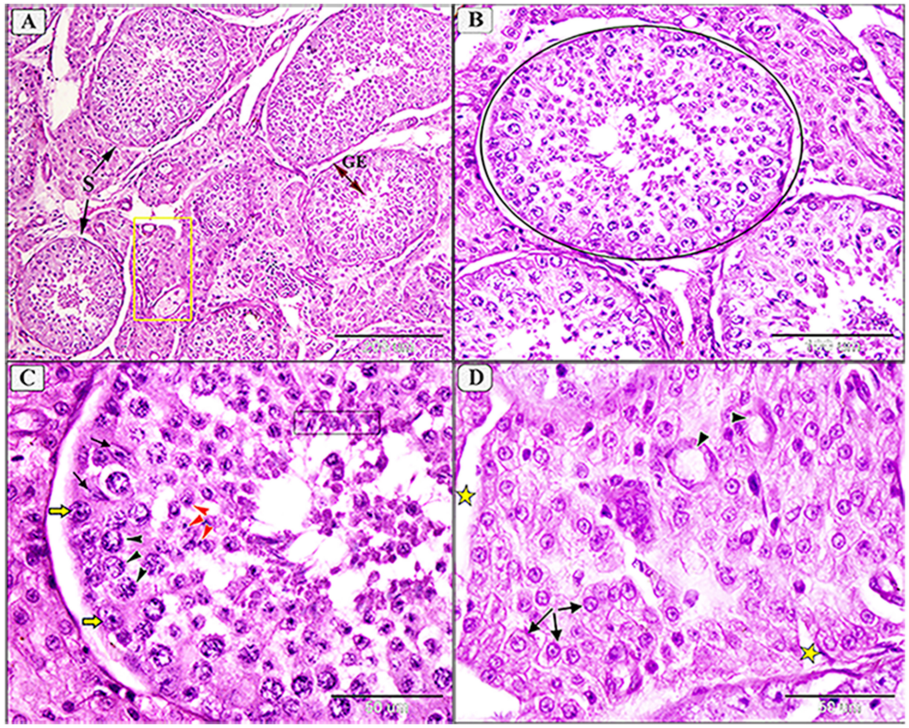

FIGURE 4
Photomicrograph showing normal histological architecture of testis in camel, *C. dromedarius*, showing: **(A)** Normal seminiferous tubules (S) full of spermatogenic cells (GE) and healthy interstitial tissue containing Lyding cells (yellow square); **(B)** High magnification of identical round seminiferous tubules with normal size; **(C)** Higher magnification showing different stages of spermatogenesis, spermatogonia (yellow arrow), primary spermatocytes (black arrowhead), secondary spermatocytes (red arrowhead), spermatids (black oblong), and many spermatocytes in the lumen; **(D)** Higher magnification of the interstitial tissue with Lyding cells (arrows) and dilated blood vessels (star).

of non-clinical infection was found (31%) of *T. evansi* in Upper Egypt (38). On the other hand, our findings were higher rate than those reported in Egypt (8), Somalia (39), and Iran (40), as well as lower than those reported in Egypt (41), Saudi Arabia (42), Iran (43), and Kenya (35). Variations in detection rates could be attributed to climate conditions, vector viability and activity, differing methodologies (31), and chronic nature of *T. evansi* infection in Egypt (44). Sobhy et al. (45) demonstrated that camels on the northwest coast may infected with *T. evansi* from hard ticks and *Stomoxys* flies. Moreover, significant amounts of *T. evansi* were reported in the skin of experimentally infected mice without detectable parasitemia (46), suggesting that the skin of negative animals might serve as a silent source of infection. The high prevalence of *T. evansi* highlights the need for regular screening and control camel challenges, which can lead to significant productivity and economic losses. We acknowledge that this prevalence rate represents a substantial proportion of infected camels, indicating that *T. evansi* is a prevalent health concern in the region. This rate suggests that a notable number of camels are at risk of the associated health issues, including infertility and other reproductive impairments. In Egypt, high prevalence rates of trypanosomes infection were detected during summer and spring, with increase vector density influenced by high temperature (12, 45). Moreover, adult camels (<4 years old) were more frequently infected with *T. evansi* than young camels (47), which align with the present study. Thus, camels within this age range are more likely to exhibit the physiological, biochemical, and pathological effects associated with chronic *T. evansi* infections.

The main finding of the current study is the close correlation between parasitism, serum protein concentrations, dyslipidemia, and testicular degeneration, alongside the upregulation of HSP70 expression. These interrelated factors present significant challenges to camel reproduction and productivity. Specifically, parasitism load and its associated physiological disruptions such as serum protein imbalances and alteration of lipid metabolism, which can lead to testicular degeneration, ultimately affecting fertility. This aligns with previous studies, which have highlighted the impact correlation between high parasitism and other diseases, including pleuropneumonia, mange, tuberculosis (TB), and trypanosomiasis, on camel fertility and overall productivity (48). Lipids, beyond their energy-storing role, are crucial for cell function, sperm maturation, and hormone production (49). Hamad et al. (50) reported that no significant effect of season on triglycerides and cholesterol. Moreover, little variations were reported between rut and non-rut seasons in healthy camels (51). Our results showed a non-significant increase in total serum lipids, cholesterol, triglycerides, and LDL/HDL ratio in the infected camels compared to the healthy animals, which still hint at underlying biological processes that warrant further investigation. Moreover, an imbalance of fatty acids,

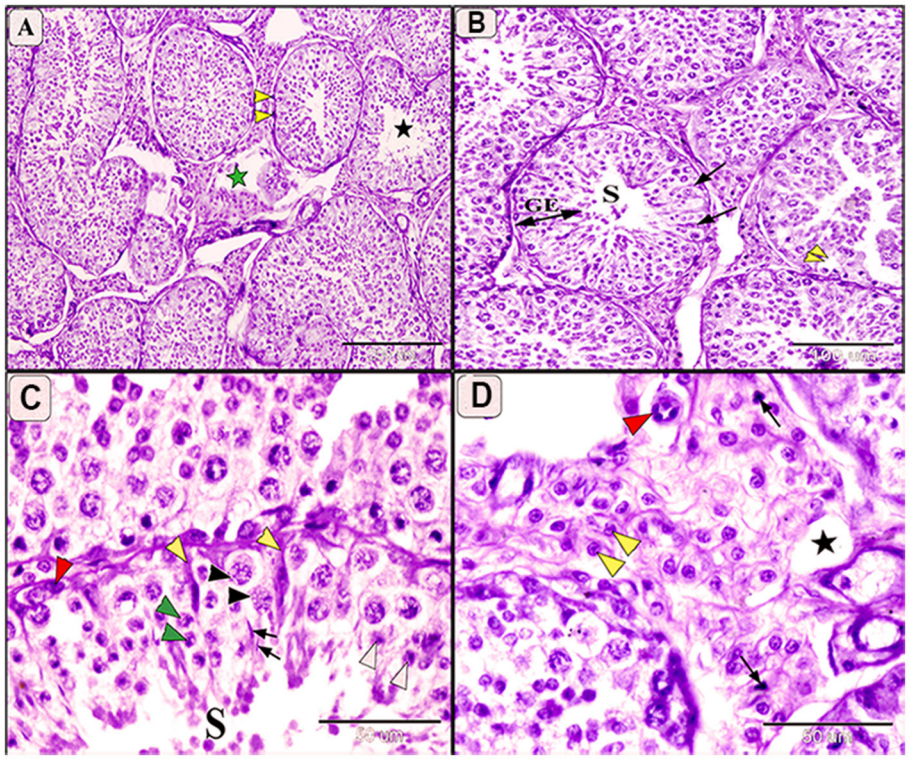

FIGURE 5
Photomicrograph of testis in camels infected with *T. evansi* showing mild degeneration in the testis of camel, *Camelus dromedarius*, showing: **(A)** Convoluted some of the seminiferous tubules, thickening the basement membrane (yellow arrowhead), inactive spermatogenesis process (black star), and necrobiotic changes in the interstitial tissue (green star); **(B)** Higher magnification showing seminiferous tubule (S), decreased the height of spermatogenic cells (GE), and mild degeneration of some Sertoli cells (arrow); **(C)** Higher magnification showing mild degeneration in spermatogenic cell, spermatogonia (red arrowhead), primary spermatocytes (black arrowhead), secondary spermatocytes (white arrowhead), spermatids (arrow), and increase size of Sertoli cells with enlarged nuclei and light eosinophilic cytoplasm (yellow arrowhead); **(D)** Higher magnification of the interstitial tissue showing decrease in the size of Lyding cells (yellow arrowhead), pyknosis of some cell (arrow), edema (star), and plumbing of the endothelial cells (red arrowhead).

including cholesterol, indicate shifts in metabolic states that may affect the overall reproductive health such as dyslipidemia, systemic oxidative stress, poor quality gametes, and infertility (52). Ferrieres (53) demonstrated that dyslipidemia, including hypertriglyceridemia, hypercholesterolemia, and reduced HDL-cholesterol, is correlated to various pathophysiological conditions. Conversely, El-Bahr and El-Deeb (54) reported significant decrease in triacylglycerol, cholesterol, HDL/cholesterol with significant increase in LDL/cholesterol in camels naturally acute infected with *T. evansi*. This variation could be due to the chronicity of infection and age of the examined camels. Although limited data is provided about the effect of trypanosomiasis and serum lipid profile, the imbalance of serum lipids in the current study may indicate sperm dysfunction under parasitism. The correlation between lipid profile and reproductive hormones, as highlighted by Bobjer et al. (55), suggested that there may be functional implications between serum triglycerides and testosterone levels in men with azoospermia. Additionally, Jones et al. (56) reported that sperm sensitivity to lipid peroxidation, due to high polyunsaturated fatty acids. This is linked to sperm mutation, dysfunction, and subsequently fertility disorders.

The breeding season is characterized by significant hormonal fluctuations, which may affect the immune system and potentially modulate susceptibility of animals to infections. Our results indicate that healthy camels aged 5 to 10 years have a high testosterone concentration (4.763 $\pm$ 0.65), whereas *T. evansi*-infected camels significantly show reduction in the concentration of serum testosterone (2.675 $\pm$ 1.47). Consistent with previous findings, our study revealed hypercholesterolemia and hypertriglyceridemia are associated with reduced sperm count, increased abnormalities, decreased testosterone levels, and testes weight (57). Similar hormonal changes were reported in *T. evansi*-infected camels, with significant reduction in luteinizing hormone and follicle-stimulating hormone, and increased cortisol level (10). Mohammed et al. (14) demonstrated similar effects in *T. evansi* infected rats and human infected with *T. gambiense* (58) which linked to hypercortisolemia impairing gonadotropin-releasing hormone secretion. These physiological changes could influence the prevalence or detectability of the infection, thus potentially impacting the representativeness of the present results.

Hematological profiles and chemical compositions have been documented in camels infected with various blood parasites, including *Theileria* (59), *Babesia* (60), and *Typanosoma* (61).

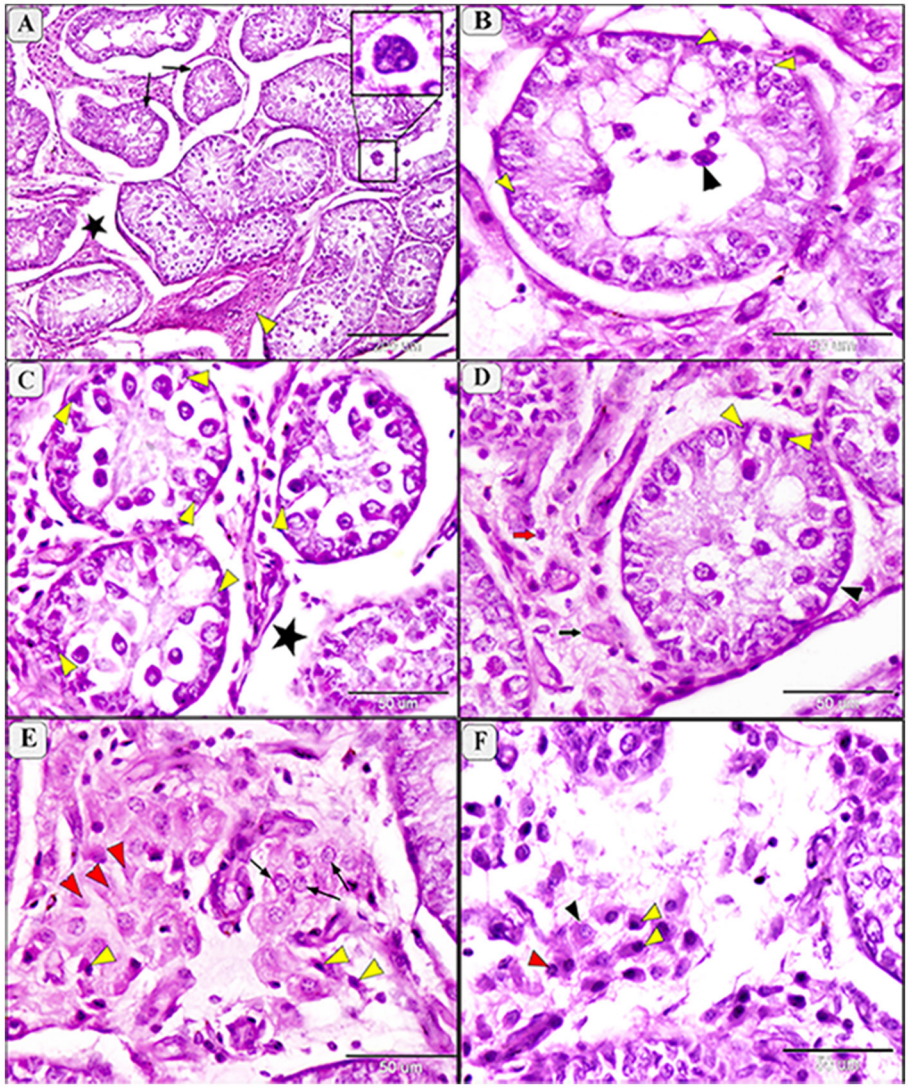

FIGURE 6
Photomicrograph of testis in camels infected with *T. evansi* showing moderate degeneration in the testis of camel, *Camelus dromedarius,* showing: **(A)** Highly convoluted and degenerative seminiferous tubules (arrow), edema (star) and necrobiotic changes (yellow arrowhead) of the interstitial tissue with formation of giant cells (higher magnification in the square); **(B)** Higher magnification showing a high loss of germinal cells and Sertoli cells (yellow arrowhead) and incomplete spermatogenesis (black arrowhead); **(C)** Necrobiotic changes in germinal epithelium (yellow arrowhead) and edema of the interstitial tissue (star); **(D)** Depletion of spermatogenic epithelium, increase thickening of the basement membrane (black arrowhead), degenerative Sertoli cells (yellow arrowhead), necrobiosis (black arrow) and pyknosis (red arrow) of Lyding cells; **(E)** Higher magnification of the interstitial tissue showing necrobiotic changes (red arrowhead), pyknosis (yellow arrowhead), and vacuolar degeneration (arrow) of Lyding cells; **(F)** Higher magnification showing edema in the interstitial tissue with vacuolar degeneration (black arrowhead) and pyknosis (yellow arrowhead) of Lyding cells.

However, the mechanism by which parasitism affects serum proteins is not well-studied. In our study, comparative SDS-PAGE analysis showed four major peaks in the serum of infected animals with molecular weights 181.72, 87.59, 30.5, and 19.5 kDa. The small molecular weight proteins 30.5 kDa and 19.5 kDa may be represent acute-phase or stress-related proteins such as small heat shock proteins. These findings align with Hoter et al. (62) who reported small molecular weight, ranging from 12 to 43 kDa in the Arabian camel (*C. dromedarius*). Additionally, the serum of *T. evansi*-infected camels exhibited a protein band at 87.59 kDa, which possibly correspond to high HSP expression. This is concurred with Rudramurthy et al. (63) who revealed the immunoreactivity of the expressed protein (~70 kDa) in serum of animals infected with *T. evansi*. On the other hand, Ulmasov et al. (64) demonstrated strong induction of a 73kDa protein coupled with HSP88 and HSP 60 after heat stress on camel lymphocytes. These findings highlight significant alterations in serum proteins patterns associated with *T. evansi* infection, with high molecular weight proteins and specific peaks serving as potential biomarkers of infection.

Amin et al. (10) indicated that immune responses influence sex hormones and contribute to infertility typically concurrent with trypanosomiasis. About 90% of blood testosterone is produced

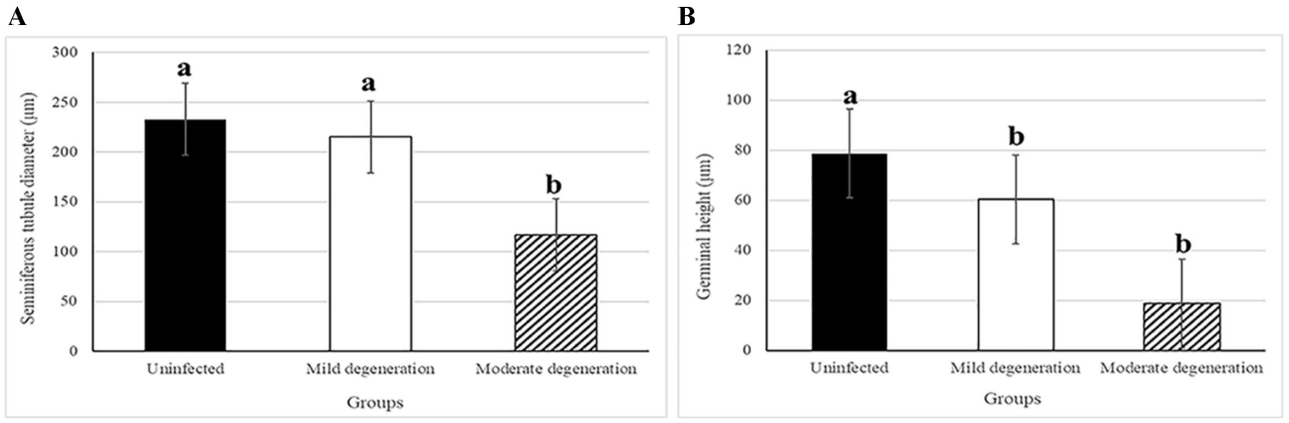

FIGURE 7
Histogram showing morphometric analysis of testicular degeneration in camels, *C. dromedarius,* infected with *T. evansi* showing: **(A)** Statistically significant reduction in the diameter of seminiferous tubules in moderate degeneration; **(B)** Statistically significant reduction in the germinal height in the mild and moderate degeneration degree compared to uninfected animals. Data are expressed as micrometer (µm), different letter refer to significant difference between groups.

from testes (10). Our findings revealed that testes of *T. evansi*-infected camels exhibit different levels of degenerative changes in seminiferous tubules. *T. evansi*-infected deer showed the same degeneration in the seminiferous tubules and sperms (65). Sekoni (66) reported that such pathological changes reduce the reproductive capacity in males, causing infertility with chronicity of the parasitism. The experimental rats infected with *T. evansi* exhibited increase in oxidative stress and lipid peroxidation in the testes, suggesting the cell injury and confirmed the pathogenicity of this parasites (11). These pathological lesions in the testicular tissue might be attributed to decrease levels of circulating luteinizing hormone and follicle-stimulating hormone due to the hypothalamic-pituitary-gonadal axis is unable to self-regulate (11). Moreover, the infected animals showed high temperature which id directly associated with parasitemia (67, 68). Since the testicular tissue is highly sensitive to temperature, the hyperthermia may have contributed to the testicular lesions such as necrosis, supporting our findings that *T. evansi* can reduce infertility either directly or indirectly.

A marked reduction in the number of seminiferous tubules with incomplete spermatogenesis and necrosis of lining epithelium were also recorded. Besides, a marked increase in the size and number of Sertoli and Lyding cells was observed. Additionally, interstitial tissue showed edema with infiltration of inflammatory cells, necrosis, and pyknosis of Lyding cells. In this aspect, the pathological changes in Lyding cells and interstitial tissue were significantly correlated with the testosterone concentration. Such results have coincided with the previous report by Amin et al. (10). Additionally, our results show a significant reduction in the diameter of seminiferous tubules and germinal height in the mild and moderate testicular degeneration of infected animals, which aligned with Bataineh and Nusier (69). This significant decrease may be attributed to the reduction of serum testosterone level due to decrease luteinizing hormone. Friedländer et al. (70) reported that testosterone production is most likely impaired only in the final stage of the Leydig cell's development during the non-breeding season. This difference is attributed to Lyding cells necrobiosis and interstitial tissue edema.

Heat shock proteins (HSPs) are essential for thermotolerance and maintaining protein homeostasis (62). The HSP70 famile, which includes both inducible (HSP72) and constitutive (HSP73) forms, plays a key role in cellular stress responses (71). Our study utilized goat anti-mouse secondary antibodies, closely related to camel HSPs. According to the phylogenetic analysis of mammalian HSPs, camel HSPs have close related to ruminant HSPs including goats (72). Cytoplasmic localization of HSP70 in spermatocytes and spermatids was noted in both normal and infected animals, aligning with Feng et al. (73) findings of HSP70 expression in normal and maturation-arrest testis. Immunohistochemical results indicate that increased HSP70 in the different germ cells (spermatogonia, spermatocytes, Sertoli cells, and Lyding cells) correlates with the degree of degeneration. This can be attributed to increase thermal stress *T. evansi* prevalence and their side effects.

Previous studies indicated that HSP 72 kDa and 73 kDa were structurally similar, having key role in the survival of cell, as well as stress severity and recovery process (74). Parallel to our SDS-PAGE results, we reported distinctive expression of HSP70 in the testes of *T. evansi*-infected camels, which can be used as cellular injury biomarker (75). Microscopic examination in our study revealed significant HSP70 cytoplasmic localization in spermatogonia, Sertoli cells, spermatocytes, and Lyding cells, which were tightly associated with cellular pathogenesis. Overexpression of HSPs reflects cellular stress responses, apoptosis, and cell survival, impacting animal performance and productivity (76). Moreover, HSPs could be considered as main diagnostic marker to trypanosomiasis due to increase of body temperature linked to parasitism peak (67). Our results align with Dix et al. (77) who reported that HSP70 gene upregulation linked to meiosis failure, germ cell apoptosis, and male infertility in mice. Additionally, upregulation

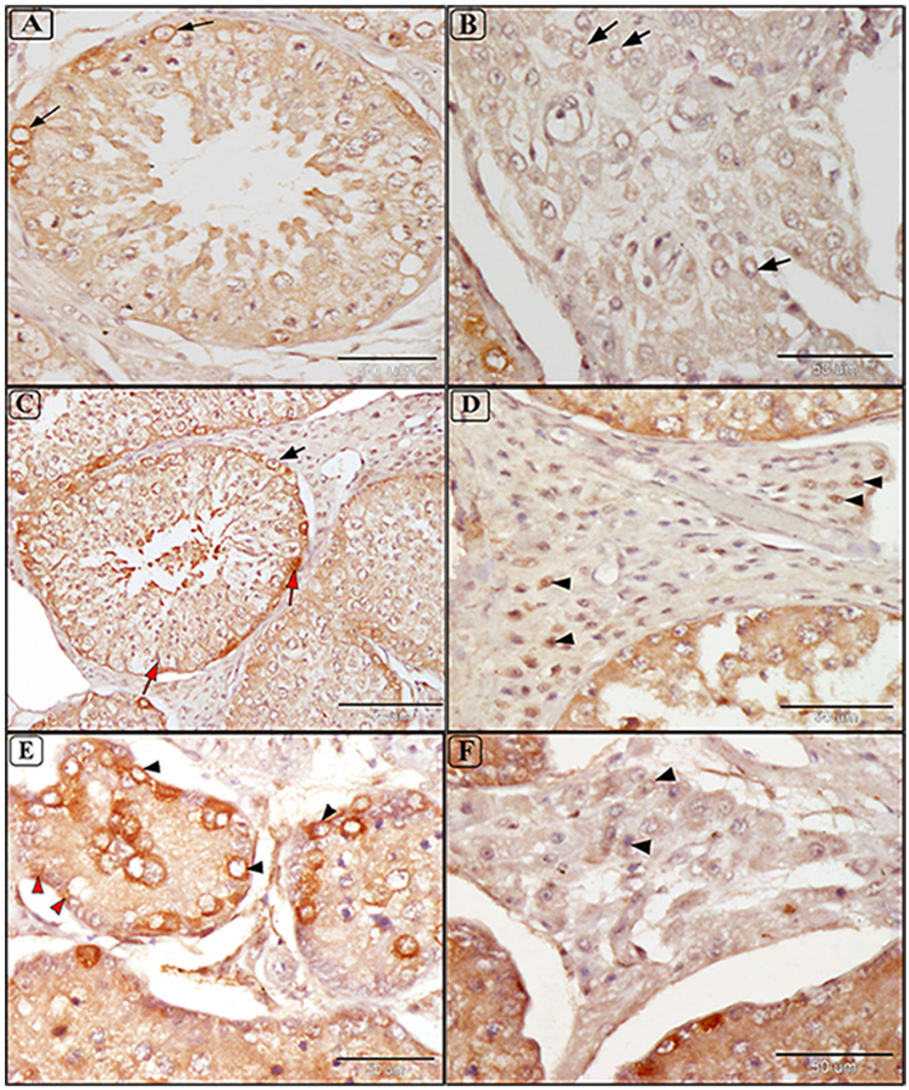

FIGURE 8
Immunostaining expression of HSP70 in the testis of camels infected with *T. evansi* showing: **(A, B)** Faint positive expression of anti-HSP70 are shown in cytoplasmic brown color in spermatogonia Lyding cells in the interstitial tissue (arrow) of normal uninfected camels (a small box represents the negative control); **(C, D)** Mild testicular degeneration in camels, *C. dromedarius,* infected with *T. evansi* showing moderate positive expression of anti-HSP70 in different germ cells including spermatogonia (black arrow), spermatids, spermatozoa, and Sertoli cells (red arrow); **(C)** and Lyding cells in the interstitial tissue (arrowhead) **(D)**; **(E, F)** Moderate testicular degeneration in camels, *C. dromedarius,* infected with *T. evansi* showing severe positive expression of anti-HSP70 in all cells and interstitial tissue (arrowhead).

of HSP70 has been linked to progress and development of inflammatory diseases including atherosclerosis (78). This could be attributed to the most of HSP genes do not have introns (79), which allow for quick expression and explain how they can be produced when RNA splicing is disrupted by stressors (80). Moreover, HSP70 have multiple cytoprotective functions including folding new proteins, refolding of denatured proteins, prevent aggregation of denatured proteins, translocation of proteins across membranous organelles, and anti-apoptotic factors (81).

Acute and chronic camel trypanosomiasis could cause anemia, loss weight, anoxia, weakness, increase body temperature up to 41°C, and immunosuppression, and perhaps death if left untreated (2, 67, 82). Moreover, it causes economic impacts including decreased production (a 30% decrease in milk and meat yield morbidity), high tendency of abortions in all age groups, and a 3% death rate (83–85).

5 Conclusion

This study explored the correlation between physiological analyses, parasitism, and pathological lesions in the testes of camels. Key findings included patterns of altered serum protein levels, dyslipidemia, HSP70 expression as a diagnostic marker to trypanosomiasis. However, the study's findings should be interpreted considering potential limitation, such as sample size, variability in parasitic load, and reliance on random sampling

from a slaughterhouse, which may not represent the overall camel population. While the study provides valuable insights into the effects of *T. evansi* infection, the findings may not fully represent the physiological baseline outside the breeding season. Further research employing advanced proteomic techniques are necessary to further identify and characterize the serum protein of *T. evansi*-infected camels, enabling a deeper understanding of their roles in infection and immune response.

Data availability statement

The datasets presented in this study can be found in online repositories. The names of the repository/repositories and accession number(s) can be found in the article/Supplementary material.

Ethics statement

This research received ethical approval from the Faculty of Science Research Ethics Committee (FSREC) at Assiut University, Egypt, in compliance with applicable Egyptian laws regarding research and publication, under approval number (01/2023/0001). The study was conducted in accordance with the local legislation and institutional requirements.

Author contributions

SA-H: Conceptualization, Data curation, Formal analysis, Investigation, Methodology, Software, Supervision, Visualization, Writing – original draft, Writing – review & editing. GM: Conceptualization, Methodology, Supervision, Writing – review & editing. AA-H: Funding acquisition, Project administration, Resources, Writing – review & editing. MT: Funding acquisition, Project administration, Resources, Writing – review & editing. YK: Data curation, Methodology, Writing – original draft, Writing – review & editing.

Funding

The author(s) declare financial support was received for the research, authorship, and/or publication of this article. The authors extend their appreciation to the Deanship of Research and Graduate Studies at King Khalid University, KSA, for funding this work through Small Research Group under grant number (RGP1/343/45).

Conflict of interest

The authors declare that the research was conducted in the absence of any commercial or financial relationships that could be construed as a potential conflict of interest.

Generative AI statement

The author(s) declare that no Gen AI was used in the creation of this manuscript.

Publisher's note

All claims expressed in this article are solely those of the authors and do not necessarily represent those of their affiliated organizations, or those of the publisher, the editors and the reviewers. Any product that may be evaluated in this article, or claim that may be made by its manufacturer, is not guaranteed or endorsed by the publisher.

Supplementary material

The Supplementary Material for this article can be found online at: https://www.frontiersin.org/articles/10.3389/fvets.2024.1506532/full#supplementary-material

References

1. El-Khabaz KA, Abdel-Hakeem SS, Arfa MI. Protozoan and helminthes parasites endorsed by imported camels (*Camel dromedaries*) to Egypt. *J Parasit Dis.* (2019) 43:607–15. doi: 10.1007/s12639-019-01138-y

2. Kaufmann BA. Reproductive performance of camels (*Camelus dromedarius*) under pastoral management and its influence on herd development. *Livestock Prod Sci.* (2005) 92:17–29. doi: 10.1016/j.livprodsci.2004.06.016

3. Hunt PA, Sathyanarayana S, Fowler PA, Trasande L. Female reproductive disorders, diseases, and costs of exposure to endocrine disrupting chemicals in the European Union. *J Clini Endocrinol Metabol.* (2016) 101:1562–70. doi: 10.1210/jc.2015-2873

4. Darwish AM, Sharaf A, Gaouar SBS, Ali NI, El-Aziz THA, Abushady AM, et al. Biochemical and genotyping analyses of camels (*Camelus dromedaries*) trypanosomiasis in North Africa. *Sci Rep.* (2023) 13:7176. doi: 10.1038/s41598-023-34086-y

5. El-Naga TRA, Barghash S. Blood parasites in camels (*Camelus dromedarius*) in Northern West Coast of Egypt. *J Bacteriol Parasitol.* (2016) 7:258. doi: 10.1016/j.parepi.2016.07.002

6. Khalphallah A, Al-Daek T, Abdelhamid M, Elmeligy E, El-Hawari SF, Khesruf KA, et al. Camel filariasis (*Dipetalonema evansi*) and its association with clinical balanoposthitis with reference to prominent changes in clinical findings, serum testosterone, semen analysis, and testicular histopathology. *BMC Vet Res.* (2024) 20:1. doi: 10.1186/s12917-023-03844-5

7. Mahmoud HY, Ali AO, Tanaka T. Molecular detection and characterization of *Anaplasma marginale* infecting cattle, buffalo, and camel populations in southern Egypt. *Front Vet Sci.* (2023) 10:1169323. doi: 10.3389/fvets.2023.1169323

8. Salman D, Sivakumar T, Otgonsuren D, Mahmoud ME, Elmahallawy EK, Khalphallah A, et al. Molecular survey of *Babesia, Theileria, Trypanosoma,* and *Anaplasma* infections in camels (*Camelus dromedaries*) in Egypt. *Parasitol Int.* (2022) 90:102618. doi: 10.1016/j.parint.2022.102618

9. Gutierrez C, Corbera JA, Juste MC, Doreste F, Morales I. Clinical, hematological, and biochemical findings in an outbreak of abortion and neonatal mortality associated with *Trypanosoma evansi* infection in dromedary camels. *Ann N Y Acad Sci.* (2006) 1081:325–7. doi: 10.1196/annals.1373.044

10. Amin YA, Noseer EA, Fouad SS, Ali RA, Mahmoud HY. Changes of reproductive indices of the testis due to *Trypanosoma evansi* infection in dromedary bulls (*Camelus dromedarius*): semen picture, hormonal profile, histopathology, oxidative parameters, and hematobiochemical profile. *J Adv Vet Anim Res.* (2020) 7:537. doi: 10.5455/javar.2020.g451

11. Faccio L, Silva AS, Tonin AA, Oberherr L, Gressler LT, Oliveira CB, et al. Relationship between testicular lesion and hormone levels in male rats infected with *Trypanosoma evansi*. *Anais da Academia Brasileira de Ciências*. (2014) 86:1537–46. doi: 10.1590/0001-3765201420130167

12. Selim A, Alafari HA, Attia K, AlKahtani MD, Albohairy FM, Elsohaby I. Prevalence and animal level risk factors associated with *Trypanosoma evansi* infection in dromedary camels. *Sci Rep*. (2022) 12:8933. doi: 10.1038/s41598-022-12817-x

13. Elhaig MM, Youssef AI, El-Gayar AK. Molecular and parasitological detection of *Trypanosoma evansi* in camels in Ismailia, Egypt. *Vet Parasitol*. (2013) 198:214–8. doi: 10.1016/j.vetpar.2013.08.003

14. Mohammed R, Darwish A, Mohamed M. Hormonal changes in *Trypanosoma evansi*-infected *Rattus norvegicus*: An approach to understand host-parasite interaction. *Parasitologists United J*. (2022) 15:303–8. doi: 10.21608/PUJ2022.174437.1196

15. Omidi A, Nazifi S, Rasekh M, Zare N. Heat-shock proteins, oxidative stress, and antioxidants in one-humped camels. *Trop Anim Health Prod*. (2024) 56:29. doi: 10.1007/s11250-023-03876-x

16. Hasi G, Wu L, Sodnompil T, Yi R, Wu R, Zhang R, et al. Differential expression and localisation of heat shock protein 70 (HSP70) and glutathione peroxidase 5 (GPX5) in the testis and epididymis of Sonid Bactrian camels. *Reprod Fertil Dev*. (2023) 35:552–62. doi: 10.1071/RD23026

17. Shevtsov M, Balogi Z, Khachatryan W, Gao H, Vígh L, Multhoff G. Membrane-associated heat shock proteins in oncology: from basic research to new theranostic targets. *Cells*. (2020) 9:1263. doi: 10.3390/cells9051263

18. Du Sert NP, Ahluwalia A, Alam S, Avey MT, Baker M, Browne WJ, et al. Reporting animal research: Explanation and elaboration for the ARRIVE guidelines 20. *PLoS Biol*. (2020) 18:e3000411. doi: 10.1371/journal.pbio.3000411

19. Soulsby E. *Helminths Arthropods and Protozoa of Domestic Animals*. London: Baillire Tindall and Cassell Ltd. (1982).

20. Songa EB, Hamers R. A card agglutination test (catt) for Veterinary use. *Ann Soc Belge Méd Trop*. (1988) 68:233–40.

21. Ali A, Tharwat M, Al-Sobayil F. Hormonal, biochemical, and hematological profiles in female camels (*Camelus dromedarius*) affected with reproductive disorders. *Anim Reprod Sci*. (2010) 118:372–6. doi: 10.1016/j.anireprosci.2009.08.014

22. Derar D, Ali A, Tharwat M, Al-Sobayil F, Zeitoun MM. Erectile dysfunction in male dromedary camels: Clinical findings and changes in the nitric oxide metabolite, cardiac troponin I and testosterone concentrations. *Theriogenology*. (2017) 89:201–5. doi: 10.1016/j.theriogenology.2016.10.022

23. Chao Y-CE, Nylander-French LA. Determination of keratin protein in a tape-stripped skin sample from jet fuel exposed skin. *Ann Occupat Hygiene*. (2004) 48:65–73. doi: 10.1093/annhyg/meg081

24. Laemmli UK. Cleavage of structural proteins during the assembly of the head of bacteriophage T4. *Nature*. (1970) 227:680–5. doi: 10.1038/227680a0

25. Mekkawy I, Mahmoud U, Salah S. Atrazine induced changes in some biochemical parameters of the early developmental stages of the african catfish *Clarias gariepinus* (Burchell, 1822). *Am J Biochem Mol Biol*. (2017) 7:21–40. doi: 10.3923/ajbmb.2017.21.40

26. Abdel-Hakeem SS, Abdel-Samiee MA, Abed GH. An insight into the potential parasitological effect of *Schistosoma mansoni* antigens in infected mice: Prophylactic role of cercarial antigen. *Microsc Microanal*. (2020) 26:708–16. doi: 10.1017/S1431927620001695

27. Abdel-Hakeem SS, Abdel-Samiee MA-Z, Youssef MSE, Abd-Elsadek SH, Abd-Elrahman SM, Abdel-Hakeem SS. Nanocurcumin: a promising therapeutic candidate for experimental trichinellosis. *Microsc Microanal*. (2024) 2024:ozae007. doi: 10.1093/micmic/ozae007

28. Abdel-Hakeem SS, Fadladdin YAJ, Khormi MA, Abd-El-Hafeez HH. Modulation of the intestinal mucosal and cell-mediated response against natural helminth infection in the African catfish *Clarias gariepinus*. *BMC Vet Res*. (2024) 20:335. doi: 10.1186/s12917-024-04153-1

29. Alnasser SM, Alotaibi M, Ramadan NK, Abd ElHafeez HH, Abdel-Hakeem SS. The efficiency of *schistosoma mansoni* crude antigens in inhibition of heat shock protein, apoptosis, and lysosomal activity: an immunohistochemical study. *Microsc Microanal*. (2023) 29:739–53. doi: 10.1093/micmic/ozac053

30. Abd-Elhafeez HH, Soliman SA, Attaai AH, Abdel-Hakeem SS, El-Sayed AM, Abou-Elhamd AS. Endocrine, stemness, proliferative, and proteolytic properties of alarm cells in ruby-red-fin shark (rainbow shark), *Epalzeorhynchos frenatum* (Teleostei: Cyprinidae). *Microsc Microanal*. (2021) 27:1251–64. doi: 10.1017/S1431927621012265

31. Barghash S. *Study of genetic variability and prevalence of Trypanosoma evansi in domestic animals in Egypt* (Ph.D thesis). Ain Shams University, Egypt. (2010).

32. Amer MM, Soliman AM DO T, Hegab AA, El-Kelesh EA Li Y, Jaroszewski J, Mohanta UK, et al. Parasitological and molecular investigation of *Trypanosoma evansi* in dromedaries from Greater Cairo, Egypt. *J Vet Med Sci*. (2024) 86:1177–84. doi: 10.1292/jvms.24-0284

33. Abdel-Rady A, Alhassan A, Mostafa W, Elhaig MM. Parasitological, serological and molecular prevalence of *Trypanosoma evansi* among Arabian camels (*Camelus dromedaries*) with evaluation of antitrypanosomal drugs. *Acta Parasitologica*. (2024) 69:465–70. doi: 10.1007/s11686-023-00770-2

34. Mossaad E, Salim B, Suganuma K, Musinguzi P, Hassan MA, Elamin E, et al. *Trypanosoma vivax* is the second leading cause of camel trypanosomosis in Sudan after *Trypanosoma evansi*. *Parasit Vectors*. (2017) 10:1–10. doi: 10.1186/s13071-017-2117-5

35. Getahun MN, Villinger J, Bargul JL, Muema JM, Orone A, Ngiela J, et al. Molecular characterization of pathogenic African trypanosomes in biting flies and camels in surra-endemic areas outside the tsetse fly belt in Kenya. *Int J Trop Insect Sci*. (2022) 42:3729–45. doi: 10.1007/s42690-022-00896-2

36. Boushaki D, Adel A, Dia ML, Büscher P, Madani H, Brihoum BA, et al. Epidemiological investigations on *Trypanosoma evansi* infection in dromedary camels in the South of Algeria. *Heliyon*. (2019) 5:e02086. doi: 10.1016/j.heliyon.2019.e02086

37. Mamman S, Dakul D, Yohanna J, Dogo G, Reuben R, Ogunleye O, et al. Parasitological, serological, and molecular survey of trypanosomosis (Surra) in camels slaughtered in northwestern Nigeria. *Trop Anim Health Prod*. (2021) 53:1–9. doi: 10.1007/s11250-021-02891-0

38. Mahran O. Some studies on blood parasites in camels (*Camelus dromedarius*) at Shalatin City, Red Sea Governorate. *Assiut Vet Med J*. (2004) 50:172–84. doi: 10.21608/avmj.2004.178964

39. Hassan-Kadle AA, Ibrahim AM, Nyingilili HS, Yusuf AA, Vieira TS, Vieira RF. Parasitological, serological and molecular survey of camel trypanosomiasis in Somalia. *Parasit Vectors*. (2019) 12:1–6. doi: 10.1186/s13071-019-3853-5

40. Jafari S, Sharifiyazdi H, Yaghoobpour T, Ghane M, Nazifi S. Molecular and hematological investigation of *Trypanosoma evansi* infection in Iranian one-humped camels (*Camelus dromedarius*). *Parasitol Res*. (2023) 122:2091–9. doi: 10.1007/s00436-023-07908-1

41. Behour TS, Abd El Fattah EM. Genotyping of Trypanosoma brucei evansi in Egyptian camels: detection of a different non-RoTat 12 Trypanosoma brucei evansi in Egyptian camels. *Trop Anim Health Prod*. (2023) 55:279. doi: 10.1007/s11250-023-03673-6

42. Metwally DM, Al-Turaiki IM, Altwaijry N, Alghamdi SQ, Alanazi AD. Molecular identification of *Trypanosoma evansi* isolated from arabian camels (*Camelus dromedarius*) in Riyadh and Al-Qassim, Saudi Arabia. *Animals*. (2021) 11:1149. doi: 10.3390/ani11041149

43. Asghari MM, Rassouli M. First identification of *Trypanosoma vivax* among camels (*Camelus dromedarius*) in Yazd, central Iran, jointly with *Trypanosoma evansi*. *Parasitol Int*. (2022) 86:102450. doi: 10.1016/j.parint.2021.102450

44. Labn NE. Investigation of *Trypanosoma evansi* infection in different animals in Northern Egyp. *Egypt Vet Med Soc Parasitol J*. (2024) 20:58–72. doi: 10.21608/evmspj.2024.371888

45. Sobhy HM, Barghash SM, Behour TS, Razin EA. Seasonal fluctuation of trypanosomiasis in camels in North-West Egypt and effect of age, sex, location, health status and vector abundance on the prevalence. *Beni-Suef Univer J Basic Appl Sci*. (2017) 6:64–8. doi: 10.1016/j.bjbas.2017.01.003

46. Capewell P, Cren-Travaillé C, Marchesi F, Johnston P, Clucas C, Benson RA, et al. The skin is a significant but overlooked anatomical reservoir for vector-borne African trypanosomes. *Elife*. (2016) 5:e17716. doi: 10.7554/eLife.17716

47. Alemu G, Abebe R. Prevalence and risk factors of trypanosomosis in dromedary camels in the pastoral areas of the Guji Zone in Ethiopia. *J Parasitol Res*. (2023) 2023:8611281. doi: 10.1155/2023/8611281

48. Merkt H, Rath D, Musa B, El-Naggar M. Reproduction in camels. a review. In: *FAO Animal Production and Health Paper*. Rome: FAO Animal Production and Health Paper Food And Agriculture Organization of the Unitednations (1990). p. 1–63.

49. Athenstaedt K, Daum G. The life cycle of neutral lipids: synthesis, storage and degradation. *Cellul Mol Life Sci CMLS*. (2006) 63:1355–69. doi: 10.1007/s00018-006-6016-8

50. Hamad B, Aggad H, Hadef L, Adaika A. Effect of seasons on blood biochemical parameters in male dromedary camels in Algeria. *Indian J Anim Res*. (2018) 52:678–82. doi: 10.18805/ijar.v0iOF.9165

51. Al-Harbi MS. Some hematologic values and serum biochemical parameters in male camels (camelus dromedarius) before and during Rut. *Asian J Anim Vet Adv*. (2012) 7:1219–26.

52. Saez F, Drevet JR. Dietary cholesterol and lipid overload: impact on male fertility. *Oxid Med Cell Longev*. (2019) e:4521786. doi: 10.1155/2019/4521786

53. Ferrieres J. Prévalence des différentes dyslipidémies en France. In: *Revues Generales Risque Cardiovasculaire*. Toulouse (2008).

54. El-Bahr S, El-Deeb W. *Trypanosoma evansi* in naturally infected dromedary camels: lipid profile, oxidative stress parameters, acute phase proteins and proinflammatory cytokines. *Parasitology*. (2016) 143:518–22. doi: 10.1017/S0031182016000123

55. Bobjer J, Naumovska M, Giwercman Y, Giwercman A. High prevalence of androgen deficiency and abnormal lipid profile in infertile men with non-obstructive azoospermia. *Int J Androl*. (2012) 35:688–94. doi: 10.1111/j.1365-2605.2012.01277.x

56. Jones R, Mann T, Sherins R. Peroxidative breakdown of phospholipids in human spermatozoa, spermicidal properties of fatty acid peroxides, and protective action of seminal plasma. *Fertil Steril.* (1979) 31:531–7. doi: 10.1016/S0015-0282(16)43999-3

57. Bashandy AS. Effect of fixed oil of *Nigella sativa* on male fertility in normal and hyperlipidemic rats. *Int J Pharmacol.* (2007) 3:27–33. doi: 10.3923/ijp.2007.27.33

58. Akinseye O, Mustapha A, Angela A. Biochemical indicators in trypanosomiasis infections. *J Analyt Pharmaceut Res.* (2020) 9:11–4. doi: 10.15406/japlr.2020.09.00346

59. Abouzaid AA. Clinicopathological studies on camels (*Camelus dromedaries*) infected with Thieleriosis in Aswan Governorate. *Aswan Univers J Environm Stud.* (2022) 3:337–45. doi: 10.21608/aujes.2022.146535.1080

60. Al-Obaidi Q, Hasan S, Alsaad K. Clinical, haematological and blood biochemical parameters in Arabian one-humped camels (*Camelus dromedarius*) with *Babesia caballi* infection. *Bulgarian J Vet Med.* (2021) 24:422–33. doi: 10.15547/bjvm.2293

61. Hussain R, Khan A, Abbas RZ, Ghaffar A, Abbas G, Ali F. Clinico-hematological and biochemical studies on naturally infected camels with trypanosomiasis. *Pakist J Zool.* (2016) 48:311.

62. Hoter A, Rizk S, Naim HY. Cellular and molecular adaptation of Arabian camel to heat stress. *Front Genet.* (2019) 10:588. doi: 10.3389/fgene.2019.00588

63. Rudramurthy GR, Sengupta PP, Ligi M, Balamurugan V, Suresh KP, Rahman H. Serodiagnosis of animal trypanosomosis using a recombinant invariant surface glycoprotein of Trypanosoma evansi. *Ind J Experi Biol.* (2017) 55:209–16.

64. Ulmasov HA, Karaev KK, Lyashko VN, Evgen'ev MB. Heat-shock response in camel (Camelus dromedarius) blood cells and adaptation to hyperthermia. *Comp Biochem Physiol B.* (1993) 106:867–72. doi: 10.1016/0305-0491(93)90043-5

65. Shehu SA, Ibrahim ND, Esievo KA, Mohammed G. Pathology of experimental trypanosoma evansi infection in savannah brown buck. *Pakistan J Biolo Sci.* (2006) 9:522–5. doi: 10.3923/pjbs.2006.522.525

66. Sekoni V. Reproductive disorders caused by animal trypanosomiases: a review. *Theriogenology.* (1994) 42:557–70. doi: 10.1016/0093-691X(94)90373-Q

67. Abera Z, Usmane A, Ayana Z. Review on camel trypanosomosis: its epidemiology and economic importance. *Acta Parasitologica Globalis.* (2015) 6:117–28. doi: 10.5829/idosi.apg.2015.6.2.94253

68. Da Silva AS, Paim FC, Santos RC, Sangoi MB, Moresco RN, Lopes ST, et al. Nitric oxide level, protein oxidation and antioxidant enzymes in rats infected by *Trypanosoma evansi*. *Exp Parasitol.* (2012) 132:166–70. doi: 10.1016/j.exppara.2012.06.010

69. Bataineh HN, Nusier MK. Effect of cholesterol diet on reproductive function in male albino rats. *Saudi Med J.* (2005) 26:398—404.

70. Friedländer M, Rosenstrauch A, Bedrak E. Leydig cell differentiation during the reproductive cycle of the seasonal breeder *Camelus dromedarius*: an ultrastructural analysis. *Gen Comp Endocrinol.* (1984) 55:1–11. doi: 10.1016/0016-6480(84)90122-9

71. Kiang JG, Tsokos GC. Heat shock protein 70 kDa: molecular biology, biochemistry, and physiology. *Pharmacol Ther.* (1998) 80:183–201. doi: 10.1016/S0163-7258(98)00028-X

72. Banerjee D, Upadhyay R, Chaudhary U, Kumar R, Singh S, Ashutosh G, et al. Seasonal variation in expression pattern of genes under HSP70 family in heat-and cold-adapted goats (*Capra hircus*). *Cell Stress Chaperones.* (2014) 19:401–8. doi: 10.1007/s12192-013-0469-0

73. Feng HL, Sandlow JI, Sparks AE. Decreased expression of the heat shock protein HSP70-2 is associated with the pathogenesis of male infertility. *Fertil Steril.* (2001) 76:1136–9. doi: 10.1016/S0015-0282(01)02892-8

74. Didomenico BJ, Bugaisky GE, Lindquist S. The heat shock response is self-regulated at both the transcriptional and posttranscriptional levels. *Cell.* (1982) 31:593–603. doi: 10.1016/0092-8674(82)90315-4

75. Yamashita N, Hoshida S, Taniguchi N, Kuzuya T, Hori M. Whole-body hyperthermia provides biphasic cardioprotection against ischemia/reperfusion injury in the rat. *Circulation.* (1998) 98:1414–21. doi: 10.1161/01.CIR.98.14.1414

76. Sadder MT, Migdadi H, Zakri A, Abdoun K, Samara E, Okab A, et al. Expression analysis of heat shock proteins in dromedary camel (*Camelus dromedarius*). *J Camel Pract Res.* (2015) 22:19–24. doi: 10.5958/2277-8934.2015.00003.X

77. Dix DJ, Allen JW, Collins BW, Mori C, Nakamura N, Poorman-Allen P, et al. Targeted gene disruption of HSP70-2 results in failed meiosis, germ cell apoptosis, and male infertility. *Proc Nat Acad Sci.* (1996) 93:3264–8. doi: 10.1073/pnas.93.8.3264

78. McCullagh K, Cooney R, O'Brien T. Endothelial nitric oxide synthase induces heat shock protein HSPA6 (HSP70B′) in human arterial smooth muscle cells. *Nitric Oxide.* (2016) 52:41–8. doi: 10.1016/j.niox.2015.11.002

79. NCBI Resource Coordinates. Database resources of the National Center for biotechnology information. *Nucleic Acids Res.* (2014) 42:D7–D17. doi: 10.1093/nar/gkt1146

80. Lindquist S. The heat-shock response. *Annu Rev Biochem.* (1986) 55:1151–91. doi: 10.1146/annurev.bi.55.070186.005443

81. Parsell D, Lindquist S. The function of heat-shock proteins in stress tolerance: degradation and reactivation of damaged proteins. *Annu Rev Genet.* (1993) 27:437–97. doi: 10.1146/annurev.ge.27.120193.002253

82. Rami M, Atarhouch T, Bendahman M, Azlaf R, Kechna R, Dakkak A. Camel trypanosomosis in Morocco: 2. A pilot disease control trial. *Vet Parasitol.* (2003) 115:223–31. doi: 10.1016/S0304-4017(03)00222-X

83. Enwezor FNC, Sackey AKB. Camel trypanosomosis-a review. *Vet Arh.* (2005) 75:439–52. doi: 10.4236/als.2014.23015

84. Njiru ZK, Ole-Mapeny IM, Ouma JO, Ndungú JM, Olaho-Mukani W. Prevalence of trypanosomosis in camel calves: A pilot study in Laikipia District of Kenya. *Revue Elev Med Vet Pays Trop.* (2000) 53:183–6.

85. Tekle T, Abebe Gebreamlak G. Trypanosomosis and helminthoses: Major health problems of camels (Camelus dromedarius) in the Southern Rangelands of Borena, Ethiopia. *J Camel Pract Res.* (2001) 8:39–42.

frontiers | Frontiers in Veterinary Science

TYPE Original Research
PUBLISHED 16 January 2025
DOI 10.3389/fvets.2024.1507496

Check for updates

OPEN ACCESS

EDITED BY
Hongbin Yan,
Chinese Academy of Agricultural Sciences, China

REVIEWED BY
Arlex Rodríguez-Durán,
Federal University of Rio Grande do Sul, Brazil
Kaiqing Zhang,
Biocytogen, United States

*CORRESPONDENCE
Chien-Chin Chen
✉ hlmarkc@gmail.com
Abid Ali
✉ uop_ali@yahoo.com

†These authors have contributed equally to this work

RECEIVED 08 October 2024
ACCEPTED 02 December 2024
PUBLISHED 16 January 2025

CITATION
Rahman S, Liu H, Shah M, Almutairi MM, Liaqat I, Tanaka T, Chen C-C, Alouffi A and Ali A (2025) Prediction of potential drug targets and key inhibitors (ZINC67974679, ZINC67982856, and ZINC05668040) against *Rickettsia felis* using integrated computational approaches. *Front. Vet. Sci.* 11:1507496. doi: 10.3389/fvets.2024.1507496

COPYRIGHT
© 2025 Rahman, Liu, Shah, Almutairi, Liaqat, Tanaka, Chen, Alouffi and Ali. This is an open-access article distributed under the terms of the Creative Commons Attribution License (CC BY). The use, distribution or reproduction in other forums is permitted, provided the original author(s) and the copyright owner(s) are credited and that the original publication in this journal is cited, in accordance with accepted academic practice. No use, distribution or reproduction is permitted which does not comply with these terms.

Prediction of potential drug targets and key inhibitors (ZINC67974679, ZINC67982856, and ZINC05668040) against *Rickettsia felis* using integrated computational approaches

Sudais Rahman[1†], Hsien Liu[2†], Mohibuallah Shah[3], Mashal M. Almutairi[4], Iram Liaqat[5], Tetsuya Tanaka[6], Chien-Chin Chen[7,8,9,10*], Abdulaziz Alouffi[11] and Abid Ali[1*]

[1]Department of Zoology, Abdul Wali Khan University, Mardan, Khyber Pakhtunkhwa, Pakistan, [2]Division of General Surgery, Department of Surgery, Ditmanson Medical Foundation Chia-Yi Christian Hospital, Chiayi, Taiwan, [3]Department of Biochemistry, Bahauddin Zakariya University, Multan, Pakistan, [4]Department of Pharmacology and Toxicology, College of Pharmacy, King Saud University, Riyadh, Saudi Arabia, [5]Microbiology Lab, Department of Zoology, Government College University Lahore, Lahore, Pakistan, [6]Laboratory of Animal Microbiology, Faculty of Agriculture, Graduate School of Agricultural Science, Tohoku University, Sendai, Japan, [7]Department of Pathology, Ditmanson Medical Foundation Chia-Yi Christian Hospital, Chiayi, Taiwan, [8]Department of Cosmetic Science, Chia Nan University of Pharmacy and Science, Tainan, Taiwan, [9]Doctoral Program in Translational Medicine, National Chung Hsing University, Taichung, Taiwan, [10]Department of Biotechnology and Bioindustry Sciences, College of Bioscience and Biotechnology, National Cheng Kung University, Tainan, Taiwan, [11]King Abdulaziz City for Science and Technology, Riyadh, Saudi Arabia

Rickettsia felis, responsible for flea-borne spotted fever, is a rising zoonotic pathogen posing an increasing global threat due to its expanding geographical distribution. The rise in antibiotic-resistant strains of this pathogen underscores the urgent need for new therapeutic interventions. This study employed a comprehensive subtractive proteomics analysis of the *R. felis* proteome, aiming to identify essential, non-host homologous, and pathogen-specific proteins, which were subsequently evaluated as potential new drug targets. These findings offer valuable insights into the development of therapeutic strategies against rickettsiosis. The analysis revealed 343 proteins that are non-homologous to the host, including 108 essential proteins, 25 unique metabolic pathways, and 11 distinct proteins. Out of these, 10 proteins were druggable in which two associated with virulence, and one related to resistance (succinate dehydrogenase). Through a rigorous screening process and extensive literature review, succinate dehydrogenase emerged as a promising drug target. Protein interaction partners for succinate dehydrogenase were identified using the STRING database. To further assess the functionality of succinate dehydrogenase, structure-based studies were conducted. Approximately 18,000 ZINC compounds were screened, leading to the finding of six potential inhibitors: ZINC67847806, ZINC67982856, ZINC67974679, ZINC67895371, ZINC05668040, and ZINC05670149. Absorption, distribution, metabolism, excretion, and toxicity (ADMET) profiling confirmed that most compounds met the preferred pharmacokinetic properties, except for ZINC67895371 and ZINC67847806, which exhibited positive ames test results, and ZINC05670149, ZINC67895371, and ZINC67847806, showed hepatotoxicity. All compounds were found to be non-sensitizing to the skin. Based on these findings, further

experimental validation of ZINC67974679, ZINC67982856, and ZINC05668040 is recommended.

KEYWORDS

Rickettsia felis, novel drug targets, succinate dehydrogenase, *in silico* screening, pharmacokinetics

1 Introduction

Rickettsia felis is a gram-negative, obligate intracellular bacterium that causes flea-borne spotted fever (1). *R. felis* is a rod-shaped bacterium, usually around 0.3 to 0.5 micrometers wide and 0.8–1.5 micrometers long (2). It possesses a rickettsial cell wall structure, with a peptidoglycan layer and an outer membrane that is essential for its ability to survive and cause disease in the host (3). *R. felis* was first discovered in 1994 in cat fleas, known as *Ctenocephalides felis*, and has since been acknowledged as a new zoonotic agent found worldwide (4). It has been found in different arthropod vectors, such as fleas (5, 6), ticks (7, 8), and mites (9), as well as in a variety of mammals hosts (10), indicating a wide ecological range. The global distribution of *R. felis* highlights its significance as a public health threat, particularly in underdeveloped regions where diagnostic facilities and awareness are limited (11–13). Its emergence as a zoonotic agent necessitates a deeper understanding of its epidemiology to mitigate its impact on global health. Cases of human infections have been reported globally (14), with occurrences documented in America (15–18), Europe (19, 20), Africa (21–25), and Asia (26–28). The pathogen's history of recognition is relatively recent compared to other rickettsial species (29). Its ability to infect diverse hosts and vectors, coupled with the increasing movement of pets and livestock, has facilitated its spread across different geographical regions (30–32). *R. felis* has been shown to cause pathology in various hosts, including humans, where it induces flea-borne spotted fever (33–36), as well as in animals such as cats (*Felis catus*) (37, 38), opossums (*Didelphis spp.*) (39–41), and rodents (42, 43), although the pathogenesis may differ between species due to variations in host susceptibility and immune responses. The epidemiology of *R. felis* is intricate, with numerous transmission cycles between arthropod vectors and vertebrate hosts, including humans (1, 44–49). In addition to the complexity of the life cycle, there is also the persistence and difficulty in controlling its spread. The increasing geographical spread and involvement of multiple hosts and vectors suggest that *R. felis* may pose a higher risk. Furthermore, its potential for outbreaks in densely populated areas underscores the urgency of identifying effective therapeutic targets and preventive measures (50). *R. felis* penetrates the endothelial cells lining the blood vessels, leading to a systemic infection characterized by fever, rashes, headache, and myalgia (51). Serious instances can result in complications like vasculitis and dysfunction in multiple organs (52).

The intracellular lifestyle of *R. felis* enables it to evade the host immune system, persist within host cells, and develop antibiotic resistance, rendering traditional therapies less effective and highlighting the need for novel therapeutic targets and specific inhibitors (53). *R. felis* typically shows resistance or reduced sensitivity to several classes of antibiotics, including beta-lactams (such as penicillin and cephalosporin), aminoglycosides (such as gentamicin and streptomycin), sulfonamides (such as sulfamethoxazole), fluoroquinolones, and macrolides (such as erythromycin) (54). Nonetheless, the process of evaluating numerous macromolecules followed by subsequent *in vivo* experimentation is both time-intensive and resource-draining in drug discovery (55). Subtractive proteomics, a comparative proteomics technique, allows for pinpointing essential, non-host homologous proteins crucial for the pathogen's survival (56).

Existing drugs used for treating infections can vary in their side effects in humans, and their misuse has accelerated the evolution of drug resistance in pathogens (57, 58). Subtractive proteomics is commonly used to evaluate the precision and relevance of potential therapeutic targets. It has been extensively applied in research to uncover and identify unique therapeutic targets specific to various pathogenic strains (59–62). This method ensures that identified targets are pathogen-specific, reducing the likelihood of off-target effects on the host (63). In this study, we aimed to identify potential drug targets and their inhibitors in *R. felis* using an integrated approach combining subtractive proteomics, molecular docking, virtual screening, and absorption, distribution, metabolism, and excretion (ADMET) profiling. This comprehensive strategy is designed to enhance our understanding of potential drug targets, offering promising avenues for developing effective treatments against this persistent and evolving pathogen.

2 Methodology

A subtractive proteomics approach was utilized in this study to analyze the entire proteome of *Rickettsia felis*, aiming to identify new potential drug targets, then followed by molecular docking, virtual screening and ADMET profiling which shown in Figure 1.

2.1 Retrieval of pathogen proteome

The entire proteome of *R. felis* was obtained from the NCBI (https://www.ncbi.nlm.nih.gov/) database in the FASTA format (Genbank ID: GCA_000804505.1, Assembly no: ASM80450v1), and was processed for the CD-HIT analysis.

2.2 Removal of paralogous sequences

Paralogous proteins were identified using the CD-HIT tool (64). All sequences were processed with CD-HIT, maintaining a sequence similarity cutoff of 60% to eliminate redundant

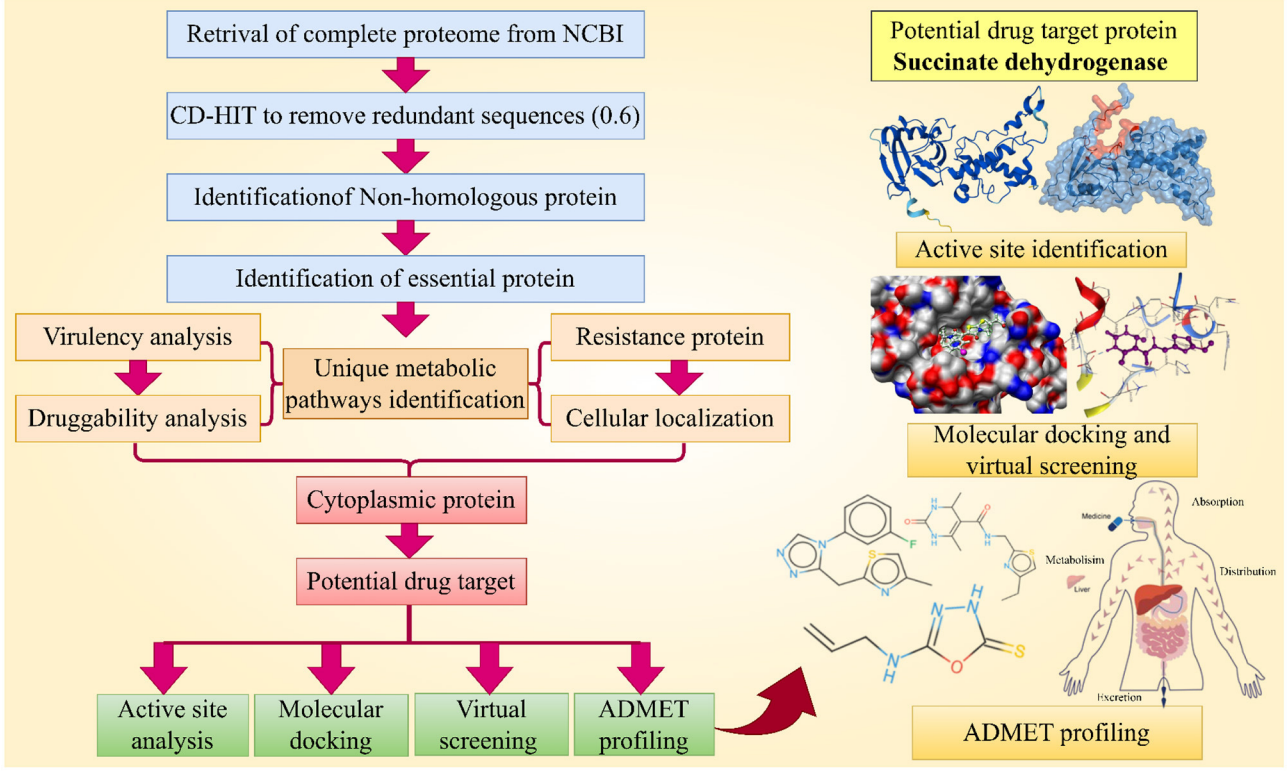

FIGURE 1
This chart illustrates the complete methodology followed for the identification of novel drug target and their inhibitors against *R. felis*. (Created with https://smart.servier.com/ and Draw.io https://app.diagrams.net/).

proteins. Paralogue proteins were eliminated from subsequent analysis, and non-paralogue proteins comprising over 100 amino acids were chosen. Proteins with <100 amino acids were deemed non-essential and therefore excluded from the analysis.

2.3 Detection of host-specific protein homologs

A BLASTp search with a bit score >100 and an E-value $<10^{-4}$ was used to identify human non-homologous proteins (65). Human homologous proteins were excluded to avoid potential drug cross-reactivity with host proteins. The non-homologous proteins with no significant similarity to human proteins were then selected for further investigation.

2.4 Identification of essential proteins

Essential proteins are crucial for an organism's survival, growth, and adaptability (66). Essential proteins were identified through a BLASTp search against the Database of Essential Genes (DEG) (http://tubic.tju.edu.cn/deg/), applying an E-value threshold of 10^{-10} and a bit score >100 (67). Non-essential proteins were excluded, focusing solely on proteins critical for pathogen survival.

2.5 Identification of unique metabolic pathways

To precisely annotate the functions of non-paralogous vital proteins, the KEGG Automatic Annotation Server (KAAS) (https://www.genome.jp/kegg/kaas/) was employed. A comparative evaluation of metabolic pathways between pathogen and host was performed using the KEGG (https://www.genome.jp/kegg/) database. KEGG used organism codes "rfe" for *R. felis* and "hsa" for *H. sapiens* to retrieve the IDs of the metabolic pathways (68). Proteins involved in pathogen-specific pathways were chosen for further identification of potential drug targets, ensuring that these targets were exclusive to the pathogen and absent in the host.

2.6 Druggability analysis

All essential non-homologous proteins were subsequently assessed using BLASTp to compare them with FDA-approved drug targets. The default E-value parameter of 10^{-5} was utilized in BLASTp to search the Drug Bank for potential novel drug targets.

2.7 Prediction of virulence protein

To assess the virulence of proteins, the VFDB (Virulence Factor Database) (http://www.mgc.ac.cn/VFs/) was utilized (69). Selected

R. felis proteins underwent a BLASTp search against the VFDB, applying an E-value threshold of 0.0001 and a bit score above 100.

2.8 Identification of resistance proteins

The Antibiotic Resistance Gene Annotation Tool (ARG-ANNOT V6) tool (https://ifr48.timone.univ-mrs.fr/blast/arg-annot_v6.html) was employed to explore novel resistance proteins by analyzing the entire pathogen proteome. The FASTA sequences of the selected proteins were analyzed using a BLASTp search against the ARG-ANNOT V6 database, with a threshold of 10^{-5} (70).

2.9 Protein localization and interaction profiling

Proper subcellular localization is vital for protein function and interactions, influencing their role as drug or vaccine targets (71). All selected proteins were analyzed using the CELLO v.2.5 (http://cello.life.nctu.edu.tw/) online tool to determine their intracellular positioning. The position-specific iterated BLAST (PSI-BLAST) feature within this tool categorized the proteins into different subcellular compartments, including the cytoplasm, membrane, periplasmic membrane, and extracellular space (72). Additionally, the STRING (https://string-db.org/) database was utilized to identify protein-protein interactions of the identified target protein. STRING is a pre-computed database used to identify PPIs based on various data sources. To ensure the reliability of the interactions, only those with a high confidence score ($\geq$0.7) were considered (73).

2.10 Protein structure modeling and validation

The 3D structure of the succinate dehydrogenase was obtained from the AlphaFold (https://alphafold.ebi.ac.uk/) database. The predicted structure included confidence scores (pLDDT) provided by AlphaFold2, with scores above 70 indicating high reliability. The quality and reliability of the predicted structure were then verified by using the Ramachandran plot and ERRAT (https://saves.mbi.ucla.edu/), ensuring the accuracy and quality of the predicted 3D model.

2.11 Active site analysis and ligand identification

Active site localization was accomplished using Molecular Operating Environment (MOE v. 2015) software. Forecasting active site residues was determined by pinpointing conserved sites across protein families, utilizing robust sequence-based scoring functions, and analyzing the features of the well-defined 3D structure, including the structural geometry of amino acid residues and their electrostatic and chemical properties. For ligand prediction, the computational tool ProBiS (Protein Binding Site) (http://probis.cmm.ki.si/) was employed (74).

2.12 Docking simulation and computational screening

The 3D structure of the protein was essential for docking studies; therefore, succinate dehydrogenase was modeled in three dimensions, and the ligand was predicted to act as an inhibitor. Docking preparation was performed for the protein-ligand complex by removing ligands and heteroatoms, including water molecules. Protein preparation was carried out using AutoDock v4.2 (75), which included adding hydrogens, merging non-polar hydrogen atoms, and assigning Kollman charges. The receptor was then saved in a local shell. Molecular docking was conducted using AutoDock with the Lamarckian Genetic Algorithm (LGA), performing 250 runs with a maximum of 27,000 generations and 2,500,000 evaluations. Redocking was performed to evaluate the program's ability to reproduce the crystal conformation of the bound ligand. The grid points on the X, Y, and Z axis were set to 64, 70, and 62, respectively. A ZINC library of 18,000 molecules was retrieved in SDF format and converted to a 3D PDB file using Open Babel. The ligand library's energy was minimized using the MMFF94 force field and the steepest descent method for 1,500 steps. Gastieger charges were added, rotatable bonds were adjusted in AutoDock, and the ligand library was saved in PDBQT format. The PDBQT library was divided into files using Vina split, with the redocking settings and grid box configuration applied for virtual screening.

2.13 ADMET profiling

Pharmacokinetic parameters, including absorption, distribution, metabolism, and excretion (ADME) (http://www.swissadme.ch/) were evaluated for the shortlisted drug-like compounds using the SwissADME tool (76). The pkCSM tool (https://biosig.lab.uq.edu.au/pkcsm/) was then employed to analyze the compounds' toxicity profiles, including immunotoxicity, mutagenicity, teratogenicity, neurotoxicity, increased penetration, and carcinogenicity (77). Additionally, the potential toxicity of the novel compounds was passed by evaluating the maximum tolerated dose (human), minnow toxicity, *Tetrahymena pyriformis* toxicity, acute oral toxicity (LD50) in rats, hepatotoxicity, and skin sensitization.

3 Result and discussion

3.1 Subtractive proteomics analysis

3.1.1 Proteome retrieval, filtration and non-host homology analysis

The *R. felis* proteome, comprising 1,393 sequences, was subjected to CD-HIT analysis, resulting in the exclusion of 333 paralogous sequences. To prevent cross-reactivity with human proteins, the remaining 1,060 non-paralogous sequences

TABLE 1 Shortlisted druggable proteins in *R. felis*.

Serial no	Protein ID	DrugBank target	DrugBank ID	Cellular localization
1	WP_011270515.1	Drugbank_target | P24752 Acetyl-CoA acetyltransferase	DB00795	Cytoplasmic
2	WP_011271493.1	Drugbank_target | P0A827 Serine hydroxymethyltransferase	DB11596	Cytoplasmic
3	WP_011270920.1	Drugbank_target | P00338 L-lactate dehydrogenase A chain	DB02701; DB09118	Cytoplasmic
4	WP_011270490.1	Drugbank_target | P21912 Succinate dehydrogenase	DB00139	Cytoplasmic
5	WP_011270625.1	Drugbank_target | P04424 Argininosuccinate lyase	DB00125	Cytoplasmic
6	WP_011270995.1	Drugbank_target | P22102 Trifunctional purine biosynthetic protein adenosine-3	DB00642	Cytoplasmic
7	WP_039594975.1	Drugbank_target | P53597 Succinyl-CoA ligase	DB00139	Cytoplasmic
8	WP_039595039.1	Drugbank_target | P13995 Bifunctional methylenetetrahydrofolate dehydrogenase/cyclohydrolase	DB00116	Cytoplasmic
9	WP_039595177.1	Drugbank_target | P10902 L-aspartate oxidase	DB03147	Cytoplasmic
10	WP_011271325.1	Drugbank_target | Q02768 Cytochrome b	DB01117	Inner membrane

underwent a BLASTp analysis against the *Homo sapiens* proteome (78). This analysis identified 717 sequences with human homology, which were excluded, leaving 343 non-homologous proteins for further analysis.

3.1.2 Evaluation of essential proteins, unique metabolic pathways, and druggability analysis

Using DEG database, we identified 108 essential proteins in *R. felis* which are pivotal to the pathogen's life cycle and represent potential targets for antibacterial drug development. Additionally, using the KEGG database, we mapped 25 distinct metabolic pathways linked to these essential proteins. Identifying these pathways is critical as it provides insights into the metabolic dependencies, which could be exploited for therapeutic interventions. Supplementary Table S1 lists these specific pathways with their identifiers, while Supplementary Table S2 presents 11 unique proteins along with their corresponding metabolic pathways. To further assess their therapeutic potential, we performed a BLASTp search of these distinct vital proteins against the Drugbank database which revealed 10 proteins with substantial similarity to FDA-approved drug targets (Table 1). These proteins, which closely aligned with known FDA-approved drug targets, were selected for further investigation.

3.1.3 Prediction of virulent and resistant proteins

Using VFDB resource, we identified two proteins from a set of 10 being associated with the virulence of *R. felis*. These proteins are of particular interest as potential drug targets, especially in the context of combating drug-resistant pathogens, which present significant challenges in the treatment and may necessitate higher doses with increased risk of adverse effects (79). Targeting virulence factors is thus a promising strategy in drug development (80). Additionally, an analysis with the ARG-ANNOT V6 tool revealed that one of the virulent proteins succinate dehydrogenase, is involved in resistance mechanisms, such as drug degradation and efflux. Despite its association with resistance, succinate dehydrogenase remains a viable drug target due to its critical role in the pathogen's biology (81).

3.1.4 Subcellular localization and protein-protein interaction

Our analysis found that 90% of proteins were cytoplasmic, with 5% in both the inner and outer membranes (Figure 2A). The identified target protein, succinate dehydrogenase, was cytoplasmic, indicating its potential as a hub protein due to its extensive interactions. Targeting succinate dehydrogenase could disrupt the function of other interacting proteins, underscoring its critical role in cellular processes (82). The protein-protein interaction (PPI) analysis showed the succinate dehydrogenase interaction with ubiquinol-cytochrome reductase (petA), NADH dehydrogenase I, chain I (nuoI), NADH dehydrogenase I, chain E (nuoE), succinyl-CoA synthase beta chain (SucC), succinyl CoA synthase alpha chain (SucD), fumarate hydratase (fumC), succinate dehydrogenase hydrophobic membrane protein (sdhD), pyruvate dehydrogenase E1 component (pdhB), succinate dehydrogenase cytochrome subunit (sdhC), and succinate dehydrogenase flavoprotein (sdhA). The PPI analysis of succinate dehydrogenase revealed a network with 11 nodes, an average node degree of 8, an average local clustering coefficient of 0.863, and a total of 44 edges (Figure 2B). The PPI enrichment *p*-value was calculated to be $6.51e^{-11}$, indicating a significant interaction network, with an expected number of 14 edges. These proteins participate in various essential functions, suggesting that inhibiting succinate dehydrogenase could potentially disrupt the activity of other interacting proteins (Figure 2C) (83). This makes succinate dehydrogenase a promising candidate for a drug target.

3.1.5 Succinate dehydrogenase as a new drug target

The succinate dehydrogenase protein in *R. felis* presents a compelling target for drug development due to its vital role in the tricarboxylic acid (TCA) cycle and electron transport chain (ETC), both essential for ATP production (84). Succinate

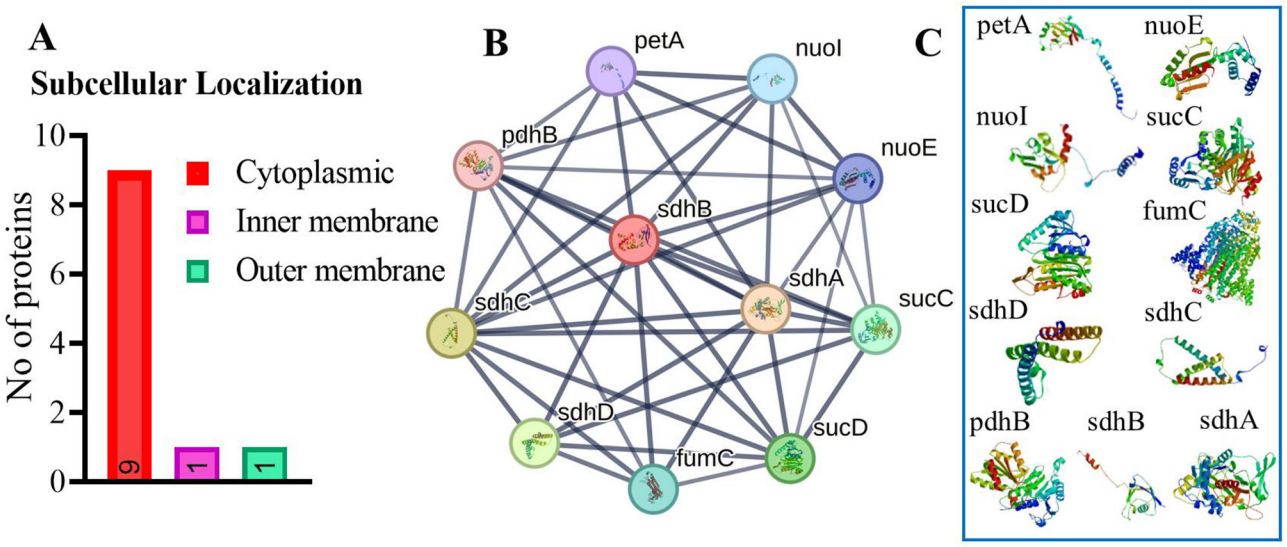

FIGURE 2
(A) Subcellular localization of vital, druggable, and pathogen-specific proteins. **(B)** Protein-protein interaction network for succinate dehydrogenase, showing various protein interactions represented as nodes and edges. Colored nodes indicate the query protein. **(C)** Illustrate the proteins which interact with succinate dehydrogenase.

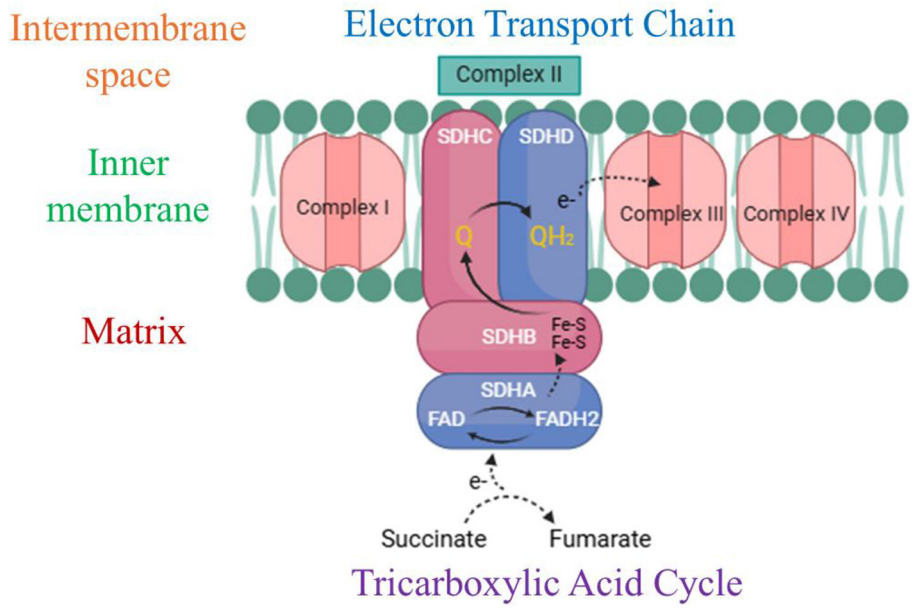

FIGURE 3
Diagrammatic representation of the succinate dehydrogenase/complex II structure and function. This complex contributes to both the tricarboxylic acid (TCA) cycle and electron transport chain (ETC) by facilitating the electron transfer process from succinate to ubiquinone (Q) via its four integral subunits: SDHA, SDHB, SDHC, and SDHD. Key elements include Fe-S clusters (iron–sulfur clusters), ubiquinone (Q), ubiquinol (QH2), the inner mitochondrial membrane, and the intermembrane space. (Created with https://smart.servier.com/ and Draw.io https://app.diagrams.net/).

dehydrogenase (SDH) is a mitochondrial enzyme that plays a pivotal role in cellular metabolism by linking the tricarboxylic acid (TCA) cycle and the electron transport chain (ETC) (85). Within the TCA cycle, succinate dehydrogenase facilitates the oxidation of succinate into fumarate, while in the ETC, it reduces ubiquinone to ubiquinol, functioning as complex II. This enzyme facilitates electron transfer through its four subunits (SDHA, SDHB, SDHC, and SDHD), enabling the movement of electrons from $FADH_2$ to ubiquinone and subsequently to complex III, contributing to the production of adenosine triphosphate (ATP), the primary energy currency of the cell. The catalytic subunit SDHA, the largest component of the succinate dehydrogenase (SDH) complex, is responsible for oxidizing succinate into fumarate, producing $FADH_2$ in the process as part of the tricarboxylic acid (TCA)

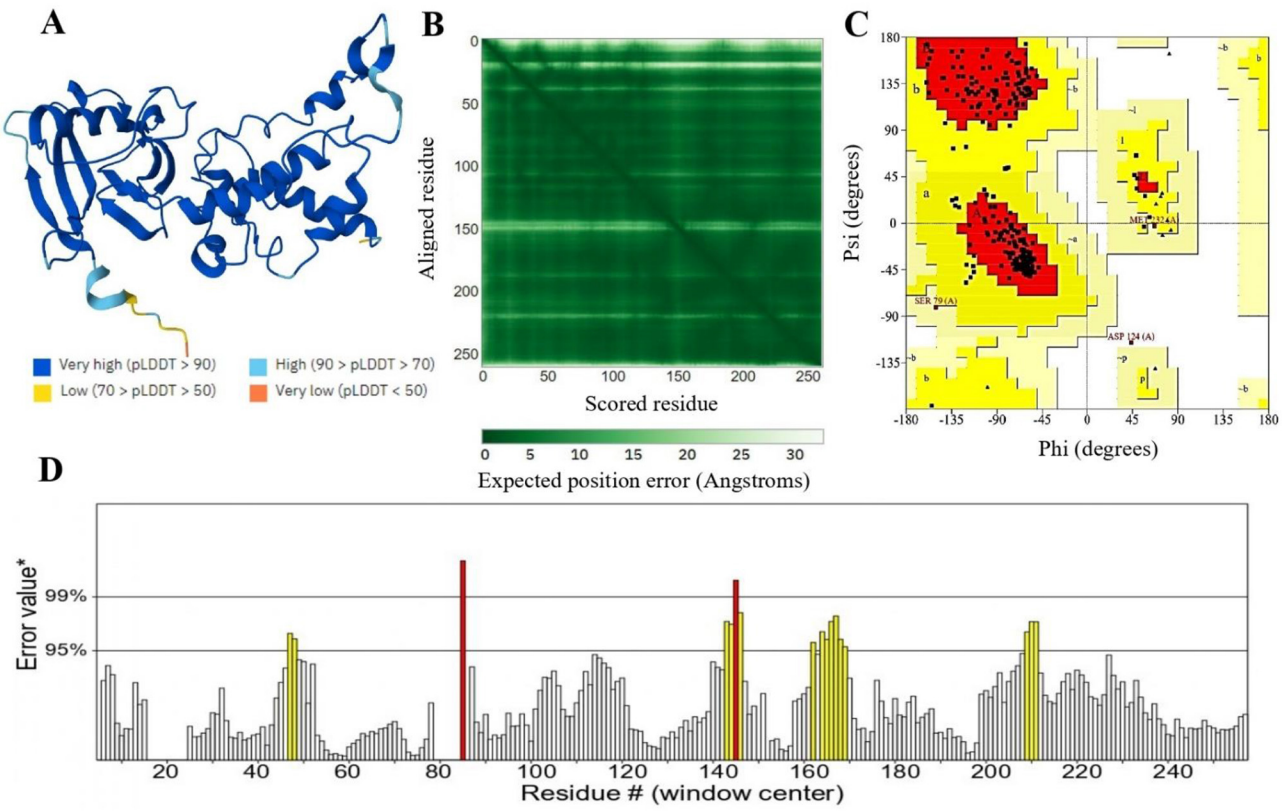

FIGURE 4
(A) The 3D structure of succinate dehydrogenase was modeled using AlphaFold2. AlphaFold2 assigns a confidence score (pLDDT) from 0 to 100 for each residue. Scores below 50 suggest unstructured regions, while higher scores indicate more reliable predictions. **(B)** The anticipated aligned error of the model is depicted, where dark green areas represent low error, and light green areas signify higher error rates. **(C)** Represents 86.3% validity by Ramachandran plot and **(D)** represents 92.7% ERRAT score of the predicted 3D structure.

cycle (86). The SDHB subunit houses three iron–sulfur clusters that facilitate electron transfer from $FADH_2$ to the membrane-embedded subunits SDHC and SDHD. These latter subunits, situated in the inner mitochondrial membrane, form the electron transport chain's (ETC) complex II and serve as the binding and reduction site for ubiquinone (Q) to ubiquinol (QH_2) (87) (Figure 3). Therefore, its disruption can lead to impaired ATP synthesis, metabolic imbalances, and increased oxidative stress, ultimately weakening the bacterium's ability to thrive and cause infection. Given its critical function in both metabolism and virulence, succinate dehydrogenase emerges as a promising target for therapeutic interventions aimed at inhibiting the survival and proliferation of *R. felis* (88).

3.1.6 3D structure prediction and its validation

The protein 3D structure provided by AlphaFold2, includes some regions of disorder, which are indicated by low pLDDT values (89). In the resulting model, most residues exhibit very high confidence scores (pLDDT > 90), indicating the model's accuracy (Figure 4A). The dark green areas in the predicted aligned error plot signify high accuracy, while the light green areas suggest higher error rates (Figure 4B) (90). The structure was validated using the PROCHECK and ERRAT servers which revealed good quality of three-dimensional models (91). Ramachandran plot categorized residues into three regions: favored (86.3%), allowed (12.3%), and disallowed (0.4%) (Figure 4C). Additionally, the ERRAT server evaluated the model's quality based on statistical interactions among non-bonded atoms of different types. ERRAT scores around 92.7% indicate high-resolution structures as shown in Figure 4D.

3.2 Molecular docking, virtual screening, and ADMET profiling

3.2.1 Active site identification and ligand prediction for the modeled protein

The functional activity of a protein depends on the binding of a ligand to its active site (92). Identifying this binding site is crucial for understanding the protein's role and for drug discovery (93). MOE utilized the 3D template structure, which shares similarities with known ligand-binding sites, to identify potential binding pockets through geometric analysis (94). Multiple active sites were found, with the site having the highest energy profile and key functional residues selected (Figure 5A). Predicting protein ligands is challenging, as similar protein folds do not always imply similar functions (95). Conversely, proteins with different folds can exhibit similar biochemical properties, emphasizing that the binding site is crucial for protein function (96). The ProBiS revealed high sequence and structural homology

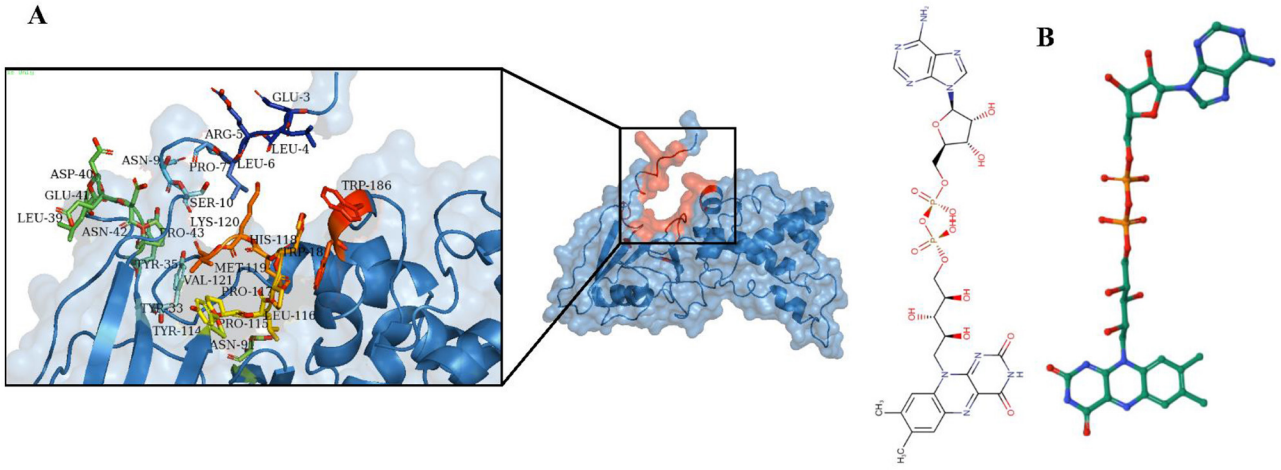

FIGURE 5
Identification of ligand and active site. **(A)** The active site of the succinate dehydrogenase is determined using MOE. **(B)** The ProBis tool predicts Flavin-adenine dinucleotide (FAD) as a ligand for succinate dehydrogenase.

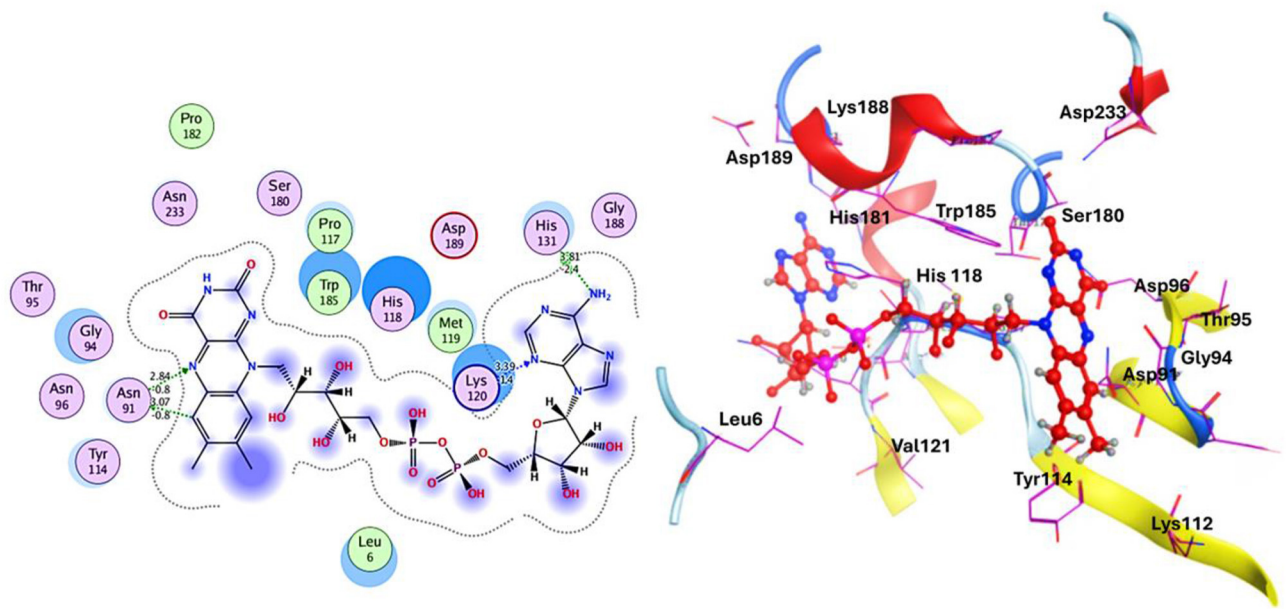

FIGURE 6
Docking analysis of the succinate dehydrogenase revealed a binding affinity of −8.47 kcal/mol for FAD at the active site.

with rhodoquinol-fumarate reductase complexed with Flavin-adenine dinucleotide (FAD) (PDB ID 3VR8) (Figure 5B). A lower binding energy, such as that observed here, suggests a stronger binding affinity, which often correlates with effective inhibition of enzyme activity.

3.2.2 Molecular docking and ligand-protein interactions analysis

Various bioinformatics tools are used for molecular docking in drug discovery (97). MOE module provides detailed graphical representations and ranks receptor-ligand binding affinities using the S-score, a measure of binding free energy (in kcal/mol), where a lower score indicates a more favorable binding (98). Docking of Flavin-adenine dinucleotide (FAD) to succinate dehydrogenase revealed five distinct conformations. Conformation 1, with a high binding energy of −8.47 kcal/mol, was selected for further analysis due to its superior binding affinity compared to the lowest score of −7.50 kcal/mol. This indicates that conformation 1 represents the most stable and potentially effective binding mode for FAD, supporting its role in the protein's function (Figure 6, Table 2) (99).

TABLE 2 Protein-ligand interaction and docking score.

Compound ID	Docking score	Amino acid			Interactions	Distance	E (kcal/mole)
DB03147	−8.47	OD1	ASN	91	H-donor	3.07	−0.8
		N	LYS	120	H-acceptor	3.39	−1.4
		ND2	ASN	91	H-acceptor	2.84	−0.8
		5-ring	HIS	131	pi-H	3.81	−2.4

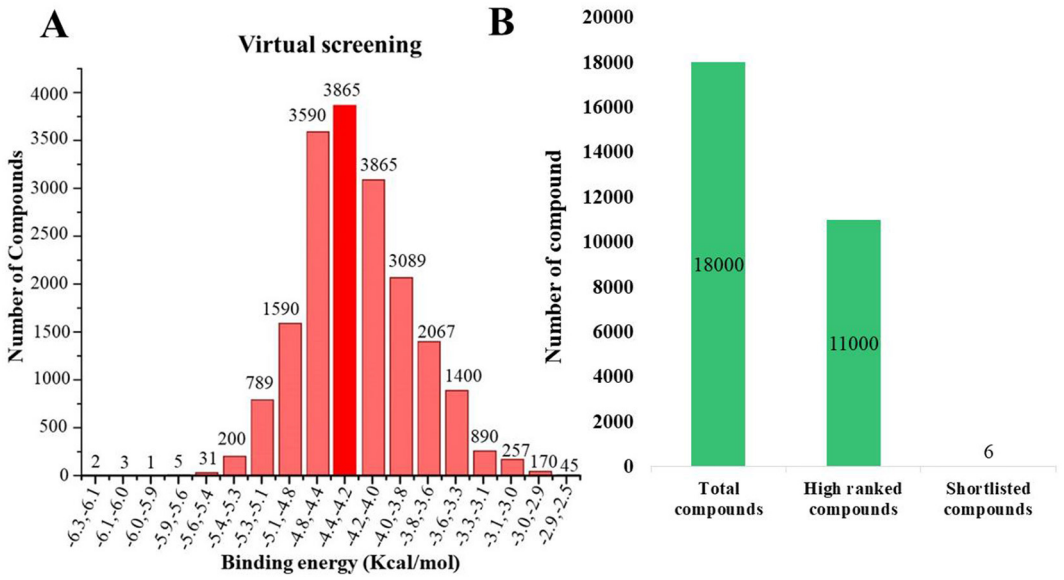

FIGURE 7
(A) Virtual screening was conducted for succinate dehydrogenase using a ZINC database containing 18,000 compounds, revealing binding affinities ranging from −2 to −6 kcal/mol. The analysis identified approximately 3,865 compounds that docked at the same binding site with energies between −4.4 and −4.2 kcal/mol (depicted in dark red). **(B)** An overview of the virtual screening process is presented, narrowing down from an initial pool of 18,000 compounds to 11,000 top-ranked candidates. This ultimately led to the discovery of six potential inhibitors: ZINC67847806, ZINC67982856, ZINC67974679, ZINC67895371, ZINC05668040, and ZINC05670149.

A comprehensive *in silico* screening of the 18,000-compound ZINC library was conducted against the active site of succinate dehydrogenase using an intensive docking approach. This process generated numerous docked conformations, ranked according to their docking scores. Compounds exhibiting lower binding affinities than the reference inhibitor, FAD with a binding energy threshold of −8.47 kcal/mol, were eliminated from further consideration as potential hit candidates. The screening identified over 11,000 compounds with binding energies surpassing that of FAD, ranging between −6.32 kcal/mol and −4.42 kcal/mol (Figure 7A, indicated in dark red). These results suggest that the inhibition of succinate dehydrogenase by these molecules could represent promising leads, as the favorable binding energies imply that these compounds form stable interactions with succinate dehydrogenase, which could effectively inhibit its function (100). Compounds demonstrating higher binding affinities than the FAD inhibitor were prioritized for further investigation due to their potent inhibitory potential against succinate dehydrogenase (Figure 7B). From this group, six compounds emerged as viable therapeutic candidates against succinate dehydrogenase in *R. felis*: ZINC67847806, ZINC67982856, ZINC67974679, ZINC67895371, ZINC05668040, and ZINC05670149 which were used for further analysis.

3.2.3 Post-docking interaction analysis of selected compounds with succinate dehydrogenase

The selected compounds were subjected to post-docking interaction analysis to gain further insights into the pharmacological characteristics and binding dynamics of succinate dehydrogenase. Multiple interactions between each ligand and the receptor were observed during the molecular docking analysis. The docking rank order, based on binding scores, is as follows: ZINC67974679 > ZINC67895371 > ZINC67982856 > ZINC67847806 > ZINC05670149 > ZINC05668040. In the docking study, ZINC67974679 demonstrated a binding energy of −6.54 kcal/mol. The compound's five-aromatic ring facilitated the formation of one pi interaction with HIS118 achieved binding energy of −0.8 kcal/mol, and two H-donor interactions with TYR184 and ASP128, with bond lengths of 3.71 and 3.07 Å, and interaction energy (E) of −0.9 and −6.3 kcal/mol, respectively

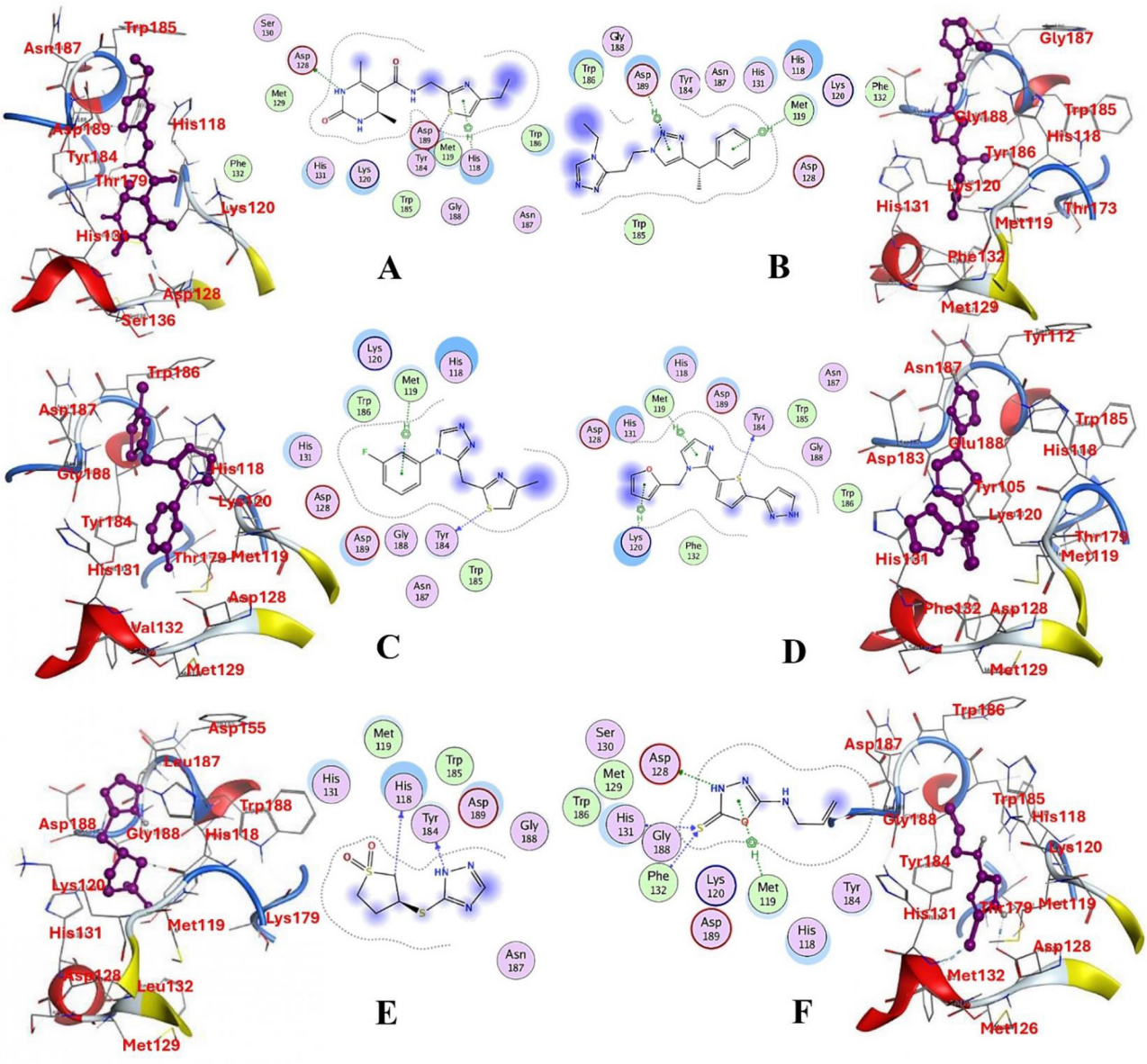

FIGURE 8
Molecular docking analysis for the shortlisted compound **(A)** ZINC67974679, **(B)** ZINC67895371, **(C)** ZINC67982856, **(D)** ZINC67847806, **(E)** ZINC05670149, **(F)** ZINC05668040.

(Figure 8A). ZINC67895371 achieved a docking score of −6.40 kcal/mol. The six and five aromatic rings of this compound established a pi-hydrogen bond with MET119 and ASP189, characterized by a bond length of 3.78 Å, 3.95 and an energy of −0.6 and −0.7 kcal/mol (Figure 8B). ZINC67982856 was highly compatible with the succinate dehydrogenase binding site, displaying a binding score of −6.02 kcal/mol. The six aromatic rings engaged in one H-donor and a pi-H interaction with TYR184 and MET119, with bond lengths ranging from 3.64 to 4.43 Å and interaction energies between −0.7 and −0.9 kcal/mol (Figure 8C). ZINC67847806 formed one hydrogen bond as a donor with TYR184, resulting in a binding energy of −6.00 kcal/mol with bond lengths ranging from 3.97 to 3.75 Å and interaction energies between −0.7 and −0.8 kcal/mol (Figure 8D). Conversely, ZINC05670149 initiated two hydrogen bonds as donors from TYR184 and HIS118. This compound demonstrated a binding score of −5.27 kcal/mol (Figure 8E). Finally, ZINC05668040 docked with succinate dehydrogenase, producing a binding energy of −4.73 kcal/mol. The compound's aromatic ring mediated a single pi-hydrogen bond with the MET119, and three hydrogen bonds as acceptors (HIS131, PHE132), and one hydrogen bond as a donor with ASP128 residue (Figure 8F). Compounds with lower docking scores, such as ZINC67974679 and ZINC67895371, are expected to show increased stability within the binding site and thus greater inhibitory potential, supporting their prioritization for further investigation. The lower binding energies observed in these interactions suggest that these compounds form stable complexes with succinate dehydrogenase, potentially disrupting the enzyme's

TABLE 3 Docking scores and identified bond types for the selected compounds were determined through the MOE tool.

Compound ID	Docking score	Receptors	Interactions	Distance	E (kcal/mole)
ZINC67974679 5-ring	−6.54	O TYR 184 OD2 ASP 128 NE2 HIS 118	H–donor H–donor pi–H	3.71 3.07 3.74	−0.9 −6.3 −0.8
ZINC67895371 6-ring 5-ring	−6.40	CG MET 119 CB ASP 189	pi–H pi–H	3.78 3.95	−0.6 −0.7
ZINC67982856 6-ring	−6.02	O TYR 184 CA MET 119	H–donor pi–H	3.64 4.43	−0.7 −0.9
ZINC67847806 S1 16 5-ring 5-ring	−6.00	O TYR 184 CG MET 119 CD LYS 120	H–donor pi–H pi–H	4.33 3.97 3.75	−0.5 −0.7 −0.8
ZINC05670149 N2 4 C6 15	−5.27	O TYR 184 O HIS 118	H–donor H–donor	3.45 3.24	−0.8 −1.2
ZINC05668040 N3 10 S1 10 S1 10 5-ring	−4.73	OD2 ASP 128 N HIS 131 N PHE 132 CG MET 119	H–donor H–acceptor H–acceptor pi–H	3.33 3.41 3.28 3.71	−1.6 −2.0 −2.8 −1.6

activity effectively (101). This correlation between docking score and inhibitory potential underscores these candidates' potential efficacy. The detailed binding interactions within succinate dehydrogenase active site for the selected compounds is presented in Table 3.

3.2.4 Pharmacokinetic assessment

A pivotal aspect of drug discovery is the examination of ADMET properties, as it significantly reduces time and expenses during clinical trials (102). The pharmacokinetic evaluation revealed key insights into the drug-likeness, ADME characteristics, and blood-brain barrier (BBB) penetration of the selected compounds (103). The Lipinski Rule of Five (RO5) served as the foundation for determining drug-likeness, stipulating that drug-like molecules should possess a molecular weight under 500 Daltons, with a maximum of 10 hydrogen bond acceptors and <5 hydrogen bond donors and a logP (lipophilicity) value below 5 (104). Following these criteria, compounds ZINC20115475, ZINC02688148, and ZINC04259566 satisfied the RO5, whereas ZINC95543764, ZINC04232055, and ZINC04231816 exhibited a single violation each. Nonetheless, all six compounds were determined to lack BBB permeability, which evaluates the compound's ability to cross the protective blood-brain barrier to reach the central nervous system. The compounds adhering to drug-likeness criteria progressed to the subsequent phase of the study. For preliminary ADME property estimation, the pkCSM tool was utilized (105). This analysis encompassed solubility in pure water (mg/L), gastrointestinal absorption (HIA), which indicates the compound's potential for oral absorption in the intestine, permeability, inhibition of liver enzymes such as CYP 2C19, CYP 2C9, CYP 2D6, and CYP 3A4, as well as Caco-2 cell permeability, a model used to predict intestinal drug absorption and permeability through cell monolayers (106). The water solubility of these compounds ranged from −2 to −5, with ZINC02688148 exhibiting high solubility. Caco-2 permeability values spanned from −0.025 to 0.94, with ZINC04259566 demonstrating high cell permeability and ZINC95543764 the lowest. The high permeability observed for ZINC04259566 aligns with studies suggesting that compounds with permeability values exceeding 0.5 tend to exhibit favorable intestinal absorption profiles, making them promising candidates for oral drug delivery (77). Additionally, all compounds displayed good potent HIA permeability, leading to the recommendation of ZINC67982856 for further experimental validation (Table 4). Moreover, an Ames mutagenicity test conducted using the pkCSM tool assessed the potential toxicity of these compounds, including maximum tolerated dose (human), minnow toxicity, *T. pyriformis* toxicity, oral rat acute toxicity (LD50), hepatotoxicity, and skin sensitization (107). The use of *T. pyriformis* as a model organism in toxicity studies is due to its sensitivity to chemical compounds, providing valuable insights into aquatic toxicity (106). All compounds except ZINC20115475 yielded a negative Ames test, indicating a lack of mutagenic potential. The LD50 values ranged from 2.8 to 4.3 mol/kg, with ZINC02688148 exhibiting the highest value, indicating lower acute oral toxicity in rats. These results are consistent with other studies where compounds with higher LD50 values demonstrated greater safety margins, particularly for therapeutic agents intended for prolonged use (108). The data for oral rat acute toxicity (LD50), hepatotoxicity, and skin sensitization were predicted computationally using the pkCSM tool, which evaluates toxicity based on chemical structure and quantitative structure-activity relationships (QSAR). Given that a chemical's toxicity is often predicted based on its molecular structure, ZINC20115475 was excluded from further studies due to its positive result in the Ames test, suggesting possible mutagenicity. While ZINC02688148, ZINC04259566, ZINC04232055, and ZINC04231816 were found to be hepatotoxic, none of the compounds induced skin sensitization. The hepatotoxic compounds were not considered for future investigation, as previous study indicate the dose-dependent liver

TABLE 4 ADME analysis of the shortlisted compounds against succinate dehydrogenase.

ZINC ID	Water solubility (log mol/L)	CaCo2 permeability (log Papp in 10-6 cm/s)	Intestinal absorption (human)	Skin permeability (log Kp)	BBB permeability (log BB)	Structure
ZINC67974679	−3.373	0.69	77.32	−3.695	−0.973	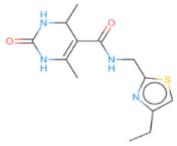
ZINC67895371	−3.162	1.247	98.70	−2.661	−0.123	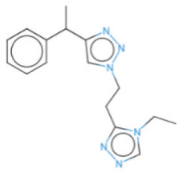
ZINC67982856	−3.45	1.327	99.92	−2.515	0.245	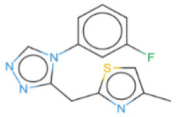
ZINC67847806	−2.835	1.341	90.18	−2.735	0.623	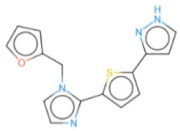
ZINC05670149	−1.957	0.571	90.13	−3.124	−1.417	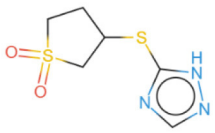
ZINC05668040	−2.184	1.155	91.39	−3.182	−0.414	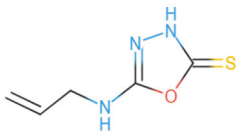

TABLE 5 Toxicity analysis of the shortlisted compounds against succinate dehydrogenase.

ZINC ID	Max. tolerated dose (human)	Minnow toxicity (logmM)	*T. pyriformis* toxicity (log μg/L)	Oral rat acute toxicity (LD50) (mol/kg)	Ames test	Hepatotoxicity	Skin sensitization
ZINC67974679	0.513	2.815	0.061	2.632	No	No	No
ZINC67895371	0.561	−0.691	0.431	2.212	Yes	Yes	No
ZINC67982856	−0.522	0.944	0.514	2.316	No	No	No
ZINC67847806	0.099	1.968	0.285	2.306	Yes	Yes	No
ZINC05670149	−0.334	2.993	0.069	2.492	No	Yes	No
ZINC05668040	0.892	2.768	−0.399	2.794	No	No	No

toxicity profiles and mitigate potential risks (109). *T. pyriformis* exhibited maximum tolerance to ZINC20115475 (0.367 log μg/L), whereas the remaining compounds were less tolerated. Detailed information can be found in Table 5.

4 Conclusions

This study employed the subtractive proteomics method to prioritize viable drug targets against the *R. felis*. The approach

involves several essential analyses at different stages, including identifying non-host homologous, essential, druggable, and pathogen-specific proteins. Several proteins, including succinate dehydrogenase, were identified as novel drug targets against *R. felis*. The selected essential proteins could serve as therapeutic targets for the development of new drugs or vaccines against *R. felis*. Additionally, a pharmacoinformatic approach was utilized to screen a natural product's ZINC library (n = 18,000) against succinate dehydrogenase for potential inhibitors. Six compounds—ZINC67847806, ZINC67982856, ZINC67974679, ZINC67895371, ZINC05668040, and ZINC05670149—were identified as promising inhibitors based on their ligand-protein binding patterns (lowest estimated binding energy). However, ADMET profiling indicated that while all compounds generally met the required ADMET properties, ZINC67895371 and ZINC67847806 showed positive Ames activity, and ZINC05670149, ZINC67895371, and ZINC67847806 exhibited hepatotoxicity, though none showed skin sensitization. Based on these findings, we recommend the ZINC67974679, ZINC67982856, and ZINC05668040 compounds for further experimental validation. Nonetheless, experimental validation is needed to enhance the efficacy of the predicted targets.

Data availability statement

The original contributions presented in the study are included in the article/Supplementary material, further inquiries can be directed to the corresponding authors.

Author contributions

SR: Writing – original draft, Writing – review & editing. HL: Writing – original draft, Writing – review & editing. MS: Writing – original draft, Writing – review & editing. MA: Writing – original draft, Writing – review & editing. IL: Writing – original draft, Writing – review & editing. TT: Writing – original draft, Writing – review & editing. C-CC: Writing – original draft, Writing – review & editing. AAlo: Writing – original draft, Writing – review & editing. AAli: Writing – original draft, Writing – review & editing.

Funding

The author(s) declare that financial support was received for the research, and/or publication of this article. The authors acknowledge the financial support provided by the Higher Education Commission (HEC), Pakistan, Pakistan Science Foundation (PSF). The researchers supporting project number (RSP2024R494), King Saud University, Riyadh, Saudi Arabia.

Conflict of interest

The authors declare that the research was conducted in the absence of any commercial or financial relationships that could be construed as a potential conflict of interest.

Publisher's note

All claims expressed in this article are solely those of the authors and do not necessarily represent those of their affiliated organizations, or those of the publisher, the editors and the reviewers. Any product that may be evaluated in this article, or claim that may be made by its manufacturer, is not guaranteed or endorsed by the publisher.

Supplementary material

The Supplementary Material for this article can be found online at: https://www.frontiersin.org/articles/10.3389/fvets.2024.1507496/full#supplementary-material

References

1. Brown LD, Macaluso KR. *Rickettsia felis*, an emerging flea-borne rickettsiosis. *Curr Trop Med Rep.* (2016) 3:27–39. doi: 10.1007/s40475-016-0070-6

2. Ogrzewalska M, Rozental T, Favacho AR, de Mello Mares-Guia MAM. Rickettsial infections, Bartonella infections, and coxiellosis. *Arthropod Borne Dis.* (2017) 2017:171–91. doi: 10.1007/978-3-319-13884-8_12

3. Helminiak L, Mishra S, Kim HK. Pathogenicity and virulence of *Rickettsia*. *Virulence.* (2022) 13:1752–71. doi: 10.1080/21505594.2022.2132047

4. Higgins JA, Sacci Jr JB, Schriefer ME, Endris RG, Azad AF. Molecular identification of rickettsia-like microorganisms associated with colonized cat fleas (*Ctenocephalides felis*). *Insect Mol Biol.* (1994) 3:27–33. doi: 10.1111/j.1365-2583.1994.tb00147.x

5. Noden BH, Davidson S, Herdlitchka HT, Williams F. First detection of *Rickettsia typhi* and *Rickettsia felis* in fleas collected from client-owned companion animals in the Southern Great Plains. *J Med Entomol.* (2017) 54:1093–7. doi: 10.1093/jme/tjx069

6. Bitam I, Parola D, De La Cruz KD, Matsumoto K, Baziz B, Rolain JM, et al. First molecular detection of *Rickettsia felis* in fleas from Algeria. *Am J Trop Med Hyg.* (2006) 74:532–5. doi: 10.4269/ajtmh.2006.74.532

7. Peniche-Lara G, Jimenez-Delgadillo B, Dzul-Rosado K. *Rickettsia rickettsii* and *Rickettsia felis* infection in *Rhipicephalus sanguineus* ticks and *Ctenocephalides felis* fleas co-existing in a small city in Yucatan, Mexico. *J Vector Ecol.* (2015) 40:422–4. doi: 10.1111/jvec.12185

8. Peniche-Lara G, Dzul-Rosado K, Perez-Osorio C, Zavala-Castro J. *Rickettsia typhi* in rodents and *R. felis* in fleas in Yucatán as a possible causal agent of undefined febrile cases. *Revista do Instituto de Medicina Tropical de São Paulo.* (2015) 57:129–32. doi: 10.1590/S0036-46652015000200005

9. Ponnusamy L, Garshong R, McLean BS, Wasserberg G, Durden LA, Crossley D, et al. *Rickettsia felis* and other Rickettsia species in chigger mites collected from wild rodents in North Carolina, USA. *Microorganisms.* (2022) 10:1342. doi: 10.3390/microorganisms10071342

10. Tsokana CN, Kapna I, Valiakos G. Current data on *Rickettsia felis* occurrence in vectors, human and animal hosts in Europe: a scoping review. *Microorganisms.* (2022) 10:2491. doi: 10.3390/microorganisms10122491

11. Low VL, Tan TK, Khoo JJ, Lim FS, AbuBakar S. An overview of rickettsiae in Southeast Asia: vector-animal-human interface. *Acta Trop.* (2020) 202:105282. doi: 10.1016/j.actatropica.2019.105282

12. Asante J, Noreddin A, El Zowalaty ME. Systematic review of important bacterial zoonoses in Africa in the last decade in light of the 'One Health'concept. *Pathogens.* (2019) 8:50. doi: 10.3390/pathogens8020050

13. Ehlers J, Krüger A, Rakotondranary SJ, Ratovonamana RY, Poppert S, Ganzhorn JU, et al. Molecular detection of *Rickettsia* spp., *Borrelia* spp., *Bartonella* spp. and *Yersinia pestis* in ectoparasites of endemic and domestic animals in southwest Madagascar. *Acta Trop.* (2020) 205:105339. doi: 10.1016/j.actatropica.2020.105339

14. Angelakis E, Mediannikov O, Parola P, Raoult D. *Rickettsia felis*: the complex journey of an emergent human pathogen. *Trends Parasitol.* (2016) 32:554–64. doi: 10.1016/j.pt.2016.04.009

15. Hoque MM, Barua S, Kelly J, Chenoweth K, Kaltenboeck B, Wang C. Identification of *Rickettsia felis* DNA in the blood of domestic cats and dogs in the USA. *Parasit Vectors.* (2020) 13:1–7. doi: 10.1186/s13071-020-04464-w

16. Hun L, Troyo A, Taylor L, Barbieri AM, Labruna MB. First report of the isolation and molecular characterization of *Rickettsia amblyommii* and *Rickettsia felis* in Central America. *Vector-Borne Zoo Dis.* (2011) 11:1395–7. doi: 10.1089/vbz.2011.0641

17. Bermúdez CSE, Troyo A. A review of the genus *Rickettsia* in Central America. *Res Reports trop. Med.* (2018) 2018:103–112. doi: 10.2147/RRTM.S160951

18. Galvão MAM, Mafra C, Chamone CB, Calic SB, Zavala-Velazquez JE, Walker DH. Clinical and laboratorial evidence of *Rickettsia felis* infections in Latin America. *Rev Soc Bras Med Trop.* (2004) 37:238–40. doi: 10.1590/S0037-86822004000300009

19. Portillo A, Santibáñez S, García-Álvarez L, Palomar AM, Oteo JA. Rickettsioses in europe. *Microbes Infect.* (2015) 17:834–8. doi: 10.1016/j.micinf.2015.09.009

20. Richter J, Fournier E, Petridou J, Häussinger D, Raoult D. *Rickettsia felis* infection acquired in Europe and documented by polymerase chain reaction. *Emerg Infect Dis.* (2002) 8:207. doi: 10.3201/eid0802.010293

21. Socolovschi C, Mediannikov O, Sokhna C, Tall A, Diatta G, Bassene H, et al. *Rickettsia felis*–associated uneruptive fever, Senegal. *Emerg Infect Dis.* (2010) 16:1140. doi: 10.3201/eid1607.100070

22. Blanton LS, Walker DH. Flea-borne rickettsioses and rickettsiae. *Am J Trop Med Hyg.* (2017) 96:53. doi: 10.4269/ajtmh.16-0537

23. Parola P. *Rickettsia felis*: from a rare disease in the USA to a common cause of fever in sub-Saharan Africa. *Clini Microbiol Infect.* (2011) 17:996–1000. doi: 10.1111/j.1469-0691.2011.03516.x

24. Mediannikov O, Socolovschi C, Edouard S, Fenollar F, Mouffok N, Bassene H, et al. Common epidemiology of *Rickettsia felis* infection and malaria, Africa. *Emerg Infect Dis.* (2013) 19:1775. doi: 10.3201/eid1911.130361

25. Keita AK, Socolovschi C, Ahuka-Mundeke S, Ratmanov A, Butel C, Ayouba A, et al. Molecular evidence for the presence of *Rickettsia felis* in the feces of wild-living African apes. *PLoS ONE.* (2013) 8:e54679. doi: 10.1371/journal.pone.0054679

26. Ferdouse F, Hossain MA, Paul SK, Ahmed S, Mahmud MC, Ahmed R, et al. *Rickettsia felis* infection among humans, Bangladesh, 2012–2013. *Emerg Infect Dis.* (2015) 21:1483. doi: 10.3201/eid2108.150328

27. Younas M, Ashraf K, Rashid MI, Ijaz M, Suleman M, Chohan TA. Expression and purification of recombinant multi-epitope protein of *rhipicephalus microplus* tick and its antigenicity in the rabbit model. *Pakistan Vet. J.* (2023) 43:4. doi: 10.29261/pakvetj/2023.08

28. Ceylan C, Ekici ÖD. Molecular investigation of ovine and caprine anaplasmosis in south-Eastern Anatolia region of Turkey. *Pakistan Vet. J.* (2023) 43:1.

29. Adams JR, Schmidtmann ET, Azad AF. Infection of colonized cat fleas, *Ctenocephalides felis* (Bouché), with a rickettsia-like microorganism. *Am J Trop Med Hyg.* (1990) 43:400–9. doi: 10.4269/ajtmh.1990.43.400

30. de Oliveira JCP, Reckziegel GH, Ramos CADN, Giannelli A, Alves LC, de Carvalho GA, et al. Detection of *Rickettsia felis* in ectoparasites collected from domestic animals. *Exp Appl Acarol.* (2020) 81:255–64. doi: 10.1007/s10493-020-00505-2

31. Eremeeva ME, Dasch GA. Challenges posed by tick-borne rickettsiae: eco-epidemiology and public health implications. *Front Public Health.* (2015) 3:55. doi: 10.3389/fpubh.2015.00055

32. Otranto D, Cantacessi C, Pfeffer M, Dantas-Torres F, Brianti E. Deplazes, et al. The role of wild canids and felids in spreading parasites to dogs and cats in Europe: Part I: Protozoa and tick-borne agents. *Vet Parasitol.* (2015) 213:12–23. doi: 10.1016/j.vetpar.2015.04.022

33. Richards AL, Jiang J, Omulo S, Dare R, Abdirahman K, Ali A, et al. Human infection with *Rickettsia felis*, Kenya. *Emerg Infect Dis.* (2010) 16:1081. doi: 10.3201/eid1607.091885

34. Raoult D, Roux V. Rickettsioses as paradigms of new or emerging infectious diseases. *Clin Microbiol Rev.* (2001) 14:694–728. doi: 10.1128/CMR.10.4.694

35. Parola P, Raoult D. Tropical rickettsioses. *Clini Dermatol.* (2005) 23:203–13. doi: 10.1016/j.clindermatol.2005.11.007

36. Azad AF, Beard CB. Rickettsial pathogens and their arthropod vectors. *Emerg Infect Dis.* (1998) 4:179. doi: 10.3201/eid0402.980205

37. Horta MC, Labruna MB, Sangioni LA, Vianna MC, Gennari SM, Schumaker TT, et al. Prevalence of antibodies to spotted fever group rickettsiae in cats and dogs in Brazil. *Am J Trop Med Hyg.* (2007) 77:1029–34. doi: 10.4269/ajtmh.2004.71.93

38. Mullins KE, Maina AN, Krueger L, Jiang J, Cummings R, Drusys A, et al. Rickettsial infections among cats and cat fleas in Riverside County, California. *Am J Trop Med Hyg.* (2018) 99:291. doi: 10.4269/ajtmh.17-0706

39. Azrizal-Wahid N, Sofian-Azirun M, Low VL. Flea-borne pathogens in the cat flea *Ctenocephalides felis* and their association with mtDNA diversity of the flea host. *Comp Immunol Microbiol Infect Dis.* (2021) 75:101621. doi: 10.1016/j.cimid.2021.101621

40. Morick D, Krasnov BR, Khokhlova IS. Molecular detection of *Rickettsia felis* in fleas from wild mammals in Israel. *J Med Entomol.* (2011) 48:818–22.

41. Boostrom A, Beier MS, Macaluso JA, Sprenger D, Hayes J, Radulovic S, et al. Geographic association of *Rickettsia felis*-infected opossums with human *murine typhus*, Texas. *Emerg Infect Dis.* (2002) 8:549–54. doi: 10.3201/eid0806.010350

42. Hornok S, Meli ML, Gönczi E, Halász E, Takács N, Farkas R, et al. Molecular investigation of fleas and ticks on rodents and lagomorphs for rickettsial pathogens. *Vector-Borne Zoon Dis.* (2010) 10:811–6.

43. Maina AN, Fogarty C, Kruger H, Odhiambo A, Farris CM, Odongo D, et al. *Rickettsia* species detected in rodent ectoparasites in Kenya. *Vector-Borne and Zoonotic Diseases.* (2019) 19:747–51.

44. Pérez-Osorio CE, Zavala-Velázquez JE, León JJA, Zavala-Castro JE. *Rickettsia felis* as emergent global threat for humans. *Emerg Infect Dis.* (2008) 14:1019. doi: 10.3201/eid1407.071656

45. Dieme C, Bechah Y, Socolovschi C, Audoly G, Berenger JM, Raoult D. Transmission potential of *Rickettsia felis* infection by *Anopheles gambiae* mosquitoes. *Proc Nat Acad Sci.* (2015) 112:8088–93. doi: 10.1073/pnas.1413835112

46. Sangioni LA, Horta MC, Vianna MC, Gennari SM, Soares RM, Galvão MA, et al. Rickettsial infection in animals and Brazilian spotted fever endemicity. *Emerg Infect Dis.* (2005) 11:265. doi: 10.3201/eid1102.040656

47. Teoh YT Hii SF, Graves S, Rees R, Stenos J, Traub RJ. The epidemiology of *Rickettsia felis* infecting fleas of companion animals in eastern Australia. *Parasit Vect.* (2018) 11:1–8. doi: 10.1186/s13071-018-2737-4

48. Yazid Abdad M, Stenos J, Graves S. *Rickettsia felis*, an emerging flea-transmitted human pathogen. *Emerg Health Threats J.* (2011) 4:7168. doi: 10.3402/ehtj.v4i0.7168

49. Álvarez-Hernández G, López-Ridaura R, Cortés-Alcalá R, Rodríguez GG, Calleja-López JT, Rivera-Rosas CN, et al. Rocky mountain spotted fever in Mexico: a call to action. *Am J Trop Med Hygiene.* (2024) 111:1070. doi: 10.4269/ajtmh.24-0265

50. Liu D. Rickettsia. In: *Molecular Medical Microbiology*. London:Academic Press. (2015) p. 2043–2056.

51. Pornwiroon W, Pourciau SS, Foil LD, Macaluso KR. *Rickettsia felis* from cat fleas: isolation and culture in a tick-derived cell line. *Appl Environ Microbiol.* (2006) 72:5589–95. doi: 10.1128/AEM.00532-06

52. Epstein SE, Stern JA, Sykes JE. Cardiovascular Infections (Bacteremia, Endocarditis, Myocarditis, Infectious Pericarditis). In: *Greene's Infectious Diseases of the Dog and Cat.* Philadelphia, PA: WB Saunders. (2021) p. 1590–1602.

53. Rolain JM, Stuhl L, Maurin M, Raoult D. Evaluation of antibiotic susceptibilities of three rickettsial species including *Rickettsia felis* by a quantitative PCR DNA assay. *Antimicrob Agents Chemother.* (2002) 46:2747–51. doi: 10.1128/AAC.46.9.2747-2751.2002

54. Singh BR, Somvanshi R. *Diseases of Animals: Diagnosis and Management*. Izatnagar, India: Indian Veterinary Research Institute. (2013).

55. Stewart MP, Sharei A, Ding X, Sahay G, Langer R, Jensen KF. *In vitro* and *ex vivo* strategies for intracellular delivery. *Nature.* (2016) 538:183–92. doi: 10.1038/nature19764

56. Rahman S, Chiou CC, Ahmad S, Islam ZU, Tanaka T, Alouffi A, et al. Subtractive proteomics and reverse-vaccinology approaches for novel drug target identification and chimeric vaccine development against *bartonella henselae* strain houston-1. *Bioengineering.* (2024) 11:505. doi: 10.3390/bioengineering11050505

57. Ali A, Ahmad S, Wadood A, Rehman AU, Zahid H, Qayash Khan M, et al. Modeling novel putative drugs and vaccine candidates against tick-borne pathogens: A subtractive proteomics approach. *Vet Sci.* (2020) 7:129. doi: 10.3390/vetsci7030129

58. Hughes D, Andersson DI. Evolutionary consequences of drug resistance: shared principles across diverse targets and organisms. *Nat Rev Genet.* (2015) 16:459–71. doi: 10.1038/nrg3922

59. Ali A, Ahmad S, de Albuquerque MM, Kamil A, Alshammari FA, Alouffi A, et al. Prediction of novel drug targets and vaccine candidates against human lice (Insecta), Acari (Arachnida), and their associated pathogens. *Vaccines.* (2021) 10:8. doi: 10.3390/vaccines10010008

60. Wu X, Wang Y, Wang Q, Wang Y, Wang H, Luo X. Acinetobacter of pigs reveals high multiple drug resistance through genomics and antimicrobial resistance monitoring. *Pak Vet J.* (2024). doi: 10.29261/pakvetj/2024.259

61. Riaz R, Zahid S, Khan MS. Designing an epitope-based vaccine against bovine viral diarrhea using immuno-informatics. *Pak Vet J.* (2024) 44:465–475. doi: 10.29261/pakvetj/2024.162

62. Rahman S, Chiou CC, Almutairi MM, Ajmal A, Batool S, Javed B, et al. Targeting yezo virus structural proteins for multi-epitope vaccine design using immunoinformatics approach. *Viruses.* (2024) 16:1408. doi: 10.3390/v16091408

63. Maxson T, Mitchell DA. Targeted treatment for bacterial infections: prospects for pathogen-specific antibiotics coupled with rapid diagnostics. *Tetrahedron.* (2016) 72:3609–24. doi: 10.1016/j.tet.2015.09.069

64. Huang Y, Niu B, Gao Y, Fu L, Li W, CD-HIT. Suite: a web server for clustering and comparing biological sequences. *Bioinformatics.* (2010) 26:680–2. doi: 10.1093/bioinformatics/btq003

65. Mahram A, Herbordt MC. NCBI BLASTP on high-performance reconfigurable computing systems. *ACM Trans Reconfigur Technol Syst.* (2015) 7:1–20. doi: 10.1145/2629691

66. Tenguria S, Ismaeel S. Essential proteins for the survival of bacteria in hostile environment. In: *Bacterial Survival in the Hostile Environment.* (London: Academic Press. (2023) p. 63–72.

67. Luo H, Lin Y, Liu T, Lai FL, Zhang CT, Gao F, et al. DEG 15, an update of the Database of Essential Genes that includes built-in analysis tools. *Nucleic Acids Res.* (2021) 49:D677–86. doi: 10.1093/nar/gkaa917

68. Kanehisa M, Furumichi M, Tanabe M, Sato Y, Morishima K, KEGG. new perspectives on genomes, pathways, diseases and drugs. *Nucleic Acids Res.* (2017) 45:D353–61. doi: 10.1093/nar/gkw1092

69. Chen L, Yang J, Yu J, Yao Z, Sun L, Shen Y, et al. VFDB: a reference database for bacterial virulence factors. *Nucleic Acids Res.* (2005) 33:D325–8. doi: 10.1093/nar/gki008

70. Gupta SK, Padmanabhan BR, Diene SM, Lopez-Rojas R, Kempf M, Landraud L, Rolain, J. ARG-ANNOT, a new bioinformatic tool to discover antibiotic resistance genes in bacterial genomes. *Antimicrob Agents Chemother.* (2014) 58:212–20. doi: 10.1128/AAC.01310-13

71. Dönnes P, Höglund A. Predicting protein subcellular localization: past, present, and future. *Genom Prot Bioinform.* (2004) 2:209–15. doi: 10.1016/S1672-0229(04)02027-3

72. Yu CS, Chen YC, Lu CH, Hwang JK. Prediction of protein subcellular localization. *Proteins: Struct Funct Bioinform.* (2006) 64:643–51. doi: 10.1002/prot.21018

73. Szklarczyk D, Kirsch R, Koutrouli M, Nastou K, Mehryary F, Hachilif R, et al. The STRING database in 2023: protein–protein association networks and functional enrichment analyses for any sequenced genome of interest. *Nucleic Acids Res.* (2023) 51:D638–D646. doi: 10.1093/nar/gkac1000

74. Konc J, JaneŽič D. ProBiS: a web server for detection of structurally similar protein binding sites. *Nucleic Acids Res.* (2010) 38:W436–W440. doi: 10.1093/nar/gkq479

75. Morris GM, Huey R, Lindstrom W, Sanner MF, Belew RK, Goodsell DS, et al. (2009). Autodock4 and AutoDockTools4: automated docking with selective receptor flexiblity. *J Computational Chemistry.* (2009) 16:2785–91. doi: 10.1002/jcc.21256

76. Daina A, Michielin O, Zoete V. SwissADME: a free web tool to evaluate pharmacokinetics, drug-likeness and medicinal chemistry friendliness of small molecules. *Sci Rep.* (2017) 7:42717. doi: 10.1038/srep42717

77. Pires DE, Blundell TL, Ascher DB. pkCSM: predicting small-molecule pharmacokinetic and toxicity properties using graph-based signatures. *J Med Chem.* (2015) 58:4066–72. doi: 10.1021/acs.jmedchem.5b00104

78. Johnson M, Zaretskaya I, Raytselis Y, Merezhuk Y, McGinnis S, Madden TL, et al. a better web interface. *Nucleic Acids Res.* (2008) 36:W5–9. doi: 10.1093/nar/gkn201

79. Lambert A. Bacterial resistance to antibiotics: modified target sites. *Adv Drug Deliv Rev.* (2005) 57:1471–85. doi: 10.1016/j.addr.2005.04.003

80. Shami A, Abdallah M, Alruways MW, Mostafa YS, Alamri SA, Ahmed AE, et al. Comparative prevalence of virulence genes and antibiotic resistance in *Campylobacter jejuni* isolated from broilers, laying hens and farmers. *Pak Vet J.* 44:200–4. doi: 10.29261/pakvetj/2024.133

81. Yushuai M, Yabing D, Mingguo Z. Research progress of the resistance to succinate dehydrogenase inhibitors. *Chin J Pesticide Sci.* (2022) 24:937–48.

82. Yu L, Yu CA. Interaction between succinate dehydrogenase and ubiquinone-binding protein from succinate-ubiquinone reductase. *Biochimica et Biophysica Acta (BBA)-Bioenergetics.* (1980) 593:24–38. doi: 10.1016/0005-2728(80)90005-5

83. Li S, Li X, Zhang H, Wang Z, Xu H. The research progress in and perspective of potential fungicides: Succinate dehydrogenase inhibitors. *Bioorg Med Chem.* (2021) 50:116476. doi: 10.1016/j.bmc.2021.116476

84. Ackrell BA, Johnson MK, Gunsalus RP, Cecchini G. Structure and function of succinate dehydrogenase and fumarate reductase. In: *Chemistry and Biochemistry of Flavoenzymes.* Boca Raton, FL: CRC Press. (2019) p. 229–297.

85. Kregiel D. Succinate dehydrogenase of *Saccharomyces cerevisiae*–the unique enzyme of TCA cycle–current knowledge and new perspectives. In: Canuto, RA, editor. *Dehydrogenases* (2012) p. 211–234.

86. Read AD, Bentley RE, Archer SL, Dunham-Snary KJ. Mitochondrial iron–sulfur clusters: Structure, function, and an emerging role in vascular biology. *Redox Biol.* (2021) 47:102164. doi: 10.1016/j.redox.2021.102164

87. Huang S, Millar AH. Succinate dehydrogenase: the complex roles of a simple enzyme. *Curr Opin Plant Biol.* (2013) 16:344–9. doi: 10.1016/j.pbi.2013.02.007

88. Richardson R. AVirulence and metabolism. *Microbiol Spect.* (2019) 7:10–1128. doi: 10.1128/microbiolspec.GPP3-0011-2018

89. Guo HB, Perminov A, Bekele S, Kedziora G, Farajollahi S, Varaljay V, et al. (2022). AlphaFold2 models indicate that protein sequence determines both structure and dynamics. *Scient Rep.* 12:10696. doi: 10.1038/s41598-022-14382-9

90. Abramson J, Adler J, Dunger J, Evans R, Green T, Pritzel A, et al. (2024). Accurate structure prediction of biomolecular interactions with AlphaFold 3. *Nature* 2024:1–3. doi: 10.1038/s41586-024-08416-7

91. DasGupta D, Kaushik R, Jayaram B. From Ramachandran maps to tertiary structures of proteins. *J Phys Chemistry B.* (2015) 119:11136–45. doi: 10.1021/acs.jpcb.5b02999

92. Stank A, Kokh DB, Fuller JC, Wade RC. Protein binding pocket dynamics. *Acc Chem Res.* (2016) 49:809–15. doi: 10.1021/acs.accounts.5b00516

93. Scott DE, Bayly AR, Abell C, Skidmore J. Small molecules, big targets: drug discovery faces the protein–protein interaction challenge. *Nat Rev Drug Discov.* (2016) 15:533–50. doi: 10.1038/nrd.2016.29

94. Shah R, Alharbi A, Hameed AM, Saad F, Zaky R, Khedr AM, et al. Synthesis and structural elucidation for new Schiff base complexes; conductance, conformational, MOE-docking and biological studies. *J Inorg Organomet Polym Mater.* (2020) 30:3595–607. doi: 10.1007/s10904-020-01505-w

95. Esmaielbeiki R, Krawczyk K, Knapp B, Nebel JC, Deane CProgress M, and challenges in predicting protein interfaces. *Brief Bioinform.* (2016) 17:117–31. doi: 10.1093/bib/bbv027

96. Zhou HX, Pang X. Electrostatic interactions in protein structure, folding, binding, and condensation. *Chem Rev.* (2018) 118:1691–741. doi: 10.1021/acs.chemrev.7b00305

97. Stanzione F, Giangreco I, Cole JC. Use of molecular docking computational tools in drug discovery. *Prog Med Chem.* (2021) 60:273–343. doi: 10.1016/bs.pmch.2021.01.004

98. Mosa FE, El-Kadi AO, Barakat K. In-depth analysis of the interactions of various aryl hydrocarbon receptor ligands from a computational perspective. *J Mol Graph Model.* (2023) 118:108339. doi: 10.1016/j.jmgm.2022.108339

99. Althagafi I, El-Metwaly N, Farghaly TA. New series of thiazole derivatives: synthesis, structural elucidation, antimicrobial activity, molecular modeling and MOE docking. *Molecules.* (2019) 24:1741. doi: 10.3390/molecules24091741

100. Manoharan JP, Nirmala Karunakaran K, Vidyalakshmi S, Dhananjayan K. Computational binding affinity and molecular dynamic characterization of annonaceous acetogenins at nucleotide binding domain (NBD) of multi-drug resistance ATP-binding cassette sub-family B member 1 (ABCB1). *J Biomol Struct Dynam.* (2023) 41:821–32. doi: 10.1080/07391102.2021.2013321

101. Moosavi B, Berry EA, Zhu XL, Yang WC, Yang GF. The assembly of succinate dehydrogenase: a key enzyme in bioenergetics. *Cellular Mol Life Sci.* (2019) 76:4023–42. doi: 10.1007/s00018-019-03200-7

102. Vrbanac J, Slauter R. ADME in drug discovery. In: *A Comprehensive Guide to Toxicology in Nonclinical Drug Development.* London: Academic Press. (2017) p. 39–67.

103. Janicka M, Sztanke M, Sztanke K. Predicting the blood-brain barrier permeability of new drug-like compounds via HPLC with various stationary phases. *Molecules.* (2020) 25:487. doi: 10.3390/molecules25030487

104. Lipinski CA. Rule of five in 2015 and beyond: Target and ligand structural limitations, ligand chemistry structure and drug discovery project decisions. *Adv Drug Deliv Rev.* (2016) 101:34–41. doi: 10.1016/j.addr.2016.04.029

105. Lohohola O, Mbala BM, Bambi SMN, Mawete DT, Matondo A, Mvondo JGM. *In silico* ADME/T properties of quinine derivatives using SwissADME and pkCSM webservers. *Int J Tropical Disease and Health.* (2021) 42:1–12. doi: 10.9734/ijtdh/2021/v42i1130492

106. Ghosh V, Bhattacharjee A, Kumar A, Ojha K. q-RASTR modelling for prediction of diverse toxic chemicals towards *T. pyriformis. SAR and QSAR Environm Res.* (2024) 35:11–30. doi: 10.1080/1062936X.2023.2298452

107. Ferrari IV. *Assessing Antibiotic Safety: A Comparative Study of Four Promising Candidates Using pKCSM Database.* Basel: MDPI Preprints-Communication (2023).

108. Keshavarz MH. *Toxicity: 77 Must-Know Predictions of Organic Compounds: Including Ionic Liquids*. Berlin: Walter de Gruyter GmbH and Co KG. (2023).

109. Meunier L, Larrey D. Hepatotoxicity of drugs used in multiple sclerosis, diagnostic challenge, and the role of HLA genotype susceptibility. *Int J Mol Sci.* (2023) 24:852. doi: 10.3390/ijms24010852

frontiers | Frontiers in Veterinary Science

TYPE Original Research
PUBLISHED 05 February 2025
DOI 10.3389/fvets.2025.1493928

Check for updates

OPEN ACCESS

EDITED BY
Mughees Aizaz Alvi,
University of Agriculture, Faisalabad, Pakistan

REVIEWED BY
Hongchao Sun,
Zhejiang Academy of Agricultural Sciences, China
Muhammad Wasim Usmani,
Ningbo University, China

*CORRESPONDENCE
Jing Jiang
✉ jiangjingxiaoyao@163.com
He-Ting Sun
✉ xiaofengsht@163.com

†These authors have contributed equally to this work

RECEIVED 12 September 2024
ACCEPTED 24 January 2025
PUBLISHED 05 February 2025

CITATION
Liu S, Li J-H, Qin S-Y, Jiang J, Wang Z-J, Ma T, Zhu J-H, Geng H-L, Yan W-L, Xue N-Y, Tang Y and Sun H-T (2025) Existence of *Pentatrichomonas hominis* in Tibetan Antelope (*Pantholops hodgsonii*). *Front. Vet. Sci.* 12:1493928. doi: 10.3389/fvets.2025.1493928

COPYRIGHT
© 2025 Liu, Li, Qin, Jiang, Wang, Ma, Zhu, Geng, Yan, Xue, Tang and Sun. This is an open-access article distributed under the terms of the Creative Commons Attribution License (CC BY). The use, distribution or reproduction in other forums is permitted, provided the original author(s) and the copyright owner(s) are credited and that the original publication in this journal is cited, in accordance with accepted academic practice. No use, distribution or reproduction is permitted which does not comply with these terms.

Existence of *Pentatrichomonas hominis* in Tibetan Antelope (*Pantholops hodgsonii*)

Shuo Liu[1,2†], Jing-Hao Li[3†], Si-Yuan Qin[3], Jing Jiang[1*], Zhen-Jun Wang[4], Tao Ma[4], Jun-Hui Zhu[4], Hong-Li Geng[2], Wei-Lan Yan[2], Nian-Yu Xue[5], Yan Tang[6] and He-Ting Sun[3*]

[1]College of Life Sciences, Changchun Sci-Tech University, Shuangyang, Jilin, China, [2]College of Veterinary Medicine, Qingdao Agricultural University, Qingdao, Shandong, China, [3]Center of Prevention and Control Biological Disaster, State Forestry and Grassland Administration, Shenyang, Liaoning, China, [4]Key Laboratory of Zoonosis Research, Ministry of Education, College of Veterinary Medicine, Jilin University, Changchun, Jilin, China, [5]College of Veterinary Medicine, Yangzhou University, Yangzhou, Jiangsu, China, [6]College of Pharmacy, Guizhou University of Traditional Chinese Medicine, Guiyang, Guizhou, China

Introduction: *Pentatrichomonas hominis* is a conditional pathogen that parasitizes the intestines of vertebrates and has been detected in various wild animals. However, its infection rate in Tibetan antelopes has not been previously studied.

Methods: In this study, 503 fecal samples from Tibetan antelopes were analyzed to determine the prevalence and molecular characteristics of *P. hominis*.

Results: Results showed that 1.19% (6/503) of the samples tested positive, and although the prevalence was low, this finding underscores the importance of monitoring wild animals population as hosts of zoonotic pathogens. Additionally, the highest prevalence in Nima County (6.25%, 4/64), followed by Shenza County (2.44%, 2/82). No *P. hominis* was detected in samples from Shuanghu, Ruoqiang, Qiemo, and Qumarlêb Counties. Seasonally, the highest prevalence was recorded in autumn (1.42%, 6/423). Interestingly, *P. hominis* was only detected in 2020 (2%, 6/300), with no infections found in 2023 (0/50) or 2024 (0/153). Additionally, the phylogenetic analysis indicated that most islolates belonged to the CC1 genotype, with one representing a potential novel genotype.

Discussion: This is the first s to report the presence of *P. hominis* in Tibetan antelopes, revealing that Tibetan antelopes may be a potential transmitter of zoontic *P. hominis*. These findings offer new insights into its epidemiology and contribute valuable data for Tibetan antelope conservation efforts.

KEYWORDS

***Pentatrichomonas hominis*, prevalence, Tibetan antelope (*Pantholops hodgsonii*), risk factors, China**

1 Introduction

Pentatrichomonas hominis is an anaerobic, unicellular protozoan characterized by five anterior flagella and a single recurrent flagellum. It belongs to the genus *Trichomonadidae* within the phylum *Parabasalia* (1). *P. hominis* demonstrates broad host adaptability, commonly parasitizing the intestines of vertebrates, including dogs, cats, and pigs (2–4). Pathological reports have also confirmed its presence in the urinary tract of bulls (5). While *P. hominis* is typically associated with gastrointestinal disturbances in non-human primates, it is increasingly recognized as a potential pathogen in human gastrointestinal diseases (6, 7). Moreover, *P. hominis* has been linked to respiratory diseases, suggesting its involvement in a broader range of health conditions beyond gastrointestinal issues (8). These

observations imply that *P. hominis* could act as a zoonotic pathogen, rather than merely existing as a commensal organism. In recent years, extensive epidemiological research has focused on *P. hominis* in a wide range of animals, such as owls, boa constrictors, Siberian tigers, cattle, sheep, and macaques (9–13). Notably, there is a related report in huamans in northern China. However, the prevalence of *P. hominis* in Tibetan antelopes remains unexplored.

The Tibetan antelope (*Pantholops hodgsonii*) is the only species within the genus *Pantholops* of the subfamily *Antilopinae*, and it is classified as a Class I protected animal in China (14). In 2016, the International Union for Conservation of Nature (IUCN) listed the Tibetan antelope as Near Threatened (15). Tibetan antelopes are known to harbor various pathogens, such as *Brucella*, *Blastocystis*, and *Cryptosporidium*. They may serve as an intermediate host, facilitating the transmission of these pathogens from livestock to humans (16–18). Therefore, this study hypothesized that Tibetan antelope could serve as a host for *P. hominis* to promote the transmission of zoonotic diseases.

This study aimed to assess the prevalence of *P. hominis*, phylogenetic analysis, and potential risk factors in Tibetan antelopes. Nested PCR was employed to detect *P. hominis* in fecal samples collected from Tibetan antelopes across Xinjiang, Tibet, and Qinghai. This study is the first to focus on the infection and prevalence of *P. hominis* in Tibetan antelopes, and provides new evidence of *P. hominis* infection in wild animals.

2 Materials and methods

2.1 Samples collection

In September 2020 and from July 2023 to May 2024, a total of 503 fecal samples were collected from Tibetan antelopes in the Tibet Autonomous Region, Xinjiang Uygur Autonomous Region, and Qinghai Province, China (Figure 1). In the field, fresh fecal samples were randomly collected using disposable sterile gloves, immediately placed in sterile sample tubes, and stored in ice boxes. They were then transported to the laboratory under cold chain conditions and stored at −80°C.

2.2 DNA extraction and PCR amplification

For each sample, 200 mg of feces was placed in 2 mL centrifuge tubes containing 200 mg of glass beads, and 0.9% saline solution was added. The mixture was homogenized using a vortex mixer (JOANLAB, Zhejiang, China). Genomic DNA was extracted following the manufacturer's protocol using the E.Z.N.A.® Stool DNA Kit (Omega Biotek, Inc., Norcross, GA, USA). The extracted DNA was stored at −20°C until PCR analysis. This study followed the guidelines and recommendations of the Animal Welfare Committee of Qingdao Agricultural University, China. The positivity rate of *P. hominis* was

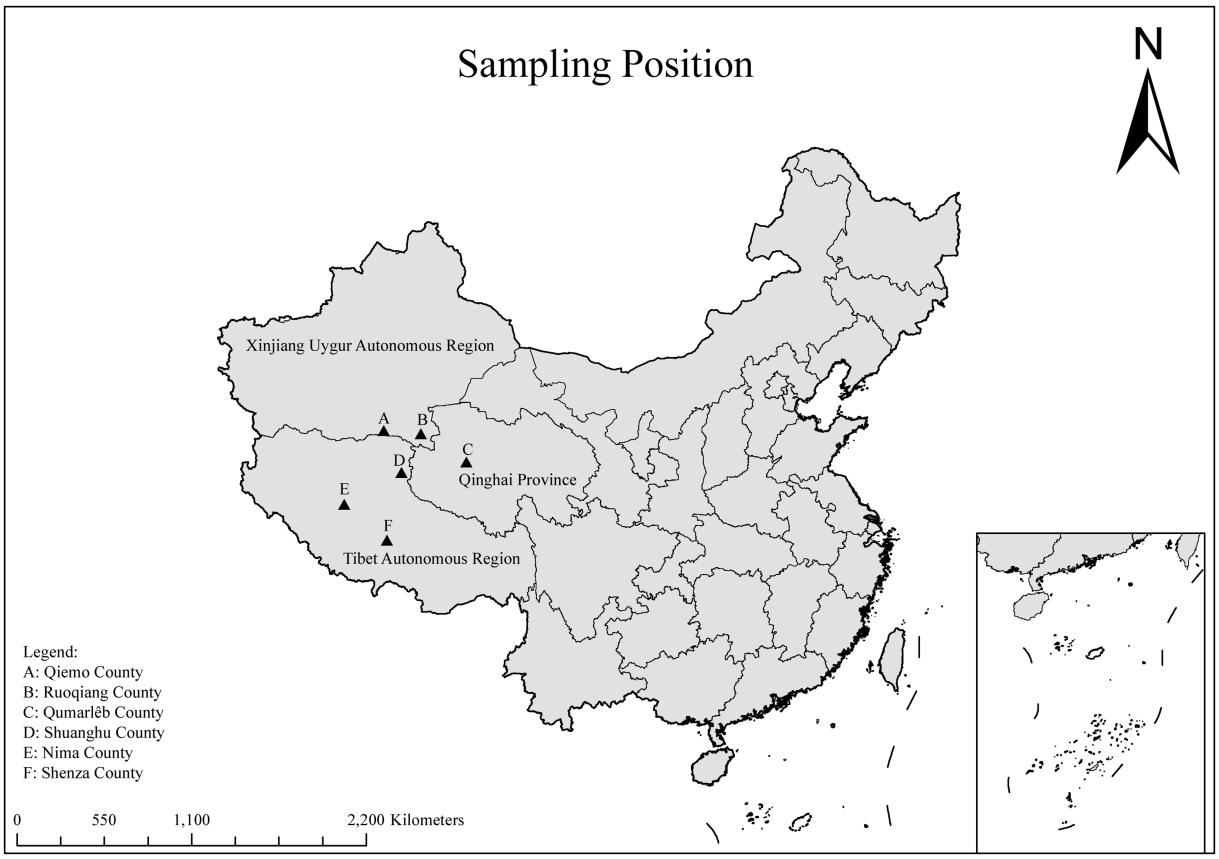

FIGURE 1
A map of the PR of China showing the sampling regions marked as triangles.

TABLE 1 Prevalence of *Pentatrichomonas hominis* infection in Tibetan antelope (*Pantholops hodgsonii*) by various factors.

Variables	Categories	No. positive/total	Positive rate % (95% CI)	Heterogeneity
				χ^2/df/I^2 (%)/p
Region	Shenza County	2/82	2.44 (0.40–7.21)	13.21/5/62.1/0.0215
	Nima County	4/64	6.25 (1.38–13.76)	
	Shuanghu County	0/204	0.00 (–)	
	Ruoqiang County	0/31	0.00 (–)	
	Qiemo County	0/30	0.00 (–)	
	Qumarlêb County	0/92	0.00 (–)	
Season	Autumn	6/423	1.42 (0.47–2.10)	0.61/2/0/0.7663
	Summer	0/30	0.00 (–)	
	Spring	0/50	0.00 (–)	
Year	2020	6/300	2.00 (0.67–3.95)	4.96/2/59.7/0.0837
	2023	0/50	0.00 (–)	
	2024	0/153	0.00 (–)	
Total		6/503	1.19 (0.44–2.56)	-

determined using nested PCR (19). In the first round of amplification, small subunit ribosomal RNA was amplified using forward primer FF (5'-GCGCCTGAGAGATAGCGACTA-3') and reverse primer RR (5'-GGACCTGTTATTGCTACCCTCTTC-3') to detect *Trichomonas* spp. A second round of amplification was performed using 2 μL of the first-round product, with forward primer HF (5'-TGTAAACG ATGCCGACAGAG-3') and reverse primer HR (5'-CAACACTGAAG CCAATGCGAGG-3') to specifically detect *P. hominis* (339 bp). Both negative and positive controls were included in each PCR. For the second-round product, 5 μL was analyzed via electrophoresis on a 1.5% agarose gel and visualized under ultraviolet light.

2.3 Sequencing and phylogenetic analysis

PCR products positive for *P. hominis* were sent to Anhui General Biotech Co., Ltd. (Anhui, China) for sequencing. The resulting contigs from bidirectional sequencing were aligned with reference sequences in GenBank using BLAST.[1] Phylogenetic trees were constructed using the neighbor-joining (NJ) method (20), with genetic distances calculated using the Kimura 2-parameter model in MEGA11 (21). The reliability of the phylogenetic trees was assessed with 1,000 bootstrap replicates. Representative nucleotide sequences were submitted to GenBank under accession numbers PQ276129-PQ276131.

2.4 Statistical analysis

The effects of sampling region ($x1$), sampling season ($x2$), and sampling year ($x3$) on the prevalence of *P. hominis* in Tibetan antelopes were analyzed using chi-square tests in the Statistical Analysis System (SAS, v9.0), with the best model selected using Fisher scoring. Logistic regression analysis was performed using Statistical Product and Service Solutions (SPSS, IBM Corp., Armonk, NY, USA), with 95% confidence intervals (95% CI) calculated. A p-value of less than 0.05 was considered statistically significant.

3 Results

3.1 Prevalence of *Pentatrichomonas hominis*

In this study, 6 out of 503 fecal samples were identified as positive for *P. hominis*, with an overall prevalence of 1.19% (6/503, 95% CI: 0.44–2.56). Nima County had the highest infection rate at 6.25% (4/64, 95% CI: 1.38–13.76), followed by Shenza County at 2.44% (2/82, 95% CI: 0.40–7.21). No *P. hominis* was detected in the remaining four counties. Seasonally, no infections were detected in spring or summer, with all positive cases found in autumn (1.42%, 6/423, 95% CI: 0.47–2.10). The prevalence of *P. hominis* was higher in 2020 (2%, 6/300, 95% CI: 0.67–3.95) compared to 2023 (0/50) and 2024 (0/153) (Table 1 and Figure 2).

3.2 Risk factors

Logistic regression analysis using the Fisher scoring method was performed to assess the influence of sampling region, season, and year on *P. hominis* prevalence. The final model did not retain any of these factors, suggesting that sampling region, season, and year had no statistically significant impact on the infection rate of *P. hominis*.

3.3 Phylogenetic analysis

Confirmed that the three representative sequences obtained in this study were all classified as *P. hominis*. Among them, sequences

1 http://www.ncbi.nlm.nih.gov/blast/

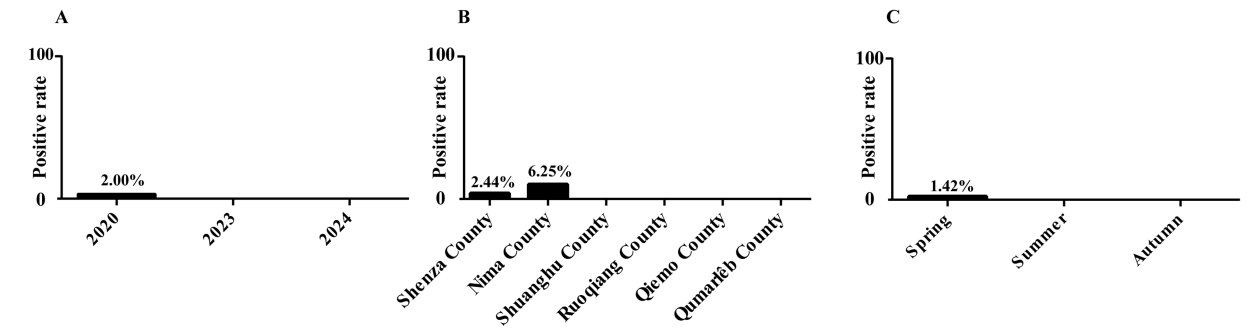

FIGURE 2
Infection rate of *P. hominis* in Tibetan antelope under various factors. **(A)** Infection rate of *P. hominis* in Tibetan antelope in different years. **(B)** Infection rate of *P. hominis* in Tibetan antelope in different regions. **(C)** Infection rate of *P. hominis* in Tibetan antelope in different seasons.

PQ276129 and PQ276130 showed 100% homology with the CC1 genotype (KJ408929). However, PQ276131 formed a distinct branch on the phylogenetic tree, indicating that this sequence may represent a novel genetic variant (Figure 3).

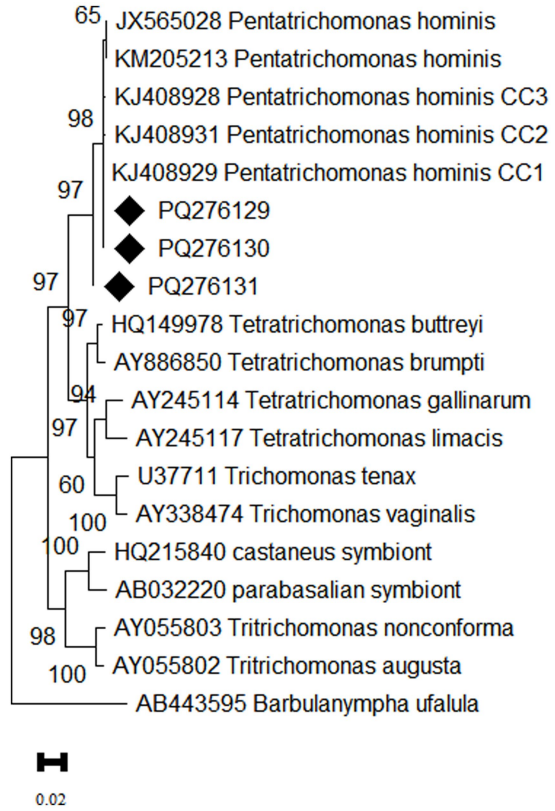

FIGURE 3
Phylogenetic tree based on the 18S rRNA gene of *P. hominis*. The phylogenetic relationship between *P. hominis* obtained in this study and other known trichomonads were inferred using the maximum likelihood analysis based on the genetic distance calculated by the Kimura 2-parameter model. Bootstrap values more than 50% are shown. The diamond shape denotes isolates from the present study.

4 Discussion

Multiple case reports have demonstrated that *P. hominis* is often isolated from patients with diarrhea, suggesting it is a likely cause of gastrointestinal symptoms (6). Furthermore, research indicates that up to 41.54% of gastrointestinal cancer patients are infected with *P. hominis*, which may imply a potential role in the development of gastrointestinal cancer in some cases (22, 23). These findings underscore the importance of not underestimating the potential dangers of *P. hominis*. There is a critical need for further research into its hosts, transmission mechanisms, pathogenicity, and specific role in gastrointestinal diseases. Such studies could lead to the development of effective prevention and treatment strategies for *P. hominis*.

In this study, *P. hominis* was detected in Tibetan antelopes with an infection rate of 1.19% (6/503). This rate is lower compared to the infection rates of *Blastocystis* (4.8%, 30/627) and *Cryptosporidium* (3.0%, 19/627) in Tibetan antelopes (17, 18). The difference may be attributed to the varying survival and transmission capabilities of these parasites in extreme environments. Although Tibetan antelopes are ruminants, their *P. hominis* infection rate is lower than that of dairy cattle (6.8%, 36/526) and beef cattle (4.6%, 15/32), indicating variability in susceptibility among species (13). Notably, the infection rates of *P. hominis* in Siberian tigers (31.3%, 41/131) and silver foxes (43.33%, 26/60) were significantly higher than that in Tibetan antelopes, suggesting that different dietary habits shape distinct gut microbiota, resulting in varying parasite susceptibility (24).

In this study, *P. hominis* was detected in Nima County (6.25%, 4/64) and Shenza County (2.44%, 2/82), while it was not found in the other four counties. Considering the small difference in altitude among the sampling sites, the influence of altitude on the parasite infection rate can be excluded. The differences in infection rates may be related to local ecological and sanitary conditions affecting parasite infection rates. Seasonally, autumn on the Qinghai-Tibet Plateau appears more conducive to *P. hominis* transmission, with an infection rate of 1.42% (6/423) observed in autumn, compared to no infections detected in summer and spring. This may relate to the migratory behavior of Tibetan antelopes, which migrate from April to June and return between August and September (25). Studies suggest that migration not only helps Tibetan antelopes evade predators but may also be a strategy to avoid parasites, thus reducing infection risk in offspring and potentially aiding population growth (26). In conclusion, although no significant effects of seasonal and regional variations on infection rates were observed in this study, the

observed trends warrant further investigation with larger sample sizes.

Interestingly, *P. hominis* prevalence was 2% (6/300) in 2020, with no infections detected in 2023 (0/50) and 2024 (0/153). This fluctuation may be linked to global warming, which can alter precipitation patterns and humidity, affecting parasite survival (27). Additionally, changes in vegetation may lead Tibetan antelopes to modify their migration routes and habitats, influencing *P. hominis* infection rates (28). However, the geographical scope of this study is limited, and the sample size is small in some years. Future studies can combine annual sampling with wider geographical coverage and larger sample size to verify this conjecture.

Epidemiological studies have shown that the CC1 genotype was first found in dogs from Changchun, later wildly distribute in *P. hominis* infection in dogs across eastern China. It has also been detected in Siberian tigers, foxes in Henan Province, and primates, including humans in north China, highlighting the strong cross-host transmission ability and potential zoonotic nature of this genotype (1, 7, 10). In this study, two representative *P. hominis* sequences from Tibetan antelopes belonged to the CC1 genotype, indicating that this genotype is the predominant one in Tibetan antelopes, further suggesting that Tibetan antelopes may serve as a potential source of infection of *P. hominis* in humans. Notably, PQ276131 exhibited genetic differences from the CC1, CC2, and CC3 genotypes, indicating that it may represent a novel genotype of *P. hominis*. The newly discovered genotype in Tibetan antelopes may represent a unique adaptation to high-altitude environments, warranting further genetic studies to gain deeper insights into its adaptation mechanisms.

Tibetan antelopes infected with *P. hominis* can easily disperse trophozoites into the environment (29). Given the lifestyle of pastoralists in the Tibetan region, there is a heightened risk of contact with contaminated water or food, increasing the risk of infection. This not only threatens the local ecosystem but also poses potential health risks to residents. Effective measures are needed to monitor and reduce environmental contamination by *P. hominis* and its impact on human health.

5 Conclusion

This study is the first to report *P. hominis* infection in Tibetan antelopes. Despite the low prevalence, which may be influenced by sampling and detection methods, it indicates that Tibetan antelopes could be potential vectors of CC1 genotype. This finding provides important data for understanding the epidemiology of *P. hominis* and suggests that Tibetan antelopes should be considered in studies and monitoring of zoonoses in Tibetan areas. Addtionally, this study recommends including other wild animals and livestock in the Tibetan region in the scope of investigation and emphasizes the importance of incorporating *P. hominis* into public health surveillance programs in areas with high human-wildlife interaction.

Data availability statement

The datasets presented in this study can be found in online repositories. The names of the repository/repositories and accession number(s) can be found in the article/supplementary material.

Ethics statement

The animal study was approved by the Research Ethics Committee for the Care and Use of Laboratory Animals in Qingdao Agricultural University, China. The study was conducted in accordance with the local legislation and institutional requirements.

Author contributions

SL: Methodology, Software, Writing – original draft. J-HL: Conceptualization, Resources, Writing – review & editing. S-YQ: Resources, Writing – review & editing. JJ: Conceptualization, Writing – review & editing. Z-JW: Resources, Writing – review & editing. TM: Resources, Writing – review & editing. J-HZ: Resources, Writing – review & editing. H-LG: Methodology, Writing – review & editing. W-LY: Methodology, Writing – review & editing. N-YX: Data curation, Writing – review & editing. YT: Data curation, Writing – review & editing. H-TS: Conceptualization, Funding acquisition, Resources, Writing – review & editing.

Funding

The author(s) declare that financial support was received for the research, authorship, and/or publication of this article. This work was supported by National Key Research and Development Program of China (2021YFC2300903).

Acknowledgments

We would like to extend our deepest gratitude to Chair Professor Hany Elsheikha, from University of Nottingham, for his invaluable assistance in revising and improving our manuscript. His insightful feedback, expert advice, and meticulous attention to detail have significantly enhanced the quality of our work.

Conflict of interest

The authors declare that the research was conducted in the absence of any commercial or financial relationships that could be construed as a potential conflict of interest.

Publisher's note

All claims expressed in this article are solely those of the authors and do not necessarily represent those of their affiliated organizations, or those of the publisher, the editors and the reviewers. Any product that may be evaluated in this article, or claim that may be made by its manufacturer, is not guaranteed or endorsed by the publisher.

References

1. Song P, Guo Y, Zuo S, Li L, Liu F, Zhang T, et al. Prevalence of *Pentatrichomonas hominis* in foxes and raccoon dogs and changes in the gut microbiota of infected female foxes in the Hebei and Henan provinces in China. *Parasitol Res*. (2023) 123:74. doi: 10.1007/s00436-023-08099-5

2. Li WC, Wang K, Zhang W, Wu J, Gu YF, Zhang XC. Prevalence and molecular characterization of intestinal *Trichomonads* in pet dogs in East China. *Korean J Parasitol*. (2016) 54:703–10. doi: 10.3347/kjp.2016.54.6.703

3. Itoh N, Iijima Y, Ogura I, Yonekura N, Kameshima S, Kimura Y. Molecular prevalence of *Trichomonad* species from pet shop puppies and kittens in Japan. *Rev Bras Parasitol Vet*. (2020) 29:e014820. doi: 10.1590/S1984-29612020098

4. Li WC, Wang K, Li Y, Zhao LP, Xiao Y, Gu YF. Survey and molecular characterization of *Trichomonads* in pigs in Anhui Province, East China, 2014. *Iran J Parasitol*. (2018) 4:602–10.

5. Silva ORE, Ribeiro L, Jesus VLT, McIntosh D, Silenciato LN, Ferreira JE, et al. Identification of *Pentatrichomonas hominis* in preputial washes of bulls in Brazil. *Rev Bras Parasitol Vet*. (2022) 31:e005322. doi: 10.1590/S1984-29612022034

6. Abdo Mohamed S, Ibrahim Ghallab MM, Elhawary Mohammed N, Elhadad H. *Pentatrichomonas hominis* and other intestinal parasites in school-aged children: coproscopic survey. *J Parasit Dis*. (2022) 46:896–900. doi: 10.1007/s12639-022-01506-1

7. Li WC, Ying M, Gong PT, Li JH, Yang J, Li H, et al. *Pentatrichomonas hominis*: prevalence and molecular characterization in humans, dogs, and monkeys in northern China. *Parasitol Res*. (2016) 115:569–74. doi: 10.1007/s00436-015-4773-8

8. Mantini C, Souppart L, Noel C, Duong TH, Mornet M, Carroger G, et al. Molecular characterization of a new *Tetratrichomonas* species in a patient with empyema. *J Clin Microbiol*. (2009) 47:2336–9. doi: 10.1128/JCM.00353-09

9. Dimasuay KG, Rivera WL. Molecular characterization of *Trichomonads* isolated from animal hosts in the Philippines. *Vet Parasitol*. (2013) 196:289–95. doi: 10.1016/j.vetpar.2013.03.019

10. Zhang H, Zhang N, Gong P, Cheng S, Wang X, Li X, et al. Prevalence and molecular characterization of *Pentatrichomonas hominis* in Siberian tigers (*Panthera tigris altaica*) in Northeast China. *Integr Zool*. (2022) 17:543–9. doi: 10.1111/1749-4877.12629

11. Dib LV, Barbosa ADS, Correa LL, Torres BDS, Pissinatti A, Moreira SB, et al. Morphological and molecular characterization of parabasilids isolated from ex-situ nonhuman primates and their keepers at different institutions in Brazil. *Int J Parasitol Parasites Wildl*. (2024) 24:100946. doi: 10.1016/j.ijppaw.2024.100946

12. Li WC, Wang K, Gu Y. Occurrence of *Blastocystis sp.* and *Pentatrichomonas hominis* in sheep and goats in China. *Parasit Vectors*. (2018) 11:93. doi: 10.1186/s13071-018-2671-5

13. Li WC, Huang JM, Fang Z, Ren Q, Tang L, Kan ZZ, et al. Prevalence of *Tetratrichomonas buttreyi* and *Pentatrichomonas hominis* in yellow cattle, dairy cattle, and water buffalo in China. *Parasitol Res*. (2020) 119:637–47. doi: 10.1007/s00436-019-06550-0

14. Song X, Shen W, Wan H, Hou P, Lin G. Dynamic monitoring of Tibetan antelope habitat suitability in the Hoh Xil nature reserve using remote sensing images. *Res Sci*. (2016) 38:17–23. doi: 10.18402/resci.2016.08.03

15. International Union for Conservation of Nature and Natural Resources. The IUCN red list of threatened species. Gland, Switzerland: International Union for Conservation of Nature and Natural Resources (2016).

16. Wu JY, Li JJ, Wang DF, Wei YR, Meng XX, Tuerxun G, et al. Seroprevalence of five zoonotic pathogens in wild ruminants in Xinjiang, Northwest China. *Vector Borne Zoonotic Dis*. (2020) 20:882–7. doi: 10.1089/vbz.2020.2630

17. Qin SY, Sun HT, Lyu C, Zhu JH, Wang ZJ, Ma T, et al. Prevalence and characterization of *Cryptosporidium* species in Tibetan Antelope (*Pantholops hodgsonii*). *Front Cell Infect Microbiol*. (2021) 11:713873. doi: 10.3389/fcimb.2021.713873

18. Geng HL, Sun YZ, Jiang J, Sun HT, Li YG, Qin SY, et al. The presence of *Blastocystis* in Tibetan Antelope (*Pantholops hodgsonii*). *Front Cell Infect Microbiol*. (2021) 11:747952. doi: 10.3389/fcimb.2021.747952

19. Wang ZR, Fan QX, Wang JL, Zhang S, Wang YX, Zhang ZD, et al. Molecular identification and survey of *Trichomonad* species in pigs in Shanxi Province, North China. *Vet Sci*. (2024) 11:203. doi: 10.3390/vetsci11050203

20. Saitou NNM. The neighbor-joining method: a new method for reconstructing phylogenetic trees. *Mol Biol Evol*. (1987) 4:406–25.

21. Tamura K, Stecher G, Kumar S. MEGA11: molecular evolutionary genetics analysis version 11. *Mol Biol Evol*. (2021) 38:3022–7. doi: 10.1093/molbev/msab120

22. Zhang N, Zhang H, Yu Y, Gong P, Li J, Li Z, et al. High prevalence of *Pentatrichomonas hominis* infection in gastrointestinal cancer patients. *Parasit Vectors*. (2019) 12:423. doi: 10.1186/s13071-019-3684-4

23. Zhang H, Yu Y, Li J, Gong P, Wang X, Li X, et al. Changes of gut microbiota in colorectal cancer patients with *Pentatrichomonas hominis* infection. *Front Cell Infect Microbiol*. (2022) 12:961974. doi: 10.3389/fcimb.2022.961974

24. Li X, Li J, Zhang X, Yang Z, Yang J, Gong P. Prevalence of *Pentatrichomonas hominis* infections in six farmed wildlife species in Jilin, China. *Vet Parasitol*. (2017) 244:160–3. doi: 10.1016/j.vetpar.2017.07.032

25. Buho H, Jiang Z, Liu C, Yoshida T, Mahamut H, Kaneko M, et al. Preliminary study on migration pattern of the Tibetan Antelope (*Pantholops hodgsonii*) based on satellite tracking. *Adv Space Res*. (2011) 48:43–8. doi: 10.1016/j.asr.2011.02.015

26. Cao Y, Foggin M, Zhao X. Tibetan Antelope migration during mass calving as parasite avoidance strategy. *Innovations*. (2022) 3:100326. doi: 10.1016/j.xinn.2022.100326

27. Wood CL, Welicky RL, Preisser WC, Leslie KL, Mastick N, Greene C, et al. A reconstruction of parasite burden reveals one century of climate-associated parasite decline. *Proc Natl Acad Sci USA*. (2023) 120:e2211903120. doi: 10.1073/pnas.2211903120

28. Shi F, Liu S, An Y, Sun Y, Zhao S, Liu Y, et al. Climatic factors and human disturbance influence ungulate species distribution on the Qinghai-Tibet plateau. *Sci Total Environ*. (2023) 869:161681. doi: 10.1016/j.scitotenv.2023.161681

29. Mahittikorn A, Udonsom R, Koompapong K, Chiabchalard R, Sutthikornchai C, Sreepian PM, et al. Molecular identification of *Pentatrichomonas hominis* in animals in central and western Thailand. *BMC Vet Res*. (2021) 17:203. doi: 10.1186/s12917-021-02904-y

frontiers | Frontiers in Veterinary Science

TYPE Original Research
PUBLISHED 19 February 2025
DOI 10.3389/fvets.2025.1514525

Check for updates

OPEN ACCESS

EDITED BY
Mughees Aizaz Alvi,
University of Agriculture, Faisalabad, Pakistan

REVIEWED BY
Zi-Guo Yuan,
South China Agricultural University, China
Zorica D. Dakić,
University of Belgrade, Serbia
Muhammad Zulqarnain Shakir,
Ningbo University, China

*CORRESPONDENCE
Jing Jiang
jiangjingxiaoyao@163.com
Jian-Xin Wen
wenjianxin@126.com

†These authors have contributed equally to this work

RECEIVED 21 October 2024
ACCEPTED 03 February 2025
PUBLISHED 19 February 2025

CITATION
Liu S, Zhang M, Xue N-Y, Wang H-T, Li Z-Y, Qin Y, Li X-M, Hou Q-Y, Jiang J, Yang X, Ni H-B and Wen J-X (2025) Prevalence and assemblage distribution of *Giardia intestinalis* in farmed mink, foxes, and raccoon dogs in northern China.
Front. Vet. Sci. 12:1514525.
doi: 10.3389/fvets.2025.1514525

COPYRIGHT
© 2025 Liu, Zhang, Xue, Wang, Li, Qin, Li, Hou, Jiang, Yang, Ni and Wen. This is an open-access article distributed under the terms of the Creative Commons Attribution License (CC BY). The use, distribution or reproduction in other forums is permitted, provided the original author(s) and the copyright owner(s) are credited and that the original publication in this journal is cited, in accordance with accepted academic practice. No use, distribution or reproduction is permitted which does not comply with these terms.

Prevalence and assemblage distribution of *Giardia intestinalis* in farmed mink, foxes, and raccoon dogs in northern China

Shuo Liu[1†], Miao Zhang[1†], Nian-Yu Xue[2,3], Hai-Tao Wang[1], Zhong-Yuan Li[4], Ya Qin[5], Xue-Min Li[1], Qing-Yu Hou[1], Jing Jiang[2*], Xing Yang[6], Hong-Bo Ni[1] and Jian-Xin Wen[1*]

[1]College of Veterinary Medicine, Qingdao Agricultural University, Qingdao, China, [2]College of Life Sciences, Changchun Sci-Tech University, Shuangyang, China, [3]College of Veterinary Medicine, Yangzhou University, Yangzhou, China, [4]Guangxi Key Laboratory of Brain and Cognitive Neuroscience, College of Basic Medicine, Guilin Medical University, The Guangxi Zhuang Autonomous Region, Guilin, China, [5]College of Animal Science and Technology, Jilin Agricultural University, Changchun, China, [6]Department of Medical Microbiology and Immunology, School of Basic Medicine, Dali University, Dali, China

Giardia intestinalis is a widespread protozoan parasite associated with significant health risks in humans and animals. However, there is a lack of epidemiological data regarding this parasite in fur-animals. The present study aimed to investigate the prevalence and assemblage distribution of *G. intestinalis* in fur-animals in northern China. A total of 871 fecal samples were detected by nested PCR. The results showed an overall infection rate of 1.15%, with the highest rate in Hebei province (2.28%), while no positive cases were observed in Jilin and Heilongjiang provinces. Although no significant differences were found in species group, raccoon dogs (1.72%) were more susceptible to infection than mink (1.40%) and foxes (0.57%). Additionally, the highest infection rate was observed in farms with fewer than 2,000 animals (1.41%), followed by farms with ≥5,000 (0.93%) and those with 2,000–5,000 animals (0.75%). The infection rate was higher in juvenile animals (1.35%) compared to adults (1.08%), and in non-diarrheal animals (1.16%) compared to diarrheal animals (1.08%). Notably, this study is the first to report assemblage A in mink, this finding highlight the potential role of mink as a reservoir for zoonotic transmission. Assemblage D was detected in foxes and raccoon dogs, further suggesting that these animals may serve as potential zoonotic reservoirs. These findings not only complements the epidemiological data of *G. intestinalis* in fur-animals but also emphasize the importance of monitoring the fur industry to mitigate public health risks.

KEYWORDS

prevalence, *Giardia intestinalis*, assemblage, mink, raccoon dog

1 Introduction

Giardia intestinalis (Syn. *G. duodenalis* or *G. lamblia*) is a flagellated protozoan parasite that widely infects the intestines of humans and various animals (1). It spreads through direct and indirect contact (via food and water) (2). Globally, *G. intestinalis* is one of the leading pathogens responsible for parasitic-related diarrhea, with infection rates strongly correlated with regional sanitation conditions. The prevalence in developed countries is significantly lower than in developing countries (3). The World Health Organization (WHO) estimated that approximately 280 million people are infected with this parasite annually, resulting in acute

diarrhea (4). Additionally, individuals infected with *G. intestinalis* may face long-term health risks, including irritable bowel syndrome, childhood malnutrition, and arthritis (5–7). Furthermore, the rise of cross-border animal trade complicates public health control efforts, blurring the lines of parasite transmission and increasing the urgency for effective global surveillance and management strategies.

Molecular biology techniques have been widely applied in the study of *G. intestinalis*. Common methods include small subunit ribosomal RNA (*SSU* rRNA) analysis and multilocus genotyping (*gdh*, *tpi*, and *bg* genes) (8). Through molecular analysis, *G. intestinalis* has been divided into eight assemblages (A–H) (9). Among these, assemblages A and B exhibit strong cross-host transmission capabilities, infecting diverse hosts, including humans, and are typical zoonotic pathogens (10–12). In contrast, assemblages C–H show distinct host specificity. Studies have shown that assemblages C and D primarily infect canines (10, 13), assemblage E mainly infects ungulates such as cattle and sheep (14, 15), assemblages F and H have been detected in marine animals (16, 17), assemblage G was specifically found in rodents (15, 18).

Interestingly, despite assemblages C and D typically being considered exclusive to canines, research has shown some exceptions. Assemblage D was detected in a German traveller, and a study in Egypt identified assemblage C as a zoonotic pathogen (19, 20). These findings suggest that the host range of *G. intestinalis* may be broader than previously known. Therefore, expanding our understanding of its host adaptability is crucial for effective disease control and prevention strategies.

The fur animal farming industry in northern China is large-scale and is one of the pillars of the local economy. However, with the development of large-scale farming, disease prevention and control face significant challenges. Research has shown that fur animals can be infected with various parasites, including *Pentatrichomonas hominis*, *Sarcocystis* spp., and *Trichinella spiralis* (21–23), indicating that fur animals may be potential hosts for zoonotic pathogens. However, reports on the infection of fur animals (mink, foxes, and raccoon dogs) with *G. intestinalis* are scarce globally. This study employs *tpi*, *gdh*, and *bg* gene analysis to test samples from mink, foxes, and raccoon dogs, aiming to investigate the infection rates of *G. intestinalis* and the diversity and distribution of assemblage in these animals as well as to assess the implications for public health and disease prevention in the farming industry.

2 Materials and methods

2.1 Sample collection

From October 2023 to May 2024, 871 fresh fecal samples were randomly collected from farmed fur animals in main fur farming provinces of China (Shandong, Hebei, Jilin, Liaoning, and Heilongjiang). The samples included mink (n = 286), foxes (n = 352), and raccoon dogs (n = 233) (Figure 1). All animals are self-breed and kept in cages, foxes and raccoon dogs are breed in individual cages, while minks are breed in group cages with three to five animals. No direct contact with animals, fresh feces were collected immediately from beneath the cages using disposable PE gloves when the animal excreted feces. Detailed records of sample's source animal, sample ID, sampling position, date, animal age, health status, species, and farm

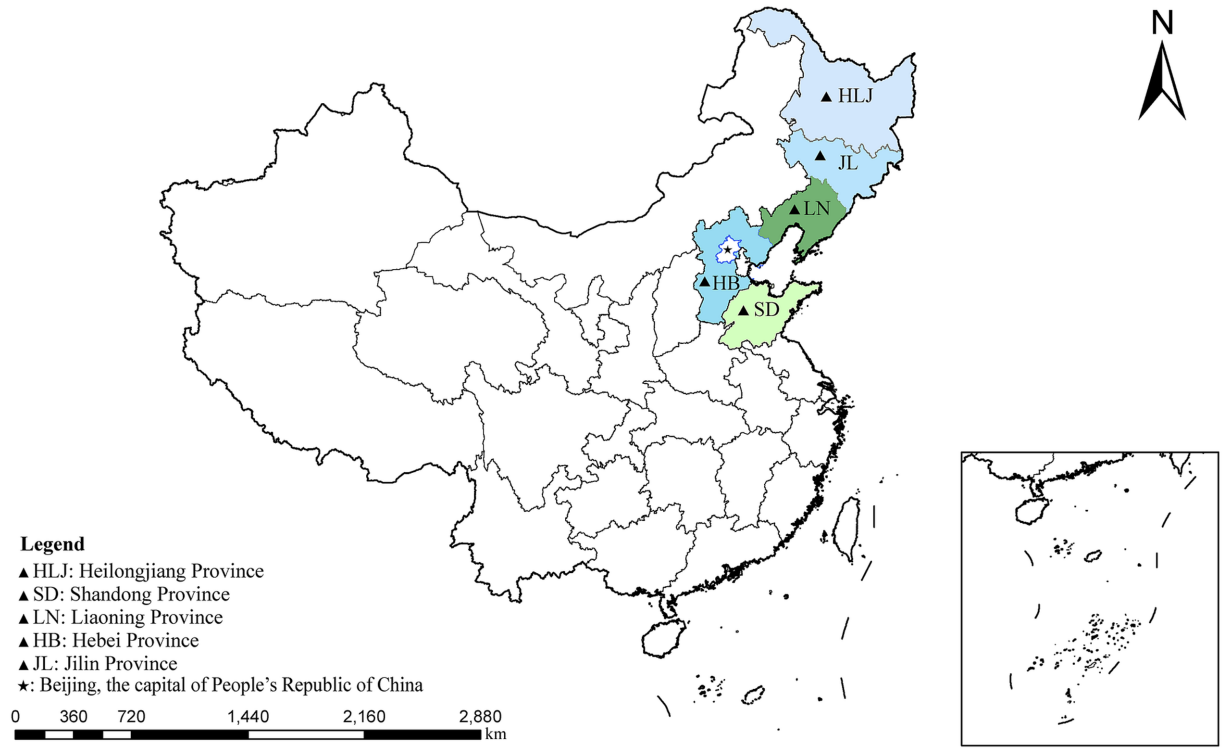

FIGURE 1
A map of the People's Republic of China showing the sampling regions marked as triangles.

size. To maintain sample integrity, samples were stored in 12 mL collection tubes, transported to the laboratory on dry ice, and preserved at −80°C.

2.2 DNA extraction and PCR amplification

According to the manufacturer's instructions, genomic DNA was extracted from each sample using the E.Z.N.A.® Stool DNA Kit (Omega Biotek, Norcross, GA, United States) and stored at −20°C until PCR analysis. First, the β-giardin (*bg*) gene was amplified using nested PCR to confirm the presence of *G. intestinalis* in the samples. Subsequently, the positive samples were subjected to amplification of the glutamate dehydrogenase (*gdh*) and triosephosphate isomerase (*tpi*) genes (24–26). The first round was performed with a 25 μL reaction mixture containing 12.5 μL of premix enzyme (dNTPs, DNA polymerase, buffer and Mg^{2+}), 8.5 μL of ddH_2O, 1 μL of forward primer, 1 μL of reverse primer, and 2 μL of template DNA. In the second round, 2 μL of the first-round product was mixed with 25 μL of premix enzyme, 21 μL of ddH_2O, 1 μL of forward primer, and 1 μL of reverse primer, in a total volume of 50 μL. Then, 5 μL of the product was tested using 1% agarose gel electrophoresis. Positive PCR products were sequenced by Anhui General Biosystems Co., Ltd. (Anhui China) using Sanger sequencing.

2.3 Sequence and phylogenetic analysis

The sequences of the *bg* and *gdh* genes were obtained from Anhui General Corporation. BLAST[1] was used to align these sequences with the corresponding *bg*, and *gdh* reference sequences in GenBank. Phylogenetic trees were constructed using the neighbour-joining (NJ) method in MEGA11 software[2] to study the relationships between different isolates and to illustrate the genetic diversity of *G. intestinalis* (27). The reliability of the phylogenetic analysis was evaluated through 1,000 bootstrap replicates.

2.4 Statistical analysis

Chi-square analysis in SAS (v9.0) software was used to evaluate the impact of sampling region ($x1$), species ($x2$), farming scale ($x3$), health status ($x4$), and age ($x5$) on the infection rate of *G. intestinalis* (y). In the multivariable regression analysis, each variable was individually included in the binary logistic model. The best model was selected using the Fisher scoring method. In the Statistical Product and Service Solutions (SPSS, IBM Corp., Armonk, NY, United States) software, chi-square tests were performed to explore the differences in the prevalence of *G. intestinalis* across various study factors while calculating the odds ratio (OR) and 95% confidence interval (95% CI). A p-value of less than 0.05 was considered statistically significant.

1 https://blast.ncbi.nlm.nih.gov/

2 http://www.megasoftware.net/

3 Results

3.1 Prevalence of *Giardia intestinalis* in mink, raccoon dogs, and foxes across the five provinces

In the present study, 10 (1.15%) positive cases of *G. intestinalis* were detected through nested PCR from 871 fecal samples. The differences in infection rates among provinces were not statistically significant ($\chi^2 = 5.88$, df = 4, $p = 0.2082$). Hebei province had the highest infection rate (2.28%, 7/307, OR = 2.86 95% CI 0.59–13.88), followed by Shandong province (0.88%, 1/113, OR = 1.09 95% CI 0.10–12.19) and Liaoning province (0.81%, 2/247), while no positive cases were observed in Jilin and Heilongjiang provinces (Table 1 and Figure 2A). Similarly, the differences in infection rates between species were not statistically significant ($\chi^2 = 2$, df = 2, $p = 0.3680$). Raccoon dogs had the highest infection rate (1.72%, 4/233, OR = 3.06 95% CI 0.56–16.83), followed by mink (1.40%, 4/286, OR = 2.48 95% CI 0.45–13.65) and foxes (0.57%, 2/352) (Table 1 and Figure 2B).

There was no statistically significant difference in the farm size group ($\chi^2 = 0.49$, df = 2, $p = 0.7837$), with the lowest infection rate was observed in farms with 2,000 to 5,000 animals (0.75%, 2/266), the highest infection rate was found in farms with fewer than 2,000 animals (1.41%, 7/498, OR = 1.88 95% CI 0.39–9.12), and the infection rate of farms with more than 5,000 was 0.94% (1/107, OR = 1.25 95% CI 0.11–13.88). Additionally, the infection rate in adult animals (1.08%, 7/649) was slightly lower than in juvenile animals (1.35%, 3/222, OR = 1.26 95% CI 0.32–4.90), the difference was not statistically significant ($\chi^2 = 0.21$, df = 1, $p = 0.6481$). The infection rate in non-diarrheal animals (1.16%, 9/778 OR = 1.08 95% CI 0.14–8.60) was slightly higher than in diarrheal animals (1.08%, 1/93), and the statistical difference was not significant ($\chi^2 = 0.07$, df = 1, $p = 0.7947$) (Table 1).

3.2 Influencing factors

The present study evaluated the influencing factors affecting the infection rate of *G. intestinalis* using logistic forward stepwise regression analysis. The final best model included sampling region and health status. The model equation is $y = -7.2133x1 + 0.8197x2 + 3.8666$.

The results show that the sampling area negatively affects the infection rate of *G. intestinalis* (OR = 0.74, 95% CI 0.09–1.81). Hebei had the highest infection rate (OR = 2.86, 95% CI 0.59–13.88), followed by Shandong (OR = 1.09, 95% CI 0.10–12.19) and Liaoning (0.81%, 2/247). No infections were observed in Jilin (OR = 0.67, 95% CI 0.03–14.07) and Heilongjiang (OR = 0.37, 95% CI 0.02–7.84). Health status positively influences infection (OR = 0.98, 95% CI 0.36–1.82), and the infection rate in diarrheal animals (1.08%, 1/93) was lower than in non-diarrheal animals (OR = 1.08, 95% CI 0.14–8.60) (Table 1).

3.3 Assemblage of *Giardia intestinalis* determined through *bg* and *gdh* sequence analysis

The present study conducted nested PCR detection on 871 fecal samples, identifying 10 positive samples for the *bg* gene and

TABLE 1 Prevalence of *G. intestinalis* determined by sequence analysis of the *bg* gene.

Variables	Categories	No. positive / No. test	% (95% CI)	Heterogeneity	OR (95% CI)
				χ^2/df/I^2(%)/*p*	
Region	Liaoning province	2/247	0.81 (0.01–2.42)	5.88/4/32/0.2082	Reference
	Shandong province	1/113	0.88 (0.00–3.76)		1.09 (0.10–12.19)
	Hebei province	7/307	2.28 (0.86–4.30)		2.86 (0.59–13.88)
	Jilin province	0/73	0.00 (—)		—
	Heilongjiang province	0/131	0.00 (—)		—
Species	Fox	2/352	0.57 (0.01–1.70)	2.00/2/0/0.3680	Reference
	Raccoon dog	4/233	1.72 (0.37–3.87)		3.06 (0.56–16.83)
	Mink	4/286	1.40 (0.30–3.16)		2.48 (0.45–13.65)
Farm size	2,000–5,000	2/266	0.75 (0.01–2.25)	0.49/2/0/0.7837	Reference
	<2,000	7/498	1.41 (0.53–2.66)		1.88 (0.39–9.12)
	≥5,000	1/107	0.93 (0.00–3.97)		1.25 (0.11–13.88)
Age	Adult	7/649	1.08 (0.40–2.04)	0.21/1/0/0.6481	Reference
	Juvenile	3/222	1.35 (0.17–3.40)		1.26 (0.32–4.90)
Condition	Diarrheal	1/93	1.08 (0.00–4.56)	0.07/1/0/0.7947	Reference
	Non-diarrheal	9/778	1.16 (0.51–2.05)		1.08 (0.14–8.60)
Total	—	10/871	1.15 (0.55–2.10)	—	—

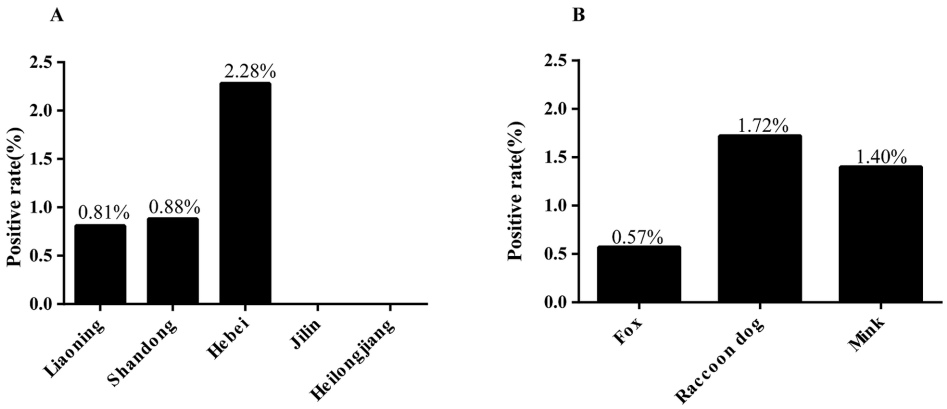

FIGURE 2
Infection rate of *G. intestinalis* in fur-animals under various factors. **(A)** Infection rate of *G. intestinalis* in fur-animals in different provinces. **(B)** Infection rate of *G. intestinalis* in different species.

obtaining six assembled sequences. Among these, three samples from mink belonged to assemblage A. Additionally, one sample from foxes and two from raccoon dogs were classified as assemblage D (Table 2).

We further tested the *bg* gene-positive samples to amplify the *gdh* gene, successfully obtaining six *gdh* sequences. Analysis of the *gdh* gene sequences showed that three mink samples belonged to assemblage A as well as two fox samples and one raccoon dog sample belonged to assemblage D. Meanwhile, we detected the *tpi* gene, but failed to obtain any sequences (Table 2).

Based on the phylogenetic analysis of the *bg* gene, the results indicated that sequences PQ416602–PQ416604 primarily cluster in the branch of assemblage A. PQ416604 is grouped with MK720260 (Calf) in the same branch, forming a sister group with PQ416602, PQ416603, and GQ329671 (Human). Meanwhile, sequences PQ416605–PQ416607 cluster with LC437444 (Canis) in the branch of assemblage D, demonstrating a high degree of phylogenetic relationship (Figure 3).

The phylogenetic analysis of the *gdh* gene shows that PQ416608–PQ416610 cluster in the branch of assemblage A and group together with EF507670 (Human) and EF507657 (Human), exhibiting a 100% bootstrap support value, indicating a high degree of phylogenetic relationship with human-derived *Giardia*. On the other hand, sequences PQ416611–PQ416613 mainly cluster in the branch of assemblage D, where they group with LC437399 (Canis), EF507619 (Dog), and KR855632 (Dog), indicating a close genetic similarity with the *Giardia* assemblages of canine hosts (Figure 4).

10.3389/fvets.2025.1514525

TABLE 2 Prevalence and assemblage distribution of *G. intestinalis*.

Variables	Categories	No. positive/No. test (%)	Assemblage of *G. intestinalis* (*n*)	
			bg	*gdh*
Region	Liaoning province	2/247 (0.81%)	0	0
	Shandong province	1/113 (0.88%)	0	D (1)
	Hebei province	7/307 (2.28%)	A (3); D (3)	A (3); D (2)
	Jilin province	0/73 (0%)	0	0
	Heilongjiang province	0/131 (0%)	0	0
Species	Fox	2/352 (0.57%)	D (1)	D (2)
	Raccoon dog	4/233 (1.72%)	D (2)	D (1)
	Mink	4/286 (1.40%)	A (3)	A (3)
Raising scale	2,000–5,000	2/266 (0.75%)	D (1)	D (1)
	<2,000	7/498 (1.41%)	A (3); D (2)	A (3); D (2)
	≥5,000	1/107 (0.93%)	0	0
Age	Adult	7/649 (1.08%)	A (3); D (2)	A (3); D (2)
	Juvenile	3/222 (1.35%)	D (1)	D (1)
Condition	Diarrheal	1/93 (1.08%)	0	0
	Non-diarrheal	9/778 (1.16%)	A (3); D (3)	A (3); D (3)
Total	—	10/871 (1.15%)	A (3); D (3)	A (3); D (3)

4 Discussion

Foodborne zoonotic diseases are a significant global public health issue, especially in regions with frequent agricultural and livestock activities. These diseases not only threaten animal health but also pose potential risks to human health, particularly when the sources of transmission are complex (28). *G. intestinalis*, a typical foodborne zoonotic pathogen, has been confirmed to transmit between humans and various animals, and it poses a severe threat to immunocompromised individuals (29). Therefore, studying the epidemiological characteristics of this parasite is of utmost importance. In this study, we tested farmed fur-animals in northern China, and the overall prevalence of *G. intestinalis* in fur-animals was 1.15% (10/871), which was lower than other animal populations in China, such as cattle in Shanxi province (28.3%, 243/858), dogs in Liaoning province (13.2%, 27/205), black bears in Heilongjiang province (8.3%, 3/36), and donkeys in Jilin, Lioning, and Shandong provinces (15.5%, 28/181) (13, 30–33). The difference may be related to species differences, sample size and living habits. Interestingly, in this study, animals showed different susceptibilities to the disease, raccoon dogs had the highest infection rate (1.72%, 4/233), followed by mink (1.40%, 4/286) and foxes (0.57%, 2/352). although, no significant differences were found among them, which may be related to the small sample size. Future studies could increase the sample size and further investigate the infection mechanisms of *G. intestinalis* to difference species.

In the present study, the sampling region negatively affected the infection rates of *G. intestinalis*. The highest infection rate was observed in Hebei province (2.28%, 7/307), followed by Shandong province (0.88%, 1/113) and Liaoning province (0.81%, 2/247). Notably, no positive cases were detected in Jilin (0/73) and Heilongjiang (0/131) provinces, suggesting a lower risk of infection in these regions. However, a report showed that the infection rate of *G. intestinalis* in diarrhea patients in Heilongjiang was 5.81%, which indicated that the epidemic prevention and control situation was still not optimistic (31). Future studies should aim to expand both the sample size and the range of animal testing. Furthermore, the present study also found that the health status of animals was an important influencing factor affecting the infection rate of *G. intestinalis*. The infection rate in non-diarrheal animals was 1.16% (9/778) higher than the 1.08% (1/93) observed in diarrheal animals. This contrasts with findings in cattle in Shanxi province and children in Zhejiang province (30, 34). This difference may be related to the stages of *G. intestinalis* infection and the pathogenic mechanisms that cause diarrhea. Additionally, the host's age, immune status, and co-infections with other pathogens may also influence the clinical manifestations and transmission patterns of *G. intestinalis* infection.

In this study, no significant differences in infection rates were observed between farms with different farming sizes. Notably, the infection rate of farms with less than 2,000 animals (1.41%, 7/498) was higher than that of farms with 2,000–5,000 animals (0.75%, 2/266) and ≥5,000 animals (0.93%, 1/107). These small-scale farms are usually family-run, and the technical level of feeding management, disease prevention and control is relatively low. Additionally, some farms have the phenomenon of raising dogs together, which may be a factor leading to the high infection rate.

Researchers have classified *G. intestinalis* into eight genotype assemblages (A–H), based on common genetic markers such as the *SSU* rRNA gene, and the *gdh*, *bg*, and *tpi* loci (9). In the present study, *G. intestinalis* in fur-animals were identified primarily as assemblages A ($n = 3$) and D ($n = 3$) through the analysis of *bg* and *gdh* genes. Among them, assemblage A was the dominant assemblage in mink, consistent with studies on ferrets in Europe and Japan, confirming that assemblage A was common in mustelids (35–37). Assemblage A

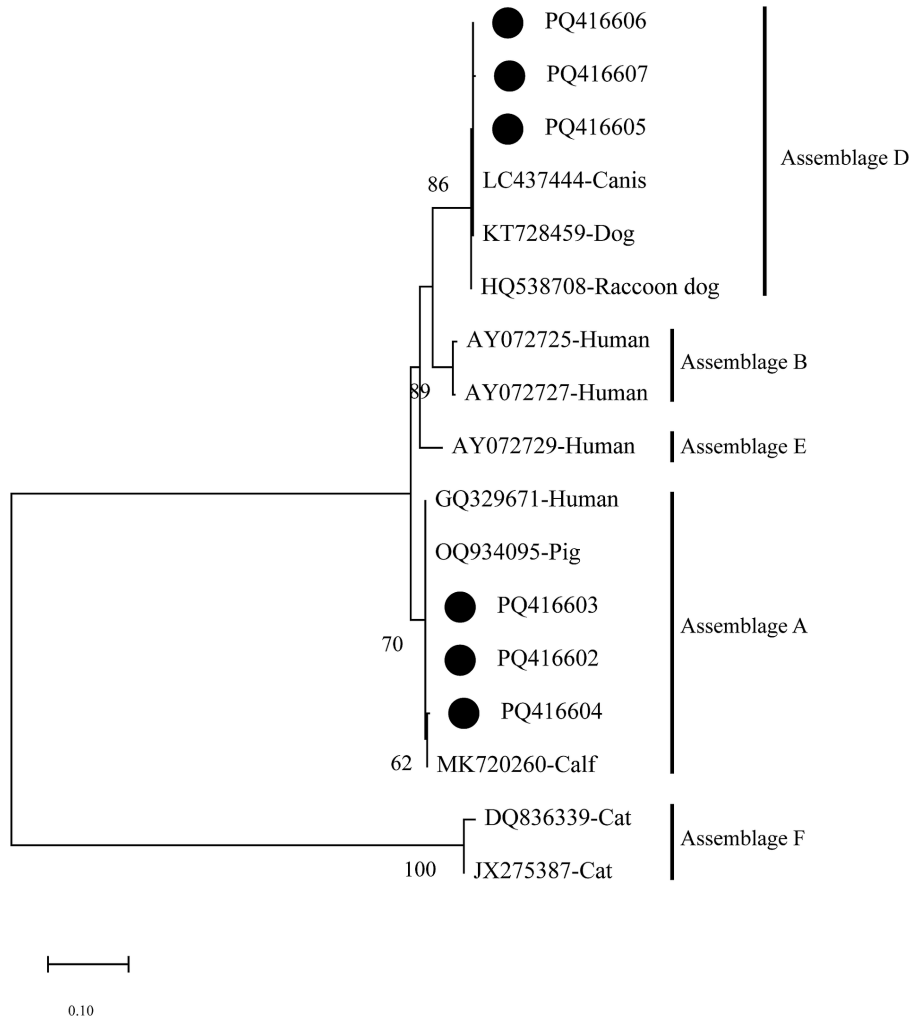

FIGURE 3
Evolutionary relationships among *Giardia intestinalis* inferred by neighbour-joining analysis using the Kimura 2-parameter model of *bg* gene sequences. Numbers on branches are percent bootstrap values from 1,000 replicates, with only those greater than 50% shown. The sequences obtained in the present study are represented by black dots.

is distributed globally across mammals and poultry and is recognised as an important pathogen responsible for human infections (3, 9, 33, 38). The discovery of assemblage A in mink in this study indicates that mink may be a potential host for human infections. Notably, pathological reports indicate that both person-to-person and person-to-animal transmission can occur through direct contact (49). Therefore, it is recommended to further investigate the infection rates among farmers and industry workers to prevent the spread to other animal populations or human communities.

Assemblages C and D were the most common genotypes in canids globally (9). They were widely reported in dogs (13, 39, 40). In China, these assemblages have also been detected in dogs from Xinjiang and raccoon dogs from Jilin (41). In the present study, assemblage D was found in foxes and raccoon dogs, consistent with studies on foxes in Australia and raccoon dogs in Poland (42, 43). However, assemblage C was not detected in this study, which may be related to sample size, sampling time, and geographic regional differences. Notably, although assemblage D was considered host-specific to canids, existing research shows that it can infect other species, including humans (9). For instance, assemblage D has been detected in German travellers, Australian kangaroos, British cattle, and American chinchillas (19, 37, 43, 44). These findings suggest that assemblage D may cross-infection between wildlife and livestock, posing a potential zoonotic risk.

In this study, the amplification success rates for the *bg* and *gdh* genes were relatively high, whereas the *tpi* gene sequences were not successfully obtained. This suggests that the amplification success rates for *bg*, *gdh*, and *tpi* genes may be associated with different assemblage types, which is consistent with previous studies. For example, Chen et al. (31) successfully obtained 20 *bg*, 19 *gdh*, and 9 *tpi* sequences from 22 positive samples of black bears, while Xiao et al. (45) obtained 70 *bg*, 32 *gdh*, and 7 *tpi* sequences from 90 positive samples of goats. These results indicate that more accurate and sensitive molecular diagnostic techniques are urgently needed to achieve a more precise genetic characterization of *G. intestinalis*.

G. intestinalis exists as cysts in vegetables, meat and other foods (29). The food source of fur-animals in mainly poultry meat, which

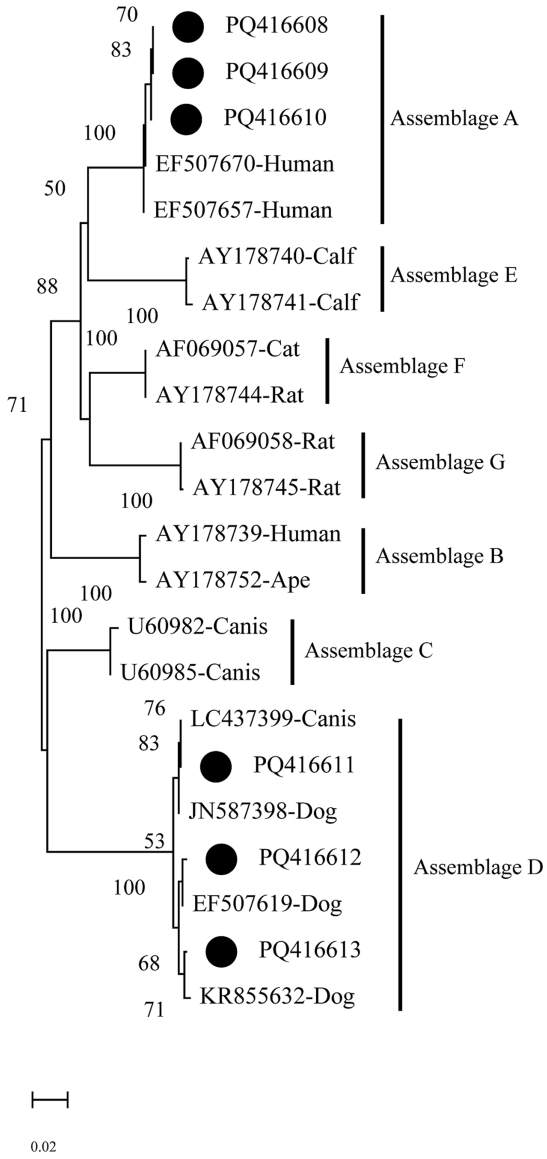

FIGURE 4
Evolutionary relationships among *Giardia intestinalis* inferred by neighbour-joining analysis using the Kimura 2-parameter model of *gdh* gene sequences. Numbers on branches are percent bootstrap values from 1,000 replicates, with only those greater than 50% shown. The sequences obtained in the present study are represented by black dots.

may be one of their infection routes. Additionally, *G. intestinalis* is also wildly present in the environment, particularly in surface water sources (46). In 2013, a waterborne outbreak of *G. intestinalis* infection was reported in South Korea, highlighting its potential for waterborne transmission (47). In addition to known hosts, there are many unknown hosts that could serve as potential sources of human infection. These potential transmission routes pose a threat to public health security. Therefore, it is essential to strengthen the quarantine of foods such as vegetables and meat, while expanding the sampling scope to include more species for detection. At the same time, treatment of the disease is also crucial. Although metronidazole is the drug of choice for treating giardiasis, its issues with resistance and potential side effects such as abdominal pain and nausea limit its use. Therefore, there is an urgent need to develop new treatment formulations, such as phytochemicals, to address this challenge (48).

5 Conclusion

The present study investigated the prevalence of *G. intestinalis* in fur-animals in northern China, first reporting the occurrence of assemblage A in mink, indicating that mink may be a potential zoonotic source of *G. intestinalis*, while also contributing to the epidemiological data on this parasite. Additionally, the detection of assemblage D in foxes and raccoon dogs suggests a similar zoonotic risk. Therefore, attention should be given to the prevalence of *G. intestinalis* among fur industry workers and their surrounding environments to effectively control and prevent potential transmission risks. However, this study has some limitations. For instance, the *tpi* gene sequence was not successfully obtained, and the effect of seasonality on prevalence was not investigated. Therefore, future studies should aim to expand the sample size and incorporate seasonal sampling to better understand the infection dynamics of *G. intestinalis* in fur-animals.

Data availability statement

The datasets presented in this study can be found in online repositories. The names of the repository/repositories and accession number(s) can be found below: https://www.ncbi.nlm.nih.gov/genbank/, PQ416602-PQ416613.

Ethics statement

The animal studies were approved by Research Ethics Committee for the Care and Use of Laboratory Animals in Qingdao Agricultural University. The studies were conducted in accordance with the local legislation and institutional requirements. Written informed consent was obtained from the owners for the participation of their animals in this study.

Author contributions

SL: Methodology, Software, Writing – original draft. MZ: Methodology, Software, Writing – original draft. N-YX: Methodology, Writing – review & editing, Data curation. H-TW: Methodology, Software, Writing – review & editing. Z-YL: Conceptualization, Writing – review & editing. YQ: Resources, Validation, Writing – review & editing. X-ML: Conceptualization, Writing – review & editing. Q-YH: Data curation, Methodology, Writing – review & editing. JJ: Conceptualization, Resources, Supervision, Writing – review & editing. XY: Conceptualization, Supervision, Writing – review & editing. H-BN: Conceptualization, Resources, Supervision, Writing – review & editing. J-XW: Conceptualization, Supervision, Writing – review & editing, Resources, Visualization.

Funding

The author(s) declare that financial support was received for the research, authorship, and/or publication of this article. This work was supported by the Special Economic Animal Industry System Project of the Modern Agricultural Industry System in Shandong Province (SDAIT-21-13).

Conflict of interest

The authors declare that the research was conducted in the absence of any commercial or financial relationships that could be construed as a potential conflict of interest.

Generative AI statement

The authors declare that no Gen AI was used in the creation of this manuscript.

Publisher's note

All claims expressed in this article are solely those of the authors and do not necessarily represent those of their affiliated organizations, or those of the publisher, the editors and the reviewers. Any product that may be evaluated in this article, or claim that may be made by its manufacturer, is not guaranteed or endorsed by the publisher.

References

1. Huang DB, White AC. An updated review on *Cryptosporidium* and *Giardia*. *Gastroenterol Clin N Am*. (2006) 35:291–314. doi: 10.1016/j.gtc.2006.03.006

2. Drake J, Sweet S, Baxendale K, Hegarty E, Horr S, Friis H, et al. Detection of *Giardia* and helminths in Western Europe at local K9 (canine) sites (DOGWALKS Study). *Parasit Vectors*. (2022) 15:311. doi: 10.1186/s13071-022-05440-2

3. Feng Y, Xiao L. Zoonotic potential and molecular epidemiology of *Giardia* species and giardiasis. *Clin Microbiol Rev*. (2011) 24:110–40. doi: 10.1128/CMR.00033-10

4. Einarsson E, Ma'ayeh S, Svärd SG. An update on *Giardia* and giardiasis. *Curr Opin Microbiol*. (2016) 34:47–52. doi: 10.1016/j.mib.2016.07.019

5. Cook DM, Swanson RC, Eggett DL, Booth GM. A retrospective analysis of the prevalence of gastrointestinal parasites among school children in the Palajunoj Valley of Guatemala. *J Health Popul Nutr*. (2009) 27:31–40. doi: 10.3329/jhpn.v27i1.3321

6. Krol A. *Giardia lamblia* as a rare cause of reactive arthritis. *Ugeskr Laeger*. (2013) 175:V05130347 PMID: 25353256

7. Allain T, Buret AG. Pathogenesis and post-infectious complications in giardiasis. *Adv Parasitol*. (2020) 107:173–99. doi: 10.1016/bs.apar.2019.12.001

8. Qi M, Dong H, Wang R, Li J, Zhao J, Zhang L, et al. Infection rate and genetic diversity of *Giardia duodenalis* in pet and stray dogs in Henan province, China. *Parasitol Int*. (2016) 65:159–62. doi: 10.1016/j.parint.2015.11.008

9. Heyworth MF. *Giardia duodenalis* genetic assemblages and hosts. *Parasite*. (2016) 23:13. doi: 10.1051/parasite/2016013

10. Berrilli F, D'Alfonso R, Giangaspero A, Marangi M, Brandonisio O, Kaboré Y, et al. *Giardia duodenalis* genotypes and *Cryptosporidium* species in humans and domestic animals in Côte d'Ivoire: occurrence and evidence for environmental contamination. *Trans R Soc Trop Med Hyg*. (2012) 106:191–5. doi: 10.1016/j.trstmh.2011.12.005

11. Covacin C, Aucoin DP, Elliot A, Thompson RC. Genotypic characterisation of *Giardia* from domestic dogs in the USA. *Vet Parasitol*. (2011) 177:28–32. doi: 10.1016/j.vetpar.2010.11.029

12. Traversa D, Otranto D, Milillo P, Latrofa MS, Giangaspero A, Cesare AD, et al. *Giardia duodenalis* sub-assemblage of animal and human origin in horses. *Infect Genet Evol*. (2012) 12:1642–6. doi: 10.1016/j.meegid.2012.06.014

13. Li W, Liu C, Yu Y, Li J, Gong P, Song M, et al. Molecular characterization of *Giardia duodenalis* isolates from police and farm dogs in China. *Exp Parasitol*. (2013) 135:223–6. doi: 10.1016/j.exppara.2013.07.009

14. Khan SM, Debnath C, Pramanik AK, Xiao L, Nozaki T, Ganguly S. Molecular evidence for zoonotic transmission of *Giardia duodenalis* among dairy farm workers in West Bengal, India. *Vet Parasitol*. (2011) 178:342–5. doi: 10.1016/j.vetpar.2011.01.029

15. Lebbad M, Mattsson JG, Christensson B, Ljungström B, Backhans A, Andersson JO, et al. From mouse to moose: multilocus genotyping of *Giardia* isolates from various animal species. *Vet Parasitol*. (2010) 168:231–9. doi: 10.1016/j.vetpar.2009.11.003

16. Lasek-Nesselquist E, Welch DM, Sogin ML. The identification of a new *Giardia duodenalis* assemblage in marine vertebrates and a preliminary analysis of *G. Duodenalis* population biology in marine systems. *Int J Parasitol*. (2010) 40:1063–74. doi: 10.1016/j.ijpara.2010.02.015

17. Reboredo-Fernández A, Ares-Mazás E, Martínez-Cedeira JA, Romero-Suances R, Cacciò SM, Gómez-Couso H. *Giardia* and *Cryptosporidium* in cetaceans on the European Atlantic coast. *Parasitol Res*. (2015) 114:693–8. doi: 10.1007/s00436-014-4235-8

18. Zhao Z, Wang R, Zhao W, Qi M, Zhao J, Zhang L, et al. Genotyping and subtyping of *Giardia* and *Cryptosporidium* isolates from commensal rodents in China. *Parasitology*. (2015) 142:800–6. doi: 10.1017/S0031182014001929

19. Broglia A, Weitzel T, Harms G, Cacció SM, Nöckler K. Molecular typing of *Giardia duodenalis* isolates from German travellers. *Parasitol Res*. (2013) 112:3449–56. doi: 10.1007/s00436-013-3524-y

20. Soliman RH, Fuentes I, Rubio JM. Identification of a novel assemblage B subgenotype and a zoonotic assemblage C in human isolates of *Giardia intestinalis* in Egypt. *Parasitol Int*. (2011) 60:507–11. doi: 10.1016/j.parint.2011.09.006

21. Song P, Guo Y, Zuo S, Li L, Liu F, Zhang T, et al. Prevalence of *Pentatrichomonas hominis* in foxes and raccoon dogs and changes in the gut microbiota of infected female foxes in the Hebei and Henan provinces in China. *Parasitol Res*. (2023) 123:74. doi: 10.1007/s00436-023-08099-5

22. Máca O, Gudiškis N, Butkauskas D, González-Solís D, Prakas P. Red foxes (*Vulpes vulpes*) and raccoon dogs (*Nyctereutes procyonoides*) as potential spreaders of *Sarcocystis* species. *Front Vet Sci*. (2024) 11:1392618. doi: 10.3389/fvets.2024.1392618

23. Zhang NZ, Li WH, Yu HJ, Liu YJ, Qin HT, Jia WZ, et al. Novel study on the prevalence of *Trichinella spiralis* in farmed American minks (*Neovison vison*) associated with exposure to wild rats (*Rattus norvegicus*) in China. *Zoonoses Public Health*. (2022) 69:938–43. doi: 10.1111/zph.12991

24. Lalle M, Pozio E, Capelli G, Bruschi F, Crotti D, Cacciò SM. Genetic heterogeneity at the beta-giardin locus among human and animal isolates of *Giardia duodenalis* and identification of potentially zoonotic subgenotypes. *Int J Parasitol*. (2005) 35:207–13. doi: 10.1016/j.ijpara.2004.10.022

25. Cacciò SM, Beck R, Lalle M, Marinculic A, Pozio E. Multilocus genotyping of *Giardia duodenalis* reveals striking differences between assemblages a and B. *Int J Parasitol*. (2008) 38:1523–31. doi: 10.1016/j.ijpara.2008.04.008

26. Sulaiman IM, Fayer R, Bern C, Gilman RH, Trout JM, Schantz PM, et al. Triosephosphate isomerase gene characterization and potential zoonotic transmission of *Giardia duodenalis*. *Emerg Infect Dis*. (2003) 9:1444–52. doi: 10.3201/eid0911.030084

27. Tamura K, Stecher G. MEGA11: molecular evolutionary genetics analysis version 11. *Mol Biol Evol*. (2021) 38:3022–7. doi: 10.1093/molbev/msab120

28. Murrell KD. Zoonotic foodborne parasites and their surveillance. *Rev Sci Tech*. (2013) 32:559–69. doi: 10.20506/rst.32.2.2239

29. Ryan U, Hijjawi N, Feng Y, Xiao L. Giardia: an under-reported foodborne parasite. *Int J Parasitol*. (2019) 49:1–11. doi: 10.1016/j.ijpara.2018.07.003

30. Zhao L, Wang Y, Wang M, Zhang S, Wang L, Zhang Z, et al. First report of *Giardia duodenalis* in dairy cattle and beef cattle in Shanxi, China. *Mol Biol Rep*. (2024) 51:403. doi: 10.1007/s11033-024-09342-7

31. Chen J, Zhou L, Cao W, Xu J, Yu K, Zhang T, et al. Prevalence and assemblage identified of *Giardia duodenalis* in zoo and farmed Asiatic black bears (*Ursus thibetanus*) from the Heilongjiang and Fujian provinces of China. *Parasite*. (2024) 31:50. doi: 10.1051/parasite/2024048

32. Zhang XX, Zhang FK, Li FC, Hou JL, Zheng WB, Du SZ, et al. The presence of *Giardia intestinalis* in donkeys, *Equus asinus*, in China. *Parasit Vectors*. (2017) 10:3. doi: 10.1186/s13071-016-1936-0

33. Wu Y, Yao L, Chen H, Zhang W, Jiang Y, Yang F, et al. *Giardia duodenalis* in patients with diarrhea and various animals in northeastern China: prevalence and multilocus genetic characterization. *Parasit Vectors*. (2022) 15:165. doi: 10.1186/s13071-022-05269-9

34. Zhao W, Li Z, Sun Y, Li Y, Xue X, Zhang T, et al. Occurrence and multilocus genotyping of *Giardia duodenalis* in diarrheic and asymptomatic children from south of Zhejiang province in China. *Acta Trop*. (2024) 258:107341. doi: 10.1016/j.actatropica.2024.107341

35. Guo Y, Li N, Feng Y, Xiao L. Zoonotic parasites in farmed exotic animals in China: implications to public health. *Int J Parasitol Parasites Wildl*. (2021) 14:241–7. doi: 10.1016/j.ijppaw.2021.02.016

36. Abe N, Tanoue T, Noguchi E, Ohta G, Sakai H. Molecular characterization of *Giardia duodenalis* isolates from domestic ferrets. *Parasitol Res*. (2010) 106:733–6. doi: 10.1007/s00436-009-1703-7

37. Pantchev N, Broglia A, Paoletti B, Globokar Vrhovec M, Bertram A, Nöckler K, et al. Occurrence and molecular typing of *Giardia* isolates in pet rabbits, chinchillas, guinea pigs and ferrets collected in Europe during 2006–2012. *Vet Rec*. (2014) 175:18. doi: 10.1136/vr.102236

38. Appelbee AJ, Thompson RC, Olson ME. *Giardia* and *Cryptosporidium* in mammalian wildlife—current status and future needs. *Trends Parasitol*. (2005) 21:370–6. doi: 10.1016/j.pt.2005.06.004

39. Yun CS, Moon BY, Lee K, Hwang SH, Ku BK, Hwang MH. Prevalence and genotype analysis of *Cryptosporidium* and *Giardia duodenalis* from shelter dogs in South Korea. *Vet Parasitol Reg Stud Rep*. (2024) 55:101103. doi: 10.1016/j.vprsr.2024.101103

40. Kabir MHB, Kato K. Examining the molecular epidemiology of *Giardia* and Eimeria species in Japan: a comprehensive review. *J Vet Med Sci*. (2024) 86:563–74. doi: 10.1292/jvms.23-0525

41. Cao Y, Fang C, Deng J, Yu F, Ma D, Chuai L, et al. Molecular characterization of *Cryptosporidium* spp. and *Giardia duodenalis* in pet dogs in Xinjiang, China. *Parasitol Res*. (2022) 121:1429–35. doi: 10.1007/s00436-022-07468-w

42. Solarczyk P, Majewska AC, Jędrzejewski S, Górecki MT, Nowicki S, Przysiecki P. First record of *Giardia* assemblage D infection in farmed raccoon dogs (*Nyctereutes procyonoides*). *Ann Agric Environ Med*. (2016) 23:696–8. doi: 10.5604/12321966.1226869

43. Ng J, Yang R, Whiffin V, Cox P, Ryan U. Identification of zoonotic *Cryptosporidium* and *Giardia* genotypes infecting animals in Sydney's water catchments. *Exp Parasitol*. (2011) 128:138–44. doi: 10.1016/j.exppara.2011.02.013

44. Minetti C, Taweenan W, Hogg R, Featherstone C, Randle N, Latham SM, et al. Occurrence and diversity of *Giardia duodenalis* assemblages in livestock in the UK. *Transbound Emerg Dis*. (2014) 61:e60–7. doi: 10.1111/tbed.12075

45. Xiao HD, Su N, Zhang ZD, Dai LL, Luo JL, Zhu XQ, et al. Prevalence and genetic characterization of *Giardia duodenalis* and *Blastocystis* spp. in black goats in Shanxi province, North China: from a public health perspective. *Animals*. (2024) 14:1808. doi: 10.3390/ani14121808

46. Xiao G, Qiu Z, Qi J, Chen JA, Liu F, Liu W, et al. Occurrence and potential health risk of *Cryptosporidium* and *Giardia* in the three gorges reservoir, China. *Water Res*. (2013) 47:2431–45. doi: 10.1016/j.watres.2013.02.019

47. Cheun HI, Kim CH, Cho SH, Ma DW, Goo BL, Na MS, et al. The first outbreak of giardiasis with drinking water in Korea. *Osong Public Health Res Perspect*. (2013) 4:89–92. doi: 10.1016/j.phrp.2013.03.003

48. Alawfi BS. A review on the use of phytochemicals for the control of zoonotic giardiasis. *Pak Vet J*. (2024) 44:592–8. doi: 10.29261/pakvetj/2024.251

49. Esch KJ, Petersen CA. Transmission and epidemiology of zoonotic protozoal diseases of companion animals. *Clin Microbiol Rev*. (2013) 26:58–85. doi: 10.1128/CMR.00067-12

frontiers | Frontiers in Veterinary Science

TYPE Case Report
PUBLISHED 12 March 2025
DOI 10.3389/fvets.2025.1500916

Check for updates

OPEN ACCESS

EDITED BY
Sirikachorn Tangkawattana,
Khon Kaen University, Thailand

REVIEWED BY
Lisa Guardone,
University of Pisa, Italy
Miloš Vučićević,
University of Belgrade, Serbia

*CORRESPONDENCE
Hebel Christiana
✉ christiana@cvrl.ae

RECEIVED 24 September 2024
ACCEPTED 04 February 2025
PUBLISHED 12 March 2025

CITATION
Christiana H, Rolf Karl S, Joerg K and Ulrich W (2025) One Health alert: zoonotic scabies from dromedary camels—A case report and call for vigilance.
Front. Vet. Sci. 12:1500916.
doi: 10.3389/fvets.2025.1500916

COPYRIGHT
© 2025 Christiana, Rolf Karl, Joerg and Ulrich. This is an open-access article distributed under the terms of the Creative Commons Attribution License (CC BY). The use, distribution or reproduction in other forums is permitted, provided the original author(s) and the copyright owner(s) are credited and that the original publication in this journal is cited, in accordance with accepted academic practice. No use, distribution or reproduction is permitted which does not comply with these terms.

One Health alert: zoonotic scabies from dromedary camels—A case report and call for vigilance

Hebel Christiana*, Schuster Rolf Karl, Kinne Joerg and Wernery Ulrich

Central Veterinary Research Laboratory, Dubai, United Arab Emirates

This case report describes the rapid transmission of sarcoptic mange, a highly contagious skin disease caused by the mite *Sarcoptes scabiei,* from one dromedary camel to a group of other dromedary camels and a group of human beings despite wearing personal protective equipment. This is the first report on an outbreak of human pseudoscabies in the United Arab Emirates, and it highlights the importance of a One Health approach managing zoonotic diseases. Early detection, treatment of infected animals, as well as adherence to hygiene and quarantine protocols are crucial to prevent zoonotic spillovers.

KEYWORDS

dromedary camel, sarcoptes scabiei, sarcoptic mange, pseudoscabies, zoonosis, One Health

1 Introduction

Dromedary camels (*Camelus dromedarius*) (following referred to as camel) are not only an important part of the cultural heritage in the Middle East by being Bedouin companions, providing transportation, milk and wool, but they also play a role in modern life as they are still bred for milk and meat, as well as for prestigious camel races (1). The bond between camels and their owners and caretakers is strong, and close contact is very common. This provides not only a lot of benefits, but does also carry the risk of disease transmission (2). Possible zoonotic transmission of different parasites from camels to human beings are described (3). One of them is sarcoptic mange, a highly contagious skin disease caused by the mite *Sarcoptes scabiei* (4). It affects various mammals, including humans, camels, and other livestock. While interspecies transmission of sarcoptic mange is common, documented cases of camel-to-human transmission are rare, and reported to occur mainly during milking (5). Transferred to humans, the sarcoptic mange is a highly contagious skin disease called "Pseudoscabies" causing a temporary infestation with mites. Unlike true scabies, which is caused in human beings by *S. scabiei* var. *hominis* and listed by the World Health Organization (WHO) as a neglected tropical disease in 2017, and which is highly contagious between humans, pseudoscabies is very rarely transmittable from person to person (6).

This case report presents the rapid transmission of sarcoptic mange from camels to a group of human beings, despite wearing personal protective equipment, highlighting the importance of a One Health approach in managing zoonotic diseases.

2 Case description

2.1 Case presentation of the camel

A 2-year old castrated, male camel was presented with a month-long history of hyperkeratosis, severe pruritus, alopecia, anorexia and dark brown color change of its skin all over the body. Several areas of the body were covered with one-centimeter-thick crusts and severely thickened involving the ears, nostrils, neck, and lower limbs (Figure 1), with several areas exhibiting half centimeter deep cracks infested with maggots of the species *Wohlfahrtia nuba*. In addition, the camel suffered from a tick (*Hyalomma dromedarii*) infestation. The camel was housed at a private farm with 19 other camels, that presented similar skin lesions of different severity. All animals were allowed to roam around the desert freely during the day.

The camel was moved to a treatment facility in Dubai, United Arab Emirates (UAE), that kept 23 camels (in groups of 3 or 4 camels), 2 donkeys and 12 sheep. Blood collection on arrival revealed an increased total white blood cell count (18.5×10^9/L), with neutrophils and eosinophils increased, a PCV of 0.21 L/L and slightly lowered iron 10 µmoL/L. Biochemistry results showed elevated CK (262 U/L) and LDH (584 U/L), while other values were within normal limits.

The camel was maintained in isolation, segregated from other animals. The only interaction occurred on the arrival day, when two resident camels had short contact by sniffing on it when it first walked into the facility. The treatment facility holding areas are simple pens with sand paddocks with iron fencing. Food troughs are made of steel. On arrival, five different people wearing Nitril gloves and working overalls handled the camel.

Within three days after the primary interaction at the treatment facility, two of the resident camels, that had less than a minute contact by only sniffing on day one, started showing typical mange lesions around the nostrils and lips (Figure 2). The camels did not share the same feeding troughs. Skin scrapings from these two camels revealed a *S. scabiei* infestation.

FIGURE 1
Index case: Camel with severe alopecia and hyperkeratosis caused by *Sarcoptes scabiei* infestation.

2.2 Case presentation of the workers

Despite wearing nitril gloves on the first day and changing their working overalls, all workers handling the camel developed intensely pruritic erythematous papules and pustules on their hands, wrists, forearms, thorax, abdomen and thighs within three days of handling the index camel. The caretakers had contact with the camel while feeding and cleaning its enclosure and treatment. Upon examination of the caretakers' skin, burrows characteristic of scabies mite infestation was identified on the affected areas. A sixth and seventh person who only started handling the camel on day four and five after arrival, also showed pruritus and erythematous papules three days after the first contact (Figure 3).

Upon investigation, the camel handlers from the original farm also confirmed that they had severe pruritus and erythematous papules at several areas of the body.

3 Management and control

The newly arrived camel was treated with a dose of 0.2 mg/kg ivermectin injection (Ivomec, Merial, details 1 mg/mL) on day one of its arrival. In addition, it received flumethrin (Bayticol, Bayer) against ticks. Furthermore, besides the antiparasitic treatment, the index camel's cracked wounds were washed with chlorhexidine 3% and the maggots were flushed out with hydrogen peroxide. Afterwards, the skin was oiled with 100% natural coconut oil to soften the crusts, and permethrin antifly repellent spray was applied topically. In addition, it received treatment with 5 mg/kg enrofloxacin (Baytril 10%, Bayer, Germany) intravenously for 5 days for secondary infections and a single dose with 0.6 mg/kg meloxicam (Metacam, Boehringer Ingelheim, Germany). Water was given orally by pouring it into the mouth, which the camel swallowed. It occasionally did take carrots and dates by hand. On day 5 the camel still showed anorexia, severe pruritus and apathy. Repeated skin scrapings taken still showed live mites. Therefore, the camel was then treated with doramectin (Dectomax, Zoetis, Egypt) injection 0.2 mg/kg subcutaneous. The camel was found dead on day 8 at the treatment facility. Postmortem examination revealed emaciation, severe anemia, alopecia and severe hyperkeratosis. All internal organs were macroscopically unremarkable. Histopathological examination of skin samples from different areas showed a marked hyperkeratotic dermatitis with perivascular inflammation including eosinophils and cocci-shaped bacteria. *Sarcoptes* mites were seen in burrows of the stratum corneum layers of the skin. Additionally, the intestine showed a marked subacute eosinophilic enteritis with severe coccidiosis.

All other 17 camels at the original private farm, as well as all 23 camels a the treatment facility and the 12 sheep, were treated thrice with subcutaneous doramectin injections of 0.2 mg/kg of body weight every two weeks and once with pour-on ivermectin (5 mg/mL Ivermectin, Durvet, Inc. Bluesprings, Missouri, USA) poured onto the hump area. Repeated skin scrapings from the infected animals showed significant reduction of live mites within 48 h from the first treatment.

FIGURE 2
Contact animal: Alopecia and hyperkeratosis caused by *Sarcoptes scabiei* infestation starting around the nostrils.

Nevertheless, 2 months after the third doramectin injection, several camels at the treatment facility started showing thickened skin and severe pruritus at different areas of the body. Skin scrapings confirmed again *Sarcoptes* mites. At this point it was decided to go for a longer treatment regime with doramectin injections of 0.2 mg/kg every two weeks for two months.

Given the composition of the enclosures, consisting primarily of sand paddocks, iron fencing and steel troughs, disinfection procedures were not implemented, and would have been very difficult. Ropes and halters of the camels were replaced with new ones after the treatment.

The handlers received topical scabicidal treatment (permethrin 5%) and symptomatic relief for itching. However, the infected handlers kept showing symptoms of the pruritic erythematous papules and pustules as well as severe pruritus up to four weeks after the first encounter. New single papules and pustules showed up occasionally in different areas of the body for two more weeks.

4 Diagnostic assessment

Deep skin scrapings from the live camel containing crusts and scabs from seven different affected areas were collected and placed on filter paper discs in petri dishes for 24 h at 38°C (7). Consequently, after only one hour a large number of mites of different development stages moved out from all samples, crawling at the base of the petri dishes. The mites were identified as *S. scabiei*. (Figure 4).

Skin scrapings collected from the 19 other camels from the private farm displaying similar skin lesions like alopecia and hyperkeratosis as well as severe pruritus, tested positive for *Sarcoptes* mites.

5 Discussion

Sarcoptic mange is a highly contagious skin disease caused by the mite *S. scabiei*. It affects various domestic and a large variety of wild mammals and is by now found in more than 140 host species (8). In the UAE, the disease was recently reported in free-roaming Arabian Oryx (*Oryx leucoryx*) (9). Direct contact between animals is the primary transmission route, and mange in camels is extremely contagious (2).

Besides the very high morbidity, *S. scabiei* can also show high mortality in species like the Arabian Oryx (9). Treatment in camelids is described as challenging and reported to take a long time (10), the same was confirmed at the treatment facility where the mange flared up after discontinuing the treatment after the third injection of doramectin. Generalized sarcoptic mange leads to weight loss, abnormal behavior, increased susceptibility to other diseases, as well as increased mortality (11). Especially in young, old or immunocompromised animals it can lead to secondary bacterial infections, emaciation and death. The severe inflammation of the skin, the biggest organ of the body, reduces the natural immunological function. The affected animals in the original farm and at the treatment facility also showed restlessness and uneasiness whilst eating, due to the intense pruritus. As documented in this case report, the camel presented to the treatment facility exhibited the profound consequences of a severe mange infection: generalized weight loss, secondary bacterial infections, and an impaired immune system likely contributing to malabsorption due to coccidiosis.

Although camel mange caused by *S. scabiei* has been reported from various countries, like Nigeria (12), Ethiopia (24, 25), Egypt (13), Saudi Arabia (14), India (15) and Pakistan (16), there are currently no known case reports of sarcoptic mange outbreaks in camels in the UAE, even though the disease is very common.

In human beings the disease is caused by a host-specific *S. scabiei* strain and it is called scabies, which was listed by the WHO as a neglected tropical disease in 2017 (17). The contact of humans with mange infected animals can cause pseudoscabies also known as zoonotic scabies, a self-limiting condition that is characterized by severe pruritus. Moroni et al. (18) reviewed the presence of *S. scabiei* in various domestic and wild animals, including new world camelids, but did not list a documented case of a zoonotic outbreak from Dromedary or Bactrian camels. The development of pseudoscabies in humans after contact with infected camels is rare (2, 3, 5, 12). But as shown in this case, even a short contact with a severely infected animal, despite wearing personal protective equipment, is enough to get infected.

Due to the high zoonotic potential, sarcoptic mange in camels should be handled by a multifaceted approach. It is important to implement robust preventive measures, including quarantine protocols and regular inspections. Early detection and immediate treatment can possibly prevent severe mange outbreaks and zoonotic spillovers. Nevertheless, as shown in this case, wearing nitril gloves when handling animals infested with mange, did not guarantee protection, most likely due to the immense number of mites. Especially the crusted "Norwegian" from, which is linked to a high mite density, seems to harbor a higher infectious potential (18).

Infestations in human beings with pseudoscabies can be challenging to identify as they presnt differently than standard

FIGURE 3
Skin lesions of the forearm of the camel caretaker showing several erythematous papules and pustules.

FIGURE 4
Sarcoptes scabiei mites 50 µm in size under the microscope 20x magnification.

human scabies. Nonetheless, careful consideration of the patient's history can lead to a definitive diagnosis (19). Especially because the distribution of the skin lesions was described as typical for zoonotic scabies (17). Infestations with pseudoscabies are usually self-limiting, but to speed up recovery up, topical treatment with 5% permethrin ointment should be considered (19).

For human scabies, different treatment protocols (oral ivermectin, repeated 1–2 weeks after) are available and treatment protocols for cattle and sheep are described in detail, but protocols for camels are based more on experience than scientific data (20–22). Doramectin in the dose of 0.2 mg/kg body weight subcutaneous biweekly for two month is the dose recommended to be used for treatment of scabies in dromedary camels (15), but pharmacological studies are missing.

This case highlights the One Health principle of interconnectedness between human, animal, and the environment. The close contact between camel handlers and infected animals, coupled with lax quarantine measures facilitated the zoonotic transmission of *S. scabiei* mites. It underscores the critical need for increased awareness among camel handlers, owners, veterinarians and public health officials, especially due to the close contact between camel handlers and their animals. It also demonstrates that even in routine animal husbandry practices, despite wearing personal protective equipment and changing clothes, the risk of transmission is still high.

Several environmental factors can contribute to the spread of sarcoptic mange in camels, including poor sanitation, overcrowding, and allowing camels to roam freely. Inadequate cleaning of stables and equipment allows mites to persist in the environment, while overcrowding in stables or during transport increases the frequency of direct contact between animals, facilitating the spread of mites. Free-roaming camels are also more likely to come into contact with infected animals. Additionally, climate and humidity can significantly influence the transmission and severity of sarcoptic mange, as these factors affect mite survival and reproduction rates. Sarcoptic mites can survive off the host for a limited time, typically a few weeks. Cool and humid conditions prolong their survival, while dry conditions at 37°C can limit their survival to less than 48 h based on our experience.

Sarcoptic mange is highly contagious and spreads easily within camel groups. Transmission primarily occurs through direct contact between infected animals, including horizontal transmission between animals within the same herd, vertical transmission from mother to offspring, and transmission between animals of different age groups. Indirect transmission can also occur through contaminated fomites such as bedding, grooming equipment, and ropes (23).

The crucial of responsible animal ownership needs to be addressed. Animal welfare is an often overlooked aspect when dealing with a severe mange infestation. Mange causes immense discomfort for the infected animals and predisposes the animals to secondary bacterial infections. Therefore, proper parasite control programmes are essential for the wellbeing of both animals and humans. Early detection and diagnosis of mange are crucial for prompt intervention and control, as evidenced by the rapid spread to the other camels and humans with just brief contact.

Veterinarians and public health officials must collaborate to implement effective prevention and control strategies. Educating the public, animal handlers and owners about the zoonotic potential of sarcoptic mange, including hygiene measures, prevention and treatment

options, is paramount. The currently missing scientific data on optimal treatment of sarcoptic mange in camels needs further research.

In conclusion, this case report highlights the One Heath relevance of scabies. It underscores the need for integrated surveillance, prevention and control strategies to safeguard both human and animal health. Collaboration can effectively help managing zoonotic disease outbreaks. By fostering collaboration we can effectively manage zoonotic diseases and create a healthier environment for all.

Data availability statement

The raw data supporting the conclusions of this article will be made available by the authors, without undue reservation.

Ethics statement

The studies involving humans were approved by the Central Veterinary Research Laboratory Ethics committee. The studies were conducted in accordance with the local legislation and institutional requirements. The participants provided their written informed consent to participate in this study. The animal studies were approved by the Central Veterinary Research Laboratory Ethics committee. The studies were conducted in accordance with the local legislation and institutional requirements. Written informed consent was obtained from the owners for the participation of their animals in this study. Written informed consent was obtained from the individual(s) for the publication of any potentially identifiable images or data included in this article. Written informed consent was obtained from the participant/patient(s) for the publication of this case report.

Author contributions

HC: Writing – original draft, Writing – review & editing. SR: Formal analysis, Writing – original draft, Writing – review & editing. KJ: Formal analysis, Writing – original draft, Writing – review & editing. WU: Supervision, Writing – original draft, Writing – review & editing.

Funding

The author(s) declare that no financial support was received for the research, authorship, and/or publication of this article.

Conflict of interest

The authors declare that the research was conducted in the absence of any commercial or financial relationships that could be construed as a potential conflict of interest.

Publisher's note

All claims expressed in this article are solely those of the authors and do not necessarily represent those of their affiliated organizations, or those of the publisher, the editors and the reviewers. Any product that may be evaluated in this article, or claim that may be made by its manufacturer, is not guaranteed or endorsed by the publisher.

References

1. Khalaf S. Camel racing in the Gulf. Notes on the evolution of a traditional cultural sport. *Anthropos*. (1999) 94:85–106.

2. Wernery U, Kinne J, Schuster R. (eds.) Camelid infectious disorders. Paris: World Organisation for Animal Health (Oie) (2014).

3. Sazmand A, Joachim A, Otranto D. Zoonotic parasites of dromedary camels: so important, so ignored. *Parasit Vectors*. (2019) 12:610. doi: 10.1186/s13071-019-3863-3

4. Sahani MS, Sharma N, Ghorui SK, Bissa UK, Chirania BL. Sarcoptic mange (Scabies) in camels-preventive measures and treatment. Bikaner, Rajanstan, India. National Research Centre on Camel (2003).

5. Schillinger D. Mange in camels - an important zoonosis. *Rec Sci Tech Off Int Epiz*. (1987) 6:479–80. doi: 10.20506/rst.6.2.299

6. WHO. (2023). Scabies. Available at: https://www.who.int/news-room/fact-sheets/detail/scabies (Accessed December 21, 2023).

7. Noeckler K, Matthes H, Hiepe T, Ziegler H. Nachweis von anti-Sarcoptes suis-IgG im Blutserumneonatal mit Sarcoptesmilben infizierter Ferkel mit dem indirekten Elisa. *Monatshefte fuer Veterinaermedizin*. (1992) 47:415–21.

8. Escobar LE, Carver S, Cross PC, Rossi L, Almberg ES, Yabsley MJ, et al. Sarcoptic mange: an emerging panzootic in wildlife. *Transbound Emerg Dis*. (2022) 69:927–42. doi: 10.1111/tbed.14082

9. Thrivikraman A, Wernery U, Baskar V, Almheiri FG, Schuster RK. An outbreak of Sarcoptic mange in free-ranging Arabian Oryx (*Oryx leucoryx*) in the United Arab Emirates, and treatment with Ivermectin-medicated pelleted feed. *J Wildl Dis*. (2023) 59:791–5. doi: 10.7589/JWD-D-22-00180

10. Deak G, Moroni B, Boncea AM, Rambozzi L, Rossi L, Mihalca AD. Case report: successful treatment of Sarcoptic mange in European camelids. *Front Vet Sci*. (2021) 8:742543. doi: 10.3389/fvets.2021.742543

11. Moerner T. Sarcoptic mange in Swedish wildlife. *Rev Sci Tech*. (1992) 11:1115–21. doi: 10.20506/rst.11.4.658

12. Basu A, Aliya A, Mohammed A. Mohammed A. Mange in Camelids: a Review. *J Camel Pract Res*. (1995) 2:131–138.

13. Ahmed MA, Elmahallawy EK, Gareh A, Abdelbaset AE, El-Gohary FA, Elhawary NM, et al. Epidemiological and histopathological investigation of Sarcoptic mange in camels in Egypt. *Animals*. (2020) 10. doi: 10.3390/ani10091485

14. Abdel-Rady A, Mostafa W, Abdel-Raouf AM. Epidemiological investigations in Sarcoptic mange in camels with special reference in treatment. *J Parasit Dis*. (2021) 45:689–94. doi: 10.1007/s12639-020-01346-x

15. Palanivelrajan M, Thangapandian M, Prathipa A. Therapeutic Management of Sarcoptic Mange in a camel (*Camelus Dromedarius*). *J. Wildlife Res*. (2015) 3:5–7.

16. Muhammad A, Bashir R, Mahmood M, Afzal MS, Simsek S, Awan UA, et al. Epidemiology of Ectoparasites (ticks, lice, and mites) in the livestock of Pakistan: a review. *Front Vet Sci*. (2021) 8:780738. doi: 10.3389/fvets.2021.780738

17. Engelman D, Cantey PT, Marks M, Solomon AW, Chang AY, Chosidow O, et al. The public health control of scabies: priorities for research and action. *Lancet*. (2019) 394:81–92. doi: 10.1016/S0140-6736(19)31136-5

18. Moroni B, Rossi L, Bernigaud C, Guillot J. Zoonotic episodes of Scabies: a global overview. *Pathogens*. (2022) 11. doi: 10.3390/pathogens11020213

19. Aydingoz IE, Mansur AT. Canine scabies in humans: a case report and review of the literature. *Dermatology*. (2011) 223:104–6. doi: 10.1159/000327378

20. Currier RW, Walton SF, Currie BJ. Scabies in animals and humans: history, evolutionary perspectives, and modern clinical management. *Ann N Y Acad Sci*. (2011) 1230:E50–60. doi: 10.1111/j.1749-6632.2011.06364.x

21. Holdsworth P, Rehbein S, Jonsson NN, Peter R, Vercruysse J, Fourie J. World Association for the Advancement of veterinary parasitology (Waavp) second edition: guideline for evaluating the efficacy of parasiticides against ectoparasites of ruminants. *Vet Parasitol*. (2022) 302:109613. doi: 10.1016/j.vetpar.2021.109613

22. Pfister K. Arhropodenbefall bei Wiederkaeuern. In: Schnieder, Thomas, editors. Paray: Veterinaermedizinische Parasitologie (2006).

23. Deplazes P, Von Samson-Himmelstjerna G, Zahner H, Joachim A, Mathis A, Taubert A, et al. Parasitologie fuer Tiermedizin. In: Deplazes P, Eckert J, Von Samson-Himmelstjerna G, Zahner H, editors. Stuttgart: New York, Thieme (2021).

24. Jarso D, Birhanu S, Wubishet Z. Review on Epidemiology of Camel Mange Mites. *Biomedical Journal of Scientific & Technical Research*. (2018) 8. doi: 10.26717/BJSTR.2018.08.001605

25. Mustefa Ame M, Mohammed M, Mohammed K, Usman M. Assessment of Camel Mange Mite Prevalence in Kumbi Woreda, Eastern Harergae, Ethiopia. *Journal of Pesticide Science and Pest Control*. (2023) 2. doi: 10.58489/2833-0943/014

frontiers | Frontiers in Veterinary Science

TYPE Original Research
PUBLISHED 18 June 2025
DOI 10.3389/fvets.2025.1517704

Check for updates

OPEN ACCESS

EDITED BY
Hussam Askar,
Al Azhar University, Egypt

REVIEWED BY
Marcos Rogério André,
São Paulo State University, Brazil
Nehaz Muhammad,
Hebei Normal University, China

*CORRESPONDENCE
Attila D. Sándor
✉ adsandor@gmail.com

RECEIVED 26 October 2024
ACCEPTED 12 May 2025
PUBLISHED 18 June 2025

CITATION
Sándor AD, Domșa C, Péter Á and Hornok S (2025) Ixodid ticks of Western Palearctic bats: ecology, host-parasite relationships, geographic distribution and zoonotic importance.
Front. Vet. Sci. 12:1517704.
doi: 10.3389/fvets.2025.1517704

COPYRIGHT
© 2025 Sándor, Domșa, Péter and Hornok. This is an open-access article distributed under the terms of the Creative Commons Attribution License (CC BY). The use, distribution or reproduction in other forums is permitted, provided the original author(s) and the copyright owner(s) are credited and that the original publication in this journal is cited, in accordance with accepted academic practice. No use, distribution or reproduction is permitted which does not comply with these terms.

Ixodid ticks of Western Palearctic bats: ecology, host-parasite relationships, geographic distribution and zoonotic importance

Attila D. Sándor[1,2,3]*, Cristian Domșa[4], Áron Péter[2] and Sándor Hornok[1,2]

[1]HUN-REN-UVMB Climate Change: New Blood-Sucking Parasites and Vector-Borne Pathogens Research Group, Budapest, Hungary, [2]Department of Parasitology and Zoology, University of Veterinary Medicine, Budapest, Hungary, [3]STAR-UBB Institute, Babes-Bolyai University, Cluj-Napoca, Romania, [4]Romanian Ornithological Society, Cluj Napoca, Romania

Bats in the Western Palearctic are host for diverse array of ectoparasites, including three ixodid ticks (*Ixodes ariadnae*, *I. simplex*, and *I. vespertilionis*), which are highly specialized to parasitize these mammals. In this study we collected and analyzed 3,965 host-tick records across 31 bat species from published literature, online sources, and unpublished field data. Individual bat-specialist ticks showed distinct host preferences, with cave-dwelling bats accounting for over 90% of all records. *Ixodes vespertilionis* was the most generalist of them, with a broad host range and distribution, while *I. simplex* was highly host-specific, primarily parasitizing a single host species, *Miniopterus schreibersii*. *Ixodes ariadnae* had a similar host spectrum as *I. vespertilionis* but more restricted geographical range, likely influenced by seasonal and life history factors. Our findings revealed substantial geographical overlap in tick distributions across Central and Eastern Europe. Free-living tick stages were predominantly found in caves, and males were observed more frequently than females. Non-bat specific, as well generalist ticks such as *Ixodes ricinus* and *Rhipicephalus sanguineus* s.l. were rare on bats, with larger bat species being the more common hosts. These ticks may host DNA of several bacterial, viral, and parasitic pathogens, suggesting an important role in pathogen transmission to bats and possibly other mammals. This study underscores the ecological significance of bat-specialist ticks and highlights the need for further research on their distribution, host interactions, and role in zoonotic disease transmission.

KEYWORDS

Chiroptera, host-specificity, Ixodidae, vector-borne pathogens, zoonotic diseases

Background

Ixodid ticks (Acari: Ixodidae) are obligate parasites of vertebrates, widely distributed across all terrestrial biomes of Earth (1). They are an ancient group, showing long coevolution with vertebrates, initially being the parasites of feathered dinosaurs/birds (2), later evolving to infest all terrestrial vertebrate groups (3). Currently, there are over 700 valid species, with high diversity in the tropics (4). Most species are specialized to feed either on birds, mammals or reptiles, however, several species are generalists, capable of feeding on most available terrestrial

vertebrates in their habitats. In contrast, some species exhibit strict host specificity, adapting to feed on a single or very few host species (5, 6). Most ixodid ticks use two or three different hosts throughout their life cycle, with each developmental stage taking a single blood meal (with the exception of males). They attach to the hosts skin, penetrate it using their hypostome and chelicerae, then extract blood from the host, through a process called engorgement. Fully engorged ticks detach from the host in specific areas, they molt into the next development stage (larva to nymph to adult) or lay eggs (females) and die. Throughout this process, ticks may transmit pathogens (viral, bacterial or protozoan) between hosts, playing a crucial role in the epidemiology of vector-borne diseases (7, 8). Ticks are likely the most important vectors of pathogens in the temperate regions and show constant adaptation to changing climatic and biotic conditions, thus being in the forefront of zoonotic disease emergence (9).

Bats are among the most widespread terrestrial mammals, with high mobility and species diversity and they are important ecosystem service providers, too (8). They also may serve as important reservoir hosts for a wide range of pathogens, including viruses, bacteria, and parasites, some of which have the potential to spill over into livestock or human populations and cause emerging infectious diseases (10).

Recent studies of bat associated ectoparasites showed that these may carry DNA of a diverse array of viral, bacterial or protozoan pathogens, some with proven zoonotic character (11), although most remain uncharacterized (12–15). Among these, DNA of several pathogenic bacteria was identified in bat specialist ticks in Europe, Africa but also in the New World (16). In addition, ixodid ticks of Palearctic bats were suggested to play a role in the cycles of several groups of protozoa (17) and viruses (18). Two of the three bat specialist ticks occurring in the Western Palearctic are known to attack humans as well (19, 20). Furthermore, research on bat ticks is important from a taxonomic point of view, as reflected by the descriptions of six new bat-specialist ticks from Europe and Asia during the last decade (21–25), while current assessments are neglected in the region (26). In conclusion, the knowledge of bat-tick relations may provide valuable insights into the mechanisms driving host–parasite interactions and the importance of bat and tick populations in the ecology and spatial evolution of pathogens they may harbor. Here we intend to construct a general spatial distribution of hard ticks hosted by bats in the Western Palearctic, using georeferenced occurrences (mostly published in literature, but also from databases and some unpublished, own records) of specialist and generalist ixodid ticks registered on bats (or in case of bat specialist ticks in bat roosts). In addition, we intend to characterize the role of both the host-, as well the tick ecology may play in building these relations, with a special focus on their role in vector-borne pathogen spread.

Methods

Database creation

Our methodology followed a three-step process. First, a keyword search was performed using terms as: 'ticks' or 'Ixodidae' + 'bats', + 'Western Palearctic', or '*Ixodes ariadnae*'/'*Ixodes simplex*' and '*Ixodes vespertilionis*' + 'Western Palearctic' in the following literature databases: PUBMED, Web of Science and Google Scholar. In the next step, duplicates were eliminated, and abstracts were verified to contain relevant data. This process resulted in a database of suitable papers. Subsequently, copies of the original publications were obtained and the references cited in these works were traced. This process was repeated until no new references were found. In the third step we extracted each individual host-tick record from the references, noting the location, date, host and parasite species, development stage (for ticks) and pathogen (if) mentioned. To complete the collated records, we traced museum specimen collections and observation records using data repositories like Global Biodiversity Information Facility,[1] Obervation.org and NBN Atlas,[2] among others. Direct internet searches using the same keywords also provided hits, verified by photos of the tick species. Unpublished data from our field studies in Algeria, Bulgaria, Hungary, and Romania (2019–2023) were also included. These records were introduced into a database and individually georeferenced to create distribution maps.

Distribution maps

For the maps, we overlaid the range of each host species with the presence data for each tick species. Each host range was set with transparency, so the more ranges overlapped, the more intense the range color appeared—a proxy for multiple host species presence. For the primary bat host species, we used freely

1 www.gbif.org

2 https://spatial.nbnatlas.org/

TABLE 1 Bat-specialist ticks recorded in the Western Palearctic.

Tick species	Free stages	Collected from host	Total number of host species	Number of primary host species	Number of non-primary hosts	Non-bat host species	Unknown/ Undefined host	Total
Ixodes ariadnae	25	107	15	6	9	0	0	132
Ixodes simplex	663	3,149	14	1	13	2	4	3,816
Ixodes vespertilionis	2,546	2,323	30	5	25	4	88	4,957
Total	3,234	5,579	31			4	92	8,905

Number of records with known hosts, free stages and host-types.

10.3389/fvets.2025.1517704

TABLE 2 Primary and non-primary bat host species of hard ticks (Ixodidae) in the Western Palearctic.

Tick species	Primary host species	Non-primary host species	Non-bat hosts
Ixodes ariadnae	*Myotis alcathoe* *Myotis bechsteinii* *Myotis daubentonii* *Myotis emarginatus* *Myotis myotis* *Plecotus auritus*	*Barbastella barbastellus* *Myotis blythii* *Myotis brandtii* *Myotis dasycneme* *Myotis nattereri* *Pipistrellus pygmaeus* *Rhinolophus ferrumequinum,* *Rhinolophus hipposideros* *Rhinolophus mehelyi*	–
Ixodes simplex	*Miniopterus schreibersii*	*Myotis alcathoe* *Myotis bechsteinii* *Myotis blythii* *Myotis daubentonii* *Myotis emarginatus* *Myotis myotis* *Myotis nattereri* *Nyctalus leisleri* *Pipistrellus kuhlii* *Rhinolophus euryale* *Rhinolophus ferrumequinum* *Rhinolophus hipposideros* *Rhinolophus mehelyi*	*Homo sapiens* *Canis lupus familiaris*
Ixodes vespertilionis	*Myotis myotis* *Myotis punicus* *Rhinolophus euryale* *Rhinolophus ferrumequinum* *Rhinolophus hipposideros*	*Asellia tridens* *Barbastella barbastellus* *Eptesicus serotinus* *Miniopterus schreibersii* *Myotis alcathoe* *Myotis bechsteinii* *Myotis blythii* *Myotis brandtii* *Myotis capaccinii* *Myotis dasycneme* *Myotis daubentonii* *Myotis emarginatus* *Myotis mystacinus* *Myotis nattereri* *Nyctalus noctula* *Pipistrellus kuhlii* *Pipistrellus pygmaeus* *Pipistrellus nathusii* *Pipistrellus pipistrellus* *Plecotus auritus* *Plecotus austriacus* *Rhinolophus blasii* *Rhinolophus mehelyi* *Rhinopoma muscatellum* *Vespertilio murinus*	*Homo sapiens* *Canis lupus familiaris* *Equus caballus* *Sus scrofa*

(Continued)

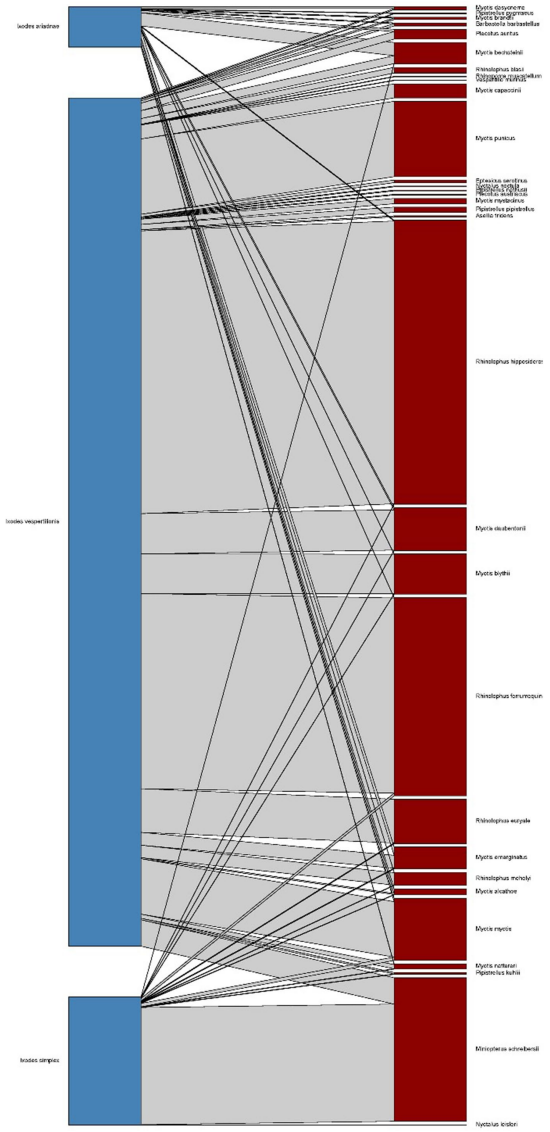

FIGURE 1
Bipartite representation of the parasite network of bats and their specific hard ticks using a quantitative interaction web based on individual host–parasite relations. Links between nodes represent the sum of individual bat tick occurrences for a given bat and tick species couple (*blue* bars – bat species, *dark red* bars – tick species, *grey* bars – host-parasite links).

available shapefiles from the International Union for Conservation of Nature (IUCN) Red List (27). IUCN ranges were used previously primarily for conservation biology of bats (28) or other mammals (29), but also for establishing the relationships between bats and argasid soft ticks (30), as well for bats' insect ectoparasites and vectored pathogens (31). In the next step, we intersected these ranges with the contour of the Western Palearctic, which was delimited according to previously published borders (30, 32, 33).

Host–parasite relationships

Using the database, we mapped each host–parasite relationship and classified hosts as primary or accidental. To determine

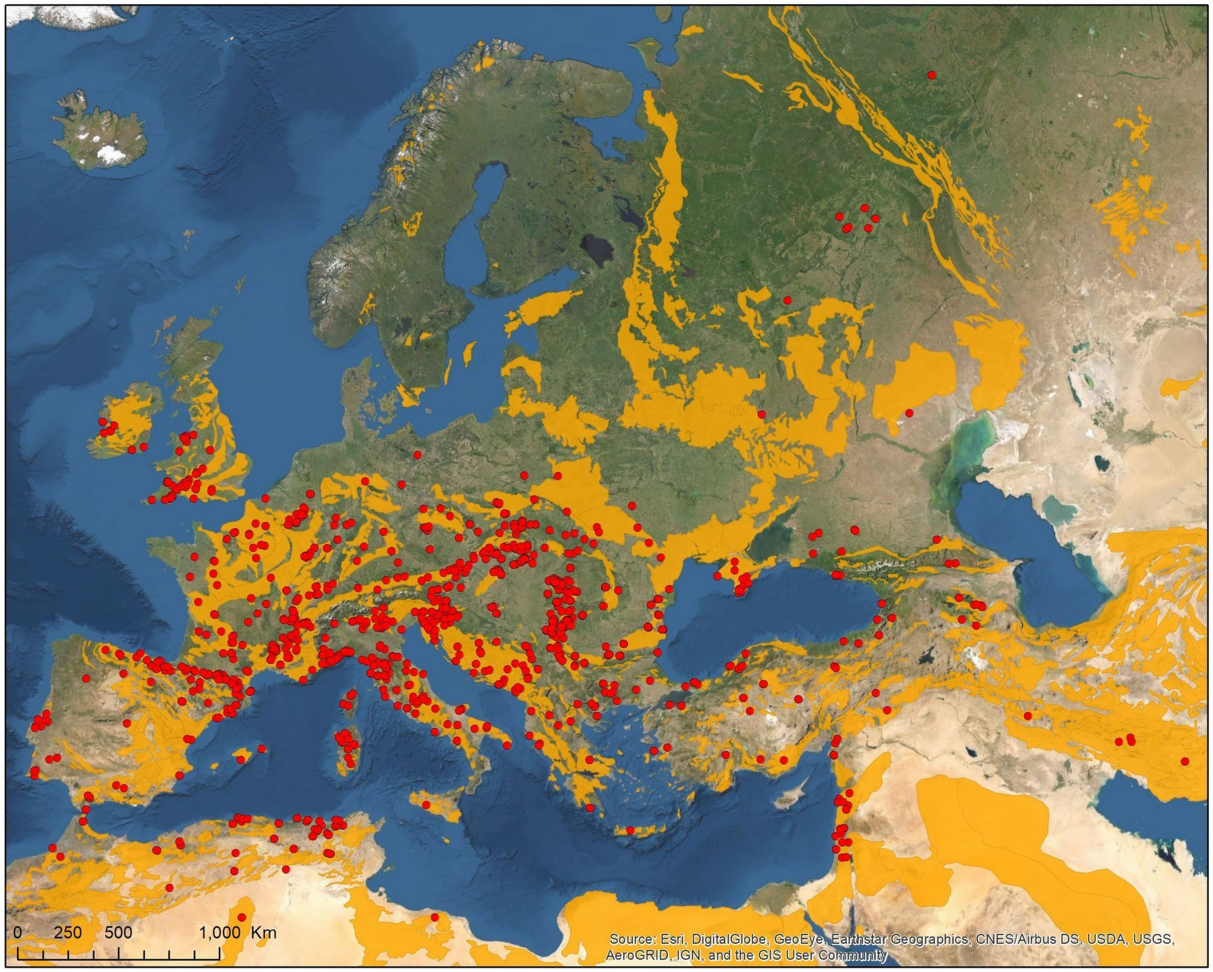

FIGURE 2
Geographic distribution of host-specialist bat ticks in the Western Palearctic (lime stone bedrock in *yellow*).

primary or accidental hosts of any ixodid tick species, we applied an arbitrary rule: any bat species with more than 5.0% of the records for a particular tick species was considered a primary host. Hosts with fewer than 5.0% of cumulative records for a particular tick species were considered non-primary or accidental hosts, following a system previously proposed for bat-fly associations (34–36). Additional host-related information, such as roosting sites or reproductive stages, was also extracted from the primary publications where available. Hosts were assigned either into cave-dwelling, or crevice dwelling group, based on their roosting preferences in their active period (37).

Results

In total, 507 published references were included in the primary reference database (Supplementary Table S1), of which 317 contained records of bat ticks. Additionally, 27 records were extracted from online sources, supplemented by 207 unpublished host–parasite records from the authors. The bat host—tick reference database contains 3,965 individual entries (Supplementary Table S1), with the three bat-specialist ticks making up to 97.3% of the total (Table 1), while ticks with generalist host selection were recorded on bats in 110 instances (Supplementary Table S1). The complete database contains 3,855 entries of bat specialist ticks (8,997 individual ticks), collected from 3,162 individual bat hosts (5,680 ticks), together with a total of 730 instances of ticks collected from the environment (3,225 individuals of unengorged, free ticks, collected generally from underground roosts' walls), while collection circumstances were unknown for 92 cases ($n = 92$ ticks, only tick species and geographic location were recorded). Altogether 31 bat species were recorded to host bat-specialist ticks, with most records noted for *I. vespertilionis* (Table 1). For 24 cases, records mentioned only generic 'Chiroptera,' while 10 cases were assigned to either *Myotis* spp., *Pipistrellus* spp., or *Plecotus* spp. Only 2 cases (0.005% of all records) involved bat ticks found on non-bat hosts—both on humans. Genetic analysis of previous blood meals identified nine cases of non-bat hosts across two tick species (all host species are listed in Table 2).

Ixodes vespertilionis had the most diverse host spectrum, with 30 different host species (5 primary and 25 non-primary hosts). *Ixodes ariadnae* had the most primary hosts (6), while *I. simplex* had a single primary host harboring 98.43% of all records. Most

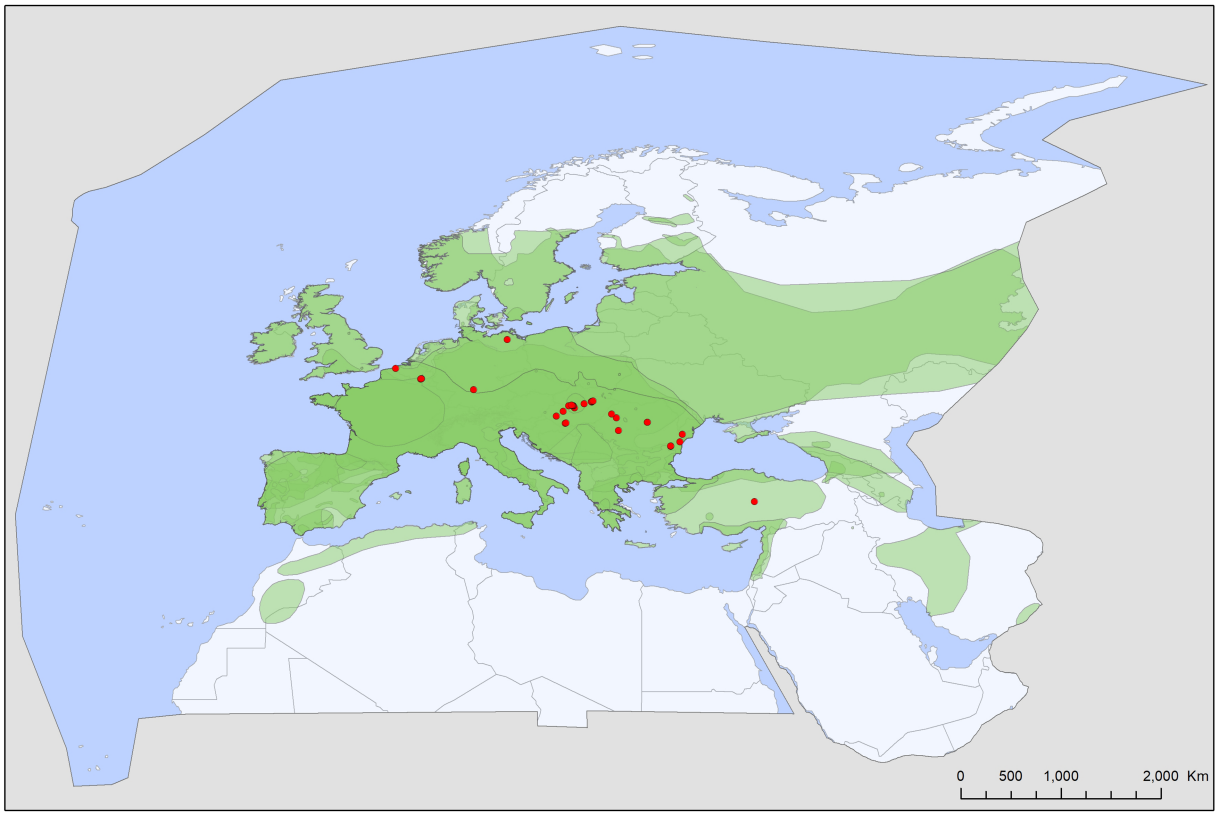

FIGURE 3
Geographic distribution of *Ixodes ariadnae* records in the Western Palearctic, overlaid to the geographic ranges for the six bat species studied as primary hosts (*Myotis alcathoe*, *M. bechsteinii*, *M. daubentonii*, *M. emarginatus*, *M. myotis*, *Plecotus auritus*) of this tick. Transparent layers were mapped on top of one another to highlight regions with dense range overlap.

ticks were recorded on cave-dwelling bat species (93.6%), with a single species (*I. ariadnae*) occurring regularly on crevice-dwelling bat hosts (these include species which rely on rock-crevices, but also tree-hole roosting ones).

Host-collected ticks were mainly subadult stages (90.2%), together with 537 adult females (9.7%) and 10 males collected from hosts (only in case of *I. vespertilionis* were males found on bats). The different tick species showed distinct host selection, with small overlap in host palette, mainly among hosts of *I. ariadnae* and *I. vespertilionis* (Figure 1). Free-stages of bat-specialist ticks were represented mainly by adults and were dominated by *I. vespertilionis* (675 individual records of 2,547 ticks, 78.7% of all free ticks), with a highly biased sex ratio toward males (1–2.32). Records of free individuals for the other two species are rare or accidental (Table 1). *Ixodes simplex* showed highly aggregated off-host presence (a single visit to a site used as nursery colony by *M. schreibersii* in the previous year resulted in 554 ticks collected from a crevice with an area of ca. 0.02 sqm, involving all tick developmental stages and sexes), but altogether only 23 instances of free individuals are known.

Tick records showed wide geographic distribution, with range overlap in Central Europe and the Mediterranean for all three species (Figures 2–6). There was a considerable overlap between the distribution of the primary hosts and the range of *I. simplex* (Figure 4) and *I. vespertilionis* (Figure 5). *Ixodes ariadnae* shows the smallest range (Figure 3), followed by *I. simplex* (Figure 4) and *I. vespertilionis* (Figure 5). Two of the three species also occurred south of the Mediterranean Sea, in Africa, though all records of *I. ariadnae* lay in Central Europe and the Middle East (Anatolia). Most host-collected ixodid ticks came from bats caught close to underground roosts (90.2%), regardless of whether the hosts were cave-dwellers (91.3%, $n = 2{,}367$) or crevice dwellers (79.3%, $n = 517$). Records of hard ticks on crevice dwellers were made mainly in the autumn (71% of all records in August–October). A single tick species, *I. ariadnae*, showed strong seasonality, with 93.4% of records occurring from August to October. Adult females of *I. simplex* also showed clumped seasonal occurrence, with over 62% collected in spring (April–June), although only 22% of tick-infested hosts were recorded in spring. We found no marked seasonal differences in the distribution of *I. vespertilionis* collected from hosts, though slightly more records came from spring. Two bat-specialist tick species were found on humans (*I. simplex* and *I. vespertilionis*, each in a single instance). Both species were also collected from dogs, and *I. vespertilionis* was found on horses and wild boars.

This survey recorded 110 host–parasite associations involving 27 bat species and other tick species (18 species, 149 individuals; Table 3). Most of these records involved generalist ticks, e.g., *Ixodes ricinus* (61 cases, 90 individuals, 60.4% of non-specialist tick records) and *Rhipicephalus sanguineus s.l.* (31 cases, 46 individuals, 30.8% of non-specialist tick records; Figures 6, 7). Even

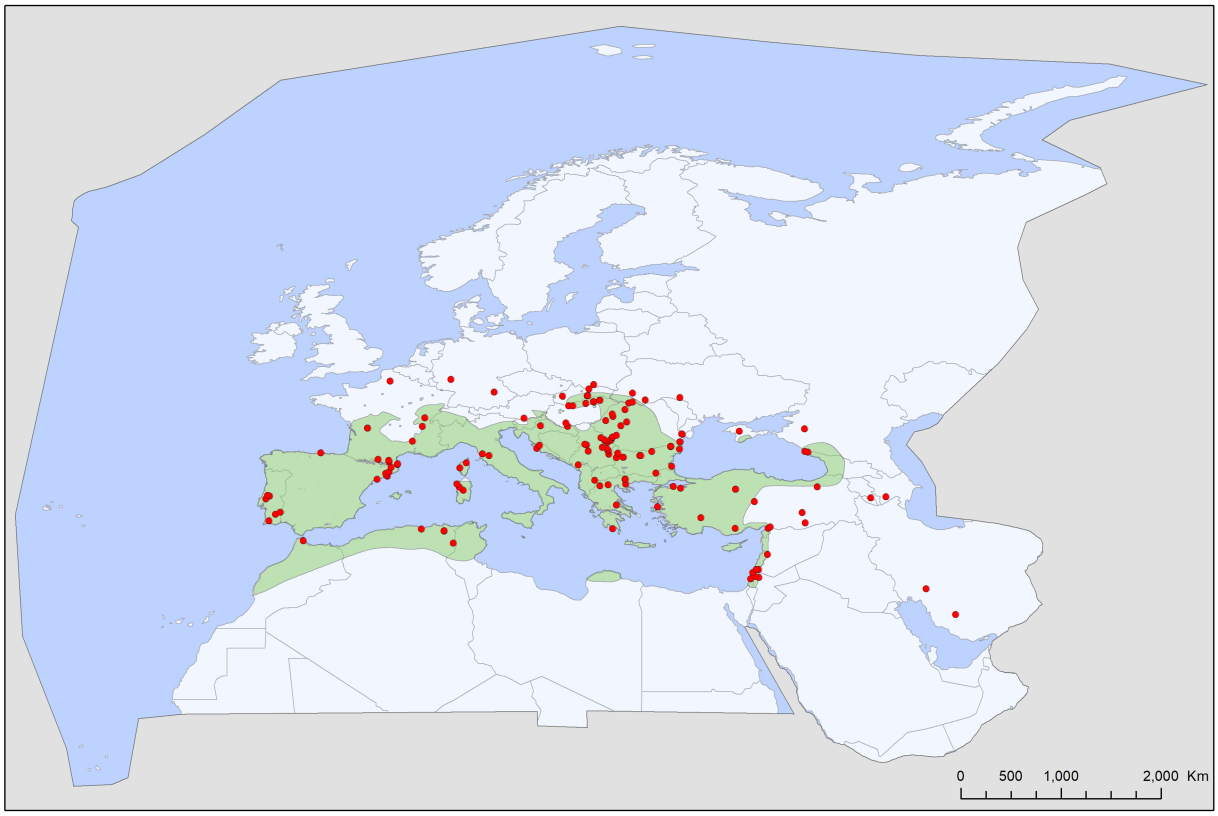

FIGURE 4
Geographic distribution of *Ixodes simplex* records in the Western Palearctic, overlaid to the geographic range for its primary host species, *Miniopterus schreibersii*.

bird-specialists (*I. arboricola*, *I. lividus*) or rodent-specialists (*I. redikorzevi*, *I. trinaguliceps*) were occasionally recorded. The geographic range of generalist tick records showed a primarily southern distribution, with most being collected in the western part of the Mediterranean region (Figure 7). Wide-range, generalist ticks (*I. ricinus* and *R. sanguineus s.l.*) were mostly found on larger, heavier bat species (mean body weight for these hosts was 16.75 g vs. 15.16 g for the rest of generalist tick's host). These ticks were evenly distributed all over the region (Figure 7, red dots), on both crevice-and cave-roosting species, with *Pipistrellus pipistrellus* hosting the most tick species (7 tick species), while most ticks were collected from *M. myotis* (16 cases) and *M. schreibersii* (11 records).

Several viral, bacterial, and apicomplexan pathogens were identified in all three bat specialist tick species. DNA of at least eight bacteria, six piroplasmids, a haemosporidian and five viruses were identified in *I. simplex*, with similar number of bacteria, but less diverse apicomplexan and virus presence in *I. vespertilionis*. The least studied species (*I. ariadnae*, four studies), harbored DNA of two bacteria and a single piroplasmid (Table 4).

Discussion

Our survey identified three ixodid ticks specialized on bats in the Western Palearctic, all of which belong to the genus *Ixodes*. These ticks were recorded from 31 bat species in the region (approximately 40% of all regularly occurring bats; Table 2), with hosts belonging to several bat families, including Hipposideridae, Miniopteridae, Molossidae, Rhinolophidae, Rhinopomatidae, and Vespertilionidae (37). The ticks primarily target cave-dwelling bat species (>90% of tick records with known hosts; see Table 2; Supplementary Table S1) but were also collected from crevice-dwellers during the swarming or hibernation periods when these bats regularly use underground habitats (37). Records of free stages for all three species were exclusively made underground, either inside active bat roosts in caves and mines (98.5%) or in large buildings and cellars with similar environmental conditions, often used by the same bat species. This co-occurrence is likely a result of shared evolutionary history or ecological limiting factors. *Ixodes ariadnae, I. simplex* and *I. vespertilionis* are close relatives, all three belong to the morphologically well documented *Pholeoixodes* subgenus, and their divergence supposedly happened only after a host shift of their common ancestor, likely originating from birds (38, 39). Ecological factors related to the hosts may also contribute to this sympatric occurrence, limiting tick-host interactions to specific spatial environments. All but one cave-dwelling bat species in the Western Palearctic are insectivorous (the fruit-eating *Rousettus aegyptiacus* is the exception, though no ixodid tick has been recorded from this bat). These bats spend most of their time in active flight away from roosts, spatially limiting the opportunity for ticks to access potential hosts to the interiors of the underground roosts.

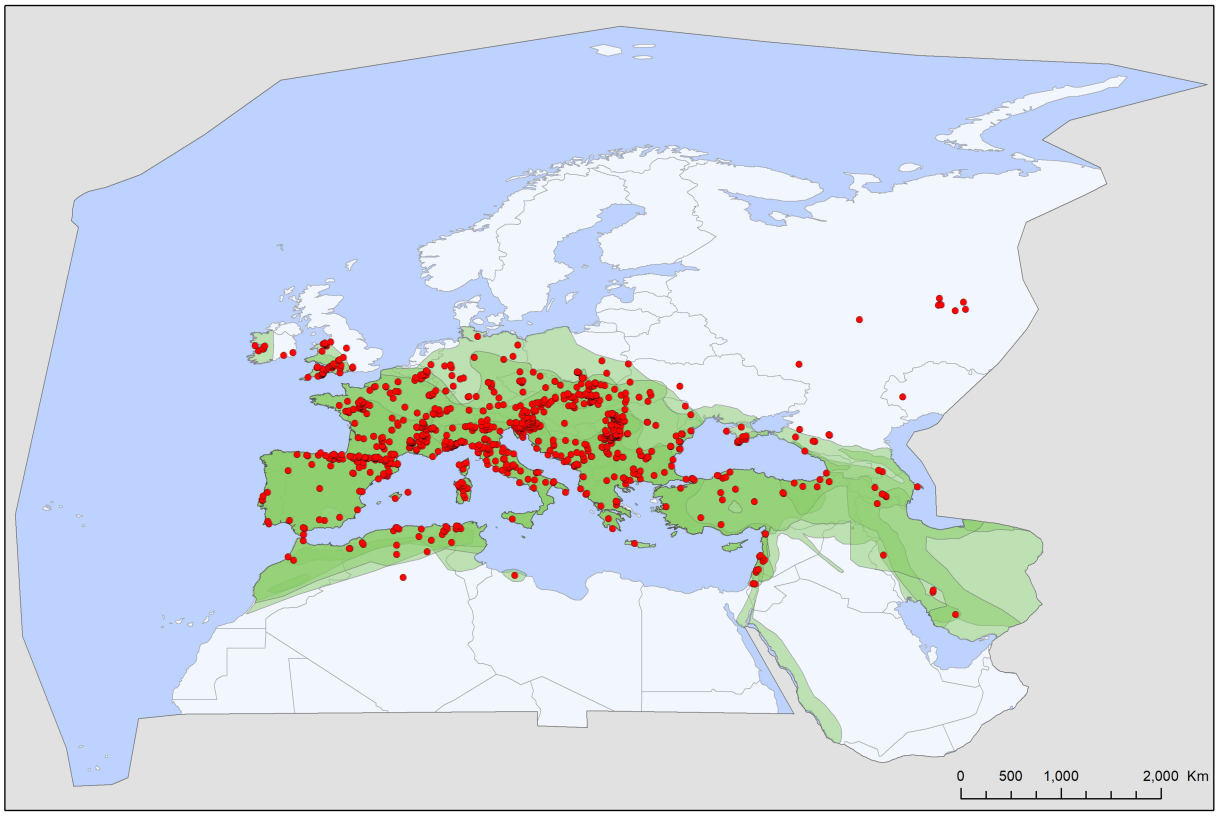

FIGURE 5
Geographic distribution of *Ixodes vespertilionis* records in the Western Palearctic, overlaid to the geographic ranges for the five bat species studied as primary hosts (*Myotis myotis, M. punicus, Rhinolophus euryale, R. ferrumequinum, R. hipposideros*) of this tick. Transparent layers were mapped on top of one another to highlight regions with dense range overlap. Some host species have additional range overlap in Africa and Central and South Asia.

Bat specialist ixodid ticks show wide distribution, two species occurring all over Europe, North Africa and the Middle East, however, the recently described *I. ariadnae* (21) was not yet found in Africa (Figure 3). The ranges of all three species overlap in Central and Eastern Europe and the Middle East, while only *I. vespertilionis* is found at northern latitudes, and *I. ariadnae* was not reported from most Mediterranean regions. There is significant overlap in the host spectrum of *I. ariadnae* and *I. vespertilionis*, with *Myotis myotis* serving as an important host for both species (Figure 1). The overlap with the hosts of *I. simplex* is less pronounced (Table 5) due to the strict host specificity of this species, which primarily parasitizes *M. schreibersii* (40, 41). Two tick species show distributions that extend well beyond the range of their primary bat host (Figures 4, 5), however, the range of *I. ariadnae* is far reduced in comparison to its primary hosts' range, with documented records laying only in the central part of the overlapping range of its primary hosts (Figure 3). We suggest that this may be caused by several factors, like potential misidentification (for example the critical evaluation of samples collected and formerly identified as *I. vespertilionis* may complete this picture) and by reduced sampling effort in the main occurrence season (the species shows high seasonality in occurrence, limiting the chances of on-host capture, see also (40)).

The geographical distribution of *I. ariadnae* and *I. vespertilionis* only partially overlaps with the distribution of their main hosts (Figures 3, 5). This discrepancy is likely due to other limiting factors beyond host range, such as climatic conditions, which may differ at the southern and northern borders of their ranges. However, the presence of bat-specialist ticks is likely not directly limited by climate, as these ticks are primarily found off-host inside underground roosts with optimal climatic conditions. This pattern is clearly visible in Figure 2, where tick distribution is plotted against limestone bedrock, which hosts more than 91% of tick occurrences due to the presence of karst formations (caves).

Ixodes vespertilionis has the largest distribution range, extending from Britain in the west to the Urals in the east and covering North Africa and the Middle East (Figure 5). The easternmost limit likely extends beyond the borders of the Western Palearctic. However, recent assessments of *I. vespertilionis* specimens from the Eastern Palearctic and Oriental regions revealed several new species (23, 24). This species is primarily associated with horseshoe bats (*Rhinolophus* spp.) but is also a common parasite of the three large *Myotis species* (*M. blythii, M. myotis*, and *M. punicus*). It is also scarcely recorded on other vesper bats which frequent caves (Table 5 and Figure 1), fact which may help to interpret its occurrences far from the main hosts' range (Figure 5). The species accounts for the bulk of unengorged tick records collected in caves, due to its habit of questing on cave walls (40). The highly biased sex ratio of free stages noted in this species may be explained by males not feeding and potentially living longer than females, which die after

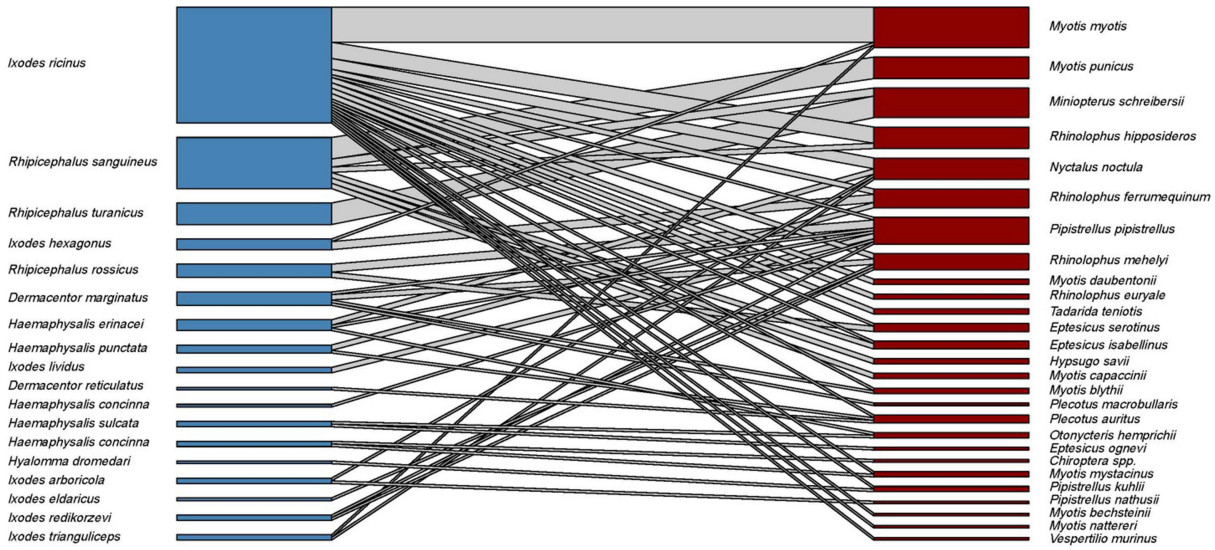

FIGURE 6
Bipartite representation of the parasite network of generalist/non-specialist ticks and their bat hosts using a quantitative interaction web based on individual host–parasite relations. Links between nodes represent the sum of individual bat tick occurrences for a given bat and tick species couple (*blue* bars – bat species, *dark red* bars – tick species, *grey* bars – host-parasite links).

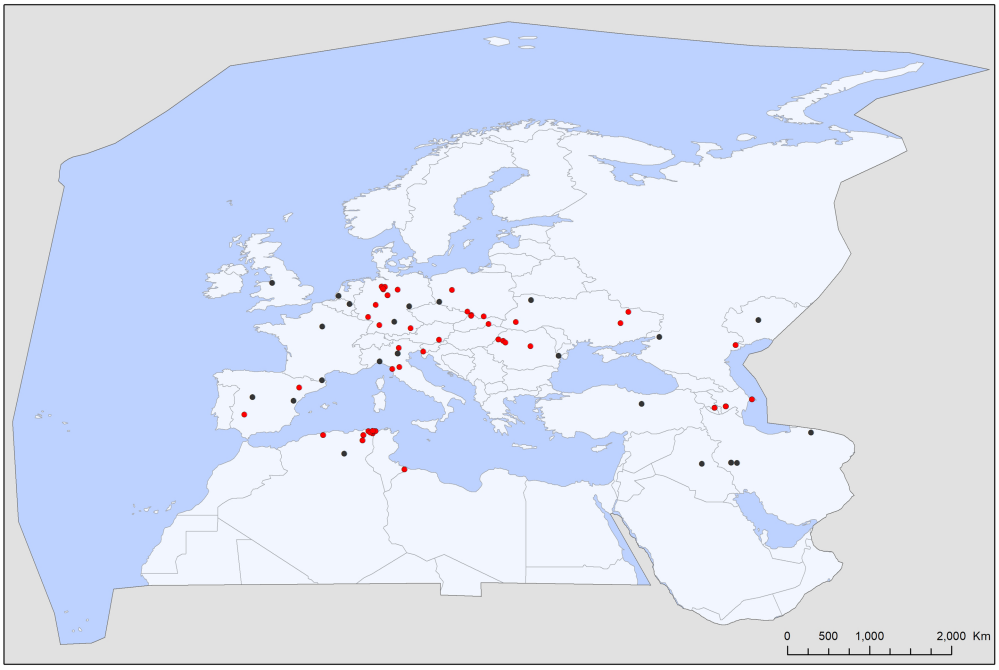

FIGURE 7
Map with the geographic distribution of other tick species (non-bat ticks) recorded on bats in the Western Palearctic.

egg laying (hence more chances of encounter on roost walls). There is a slight seasonality in the occurrence of adult free stages, with more records noted during summer months, though this may be due to more frequent cave visits during this period rather than actual seasonality of the species. Several studies detected DNA of pathogenic bacteria (16, 42–46), piroplasms (17, 47) and viruses (48, 49) in *I. vespertilionis* individuals, both in host collected and free ticks (Table 4). While definitive proof of a vectorial role of this tick species for these pathogens is lacking, its wide distribution, diverse host range, and ubiquitous presence in most bat shelters suggest a significant potential role in pathogen transmission. Moreover, a recent study performing blood-meal analyses managed to detect DNA of non-bat provenience in several adult tick individuals, thus highlighting

10.3389/fvets.2025.1517704

TABLE 3 List of other (generalist or bird specialist) tick species recorded on bats, with bat host species and number of occurrences.

Tick species	Host species	Number of cases
Dermacentor marginatus	*Myotis blythii*	1
	Pipistrellus pipistrellus	1
	Plecotus macrobullaris	1
	Rhinolophus mehelyi	2
Dermacentor reticulatus	*Plecotus auritus*	1
Haemaphysalis concinna	*Pipistrellus pipistrellus*	1
Haemaphysalis erinacei	*Nyctalus noctula*	2
	Otonycteris hemprichii	1
	Pipistrellus pipistrellus	1
Haemaphysalis punctata	*Plecotus auritus*	1
	Rhinolophus ferrumequinum	2
Haemaphysalis sulcata	*Eptesicus ognevi*	1
	Otonycteris hemprichii	1
Haemophysalis concinna	*Chiroptera* spp.	1
	Myotis mystacinus	1
Hyalomma dromedari	*Pipistrellus kuhlii*	1
Ixodes arboricola	*Nyctalus noctula*	1
	Pipistrellus nathusii	1
Ixodes eldaricus	*Rhinolophus mehelyi*	1
Ixodes hexagonus	*Myotis myotis*	1
	Rhinolophus ferrumequinum	3
Ixodes lividus	*Pipistrellus pipistrellus*	2
Ixodes redikorzevi	*Pipistrellus pipistrellus*	1
	Rhinolophus mehelyi	1
Ixodes ricinus	*Eptesicus isabellinus*	1
	Eptesicus serotinus	1
	Myotis bechsteinii	1
	Myotis blythii	1
	Myotis daubentonii	2
	Myotis myotis	13
	Myotis mystacinus	1
	Myotis nattereri	1
	Nyctalus noctula	4
	Pipistrellus kuhlii	1
	Pipistrellus pipistrellus	1
	Plecotus auritus	1
	Rhinolophus euryale	2
	Rhinolophus ferrumequinum	2
	Rhinolophus hipposideros	6
	Rhinolophus mehelyi	2
	Tadarida teniotis	2
	Vespertilio murinus	1
Ixodes trianguliceps	*Myotis myotis*	1
	Nyctalus noctula	1
Rhipicephalus rossicus	*Eptesicus serotinus*	2
	Pipistrellus pipistrellus	3
Rhipicephalus sanguineus	*Eptesicus isabellinus*	2
	Hypsugo savii	2
	Miniopterus schreibersii	3
	Myotis capaccinii	2
	Myotis punicus	8
	Rhinolophus hipposideros	2
Rhipicephalus turanicus	*Miniopterus schreibersii*	8

10.3389/fvets.2025.1517704

TABLE 4 DNA of pathogens detected in bat specialist ticks of the Western Palearctic bats.

Tick	Pathogen group	Pathogen species	Reference
Ixodes ariadnae	Bacteria	*Bartonella* sp.	Hornok et al. (43) and McKee et al. (31)
		Wolbachia sp.	Szentiványi et al. (45)
	Piroplasmida	*Babesia vesperuginis*	Hornok et al. (17)
Ixodes simplex	Bacteria	*Mycoplasma* spp.	Hornok et al. (16), Corduneanu et al. (11) and Wang et al. (51)
		Anaplasma phagocytophilum	Hornok et al. (16)
		Anaplasma ovis	Moraga-Fernández et al. (18)
		Bartonella spp.	Hornok et al. (16)
		Rickettsia slovaca	Moraga-Fernández et al. (18)
		Rickettsia aeschlimanii	Moraga-Fernández et al. (18)
		Coxiella burnetii	Moraga-Fernández et al. (18)
		Occidentia massiliensis	Moraga-Fernández et al. (18)
		Neoehrlichia mikurensis	Szentiványi et al. (45)
	Piroplasmida	*Babesia crassa*	Hornok et al. (17)
		Babesia venatorum-like	Hornok et al. (17)
		Babesia canis	Hornok et al. (17)
		Theileria capreoli	Hornok et al. (17)
		Theileria orientalis	Hornok et al. (17)
		Theileria sp. OT3	Hornok et al. (17)
	Haemosporida	*Polycromophilus melanipherus*	Sándor et al. (30)
	Virus	Jingmen tick virus	Dincer et al. (52)
		Lloviu virus	Kemenesi et al. (53)
		Flavivirus	Moraga-Fernández et al. (18)
		Crimean Congo Hemoragic Fever virus	Moraga-Fernández et al. (18)
		Nairovirus	Moraga-Fernández et al. (18)
		Orthonairovirus	Moraga-Fernández et al. (18)
Ixodes vespertilionis	Bacteria	*Bartonella* sp.	Hornok et al. (16, 43) and Szentiványi et al. (45)
			Hornok et al. (16)
			Szentiványi et al. (45)
		Bartonella tamiae	Leulmi et al. (44)
		Wolbachia sp.	Hornok et al. (43)
			Tian et al. (46)
		Rickettsia sp.	Tian et al. (46)
		Rickettsia africae	Tian et al. (46)
		Coxiella burnettii	Leulmi et al. (44)
		Coxiella sp.	Tian et al. (46)
		Neoehrlichia mikurensis	Szentiványi et al. (45)
		Midichloria sp.	Cafiso et al. (42)
	Haemosporida	*Polycromophilus murinus*	Sándor et al. (30)
	Piroplasmida	*Babesia vesperuginis*	Hornok et al. (17)
		Babesia crassa	Hornok et al. (17)
	Virus	Iflavirus IvespIV	Daveu et al. (48)
		Issyk-Kul virus	L'vov et al. (49)

TABLE 5 List of bat species (Chiroptera) and their role as primary and non-primary bat-specialist hard tick (Ixodidae) hosts in the Western Palearctic (N—number of hosts with ticks).

Bat species	N	Primary tick species	Non-primary tick species
Asellia tridens	2	–	*Ixodes vespertilionis*
Barbastella barbastellus	7	–	*Ixodes ariadnae, Ixodes vespertilionis*
Eptesicus serotinus	8	–	*Ixodes vespertilionis*
Miniopterus schreibersii	1,507	*Ixodes simplex*	*Ixodes vespertilionis*
Myotis alcathoe	13	*Ixodes ariadnae*	*Ixodes ariadnae, Ixodes vespertilionis*
Myotis bechsteinii	35	*Ixodes ariadnae*	*Ixodes ariadnae, Ixodes vespertilionis*
Myotis blythii	54	–	*Ixodes ariadnae, Ixodes simplex, Ixodes vespertilionis*
Myotis brandtii	6	–	*Ixodes ariadnae, Ixodes vespertilionis*
Myotis capaccinii	19		*Ixodes vespertilionis*
Myotis dasycneme	8	–	*Ixodes ariadnae, Ixodes vespertilionis*
Myotis daubentonii	86	*Ixodes ariadnae*	*Ixodes simplex, Ixodes vespertilionis*
Myotis emarginatus	68	*Ixodes ariadnae*	*Ixodes simplex, Ixodes vespertilionis*
Myotis myotis	195	*Ixodes ariadnae, Ixodes vespertilionis*	*Ixodes simplex*
Myotis mystacinus	44	–	*Ixodes vespertilionis*
Myotis nattereri	37	–	*Ixodes ariadnae, Ixodes simplex, Ixodes vespertilionis*
Myotis punicus	186	*Ixodes vespertilionis*	–
Nyctalus leisleri	2	–	*Ixodes simplex, Ixodes vespertilionis*
Nyctalus noctula	2	–	*Ixodes vespertilionis*
Pipistrellus kuhlii	5	–	*Ixodes simplex, Ixodes vespertilionis*
Pipistrellus nathusii	2	–	*Ixodes vespertilionis*
Pipistrellus pipistrellus	6	–	*Ixodes vespertilionis*
Pipistrellus pygmaeus	2	–	*Ixodes ariadnae, Ixodes vespertilionis*
Plecotus auritus	17	*Ixodes ariadnae*	*Ixodes vespertilionis*
Plecotus austriacus	2	–	*Ixodes vespertilionis*
Rhinolophus blasii	10	–	*Ixodes vespertilionis*
Rhinolophus euryale	95	*Ixodes vespertilionis*	*Ixodes simplex*
Rhinolophus ferrumequinum	671	*Ixodes vespertilionis*	*Ixodes ariadnae, Ixodes simplex*
Rhinolophus hipposideros	463	*Ixodes vespertilionis*	*Ixodes ariadnae, Ixodes simplex*
Rhinolophus mehelyi	24	–	*Ixodes ariadnae, Ixodes simplex*
Rhinopoma muscatellum	1	–	*Ixodes vespertilionis*
Vespertilio murinus	1	–	*Ixodes vespertilionis*

the chances for pathogen transfer between wide range of host species (31 known species of bat hosts) and other mammals (e.g., dogs, horse and wild boar, (45)), or humans (19).

Ixodes simplex is a nest-dwelling tick, highly gregarious by nature, staying hidden in crevices near its main host colonies (*M. schreibersii*) (40). It is strictly host-specific, being parasitic almost exclusively on *M. schreibersii* and rarely found on other bat species (<1.5% of occurrences collected from 13 different bat species, mainly cave-dwellers roosting in sympatry with *M. schreibersii*). The geographic distribution strongly overlaps with the main distribution of its host, showing a strong mutual relationship with this bat species. Northern outlier records were reported from areas where its host was present in the past (50), while records in the Middle East mostly represent observations on its sister species, the pale bent-winged bat (*Miniopterus pallidus*). It is common on its hosts, occurring in every roost regularly used by *M. schreibersii*, showing a constant presence and likely influencing the spatial organization of these bats (41). This tick shows high seasonality in its on-host occurrences, with the highest prevalence and intensity recorded in spring/early summer, sometimes causing detrimental effects on specific host individuals (20). While *I. simplex* is suspected to vector several bacterial (11, 16, 18, 45, 51), parasitic (17, 47), and viral pathogens (18, 52, 53), there is no unequivocal proof for these roles.

Ixodes ariadnae was recently described from Central European bats (21, 38) and remains a rare bat ectoparasite, with most records geographically limited to a narrow east–west belt between 44° and 51°N latitude, primarily in Europe. Compared to the distribution range of its primary hosts, *I. ariadnae* shows a highly reduced distribution area. We suggest that this range reflects the spatial extent of recent bat-tick studies rather than the actual distribution, which is expected to increase with future research efforts. This species displays strong seasonality, with 92.2% of host-collected ticks recorded during

August–September, coinciding with the autumn swarming of bats (45). While there are fewer than 100 records of *I. ariadnae*, it has a relatively diverse host range, with 15 known bat hosts (Figure 1; Tables 1, 2). Most hosts (n = 10, 67%) are crevice-dwelling forest bats, which only use underground roosts during swarming or hibernation. Questing adults of *I. ariadnae* were mainly collected during winter months, though this is likely due to limited access to cave sections occupied by this species (S. Hornok, pers. comm.) rather than true seasonal activity peaks. Only a handful of studies have recorded pathogens in *I. ariadnae* (Table 4), detecting DNA from bacteria (16, 31, 45) and piroplasms (17).

All, but one Western Palearctic bat species are insectivorous and most species are hunting during flight, relying mainly on insects in flight. In consequence, ticks not using caves or other bat roosts rarely gain access to bat hosts. Thus, presence of generalist ticks on bats is a rare phenomenon, with <1.7% of all tick encounters related to bats represent other species than the three bat-specialist *Ixodes*. Truly generalist ticks (*I. ricinus, R. sanguineus* s.l.) made up the bulk of these records and these mainly targeted large-bodied species regularly hunting on the ground (*M. blythii, M. myotis*, and *M. punicus*). Other tick species are rarely recorded on bats and are mostly accidentals. Some of these ticks are bird-specialist nest-dwellers, e.g., *I. arboricola* (regular in tree crevices and bird nest boxes) or *I. lividus* (a tick species using nest-holes dug by sand martins, *Riparia riparia* (54)), species which may get access to bats roosting in these bird-nests. Other species are ticks associated to carnivora, which regularly occur in caves (*Haemaphysalis erinacei* and *I. hexagonus* (55)).

Bats are frequently parasitized by ticks, and these ticks can host pathogenic bacteria, parasites, or viruses. Certain bat species may act as bridging hosts, carrying not only bat-specialist ticks but also generalist ticks, thus they may have a particular importance from One Health perspective (56). Additionally, a recent study detected high levels of non-bat host DNA in free-living bat ticks, further highlighting the potential for bridging bat-related pathogens to other hosts.

Data availability statement

The original contributions presented in the study are included in the article/Supplementary material, further inquiries can be directed to the corresponding author.

Ethics statement

The animal study was approved by Underground Heritage Commission (Romania) and the Bulgarian Ministry of Environment and Water (permit no. 718/24.08.2017 and 973/14.04.2023). Bat banding license numbers are 305/2015, 46/2016, 24/2017, 111/2018, 103/2019, 81/2021, and 122/2022. The study was conducted in accordance with the local legislation and institutional requirements.

Author contributions

AS: Conceptualization, Data curation, Formal analysis, Funding acquisition, Investigation, Methodology, Project administration, Resources, Writing – original draft, Writing – review & editing. CD: Formal analysis, Investigation, Methodology, Visualization, Writing – original draft, Writing – review & editing. ÁP: Conceptualization, Data curation, Formal analysis, Investigation, Methodology, Resources, Visualization, Writing – review & editing. SH: Conceptualization, Data curation, Funding acquisition, Investigation, Methodology, Project administration, Resources, Supervision, Writing – review & editing.

Funding

The author(s) declare that financial support was received for the research and/or publication of this article. While working for this study, AS and SH were funded by the Office for Supported Research Groups, Hungarian Research Network (HUN-REN), Hungary (Project No. 1500107), and also supported by OTKA K-132794 of the National Research, Development and Innovation Office. ÁP was supported by the PD143382 NKFIH postdoctoral grant.

Acknowledgments

We thank for help provided by T. Szentiványi, M.L. Bendjeddou and M. Sevcik in gathering hard-to-find references.

Conflict of interest

The authors declare that the research was conducted in the absence of any commercial or financial relationships that could be construed as a potential conflict of interest.

The author(s) declared that they were an editorial board member of Frontiers, at the time of submission. This had no impact on the peer review process and the final decision.

Generative AI statement

The authors declare that no Gen AI was used in the creation of this manuscript.

Publisher's note

All claims expressed in this article are solely those of the authors and do not necessarily represent those of their affiliated organizations, or those of the publisher, the editors and the reviewers. Any product that may be evaluated in this article, or claim that may be made by its manufacturer, is not guaranteed or endorsed by the publisher.

Supplementary material

The Supplementary material for this article can be found online at: https://www.frontiersin.org/articles/10.3389/fvets.2025.1517704/full#supplementary-material

References

1. Randolph SE. Ticks and tick-borne disease systems in space and from space. *Adv Parasitol*. (2000) 47:217–43. doi: 10.1016/S0065-308X(00)47010-7

2. de la Fuente J. The fossil record and the origin of ticks (Acari: Parasitiformes: Ixodida). *Exp Appl Acarol*. (2003) 29:331–44. doi: 10.1023/A:1025824702816

3. Beati L, Klompen H. Phylogeography of ticks (Acari: Ixodida). *Annu Rev Entomol*. (2019) 64:379–97. doi: 10.1146/annurev-ento-020117-043027

4. Guglielmone AA, Robbins RG, Apanaskevich DA, Petney TN, Estrada-Peña A, Horak IG. The hard ticks of the world. Dordrecht: Springer (2014).

5. Nava S, Guglielmone AA, Mangold AJ. An overview of systematics and evolution of ticks. *Front Biosci*. (2009) 14:2857–77. doi: 10.2741/3418

6. Durden LA. Taxonomy, host associations, life cycles and vectorial importance of ticks parasitizing small mammals In: S Morand, BR Krasnov and R Poulin, editors. Micromammals and macroparasites. Tokyo: Springer Japan (2006). 91–102.

7. Sonenshine DE, Roe RM. Biology of ticks, vol. *2*. Oxford: Oxford University Press, USA (2014).

8. McCoy KD, Léger E, Dietrich M. Host specialization in ticks and transmission of tick-borne diseases: a review. *Front Cell Infect Microbiol*. (2013) 3:57. doi: 10.3389/fcimb.2013.00057

9. Parola P, Raoult D. Ticks and tickborne bacterial diseases in humans: an emerging infectious threat. *Clin Infect Dis*. (2001) 32:897–928. doi: 10.1086/319347

10. Poel WHMVD, Lina PHC, Kramps JA. Public health awareness of emerging zoonotic viruses of bats: a European perspective. *Vector-Borne Zoonotic Dis*. (2006) 6:315–24. doi: 10.1089/vbz.2006.6.315

11. Corduneanu A, Zając Z, Kulisz J, Wozniak A, Foucault-Simonin A, Moutailler S, et al. Detection of bacterial and protozoan pathogens in individual bats and their ectoparasites using high-throughput microfluidic real-time PCR. *Microbiol Spectr*. (2023) 11:e0153123. doi: 10.1128/spectrum.01531-23

12. Tuttle MD. Give bats a break: searches for new viruses in bats are unlikely to contribute substantially to human health, but they may threaten the future of bats. *Issues Sci Technol*. (2017) 33:41–51.

13. Zheng X, Zhang X, Huang X, Yue X, Wang Y. Biodiversity of Ectoparasites and molecular detection of Bartonella in Ectoparasites infesting *Rhinolophus Affinis* in Yunnan Province, China. *Pak Vet J*. (2024) 44:699–706.

14. Perumalsamy N, Sharma R, Subramanian M, Nagarajan SA. Hard ticks as vectors: the emerging threat of tick-borne diseases in India. *Pathogens*. (2024) 13:556. doi: 10.3390/pathogens13070556

15. Yu Z, Wang H, Wang T, Sun W, Yang X, Liu J. Tick-borne pathogens and the vector potential of ticks in China. *Parasites Vectors*. (2015) 8:24. doi: 10.1186/s13071-014-0628-x

16. Hornok S, Szoke K, Meli ML, Sándor AD, Görföl T, Estók P, et al. Molecular detection of vector-borne bacteria in bat ticks (Acari: Ixodidae, Argasidae) from eight countries of the old and new worlds. *Parasites and Vectors*. (2019) 12:50. doi: 10.1186/s13071-019-3303-4

17. Hornok S, Szőke K, Kováts D, Estók P, Görföl T, Boldogh SA, et al. DNA of piroplasms of ruminants and dogs in ixodid bat ticks. *PLoS One*. (2016) 11:e0167735. doi: 10.1371/journal.pone.0167735

18. Moraga-Fernández A, Sánchez-Sánchez M, Muñoz-Hernández C, Pardavila X, Sereno-Cadierno J, Queirós J, et al. Beware with the backpack! New hosts and pathogens identified for *Ixodes simplex* ticks collected from bats in the Iberian Peninsula. *Res Vet Sci*. (2024) 176:105316. doi: 10.1016/j.rvsc.2024.105316

19. Piksa K, Nowak-Chmura M, Siuda K. First case of human infestation by the tick *Ixodes vespertilionis* (Acari: Ixodidae). *Int J Acarol*. (2013) 39:1–2. doi: 10.1080/01647954.2012.737831

20. Péter Á, Barti L, Corduneanu A, Hornok S, Mihalca AD, Sándor AD. First record of *Ixodes simplex* found on a human host, with a review of cases of human infestation by bat tick species occurring in Europe. *Ticks Tick-Borne Dis*. (2021) 12:101722. doi: 10.1016/j.ttbdis.2021.101722

21. Hornok S, Kontschán J, Kováts D, Kovács R, Angyal D, Görföl T, et al. Bat ticks revisited: *Ixodes ariadnae* sp. nov. and allopatric genotypes of *I. vespertilionis* in caves of Hungary. *Parasit Vectors*. (2014) 7:202. doi: 10.1186/1756-3305-7-202

22. Hornok S, Kontschán J, Estrada-Peña A, de Mera IGF, Tomanović S, de la Fuente J. Contributions to the morphology and phylogeny of the newly discovered bat tick species, *Ixodes ariadnae* in comparison with *I. vespertilionis* and *I simplex*. *Parasit Vectors*. (2015) 8:47. doi: 10.1186/s13071-015-0665-0

23. Hornok S, Görföl T, Estók P, Tu VT, Kontschán J. Description of a new tick species, *Ixodes collaris* n. sp. (Acari: Ixodidae), from bats (Chiroptera: Hipposideridae, Rhinolophidae) in Vietnam. *Parasit Vectors*. (2016) 9:322. doi: 10.1186/s13071-016-1608-0

24. Takano A, Yamauchi T, Takahashi M, Shimoda H, Gotoh Y, Mizuno J, et al. Description of three new bat-associated species of hard ticks (Acari, Ixodidae) from Japan. *ZooKeys*. (2023) 1180:1–26. doi: 10.3897/zookeys.1180.108418

25. Hornok S, Kontschán J, Takano A, Gotoh Y, Hassanin A, Tu VT. Description of *Ixodes lanigeri* sp nov., a new hard tick species (Acari, Ixodidae) collected from mouse-eared bats (Vespertilionidae, Myotis) in Vietnam. *ZooKeys*. (2024) 1215:107–25. doi: 10.3897/zookeys.1215.123624

26. Bendjeddou ML, Khelfaoui F, Abiadh A, Mechouk N, Mihalca AD, Sándor AD. Bat Ectoparasites (Acari, Diptera, Hemiptera, Siphonaptera) in the grand Maghreb (Algeria, Libya, Mauritania, Morocco and Tunisia): a literature review and new data. *Acta Parasit*. (2024) 69:106–20. doi: 10.1007/s11686-023-00732-8

27. IUCN. The IUCN red list of threatened species. Version 2024–1. (2024). Available at: https://www.iucnredlist.org (Accessed October 21, 2023).

28. Frick WF, Kingston T, Flanders J. A review of the major threats and challenges to global bat conservation. *Ann N Y Acad Sci*. (2019) 1469:5–25. doi: 10.1111/nyas.14045

29. Sándor AD. Underground life is still safest: comments on 'danger underground and in the open – predation on blind mole rats (Rodentia, Spalacinae) revisited'. *Mammal Rev*. (2017) 47:230–5. doi: 10.1111/mam.12089

30. Sándor AD, Mihalca AD, Domşa C, Péter Á, Hornok S. Argasid ticks of Palearctic bats: distribution, host selection, and zoonotic importance. *Front Vet Sci*. (2021) 8:684737. doi: 10.3389/fvets.2021.684737

31. McKee CD, Krawczyk AI, Sándor AD, Görföl T, Földvári M, Földvári G, et al. Host phylogeny, geographic overlap, and roost sharing shape parasite communities in European bats. *Front Ecol Evol*. (2019) 7:69. doi: 10.3389/fevo.2019.00069

32. Ficetola GF, Falaschi M, Bonardi A, Padoa-Schioppa E, Sindaco R. Biogeographical structure and endemism pattern in reptiles of the Western Palearctic. *Prog Phys Geogr Earth Environ*. (2018) 42:220–36. doi: 10.1177/0309133318765084

33. Masseti M, Bruner E. The primates of the western Palaearctic: a biogeographical, historical, and archaeozoological review. *J Anthropol Sci*. (2009) 87:33–91.

34. Patterson BD, Dick CW, Dittmar K. Nested distributions of bat flies (Diptera: Streblidae) on Neotropical bats: artifact and specificity in host-parasite studies. *Ecography*. (2009) 32:481–7. doi: 10.1111/j.1600-0587.2008.05727.x

35. Wenzel RL. The streblid batflies of Venezuela (Diptera: Streblidae). *Brigham Young Univ Sci Bull Biol Ser*. (1976) 20:1–177. doi: 10.5962/bhl.part.5666

36. Sándor AD, Corduneanu A, Hornok S, Mihalca AD, Péter Á. Season and host-community composition inside roosts may affect host-specificity of bat flies. *Sci Rep*. (2024) 14:4127. doi: 10.1038/s41598-024-54143-4

37. Dietz C, von Helversen O, Nill D. Bats of Britain, Europe and Northwest Africa. London: A&C Black. (2009). 1–400 p.

38. Hornok S, Estrada-Peña A, Kontschán J, Plantard O, Kunz B, Mihalca AD, et al. High degree of mitochondrial gene heterogeneity in the bat tick species *Ixodes vespertilionis, I ariadnae* and *I simplex* from Eurasia. *Parasit Vectors*. (2015) 8:457. doi: 10.1186/s13071-015-1056-2

39. Hornok S, Sándor AD, Beck R, Farkas R, Beati L, Kontschán J, et al. Contributions to the phylogeny of *Ixodes (Pholeoixodes) canisuga, I. (Ph.) kaiseri, I. (Ph.) hexagonus* and a simple pictorial key for the identification of their females. *Parasit Vectors*. (2017) 10:545. doi: 10.1186/s13071-017-2424-x

40. Sándor AD, Corduneanu A, Péter Á, Mihalca AD, Barti L, Csősz I, et al. Bats and ticks: host selection and seasonality of bat-specialist ticks in eastern Europe. *Parasit Vectors*. (2019) 12:605. doi: 10.1186/s13071-019-3861-5

41. Sándor AD, Péter Á, Beke B, Boldogh SA, Bücs SL, Hornok S. Ectoparasite-posed risk may affect the spatial organization of hibernating clusters of a social bat. *Preprint*. (2024). doi: 10.21203/rs.3.rs-4141372/v1

42. Cafiso A, Bazzocchi C, De Marco L, Opara MN, Sassera D, Plantard O. Molecular screening for *Midichloria* in hard and soft ticks reveals variable prevalence levels and bacterial loads in different tick species. *Ticks Tick-Borne Dis*. (2016) 7:1186–92. doi: 10.1016/j.ttbdis.2016.07.017

43. Hornok S, Kovács R, Meli ML, Gönczi E, Hofmann-Lehmann R, Kontschán J, et al. First detection of bartonellae in a broad range of bat ectoparasites. *Vet Microbiol*. (2012) 159:541–3. doi: 10.1016/j.vetmic.2012.04.003

44. Leulmi H, Aouadi A, Bitam I, Bessas A, Benakhla A, Raoult D, et al. Detection of *Bartonella tamiae, Coxiella burnetii* and rickettsiae in arthropods and tissues from wild and domestic animals in northeastern Algeria. *Parasit Vectors*. (2016) 9:27. doi: 10.1186/s13071-016-1316-9

45. Szentiványi T, Takács N, Sándor AD, Péter Á, Boldogh SA, Kováts D, et al. Bat-associated ticks as a potential link for vector-borne pathogen transmission between bats and other animals. *PLoS Negl Trop Dis*. (2024) 18:e0012584. doi: 10.1371/journal.pntd.0012584

46. Tian J, Hou X, Ge M, Xu H, Yu B, Liu J, et al. The diversity and evolutionary relationships of ticks and tick-borne bacteria collected in China. *Parasit Vectors*. (2022) 15:352. doi: 10.1186/s13071-022-05485-3

47. Sándor AD, Péter Á, Corduneanu A, Barti L, Csősz I, Kalmár Z, et al. Wide distribution and diversity of malaria-related haemosporidian parasites (*Polychromophilus* spp.) in bats and their ectoparasites in eastern Europe. *Microorganisms*. (2021) 9:230. doi: 10.3390/microorganisms9020230

48. Daveu R, Hervet C, Sigrist L, Sassera D, Jex A, Labadie K, et al. Sequence diversity and evolution of a group of iflaviruses associated with ticks. *Arch Virol*. (2021) 166:1843–52. doi: 10.1007/s00705-021-05060-8

49. Lvov DK, Kostiukov MA, Daniiarov OA, Tukhtaev TM, Sherikov BK. Outbreak of arbovirus infection in the Tadzhik SSR due to the Issyk-Kul virus (Issyk-Kul fever). *Vopr Virusol*. (1984) 29:89–92.

50. Aulagnier S, Presetnik P. Schreibers' Bent-Winged Bat *Miniopterus schreibersii* (Kuhl, 1817) In: K Hackländer and FE Zachos, editors. Handbook of the mammals of Europe. Cham: Springer International Publishing (2020). 1–26.

51. Wang R, Li Z-M, Peng Q-M, Gu X-L, Zhou C-M, Xiao X, et al. High prevalence and genetic diversity of hemoplasmas in bats and bat ectoparasites from China. *One Health*. (2023) 16:100498. doi: 10.1016/j.onehlt.2023.100498

52. Dincer E, Timurkan MO, Yalcınkaya D, Hekimoglu O, Nayır MB, Sertkaya TZ, et al. Molecular detection of Tacheng tick Virus-1 (TcTV-1) and Jingmen tick virus in ticks collected from wildlife and livestock in Turkey: first indication of TcTV-1 beyond China. *Vector-Borne Zoonotic Dis*. (2023) 23:419–27. doi: 10.1089/vbz.2023.0029

53. Kemenesi G, Tóth GE, Mayora-Neto M, Scott S, Temperton N, Wright E, et al. Isolation of infectious Lloviu virus from Schreiber's bats in Hungary. *Nat Commun*. (2022) 13:1706. doi: 10.1038/s41467-022-29298-1

54. Keve G, Sándor AD, Hornok S. Hard ticks (Acari: Ixodidae) associated with birds in Europe: review of literature data. *Front Vet Sci*. (2022) 9:928756. doi: 10.3389/fvets.2022.928756

55. Hornok S, Wang Y, Otranto D, Keskin A, Lia RP, Kontschán J, et al. Phylogenetic analysis of *Haemaphysalis erinacei* Pavesi, 1884 (Acari: Ixodidae) from China, Turkey, Italy and Romania. *Parasit Vectors*. (2016) 9:643. doi: 10.1186/s13071-016-1927-1

56. Martinez S, Sullivan A, Hagan E, Goley J, Epstein JH, Olival KJ, et al. Living safely with bats: lessons in developing and sharing a global one health educational resource. *Glob Health Sci Pract*. (2022) 10:e2200106. doi: 10.9745/GHSP-D-22-00106

Frontiers in Veterinary Science

Transforms how we investigate and improve animal health

The third most-cited veterinary science journal, bridging animal and human health with a comparative approach to medical challenges. It explores innovative biotechnology and therapy for improved health outcomes.

Discover the latest Research Topics

See more →

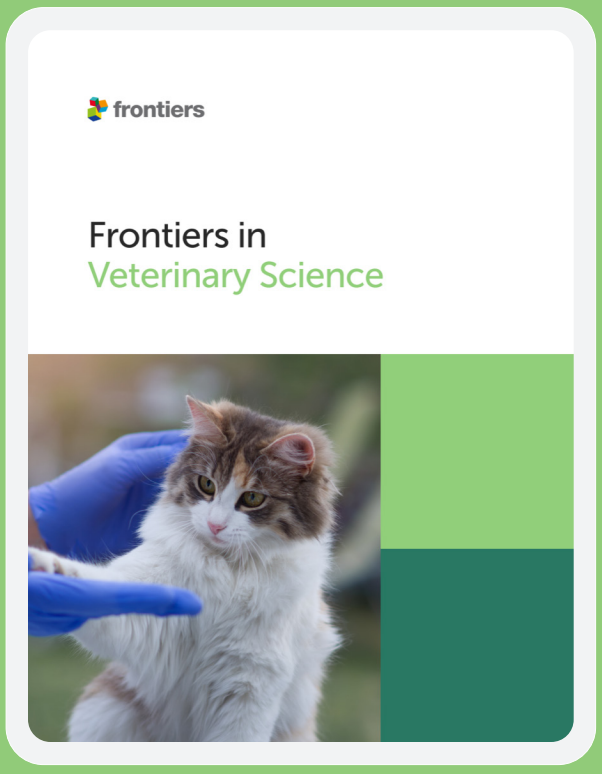

Frontiers

Avenue du Tribunal-Fédéral 34
1005 Lausanne, Switzerland
frontiersin.org

Contact us

+41 (0)21 510 17 00
frontiersin.org/about/contact